



PHD

Targeting estrogen biosynthesis and hormone receptor pathways for the treatment of cancer

Mottinelli, Marco

Award date:
2014

Awarding institution:
University of Bath

[Link to publication](#)

Alternative formats

If you require this document in an alternative format, please contact:
openaccess@bath.ac.uk

Copyright of this thesis rests with the author. Access is subject to the above licence, if given. If no licence is specified above, original content in this thesis is licensed under the terms of the Creative Commons Attribution-NonCommercial 4.0 International (CC BY-NC-ND 4.0) Licence (<https://creativecommons.org/licenses/by-nc-nd/4.0/>). Any third-party copyright material present remains the property of its respective owner(s) and is licensed under its existing terms.

Take down policy

If you consider content within Bath's Research Portal to be in breach of UK law, please contact: openaccess@bath.ac.uk with the details. Your claim will be investigated and, where appropriate, the item will be removed from public view as soon as possible.

Targeting of estrogen biosynthesis and hormone receptor signalling pathways for the treatment of cancer

Marco Mottinelli

A thesis submitted for the degree of Doctor of Philosophy
University of Bath, Department of Pharmacy and Pharmacology

October 2013

COPYRIGHT

Attention is drawn to the fact that copyright of this thesis rests with the author. A copy of this thesis has been supplied on condition that anyone who consults it is understood to recognise that its copyright rests with the author and that they must not copy it or use material from it except as permitted by law or with the consent of the author.

This thesis may be made available for consultation within the University Library and may be photocopied or lent to other libraries for the purposes of consultation.

Signed.....

Date.....

Abstract

The tetrahydroisoquinoline (THIQ) core structure is explored as a steroidomimetic nucleus with attractive pharmaceutical properties. A library was synthesised employing Pomeranz-Fritsch, Pictet-Spengler, Bischler-Napieralski strategies yielding 77 final targets, substituted at every position, for biological evaluation. Complementary strategies overcame synthetic difficulties, sometimes yielding two products in a single cyclisation. Three compounds were initially tested against a panel of 19 nuclear receptors (NRs) and exhibited broad substitution-dependent activity. 2-(4-Chlorophenyl)-1-isopropyl-1,2,3,4-tetrahydroisoquinolin-6-ol fully inhibited every NR at 100 μ M, confirming the THIQ as a lead for optimisation. Compounds were evaluated for cytotoxicity against 60 cell lines by the NCI (USA), exhibiting moderate to insignificant cytotoxicity. Three compounds showed *ca.* 30-90% of average growth inhibition and were selected for a five dose test. Off-target evaluation highlighted compounds with activity against glucagon-like peptide 1 secretion, calcitonin gene-related peptide receptor antagonism and with >100% inhibition against the metabotropic glutamate receptor 2. Estrogen receptor-related receptor α (ERR α), a constitutively active orphan NR, is a hormone-dependent cancer target and diethylstilboestrol (DES), a known inverse agonist, possesses similarities to THIQs. THIQs tested against ERR α revealed no general SAR rules, but showed a lower degree of efficacy in a commercial TR-FRET assay, with 1-benzyl-2-(4-chlorophenyl)-4-methyl-1,2,3,4-tetrahydroisoquinolin-6-ol showing 79% efficacy at 100 μ M as an inverse agonist, being more active than DES (64% at 100 μ M). Inhibition of steroidogenic enzymes like 17 β -hydroxysteroid dehydrogenase type 1 (17 β -HSD1) is an emerging approach for the treatment of HDBC, compared to other current clinical strategies. THIQs evaluated against 17 β -HSD1 showed good activity in both whole cell and cell lysate assays, with the best inhibitor, 2-(4-chlorophenyl)-4-isopropyl-1,2,3,4-tetrahydroisoquinolin-6-ol, possessing an IC₅₀ value of 336 nM. The value of THIQ as a drug-like steroidomimetic scaffold is thus established and this work reveals straightforward strategies to optimise potency and selectivity for a range of potential targets by structural and stereochemical iteration.

Acknowledgements

I need to start by stating that this first section will be rather informal because I have read many acknowledgements in other theses and they are really dry and cold. This is not my way. The order does not reflect the importance of the people. After my family you are all important to me, each of you in a unique way.

In primis, I will never thank enough my family: mum, dad and Grazia. Without the support you gave me throughout my life I would have not made it to this point. You raised me to be a good person, or at least I think I am, and I am going to use the life you gave me to try to help others with every single thing that I will achieve in my life, be it small or big. Grazia, you might have not realised it but I always looked up to you. You are strong even though sometimes bitter, but without you taking care of everything dad and I would have made a mess during the time that mum was ill. Please, don't ever think low of yourself. These words were just to say I love you.

Then it comes to Manuel. Sometimes I don't know if I should thank you or if I should just strangle you. You tried hard and we are still together and you put up with me during these last months where I have shown the worst of me. I should definitely thank you. You hurt me sometimes but I still love you.

I really have to thank Prof. Potter and Dr. Leese, namely Barry and Matt. I wanted to do a PhD abroad since I started my undergraduate studies, so thank you for making one of my many dreams come true. Barry, thanks to all of your comments I think I have grown up a lot in these years and Matt, you have been a true inspiration for every day I was able to spend with you. There was nothing more exciting than our informal meetings where I came out so full of ideas and so enthused about this project. Thank you both.

I realise now that I would have to write at least ten pages to thank everyone in this way so I will try to be a bit briefer. I have to thank Kat, probably I will never be able to thank her enough but I will try within the next years. Thanks for all the time we spent together and if there is one thing that I learned, it is definitely that I will never want to see you angry.

Jo, my light in the darkness, the breeze in the cave that shows you the way out, the life vest under the seat of a crashing plane. Since you moved into the lab, after almost

everyone else left, you helped me a lot. You helped me with everything and you probably do not realise how much. And just so you know, there are not many people in front of whom I would sing happily like I was doing in the lab. This is just one thing that shows how much I trusted you. Also thank you for helping me with the chemistry section of this thesis.

Gyles, you guided me through all the biochemistry and you also helped me with the biochemistry section of the thesis. Thank you for that and also for being able to stand my questions all the time. Pauline, thank you for helping me with the cell work and for giving me hope every time that those crazy cells misbehaved (i.e. every single time). Thanks to everyone else in the group, Wolfgang and Xiangdong the only ones left from Sterix together with Gyles and Mark. Mark, thank you for the computational chemistry you did for me. With all the conformation and chirality issues I always ended up giving you a lot of work. Thank you also for the tedious job of proof reading the whole thesis written in my ominous English. I agree with you, tests and testes are not the same. Thanks also to Andy, Steve and Jasmine, who were always there when I needed help.

I want to thank everyone that has been there almost since the first day: Elvis, who has also become my bro' in the past four years, Alex, Amit, Chris, Dan (who managed to drag me out of the lab when everybody else failed), Helen, Jeremy, Kim, Maks, Nat, Nour, Patri, Ricardo and Terrence. Thanks to those who were there at the beginning and then had to leave: Christelle, Francesca, Liz and Riccardo. And thanks to those who just recently joined the group: Kunal, Ruggero and Tiago.

I want also to thank all the people that are always waiting for me back in Italy. Friends that are always there, no matter the distance: Andrea, Elena, Luca and Matteo. The friends from high school Marco, Andrea, Francesca, Alessandro and everyone else. The friends from uni, Fiora and Simona, we studied a lot together and we surely had many coffees together. Thanks to Ema, who is one of my best friends. We have passed many moments together, some bad and some good, and we have raised a bunch of kids trying to teach them not only karate but also how to become good people. Among our students, I need to thank Lorenzo who is now looking after me like the good man that he has become. Thanks to my two sensei Alessandro and Nicola, who have become my second family together with the others of the karate club, especially Dario and Andrea. Even if we disagree on many things, I owe you a lot Ale. You helped me to grow stronger, you are the one that taught me how to overcome my limit, how to never get

down. How to rise my head up after being punch to the ground when life shows no mercy. How to be strong but just. You are the one that completed the job that my parents have done.

I need to thank Prof. Mike Threadgill, who told me off the first time that I called him Professor instead of Mike. So thank you Mike for letting me use the equipment for the cell work and for refreshing my NMR knowledge during the workshops. Thanks to Tim Woodman, who has run almost every NMR sample and who was always excited when I brought him requests of difficult samples to analyse. Thanks to Christian Rebheim who has run every mass spectrometry sample and found out that some samples are fine in negative mode while not in positive mode. I would have never thought of trying it. Thanks to Pascal, the most efficient IT technician, you just need an email and every computer problem is solved. Thanks to Paul De Bank who sometimes let me use his plate reader. Thanks to Dr. Charareh Pourzand and her group, Olivier and Tina, that accompanied me in the weekends spent taking care of the misbehaving cells. And thanks to Dr. Atul Purohit who donated the cells. Even if I couldn't make the assay work, it was really good experience. Thanks to Mary Mahon who has done the X-ray diffraction for one of the compounds. Thanks to Prof. Tea Lanisnik-Ritzner and her PhD student Maša Sinreih for the testing against 17 β -HSD1. Thanks to Prof. Geff Holman who allowed me to use his plate reader for the TR-FRET assay. Especially thanks to Francoise Koumanov who answered my last desperate email when I was giving up any hope of finding a plate reader for running the TR-FRET assay.

I want to finish thanking Prof. Minutolo, who is the one that ignited my spark for research and who I still look up to, even after five years.

My favourite motto: you give the best of yourself when you have nothing left to give.

Abbreviations

17 β -HSD1	17 β -hydroxysteroid dehydrogenase type 1
17 β -HSD2	17 β -hydroxysteroid dehydrogenase type 2
3 β -HSDs	17 β -hydroxysteroid dehydrogenases
4-OHT	4-Hydroxytamoxifen
Å	Ångström
Ac	Acetyl
AcCl	Acetylchloride
AcOH	Acetic acid
ADMET	Administration, Distribution, Metabolism, Excretion, Toxicity
Ar	Aryl
Bn	Benzyl
BN	Bischler-Napieralsky
bs	Broad singlet (NMR spectra)
CBZ	Carboxybenzyl
Conc.	Concentrated
CSM	Charcoal stripped serum supplemented medium (biology)
CSR	Chiral Shift Reagent
CYP	Cytochrome P450
d	Doublet (NMR spectra)
dd	Double doublet (NMR spectra)
ddd	Double double doublet (NMR spectra)
dt	Double triplet (NMR spectra)
DABAL	Bis(trimethylaluminum)-1,4-diazabicyclo[2.2.2]octane adduct
DBD	DNA Binding Domain
DCE	Dichloroethane
DCM	Dichloromethane
DES	Diethylstilbestrol
DHEA	Dehydroepiandrosterone
DHIQ	Dihydroisoquinoline
DIPEA	<i>N,N</i> -Diisopropylethylamine
DMF	<i>N,N</i> -Dimethylformamide

DMSO	Dimethylsulphoxyde
DNA	Deoxyribonucleic acid
DTT	Dithiothreitol
E1	Estrone
E1S	Estrone sulphate
E2	Estradiol
E3	Estriol
EC ₅₀	Concentration to activate 50% of the target (agonists); Concentration to block 50% of the constitutively active target (inverse agonists)
EDCI	1-Ethyl-3-(3-dimethylaminopropyl)carbodiimide
eq.	Equivalent
ER	Estrogen receptor
ER-	Estrogen receptor negative
ER+	Estrogen receptor positive
ERE	Estrogen response elements
ERR	Estrogen receptor-related receptor
ERRE	Estrogen-related response elements
Et	Ethyl
Eu(hfc) ₃	Europium tris[3-(heptafluoropropylhydroxymethylene)-(+)- camphorate]
FRET	Fluorescence Resonance Energy Transfer
Glu	Glutamate
GST	Glutathione <i>S</i> -transferase
HER2	Human Epidermal Growth Factor Receptor 2
HIF	Hypoxia-Inducible factor
His	Histidine
HPLC	High Performance Liquid Chromatography
HSQC	Heteronuclear single quantum coherence spectroscopy
Hz	Hertz
IC ₅₀	Concentration to inhibit 50% of the target activity
<i>i</i> -Pr	isopropyl
<i>J</i>	Coupling constant (NMR spectra)

KHMDS	Potassium hexamethyldisilazane
LBD	Ligand Binding Domain
LC-MS	(HPLC-MS) High pressure liquid chromatography - Mass spectroscopy
LDA	Lactate dehydrogenase (enzyme)
LDA	Lithium diisoprylamine (chemical)
Leu	Leucine
M	Molar (concentration), Molecular ion (mass spectroscopy)
m	milli, multiplet (NMR spectra)
Me	Methyl
mp	Melting point
MTS	3-(4,5-Dimethylthiazol-2-yl)-5-(3-carboxymethoxyphenyl)-2-(4-sulfophenyl)-2 <i>H</i> -tetrazolium, inner salt
MS	4Å molecular sieves
NAD ⁺	Nicotinamide Adenine Dinucleotide (oxidised)
NADH	Nicotinamide Adenine Dinucleotide (reduced)
NADP ⁺	Nicotinamide Adenine Dinucleotide Phosphate (oxidised)
NADPH	Nicotinamide Adenine Dinucleotide Phosphate (reduced)
NCI	National Cancer Institute of America
NHR	Nuclear Hormone Receptor
NM	Normal serum supplemented medium (biology)
NMR	Nuclear Magnetic Resonance
NOESY	Nuclear Overhauser Effect spectroscopy
NR	Nuclear Receptor
OIDD	Open Innovation Drug Discovery
OXPHOS	Oxidative phosphorylation
PD ²	Phenotypic Drug Discovery
Pd/C	Palladium on carbon
PES	Phenazine ethosulfate
pet. ether	Petroleum ether 40-60 °C
PF	Pomeranz-Fritsch
PGC-1α	Peroxisome proliferator-activated receptor gamma co-activator 1-alpha

ppm	Parts per million
PR	Progesterone Receptor
PS	Pictet-Spengler
PTSA	<i>para</i> -Toluene sulphonic acid
q	Quartet (NMR spectra)
rt	Room temperature
s	Singlet (NMR spectra)
SAR	Structure activity relationship
Ser	Serine
SERD	Selective estrogen receptor down-regulator
SERM	Selective estrogen receptor modulator
STS	Steroid Sulphatase
t	Triplet (NMR spectra)
TargetD ²	Target Drug Discovery
Tb	Terbium
TBAI	Tetrabutylammonium iodide
<i>t</i> -Bu	<i>tert</i> -Butyl, tertiary butyl
TCA	Tricarboxylic acids
TFA	Trifluoroacetic acid
TfOH	Trifluoromethanesulphonic acid (triflic acid)
THF	Tetrahydrofuran
THIQ	1,2,3,4-Tetrahydroisoquinoline
TLC	Thin layer chromatography
TNBC	Triple Negative Breast Cancer
TR-FRET	Time Resolved FRET
Tyr	Tyrosine
Val	Valine
VEGF	Vascular Endothelial Growth Factor
δ	Delta (chemical shift)

Index

LIST OF FIGURES	XV
LIST OF SCHEMES	XIX
LIST OF TABLES	XXI
CHAPTER 1 - INTRODUCTION	1
1.1. Breast cancer statistics	1
1.2. Current breast cancer treatments	1
1.3. Endocrine therapy	2
1.3.1. Selective estrogen receptor modulators (SERMS).....	3
1.3.2. Estrogens biosynthesis	4
1.3.3. Aromatase inhibitors	5
1.3.4. Steroid sulphatase inhibitors	6
1.4. 17-beta hydroxysteroid dehydrogenases (17B-HSDs).....	7
1.4.1. 17 β -HSD1.....	7
1.5. Known inhibitors of 17 β -HSD1	9
1.5.1. Steroidal inhibitors of 17 β -HSD1	10
1.5.1.1. Derivatives of E1 substituted at C2	10
1.5.1.2. Derivatives of E1 and E2 substituted at C6	11
1.5.1.3. Derivatives of E1 substituted at C15	12
1.5.1.4. Derivatives of E1 substituted at C16	13
1.5.2. Non-steroidal inhibitors of 17 β -HSD1	14
1.5.2.1. Biphenylketones.....	15
1.5.2.2. Phenylanthracene and phenylquinoline derivatives.....	18
1.5.2.3. Bis(hydroxyphenyl) substituted thiophenes, azoles, benzenes and pyridines ..	21
1.5.2.4. Benzothienopyrimidones	25
1.5.2.5. Coumarin derivatives.....	28
1.6. Estrogen receptor-related receptor alpha.....	29
1.6.1. ERR α and breast cancer	32
1.6.2. Known inhibitors of ERR α	33
1.7. The importance of drug-like properties in drug discovery.....	36
1.8. Aims of the project.....	37
CHAPTER 2 – RESULTS AND DISCUSSION: CHEMISTRY	41
2.1. Pomeranz-Fritsch approach.....	42
2.1.1. Synthesis of <i>N</i> -(2,2-dialkoxy)aniline	42

2.1.2. Synthesis of <i>N</i> -benzyl- <i>N</i> -(2,2-dimethoxyethyl)anilines.....	44
2.1.3. The Pomeranz-Fritsch cyclisation.....	51
2.1.4. Dehydroxylation of 4-hydroxytetrahydroisoquinolines.....	63
2.1.5. Methoxy deprotection of final THIQs.....	68
2.1.6. Further functionalisation of the 4-hydroxy THIQs.	69
2.2. The Pictet-Spengler (PS) and Bischler-Napieralski (BN) approach	70
2.2.1. Synthesis of the amides 178	71
2.2.2. Reduction of the amides 178a-h	71
2.2.3. The Pictet-Spengler cyclisation.....	72
2.2.4. The Bischler-Napieralski cyclisation.	74
2.2.5. Methoxy deprotection of final THIQs.....	78
2.2.6. The Pictet-Spengler approach modification: towards 3-substituted THIQs.	78
2.2.7. Weinreb reaction: alkylation of amide 208	82
2.2.8. Reductive amination of ketones 209a,b,d,e	83
2.2.9. The Pictet-Spengler cyclisation: towards 3-substituted THIQs.	84
2.2.10. The Pictet-Spengler approach modification: towards 4-substituted THIQs.	85
2.2.11. Alkylation of ester 226	89
2.2.12. Ester to amide conversion.	90
2.2.13. Reduction of amides 224a-f	91
2.2.14. PS cyclisation of amines 225a-f	92
2.2.15. The Bischler-Napieralski approach modification: towards 1,4-disubstituted THIQs.....	93
2.2.16. Deprotection of the final THIQs synthesised through the modified PS and BN approaches.....	99
2.3. General conclusions.	100
CHAPTER 3 – RESULTS AND DISCUSSION: BIOLOGICAL EVALUATION AND COMPUTATIONAL CHEMISTRY	101
3.1. 17 β -hydroxysteroid dehydrogenase type 1 (17 β -HSD1)	101
3.1.1. Protein expression and purification.....	101
3.1.2. Protein crystallisation.....	105
3.1.3. Colourimetric enzymatic assay.	107
3.1.4. Qualitative whole cell assay.....	114
3.1.5. Structure activity relationship of the synthesised compounds against 17 β HSD1. 120	
3.1.5.1. Comparison between the assays from Ipsen and Prof. Rizner's group	122
3.1.5.2. Effects of the nature of substituents on the <i>N</i> -phenyl ring	123

3.1.5.3. Effect of hydroxyl group in position 4, 5, 6 and 7	125
3.1.5.4. Effect of the position of the substituent on the <i>N</i> -phenyl ring	126
3.1.5.5. Effect of multiple substituents in positions 4, 5, 6 and 7 of the THIQ ring....	128
3.1.5.6. Effect of substitution in position 1	129
3.1.5.7. Effect of substitution on the <i>N</i> -phenyl ring for the 1-substituted THIQs	130
3.1.5.8. Effect of substitution in position 3	131
3.1.5.9. Effect of substitution in position 4	131
3.1.5.10. effect of disubstitution in position 1 and 4	133
3.1.5.11. Comparison between THIQs and the open ring analogues	133
3.1.6. Conclusions	134
3.2. Estrogen receptor-related receptor α (ERR α)	137
3.2.1. LanthaScreen TM TR-FRET assay description	138
3.2.2. Structure activity relationship of the synthesised compounds against ERR α ..	140
3.2.2.1. Effects of the nature of substituents on the <i>N</i> -phenyl ring	143
3.2.2.2. Effect of the position of the substituent on the <i>N</i> -phenyl ring	146
3.2.2.3. Effect of substituents in positions 4, 5, 6, 7 and 8 of the THIQ ring	147
3.2.2.4. Effect of multiple substituents in positions 4, 5, 6 and 7 of the THIQ ring....	147
3.2.2.5. Effect of hydroxyl in position 4	148
3.2.2.6. Effect of substitution in position 1	149
3.2.2.7. Effect of substitution on the <i>N</i> -phenyl ring for the 1-substituted THIQs	150
3.2.2.8. Effect of substitution in position 3	151
3.2.2.9. Effect of substitution in position 4	152
3.2.2.10. effect of disubstitution in position 1 and 4	153
3.2.2.11. Comparison between THIQs and the open ring analogues	154
3.2.3. Conclusions	155
3.3. Nuclear hormone receptors (NHRs) screening.	157
3.4. National cancer institute of america (NCI) – developmental therapeutics program (DTP)	162
3.5. Eli Lilly – Open Innovation Drug Discovery (OIDD)	168
3.5.1. PD ² – Wnt pathway activator	170
3.5.2. PD ² – GLP1 secretion	170
3.5.3. PD ² – Kras/Wnt synthetic lethal	170
3.5.4. TargetD ² – GPR119 receptor antagonist	173
3.5.5. TargetD ² – Apelin receptor (APJ) agonist	173
3.5.6. TargetD ² – Calcitonin gene-related peptide receptor (CGRP) antagonist	173

3.5.7. TargetD ² – Metabotropic glutamate receptor 2 (mGluR2) allosteric antagonist	173
3.5.8. TargetD ² – Hexokinase 2 (HK2) inhibitor	174
3.5.9. TargetD ² – Enhancer of zeste homolog 2 (EZH2) inhibitor	174
3.5.10. Conclusions	175
3.6. Summary	176
CHAPTER 4 - EXPERIMENTAL	185
4.1. Chemistry: materials and methods	185
4.1.1. General reaction procedures	185
4.1.2. Experimental data	189
4.2. Biology: materials and methods	330
4.2.1. Glycerol stock	330
4.2.2. Expression of His-17-βHSD1	330
4.2.3. Purification of His-17-βHSD1	331
4.2.3.1. Histrap column purification	331
4.2.3.2. Q-Sepharose column purification	332
4.2.4. SDS polyacrylamide gel electrophoresis (SDS-PAGE)	332
4.2.5. Protein concentration determination	333
4.2.6. 17β-HSD1 inhibition: MTS assay	333
4.2.7. Crystallisation	334
4.2.8. T-47D and MCF-7 cell culture	335
4.2.9. T47D and MCF-7 growth inhibition assay	335
4.2.10. Inhibition of ERRα	337
4.2.11. Outsourced assays	338
4.2.11.1. 17β-HSD1 inhibition: whole cell radio-assay	338
4.2.11.2. 17β-HSD1 inhibition: cell homogenate radio-assay	339
4.2.11.3. Nuclear receptors screening from DiscoverX	339
4.2.11.4. Eli Lilly	341
4.2.11.5. National Cancer Institute Of America (NCI) – Developmental Therapeutics Program (DTP)	343
BIBLIOGRAPHY	346
APPENDIX A	360
Crystallographic data for compound 164j	360
APPENDIX B	366
NCI raw data	366
Graphic data by cancer type	373

List of figures

Figure 1. Chemical structure of the SERM Tamoxifen and the SERD Fulvestrant.	3
Figure 2. Structure of Anastrozole, the aromatase inhibitor most commonly used in therapy.....	6
Figure 3. Structure of the steroidal STS inhibitor EMATE and non-steroidal inhibitor STX64.....	6
Figure 4. Postulated catalytic mechanism for the reduction of E1 by 17 β -HSD1.....	8
Figure 5. Catalytic conversion of E1 to E2 by 17 β -HSD1 and of E2 to E2 by 17 β -HSD2.	9
Figure 6. Structure of the steroidal inhibitor of 17 β -HSD1 STX1040, developed at the University of Bath.....	9
Figure 7. Structure of some inhibitors of 17 β -HSD1 based on 2-substituted E1.....	10
Figure 8. Structure of some 6-oxo and 6-oxime derivatives of E1 and modified E1 as 17 β -HSD1 inhibitors.....	11
Figure 9. Structure of some 6-substituted E2 derivatives	12
Figure 10. Structure of some 15-substituted E1 derivatives.....	12
Figure 11. The first E2-adenosine hybrid inhibitor reported, EM-1745 (25).	13
Figure 12. Structure of the C16 modified E2 dual site inhibitors with different linker lengths.....	13
Figure 13. Structure of the compounds synthesised as modification of the hydroxyl moiety.....	24
Figure 14. Structure of the phenyl and pyridyl derivatives.....	25
Figure 15. Lead compound of the benzothienopyrimidones series.....	26
Figure 16. Structure of the series of benzothienopyrimidones and relative activities against 17 β -HSD1 in both cell-free and cell based assays.....	26
Figure 17. 7,4'-Dihydroflavone 92 . The best flavone inhibitor resulted from the evaluation of Starčević <i>et al.</i> ⁶⁸	28
Figure 18. Structure of simple coumarin derivatives as inhibitor of 17 β -HSD1.....	28
Figure 19. Series of 7-phenyl substituted coumarin as inhibitors of 17 β -HSD1.....	29
Figure 20. Level of homology among the ERs and ERRs at the DBD (DNA binding domain) and LBD (ligand binding domain).....	30
Figure 21. Principal regulatory roles played by ERR α in the different tissues of the body.....	31
Figure 22. Two compounds reported by Novartis as ERR α inhibitors.....	33
Figure 23. Crystal structure of ERR α reported from Novartis of the unbound receptor (A) in complex with PGC-1 α and of the receptor in complex with the inhibitor (B).....	34
Figure 24. Structure of the three inhibitors of ERR α : DES, hexoestrol and dienestrol.....	35
Figure 25. Structure of the ERR γ inverse agonist 4-OHT 100	35
Figure 26. Structure of the flavonoid kaempferol as a weak inverse agonist of ERR α	35
Figure 27. Structure of the potent ERR α inhibitor XCT790 and the lead compound from which it originated.....	36
Figure 28. Rationale behind the choice of THIQ as the scaffold for development as an inhibitor of 17 β -HSD1 and inverse agonist of ERR α	38
Figure 29. Structure of some natural alkaloids that contain a THIQ moiety, namely carnegine, salsolinol, norcoclaurine, pavine, tubocurarine and tetrandrine.....	41
Figure 30. Steric and electronic effects of the substituent on the nucleophilicity of the aniline.....	46

Figure 31. List of substitutions of aldehydes (129a-h) and ketones (129i,j) tested for the benzoxazine ring formation.	48
Figure 32. Possible intramolecular charge stabilisation of the protonated 123k	55
Figure 33. The stacked spectra refer, from the bottom to the top, to the starting material 123i (SM), the samples at 0, 10, 20, 40 min and the last one is the worked up reaction after 60 min..	57
Figure 34. ¹ H NMR of the crude reaction mixture of compound 154d	59
Figure 35. ¹ H NMR of the non-purified compound 143a	61
Figure 36. Structure of substitutions for the final THIQs.	67
Figure 37. Structure of substitutions for the hydroxytetrahydroisoquinolines.	69
Figure 38. Compounds isolated after attempted alkylation of amide 178	80
Figure 39. Representation of a Soxhlet extractor used during the Fisher esterification.	88
Figure 40. ¹ H NMR of crude amide 224a	91
Figure 41. ¹ H NMR of the crude amine 225a	92
Figure 42. Chiral HPLC chromatogram of compound <i>trans</i> - 234j	95
Figure 43. Three dimensional conformation of compound <i>trans</i> - 234j seen from the “top” (on the left) and from the “side” (on the right).	96
Figure 44. NOESY spectrum of compound <i>trans</i> - 234j	96
Figure 45. Stacked ¹ H NMR spectra of <i>trans</i> - 234j during the CSR experiment.	97
Figure 46. ¹ H- ¹³ C HSQC analysis of <i>trans</i> - 234j + 6.0 mg of Eu(hfc) ₃	98
Figure 47. Schematic representation of the insertion of the 17βHSD1 gene into the pET-24a(+) from the pCEP4 mammalian vector.	102
Figure 48. Map of the protein cloning expression region of pET-24a showing the promoter, lac operator, NheI and XhoI restriction enzyme binding sites, His-tag coding region and the terminator sequence.	103
Figure 49. Structure of allolactose and its mimic IPTG.	103
Figure 50. Structure of histidine and imidazole.	104
Figure 51. Structure of compound 170i used for the crystallisation trials.	106
Figure 52. Pictures of a hanging drop of buffer with crystals of apo-17βHSD1.	106
Figure 53. Pictures of a hanging drop of buffer with crystals of 17βHSD1 after the addition of NADP ⁺	107
Figure 54. Pictures of a crystal of 17βHSD1 obtained with a SEM.	107
Figure 55. Schematic representation of the conversion of E1 to E2 by 17βHSD1.	108
Figure 56. Structure of the initial set of compounds tested against 17βHSD1 on the colourimetric assay and the control steroidal inhibitor STX1040.	110
Figure 57. Graph of the measured V ₀ of 17βHSD1 without E2 or 170i , with E2 but no 170i , with E2 and 170i and with 170i but no E2.	112
Figure 58. Docking of compound 170i	113
Figure 59. Flow chart depicting the information obtainable by treating T47-D cells with an inhibitor and with or without E1 or E2.	114
Figure 60. Initial set of compounds used for the screening.	115
Figure 61. Growth percentage of T47-D cells treated only with the set of THIQs.	115
Figure 62. Growth percentage of T47-D cells treated with E2 the set of THIQs.	115
Figure 63. Growth percentage of T47-D cells treated with E1 the set of THIQs.	116
Figure 64. Effect of the vehicle DMSO on the T47-D cell growth.	116
Figure 65. Growth curves of T47-D cells with or without ethanol or either E1 or E2.	117
Figure 66. Growth of untreated cells at different passages.	118
Figure 67. Graph A: cell growth of the original stock of cells used for every experiment previously mentioned. Graph B: early passage of a new stock of cells. Graph C: late passage of the same stock of cells used in graph B..	119

Figure 68. Structure and substitution pattern of the compounds selected and tested against 17 β HSD1..	120
Figure 69. Structure of the non-cyclic compounds tested against 17 β HSD1.	122
Figure 70. Structure of the compounds tested to evaluate the effect of the nature of groups R ₁ and R ₂ .	122
Figure 71. Structures of E1 (on the left) and the tested series of THIQs (on the right). At the centre, the overlap of the two structures highlights the similar spatial disposition of the steroidal phenol and R ₁ .	124
Figure 72. Craig plot with the R ₂ substituents (Figure 70) highlighted.	125
Figure 73. Structure of compounds 143z , 163a,z , 170i , 171 and 172 and relative percentage of inhibition at 6 μ M.	126
Figure 74. Structure of the compounds tested to evaluate the influence of the position of the group R ₂ on the N-phenyl ring.	127
Figure 75. Crystal structure of compound 164j (Table 17, page 67) which show the planarity of the molecule;	127
Figure 76. Superimposition of the minimised 3D structure of E2 and the core structure of THIQ.	128
Figure 77. Structure of compounds 163s , 167 and 146x with relative percentage of inhibition at 6 μ M.	128
Figure 78. Structure of compounds 170s , 173 and 174 with relative percentage of inhibition at 6 μ M.	129
Figure 79. Structure of compounds 144h , 145h with relative percentage of inhibition at 6 μ M compared with compound 163a .	129
Figure 80. Structure of the compounds tested to evaluate the influence of the substituent R in position 1.	130
Figure 81. Structure of the 1-benzyl substituted compounds 181f,h-i .	131
Figure 82. Structure of 3-substituted compounds 234a-b and their relative percentage of inhibition at 6 μ M in comparison with the unsubstituted compound 170i .	131
Figure 83. Structure of 4-substituted compounds 234c-f,h and the parent unsubstituted compound 170i .	132
Figure 84. Relationship between 234c and 234h . 234h possess the groups of both enantiomer of 234c at the same time.	133
Figure 85. Structure of 1,4-disubstituted compounds 234i-k .	133
Figure 86. Structure and activity of the THIQs 170i,a and 234c,h compared with the open ring analogues 139n and 140n .	134
Figure 87. Picture of the SAR conclusions for each position of the THIQ.	136
Figure 88. Scheme representing the excitation-relaxation steps coupled with the absorbance and emission of light in normal fluorescence (A) and in FRET (B).	138
Figure 89. Representation of the ERR α TR-FRET assay.	139
Figure 90. Binding saturation curve of ERR α for XCT790.	140
Figure 91. Structure and substitution pattern of the compounds selected and tested against ERR α .	141
Figure 92. Structure of the compounds tested to evaluate the effect of the nature of groups R ₁ and R ₂ .	144
Figure 93. Craig plot graph used to highlight the effects of substitution in position 4' of the 6-methoxy series.	145
Figure 94. Craig plot graph used to highlight the effects of substitution in position 4' of the 6-hydroxy series.	145
Figure 95. Structure of the compounds tested to evaluate the effect of the position of substituent R ₂ on the N-phenyl ring.	146

Figure 96. Structure of the compounds used to evaluate the effect of substituents in positions 4, 5, 6 and 7.	147
Figure 97. Structure of the compounds used to evaluate the effect of multiple substituents in positions 4, 5, 6 and 7.	148
Figure 98. Structure and relative efficacy of compounds 170i , 143n and 175n	149
Figure 99. Structure and relative efficacy of compounds 144h and 145h	149
Figure 100. Structure of tested compounds used to evaluate substituents in position 1..	150
Figure 101. Structure of the compounds used to re-evaluate the influence of the substituent on the <i>N</i> -phenyl ring and to evaluate the influence of the substituent in position 8.	151
Figure 102. Structure of compounds used to evaluate the effect of substituents in position 3.	152
Figure 103. Structure of compounds used to evaluate the effect of substituents in position 4.	153
Figure 104. Structure and relative efficacy of the THIQs 170i,s and the respective open ring derivative 122n,p	155
Figure 105. Structure and relative activity and CLogP values of compounds 191f , 191i and 234i , and compounds of possible future interest 235 and 236	156
Figure 106. Structure and relative activity of compounds 163s and 166s , respectively an inverse agonist and an agonist of ERR α	157
Figure 107. Structure of the three compounds tested against a wide range of NHRs. .	157
Figure 108. Schematic representation of the PathHunter assay from DiscoverX.	158
Figure 109. General structure for the compounds tested on the NCI 60 cell line panel.	162
Figure 110. Results from the NCI 60 cell line panel for every compound tested reported in a single graph.	166
Figure 111. Five dose curve response against the all 60 cell line panel for compound 164j	167
Figure 112. Five dose curve response against the all 60 cell line panel for compound 176x	167
Figure 113. General structure for the compounds tested on the Eli Lilly OIDD screening panel.	169
Figure 114. The comparison between the structure of THIQ, E2 and DES gave the rationale for choosing THIQ as core structure.	177
Figure 115. During both the PF and PS reactions, it was sometime possible to isolate two regioisomers in one single cyclisation step.	178
Figure 116. TOP: structure of compound 234a . BOTTOM: Cyclisation of the amides 231a,b,d under the BN conditions led to only the <i>trans</i> diastereoisomer.	178
Figure 117. Structure of the three compounds selected for the NHR screening.	179
Figure 118. Structure of the three compounds that showed cytotoxic activity in the NCI 60 cell line panel.	180
Figure 119. SAR for 17 β -HSD1 of substitutions around the core THIQ structure.	182
Figure 120. Scheme of the transfer of aliquots from the 96 well plate to the 384 well plate.	338

List of schemes

Scheme 1. Steroidogenesis.....	5
Scheme 2. Synthetic approaches considered for the synthesis of the THIQ core.....	41
Scheme 3. Proposed synthesis for the substituted THIQ through the PF ring closure. ..	42
Scheme 4. Aniline Alkylation. Refer to Table 11 for reagents and conditions.	42
Scheme 5. 2,2-dimethoxyacetaldehyde reductive amination.....	44
Scheme 6. Double reductive amination approach.....	44
Scheme 7. Double reductive amination did not yield the desired product 123c (Table 12) but the C-alkylated product 124	46
Scheme 8. Possible mechanism of the intramolecular rearrangement leading to the formation of 124	47
Scheme 9. Competition between the formation of benzoxazine 126 vs. Vilsmeier-like product 127	48
Scheme 10. Synthesis of benzoxazines.....	48
Scheme 11. Synthesis of the analogues of 123t and 123v , namely 131t , 131v	50
Scheme 12. Proposed strategy for the synthesis of 1 and 3-substituted THIQ.....	50
Scheme 13. Synthesis of compounds 138i and 138s	50
Scheme 14. Synthesis of compounds 122n,p , 139n , and 140n via reductive amination.	51
Scheme 15. Original Pomeranz reaction.	52
Scheme 16. <i>Para</i> -activating effect of the methoxy group..	52
Scheme 17. Electron-withdrawing effects on the PF ring closure.	53
Scheme 18. <i>Ortho</i> vs. <i>para</i> competition for ring closure.....	54
Scheme 19. Cyclisation of compound 123x occurred only in the <i>para</i> position (146x).	54
Scheme 20. Ring closure of compounds 123y and 123k	55
Scheme 21. Possible pathways for the PF reaction.....	56
Scheme 22. Kinetic NMR study of the PF reaction.	56
Scheme 23. Methyl ethers 153f , 151l-o vs. alcohols 144f , 143l-o formation in the PF reaction. 123f,l-o (Table 12, Scheme 6, page 43).	57
Scheme 24. 5- vs. 6-membered ring formation.	59
Scheme 25. 6- vs. 7-membered ring formation from the cyclisation of compound 155	60
Scheme 26. Regioselectivity of the PF reaction under electronic control.	61
Scheme 27. Scheme of the of the PF ring closure.....	62
Scheme 28. PF ring closure of compounds 162i and 162s	63
Scheme 29. Dehydroxylation of compounds 144f,j and 145f,j	64
Scheme 30. Dehydroxylation of compounds 146x and 148y	64
Scheme 31. Attempts to dehydroxylate compounds 143e and 143l	65
Scheme 32. Possible mechanism for dehydroxylation with triethylsilane.....	66
Scheme 33. Benzylation of the 4-hydroxy THIQs 143n and 143x	70
Scheme 34. Proposed synthesis for the substituted THIQs through the PS and BN ring closure.	70
Scheme 35. Synthesis of intermediates 178a-h	71
Scheme 36. Reduction of amides 178a-h	72
Scheme 37. Scheme of the original PS condensation.	72
Scheme 38. Cyclisation of compounds 179d-g,aa	73
Scheme 39. Application of the BN reaction to the synthesis of THIQs.	74
Scheme 40. Synthesis of amides 180a-i (refer to Table 22 for compound substitution).	74

Scheme 41. Mechanism of cyclisation during the BN reaction.	75
Scheme 42. BN cyclisation of amides 180a-i	76
Scheme 43. Synthesis of amides 180j-l	77
Scheme 44. Attempted synthesis of THIQs 181m-n	77
Scheme 45. Deprotection of THIQs 181a-i	78
Scheme 46. Synthesis of THIQ 143 through the PS approach.	79
Scheme 47. Deprotonation of amide 178 by a simple carbanion.	79
Scheme 48. Envisaged mechanism for the alkylation of amide 178	79
Scheme 49. Possible explanation for the formation of the amides 196 and 197	80
Scheme 50. Weinreb reaction mechanism.	81
Scheme 51. Planned synthetic strategy towards the 3-substituted THIQs 211	82
Scheme 52. Synthesis of the Weinreb amide 208	82
Scheme 53. Weinreb reaction of amide 208 with the nucleophiles 213a-e	82
Scheme 54. Degradation of the Weinreb amide 208 in the presence of poorly nucleophilic strong bases such as a non-nucleophilic Grignard.	83
Scheme 55. Reductive amination of ketones 209a,b,d,e	84
Scheme 56. PS cyclisation of amines 210a,b,e	84
Scheme 57. Deprotonation-alkylation of unprotected and protected amide 178b	86
Scheme 58. Planned synthetic scheme for the introduction and cleavage of the CBZ protecting group within the existing synthetic steps.	86
Scheme 59. Fischer esterification of the 3-methoxyphenylacetic acid 177	88
Scheme 60. Planned strategy for the synthesis of 4-substituted THIQs 228	89
Scheme 61. Alkylation of ester 226	89
Scheme 62. Direct conversion of the ester 226 into the amide 178b	90
Scheme 63. Synthesis of amides 224a-f	91
Scheme 64. Reduction of amides 224a-f	92
Scheme 65. PS cyclisation of the amines 225a-f	92
Scheme 66. Acylation of amines 225a-d	93
Scheme 67. BN cyclisation of amides 231a,b,d	94
Scheme 68. Demethylation of the disubstituted THIQs <i>trans</i> - 232a-d	95
Scheme 69. Deprotection of 3- and 4-substituted (166i , 211b and 228a-f , respectively) and 1,4-disubstituted THIQs (232a-e).	99
Scheme 70. Conversion of the tetrazolium salt form of MTS into the formazan form.	109
Scheme 71. Redox cascade that leads to the reduction of the tetrazolium salt MTS to the formazan.	110
Scheme 72. Structure of the 1,4-disubstituted compounds used to evaluate the effects of the substituent in position 4.	154

List of tables

Table 1. Activity and relative substitution pattern of the C16 modified E2 dual site inhibitors measured in a recombinant 17 β -HSD1 assay.	14
Table 2. Structure and biological activity of a series of biphenylketones as non-steroidal inhibitors of 17 β -HSD1.....	15
Table 3. Series of non-steroidal inhibitors of 17 β -HSD1 based on the phenyl-naphthalene core.....	18
Table 4. Series of non-steroidal inhibitors of 17 β -HSD1 based on the phenylquinoline core.....	20
Table 5. Structure and biological activity of bis(hydroxyphenyl) derivatives evaluated in a recombinant 17 β -HSD1 assay.....	22
Table 6. Substituents and biological activity of compounds without a 4-hydroxyl group.	24
Table 7. Substitution and biological evaluation of the series of phenyl and pyridyl derivatives.	25
Table 8. Substitution pattern and biological activity of a series of benzothio-pyrimidones.	27
Table 9. Substituents and biological evaluations of the coumarins 93a-c against 17 β -HSD1.	28
Table 10. Substituents and biological evaluations of the 7-phenyl substituted coumarins 94a-d against 17 β -HSD1.	29
Table 11. Aniline alkylation conditions.....	43
Table 12. Double reductive amination.....	45
Table 13. Results and conditions for the benzoxazines formation.....	49
Table 14. Acids screened for the PF cyclisation with or without <i>para</i> -activating group.	53
Table 15. Ratio between the formation of 143l-o , 144f and 151l-o , 153f at different reaction concentrations.....	58
Table 16. Summary of PF results.	62
Table 17. Summary of the results for the dehydroxylation reaction.....	67
Table 18. Summary of the results for the deprotection of the arylmethoxy THIQs.	69
Table 19. Summary of the results for the synthesis of amides 178a-h	71
Table 20. Summary of the results for the reduction of amides 179a-h	72
Table 21. Yields of the PS cyclisation.	73
Table 22. Summary of the synthesis of amides 180a-i	74
Table 23. Results of the BN cyclisation of amides 180a-i	76
Table 24. Results for the synthesis of amide 180j-l	77
Table 25. Summary of the results for the deprotection of THIQs 181a-i	78
Table 26. Summary of results for the Weinreb reaction.	83
Table 27. Reductive amination of ketones 209a,b,d,e	84
Table 28. Results of the PS cyclisation of amines 210a,b,e	85
Table 29. Summary of the results for the alkylation of ester 226	89
Table 30. Summary of the results for the synthesis of amides 224a-f	91
Table 31. Summary of the results for the cyclisation of amines 225a-f	93
Table 32. Results of the acylation of the amines 225a,b,d	93
Table 33. Results of the BN cyclisation of amides 231a,b,d	94
Table 34. Results of the deprotection of the THIQs obtained through the modified PS and BN approaches.	99

Table 35. Results for the compounds tested against 17 β HSD1 at 10 μ M in the colourimetric assay.	111
Table 36. Comparison between the colourimetric assay and the results from Ipsen. ...	111
Table 37. Comparison of the activity of STX1040 and 170i at three different pHs: 6.5, 7.5, 9.2.....	112
Table 38. List of compounds selected for screening against 17 β HSD1.	120
Table 39. Non-cyclic intermediates tested against 17 β HSD1.....	122
Table 40. Comparison of the results from the assays from Ipsen and the assay from Prof. Lanisnik's group.	123
Table 41. Influence of the position of R ₂ on the inhibitory activity against 17 β HSD1.	127
Table 42. Influence of the substituent in position 1 on the inhibitory activity against 17 β HSD1.....	130
Table 43. Influence of the <i>N</i> -phenyl substituent on the activity of compounds 181f,h-i	131
Table 44. Influence or the substituent in position 4 on the activity of compounds 234c-f,h compared with the activity of the unsubstituted compound 170i	132
Table 45. Effect of the substituent in position 4 on the activity of compounds 234i-k	133
Table 46. Chemicophysical descriptors of compound 234e and relative compliance with some drug-like rules.....	137
Table 47. Full list of compounds tested against ERR α , their relative substitutions and their activity expressed in percentage of inhibition.	141
Table 48. Results of the two series of 4'-substituted compounds tested against ERR α	144
Table 49. Effect of the position of substituent R ₂ on the activity of the two series of compounds tested.....	146
Table 50. Effect on the activity of the position of the substituent R on the THIQ ring.	147
Table 51. Effect of the presence of multiple substituents on the THIQ ring.	148
Table 52. Effects of the substituent in position 1 for the two series of compounds tested.	150
Table 53. Effect of the substituent in 4' position of the 1-benzyl substituted compounds.	151
Table 54. Effect of the substituents in position 3.....	152
Table 55. Effect of the substituents in position 4.....	153
Table 56. Effect of the substituents in position 4 of the 1-benzyl substituted compounds.	154
Table 57. Results of the screening against the NHRs panel in agonist mode.....	160
Table 58. Results of the screening against the NHRs panel in Antagonist mode.....	161
Table 59. List of the 54 compounds tested on the NCI 60 cell line panel with relative substituents description.	163
Table 60. Area of research and relative targets for both TargetD ² and PD ²	168
Table 61. List of the 28 compounds tested on the Eli Lilly OIDD screening panel with relative substituents description.	169
Table 62. Table of the activity of the tested compounds against the PD ² assay modules.	172
Table 63. Table of the activity of the tested compounds against the TargetD ² assay modules.	175

CHAPTER 1

Introduction

Around 309,500 new cases of cancer are diagnosed each year in the UK and between 1979 and 2008 the incidence rates for cancer increased by 26%.¹ Cancer occurs predominantly in older people with 75% of cases diagnosed in people aged 60 but one in ten of all cancer cases occur in adults aged 25-49 years. Breast cancer accounts for nearly half of all cancers diagnosed in the UK in women aged 29-49 years.¹ Of the many types of cancer, breast, lung, colorectal and prostate are the four most commonly diagnosed. In addition, breast, prostate, ovarian and uterine cancers represent 32% of the total cancer diagnoses in the UK and these cancers can develop in hormone sensitive forms.¹

1.1. Breast cancer statistics

Cancer incidence varies by sex and breast cancer, which is overall the most common in the UK with 48,034 new diagnoses in 2012, is quite rare in men for whom prostate cancer is the most common with 37,051 diagnoses.¹ Between 1999-2001 and 2008-2010, the incidence of breast cancer in women has increased by 6% but, in contrast, the mortality rate in the same time span has reduced by 19%.¹ This reduction in mortality is connected to the increase in therapeutic options, better screening services and enhanced and more effective surgical techniques. Nevertheless, 12,047 deaths for breast cancer in only 2008 is still a frightening number.¹

Even though the exact cause of cancer is unknown, breast cancer is known to have some degree of heredity. In fact, mutation in the genes BRCA1 and BRCA2 are associated with a greater incidence of breast cancer. Together, BRCA1 and BRCA2 mutations account for the 20-25% of hereditary breast cancer.² These two genes are related to the expression of tumour suppressing proteins and therefore mutations might deprive the cells of a protecting factor and ultimately increase the risk of cancer.³

1.2. Current breast cancer treatments

The best treatment options to undertake are decided after the status of the cancer has been identified (e.g. type, size, stage and grade of breast cancer) and depending on other

patient related factors such as whether the patient has had her menopause or not or other general health issues.⁴

Surgery is generally the first line treatment and is often coupled with radiotherapy to reduce the risk of remaining tumoural tissues. After a positive screening for BRCA1 and BRCA2, the patient might even decide to have a preventive mastectomy (breast removal) such has been the case for the actress Angelina Jolie. Before surgery, if the tumour mass is too large, chemotherapy can be used to shrink the tumour for better results. Chemotherapy is also used when the tumour has already metastasised (spread through the body) or to treat recurrent breast cancer.⁴

After surgery, to prevent breast cancer recurrence, endocrine therapy or biological therapy can be used. The use of these therapies depends on the status of three receptors in breast cancer cells, i.e. estrogen receptor (ER), progesterone receptor (PR), and human epidermal growth factor receptor 2 (HER2). Breast cancer cells that do not express any of the three receptors are classified as triple-negative and in this case chemotherapy is the only treatment option in addition to surgery and radiotherapy. Triple-negative breast cancer (TNBC) accounts for 15-25% of all breast cancers and is associated with bad prognosis.⁵

1.3. Endocrine therapy

The lifecycle of breast cells is normally regulated by the female sex hormones (estrogens) and, as might be expected, the proliferation of neoplastic cells in these tissues is often stimulated by these same hormones. Tumours which develop from these cells and whose growth is stimulated by these hormones are thus termed hormone dependent. To be stimulated by estrogens, cells must express functional ERs. For this reason, hormone dependent breast cancer is also referred to as estrogen receptor positive (ER+) breast cancer. Therefore, hormone independent breast cancer is often referred to as estrogen receptor negative (ER-). From recent studies, it seems that the transition from ER+ to ER- may occur as a step-wise process involving first the acquisition of estrogen insensitivity, even if ER expression remains, and subsequently the down-regulation of ER expression.^{6,7} The endocrine therapy aims to disrupt the stimulation activity of estrogens on ER+ breast cancer by either preventing their binding to the ER or reducing their biosynthesis.

1.3.1. Selective Estrogen Receptor Modulators (SERMs)

The estrogen receptor was the first target to be addressed for treatment of hormone dependent breast cancer. This approach relies on the inhibition of ER binding by estradiol (E2), thus preventing the E2 initiated signalling cascade. The first compounds showing tissue selective anti-estrogen effects were named selective estrogen receptor modulators (SERMs) and tamoxifen (Figure 1) is the most commonly used in therapy.

There are two known isoforms of the estrogen receptor, namely ER α and ER β , which are diversely expressed in different tissues. Of the two receptors, ER α has been reported to have greater influence on hormone dependent tumours while ER β has a major role in controlling bone formation and calcium and phosphate homeostasis.⁸

Unfortunately, SERMs have proved not to be pure antagonists and the agonist vs. antagonist activity has revealed to be tissue dependent. Due to this issue, the use of SERMs in therapy is associated, for instance, with an increased incidence in uterine cancer, a risk that is, however, usually outweighed by their positive effects. More recently, a new generation of compounds named Selective Estrogen Receptor Down-regulators (SERDs) have shown reduced risks.⁹ SERDs act as potent antagonists by increasing ER turnover and display no agonist activity thus differing markedly from SERMs, which always possess a partial agonist character. Fulvestrant (Figure 1) is an example of a SERD but its use in therapy is limited by its costs.

Recently, *N*-substituted tetrahydroisoquinolines (THIQs) have been demonstrated as effective ER α selective or ER β selective estrogen mimetics presenting a good agonist/antagonist ratio with nM activity.¹⁰

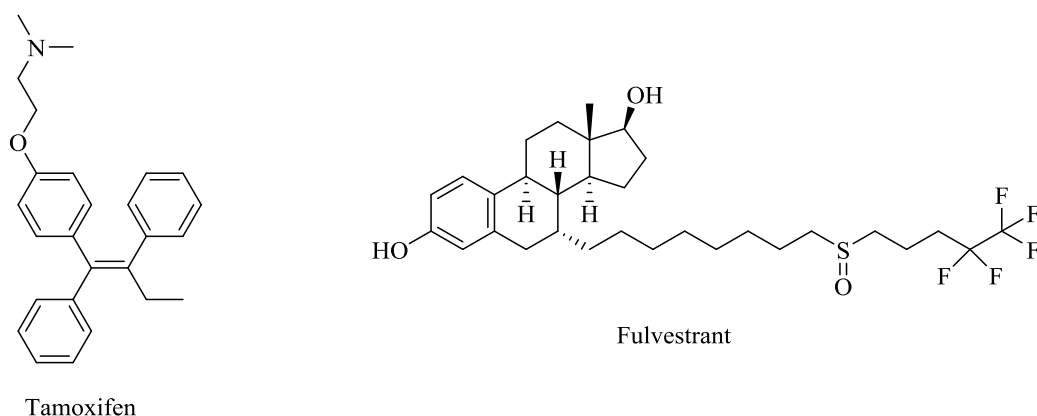


Figure 1. Chemical structure of the SERM Tamoxifen and the SERD Fulvestrant.

1.3.2. Estrogens biosynthesis

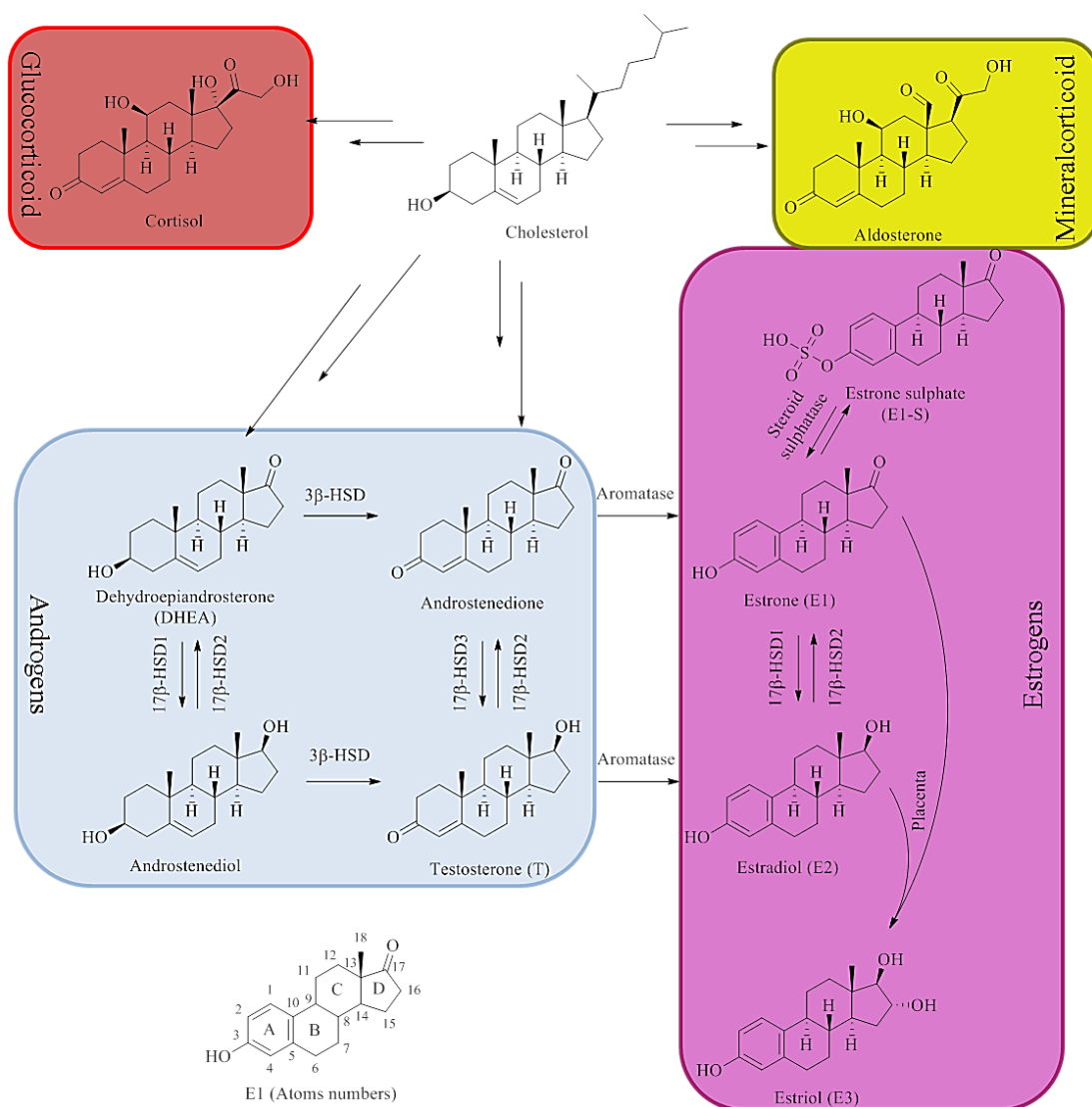
Every steroid hormone (glucocorticoids, mineralcorticoids, androgens and estrogens) is synthesised from cholesterol and each shares the same basic cyclopentanphenantrenic structure (three six-membered rings and one five-membered ring, respectively A, B, C and D) (Scheme 1).

The conversion of dehydroepiandrosterone (DHEA) to androstenedione and the conversion of androstenediol to testosterone (T) are catalysed by a family of enzymes named 3-beta hydroxysteroid dehydrogenases (3β -HSDs) (Scheme 1). The most common isoform is 3β -HSD1, which catalyses the conversion of pregnenolone to progesterone and the conversion of 17β -hydroxypregnenolone to 17β -hydroxyprogesterone (not shown in Scheme 1). Progesterone and 17β -hydroxyprogesterone are the precursors of aldosterone and cortisol, respectively.¹¹

The interconversion of androgens is catalysed by another family of enzymes, namely 17-beta hydroxysteroid dehydrogenases (17β -HSDs). 17β -HSD1 catalyses the conversion of DHEA to androstenediol and 17β -HSD3 catalyses the conversion of androstenedione to T. The conversion of T and androstenediol to their respective precursors is catalysed instead by the same isoform, 17β -HSD2 (Scheme 1). T can also be converted to the more active dihydrotestosterone (DHT) by the enzyme 5α -reductase (not shown in Scheme 1).

The androgens androstenedione and T are converted by the enzyme aromatase to the estrogens estrone (E1) and estradiol (E2), respectively. E1 can also be converted to E2 by 17β -HSD1 while the reverse reaction is catalysed by 17β -HSD2. In addition, E1 can also be converted to the inactive estrone sulphate (E1-S) and stored intracellularly. Moreover, in placental tissues, the E1 and E2 can be converted into the estriol (E3) (Scheme 1).

Among the three estrogens (E1, E2 and E3), E2 is the most potent and binds to the ER with nM affinity.



Scheme 1. Steroidogenesis. Cholesterol is the starting point for the synthesis of glucocorticoids (red), mineral corticoids (yellow), androgens (blue) and estrogens (pink).

1.3.3. Aromatase inhibitors

Aromatase is one of the last enzymes involved in the synthesis of E2 (Scheme 1) and as such has been exploited for the treatment of hormone dependent breast cancer. Anastrozole (Arimidex, AstraZeneca, Figure 2) is the most common aromatase inhibitor used in therapy and is generally administered after an initial treatment with Tamoxifen.

The ATAC (Arimidex, Tamoxifen, Alone or in Combination) trial was a randomised controlled trial that studied a group of 9366 women who received breast cancer treatment with either Anastrozole, Tamoxifen or both for five years. The study continued until further five years from the end of the treatment and concluded that the group that received Anastrozole has significant better clinical results than the group

which received Tamoxifen only. The same study suggested that Anastrozole should be the preferred clinical approach for the treatment of post-menopausal women with localised ER+ breast cancer.¹²

Another study associated Anastrozole with a 40% decrease in recurrence of cancer but also with an increased grade of bone frailty. The same study suggest that the treatment regimen should be two years with Tamoxifen followed by three years with Anastrozole.¹³

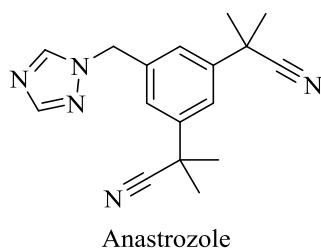


Figure 2. Structure of Anastrozole, the aromatase inhibitor most commonly used in therapy.

1.3.4. Steroid sulphatase inhibitors

Steroid sulphatase (STS) is also another important enzyme involved in the biosynthesis of E2 especially in post-menopausal women. In fact, when a woman reaches menopause, the synthesis of estrogens in the ovaries stops and most estrogens are instead synthesised in peripheral tissues by the conversion of androstenedione to E1. E1 is then converted to E1 sulphate (E1-S) which is the main form of circulating estrogens. In the target tissues (e.g. ovaries), E1-S is converted back to E1 and then reduced to E2 by 17 β -HSD1 (Scheme 1).^{14, 15}

Some inhibitors of STS, both steroidal (e.g. EMATE, Figure 3) and non-steroidal (e.g. STX64, Figure 3), are reported in the literature and inhibitors recently developed at the University of Bath are currently in clinical trial.^{15, 16}

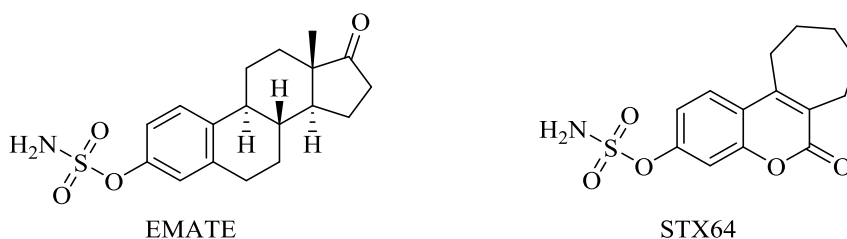


Figure 3. Structure of the steroidal STS inhibitor EMATE and non-steroidal inhibitor STX64.

1.4. 17-Beta hydroxysteroid dehydrogenases (17 β -HSDs)

At present, fifteen types of 17 β -HSDs have been reported in the literature.¹⁷⁻²⁹ 17 β -HSDs are responsible for the reduction or oxidation of hormones, fatty acids and bile acids and they all require nicotinamide adenine dinucleotide (phosphate or not, in its reduced or oxidised state (NAD(P)(H))), for their activity. Of the fifteen isoforms identified, 17 β -HSD5 is the only aldo-keto reductase (AKR) while the other isoforms are all short-chain dehydrogenases/reductases.^{30, 31}

Even though they are named 17 β -HSDs, the redox activity in position 17 β is only the major one with most of the 17 β -HSDs being capable of converting different substrates at different sites (e.g. position 3 on the steroid ring). In addition, most of 17 β -HSDs have bidirectional capabilities *in vitro* but they appear to work unidirectionally *in vivo*. Although they have similar dimensions (250-350 amino acids) and they have highly conserved portions, the overall homology among the different 17 β -HSDs is rather low. Moreover, they have been found to have different cellular localisations in the cytosol (17 β -HSD1), microsomes (17 β -HSD3), mitochondria (17 β -HSD10) and peroxisomes (17 β -HSD4) and to differ in tissue distribution.^{30, 31}

The two highly conserved regions are the catalytic domain which contains the sequence Tyr-X-X-X-Lys (where X is any amino acid) and the Rossmann fold.³² The Rossmann fold is a sequence of alternating α -helices and β -strands that constitutes the co-factor (NAD(P)(H)) binding domain.³²

Of the fifteen types, only 17 β -HSD1, 17 β -HSD2, 17 β -HSD3 and 17 β -HSD5 are strictly related to hormone dependent cancer. Of these, 17 β -HSD1 and 17 β -HSD2 are of interest in ER+ breast cancer because they catalyse the interconversion of E1 and E2.³³

1.4.1. 17 β -HSD1

17 β -HSD1 is the primary enzyme that catalyses the conversion of E1 to E2 by reducing the carbonyl at position 17. To do so, 17 β -HSD1 requires NADPH as co-factor. 17 β -HSD1 was also the first among the 17 β -HSDs to have a crystal structure elucidated.^{34,35}

The core of the structure is the seven-stranded parallel β -sheet (β A to β G), surrounded by six parallel α -helices (α B to α G), three on each side of the β -sheet.³⁶ The steroid binding site is a hydrophobic pocket that shows a high degree of

complementarity with the substrate and these hydrophobic interactions are thought to provide a significant contribution to the thermodynamic force of binding.³⁶

The proposed mechanism involves the residues Ser142, Tyr155, Lys159 and Asn114, which stabilise the carbonyl of E1 through a net of hydrogen bonds and the same hydrogen bonds facilitate the second proton transfer from water. The hydride is instead transferred directly from the co-factor, which is in close proximity to the substrate. The pro-*S* hydrogen of the nicotinamide ring is transferred to the carbonyl to form the 17 β -hydroxyl group that characterises E2 (Figure 4).³⁷

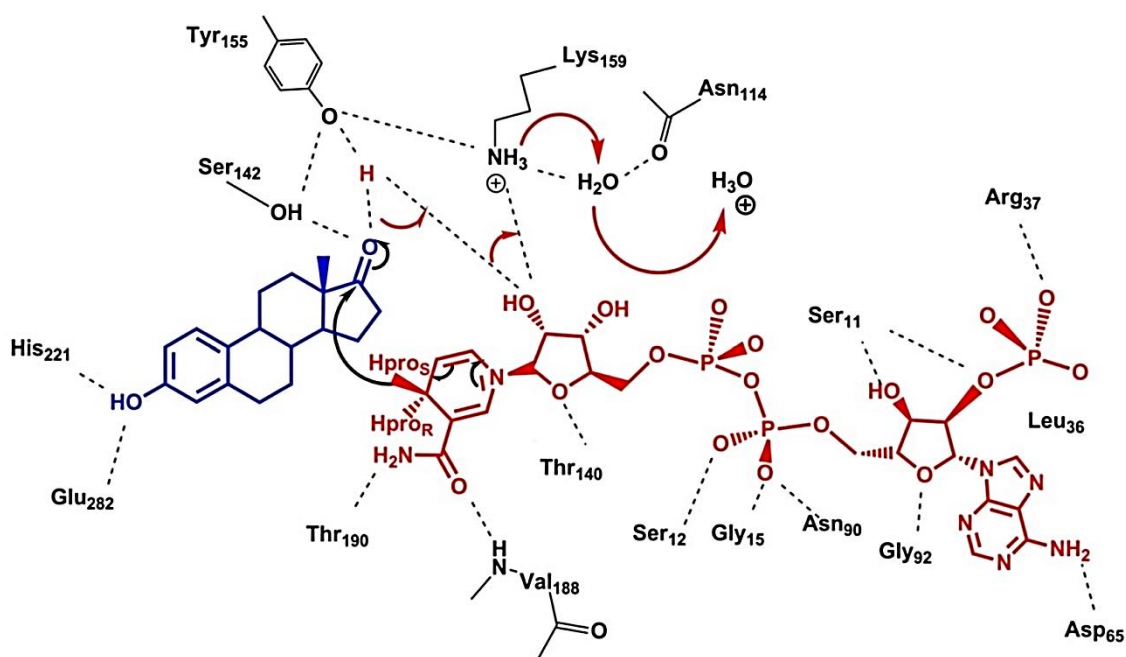


Figure 4. Postulated catalytic mechanism for the reduction of E1 by 17 β -HSD1. The substrate E1 is depicted in blue while the co-factor NADPH is in red.³⁷

The ratio between the expression of 17 β -HSD1 and 17 β -HSD2 has been directly correlated with the intracellular ratio between the concentrations of E1 and E2. This ratio, in addition to the ratio between the two enzymes, depends also on the concentration of the co-factor. It has been demonstrated in more than one cell line that breast cancer cells highly expressing 17 β -HSD1 have an [E2]/[E1] of 9/1.³⁸ When the gene expressing 17 β -HSD1 is silenced or when the overexpression of 17 β -HSD2 is induced, the ratio is reduced. A further decrease in the ratio is obtained by increasing NAD⁺ concentrations when 17 β -HSD2 is expressed.³⁸ In fact, 17 β -HSD2 uses E2 and NAD⁺ as a substrate and low concentration of the co-factor inhibits the reaction (Figure 5). In living cells, the NADH/NAD⁺ ratio is greatly in favour of the reduced NADH.

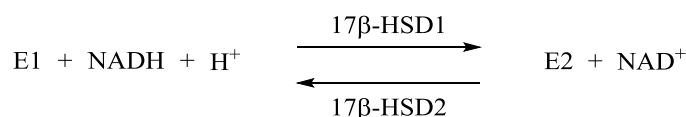


Figure 5. Catalytic conversion of E1 to E2 by 17 β -HSD1 and of E2 to E1 by 17 β -HSD2. Though 17 β -HSD1 can use both NADH and NADPH (with a greater affinity for NADPH), 17 β -HSD2 is more NAD⁺ specific.

The ratio 17 β -HSD1/17 β -HSD2 is increased in post-menopausal women with hormone dependent breast cancer.³⁹ This is reflected in an increased concentration of E2, which stimulates cell growth *via* ER activation. Hence, inhibiting 17 β -HSD1 would potentially lower the intracellular E2 concentration and consequently reduce tumour growth. Studies reveal that high levels of expression of 17 β -HSD1 mRNA are associated with bad prognoses and lower survival rates.⁴⁰

Many examples of 17 β -HSD1 inhibitors are reported in the literature, showing a great interest for this novel target.⁴¹⁻⁴⁵ The drug candidate STX1040 (**1**, Figure 6) developed at the University of Bath has inhibited *in vitro* the proliferation of T-47D cells stimulated by E1 and significantly decreased tumour volume and plasma level of E2 *in vivo*.⁴³

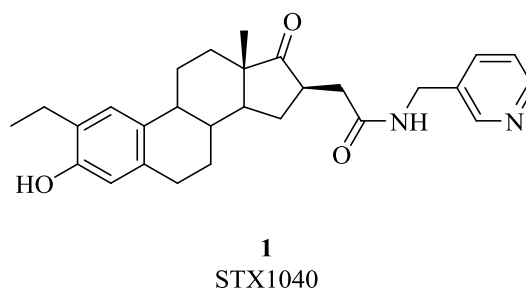


Figure 6. Structure of the steroidal inhibitor of 17 β -HSD1 STX1040, developed at the University of Bath.

1.5. Known inhibitors of 17 β -HSD1

The inhibitors of 17 β -HSD1 are of two types: steroidal and non-steroidal. The steroidal inhibitors tend to have somewhat a worse drug-like profile, thus growing interest is cast on the development of new non-steroidal inhibitors. Even though the number of patents related to the inhibition of 17 β -HSD1 has significantly increased in recent years, no inhibitor has yet reached the market to date. This highlights the potential impact that the development of good 17 β -HSD1 inhibitors may have on the pharmaceutical industry.

1.5.1. Steroidal inhibitors of 17 β -HSD1

The majority of 17 β -HSD1 inhibitors are based on the steroid structure. These compounds are based on modification of the substrate E1 or the product E2. The core steroidal structure can be substituted at different positions (C2, C6, C15, and C16) and small modifications of the core are possible. These allow the development of a structure activity relationship around the core structure of E1 or E2.

1.5.1.1. Derivatives of E1 substituted at C2

The works of Hillish *et al.*⁴⁶ and Gege *et al.*⁴⁷ describe the synthesis and evaluation of 2-substituted E1 derivatives. Introduction of large groups in this position leads to rather active compounds with IC₅₀ values of 56 nM (**2**, Figure 7) and 47 nM (**3**, Figure 7). This indicates that the binding pocket is large enough to accommodate such bulky groups. Compound **4** (Figure 7), bearing a chlorine in position 2, has an IC₅₀ value of 140 nM but the activity is drastically increased when a fluorine is introduced in position 16. The stereochemistry of this group plays a pivotal role in the activity of the compound and while compound **5** (Figure 7) shows only marginal increase in activity, compound **6** (Figure 7) has an IC₅₀ of 35 nM. Interestingly, when the same substitution is attempted in compound with a D ring expanded to a six-membered ring, the effect is reversed and derivative **8** (Figure 7) shows lower activity than **7** (Figure 7).

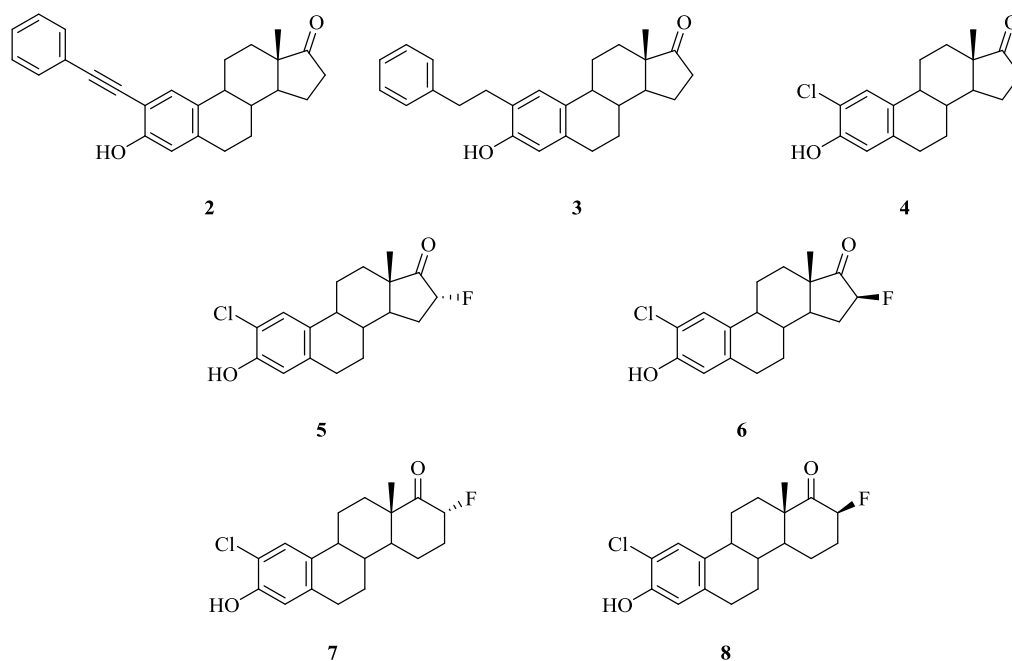


Figure 7. Structure of some inhibitors of 17 β -HSD1 based on 2-substituted E1.

The advantage of substitutions in position 2 is the enhanced stability. In fact, C2 is the prevalent position for metabolic oxidation by cytochrome P450 (CYP). Blocking the position reduces drastically the metabolism of the compounds with consequent increased half-life.⁴⁸

1.5.1.2. Derivatives of E1 and E2 substituted at C6

A few examples of modification at C6 of the E1 structure are reported by Allan *et al.*⁴⁹ The idea of this group was led by the observation of the presence in computational analysis of the residue of Ser222 in proximity with the C6 position. Thus, they expected substitution in this position to positively contribute to the activity of the compounds. Nevertheless, introduction of a ketone at C6 in compounds **9-11** (Figure 8) did not increase the activity compared to the non-oxo counterpart.⁴⁹ It was concluded that, even though the position was tolerated, the carbonyl was not interacting with Ser222. The introduction of an oxime group at position 6 (**12**, Figure 8) led to a drastic loss of activity.⁴⁹

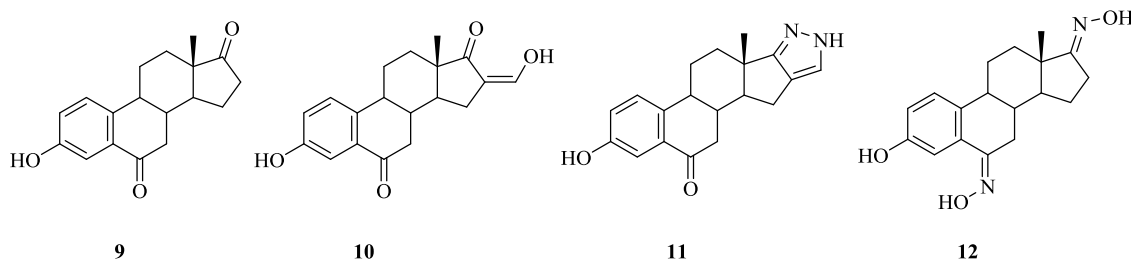


Figure 8. Structure of some 6-oxo and 6-oxime derivatives of E1 and modified E1 as 17 β -HSD1 inhibitors.

Other examples of longer chains in position 6 are reported by Poirer *et al.* based on the anti-estrogen **13** (Figure 9) which is modified at position 7. Compound **14** (Figure 9) was then synthesised by transposition and optimisation of the substituent from position 7 to position 6 and showed an IC₅₀ value of 0.17 μ M (IC₅₀ value of E1 is approximately 300 nM).⁵⁰ Similarly to what observed for the 16-fluoro derivatives **5-8** (Figure 7) the stereochemistry of the group introduced is important and compound **15** is 70 fold more potent than **16** (Figure 9).

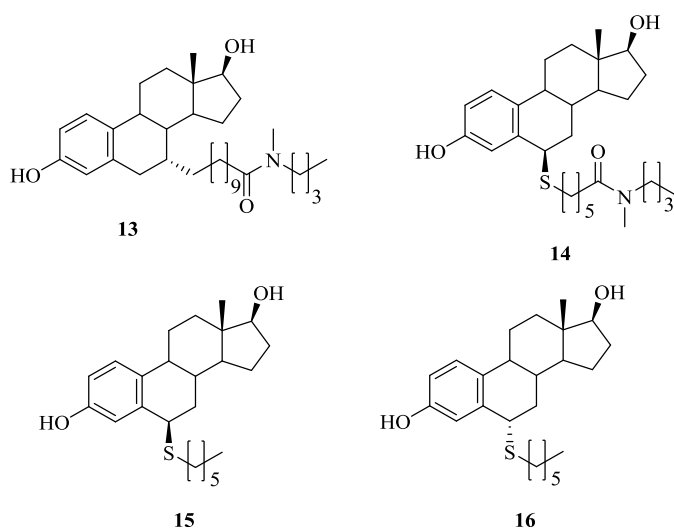


Figure 9. Structure of some 6-substituted E2 derivatives^{50,51}

1.5.1.3. Derivatives of E1 substituted at C15

Examples of E1 derivatives substituted at position 15 can be found in two patents from Solvay Pharmaceuticals.^{52, 53} The range of chain length and type of substitutions suggests that groups in position 15 are well tolerated (**17-24**, Figure 10). Analysis of the crystal structure of 17 β -HSD1 performed by Messinger *et al.* pointed out the presence of an opening in the proximity of the D ring.⁵⁴

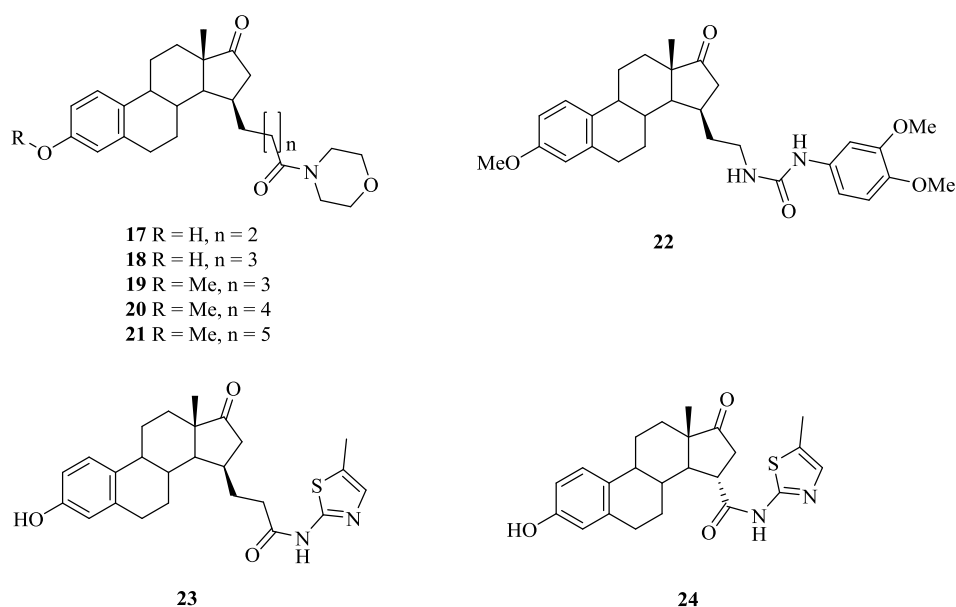


Figure 10. Structure of some 15-substituted E1 derivatives.^{52, 53}

Compound **23** showed 87% inhibition at 100 nM in a recombinant 17 β -HSD1 assay and an IC₅₀ value of 4 nM. Compound **17**, instead, proved effective at a dose of

5 $\mu\text{M/kg/day}$ *in vivo*, causing a 60% reduction of tumour size in mice inoculated with MCF-7 breast cancer cells.

1.5.1.4. Derivatives of E1 substituted at C16

From docking studies, it has been postulated that a side chain substitution at position 16 may possibly interact with the co-factor binding region, thereby generating dual site inhibitors. Poirier *et al.* showed that substituents at position 16 are well tolerated.⁵⁵ The dual site inhibitors are very interesting because they take advantage of the interactions in both the E1 and NADPH binding pockets to obtain greater thermodynamic stability.

Qui *et al.* were the first group to publish a hybrid dual inhibitor containing E1 and adenosine connected with an aliphatic linker (EM-1745, **25**, Figure 11).⁵⁶

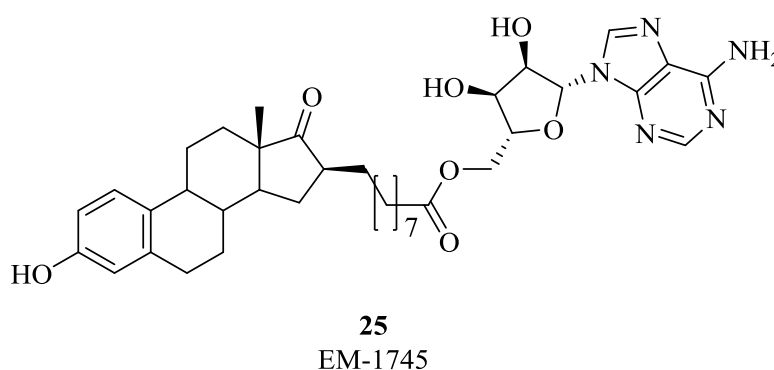


Figure 11. The first E2-adenosine hybrid inhibitor reported, EM-1745 (**25**).⁵⁶

Poirier *et al.* studied further modification of the linker to identify the optimal chain length. It was found that a spacer of 7-8 carbons (**26-31**, Figure 12, Table 1) between the ester and C16 was the optimal one giving compound **25** that has an IC_{50} value of 52 nM.

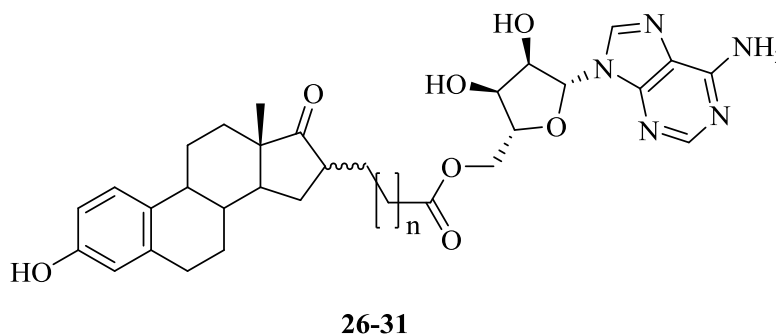


Figure 12. Structure of the C16 modified E2 dual site inhibitors with different linker lengths.

Table 1. Activity and relative substitution pattern of the C16 modified E2 dual site inhibitors measured in a recombinant 17 β -HSD1 assay.

Compound	C16 orientation	Spacer length	IC ₅₀ (nM)
26	α	10	310
27	β	10	120
28	β	11	1000
25	β	8	52
30	β	7	93
31	β	6	430

Investigations by Fournier *et al.*⁵⁷ highlighted two major flaws in the use of compound **25** as an inhibitor. Despite its high activity in a purified 17 β -HSD1 assay and in a cell lysate assay, the compound was inactive in a whole cell assay. It is possible that **25** is not capable of passing through the cell membrane or that it is being metabolised before encountering the target.⁵⁷

This stability issue has challenged the synthesis of new derivatives with simplified structures and lead ultimately to the synthesis of STX1040 (**1**, Figure 6, page 9). STX1040 **1** is the most potent inhibitor of 17 β -HSD1 reported to date with the lowest IC₅₀ value of 27 nM in a whole-cell based assay.⁴³

1.5.2. Non-steroidal inhibitors of 17 β -HSD1

Of growing interest is the development of non-steroidal inhibitors of 17 β -HSD1. These have several advantages over to the steroidal inhibitors, such as ease of synthesis, drug-likeness and may give easier access to selectivity and non-estrogenicity features. Moreover, it is difficult to introduce substituents in every position of the steroidal core. The selection of an opportune steroidal core structure can instead enable a more in depth SAR study of the binding region.

Some basic features are retained by most of the compounds synthesised and include a phenol moiety and a hydrophobic scaffold that mimic the steroid core. The scaffolds used include biphenyl compounds, phenylnaphthalenes, benzothienopyrimidones and coumarin derivatives.

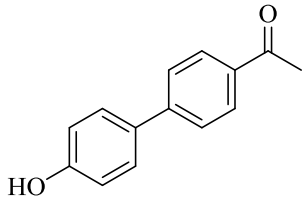
1.5.2.1. Biphenylketones

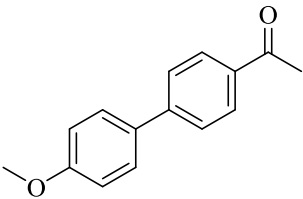
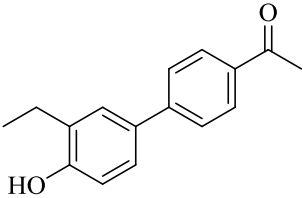
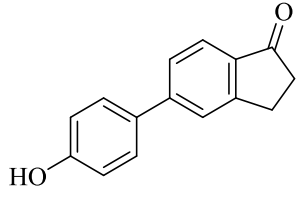
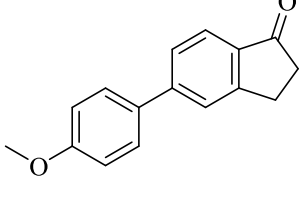
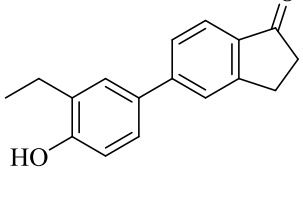
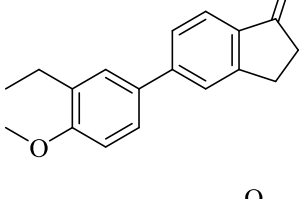
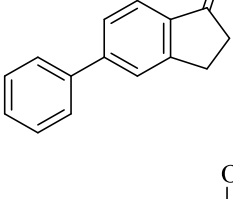
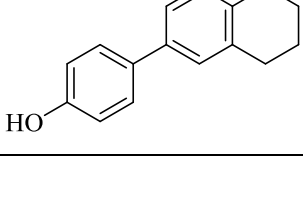
Vicker *et al.*⁵⁸ used biphenylketones to mimic the core features of E1, i.e. the phenol moiety and ketone. Compounds were easily synthesised from the respective boronic acid and arylbromide *via* Suzuki coupling.

Compounds were assessed for their inhibitory activity against 17 β -HSD1 using T-47D human breast cancer cells. The initial compound **32** (Table 2) showed promising results with 97% of inhibition at 10 μ M and an IC₅₀ value of 3.7 μ M. Introduction of an ethyl group in the *ortho* position to the phenol moiety (**34**, **37**, **42**, Table 2) was tolerated but somewhat lower activities were registered. In addition, the ethyl group was also reducing the selectivity of the compounds against 17 β -HSD1 as shown by the couple of compounds **35** and **37** (Table 2). Changing the phenol group into a methoxy group (**33**, **36**, **38**, **41** and **43**, Table 2) or removing it (**39**, Table 2) led generally to inactive compounds. Compared to **32** (Table 2), the indanone **35** (Table 2) showed improved efficacy with an IC₅₀ value of 1.7 μ M whereas the compound **40** (Table 2) containing the tetralone ring had significantly lower activity. As a further modification, the same pyridyl moiety that characterises STX1040 **1**, was introduced (**44-47**, Table 2) but with no improvement in the activity. The position of the nitrogen in the pyridyl ring proved very important and, even if the 3-pyridyl derivatives **44** and **46** (Table 2) retained the activity of the parent compounds, the 2-pyridyl derivatives **45** and **47** (Table 2) were completely inactive.⁵⁸

The preliminary data on this series of compounds is very encouraging but further optimisation is necessary to increase the activity of the compounds.

Table 2. Structure and biological activity of a series of biphenylketones as non-steroidal inhibitors of 17 β -HSD1⁵⁸

Compound	Structure	% Inhibition of 17 β -HSD1 @ 10 μ M	% Inhibition of 17 β -HSD2 @ 10 μ M	IC ₅₀ (μ M)
32		97	Nt	3.7

33		Inactive	Nt	Nt
34		73	51	5.4
35		81	17	1.7
36		Inactive	Nt	Nt
37		86	48	2.0
38		Inactive	Nt	Nt
39		Inactive	Nt	Nt
40		89	Nt	15.6

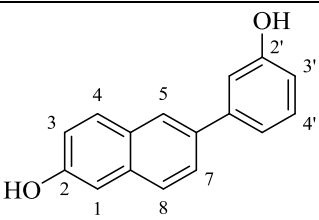
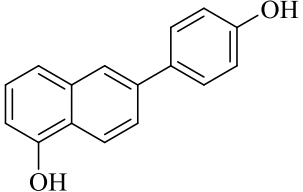
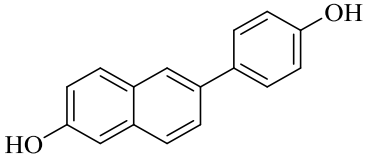
41		Inactive	Nt	Nt
42		51	Nt	Nt
43		71	Nt	8.3
44		24	12	3.7
45		Inactive	Nt	Nt
46		39	Nt	4.7
47		Inactive	Nt	Nt

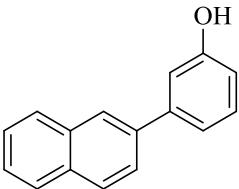
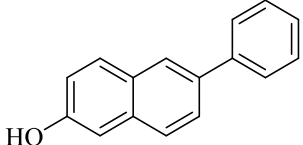
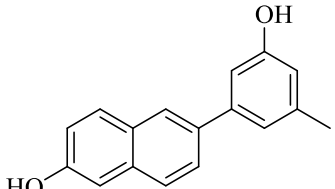
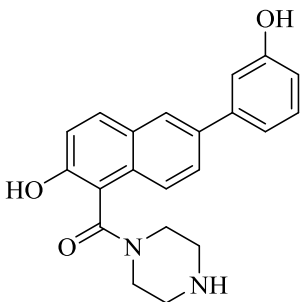
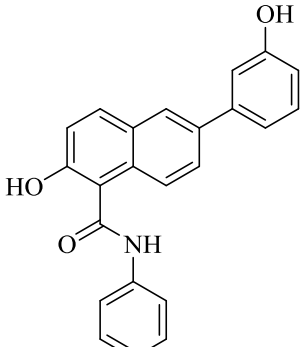
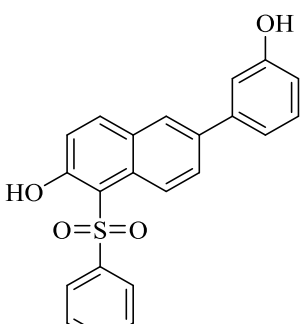
Nt = not tested

1.5.2.2. Phenyl naphthalene and phenylquinoline derivatives

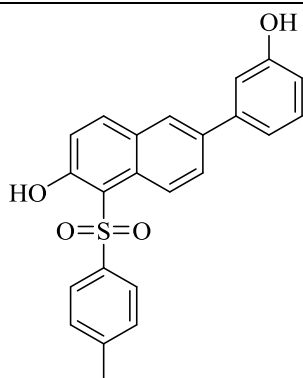
Hartmann *et al.*^{41, 59, 60} reported the use of phenyl naphthalene based non-steroidal structures as inhibitors of 17 β -HSD1. When the phenol group was in position 1 of the naphthalene ring (**49**, Table 3) the compound was moderately active with only 55% inhibition at 1 μ M but when two hydroxyls were present in position 2 and 2' (**48**, Table 3) the compound showed high percentage of inhibition. The calculated IC₅₀ value for compound **48** was of 116 nM in a recombinant placental 17 β -HSD1 assay. Both hydroxyl groups of compound **48** appeared to be very important as the removal of one or the other (**87**, **88**, Table 3) lead to complete loss of activity. The introduction of substituents in position 1 turned out to be a more interesting approach. Aromatic rings separated by a spacer (**55-57**, Table 3) reduced the activity but a bromine (**58**, Table 3) or a phenyl ring (**59**, Table 3) with no linker showed good inhibition. Compounds **58** and **59**, with IC₅₀ values of 40 nM and 20 nM, respectively, have improved activities compared to **48**. It is not clear how the bromine in compound **58** may have such a positive effect, but electronic effects might be an explanation. In fact, the hydrogen bond from the hydroxyl in position 2 is very important and a hydrogen bond is stronger when the two groups involved have a similar pKa. Hence, modulation of the acidity of the hydroxyl group adjacent to the bromine might be a possible explanation.

Table 3. Series of non-steroidal inhibitors of 17 β -HSD1 based on the phenyl naphthalene core.

Compound	Structure	% of inhibition	
		@ 100 nM	@ 1 μ M
48		91	94
49		Ni	55
50		Ni	Ni

51		26	61
52		Ni	Ni
53		14	42
54		Ni	45
55		40	80
56		Nt	33

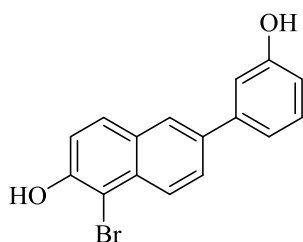
57



Nt

75

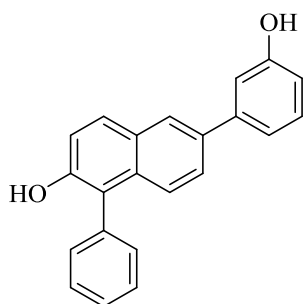
58



83

88

59



76

89

Ni = No inhibition; Nt = Not tested.

It was hypothesised that the introduction of a heteroatom into the naphthalene could enhance activity by establishing a favourable interaction with a Tyr or a Ser residue, which appear to be in proximity to the C6 position of E1. To investigate this possibility, the quinoline derivatives 60 and 61 (Table 4) were synthesised but their activity was much lower than that of compound **48** (Table 3).⁶¹

Table 4. Series of non-steroidal inhibitors of 17 β -HSD1 based on the phenylquinoline core.⁶¹

Compound	Structure	% of inhibition	
		@ 100 nM	@ 1 μ M
60		24	57
61		14	63

1.5.2.3. Bis(hydroxyphenyl) substituted thiophenes, azoles, benzenes and pyridines

Persisting in the research of new polar interactions with Tyr218 and Ser222, Hartmann *et al.* discovered a new pharmacophore for the inhibition of 17 β -HSD1. This new scaffold was based on biphenyl substituted heterocyclic rings such as azoles, oxazoles, thiazoles and thiophenes.⁶²

To investigate the potential of these compounds, different substitution patterns in the central heterocyclic ring and on the biphenyl groups were synthesised and evaluated. The different heterocycles, 1,2,3-triazole, the oxazole or the isoxazole (**62**, **63** and **64**, respectively, Table 5) were active with IC₅₀ values of 0.84 μ M, 1.61 μ M and 0.31 μ M, respectively. Introduction of a third substituent, such as a methyl or phenyl group (**65** and **66**, respectively, Table 5), lead to complete inactivity. The thiazole and thiophene (**67** and **68**, Table 5) series proved to be more active with no significant difference in IC₅₀ values, i.e. 0.05 μ M and 0.069 μ M, respectively. This means that the nitrogen in the ring is not involved in any significant polar interaction.

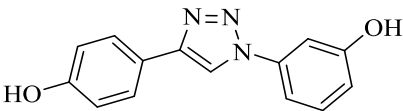
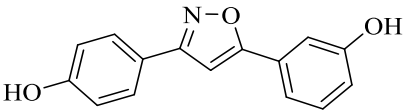
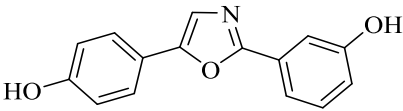
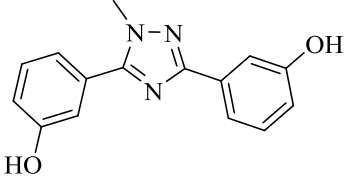
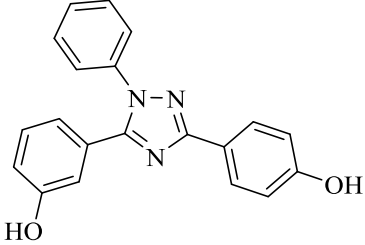
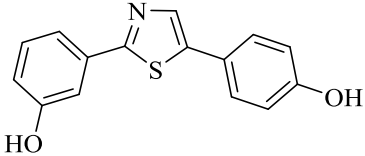
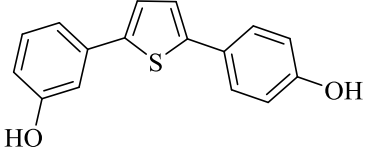
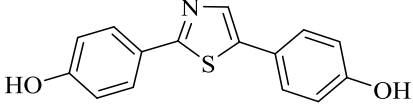
Investigation of the influence of the relative position of the hydroxyl group demonstrated that the substitution in position 3 and 4' was the best pattern. In fact, the symmetric substitution in positions 3 and 3' of the two phenyl rings (**70**, Table 5) reduced the activity and substitution in positions 4 and 4' (**69**, Table 5) made the compound completely inactive.

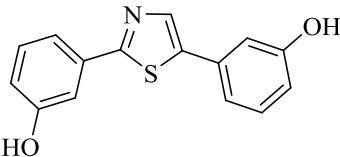
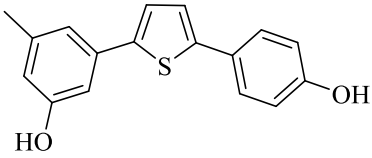
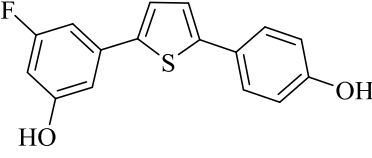
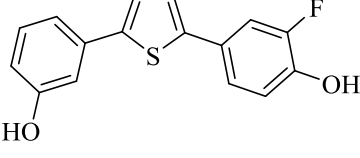
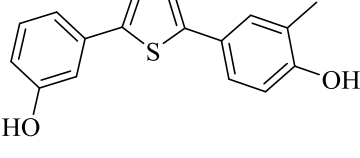
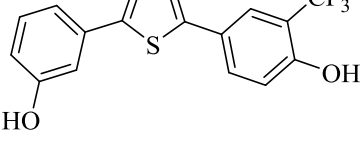
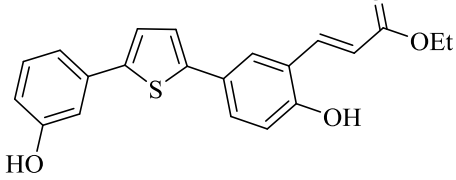
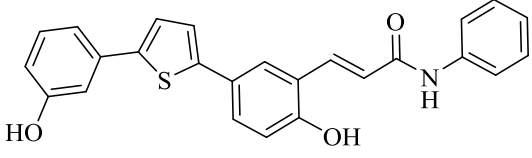
The introduction of a methyl in position 5 of the *meta*-hydroxyphenyl group (**71**, Table 5) decreased the activity but substitution in the same position with a fluorine (**72**, Table 5) led to a slight increase in activity compared to the unsubstituted compound **68** (Table 5).

When a small electron-withdrawing group, such as a fluorine, was introduced in position 3 of the *para*-hydroxyphenyl ring (**73**, Table 5), the activity was significantly increased. However, slightly larger groups as methyl or trifluoromethyl (**74**, **75**, Table 5) led only to a slight improvement compared to the parent compound **68** (Table 5). Instead, introduction of a larger group (**76**, **77**, Table 5) was not very well tolerated and the activity of the compounds was lower than that of the parent compound **68** (Table 5).

Ortho- substitution was not investigated because it would disrupt the planarity of the molecule forcing the adjacent rings to twist. Planarity was found to be important for the activity of these compounds.⁶²

Table 5. Structure and biological activity of bis(hydroxyphenyl) derivatives evaluated in a recombinant 17 β -HSD1 assay.

Compound	Structure	IC ₅₀ (μ M)
62		0.84
63		1.61
64		0.31
65		Ni
66		Ni
67		0.05
68		0.069
69		Ni

70		0.243
71		0.629
72		0.042
73		0.008
74		0.046
75		0.038
76		0.130
77		0.427

Ni = No inhibition

All of the compounds showed very low affinity for ER- α and ER- β . Inhibition of 17 β -HSD1 for compounds **73** and **74** (Table 5) was also evaluated in a whole-cell assay using T-47D cells. The respective IC₅₀ values were 426 nM and 282 nM and proved that the two compounds were able to penetrate cells and inhibit the 17 β -HSD1 dependent conversion of E1 to E2. Further biological studies demonstrated some inhibitory activity against CYP3A4 with IC₅₀ values of 0.50 μ M and 0.82 μ M for **73** and **74**, respectively.

Inhibition of CYP is usually undesired because brings cross interactions in multi-drug therapies and thus has to be taken into consideration during further optimisation of the compounds.⁶²

To address the metabolic problems encountered, substitution of the hydroxyl group with different substituents was attempted. The *meta*-hydroxyphenyl group was left unvaried and the other hydroxyl group was substituted with other hydrogen bond donor (e.g. NH₂, SH) or lipophilic (e.g. F) groups.

Substitution of the 4-hydroxyl group with an amine or a thiol (**79** and **80**, respectively, Table 6) led to a complete loss of activity. The activity of the compounds bearing a fluorine in position 4 or 3 (**78** and **81**, Table 6) did not differ much from the unsubstituted compound **84** (Table 6). Substitution in position 3 with the more polar sulphonamides (**82** and **83**, Table 6) led to a small loss of activity compared to **84**. Nevertheless, these compounds stressed even more the importance of the two hydroxyl groups and all the modifications shown in Table 6 led to a substantial drop in activity.

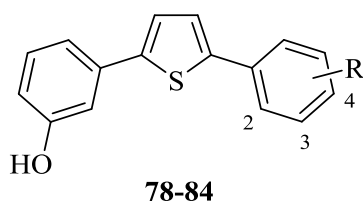


Figure 13. Structure of the compounds synthesised as modification of the hydroxyl moiety.

Table 6. Substituents and biological activity of compounds without a 4-hydroxyl group. IC₅₀ values were determined in a recombinant 17 β -HSD1 assay.⁶³

Compound	R	IC ₅₀ (nM)
78	4-F	717
79	4-NH ₂	>5000
80	4-SH	>5000
81	3-F	535
82	3-NHSO ₂ CH ₃	523
83	Tosylamide	350
84	H	342

In the search for molecular diversity, a series of phenyl and pyridine derivatives was synthesised. These compounds were lacking a second hydroxyl group but the sulphur of

the thiophene ring was expected to be able to participate in the hydrogen bond in place of the oxygen.

The series was generally less active than the previous one (**62-77**, Table 5, page 22), however, compounds possessed IC₅₀ values in the nM range. Between the phenyl derivatives **85** and **86** (Table 7), the compound bearing an additional phenyl ring (**86**, Table 7) showed better activity with an IC₅₀ value of 137 nM.

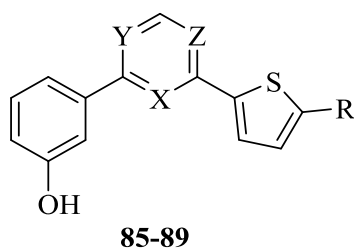


Figure 14. Structure of the phenyl and pyridyl derivatives.

Table 7. Substitution and biological evaluation of the series of phenyl and pyridyl derivatives.⁶⁴

Compound	R	X	Y	Z	IC ₅₀ (nM)
85	Cl	C	C	C	560
86	Ph	C	C	C	137
87	Cl	N	C	C	139
88	Cl	C	N	C	850
89	Cl	C	C	N	238

In the pyridyl series, instead, the position of the nitrogen was found to be important for the activity and when the *N* was far from the thiophene point of substitution (**88**, Table 7), the activity was significantly lower than in the other cases (**87** and **89**, Table 7). Despite the somewhat lower activity compared to other series of compounds, the phenyl and pyridyl derivatives showed very low affinity for ER- α and ER- β and a good selectivity between 17 β -HSD1 and 17 β -HSD2.⁶⁴

1.5.2.4. Benzothienopyrimidones

In their research for new non-steroidal therapeutics for breast cancer, Lilienkamp *et al.* screened a small commercial library of compounds. Based on molecular modelling experiments,⁶⁵ compounds that met the structural hydrophobic requirement to fit in the

active site were selected. Compound **90** (Figure 15) was identified as a lead compound showing a percentage inhibition against 17 β -HSD1 of 41% at 1 μ M.⁶⁶

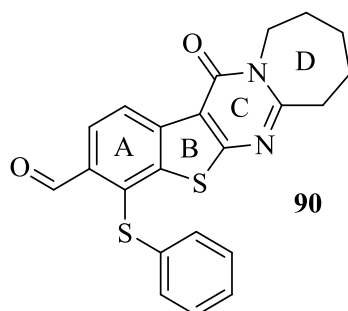


Figure 15. Lead compound of the benzothienopyrimidones series

In an attempt to improve the activity of compound **90**, some modifications were introduced at the sulphur position. Homologation of the D ring was also evaluated.

Most of the compounds showed very good activity in both cell-free and cell based assay demonstrating their ability to penetrate inside the cells. Compounds substituted with different aliphatic chains did not show significantly different activity (**91a-d**, Table 8). The carboxylic acid group was not tolerated and the activity of compounds **91e** and **91h** (Table 8) was almost completely lost compared to the rest of the series. Both hydrophilic and lipophilic moieties were well accepted but compounds bearing a substituted phenyl group (**91f-l**, Table 8) showed a lack of selectivity between 17 β -HSD1 and 17 β -HSD2, with the less selective compounds being **91j-l** (Table 8).⁶⁷ Even though by expanding the D ring (**91n**, Table 8) the biological activity was mostly retained, when the ring was reduced to a five-membered ring (**91m**, Table 8) the activity was almost lost. This indicates that the D ring is involved in some hydrophobic interactions that are very important for the activity.⁶⁷

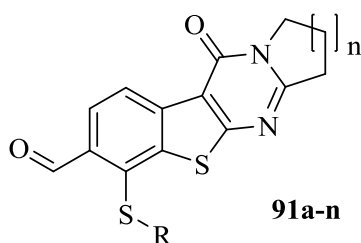
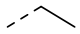
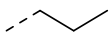
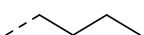
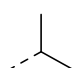
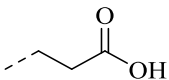
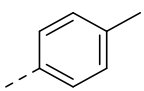
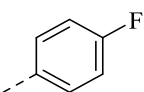
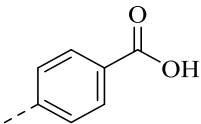
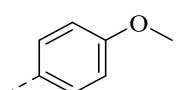
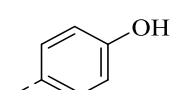
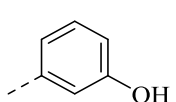
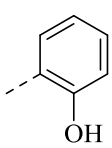
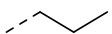
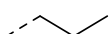


Figure 16. Structure of the series of benzothienopyrimidones and relative activities against 17 β -HSD1 in both cell-free and cell based assays

Table 8. Substitution pattern and biological activity of a series of benzothioipyrimidones.⁶⁷

Compound	R	n	% of inhibition of 17 β -HSD1 (cell-free assay)		% of inhibition of 17 β -HSD1 (cell based assay)	
			0.1 μ M	1 μ M	0.1 μ M	1 μ M
91a		3	72	95	66	100
91b		3	73	92	74	100
91c		3	68	93	54	100
91d		3	65	93	72	100
91e		3	0.3	3	Nt	Nt
91f		3	63	85	41	99
91g		3	87	92	37	77
91h		3	4	22	Nt	Nt
91i		3	89	90	25	72
91j		3	59	92	37	77
91k		3	94	97	53	84
91l		3	86	91	18	90
91m		1	17	67	Nt	Nt
91n		4	63	75	Nt	Nt

Nt = Not tested

1.5.2.5. Coumarin derivatives.

Starčević *et al.* recently reported a number of inhibitors of 17 β -HSD1 based on the coumarin structure.⁶⁸⁻⁷⁰ The group initially screened a series of flavonoid compounds and found that many showed good percentage of inhibition at 6 μ M. Among the tested flavones compound **92** (Figure 17) showed the highest activity with more than 90% of inhibition at 6 μ M and 41% of inhibition at 0.6 μ M.

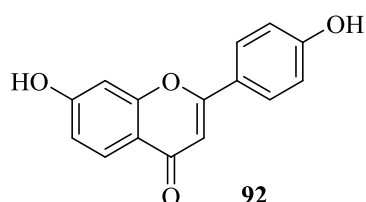


Figure 17. 7,4'-Dihydroflavone **92**. The best flavone inhibitor resulted from the evaluation of Starčević *et al.*⁶⁸

Among the simple flavones tested, **93a** (Table 9) showed good inhibition even at 0.6 μ M with an IC₅₀ value of 360 nM. When the triflate was replaced by a methoxy group the activity dropped drastically and compound **93b** (Table 9) showed only 23% inhibition at 0.6 μ M. Similarly, substituting the ketone (**93c**, Table 9) with an ester was not tolerated and the activity was completely lost.⁶⁸

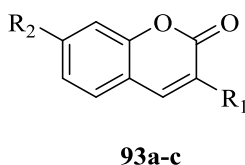


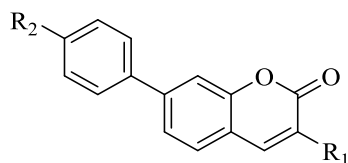
Figure 18. Structure of simple coumarin derivatives as inhibitor of 17 β -HSD1.

Table 9. Substituents and biological evaluations of the coumarins **93a-c** against 17 β -HSD1.⁶⁸

Compound	R1	R2	% of inhibition of 17 β -HSD1	
			0.6 μ M	6 μ M
93a			60	100
93b		OMe	23	23
93c			Ni	Ni

Ni = No inhibition

When the triflate group was replaced with a phenyl ring, the activity dropped significantly (**94a**, Table 10). The introduction of a methyl group on the phenyl ring (**94b**, Table 10) did not increase the activity. However, the introduction of a hydroxyl group restored the activity and compound **94c** (Table 10) was even slightly more active than **93a** (Table 9) with an IC₅₀ value of 270 nM. In addition, similarly to the previous example, substitution of the ketone with an ester (**94d**, Table 10) was not tolerated and the activity was lost completely.⁶⁸



94a-d

Figure 19. Series of 7-phenyl substituted coumarin as inhibitors of 17 β -HSD1.

Table 10. Substituents and biological evaluations of the 7-phenyl substituted coumarins **94a-d** against 17 β -HSD1.⁶⁸

Compound	R1	R2	% of inhibition of 17 β -HSD1	
			0.6 μ M	6 μ M
94a		H	57	63
94b		Me	40	72
94c		OH	76	100
94d		H	Ni	7

Ni = No inhibition

None of the coumarin derivatives showed any inhibitory activity against 17 β -HSD2 and none of them showed affinity for either ER α or ER β . These results were promising, even though further development was still necessary.

1.6. Estrogen receptor-related receptor alpha

The nuclear receptor (NR) superfamily was originally defined as a group of ligand activated transcription factors that had structural similarity. However, it was soon clear that the number of NR exceeded the number of ligands (e.g. steroid hormones, thyroid hormones, etc.).⁷¹ The NRs that could not be associated to a ligand were then named

orphan nuclear receptors.^{72, 73} The first orphan NRs identified were the estrogen receptor-related receptors (ERRs) known also as NR3B.

The NR3B subgroup of nuclear receptors consist of ERR α (NR3B1), ERR β (NR3B2) and ERR γ (NR3B3). The NR3B members belong to the a larger class of nuclear receptor which include also the two estrogen receptors, ER α and ER β .⁷³ In addition to mammals, ERRs are widely expressed in different organisms such invertebrates,⁷⁴ amphioxus⁷⁵ and also in simpler animal that lack ERs.⁷⁶ This has led to the hypothesis that ERRs might be ancestral evolutionary precursors of the ERs.⁷⁶ Of the three ERRs, ERR α is more abundant than ERR γ which in turn is more abundant than ERR β .

ERR α was the first to be discovered and is formed by a single peptide of 423 amino acids. They are composed by three main sections: the regulatory amino-terminal domain, the DNA binding domain (DBD) and the ligand binding domain (LBD). All the three ERRs show a high sequence identity with the ERs with *ca.* 70% homology at the DBD. However, the homology at the LBD is much lower and is only 37% for ERR α (Figure 20).⁷⁷

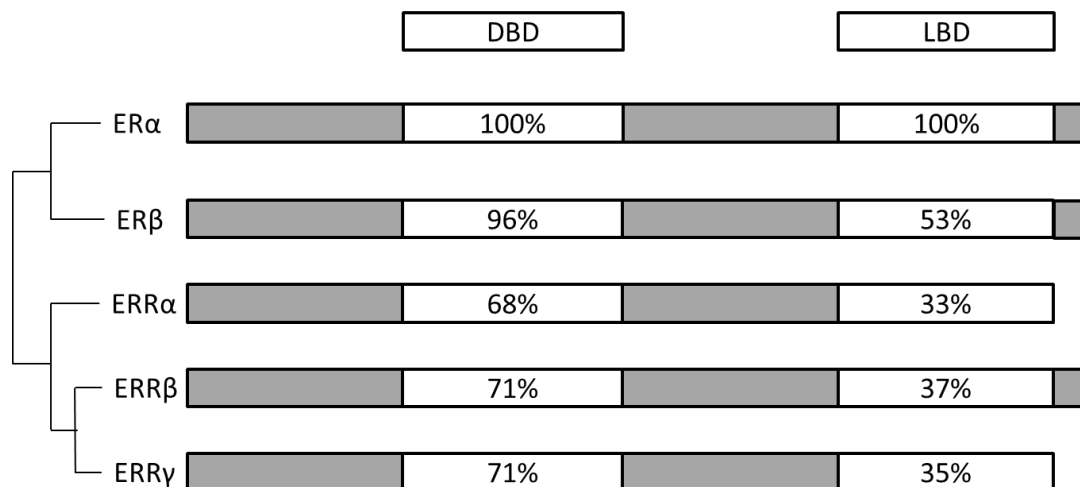


Figure 20. Level of homology among the ERs and ERRs at the DBD (DNA binding domain) and LBD (ligand binding domain).

ERR α is ubiquitously present in every tissue but its activity is tissue specific. Despite its main functions seems related to energy metabolism, ERR α orchestrate myriad of functions (Figure 21).

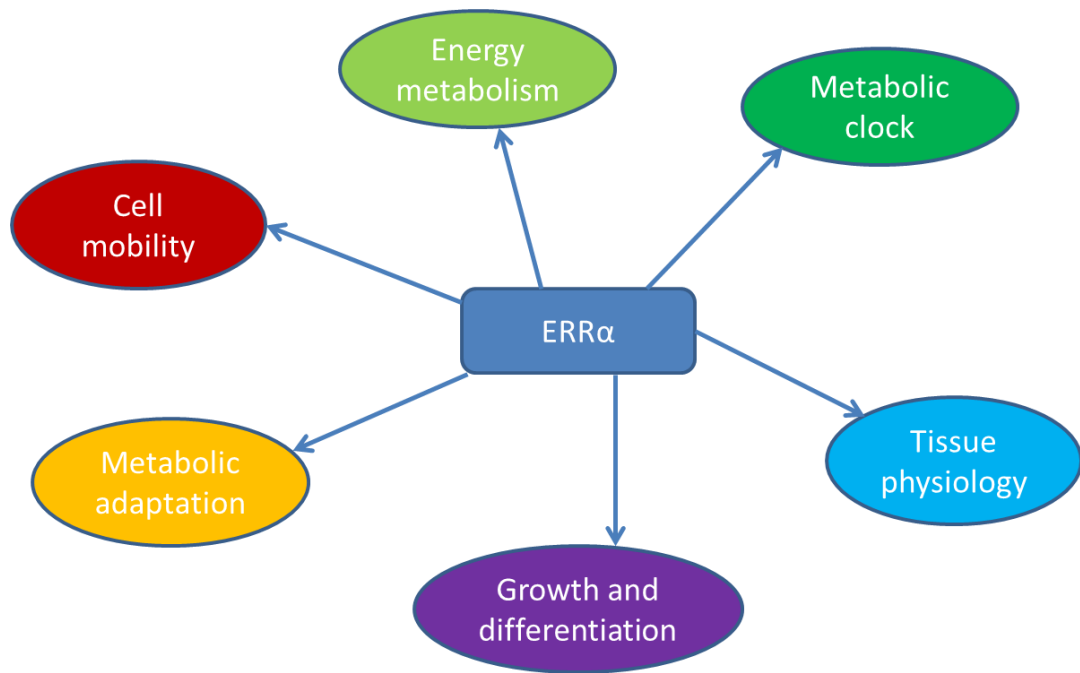


Figure 21. Principal regulatory roles played by ERR α in the different tissues of the body.

ERR α is involved in osteoblast cell differentiation and bone homeostasis and ERR α deficient mice have a higher bone mass and bone density.⁷⁸⁻⁸¹ Whereas in brown adipose tissue (BAT) ERR α stimulates the metabolism of fats, in white adipose tissue (WAT) it induces adipogenesis. BAT is abundant in hibernating mammals and human infants and its function is to produce heat. BAT produces heat through a “short-circuit” in oxidative phosphorylation (OXPHOS) in the inner membrane of the mitochondria. ERR α enhances BAT activity by inducing expression of OXPHOS related genes. In WAT, ERR α stimulates accumulation of fats and for this it has been proposed as a possible target for metabolic diseases.^{82, 83} ERR α deprived mice are generally healthy and show lower fat accumulation, lower body weight and leaner muscles.⁸⁴

ERR α helps regulating OXPHOS activity in other tissues such as heart, skeletal muscles and liver. ERR α is involved in the circadian adaptation of metabolism showing regular fluctuation of mRNA levels during the day-night cycle.⁸⁵

Controversially, ERR α has been demonstrated to be important in the tumour adaptation to hypoxic conditions.⁸⁶ Tumour masses often grow independent of OXPHOS because of their high metabolic rate in association with a surrounding environment incapable of properly distributing oxygen. ERR α is important for the adaptation during the transition from normoxic to hypoxic condition and ERR α silencing or inhibition affects hypoxic tissues. In contrast, ERR α inhibits the transcription of lactate dehydrogenase A (LDA) which is an essential enzyme for

hypoxic metabolism. It appears that the beneficial effects of ERR α in hypoxic conditions are related to the increased transcription of proteins related to the tricarboxylic acid (TCA) cycle that take place in the mitochondria.⁸⁷ In fact, the intermediates of this cycle play important roles in the catabolic activity that in tumour cells is enhanced in order to sustain their multiplication.⁸⁰ In addition, ERR α transcription is directly increased by the hypoxia-inducible factor (HIF) and the association of the two elements has been proven to be a key step in phenotypic differentiation and hypoxic adaptation.⁸⁸

ERR α has also been associated with high expression of the vascular endothelial growth factor (VEGF) which is necessary for the angiogenesis, the formation of blood vessels, necessary to sustain tumour growth.^{89, 90} Probably due to the effects on VEGF expression, ERR α is implicated in tumour progression and also in metastasis formation. In fact, using a trans-well migration assay Stein *et al.*⁹¹ demonstrated how ERR α knockdown resulted in a 65% reduction of cell migration.

1.6.1. ERR α and breast cancer

In addition to the other physiological functions, ERR α has been linked to breast cancer. ERR α has been reported to have a prognostic value in cancer treatment outcomes and elevated ERR α expression is associated with bad prognosis, more malignant phenotypes and a higher risk of recurrence.^{77, 83} Some studies have also correlated ERR α to the expression of ErbB2 which in turn is associated to an increase risk of tamoxifen resistance.⁹² ERR α is capable of both inhibiting and enhancing the expression of ErbB2 depending on the concentration of the co-activator glucocorticoid receptor interacting protein 1 (GRIP1). At a high concentration of GRIP1, ERR α is capable of overexpressing ErbB2 even in the absence of any ligand mediated response by ER α .⁹³

Another important correlation between ERR α and breast cancer lies in the cross-talk between the latter and ER α . In fact, ERR α and ER α not only share a great homology at the LDB but also in their target genes.

As with many NRs, ERR α requires the binding of certain co-activators and has to dimerise to initiate transcription. Whereas ERR α is constitutively active, ER α is able to initiate transcription only in response to a ligand (E2) activation. Even though the type

of protein expressed by both transcription factors are mostly similar, they do so activating their own separated genes. Deblois *et al.*⁹⁴ found that only 18% of the total pool of genes was common to the two receptors.

ERR α and ER α bind DNA recognising different promoters, namely estrogen receptor-related receptor response element (ERRE) and estrogen receptor response element (ERE), respectively. The common genes possess a modified promoter termed ERRE/ERE, in which an ERRE (underlined) merges with a classical ERE (**bold**) (**TNAAGGTCANNNTGACCT**). These ERRE/ERE sites can be occupied by only a single receptor at a time (ERR α or ER α).⁹⁵

Among ERR α target genes, there are genes taking part in the estrogen mediated signalling pathways. In fact, ERR α induces expression of aromatase and dehydroepiandrosterone (DHEA) sulphotransferase (SULT2A1), which increase E2 cellular content.⁹⁶

Most importantly, even if there is disagreement in the literature concerning the effects of ERR α inhibition in ER+ breast cancer,^{80, 83, 97, 98} ERR α is well accepted as a potential therapeutic target in breast cancer, especially ER- breast cancer.^{80, 83, 85, 99, 100}

1.6.2. Known inhibitors of ERR α

The most interesting piece of literature concerning ERR α inhibitors probably comes from Novartis laboratories.¹⁰¹ The group published the crystal structure of the receptor binding a small molecule inverse agonist (**96**, Figure 22).

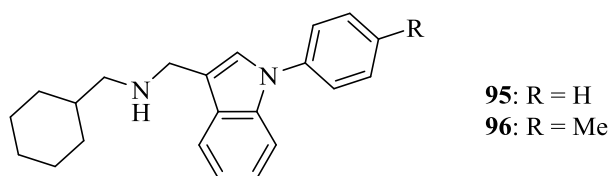


Figure 22. Two compounds reported by Novartis as ERR α inhibitors.

The crystal structure, compared to the unbound receptor (**A**, Figure 23), shows how a key interaction lies between the inhibitor and Phe328. The secondary amine place the compound near the residue of Glu331 in a region normally occupied by Phe328. Hence, the inhibitor forces the residue of Phe328 away, which in turn clashes with the Phe510. The displacement of Phe510 ultimately generates a distortion in the alpha helix named H12. The displaced H12 then occupies the co-regulator peroxisome proliferator-

activated receptor gamma co-activator 1-alpha (PGC-1 α) binding region (**B**, Figure 23). Hence, PGC-1 α cannot bind anymore to ERR α .

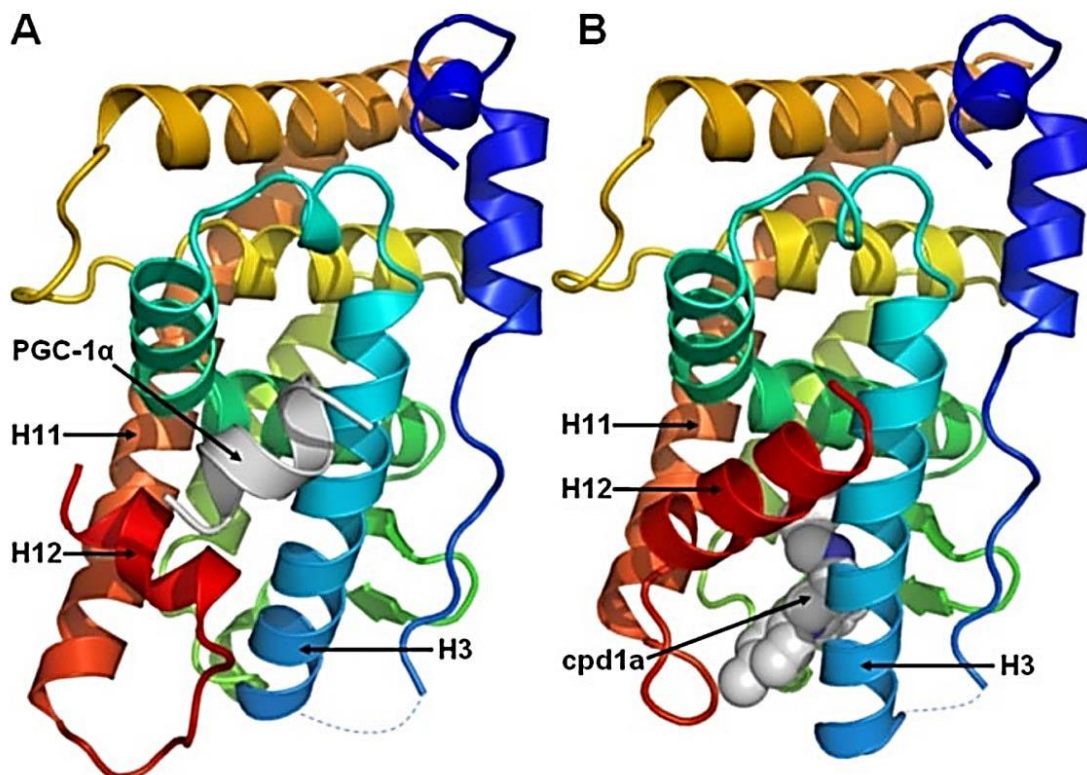


Figure 23. Crystal structure of ERR α reported from Novartis of the unbound receptor (**A**) in complex with PGC-1 α and of the receptor in complex with the inhibitor (**B**)¹⁰¹. Cpd1a correspond to compound **96**. The presence of the inhibitor displaces the alpha helix H12 which in turn occupies the co-regulator binding site.

The EC₅₀ values reported for the two compounds are 700 nM and 190 nM for **95** and **96**, respectively. It is rather interesting to notice the effect that the small methyl group have on the activity, considering that the group lies in the edge of the enzyme.¹⁰¹

Noteworthy is also the enormous difference in the binding site of the unbound and bound receptor. In fact, the ligand binding domain does not naturally have enough space to accommodate the compound. Nevertheless, the flexibility of the chains allows the compound to penetrate and a new thermodynamic equilibrium is generated which leads to the displacement of the helix H12.

Diethylstilbestrol (DES, **97**, Figure 24) and the similar hexoestrol (**98**, Figure 24) and dienestrol (**99**, Figure 24) show significant activity against ERR α . DES has been reported to have an EC₅₀ value of 1 μ M.^{99, 102}

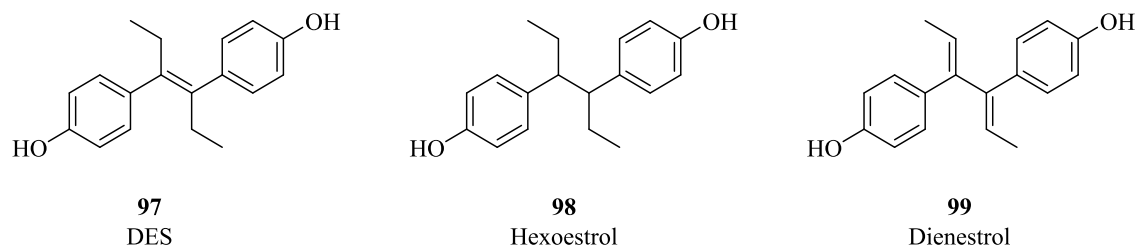


Figure 24. Structure of the three inhibitors of ERR α : DES, hexoestrol and dienestrol.

4-Hydroxytamoxifen (4-OHT, **100**, Figure 25) is an ERR γ inverse agonist with no affinity for ERR α . This was found to be due to a clash with Phe328 in ERR α .¹⁰³

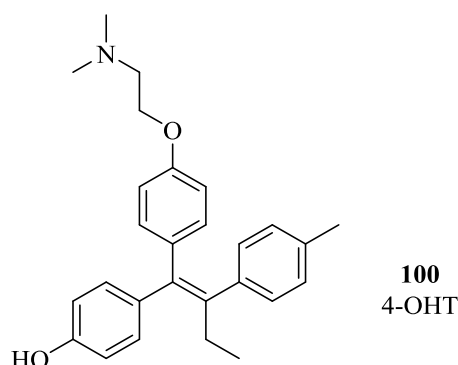


Figure 25. Structure of the ERR γ inverse agonist 4-OHT **100**.

Wang *et al.*¹⁰⁴ demonstrated the activity against ERR α of the flavonoid kaempferol (**101**, Figure 26) with a luciferase assay. In this whole cell system, **101** had the same effect at 20 μ M as XCT790 (**103**, Figure 27) at 10 μ M. Kaempferol has a much stronger affinity for ER β (for which is an activator) and at the concentration at which it shows effects against ERR α , it also activates ER α .

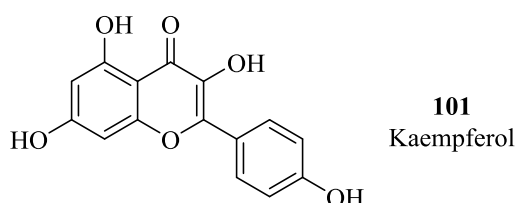


Figure 26. Structure of the flavonoid kaempferol as a weak inverse agonist of ERR α .

In 2004, Busch *et al.*¹⁰⁵ reported the synthesis of XCT790 (**103**, Figure 27) as optimisation of the lead compound **102** (Figure 27) identified with a high throughput screen (HTS). **102** (Figure 27) showed an EC₅₀ value of 2.0 μ M in a fluorescence polarisation assay. The ether linker and the thiadiazole moiety of compound **102** (Figure 27) were optimised to ultimately obtain XCT790 (**103**, Figure 27), which showed an EC₅₀ of 0.37 μ M.

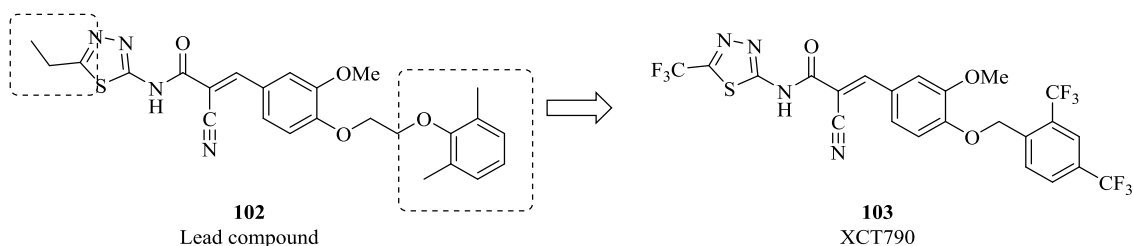


Figure 27. Structure of the potent ERR α inhibitor XCT790 and the lead compound from which it originated.

None of the few examples of ERR α inhibitors reported in the literature has reached clinical trials. This leaves the field open for the development of new potent and selective inhibitors of ERR α for the treatment of cancer.

1.7. The importance of drug-like properties in drug discovery

When developing new drugs, potency is not the only feature a molecule needs to possess. It is too often forgotten that it does not matter how active a molecule is against a target if, when administered to the patient, it cannot reach the target itself.

In 1988 an important piece of literature was published by Prentis *et al.*¹⁰⁶ concerning the reasons for failure of drug development. The article revealed that *ca.* 39% of drugs were failing in development because of poor biopharmaceutical properties. In fact, compounds were developed only for their potency and concerns about the administration, distribution, metabolism, excretion and toxicity (ADMET) properties were left to a later stage.

In subsequent years, the discovery process was enhanced by including the physiochemical properties in the criteria for the selection of the lead compounds. As a result, the failure rate because of biopharmaceutical problems dropped from 39% in 1988 to 10% in 2000.¹⁰⁷

During the optimisation period, a new concept was introduced to describe how probable would be the transformation of a lead compound into a marketed drug. This concept is drug-likeness. As a definition by Christopher A. Lipinski: “Drug-like is defined as those compounds that have sufficiently acceptable ADME properties and sufficiently acceptable toxicity properties to survive through the completion of human Phase I clinical trials.”¹⁰⁸

Rules were then introduced to define the drug-likeness compounds during their development. These rules are not absolute but a guide for choosing better candidates

and a way to keep the physicochemical parameters under control during drug development. Very well-known is the Lipinski “rule of five”, also referred as “Lipinski rules”.

In his article, Lipinski states that “poor absorption or permeation are more likely when”:

- The molecule has five or more hydrogen bond donors.
- The molecular weight is higher than 500 Daltons.
- The logP is higher than five
- The molecule has more than ten hydrogen bond acceptors¹⁰⁸

These rules were set for the development of orally active compounds. In fact, the rules need to be set keeping in mind the target of the molecule. For instance, for the development of drugs that act on the brain, the molecules need to be lipophilic to pass the blood-brain barrier (BBB). Alternatively, compounds that need to be administered by infusion may require less strict parameters than the ones for oral administration.

Other rules have been fixed, such as Veber rules, Ghose rules, lead-likeness, and the choice is at the developer discretion.

1.8. Aims of the project

This project is focused on the development and subsequent optimisation of lead compounds for the treatment of breast cancer targeting the estrogen biosynthesis or the estrogen signalling pathways. The main targets are 17 β -HSD1 and ERR α , which have been shown to play pivotal roles in ER+ and ER- breast cancer, respectively, as described in the previous sections.

The 1,2,3,4-tetrahydroisoquinoline is chosen as the core scaffold based on its structural similarities to E1, E2 and DES, respectively the substrate and product of 17 β -HSD1 and a known inhibitor of ERR α (Figure 28). There are good precedents in the literature and from our own work to support this choice.^{10, 109} Furthermore, in addition to low molecular weight, good hydrophilic-lipophilic balance and other drug-like properties, the THIQ scaffold possesses potential for broad functionalisation, thus enabling an investigation of the active site of the primary targets.

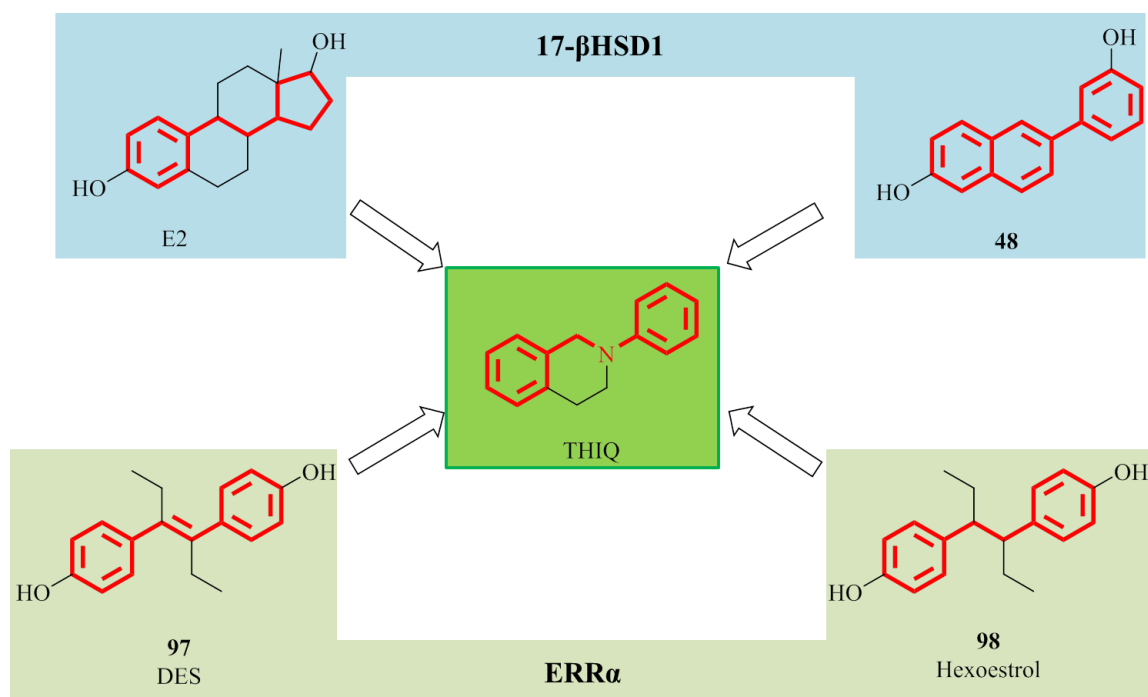


Figure 28. Rationale behind the choice of THIQ as the scaffold for development as an inhibitor of 17β-HSD1 and inverse agonist of ERRα. Structure of the core THIQ compared with compound **48** (Table 3, page 18), E2, DES (**97**, Figure 24, page 35) and hexoestrol (**98**, Figure 24, page 35)

The chemical aspect of the project involves the planning and, when necessary, the development of short, robust and cost effective synthetic routes that would give access to the whole range of differently substituted THIQs. High yielding reactions are desirable but this is considered a secondary matter in order to achieve the main objectives. A set of substituted THIQs is to be obtained through the chosen routes using the Topliss¹¹⁰ approach and similar logic-driven processes.

The synthesised compounds are to be subsequently evaluated against the two primary targets. In order to have a prompt access to their biological activity, an assay for the 17β-HSD1 inhibition was to be developed carrying on previous work from our group. Alternatively, the compounds were going to be evaluated through a collaboration with the external sponsor Ipsen or other external groups.

Development of a cellular assay is to be considered to obtain information not only regarding the enzyme inhibition but also the estrogenicity or anti-estrogenicity that the test compounds might possess. Crystallisation of a few selected compounds with the enzyme was also attempted in order to obtain a better insight into the binding conformation and possible interactions.

The target compounds were evaluated against ER α using a commercially available assay. The biological data thus obtained are used to optimise the test structure of the compounds in an iterative process.

In addition, general cytotoxicity was evaluated with the help of the NCI through their screening panel of 60 cell lines. At the same time, off-target activity against other nuclear receptors and against other different targets was considered and investigated.

CHAPTER 2

Results and discussion

Chemistry

1,2,3,4-Tetrahydroisoquinolines (THIQ) are common compounds present in a large number of natural alkaloids. Examples are the simple salsolinol,¹¹¹ carnegine¹¹² and norcoclaurine (**105**, **104** and **106**, respectively, Figure 29) or the more complex pavine, tubocurarine and tetrandrine (**107**, **108** and **109**, respectively, Figure 29).¹¹³ Due to the importance of THIQs in drug discovery, a wide range of synthetic methods have been reported in the literature.¹¹³⁻¹¹⁹

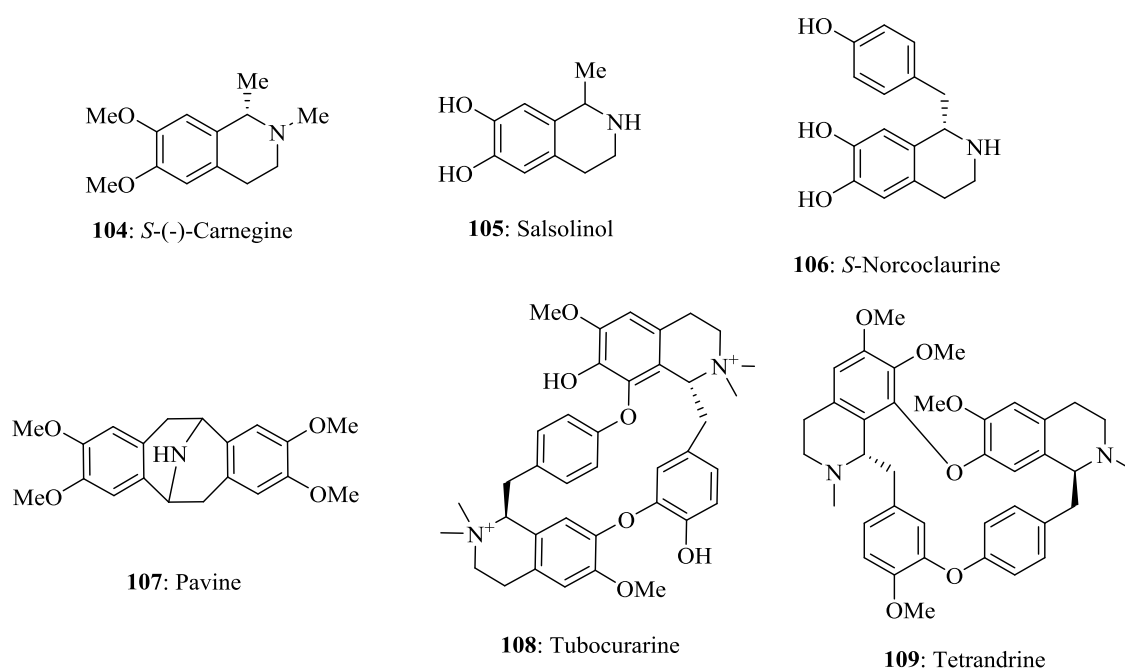
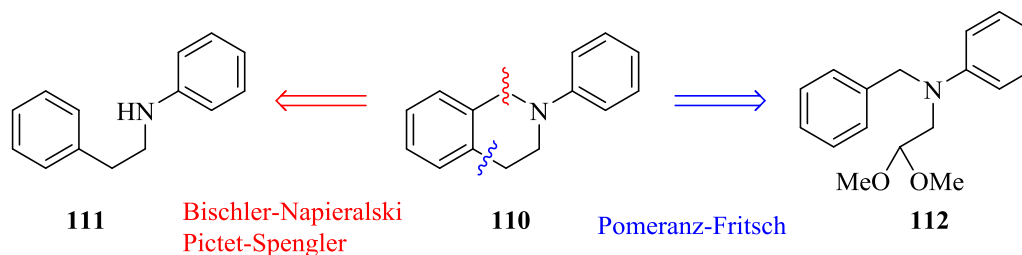


Figure 29. Structure of some natural alkaloids that contain a THIQ moiety, namely carnegine, salsolinol, norcoclaurine, pavine, tubocurarine and tetrandrine.

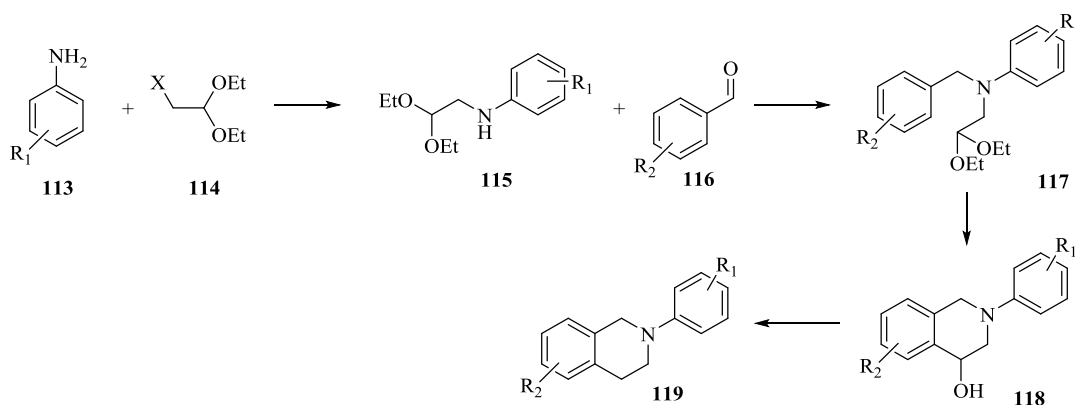
It was envisaged that the construction of the reduced ring offered the best approach to access substitutions in every position available. This could be achieved through already established reactions namely Pomeranz-Fritsch (PF), Pictet-Spengler (PS) and Bischler-Napieralski (BN) (Scheme 2).



Scheme 2. Synthetic approaches considered for the synthesis of the THIQ core.

2.1. Pomeranz-Fritsch approach

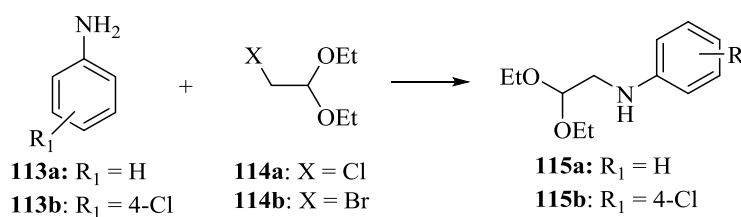
The Pomeranz-Fritsch approach was the first to be investigated because it was expected to give flexibility for the introduction of substitutions and because the reaction was to some extent less represented in the literature, making it more appealing for future patent purposes. The proposed synthesis of the THIQs was to be achieved starting from the appropriately substituted and commercially available benzaldehydes (**116**, Scheme 3), anilines (**113**, Scheme 3) and dialkyl acetals (**114**, Scheme 3). It involved an initial alkylation of the starting aniline **113** with the haloacetaldehyde diethylacetal **114** to obtain the secondary aniline **115**, which could then be reductively alkylated with a substituted benzaldehyde **116** to give intermediate **117**. The resultant acetal **117** could then be cyclised to the 4-hydroxy-THIQ **118** and reduced to yield the target THIQ **119**.



Scheme 3. Proposed synthesis for the substituted THIQ through the PF ring closure.

2.1.1. Synthesis of *N*-(2,2-dialkoxy)aniline

For the aniline (**113a,b**, Scheme 4) alkylation many reaction conditions were explored. Interestingly, the alkylchloride **114a** (Scheme 4) was not effective as an electrophile and no product was obtained under any of the conditions tested (Table 11, entries **1-16**).



Scheme 4. Aniline alkylation. Refer to Table 11 for reagents and conditions.

Table 11. Aniline alkylation conditions^a

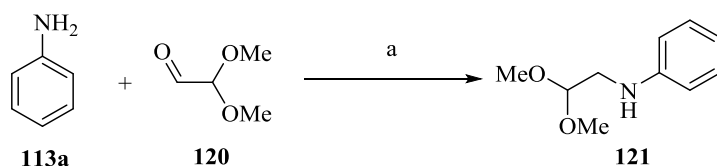
Entry	R ₁	X	Base	Solvent	Catalyst	T (°C)	Time (h)	Yields
1	4-Cl	Cl	NaH	Et ₂ O	none	rt	4	0%
2	4-Cl	Cl	NaH	Et ₂ O	NaI	reflux	2	0%
3	4-Cl	Cl	K ₂ CO ₃	MeCN	TBAI	reflux	24	0%
4	4-Cl	Cl	NaH	DMSO	none	80	24	0%
5 ^b	4-Cl	Cl	none	MeCN	KI	150	15 min	0%
6 ^b	4-Cl	Cl	none	MeCN	KI	170	10 min	0%
7 ^b	H	Cl	none	MeCN	KI	100	10 min	0%
8 ^b	H	Cl	none	MeCN	KI ^c	100	10 min	0%
9	H	Cl	NaHCO ₃	EtOH	none	reflux	72	0%
10	H	Cl	NaH	DMSO	none	rt	5	0%
11	H	Cl	NaH	DMSO	none	80	8	0%
12 ^b	H	Cl	NaH	DMSO	none	100	15 min	0%
13 ^b	H	Cl	NaH	DMSO	none	150	15 min	0%
14	H	Cl	KHMDS	DMSO	none	rt	24	0%
15	H	Cl	NaH	DMF	none	60	24	0%
16	H	Cl	Et ₃ N	none	none	60	24	0%
17	H	Br	NaH	DMSO	none	rt	24	50% <i>ca.</i> ^{d, e}
18	H	Br	NaH	DMF	none	rt	18	52% <i>ca.</i> ^{d, e}
19 ^f	H	Br	NaH	DMF	none	rt	24	30% <i>ca.</i>
20	H	Br	K ₂ CO ₃	EtOH	none	80	18	75% ^d
21	H	Br	KOH	EtOH	none	80	18	50% ^d
22	H	Br	Et ₃ N	EtOH	none	80	18	75% ^d

^aReactions were conducted at 1.0 M concentration. ^bReactions were performed in a microwave. ^c6.0 eq. of KI were used. ^dYield based on NMR of crude. ^e5-15% of double alkylated aniline formed. ^fReaction was conducted at 0.1 M concentration.

In contrast, the alkylbromide (**114b**, Scheme 4) proved to be reactive at rt and, indeed, double alkylation became an issue (Table 11, entries **17-18**), which could be partly overcome by changing the procedures (e.g. the dilution), albeit at the cost of a reduced yield (Table 11, entry **19**). Best results were obtained with the use of weaker bases such as K₂CO₃ and Et₃N (Table 11, entries **20, 22**).

An alternative approach for the synthesis involving a direct reductive amination was evaluated (Scheme 5). The reaction parameters (e.g. solvent and reducing agent) were chosen upon literature examples.¹²⁰ The reaction reached completion within 1 h at rt and

the amine **121** (Scheme 5) was obtained with a yield higher than 95%. An excess of sodium triacetoxyborohydride ($\text{NaBH}(\text{OAc})_3$) was necessary to drive the reaction to completion but the reagents were used in stoichiometric ratio and no double alkylation was observed.

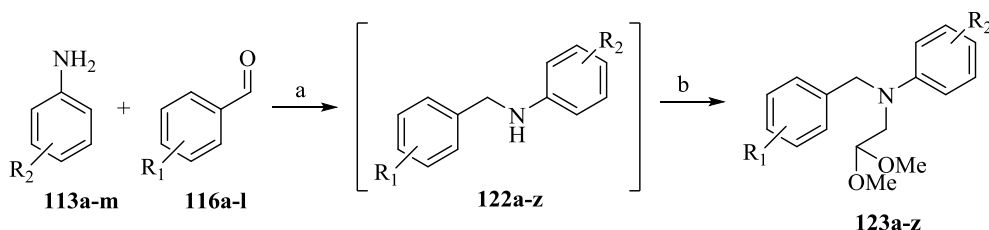


Scheme 5. 2,2-dimethoxyacetaldehyde reductive amination. Reagents and conditions: a) $\text{NaBH}(\text{OAc})_3$, CHCl_3 , rt.

With these results in hand, the synthesis of THIQ could be accelerate by carrying out two sequential reductive aminations in one pot and thus moved to explore this possibility.

2.1.2. Synthesis of *N*-benzyl-*N*-(2,2-dimethoxyethyl)anilines

The synthesis of compounds **123a-z** using two sequential reductive aminations in one pot is shown in Scheme 6 and the results obtained are presented in Table 12. The yields range from good to very good with a range of substituents on both the aromatic rings. Unsurprisingly, the reaction was unsuccessful when using 3-chloroaniline and 2-chloroaniline as starting materials (products **123t** and **123v**, Table 12) and only the intermediates **122t,v** (Table 12) were recovered. In these cases, the reaction stopped after the first alkylation.



Scheme 6. Double reductive amination approach. Reagents and conditions: a) $\text{NaBH}(\text{OAc})_3$, CHCl_3 , rt. b) 2,2-dimethoxyacetaldehyde, $\text{NaBH}(\text{OAc})_3$, rt.

Table 12. Double reductive amination.

Benzaldehyde	R ₁	Aniline	R ₂	Product	Yields (%)
116a	H	113a	H	123a	99
116a	H	113c	3-OMe	123b	73
116a	H	113d	3,5-(OMe) ₂	123c	Nf ^a
116a	H	113e	3,4,5-(OMe) ₃	123d	85
116b	4-OMe	113a	H	123e	85
116c	3-OMe	113a	H	123f	66
116d	4-Cl	113a	H	123g	89
116e	3-Br	113a	H	123h	54
116b	4-OMe	113b	4-Cl	123i	91
116c	3-OMe	113b	4-Cl	123j	90
116f	2-OMe	113b	4-Cl	123k	96
116g	4-OH	113a	H	123l	90
116g	4-OH	113c	4-Me	123m	94
116g	4-OH	113b	4-Cl	123n	66
116g	4-OH	113d	4-OMe	123o	90
116g	4-OH	113e	4-OH	123p	Nf ^a
116b	4-OMe	113f	4-Me	123q	91
116b	4-OMe	113g	4-Et	123r	86
116b	4-OMe	113d	4-OMe	123s	97
116b	4-OMe	113h	3-Cl	123t	Nf ^a
116b	4-OMe	113i	3-OMe	123u	89 ^b
116b	4-OMe	113l	2-Cl	123v	Nf ^a
116b	4-OMe	113m	2-OMe	123w	81 ^b
116h	3,4-(OMe) ₂	113d	4-OMe	123x	91
116i	3,4,5-(OMe) ₃	113d	4-OMe	123y	98
116l	H	113b	4-Cl	123z	82

^aNf = product did not form. ^bReaction was concentrated during the second step.

Difficulties occurred also when 3- and 2-methoxyaniline were used (products **123u** and **123w**, Table 12) but in this case it was possible to force product formation by concentrating the reaction mixture under reduced pressure and increasing the reaction time. These behaviours could easily be explained taking into consideration the

electronic and steric effect of the substituents on the nucleophilicity of the nitrogen. Substituents *ortho* to the nitrogen created steric hindrance that made the nucleophilic attacks more difficult (entries **123v**, **123w**, Table 12). Additionally, the electron-withdrawing effect of the chlorine reduced the electron-density on the nitrogen consequently reducing its nucleophilicity. An opposite effect was exerted by electron-donating groups. The sum of these steric and electronic effects could thus explain the reactivity issues of compounds **123t-w** (Table 12) as shown in Figure 30.

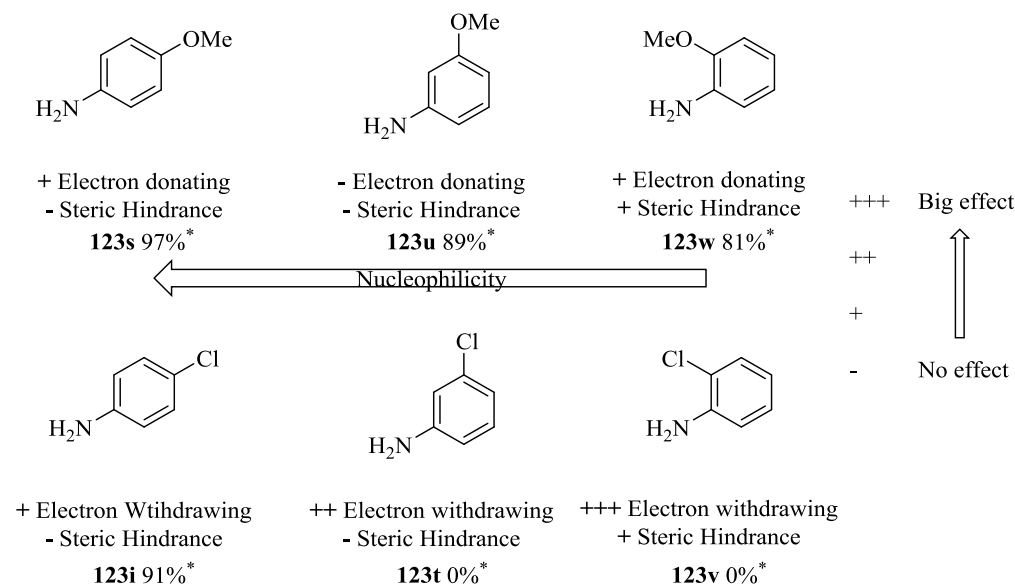
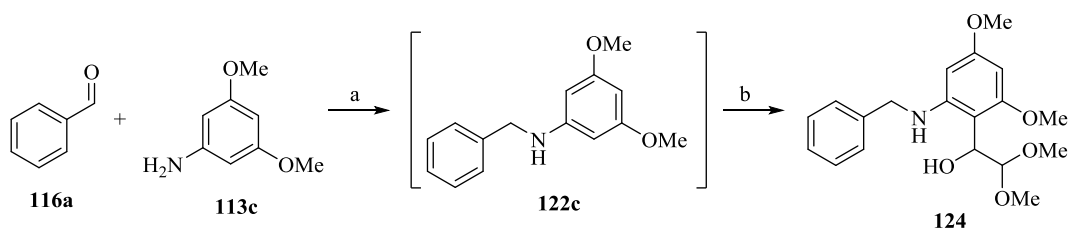


Figure 30. Steric and electronic effects of the substituent on the nucleophilicity of the aniline. *Yields refer to the product having the respective aniline as starting material.

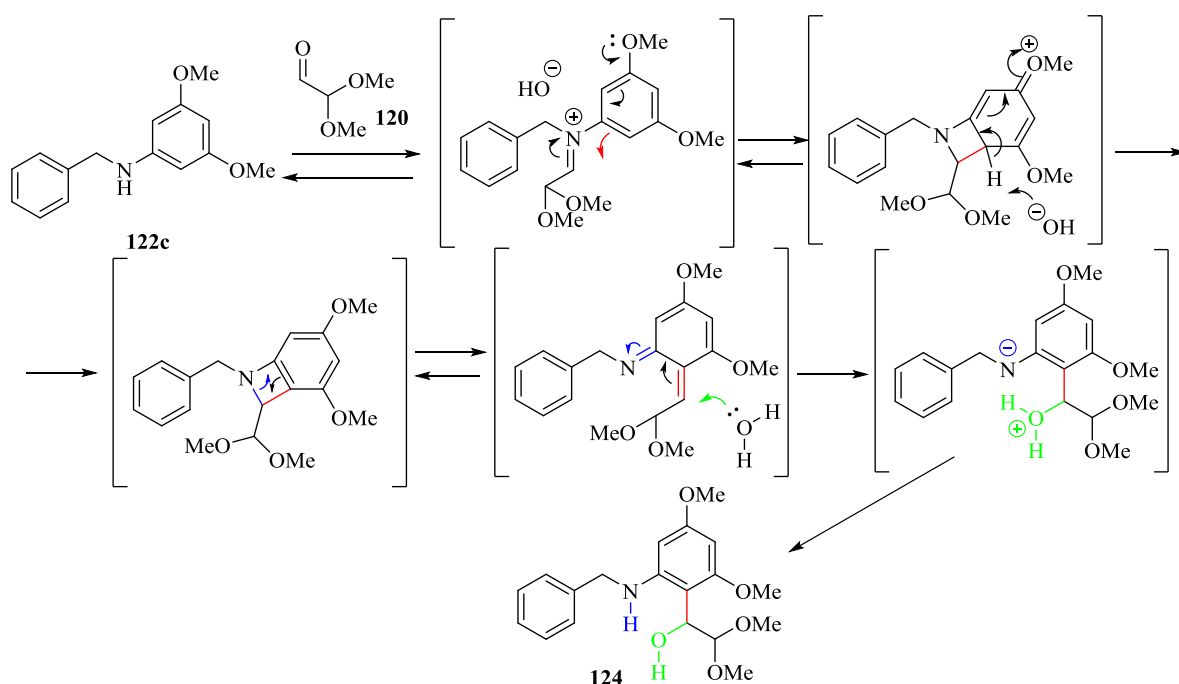
The 4-hydroxyaniline gave initial solubility problems in chloroform that could be overcome using THF as the solvent. However, solving the solubility issue did not lead to the desired product **123p** (Scheme 6, Table 12) and again only the intermediate *N*-benzylaniline **122p** (Scheme 6, Table 12) was recovered.

An interesting side reaction was observed when the synthesis of compound **123c** (Scheme 6, Table 12) was attempted. In this case the desired product **123c** was not obtained and **124** (Scheme 7) was obtained instead with a 62% yield.



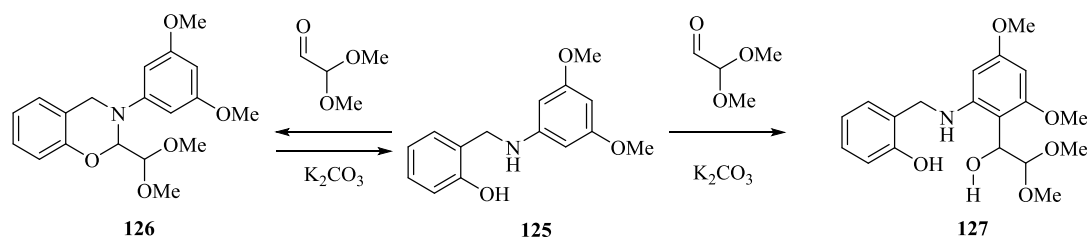
Scheme 7. Double reductive amination did not yield the desired product **123c** (Table 12) but the C-alkylated product **124**. Reagents and conditions: a) $\text{NaBH}(\text{OAc})_3$, CHCl_3 , rt. b) 2,2-dimethoxyacetaldehyde, $\text{NaBH}(\text{OAc})_3$, rt.

It appeared that the intermediate iminium ion, in place of the expected reduction, underwent an intramolecular rearrangement through a Vilsmeier like mechanism to yield **124** (Scheme 8). The same product **124** was formed when a solution of the secondary aniline (**122c**, Scheme 8) and 2,2-dimethoxyacetaldehyde (**120**, Scheme 8) were stirred in chloroform in the absence of $\text{NaBH}(\text{OAc})_3$, proving that the reducing agent was not involved in the rearrangement.



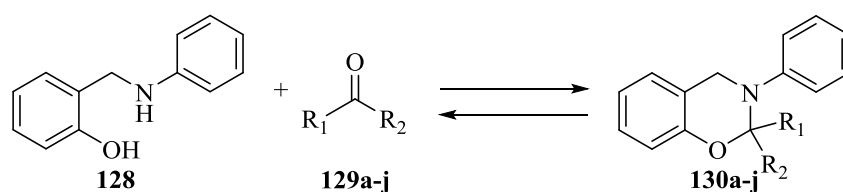
Scheme 8. Possible mechanism of the intramolecular rearrangement leading to the formation of **124**.

A kinetic ^1H -NMR experiment was performed in an attempt to gain insight into the mechanism. Unfortunately, even though the starting material and the product had quite different NMR spectra, the reaction mixture proved too convoluted for clear interpretation. Some signals, not belonging to the starting material or the product, were visible but the identity of the intermediate could not be determined. This side reaction was, however, clearly faster than the reduction and this suggested that it was an intramolecular rearrangement process. Even when the reaction was performed with a deprotonated hydroxyl (a good nucleophile) near the carbon of the iminium ion (compound **125**, Scheme 9) the alkylation occurred mainly on the aromatic ring (compound **127**, Scheme 9) and the benzoxazine **126** (Scheme 9) was recovered only with a 16% yield.



Scheme 9. Competition between the formation of benzoxazine **126** vs. Vilsmeier-like product **127**.

This Vilsmeier-like process intriguingly only occurred when the aniline was 3,5-dimethoxy substituted, as none of the other anilines assayed gave this product (Table 12, page 45). It had to be considered, that the benzoxazine formation was a reversible reaction and that the stability of **126** (Scheme 9) influenced the irreversible formation of **127** (Scheme 9). The stability of the benzoxazine ring was then briefly evaluated to understand if that might have influenced the formation of compound **127** (Scheme 9). Moreover, the benzoxazine structure was similar to THIQ giving rise to an interest in its potential use as alternative core structure. The benzylamine **128** (Scheme 10) was chosen as the candidate for the synthesis of the respective benzoxazines **130a-j** (Scheme 10). The choice of **128** was motivated by the lack of a methoxy group on the aniline ring, which allowed control of the reactivity towards formation of compounds like **124** (Scheme 6, page 44) and **127** (Scheme 9). The benzylamine **128** was duly subjected to reaction with a range of different aldehydes (compounds **129a-h**, Figure 31) and ketones (compounds **129i,j**, Figure 31).



Scheme 10. Synthesis of benzoxazines. Reactions and conditions: **129a-j** (Figure 31); CHCl₃, rt.

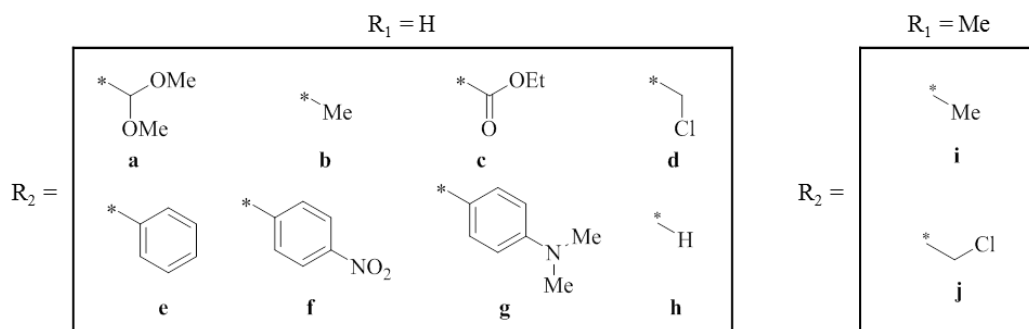


Figure 31. List of substitutions of aldehydes (**129a-h**) and ketones (**129i,j**) tested for the benzoxazine ring formation.

Table 13. Results and conditions for the benzoxazines formation^a

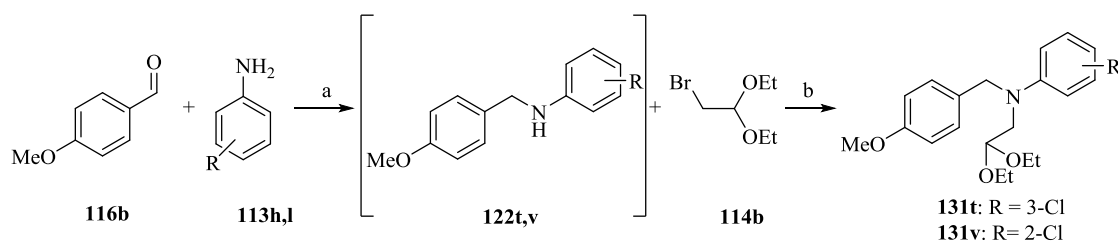
Entry	SM	Cond.	Solvent	Conv.	Entry	SM	Cond.	Solvent	Conv.
								t	
1	129a ^b	K ₂ CO ₃	CHCl ₃	Quant	11	129e	MS	CHCl ₃	0%
2	129b	K ₂ CO ₃	CHCl ₃	0%	12	129f	K ₂ CO ₃	CHCl ₃	0%
3	129b	K ₂ CO ₃	H ₂ O/CHCl ₃	0%	13	129g	K ₂ CO ₃	CHCl ₃	0%
4	129c	K ₂ CO ₃	CHCl ₃	50%	14	129h ^b		CHCl ₃	26%
5	129c	K ₂ CO ₃	H ₂ O/CHCl ₃	90%	15	129h ^b	K ₂ CO ₃	CHCl ₃	0%
6	129d	K ₂ CO ₃	CHCl ₃	15%	16	129h ^b	MS	CHCl ₃	11%
7	129d	MS	CHCl ₃	30%	17	129i		CHCl ₃	0%
8	129d		H ₂ O/CHCl ₃	58%	18	129i	K ₂ CO ₃	CHCl ₃	0%
9	129e	K ₂ CO ₃	CHCl ₃	0%	19	129j		CHCl ₃	0%
10	129e	PTSA	CHCl ₃	0%	20	129j	MS	CHCl ₃	0%

SM = Starting Material (referring to the compound reacted with **128**); MS = 4Å molecular sieves; Cond. = Conditions; Quant = Quantitative; ^aReaction was followed by LC-MS. ^bCompound is commercially available as aqueous solution.

It was possible to form the desired benzoxazine only with compounds **129a,c,d,h** (Table 13) and, of these, only **129a** (Table 13) led to quantitative conversions. An aromatic ring α to the carbonyl group had a drastic effect on reactivity and resulted in no product formation. It was not possible to precisely determine the contribution of the substituents but it appears that an inductively electron withdrawing group α to the carbonyl had a positive effect in formation of the benzoxazine ring. The reaction itself is a condensation with the elimination of a molecule of water (dehydration) and for this reason water itself might be expected to have a negative influence on the course of the reaction but this was not found to be the case. In practice, the addition of water delivered enhanced conversions for compounds **129c**, **129d** and **129h** (entries 4-8 and 14-16, Table 13).

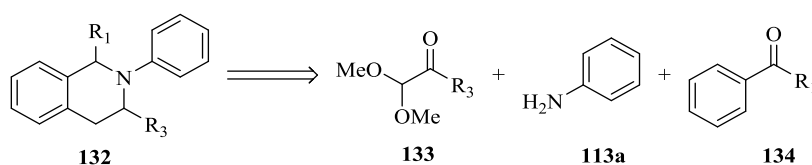
The stability of compound **130a** (Scheme 10, page 48) was tested in neutral water, 1N NaOH and 1N HCl. Intriguingly, the compound was revealed to be rather unstable and after 4 h the amount of the starting material **128** (Scheme 10, page 48) was respectively 77%, 87% and 100% by LC-MS. Thus, the instability of compounds **130a-j** in aqueous media prevents their use for biological testing, which are commonly performed in aqueous buffers. In addition, the same instability might be the reason why the formation of **126** (Scheme 9, page 48) could not compete with the formation of **127** (Scheme 9, page 48).

Analogues of compounds **123t** and **123v** (Table 12, page 45), that were not accessible *via* the double reductive amination approach, were made according to the synthesis initially planned (**131t,v**, Scheme 11) with yields of 21% and 34%, respectively.



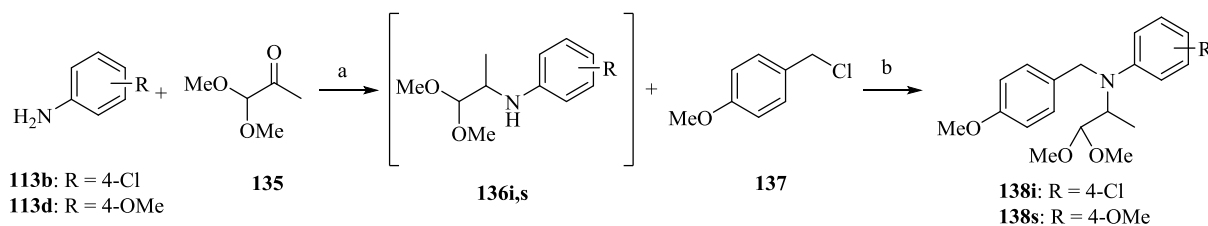
Scheme 11. Synthesis of the analogues of **123t** and **123v**, namely **131t**, **131v**. a) $\text{NaBH}(\text{OAc})_3$, CHCl_3 , rt; b) NaH , DMF, $60\text{ }^\circ\text{C}$.

According to the planned synthesis, 1- and 3-substituted THIQ could be achieved starting from the opportunely substituted benzaldehyde and dimethylacetal, respectively (Scheme 12).



Scheme 12. Proposed strategy for the synthesis of 1 and 3-substituted THIQ.

Interestingly, when the synthesis of acetals **138i** and **138s** (Scheme 13) was attempted, the compounds could not be obtained through the standard double reductive amination and the synthesis was then modified accordingly (Scheme 13) similarly to what described for the analogues of compounds **123t** and **123v** (Scheme 11).

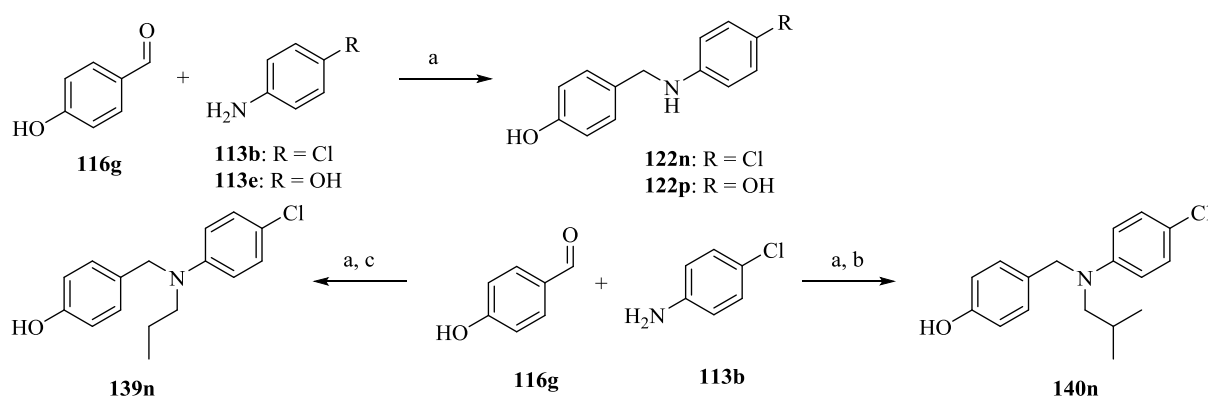


Scheme 13. Synthesis of compounds **138i** and **138s**. a) $\text{NaBH}(\text{OAc})_3$, CHCl_3 , rt; b) NaH , THF, reflux.

The acetal **138s** (Scheme 13) was obtained with a 24% yield while compound **138i** (Scheme 13) proved problematic to be fully purified by flash chromatography and was then used for the next step without being isolated. Due to the low yields and the somewhat difficult purification, the investigation of this pathway for the synthesis of 1-

substituted THIQs was postponed (see chapter 2.2 for the synthesis of 1-substituted THIQs).

With the same reductive amination, compounds **122n,p**, **139n**, and **140n** (Scheme 14) were also synthesised as open ring analogues of the parent THIQs.



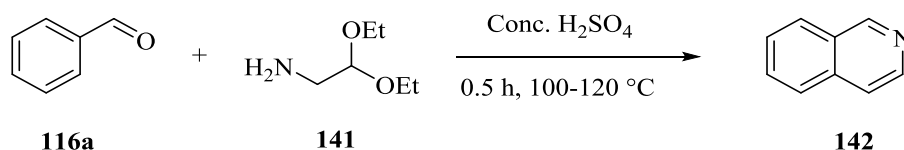
Scheme 14. Synthesis of compounds **122n,p**, **139n**, and **140n** via reductive amination. a) $\text{NaBH}(\text{OAc})_3$, CHCl_3 , rt; b) $\text{NaBH}(\text{OAc})_3$, propanal, CHCl_3 , rt; c) $\text{NaBH}(\text{OAc})_3$, isobutyraldehyde, CHCl_3 , rt;

In conclusion, the double reductive amination step was generally successful with good yields on simply substituted compounds. In addition, the reaction was performed at room temperature and, considering the mild nature of the reducing agent, it was not necessary to perform the reaction under inert atmosphere conditions. The reductive amination was also used to readily access the benzyanilines necessary for the synthesis of the acetals **131t,v** and **138i,s**, which were not accessible through the standard double reductive amination (Scheme 11 and Scheme 13). Further investigation of the formation of compound **124** (Scheme 8, page 47) and on the stability of the benzoxazines **130a-j** (Scheme 10, page 48), even though interesting, would have also been time consuming and would have lain outside the main objectives of this project.

2.1.3. The Pomeranz-Fritsch cyclisation.

The acid catalysed ring closure reaction of a dialkyl acetal is an established reaction named Pomeranz-Fritsch (PF). The reaction is an intramolecular aromatic electrophilic substitution and is controlled by the same electronic factors that control this family of reactions. The presence of electron donating groups on the aromatic ring facilitates the reaction and they exert, to some extent, a directing effect, thus delivering a level of regioselectivity. The PF was firstly reported for the synthesis of isoquinoline (**142**,

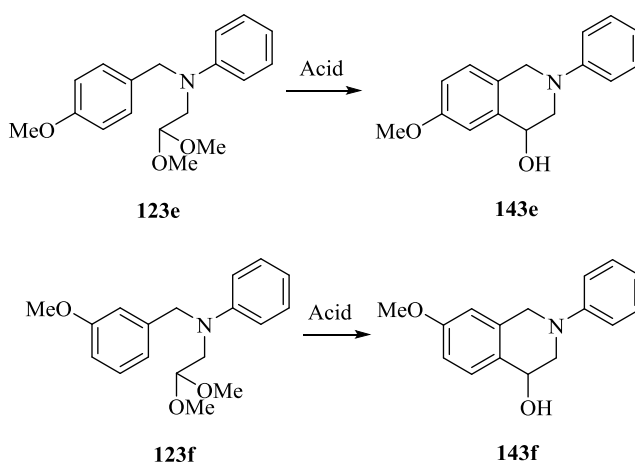
Scheme 15) involving a one-pot condensation of a benzaldehyde (**116a**, Scheme 15) with aminoglyoxal diethylacetal (**141**, Scheme 15).^{121, 122}



Scheme 15. Original Pomeranz reaction.

Since it was originally reported in 1893 there have been only a few reports on the applicability of this reaction to diversely substituted systems. The PF reaction is mainly reported in the literature for ring closure for compounds bearing more than one activating group to facilitate the reaction.^{117, 123-125} However, most of the acids used have proved to be ineffective catalysts when the position for ring closure was not electronically activated. The present studies contribute in part to better understand how diversely substituted systems undergo PF reaction and the regioselectivity observed in these cases.

In the present work and according to the results of Suzuki *et al.*,¹²⁶ when a mesomeric electron donating group, such as a methoxy group, is present *para*- to the position for the ring closure 6 N HCl (entry 1, Table 14) is strong enough to bring the reaction to completion. On the contrary, when the same methoxy group was in the *meta* position the only acid that was capable of catalysing the reaction was 70% HClO₄ (entry 11, Table 14). To some extent understandable, was the effect of the latter acid on the more active system (entry 5, Table 14) which led to a complete degradation of the starting material.



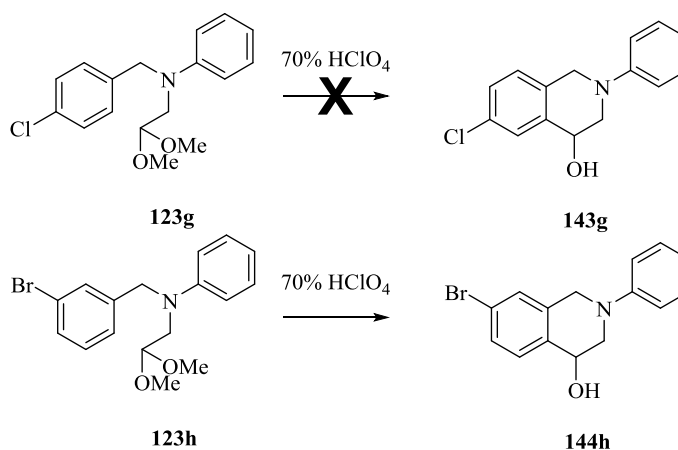
Scheme 16. *Para*-activating effect of the methoxy group. Reagents and conditions: Acid used are shown in Table 14 and reactions are performed rt.

Table 14. Acids screened for the PF cyclisation with or without *para*-activating group.

Entry	SM	Acid	pKa [*]	SM ^{**}	Product
1	123f	6 N HCl	-0.4 ^e	0%	Quant.
2	123f	Conc. HCl (36%)	-0.4 ^e	0%	Quant.
3	123f	Conc. H ₂ SO ₄ (97%)	-2.5 ^e	0%	0% ^b
4	123f	TFA		100%	0%
5	123f	Conc. HClO ₄ (70%)	-13.0 ^e	0%	0% ^b
6	123e	6 N HCl	-0.4 ^e	0%	0% ^c
7 ^a	123e	6 N HCl	-0.4 ^e	0%	0% ^d
8	123e	Conc. HCl (36%)	-0.4 ^e	0%	0% ^d
9	123e	Conc. H ₂ SO ₄ (97%)	-2.5 ^e	0%	0% ^b
10	123e	TFA		100%	0%
11	123e	Conc. HClO ₄ (70%)	-13.0 ^e	0%	Quant.

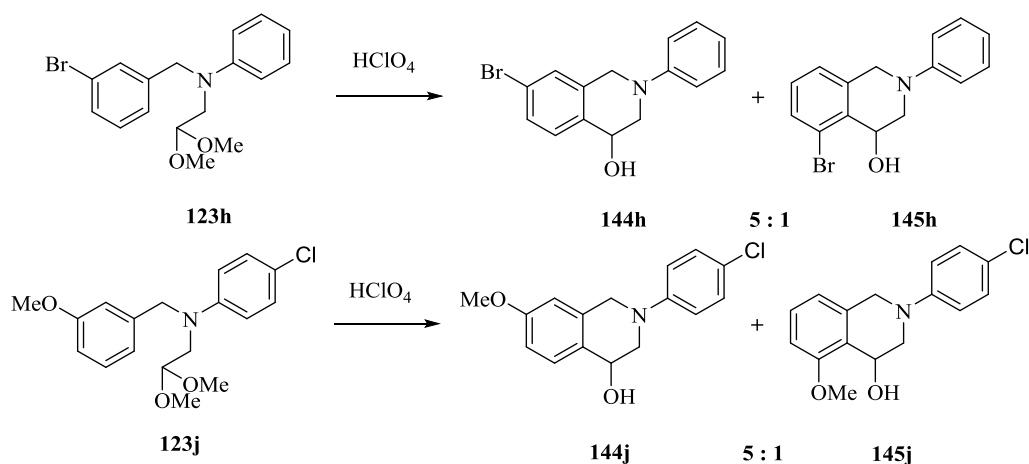
^{*}pKa referred to the acid catalyst used in the reaction; ^{**}SM = Starting Material; ^aReaction was performed in a microwave at 100 °C for 30 min; ^bDegraded to unknown compound; ^cThe hemiacetal was formed; ^dThe aldehyde was formed; ^epKa measured in DCE¹²⁷

The PF reaction was unsuccessful when the cyclisation of compound **123g**, bearing a rather electron withdrawing chlorine group, was attempted but the cyclisation of **123h**, bearing the less deactivating bromine, proceeded smoothly towards the desired product (Scheme 17).

**Scheme 17.** Electron-withdrawing effects on the PF ring closure.

At this stage of the study, the size of the reactions was scaled up to a few grams. A minor product, the amount of which was negligible at smaller scales, became clearly identifiable and was successfully isolated. It could be expected that the regiochemistry of the reaction would have greatly favoured *para*- substitution giving the 7-substituted THIQs **144h** and **144j** (Scheme 18). Nevertheless, it was possible to isolate a significant

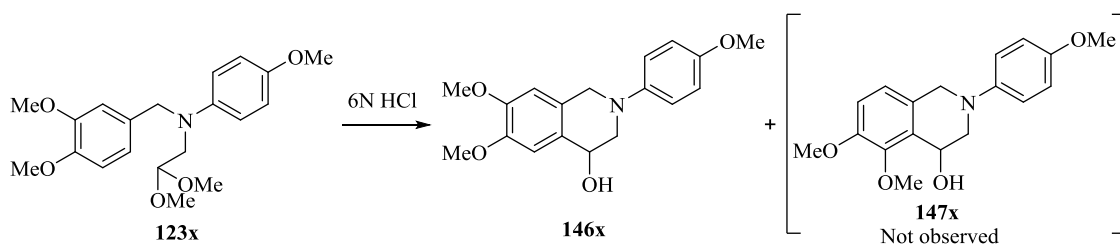
amount of the 5-substituted THIQs **145h** and **145j** (Scheme 18). The ratio between the two regioisomers was found to be constant, with a ratio of 5:1 in favour of the *para*-substituted compounds **144j** and **144h** (Scheme 18).



Scheme 18. *Ortho* vs. *para* competition for ring closure.

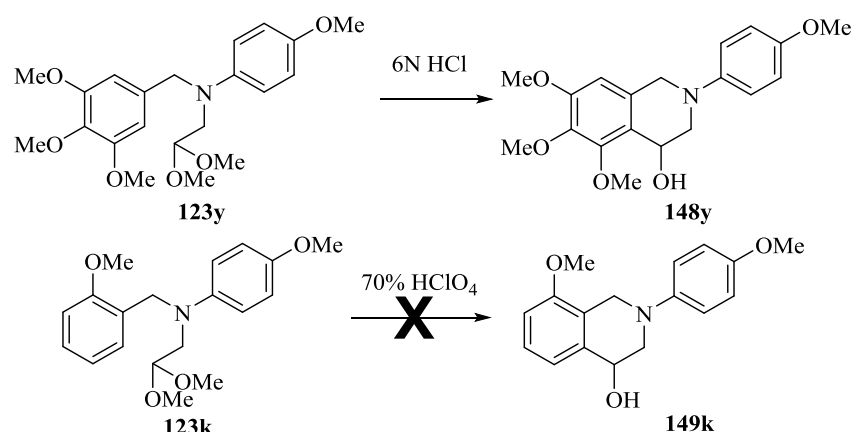
It was predictable that the electron donating mesomeric effect of the methoxy group was virtually identical in both *para* and *ortho* positions and that the regio-selectivity would be controlled by merely steric factors. Inexplicably the ratio remained constant even with the bromine as substituent. Bromine is mainly inductively electron withdrawing and this effect, differently from the mesomeric effect, is much stronger in the *ortho* position. Thus, the formation of **145h** (Scheme 18) was expected to be disfavoured not only by steric factors but also by electronic effects. Nevertheless, access to compounds like **145j** and **145h** (Scheme 18) was much easier than originally envisaged and a more elaborate route to access them was not necessary.

Contrary to **144j** (Scheme 18), the presence of an extra methoxy group, i.e. **123x** (Scheme 19), led to no *ortho* substitution and only compound **146x** (Scheme 19) was recovered. This result was in line with the tendency observed in the literature to obtain only the *para* substitution considering that, as stated before, the majority of the systems investigated were highly activated like **123x** (Scheme 19).



Scheme 19. Cyclisation of compound **123x** occurred only in the *para* position (**146x**). No *ortho* cyclised product (**147x**) was observed.

The reaction proceeded without problems even when only the *ortho* position was available for ring closure as for **123y** (Scheme 20). More difficult to explain was the behaviour of **123k** (Scheme 20), which did not generate any product when subjected to the PF reaction with 70% HClO₄. This lack of reactivity might be explained by the steric hindrance provided by the methoxy group, which might reduce the rotational freedom of the benzyl group necessary for proper conformation for the ring closure. In addition, this effect might be enhanced by intramolecular charge stabilisation of the protonated nitrogen from the lone pair of the methoxy group (Figure 32).¹²⁸



Scheme 20. Ring closure of compounds **123y** and **123k**.

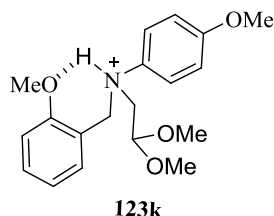
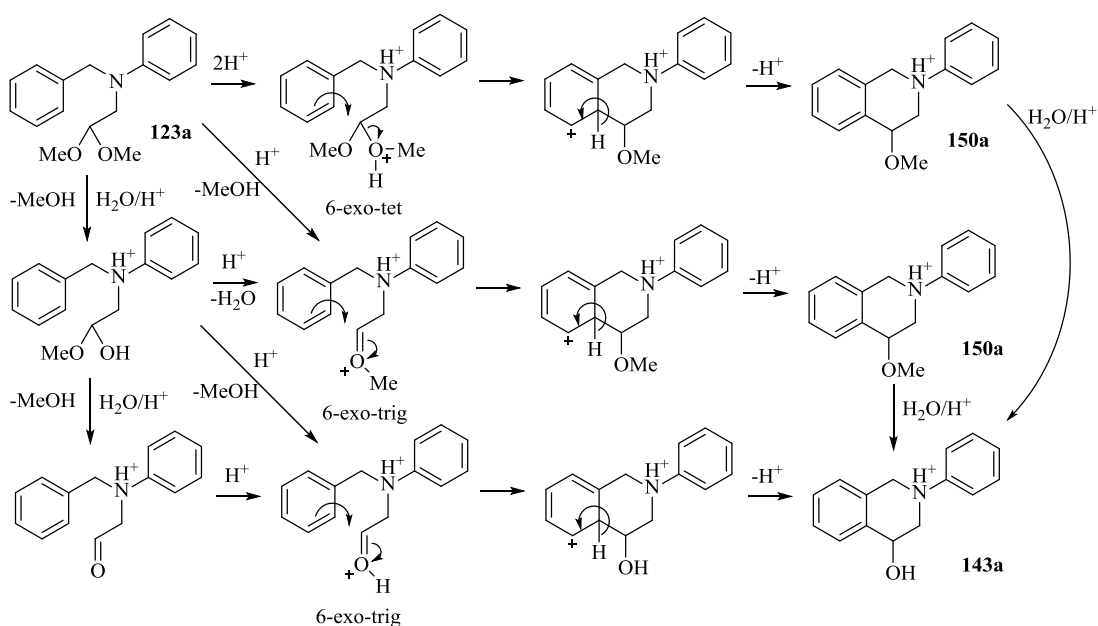


Figure 32. Possible intramolecular charge stabilisation of the protonated **123k**.

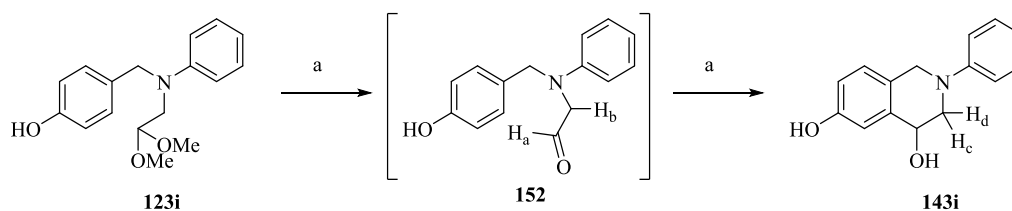
The PF reaction itself can proceed through different pathways to give the same product (**143a**, Scheme 21). Even though all of the pathways can happen at the same time and all of them are favoured according to Baldwin rules, the 6-*exo-trig* cyclisation should be energetically favoured because it involves only rearrangement of electrons hosted in π orbitals.



Scheme 21. Possible pathways for the PF reaction.

A kinetic experiment aiming to explore the cyclisation of compound **123i** and thus identify any long lifetime intermediates was performed directly in an NMR tube. However, the strongly ionic environment led to very convoluted ^1H NMR spectra, which were very difficult to interpret. The kinetic experiment was then repeated by performing the reaction normally and taking aliquots at regular intervals to give samples for ^1H NMR analysis.

Acetal **123i** (Scheme 22, Figure 33) was clearly converted immediately to the aldehyde which subsequently ring closed. It is possible to see how the two protons of the aldehyde (H_a and H_b , Scheme 22, Figure 33) disappeared quickly together with the emergence of two protons of the product (H_c and H_d , Scheme 22, Figure 33).



Scheme 22. Kinetic NMR study of the PF reaction. Reagents and conditions: a) 70% HClO_4 , rt.

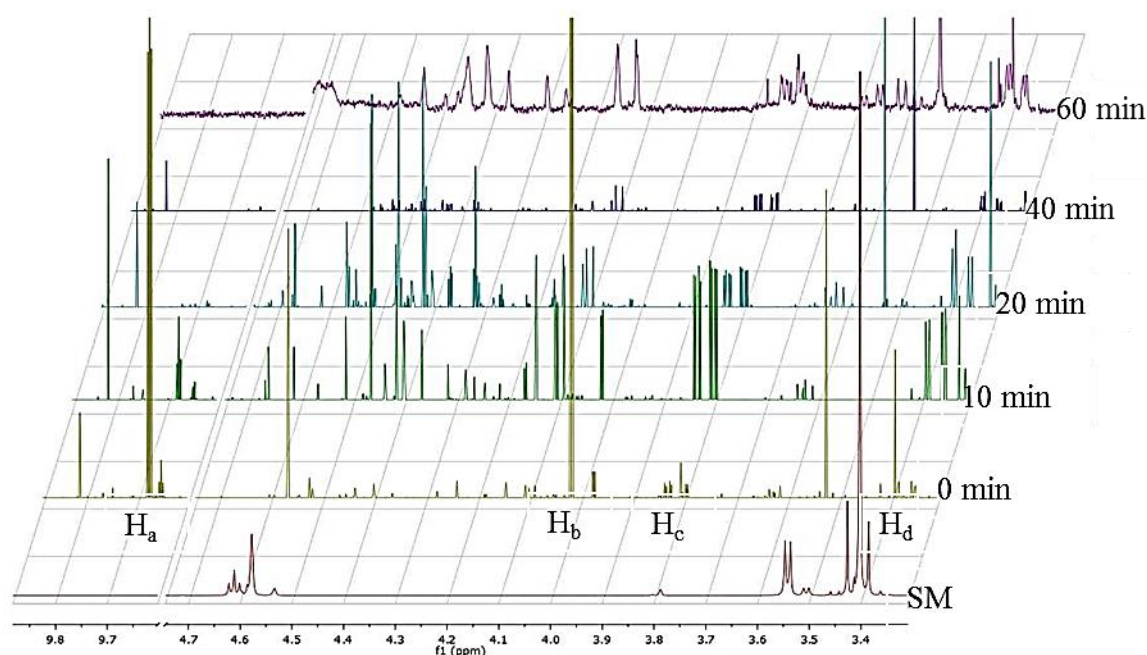
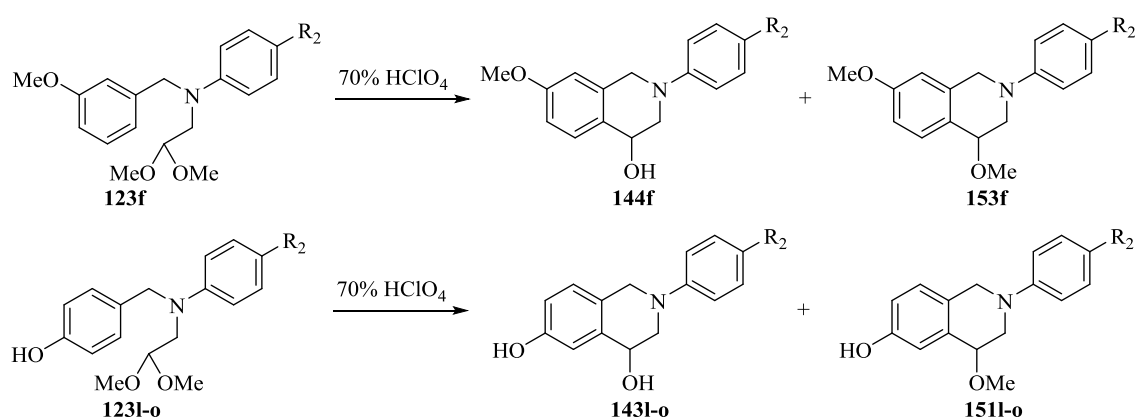


Figure 33. The stacked spectra refer, from the bottom to the top, to the starting material **123i** (SM), the samples at 0, 10, 20, 40 min and the last one is the worked up reaction after 60 min. Spectra have been elaborated for a better visualisation.

Though the kinetic experiment seemed to demonstrate that the preferred pathway would proceed through aldehyde formation, contrasting results were found. As a matter of fact, the formation of the methyl ether (**151l-o**, **153f**, Scheme 23) was noticed to occur in parallel with the free alcohol formation (**143l-o**, **144f**, Scheme 23) and this implied that the other pathways had to be involved in a certain proportion. In some following experiments it was noticed that the ratio between the two products could be controlled by varying the reaction concentration (Scheme 23).



Scheme 23. Methyl ethers **153f**, **151l-o** vs. alcohols **144f**, **143l-o** formation in the PF reaction. **123f,l-o** (Table 12, Scheme 6, page 44).

Formation of the methyl ether **151l-o** was minimised by reducing the reaction concentration to 0.3 M (entry 2, Table 15), which was then considered the optimal concentration for the reaction. A rather different ratio was observed when the reaction

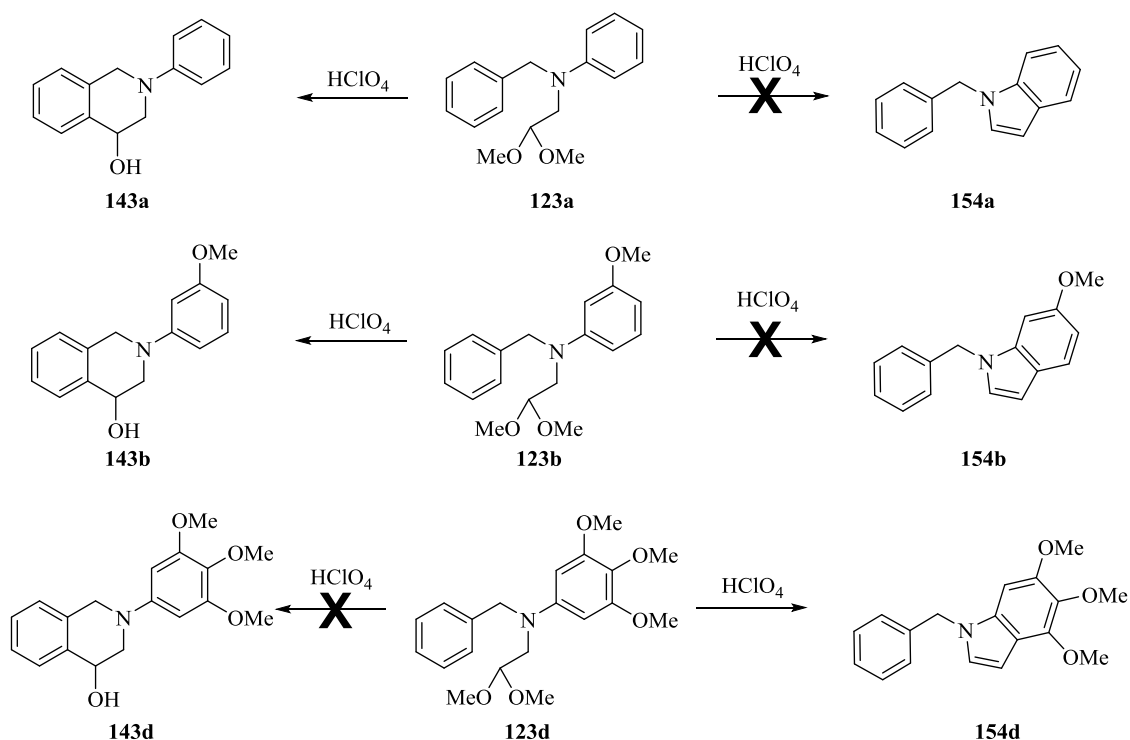
was performed with 6 N HCl, where only *ca.* 15% of the ether **153f** formed in the reaction at 1.0 M concentration. Notably, 6 N HCl (6 N \approx 18%) has a higher water content than 70% HClO₄ and that water was necessary for the hydrolysis of the acetal to the hemiacetal and from the latter to the aldehyde. Hence, it was possible to postulate that the amount of water in the reaction, more than the acid strength, was the factor that controls the ratio among the three different reaction processes and consequently the ratio between the two products **143l-o**, **144f** and **151l-o**, **153f**.

Table 15. Ratio between the formation of **143l-o**, **144f** and **151l-o**, **153f** at different reaction concentrations.

Entry	SM	Conc. (M)	Products	R ₁	R ₂	Ratio ^a
1	123f ^b	1.0	144f + 153f	7-OMe	H	5:1
2	123l	0.9	143l + 151l	6-OH	H	2:1
3	123l	0.3	143l + 151l	6-OH	H	1:0
4	123m	0.7	143m + 151m	6-OH	CH ₃	1:1
5	123n	0.9	143n + 151n	6-OH	Cl	1:1
6	123o	0.8	143o + 151o	6-OH	OMe	1:1

^aRatios alcohol vs. ether were calculated by ¹H NMR of the crude reaction mixture; ^bReaction was performed with 6N HCl.

It is reported in the literature that the PF reaction can be used in some cases for the synthesis of indoles.^{129, 130} The indole formation would compete with the THIQ formation possibly leading to lower yields of THIQs up to the complete inability to obtain the desired THIQs. For this reason, the possible competition between the formation of 5- (**154a,b,d**, Scheme 24) and 6-membered (**143a,b,d**, Scheme 24) ring was investigated, as that could have become an issue for some future substitution on the aniline ring. When compound **123a** (Scheme 24) was treated with 70% HClO₄, the reaction proceeded towards the formation of the THIQ **143a** (Scheme 24). Even when the position for the indole formation was activated by one single methoxy group (**123b**, Scheme 24), the 6-membered ring formation was more competitive and only the THIQ **143b** (Scheme 24) was recovered while no indole **154b** (Scheme 24) formation was observed. Nevertheless, when the system was highly activated (**123d**, Scheme 24), the indole **154d** (Scheme 24) became the only product and no THIQ **143d** (Scheme 24) was identifiable.



Scheme 24. 5- vs. 6-membered ring formation.

The indole **154d** (Figure 34) was not isolated but the ^1H NMR of the reaction mixture was clear enough to leave no doubts. The only side product that was visible on the spectrum was the debenzylated analogue of the indole **154d** (Figure 34).

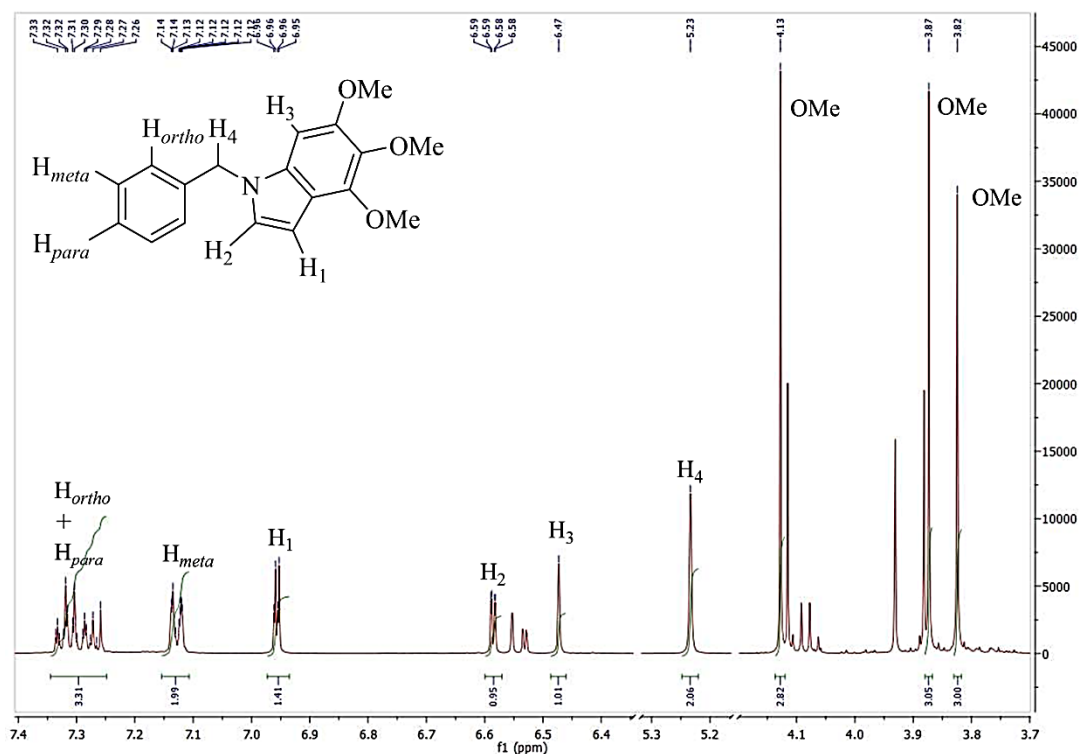
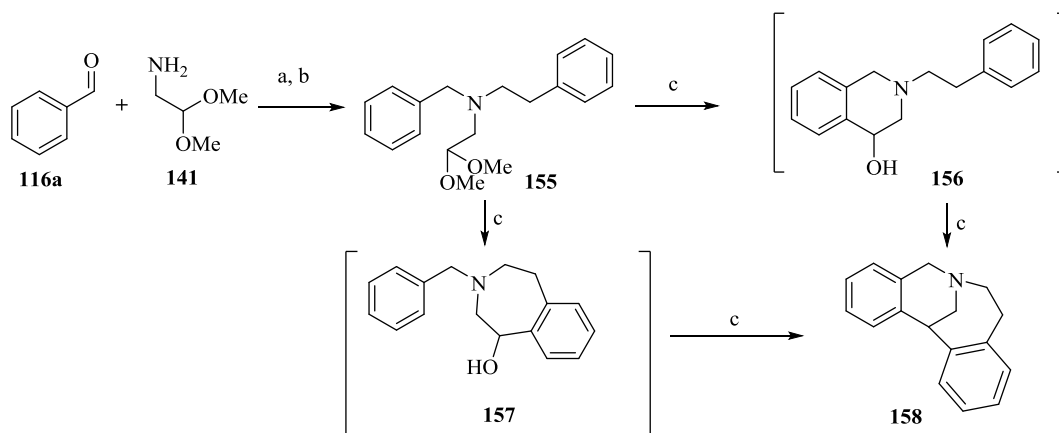


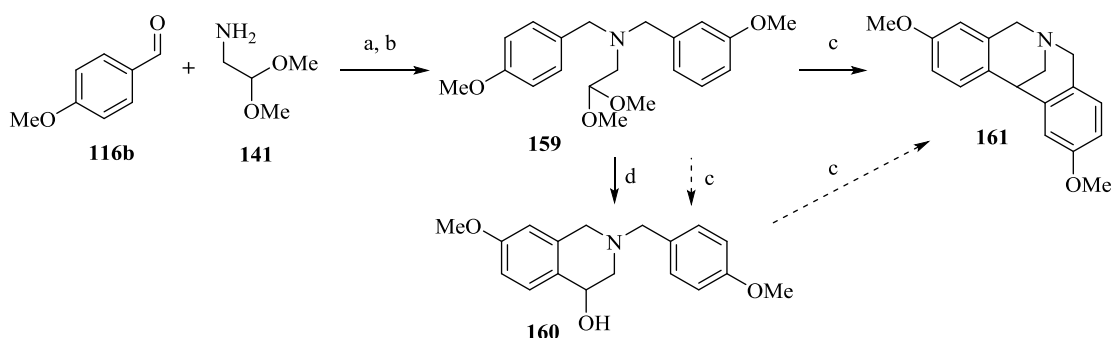
Figure 34. ^1H NMR of the crude reaction mixture of compound **154d**. The sections of spectrum 4.1–5.2 ppm and 5.3–6.4 ppm has been digitally removed for a clearer view. No signal was visible in the removed sections.

The possible competition between the formation of 6- and 7-membered ring was also investigated. The appropriate precursor **155** (Scheme 25) was synthesised from benzaldehyde and 2,2-dimethoxyethylamine (respectively **116a** and **141**, Scheme 25) *via* a double reductive amination and duly cyclised with 70% HClO₄. However, it was not possible to stop the reaction after the initial PF ring closure (**156** and **157**, Scheme 25). Instead, only the double ring closed compound **158** (Scheme 25) was recovered. Hence, in the reaction conditions tested, unlike in the previous example (Scheme 24, page 59), it was not possible to determine if there was a significant competition between the 6- and 7-membered ring closure.



Scheme 25. 6- vs. 7-membered ring formation from the cyclisation of compound **155**. Reagents and conditions: a) NaBH(OAc)₃, CHCl₃, rt. b) 2-Phenylacetaldehyde, NaBH(OAc)₃, rt. c) 70% HClO₄, rt.

Since HClO₄ was able to cyclise compounds even when no methoxy group was present *para*- to the site of ring closure while 6 N HCl was not, a possible selectivity between *meta*- and *para*- cyclisation was investigated. The acetal **159** was synthesised from 4-methoxybenzaldehyde (**116b**, Scheme 26) and 2,2-dimethoxyethylamine (**141**, Scheme 26) *via* a double reductive amination approach and then cyclised with 70% HClO₄. The only product recovered was the double alkylated compound **161** (Scheme 26). Instead, the cyclisation using 6 N HCl led to a single cyclisation giving only compound **160** (Scheme 26). HCl was able to catalyse the ring closure only *para*- to the activating group, therefore only the 7-methoxy substituted THIQ (**160**, Scheme 26) was formed.



Scheme 26. Regioselectivity of the PF reaction under electronic control. In presence of 70% HClO₄, compound **159** cyclise to compound **161** while in presence of 6 N HCl only compound **160** is recovered. Reagents and conditions: a) NaBH(OAc)₃, CHCl₃, rt. b) 3-Methoxybenzaldehyde, NaBH(OAc)₃, rt. c) 70% HClO₄, rt. d) 6 N HCl, rt.

In many cases, when all of the acetals **123a-y** (Scheme 6, Table 12, pages 44-45) and **131t,v** (Scheme 11, page 50) were subjected to the PF cyclisation, the reaction proceeded so cleanly that the degree of purity was sufficient to proceed to the following step without any further purification. An example of the purity of the crude compound **143a** is given in Figure 35.

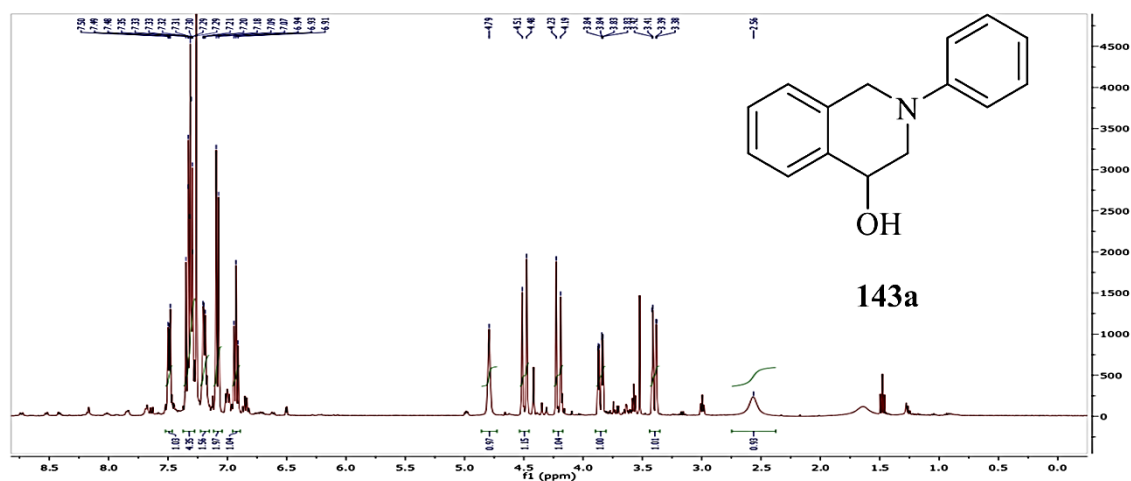
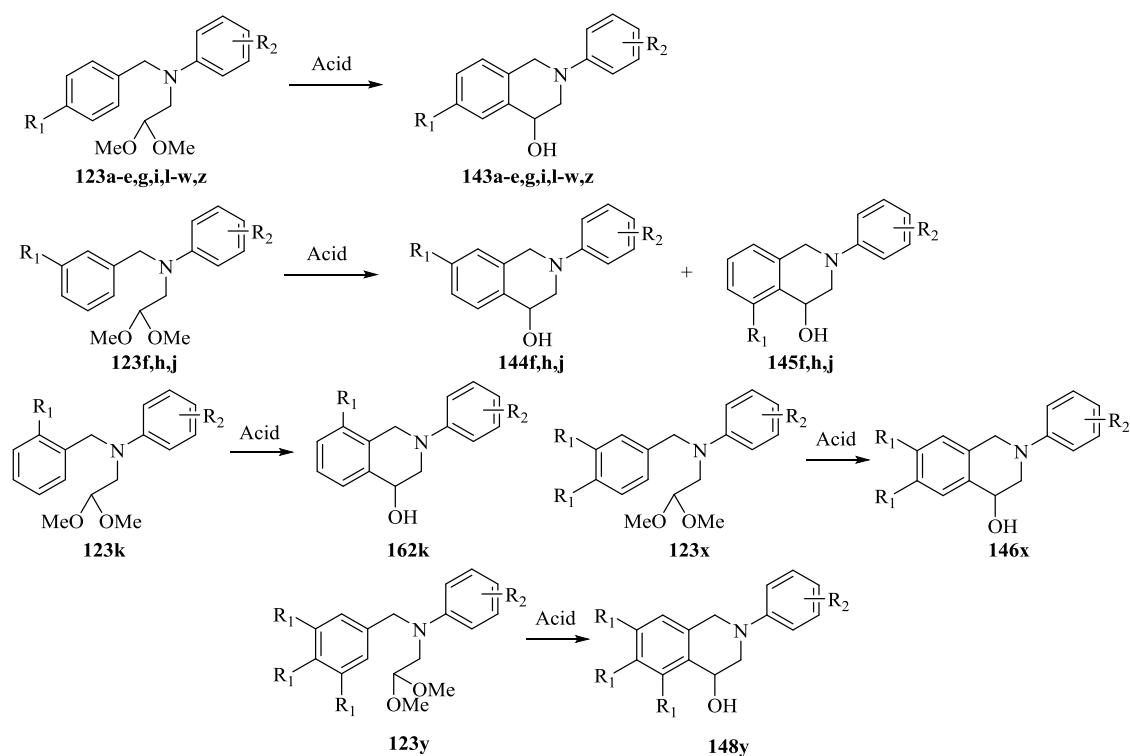


Figure 35. ^1H NMR of the non-purified compound **143a**.

The results of the successful ring closure *via* the PF reaction (Scheme 27) are summarised in Table 16. With the exception of **123g** (Scheme 17, page 53) and **123k** (Scheme 20, page 55), which have been previously discussed, and **131v** (Scheme 11, page 50), all the compounds were successfully ring closed in the experimental conditions used. Moreover, when it was judged unnecessary, the compound was not purified after the work up. The two diastereoisomers **144h** and **145h** were separated, while the mixtures of diastereoisomers **144f-145f** and **144j-145j** were not separated and the ratios were determined by ¹H NMR.



Scheme 27. Scheme of the of the PF ring closure.

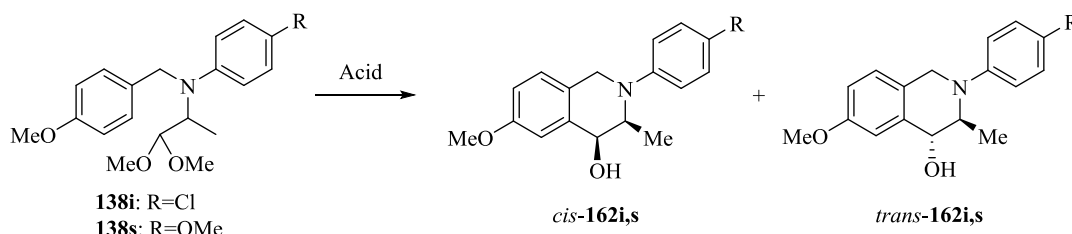
Table 16. Summary of PF results.

SM	R ₁	R ₂	Acid	Product	Yield (%)
123a	H	H	70% HClO ₄	143a	67
123b	H	3-OMe	70% HClO ₄	143b	Np
123e	OMe	H	70% HClO ₄	143e	45
123f	OMe	H	6N HCl	144f + 145f	71 ^b
123g	Cl	H	70% HClO ₄	143g	Nf
123h	Br	H	70% HClO ₄	144h 145h	48 ^c 10 ^c
123i	OMe	4-Cl	70% HClO ₄	143i	Np
123j	OMe	4-Cl	6N HCl	144j + 145j	31 ^d
123k	OMe	4-Cl	70% HClO ₄	162k	Nf
123l	OH	H	70% HClO ₄	143l	Np
123m	OH	4-Me	70% HClO ₄	143m	Np
123n	OH	4-Cl	70% HClO ₄	143n	Np
123o	OH	4-OMe	70% HClO ₄	143o	Np
123q	OMe	4-Me	70% HClO ₄	143q	Np
123r	OMe	4-Et	70% HClO ₄	143r	31
123s	OMe	4-OMe	70% HClO ₄	143s	Np

131t^a	OMe	3-Cl	70% HClO ₄	143t	41
123u	OMe	3-OMe	70% HClO ₄	143u	36
131v^a	OMe	2-Cl	70% HClO ₄	143v	Nf
123w	OMe	2-OMe	70% HClO ₄	143w	26
123x	OMe	4-OMe	6N HCl	146x	62
123y	OMe	4-OMe	6N HCl	148y	82
123z	H	4-Cl	70% HClO ₄	143z	61

^aCompounds **131t** and **131v** are diethyl acetal instead of dimethyl acetal. ^bRefers to the sum of **144f** and **145f** that were not separated (ratio **144f**/**145f** 5:1). ^c**144h** and **145h** were isolated from the same reaction. ^dRefers to the sum of **144j** and **145j** that were not separated (ratio **144j**/**145j** 4:1). SM = Starting Material. Nf = Not formed. Np = Not purified.

Compounds **138i** and **138s** were also successfully ring closed using 70% HClO₄ as catalyst (Scheme 28). Again, the two diastereoisomers formed were not isolated and were carried through to the next reaction as a mixture.



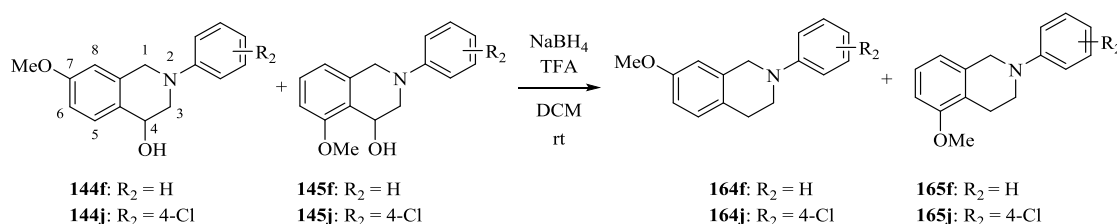
Scheme 28. PF ring closure of compounds **162i** and **162s**.

In conclusion, the PF reaction was versatile and robust, allowing us to obtain a wide range of 4-hydroxytetrahydroisoquinolines. The alcohol that was formed as a product of the PF reaction might represent an advantageous point for further strategic modification. The site of ring closure might be predicted based on the starting material structure and the reaction conditions chosen and also be controlled by carefully selecting the conditions or strategically placing activating groups. In addition, the reaction gave products with moderate to good yields and proved to be clean to the extent that in some cases purification was not essential. Moreover, in some cases (ring closure of **123f**, **123h**, **123j**) it was possible to obtain two different regioisomers with one single reaction.

2.1.4. Dehydroxylation of 4-Hydroxytetrahydroisoquinolines.

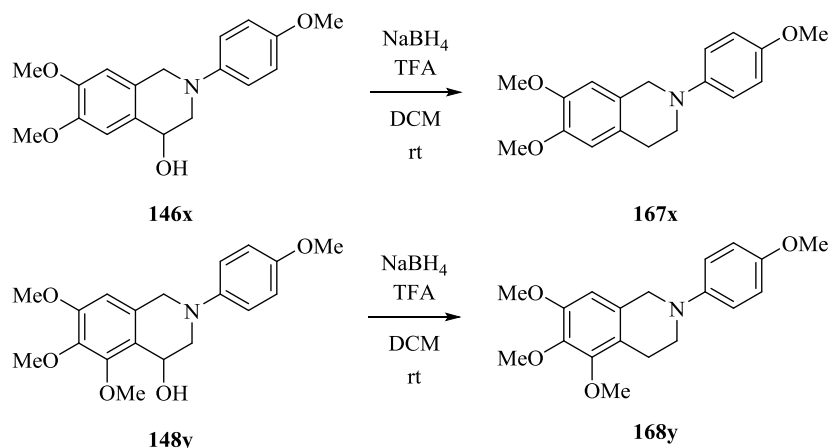
The last step of the synthesis was the dehydroxylation of compounds **143a-e,g,i,l-w,z**, **144f,j**, **145f,j** and **162i,s** to give the respectively final THIQ. The dehydroxylation of compounds similar to **144f** is reported in the literature using NaBH₄ as reducing

agent and TFA as catalyst.¹³¹ The aforementioned conditions were not appropriate for all the compounds synthesised. In fact, only compounds **144f,j** and **145f,j** bearing a methoxy substituent in position 7 or 5 of the THIQ ring underwent a successful dehydroxylation. Compounds **144f** and **145f**, as well as compounds **144j** and **145j**, were reduced as a mixture and the two isomers **164f,j** and **165f,j** could be successfully separated *via* standard flash chromatography (Scheme 29).



Scheme 29. Dehydroxylation of compounds **144f,j** and **145f,j**.

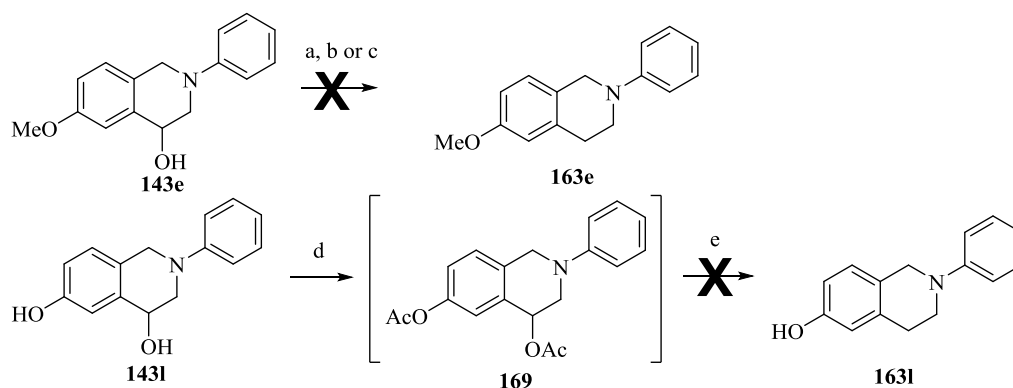
Similarly compounds **146x** and **148y** underwent a reduction using the same reaction conditions to give compounds **167x** and **168y**, respectively (Scheme 30).



Scheme 30. Dehydroxylation of compounds **146x** and **148y**.

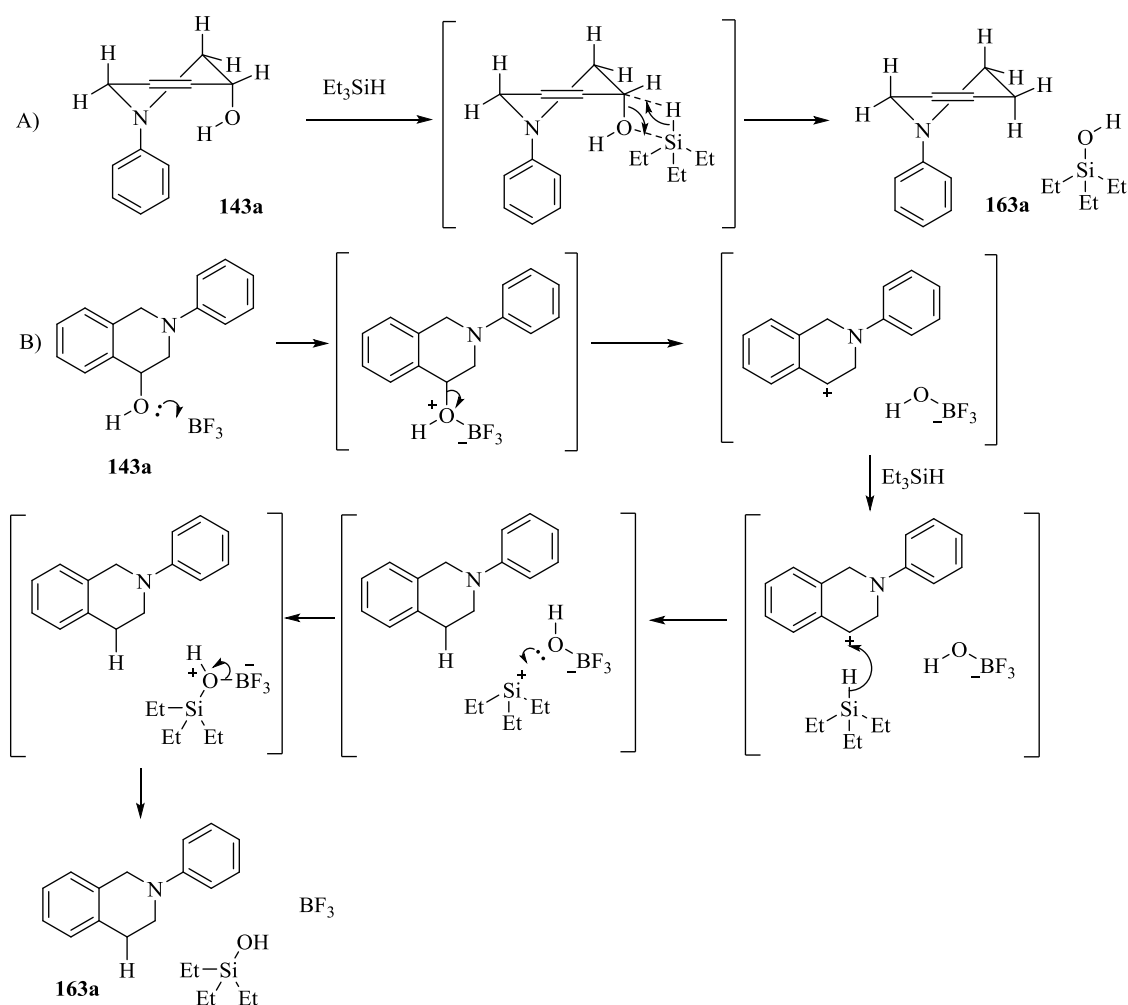
As stated above, any attempt to reduce compounds like **143e** (method a, Scheme 31) using NaBH₄/TFA failed and the use of a stronger Brønsted acid such as TfOH (method b, Scheme 31) did not improve the results. The catalytic hydrogenation of compound **143e** with a Pd/C catalyst (method c, Scheme 31) as a means to remove the 4-hydroxyl group was also evaluated. A range of common hydrogenation solvents was tested, but none of them could yield the desired product **163e** (Scheme 31). The reaction was also attempted in a flow reactor at 100 °C (in THF/MeOH with a 0.5 mL/min flow and 70 bar of H₂) but, as with the previous attempts, no product **163e** (Scheme 31) was formed. The free hydroxyl **143i** (Scheme 31) was then converted to the corresponding acetyl ester **169** (Scheme 31) as literature reports suggested that the acyloxy derivative would

be more labile than the corresponding hydroxyl group,¹³¹ but this proved not to be the case for compounds that did not bear a methoxy group in position 7 (e.g. **143e,l**, Scheme 31).



Scheme 31. Attempts to dehydroxylate compounds **143e** and **143l**. Reagents and conditions: a) NaBH₄, TFA, DCM, rt; b) NaBH₄, TfOH, DCM, rt; c) Pd/C, H₂ 1 atm; d) AcCl, AcOH; e) Pd/C, H₂ 1 atm.

Other reducing agents such as triethylsilane were then evaluated. Reduction with triethylsilane is known in the literature with a wide range of substrates.¹³²⁻¹³⁶ Triethylsilane proved to be capable of giving the desired product in the presence of boron trifluoride etherate as a Lewis acid and DCM as a solvent. Even though the reaction was slow at rt, at reflux it was possible to obtain full conversion in 12-18 h. It is reported in the literature that the reduction with silanes might undertake two principal pathways depending on the nature of the reactant and more importantly on the polarity of the solvent. A concerted mechanism is favoured in apolar or moderately polar solvents¹³⁷ (example A, Scheme 32) while with highly polar solvents a pathway that involves charged intermediates might take place¹³⁸ (example B, Scheme 32). In the experimental conditions attempted, the concerted mechanism is believed to be predominant and this could explain why it was possible to reduce compounds that do not have the ability to stabilise the benzylic cation. These conditions successfully led to product formation even with unsubstituted THIQs. Notably, the same compounds that underwent facile cyclisation with the less strong hydrochloric acid were also successfully reduced by the TFA/NaBH₄ system and compounds that needed harsher cyclisation conditions could be successfully reduced only by Et₃SiH/BF₃·Et₂O.



Scheme 32. Possible mechanism for dehydroxylation with triethylsilane. A) Concerted mechanism involving non-ionic species; B) Mechanism involving charged species.

After initial optimisation of the reaction conditions, the whole range of THIQs synthesised were subjected to dehydroxylation with Et₃SiH. When the dehydroxylation of compounds **143l-o** (Table 17), which bear a free phenolic group, was attempted, the expected product was visible by ¹H NMR of the crude reaction mixture but it was not possible to isolate it by standard purification methods. It was never possible to recover the products by normal phase flash chromatography and crystallisation attempts were unsuccessful probably due to the low purity of the compound in the crude reaction mixture. Reverse phase column chromatography was found to be the only method that could deliver the desired product with a high grade of purity and in reasonable amounts. Driven by this unfortunate discovery it was decided to use only THIQs with a protected phenol. THIQs bearing a methoxy group (e.g. **143b**, Table 16, page 62) synthesised were chosen as a protected THIQs, which could be subsequently easily deprotected with high yields and low purification requirements. The results of the dehydroxylation reaction are shown in Table 17 below.

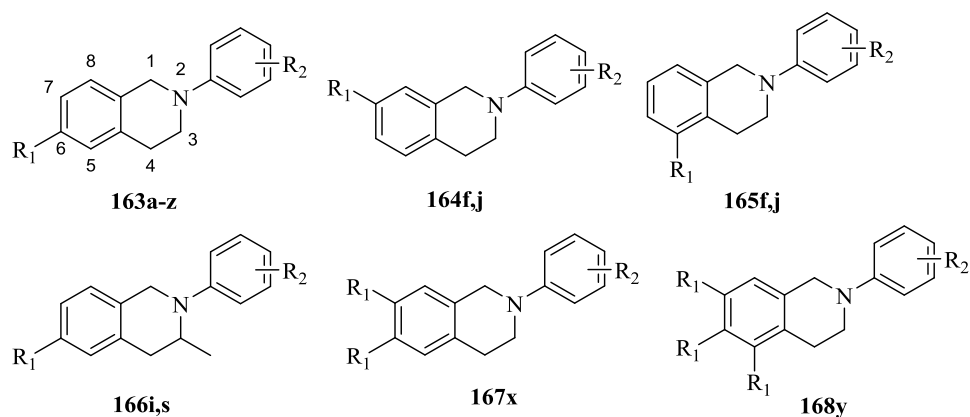


Figure 36. Structure of substitutions for the final THIQs.

Table 17. Summary of the results for the dehydroxylation reaction.

SM	Product	R1	R2	Conditions	Yields (%)
143a	163a	H	H	B	67
143b	163b	H	3-OMe	B	11
143e	163e	OMe	H	B	35
144f + 145f^a	164f + 165f	OMe	H	A	85 ^c
143i	163i	OMe	4-Cl	B	20 ^d
144j^b	164j	OMe	4-Cl	A	51 ^d
145j^b	165j	OMe	4-Cl	A	11 ^d
143l	163l	OH	H	B	35 ^e
143m	163m	OH	4-Me	B	45 ^e
143n	163n	OH	4-Cl	B	50 ^e
143o	163o	OH	4-OMe	B	20 ^d
143q	163q	OMe	4-Me	B	25 ^d
143r	163r	OMe	4-Et	B	51
143s	163s	OMe	4-OMe	B	21 ^d
143t	163t	OMe	3-Cl	B	52
143u	163u	OMe	3-OMe	B	44
143w	163w	OMe	2-OMe	B	38
146x	167x	6,7-(OMe) ₂	4-OMe	A	29
148y	168y	5,6,7-(OMe) ₃	4-OMe	A	49
143z	163z	H	4-Cl	B	76
162i	166i	OMe	4-Cl	B	4 ^d
162s	166s	OMe	4-OMe	B	6 ^d

^aCompounds were reacted as a mixture and not separated afterwards. ^bCompounds were reacted as a mixture and separated afterwards. ^cReaction was performed on a 10 mg scale and the yield refers to the conversion as measured by LC-MS. ^dYield of the last three steps. ^eConversion measured by LC-MS; compound was not purified successfully. SM = Starting material. Conditions: A = TFA, NaBH₄, DCM, rt, 6 h; B = Et₃SiH, BF₃·Et₂O, DCM, reflux, 12–18 h, inert atmosphere.

The dehydroxylation of the 4-hydroxytetrahydroisoquinoline derivatives could be successfully accomplished by selecting the appropriate conditions. The same electronic factors that controlled the PF ring closure, control to a similar extent also the dehydroxylation itself. Even though the NaBH₄/TFA system was effective only in a few cases, it was possible to dehydroxylate the remaining compounds using Et₃SiH and BF₃·Et₂O. The latter conditions gave apparently lower yields, they referred mostly to the sum of the two last steps and did not differ significantly from the overall two-step yield when NaBH₄/TFA was used for the reduction. The main concern of the project was to secure as large a number of compounds as possible, therefore the results obtained were accepted and no further optimisation of the reaction was attempted.

2.1.5. Methoxy deprotection of final THIQs

As previously stated, after the difficulties encountered during the purification of compounds bearing a phenolic group (Compounds **163l-o**, Table 17) it was decided to access these type of compounds from the methoxy compounds like **143b** (Table 16, page 62).

One last step for the deprotection of the methoxy derivatives was introduced to obtain the free phenol derivatives. It was very important to obtain the phenolic derivatives because they are more closely related to the structure of E2 and it was envisaged they could possess higher potency. Further detail concerning the structure activity relationship of these compounds will be discussed in detail in CHAPTER 3 (from page 101).

Many procedures are reported in the literature for the demethylation of an arylmethoxy group to give the free phenol.^{139, 140} The problem was initially addressed using 48% aqueous HBr at 100 °C and the clean product could be obtained as the hydrobromide salt by simple filtration after the reaction was cooled to rt.

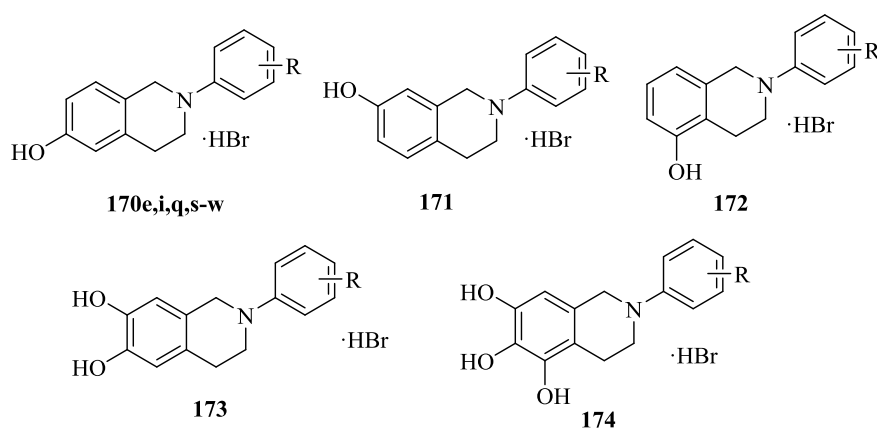


Figure 37. Structure of substitutions for the hydroxytetrahydroisoquinolines.

Table 18. Summary of the results for the deprotection of the arylmethoxy THIQs.

SM	R	Product	Conditions	Yield (%)
163e	H	170e	A	90
163i	4-Cl	170i	A	79
164j	4-Cl	171	A	74
165j	4-Cl	172	A	75
163q	4-Me	170q	A	95
163s	4-OH	170s	A	91
163t	3-Cl	170t	A	64
163u	3-OH	170u	A	67
163w	2-OH	170w	A	Nr
167	4-OH	173	B	74
168	4-OH	174	B	99

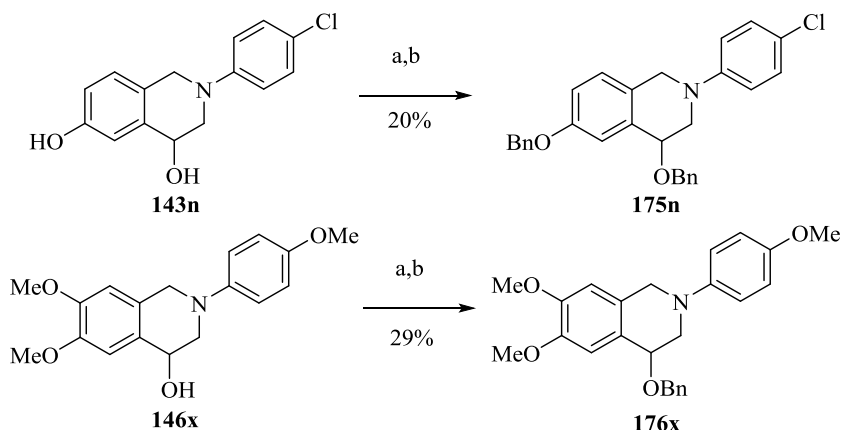
Conditions: A) 48% aq. HBr, 100 °C, 1-2 h, inert atmosphere; B) BBr₃, DCM, -78 °C to rt, 2 h, inert atmosphere. SM = Starting material. Nr = Not recovered.

Under these conditions it was not possible to easily recover every compound and BBr₃ in DCM was later found to be a better demethylating agent. Even when using BBr₃ in DCM, the clean product could be obtained as the hydrobromide by filtration after quenching the reaction with water. These conditions gave better results and were used as the standard procedure for the deprotection of the phenols **170e,i,q,s-w**, **171-174** (Figure 37, Table 18).

2.1.6. Further functionalisation of the 4-hydroxy THIQs.

To simply prove the possibilities of functionalisation and to introduce bigger groups, the 4-hydroxy THIQs **143n** and **146x** were benzylated following their deprotonation

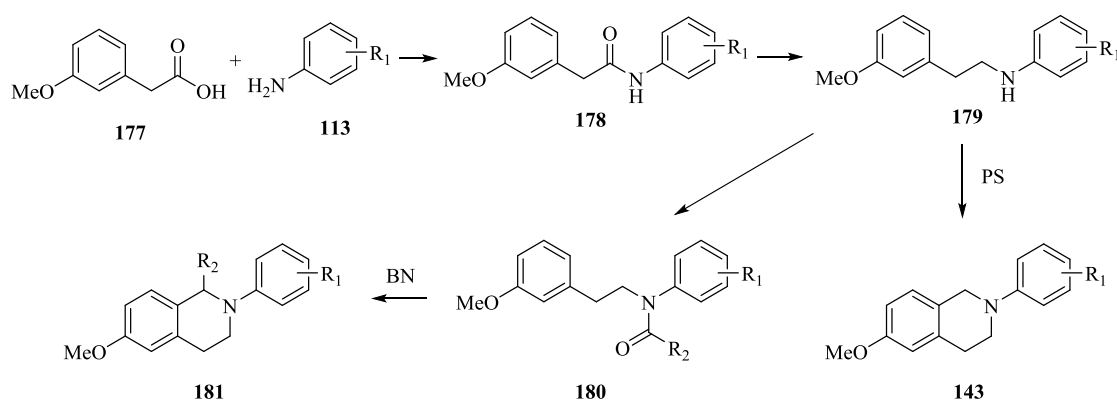
with NaH (Scheme 33). Initially, the reactions did not proceed well but the addition of crown ether 15-crown-5 gave moderate yields of the product.



Scheme 33. Benzylation of the 4-hydroxy THIQs **143n** and **143x**. a) NaH, 12-crown-5, THF, 1 h, rt; b) BnBr, THF, 4-6 h, rt.

2.2. The Pictet-Spengler (PS) and Bischler-Napieralski (BN) approach

As a means to expand the synthetic possibilities and flexibility offered by the PF approach, as stated at the beginning of CHAPTER 2, an alternative synthetic approach was investigated (Scheme 34). Both the PS and BN reactions are exploited in the literature for the syntheses of a wide range of compounds.^{113, 141}



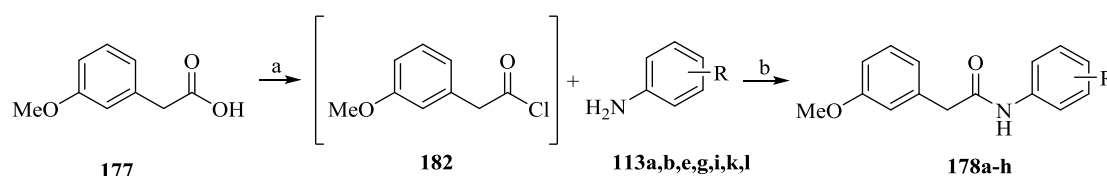
Scheme 34. Proposed synthesis for the substituted THIQs through the PS and BN ring closure.

Both pathways share the key intermediates **178** and **179** and differ only during the cyclisation process. Commercially available 3-methoxyphenylacetic acid **177** and an appropriately substituted aniline could be combined to give amide **178** that could be subsequently reduced to amine **179**. The latter intermediate **179** was cyclised in the PS conditions to give the final THIQ **143**. Alternatively, amide **180** could be obtained by

condensation of amine **179** with the appropriately substituted acid. The same amide **180** could then be cyclised under the BN conditions to give the final THIQ **181**.

2.2.1. Synthesis of the amides **178**

The synthesis of the amides **178a-h** was carried out by converting commercially available 3-methoxyphenylacetic acid into the corresponding acid chloride using SOCl_2 as shown in Scheme 35. The acid chloride obtained was then reacted with the appropriately substituted aniline in refluxing toluene to give the desired amides **178a-h** (Scheme 35, Table 19). The unreacted starting materials could be easily removed by washing the reaction mixture sequentially with aqueous 1 M HCl and 1M NaOH and the products were subsequently purified by recrystallisation from EtOAc/pet. ether when necessary. If the product had a purity higher than 95% by ^1H NMR then no recrystallisation was performed (Table 19).



Scheme 35. Synthesis of intermediates **178a-h**. Conditions: a) SOCl_2 , DCM, rt, 1 h, inert atmosphere; b) Na_2CO_3 , Toluene, reflux, 12-16 h, inert atmosphere.

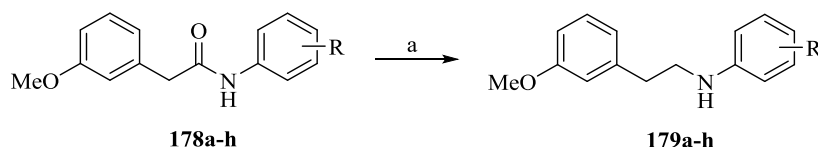
Table 19. Summary of the results for the synthesis of amides **178a-h**.

Compound	R	Yield (%)
178a	H	46
178b	4-Cl	85
178c	4-OMe	51
178d	3-Cl	80
178e	3-OMe	87
178f	2-Cl	66
178g	2-OMe	93
178h	3,4-Cl ₂	76

2.2.2. Reduction of the amides **178a-h**.

Amides **178a-h** were reduced using LiAlH_4 as the reducing agent and the reactions were performed in refluxing anhydrous THF under inert atmosphere to yield amines

179a-h as shown in Scheme 36. The products **179a-h** could generally be obtained by precipitating it as hydrochloride salt from the crude reaction mixture (Table 20).



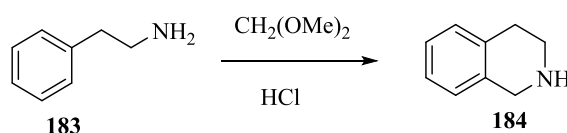
Scheme 36. Reduction of amides **178a-h**. a) LiAlH₄, THF, 80 °C, 4-6 h.

Table 20 Summary of the results for the reduction of amides **179a-h**.

Compound	R	Yield (%)
179a	H	64
179b	4-Cl	64
179c	4-OMe	59
179d	3-Cl	74
179e	3-OMe	68
179f	2-Cl	97
179g	2-OMe	45
179h	3,4-Cl ₂	75

2.2.3. The Pictet-Spengler cyclisation.

The Pictet-Spengler (PS) reaction originally involved the condensation of β-phenylalanine **183** and formaldehyde dimethylacetal to yield THIQ (Scheme 37).

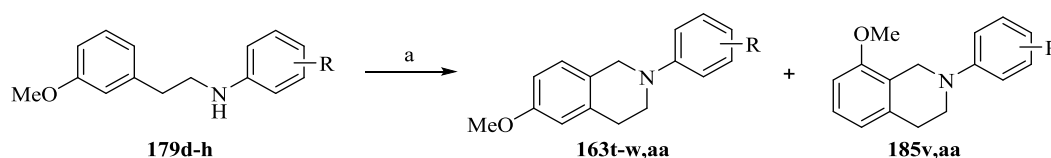


Scheme 37. Scheme of the original PS condensation.¹⁴²

The reaction has recently celebrated 100 years of success in the laboratory following its first discovery and the reaction has been implemented in the synthesis of many alkaloids.^{113, 143} Further investigations of the reaction have led to conditions that allowed not only the introduction of substituents, but also a certain degree of diastereo- and enantio-selectivity at the newly formed stereogenic centre.¹¹³ The reaction was also studied under enzymatic catalytic conditions and the enzyme was named Pictet-Spenglerase from the homonymous reaction.¹¹³

Due to previous work undertaken by our group, the conditions used were different from the ones originally reported by Pictet and Spengler.¹⁴² These conditions required the use of paraformaldehyde as the formaldehyde source and *p*-toluenesulphonic acid

(PTSA) as the acid catalyst (Scheme 38). Under these conditions and in refluxing toluene, amines **179d-h** cyclised to THIQs **163t-w,aa** with acceptable yields (Scheme 38, Table 21). Similarly to what was observed with the PF reaction, cyclisation occurred with an incomplete regioselectivity, affording the regioisomers **185v,aa** alongside the major products **143v,aa** (Scheme 38, Table 21). The two isomers were easily separated by flash column chromatography.



Scheme 38. Cyclisation of compounds **179d-g,aa**. Reagents and conditions: a) paraformaldehyde, PTSA, toluene, reflux, 12-18 h.

Table 21. Yields of the PS cyclisation.

SM	R	Product	Yield (%)	Product	Yield (%)
179d	3-Cl	163t^a	23		
179e	3-OMe	163u	Nf		
179f	2-Cl	163v	57	185v	4
179g	2-OMe	163w	Nf		
179h	3,4-Cl ₂	163aa	55	185aa	4

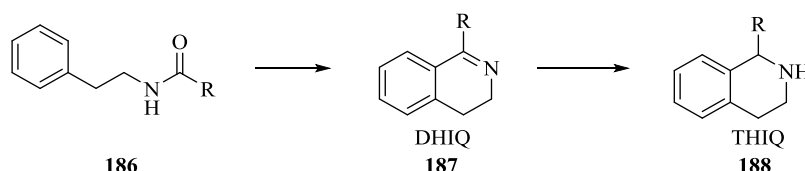
^a Formation of isomer **185t** was not observed. SM = Starting Material; Nf = Not formed

Through the PS cyclisation it was possible to obtain compounds like **163t**, **163v** and **163aa** (Scheme 38, Table 21) that proved difficult to be obtained by the PF pathway (Table 16, page 62). In fact, compounds with highly electron-withdrawing groups on the aniline ring as for **163aa** (Scheme 38, Table 21) showed synthetic difficulties during the initial alkylation step (**131t,v**, Scheme 11, page 50) and compounds bearing a chlorine in the *ortho* position to the nitrogen did not cyclise under the PF conditions (**131v**, Table 16, page 62). Moreover, THIQs such as **185v** and **185aa** (Scheme 38, Table 21) have proven inaccessible through the PF cyclisation (cyclisation of **123k**, Table 16, page 62).

Conversely, the THIQs **163u** and **163w** (Scheme 38, Table 21) did not form under the experimental conditions used but the causes were not investigated as the same compounds had been previously obtained by the PF route (Table 16, page 62).

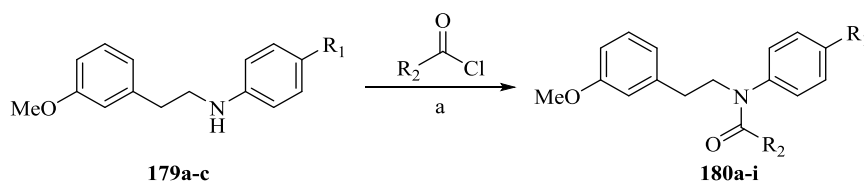
2.2.4. The Bischler-Napieralski cyclisation.

The BN reaction was first discovered in 1893¹⁴⁴ and allowed the cyclisation of β -arylethylamides to form 3,4-dihydroisoquinolines. The application of this reaction for the synthesis of THIQs involves *de facto* two steps, cyclisation to form a 3,4-dihydroisoquinoline (DHIQ) followed by a reduction to obtain the THIQ (Scheme 39).



Scheme 39. Application of the BN reaction to the synthesis of THIQs.

The advantage of the BN reaction was that it allowed the facile introduction of substituents in position 1 of the THIQ ring. On the other hand, it was not possible to obtain THIQs with no substituents in the same position 1 by this method. The reaction is carried out under dehydrating conditions and phosphorous oxychloride (POCl_3) is often used as the dehydrating agent even though other reagents such as phosphorous pentoxide (P_2O_5) are reported in the literature.^{118, 141}



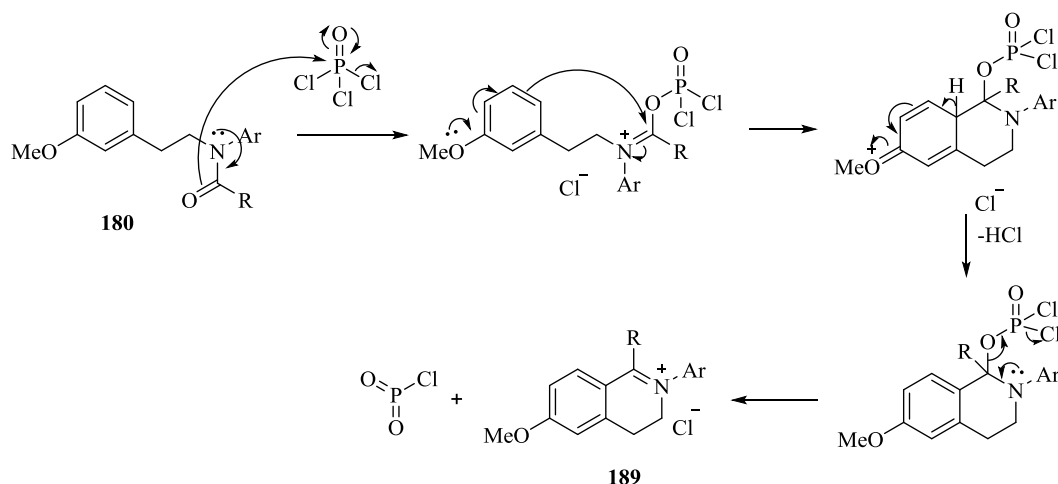
Scheme 40. Synthesis of amides **180a-i** (refer to Table 22 for compound substitution). a) The appropriate commercially available acid chloride, pyridine, DCM, rt, 12–18 h.

Table 22. Summary of the synthesis of amides **180a-i**.

SM	Product	R ₁	R ₂	Yield (%)
179b	180a	Cl	Me	91
179b	180b	Cl	Et	96
179b	180c	Cl	<i>i</i> -Pr	93
179b	180d	Cl	<i>t</i> -Bu	70
179b	180e	Cl	Ph	89
179b	180f	Cl	Bn	98
179b	180g	Cl	(CH ₂) ₂ Ph	76
179a	180h	H	Bn	73
179c	180i	OMe	Bn	84

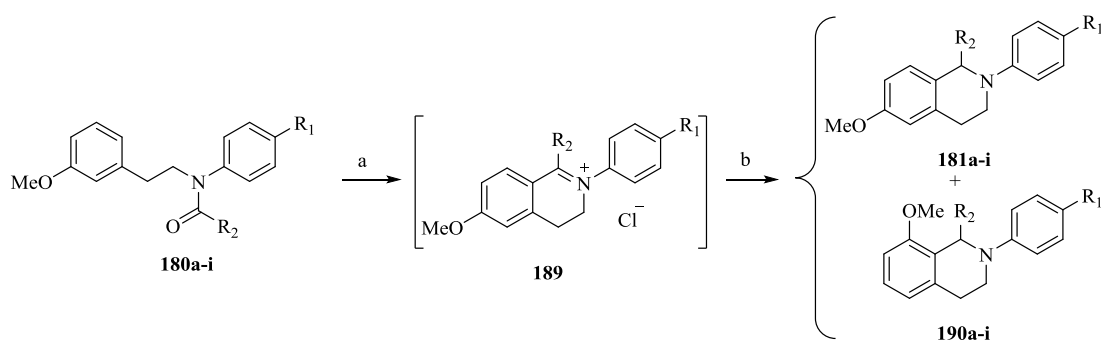
In order to proceed with the synthesis it was necessary to obtain first the amides **180a-i** (Scheme 40, Table 22) which could be subsequently cyclised under BN reaction conditions.

The amides thus synthesised were subjected to the BN reaction conditions with POCl₃ in refluxing toluene. After initial addition of the amide to the POCl₃, the iminium ion generated cyclises and after aromatisation is restored, phosphenic chloride is expelled and the 3,4-dihydroisoquinolinium ion **189** is formed (Scheme 41).



Scheme 41. Mechanism of cyclisation during the BN reaction.

When no substituent was present on the nitrogen of the starting phenylethylamide the obtained product was neutral and could be easily isolated. Conversely, intermediate **189** (Scheme 41) was charged and work up of the reaction in aqueous media to remove excess reagents would have led to reduced yield. Therefore, product formation was confirmed by thin layer chromatography (TLC) and when all the starting material had reacted only a spot on the base line remained visible. This spot was easily visualised under a UV lamp at 254 nm and had a typical blue fluorescence at 365 nm. The reaction was then quenched with methanol and the excess of POCl₃ was converted to trimethylphosphate, which did not interfere with the reduction step. The solvents were evaporated and the crude residue reduced with NaBH₄ using methanol as the solvent to yield the final THIQ **181a-i** (Scheme 42, Table 23). Similarly to what was observed with the PS reaction, the other isomers **190a-i** could be isolated, albeit in very poor yields (Scheme 42, Table 23).



Scheme 42. BN cyclisation of amides **180a-i**. a) POCl₃, anhydrous toluene, reflux, 12-18 h, quenched with MeOH. b) NaBH₄, MeOH, rt, 6 h.

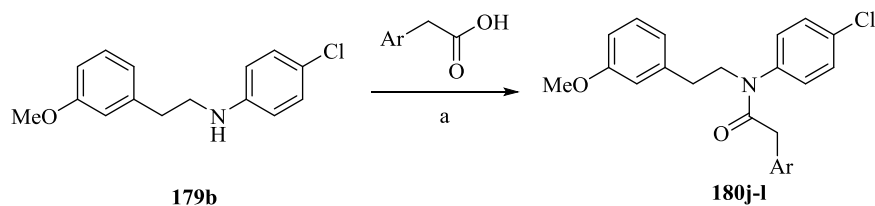
Table 23. Results of the BN cyclisation of amides **180a-i**.

SM	R ₁	R ₂	Product	Yield (%)	Product	Yield (%)
180a	Cl	Me	181a	69	190a	3
180b	Cl	Et	181b	71	190b	5
180c	Cl	<i>i</i> -Pr	181c	56	190c	12
180d	Cl	<i>t</i> -Bu	181d	Nf	190d	Nf
180e	Cl	Ph	181e	68	190e	2
180f	Cl	Bn	181f	78	190f	4
180g	Cl	Phenylethyl	181g	67	190g	3
180h	H	Bn	181h	58	190h	6
180i	OMe	Bn	181i	61	190i	8

SM = Starting material; Nf = Not formed.

Only amide **180d** did not cyclise under the experimental conditions used and this was probably due to steric hindrance of the substituent. In fact, the *t*-butyl group could possibly clash with the proton *ortho* to the cyclisation position not allowing a proper conformation for the ring closure.

Some of the THIQs thus synthesised possessed CLogP values that were marginally outside the Lipinski rules (Chapter 1.7, page 36) and, in order to try to address the problem at an early stage, the introduction of a more polar group was attempted. Therefore, amides **180j-l** (Scheme 43, Table 24) were synthesised but it was necessary to use a coupling agent such as EDCI to generate amides **180j-l** (Scheme 43, Table 24) because attempts to obtain the amide from the acid chloride failed.



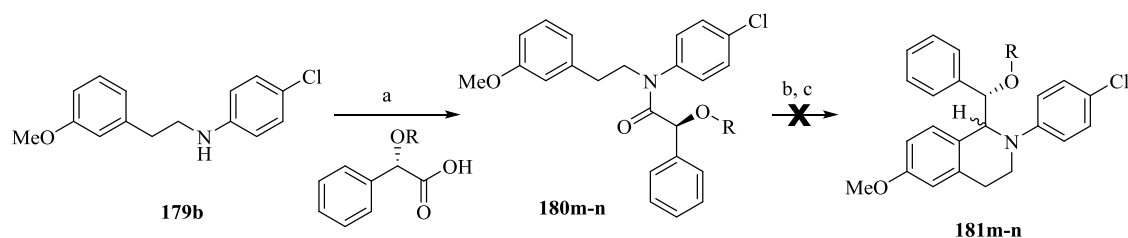
Scheme 43. Synthesis of amides **180j-l**. a) The opportune pyridylacetic acid hydrochloride, EDCI, Et₃N, DCM, rt, 12-18 h.

Table 24. Results for the synthesis of amide **180j-l**.

Product	Ar	Yield (%)
180j	4-Pyridyl	64
180k	3-Pyridyl	60
180l	2-Pyridyl	67

Interestingly, every attempt to cyclise amides **180j-l** failed, giving back the starting material with no clear explanation.

During the BN cyclisation, a new stereogenic centre was generated thus leading to the formation of two different enantiomers. Considering that the two enantiomers were likely to possess different biological activity, a method to obtain one single enantiomer was investigated. There are examples in the literature of asymmetric BN reaction¹⁴¹ but they generally involve the use of expensive catalysts. Alternatively, the two enantiomers could be separated from the racemic mixture by chiral chromatography. Instead, the synthesis from a chirally pure acid was planned using an appropriately *O*-protected mandelic acid (Scheme 44). The amides **180m-n** (Scheme 44) were synthesised and then subjected to the BN conditions, however, both the amides failed to cyclise and for **181n** (Scheme 44) the starting material was recovered.



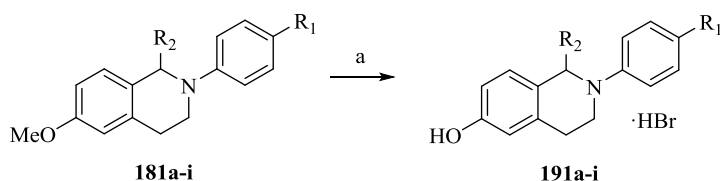
Scheme 44. Attempted synthesis of THIQs **181m-n**. a) The opportunely protected mandelic acid, EDCI, Et₃N, DCM, rt, 12-18 h. b) POCl₃, anhydrous toluene, reflux, 12-18 h, quenched with MeOH. c) NaBH₄, MeOH, rt, 6 h. **180m**: R = Me; **180n**: R = Ac.

In conclusion, the BN cyclisation was generally very efficient for the introduction of simple substituents to position 1, while the pyridyl ring was not tolerated in the same experimental conditions. Moreover, though compounds **180f**, **180h** and **180i** (Scheme

43, Table 24), bearing a benzyl group, cyclised with no problems, the addition of an electron-withdrawing substituted oxygen on the benzylic position, as for the amides **180m** and **180n** (Scheme 44), prevented the cyclisation from happening.

2.2.5. Methoxy deprotection of final THIQs

As previously seen in chapter 2.1.5 (page 68), one last step for the deprotection of the methoxy-substituted THIQs was introduced in order to obtain the free phenol derivatives **191a-i** (Scheme 45, Table 25).



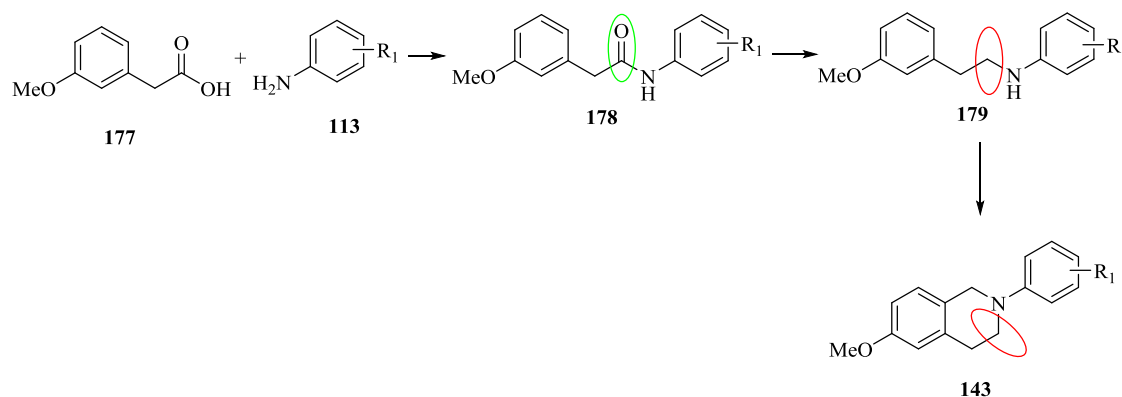
Scheme 45. Deprotection of THIQs **181a-i**. a) BBr₃, DCM, -78 °C to rt, 2 h, inert atmosphere.

Table 25. Summary of the results for the deprotection of THIQs **181a-i**.

Product	R1	R2	Yield (%)
191a	Cl	Me	41
191b	Cl	Et	61
191c	Cl	<i>i</i> -Pr	58
191e	Cl	Ph	79
191f	Cl	Bn	44
191g	Cl	Phenethyl	61
191h	H	Bn	87
191i	OH	Bn	96

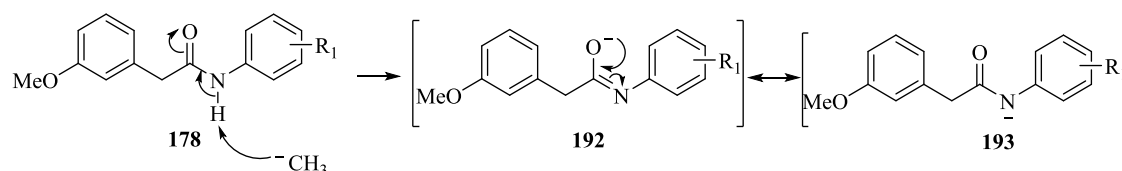
2.2.6. The Pictet-Spengler approach modification: towards 3-substituted THIQs.

Due to the difficulties encountered during the synthesis of 3-substituted THIQs with the PF approach (see synthesis of precursors to the THIQs **165i,s** in chapters 2.1.2 to 2.1.4, pages 50 to 67) an alternative method was investigated. It was decided to attempt to introduce an alkylation step during the synthesis by using a PS approach. Analysing the synthetic steps, amide **178** (Scheme 46) was chosen as the substrate for the alkylation reaction. In fact, when amide **178** (Scheme 46) was reduced to amine **179** (Scheme 46) prior to its PS cyclisation, it would become rather difficult to introduce a group α to the nitrogen (Scheme 46).



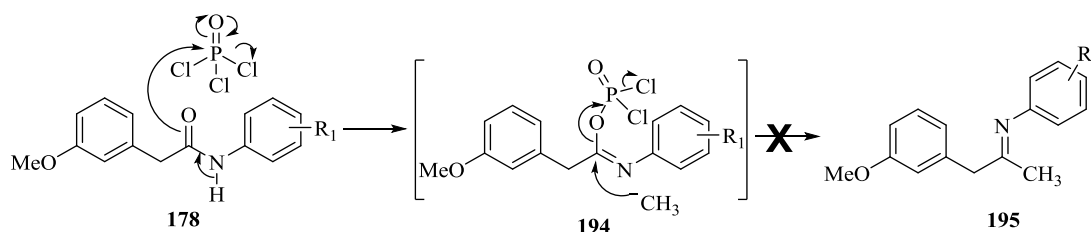
Scheme 46. Synthesis of THIQ **143** through the PS approach. In red are highlighted the positions that are strategically difficult to exploit for an alkylation reaction. In green is highlighted the position with higher functionalisation capabilities.

A carbonyl can be easily alkylated with a wide range of nucleophiles but amides are much less reactive due to the O-C-N electron delocalisation. Moreover, a carbanionic nucleophile is also a strong base and under these conditions, deprotonation of the amide would happen first nullifying any chance of C-alkylation (Scheme 47).



Scheme 47. Deprotonation of amide **178** by a simple carbanion.

It was hoped that converting the oxygen into a good leaving group would lead to a successful C-alkylation that would not require any additional steps. Revising the mechanism of the BN reaction (Scheme 41, page 75), POCl₃ was expected to be a good starting point for such investigations.

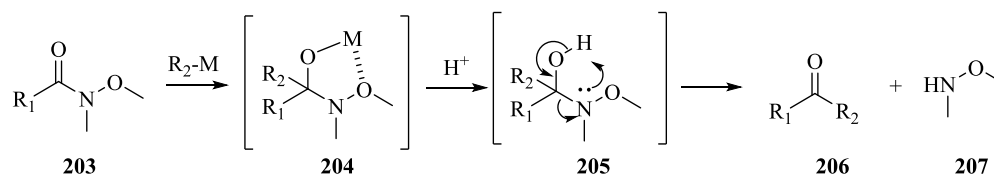


Scheme 48. Envisaged mechanism for the alkylation of amide **178**. a) Toluene, 100 °C, 18 h; b) MeMgBr, toluene, rt for 1 day then reflux for 1 day.

The amide **178** (Scheme 48) did not react at all with POCl₃ at rt but full conversion occurred at 100 °C as judged by TLC. Excess solvents and reagents were evaporated and the residue was dissolved in toluene and reacted with MeMgBr at rt for one day. No conversion occurred so the mixture was heated to refluxing conditions. Surprisingly, the

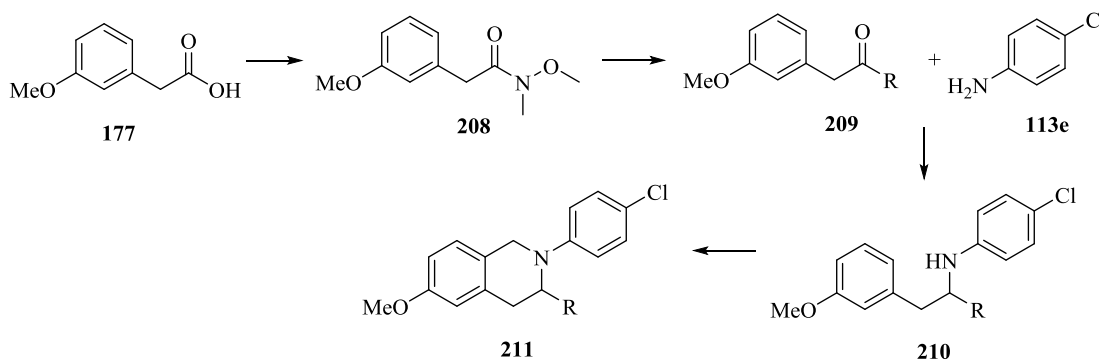
converted to the amide **197** (Scheme 49) during the quenching itself. This hypothesis, though, is yet to be proved and further in depth mechanistic investigations would be required. Nevertheless, the formation of the intermediate **202** (Scheme 49) seemed both plausible and a good explanation for the formation of the unexpected products **196** and **197** (Scheme 49).

An alternative procedure to obtain the desired 3-substituted THIQs was then evaluated. The direct alkylation of a carboxylic acid is possible with an organolithium¹⁴⁶ but only few of this type of compounds are commercially available. Conversely, a wide range of Grignard reagents are readily commercially available and, in addition, they can be handled and stored more easily. However, Grignard reagents are not able to directly alkylate carboxylic acids unlike the organolithium reagents and their addition to esters usually give significant problems of dialkylation. The Weinreb reaction was used to overcome this limitation and to access a wide range of substitutions. The Weinreb reaction was firstly reported by Weinreb and Nahm in 1981¹⁴⁷ and is a useful tool to access mono-alkylation of acids to give ketones. The reaction uses *N,O*-dimethylhydroxylamides as the substrate, which are named Weinreb amides from the same reaction and the alkylation can be performed with a variety of nucleophiles even though Grignard and organolithium reagents are most extensively used. The peculiarity of this reaction lays in the stabilisation of the intermediate anion by metal chelation, which prevents the compound from undergoing a second alkylation (**204**, Scheme 50). Only when the reaction is quenched, and the alkylating agent (usually in excess) destroyed, is the anion protonated generating the intermediate species (**205**, Scheme 50), which collapses to give the final ketone and *N,O*-dimethylhydroxylamine (respectively **206** and **207**, Scheme 50). The Weinreb amide and the chelated intermediate are so stable under the reaction conditions that is possible to perform an *in situ* metalation of alkyl- or arylhalides¹⁴⁷ to give the respective Grignard reagents that then react immediately to give the final ketone.



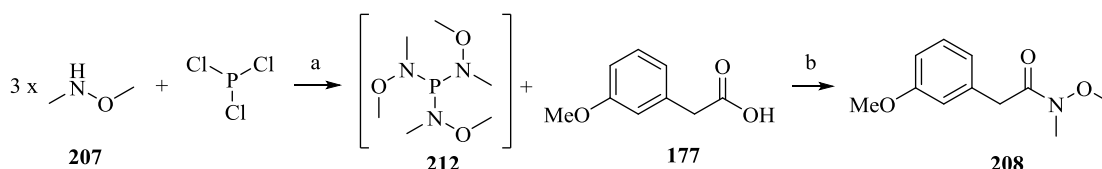
Scheme 50. Weinreb reaction mechanism.

Based on this reaction a modified synthetic scheme towards 3-substituted THIQs was planned (Scheme 51) and the Weinreb amide **208** (Scheme 51) was synthesised from commercially available 3-methoxyphenylacetic acid (**177**, Scheme 51) and *N,O*-dimethylhydroxylamine hydrochloride.



Scheme 51. Planned synthetic strategy towards the 3-substituted THIQs **211**.

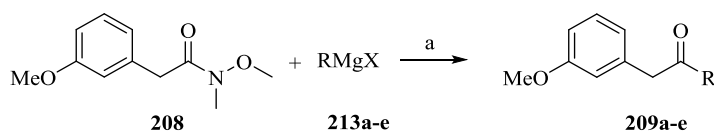
When amide **208** (Scheme 51) was synthesised by converting the acid into the acid chloride and then reacting the latter with *N,O*-dimethylhydroxylamine **207**, the yield was 48%. This was due to the low nucleophilicity of the amine and it was possible to increase the yield to 64% by converting the amine into a more reactive species according to the literature procedure (Scheme 52).¹⁴⁸ The amine was initially reacted with PCl_3 to give adduct **212**, which was then reacted with the acid to give **208**.



Scheme 52. Synthesis of the Weinreb amide **208**. a) DIPEA, Et_2O , 1 h at 0 °C then 12 h at rt; b) Toluene, 60 °C.

2.2.7. Weinreb reaction: alkylation of amide **208**.

The Weinreb reaction was conducted under the original experimental conditions¹⁴⁷ and the Grignard's **213a-e** were used as nucleophiles (Scheme 53, Table 26).



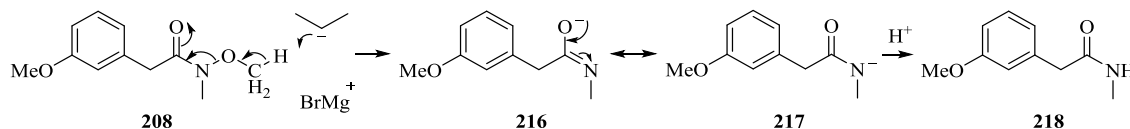
Scheme 53. Weinreb reaction of amide **208** with the nucleophiles **213a-e**. a) THF, rt.

Table 26. Summary of results for the Weinreb reaction.

Product	R	X	Yield (%)
209a	Me	Br	93
209b	Et	Br	86
209c	<i>i</i> -Pr	Br	Nf [*]
209d	Ph	Br	66
209e	Bn	Cl	28

^{*} *N*-demethoxylation occurred and amide **218** formed instead with a 62% yield. Nf = Not formed.

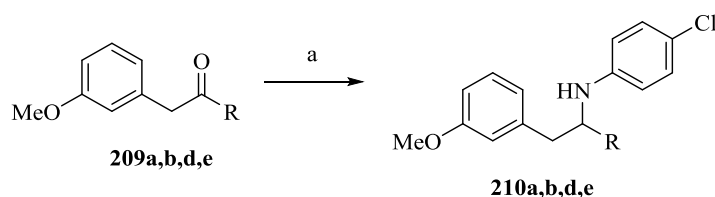
Ketones **209a**, **209b** and **209d** formed in good yield, while the yield for ketone **209e** was poor. Conversely, ketone **209c** did not form and amide **218** formed instead. In fact, it is reported in the literature that the reaction of Weinreb amides like **208** with poorly nucleophilic Grignard's such as *i*-PrMgBr would proceed towards *N*-demethoxylation (Scheme 54).¹⁴⁹ The reaction is initiated by deprotonation of the *N*-methoxy group and proceeds by elimination of formaldehyde to give the stabilised anion, which is then protonated to deliver the final amide **218**.

**Scheme 54.** Degradation of the Weinreb amide **208** in the presence of poorly nucleophilic strong bases such as a non-nucleophilic Grignard.

2.2.8. Reductive amination of ketones **209a,b,d,e**.

The ketones **209a,b,d,e** obtained through the Weinreb reaction were reductively aminated to give the amines **210a,b,d,e** using the conditions described in chapter 2.1.2 modified according to the literature procedures¹²⁰ for ketones (Scheme 55, Table 27).

When synthesis of amine **210a** (Scheme 55, Table 27) was first attempted in chloroform the yield was only 14%. Similarly to what observed during the synthesis of amines **138i,s** (Scheme 13, page 50) the ketones were sterically more hindered than aldehydes and the direct reductive amination was more difficult but the reactivity of the ketone could be improved by an acid catalyst such as acetic acid.



Scheme 55. Reductive amination of ketones **209a,b,d,e**. a) 4-Chloroaniline, NaBH(OAc)₃, DCE, AcOH, rt, 6-12 h.

Table 27. Reductive amination of ketones **209a,b,d,e**.

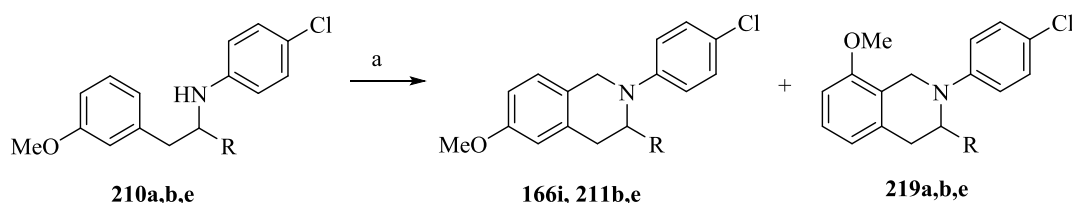
Product	R	Yield (%)
210a	Me	48
210b	Et	49
210d	Ph	Nf
210e	Bn	28

Nf = Not formed.

It was not possible to obtain amine **210d** (Scheme 55, Table 27) even with an acid catalyst and this was probably due to the lower reactivity of the compound. In fact, the ketone **209d** (Scheme 55) was the only compound of the series in which the carbonyl was conjugated to an aromatic ring. The other three compounds could be obtained in low to moderate yields and no further optimisation was attempted.

2.2.9. The Pictet-Spengler cyclisation: towards 3-substituted THIQs.

Amines **210a,b,e** (Scheme 56, Table 28) were cyclised under PS conditions to give 3-substituted THIQs **211b,e** and **166i** (Scheme 56, Table 28). Under these conditions amine **210e** (Scheme 56, Table 28) failed to cyclise and the only product obtained were **166i** and **211b** (Scheme 56, Table 28). Again, as observed before (chapter 2.2.3, page 72) when the amine did cyclise, a small amount of the regioisomer **219** was observed and isolated if possible.



Scheme 56. PS cyclisation of amines **210a,b,e**. Reagents and conditions: a) paraformaldehyde, PTSA, toluene, reflux, 12-18 h.

Table 28. Results of the PS cyclisation of amines **210a,b,e**.

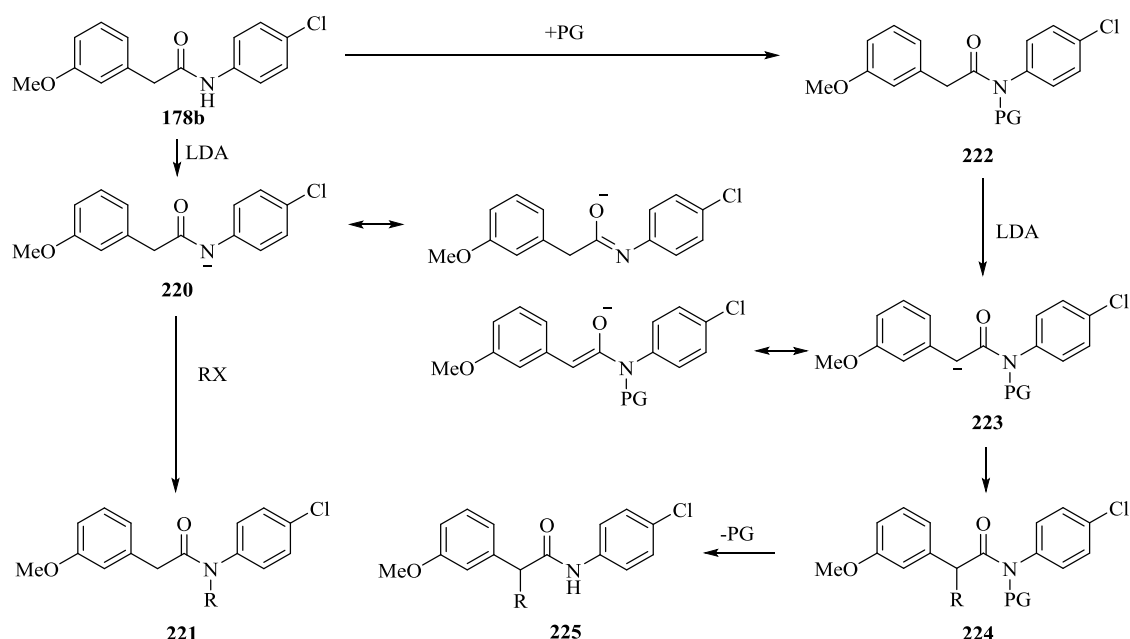
SM	R	Product	Yield (%)	Product	Yield (%)
210a	Me	166i	79	219a	No
210b	Et	211b	44	219b	4
210e	Bn	211e	Nf	219e	Nf

SM = Starting material; Nf = Not formed; No = Not observed.

Compound **166i** (Scheme 56) was resynthesised in order to have a direct comparison between the PF and PS approaches to obtain 3-substituted THIQs. The overall yield for compound **166i** (Scheme 56) was 4% when synthesised using the PF approach, while the yield increased to *ca.* 23% when the modified PS approach was used. In addition, even though the pathway was unsuccessful at different stages, it has to be stated that reactions were not optimised.

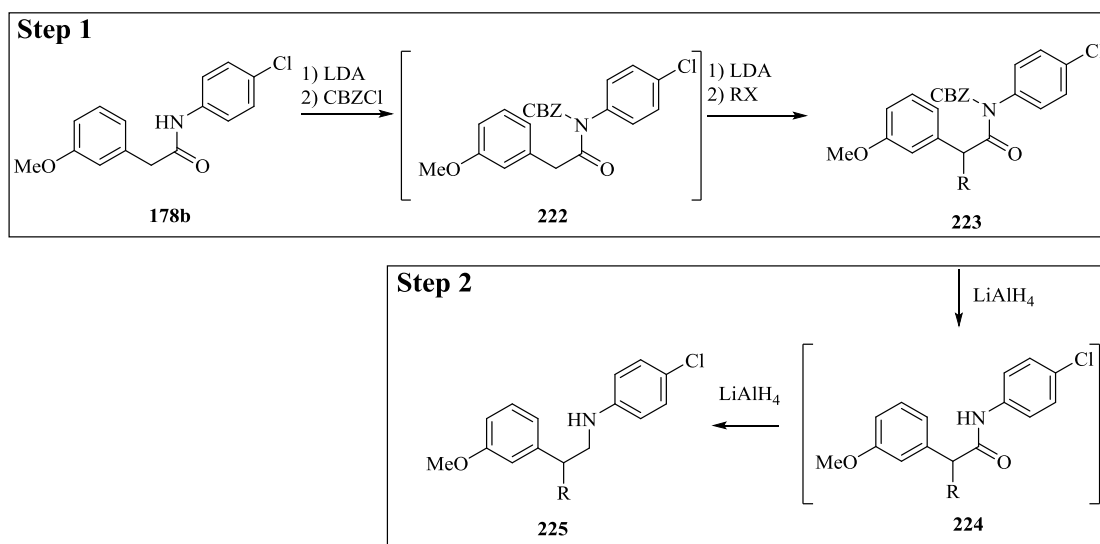
2.2.10. The Pictet-Spengler approach modification: towards 4-substituted THIQs.

Analogously to the synthesis of the 3-substituted THIQs, the first approach investigated for the synthesis of 4-substituted THIQ was alkylation of amide **178b** (Scheme 57). In order for alkylation to occur α to the carbonyl the amide needed to be protected or deprotonation would occur on the nitrogen, generating the stabilised anion **220** (Scheme 57) which would lead to the *N*-alkylated amide **221** (Scheme 57). Instead, the protected amide **222** (Scheme 57) could only be deprotonated α to the carbonyl to give anion **223** (Scheme 57), alkylation of which would lead to amide **224** (Scheme 57). Subsequent deprotection of amide **224** (Scheme 57) would yield the desired product **225** (Scheme 57). The negative aspect of this approach would have been the introduction of two additional steps, both lengthening the time for the synthesis and reducing the overall yield of the process. Even if the yield was of secondary importance, the need to access the final THIQs quickly was pivotal.



Scheme 57. Deprotonation-alkylation of unprotected and protected amide **178b**.

In order to limit the number of additional steps, a protecting group that could be introduced and removed during different steps of the current synthesis was evaluated. The carboxybenzyl (CBZ) group was chosen, following a literature analysis of its introduction and cleavage conditions. In fact, there are examples of CBZ protection in the literature under conditions that deprotonate the amine¹⁴⁰ and cleavage of the same CBZ group by metal hydrides.¹⁵⁰ The possibility of a synthesis such as the one shown in Scheme 58 was then explored.



Scheme 58. Planned synthetic scheme for the introduction and cleavage of the CBZ protecting group within the existing synthetic steps.

To evaluate this hypothesis, protected amide **222** (Scheme 58) was synthesised and isolated, and subjected to cleavage with LiAlH_4 to give the starting amide **178b**

(Scheme 58). The synthesis of **222** (Scheme 58) proceeded smoothly but when the obtained protected amide was reacted with LiAlH_4 , a convoluted mixture of products was obtained. The same amide **222** (Scheme 58) could not be deprotected by catalytic hydrogenation with Pd/C and H_2 , a procedure considered standard for the removal of the CBZ protecting group. The very optimistic plan depicted in Scheme 58 was then abandoned in favour of a more robust approach.

Due to the above-mentioned difficulties with direct alkylation of amide **178b** (Scheme 58) and the greater difficulties for direct alkylation of the starting 3-methoxyphenylacetic acid (**177**, Scheme 59), the methyl ester **226** (Scheme 59) was chosen as the substrate for the alkylation reaction. Though the methyl ester **226** (Scheme 59) was commercially available, for the present work it was obtained by Fischer esterification. When 3-methoxyphenylacetic acid **177** was refluxed in methanol in the presence of catalytic amounts of conc. H_2SO_4 the reaction did not proceed. The Fischer esterification is a condensation reaction with elimination of water, thus anhydrous conditions were required to drive the equilibrium of the reaction towards formation of the product. These conditions were obtained by the introduction of CaH_2 as dehydrating agent and the use of a Soxhlet extractor to keep it separated from the reaction environment. In fact, the CaH_2 would react with the 3-methoxyphenylacetic acid (**177**, Scheme 59) deprotonating it and preventing it from esterification and the same hydride would also neutralise the H_2SO_4 in solution. Using the Soxhlet extractor the refluxing solvent evaporated and condensed into the apparatus where it was dehydrated and then returned to the reaction mixture.

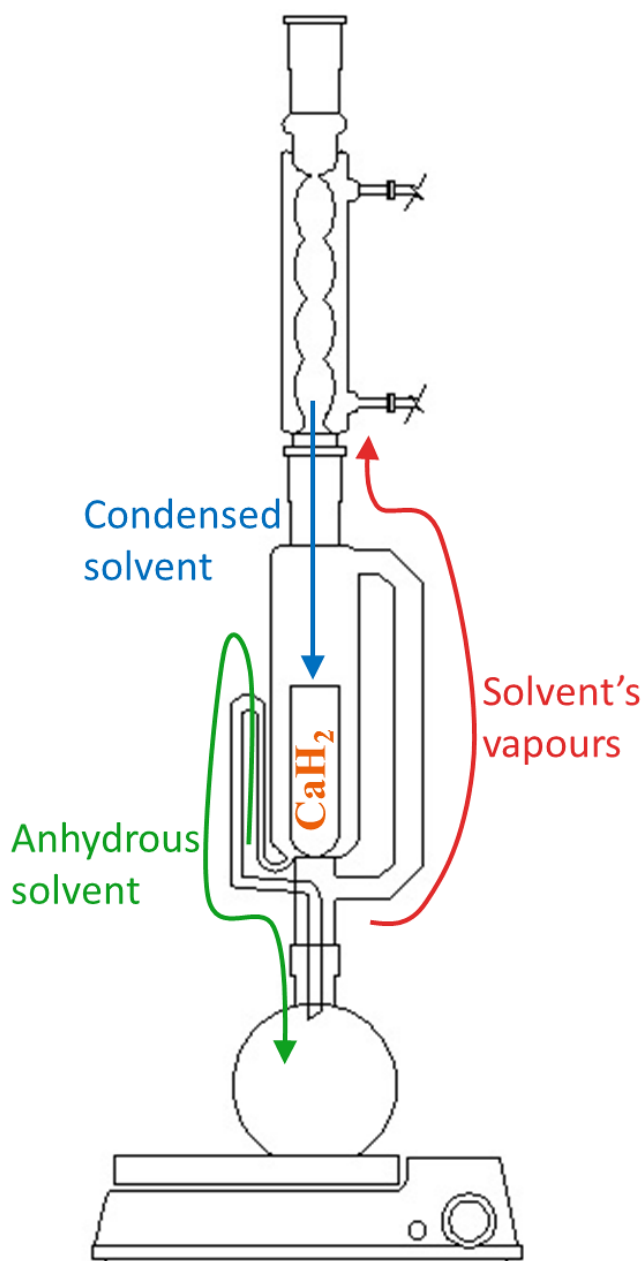
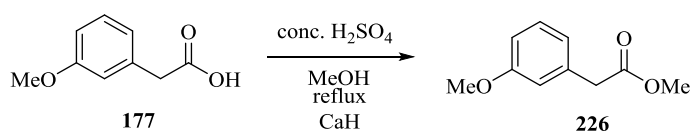


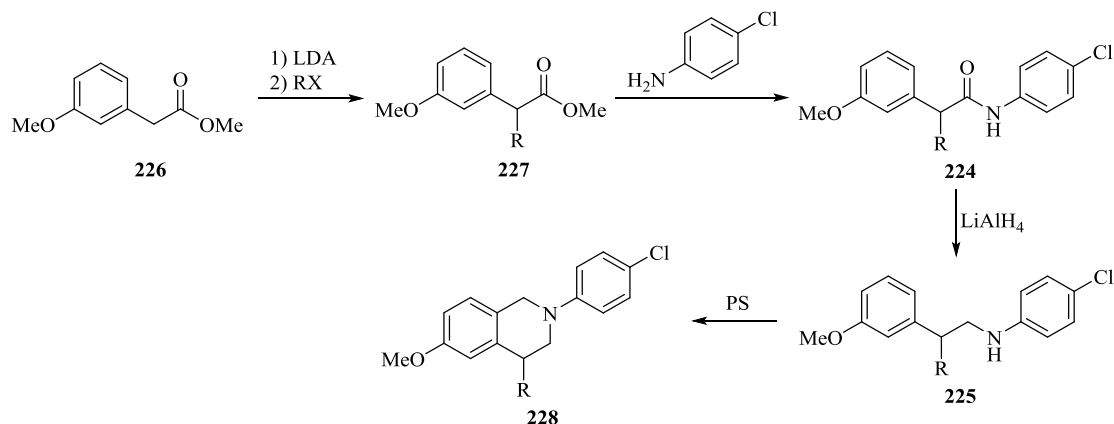
Figure 39. Representation of a Soxhlet extractor used during the Fischer esterification. The solvent is heated to reflux and the vapours (in red) are condensed (in blue) and dried by CaH_2 . CaH_2 is retained by a paper filter and the anhydrous solvent (in green) is returned in the reaction flask.

After refluxing for 3 h under these conditions, the solvent was evaporated and the residue was dissolved in EtOAc and washed with 1 N NaOH to neutralise the H_2SO_4 and to remove any unreacted starting material. In this way, the product **226** (Scheme 59) was obtained in 88% yield and did not require any further purification.



Scheme 59. Fischer esterification of the 3-methoxyphenylacetic acid **177**.

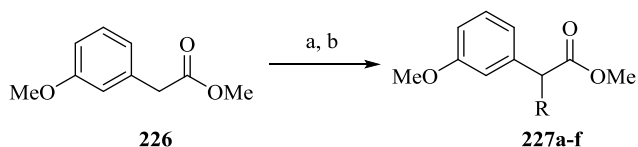
Ester **226** (Scheme 60) was then considered the starting point for the synthesis of 4-substituted THIQs (Scheme 60). The planned synthesis was only one step longer than the previous method involving the PS approach (Scheme 34, page 70)



Scheme 60. Planned strategy for the synthesis of 4-substituted THIQs **228**.

2.2.11. Alkylation of ester **226**.

To alkylate ester **226** (Scheme 61, Table 29), it was first deprotonated with LDA at $-78\text{ }^{\circ}\text{C}$ and then treated with an alkylhalide. The reaction proceeded generally with good yield and in some cases, the product was significantly clean as judged by ^1H NMR and no purification was performed. The iodo derivatives were more reactive and gave superior yields. In addition, the geminal dimethylated compound **227f** could be obtained simply using two equivalents of iodomethane and LDA.



Scheme 61. Alkylation of ester **226**. a) LDA, THF, $-78\text{ }^{\circ}\text{C}$, 1 h; b) RX, THF, $-78\text{ }^{\circ}\text{C}$ to rt, 4-6 h.

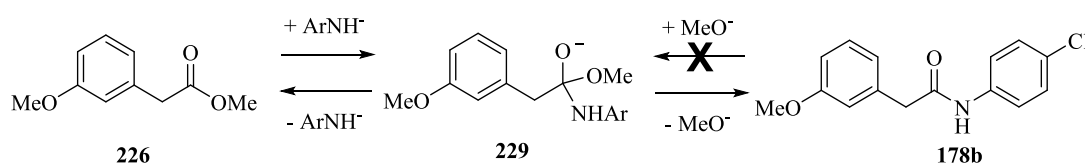
Table 29. Summary of the results for the alkylation of ester **226**.

Product	R	X	Yield (%)
227a	Me	I	Np
227b	Et	I	Np
227c	<i>i</i> -Pr	Br	20
227d	Bn	Br	86
227e	2-methoxyethyl	Br	33
227f	(Me) ₂ [*]	I	Np

X describes the halide used for the reaction of the type RX. Np = Not purified. ^{*} **116f** is geminal dimethylated.

2.2.12. Ester to amide conversion.

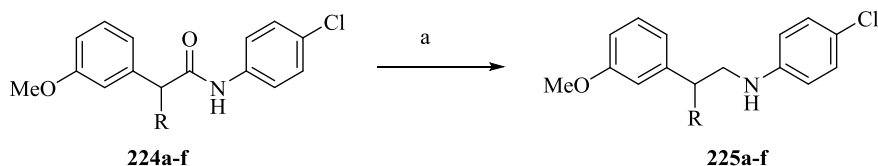
The conversion of esters **226** (Scheme 62) into amides is an equilibrium reaction and the driving force is the $pK_{a_{AH}}$ (pK_a of the conjugated acid) of the leaving species (Scheme 62). The pK_a of MeOH is 29 (in DMSO)¹⁵¹ while the pK_a of 4-chloroaniline (**113b**) is 29.4 (in DMSO).¹⁵² The difference between the two pK_a s was too narrow and it would not be enough to drive the equilibrium towards the amide **178b** (Scheme 62) formation but another factor played an important role and this was the stability of the compound formed. In fact, the amide **178b** (Scheme 62) that formed was much less electrophilic and it could not be converted to the ester **226** (Scheme 62) anymore.



Scheme 62. Direct conversion of the ester **226** into the amide **178b**.

The reaction was usually performed without solvent, at high temperature but no conversion to amide **178b** (Scheme 62) occurred even when catalytic amounts of KO^{*t*}Bu or NaH were added. Driven by the need for a reliable method for conversion of ester **226** (Scheme 62) into amide **178b** (Scheme 62), the investigation moved to the use of Al(CH₃)₃. Al(CH₃)₃ itself is extremely pyrophoric and very difficult to handle but in the recent years the use of bis(trimethylaluminum)-1,4-diazabicyclo[2.2.2]-octane (DABAL) as a source of Al(CH₃)₃ has been reported with very good results.^{153, 154} The conversion of esters to amides has been shown to proceed with very good yield for a range of substrates.¹⁵⁴ DABAL is non-pyrophoric and, although moisture sensitive, it can be weighed on the bench and reactions open to the air have been reported.¹⁵³ The reaction was very clean and excess aniline could easily be washed away during the workup (Scheme 63, Table 30). For these reasons, in most cases any further purification was considered unnecessary. As an example, the ¹H NMR spectrum of crude amide **224a** is reported in Figure 40.

necessary and as an example, the ^1H NMR spectrum of amine **225a** (Scheme 64) is reported in Figure 41.



Scheme 64. Reduction of amides **224a-f**. a) LiAlH_4 , THF, 80°C , 6-12 h.

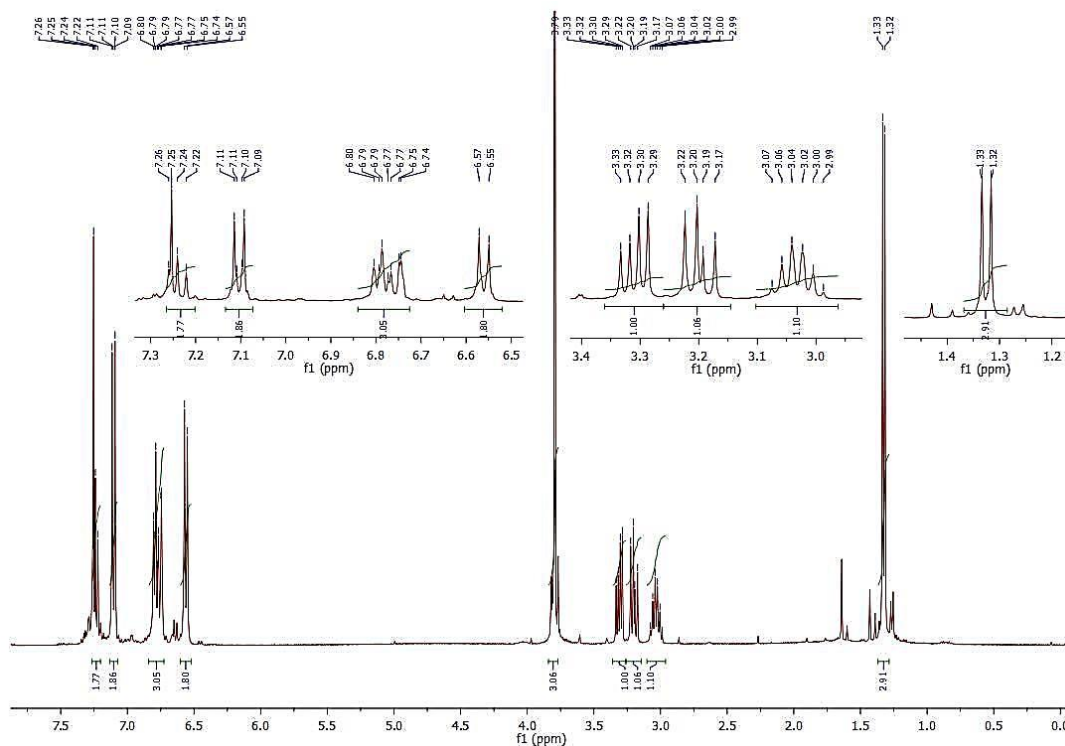
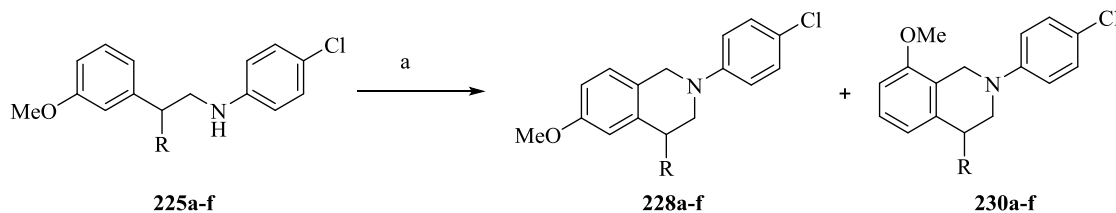


Figure 41. ^1H NMR of the crude amine **225a**.

2.2.14. PS cyclisation of amines **225a-f**.

Amines **225a-f** (Scheme 65) were cyclised under the PS conditions already described in chapter 2.2.3 (page 72) to give the THIQs **228a-f** (Scheme 65). As stated in the same chapter, small amounts of the 8-substituted THIQs **230a-f** (Scheme 65) were observed and if possible isolated (Scheme 65, Table 31).



Scheme 65. PS cyclisation of the amines **225a-f**. Conditions: a) paraformaldehyde, PTSA, toluene, reflux, 12-18 h.

Table 31. Summary of the results for the cyclisation of amines **225a-f**.

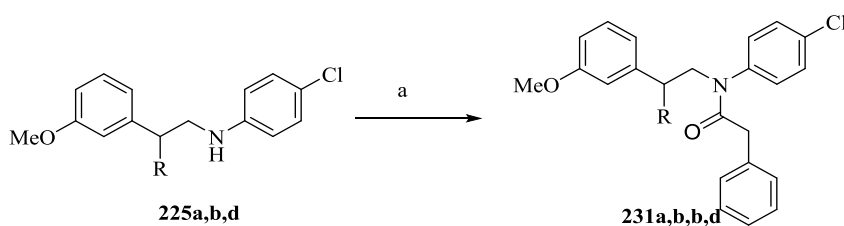
SM	R	Product	Yield (%)	Product	Yield (%)
225a	Me	228a	37 ¹	230a	2 ¹
225b	Et	228b	53 ¹	230b	No
225c	<i>i</i> -Pr	228c	27 ²	230c	No
225d	Bn	228d	39 ³	230d	2 ³
225e	2-methoxyethyl	228e	15 ³	230e	No
225f	(Me) ₂ [*]	228f	6 ¹	230f	No

SM = Starting Material; No = Not observed; ^{*} 225f and 228f are geminal dimethylated; ¹Yield of the last 4 steps; ²Yield of the last 2 steps; ³Yield of the last 3 steps.

The yields were generally good and it is noteworthy that compounds **228a**, **228b**, **228f** and **230a** were obtained without thorough purification until the last step of the whole synthesis.

2.2.15. The Bischler-Napieralski approach modification: towards 1,4-disubstituted THIQs.

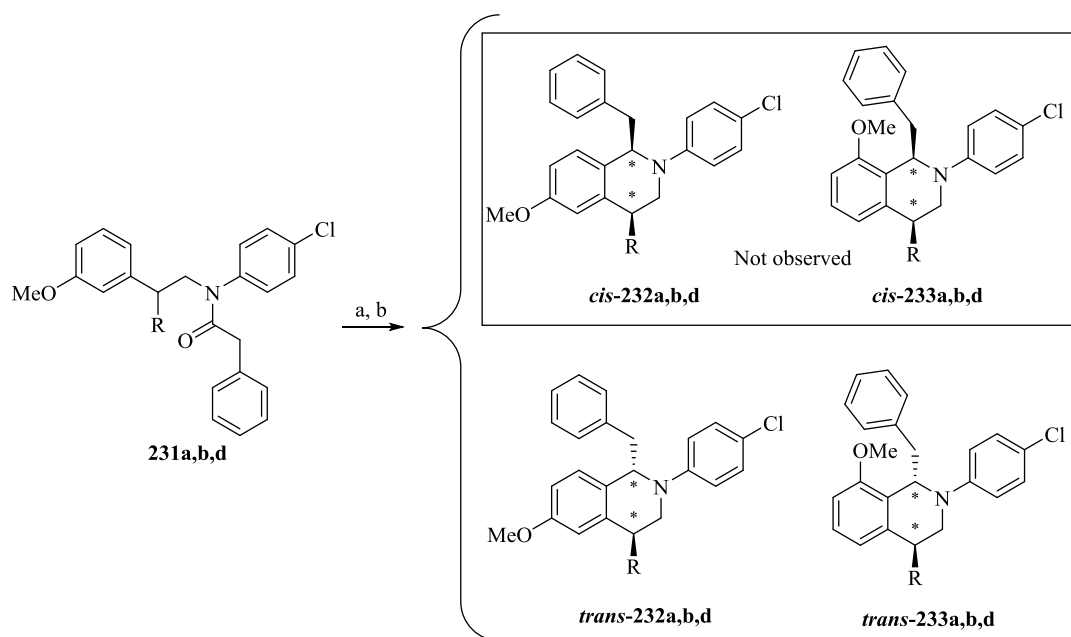
As previously mentioned in chapter 2.2.4 (page 74), the BN reaction can be used to introduce a substituent in position 1 of the THIQ ring. To test the versatility of the syntheses conducted in this work, the synthesis of 1,4-disubstituted THIQ was attempted. In order to proceed with the BN cyclisation, amines **225a**, **225b** and **225d** (Scheme 66, Table 32) were converted to the corresponding phenacetamides **231a**, **231b** and **231d** (Scheme 66, Table 32).

**Scheme 66.** Acylation of amines **225a-d**. a) Phenacetyl chloride, Et₃N, DCM, rt.**Table 32.** Results of the acylation of the amines **225a,b,d**.

Product	R	Yield (%)
231a	Me	34 ¹
231b	Et	62 ¹
231d	Bn	23 ²

¹Yield of the last 4 steps. ²Yield of the last 3 steps.

Amides **231a,b,d** (Scheme 67) were duly subjected to cyclisation under BN conditions to give the corresponding THIQs. The introduction of a second substituent increases the molecule complexity and during the BN reaction a second stereocentre is generated. Therefore, a mixture of four diastereoisomers was anticipated. Very interestingly, only two diastereoisomers formed, the THIQs *trans*-**232a,b,d** and *trans*-**233b,d** (Scheme 67, Table 33) which were successfully separated by flash column chromatography.

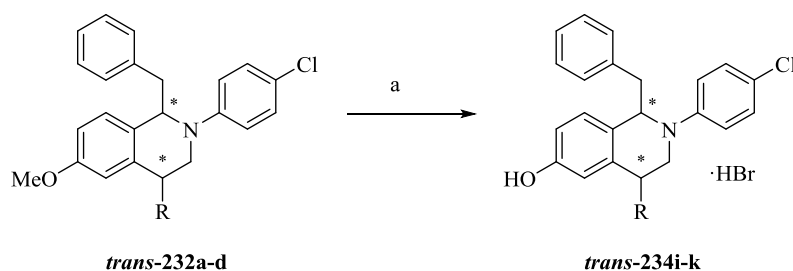


Scheme 67. BN cyclisation of amides **231a,b,d**. a) POCl₃, anhydrous toluene, reflux, 12-18 h. b) NaBH₄, MeOH, rt, 6 h.

Table 33. Results of the BN cyclisation of amides **231a,b,d**.

SM	R	Product	Yield (%)	Product	Yield (%)
231a	Me	<i>trans</i> - 232a	36	<i>trans</i> - 233a	0
231b	Et	<i>trans</i> - 232b	46	<i>trans</i> - 233b	12
231d	Bn	<i>trans</i> - 232d	46	<i>trans</i> - 233d	8

It was not possible to determine the composition of the mixture at this stage and compounds *trans*-**232a,b,d** were deprotected to give the free phenolic derivatives *trans*-**234i-k** (Scheme 68, results are reported in the following chapter 2.2.16 at page 99).



Scheme 68. Demethylation of the disubstituted THIQs *trans*-232a-d. a) BBr₃, DCM, -78 °C to rt.

In an attempt to disclose the real composition of the mixture, X-ray diffraction analysis was performed on a small crystal obtained but the signal quality was too low and the structure was not determined. In addition, the small amount of compound available limited the number of recrystallisation attempts. For this reason, other analytical methods to identify the composition of the mixture were considered.

Chiral HPLC analysis of *trans*-234j yielded a chromatogram which showed only two peaks (Figure 42). From the chromatogram it was deduced that only two enantiomers are present or otherwise four peaks should have been visible on the chromatogram itself.

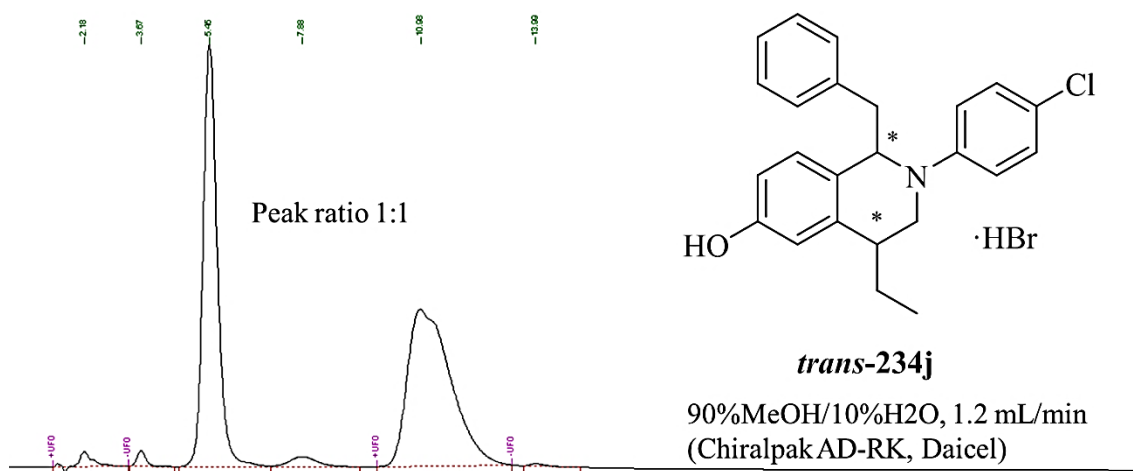


Figure 42. Chiral HPLC chromatogram of compound *trans*-234j.

Another indication of the absence of a diastereoisomeric mixture came from ¹H and ¹³C NMR analysis. The spectra showed only one peak per nucleus, while the presence of a second diastereoisomer should have shown two peaks for each nucleus or at least for the ones near the stereocentres. This data suggested that only one diastereoisomer was present but did not give any information regarding the relative stereochemistry of the two chiral centres. The answer came from a ¹H-¹H NOESY NMR analysis which is reported in Figure 44 below.

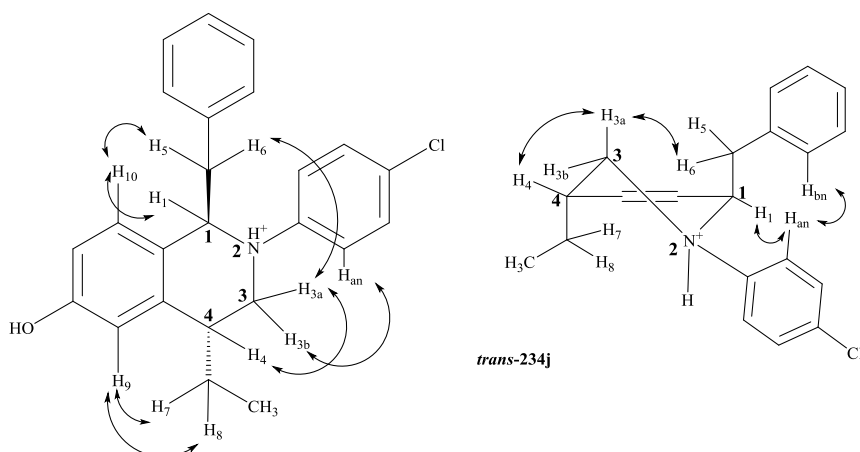


Figure 43. Three dimensional conformation of compound *trans*-234j seen from the “top” (on the left) and from the “side” (on the right). NOESY interactions are represented by double headed arrows.

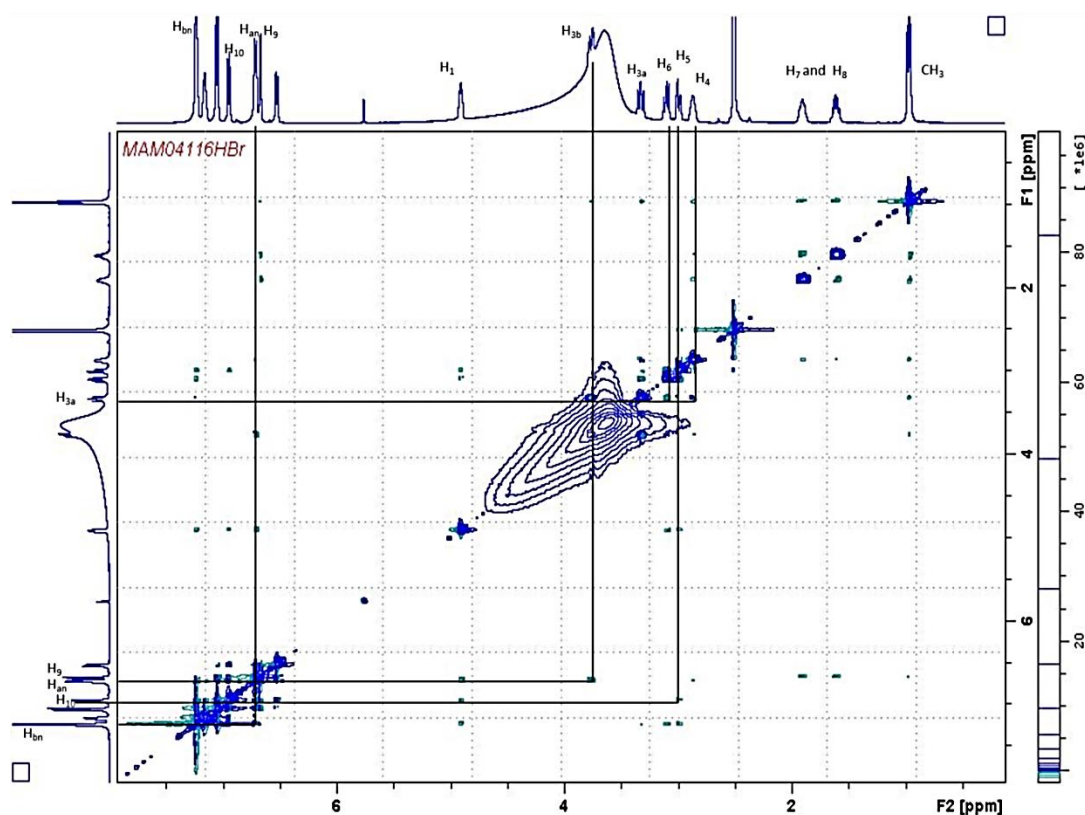


Figure 44. NOESY spectrum of compound *trans*-234j. Spatial interactions appear as cross-peaks outside the diagonal and the signals corresponding to the interactions highlighted in **Figure 43** are traced by black lines.

From the spectrum, H_{3a} interacted with both H_4 and H_6 and this was possible only if the spatial relationship between the substituents in position 1 and 4 was *trans*. Interestingly, only H_6 was able to sense H_{3a} , while on the contrary H_5 could sense H_{10} suggesting a possible locked conformation for the benzyl group in position 1. This hypothesis was also reinforced by the strong interaction between the aromatics of the *N*-phenyl ring and the 1-benzyl substituent, which might be due to intramolecular π - π stacking between the two rings. This interaction might prevent the free rotation of the 1-

benzyl substituent. It is also important to note that the NOESY signals were only visible on the salt of compound **trans-234j** and when the same experiment was attempted on the free base the signals disappeared. This was due to the fact that the protonated nitrogen was no longer capable of undergoing a fast pyramidal inversion preventing the saturated ring from flipping between the two possible twisted chair conformations. Consequently, the chance of strong spatial interactions was increased from the generated rigidity.

In order to emphasise the enantiomeric content of the sample, a NMR chiral shift reagent (CSR) analysis was performed to yield the spectra reported in Figure 45. The experiment was executed through a portion-wise addition of chiral shift agent, namely Europium(III) tris[3-(heptafluoropropylhydroxymethylene)-d-camphorate] (Eu(hfc)_3), to the solution of compound **trans-234j** in deuterated DMSO.

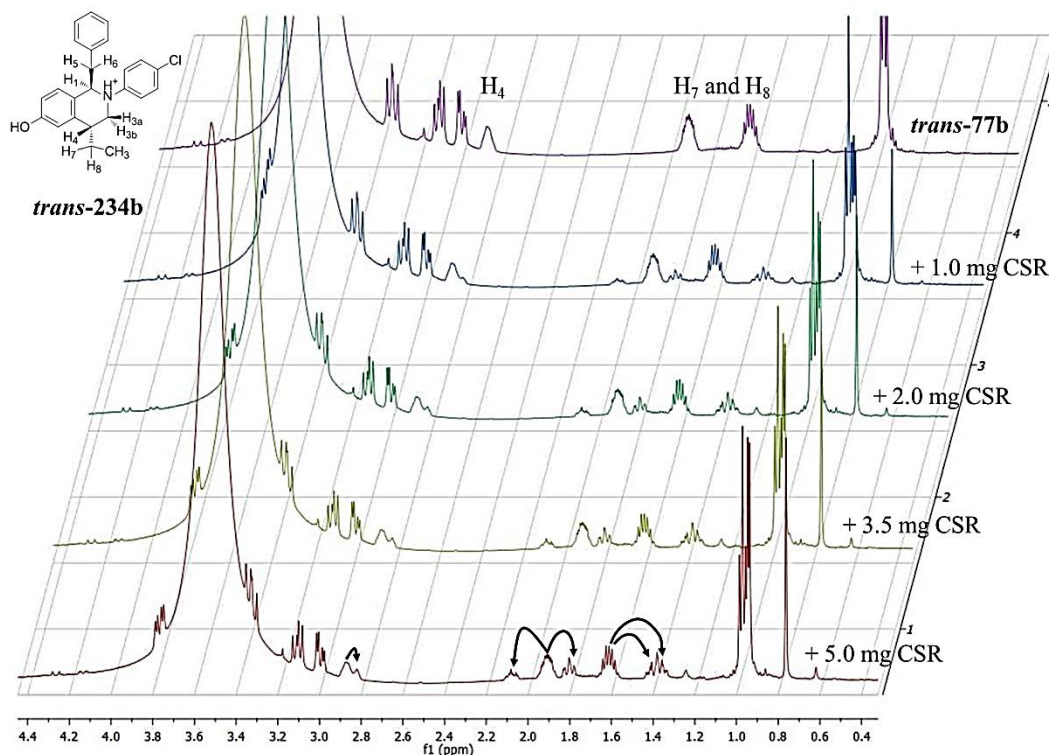


Figure 45. Stacked ^1H NMR spectra of **trans-234j** during the CSR experiment. Compound amount was 1.5 mg, and the spectra refer from top to bottom to the sequential addition of Eu(hfc)_3 . On the right of the spectrum is expressed the total amount of Eu(hfc)_3 present in the tube at the moment of the analysis. Signal splitting is highlighted by black arrows.

The peaks started to separate when the mass ratio between the compound and the CSR was 3:1 and maximise at a ratio of 1:2, and no peak deterioration was observed even at a mass ratio of 1:6. The final solution obtained was subjected to a full NMR analysis (1D and 2D, ^1H - ^{13}C HSQC reported in Figure 46). The signals corresponding

to H₇ and H₈ split into two new peaks each, while for H₄ only one new peak was visible and maybe the other peak was covered by the water peak in the spectrum. Interestingly, no change was visible for any other proton and in addition, when the same analysis was performed on the corresponding free base of **trans-234j**, the peaks appeared broader and, for similar reasons to the NOESY experiment, no signal splitting was observed.

In a similar way, the ¹³C attached to H₇ and H₈ and the one attached to H₄ had new signals that could be related to the corresponding protons by HSQC as shown in Figure 46.

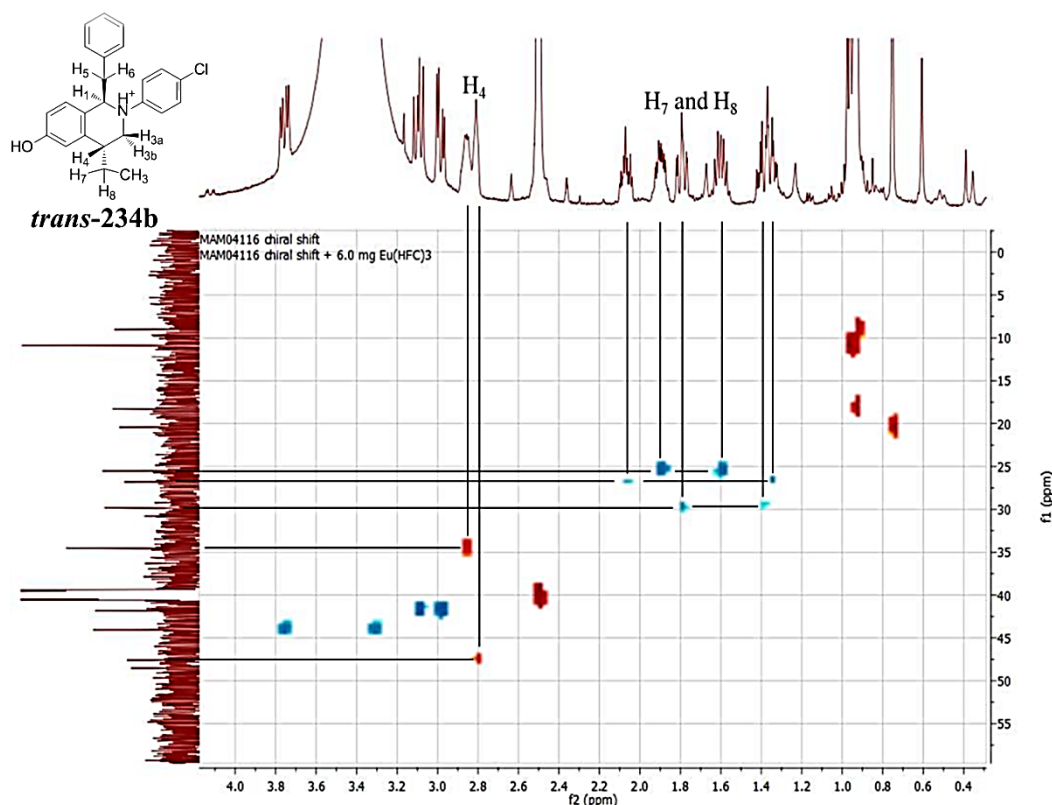
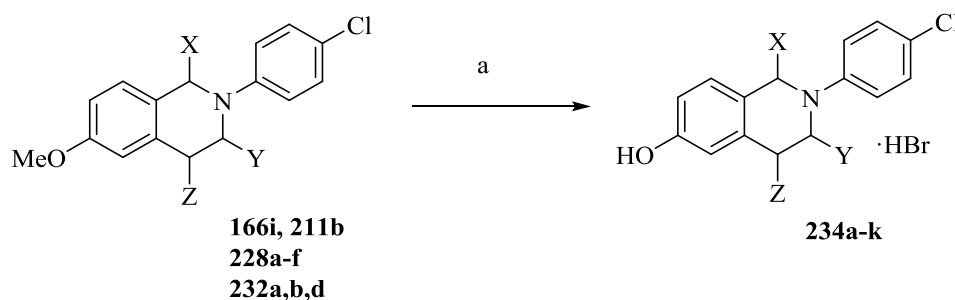


Figure 46. ¹H-¹³C HSQC analysis of **trans-234j** + 6.0 mg of Eu(hfc)₃. ¹H-¹³C correlation is highlighted by black lines.

Having proved that only the *trans*- isomers were formed, it was still unclear how this was possible considering that each step involved in the synthesis was completely achiral. It is necessary to consider that the first chiral centre was introduced in the first step of the synthesis, while the second centre was formed only at a later stage. In this way, the first chiral group could possibly induce the chirality of the second one during a later step of the reaction. Examples of stereo-induction from substituents in position 3 is well noted and exploited in the literature,¹⁴¹ therefore induction from a group in position 4 was plausible.

2.2.16. Deprotection of the final THIQs synthesised through the modified PS and BN approaches.

One last time, the protected THIQs synthesised were demethylated to yield the corresponding phenolic derivatives. The reaction was carried out under the same conditions described in chapter 2.1.5 (page 68) using BBr₃ as demethylating agent and DCM as reaction solvent. The results of the reaction represented in Scheme 69 are reported in Table 34 below.



Scheme 69. Deprotection of 3- and 4-substituted (**166i**, **211b** and **228a-f**, respectively) and 1,4-disubstituted THIQs (**232a-e**). Reagents and conditions: a) BBr₃, DCM, -78 °C to rt, 2 h, inert atmosphere.

Table 34. Results of the deprotection of the THIQs obtained through the modified PS and BN approaches.

SM	X	Y	Z	Product	Yield (%)
166i	H	Me	H	234a	87
211b	H	Et	H	234b	24
228a	H	H	Me	234c	58
228b	H	H	Et	234d	47
228c	H	H	<i>i</i> -Pr	234e	31
228d	H	H	Bn	234f	66
228e	H	H	2-methoxyethyl	234g	Ni
228f	H	H	(Me) ₂ [*]	234h	85
232a	Bn	H	Me	234i	63
232b	Bn	H	Et	234j	86
232d	Bn	H	Bn	234k	45

SM = Starting material; Ni = Not isolated; ^{*} Compounds **228f** and **234h** are geminal dimethylated.

The reaction proceeded with variable yields but with no significant deviation from the standard course for the reaction itself apart from compound **228e**, which did not yield the desired product.

2.3. General conclusions.

The chemistry reported in this work demonstrates that it is possible to obtain simple substitutions in every position of the THIQ scaffold. The short synthetic strategies applied have led to a reasonable number of compounds in short time. Also noteworthy is the overall use of cost effective procedures and inexpensive starting materials. In addition, it was possible to carry out many intermediate steps without purification. This not only contributed to rapidly accessing the desired compounds but also had a positive impact on the average synthetic costs. In addition, the majority of the reactions were carried out at temperatures near rt, which will be useful in future when an industrial adaptation process is evaluated.

The three cyclisation methods used compensate for the limitations of each other and together formed a reliable synthetic approach though increasing the complexity of the molecules required small adjustments to the synthesis itself. Future optimisation of the reactions applied might lead to increased yields. The problem of the stereochemistry still remains to be fully addressed but particularly appealing is the stereo-induction obtained in the 1,4-disubstituted compounds.

Interesting would be to establish if the ratio between the two regioisomers that were obtained during the cyclisation reactions could be influenced by temperature and concentration.

In conclusion, though improvements might be necessary, the synthetic approaches allowed to reach the objectives initially determined.

CHAPTER 3

Results and discussion

Biological evaluation and computational chemistry

The synthesised THIQs and some basic intermediates were evaluated against the two main targets: 17 β HSD1 and ERR α . The activity of the compounds was also evaluated against non-primary targets in order to obtain information on their selectivity and their possible applications outside the aim of the project was also considered. Moreover, to have prompt access to the biological results against 17 β HSD1, attempts to develop a colourimetric assay were made. In addition, to obtain information on the binding mode of the synthesised compounds, co-crystallisation with the enzyme was evaluated. Molecular modelling was used to evaluate possible binding modes.

3.1. 17 β -hydroxysteroid dehydrogenase type 1 (17 β HSD1)

To investigate the inhibitory capabilities of the synthesised THIQs against 17 β HSD1, the development of an in-house assay was considered. Commonly, activity of 17 β HSD1 is evaluated using a radiochemical assay which involves the use of HPLC combined with radioflow detectors in order to separate and quantify the amount of E1 and E2, respectively the substrate and the product of the enzymatic reaction.⁶⁹ Alternatively, the separation of the two components is performed by TLC and each sample is then analysed by a radiodetector.¹⁵⁵ To simplify the assay procedure and avoid the use of radiochemicals, previous work from our group developed a colourimetric assay (see chapter 3.1.3, page 107). For this assay the enzyme needed to be expressed and purified, and the conditions for the assay optimised. Moreover, to obtain as much information as possible on the binding of the synthesised compounds, co-crystallisation of the enzyme with a selected THIQ was performed, so milligram quantities of enzyme were required.

3.1.1. Protein expression and purification.

17 β HSD1 is naturally expressed in certain human cell lines or can be overexpressed using transfected expression vectors. However, the amount of enzyme produced in these cells is not enough to obtain the quantity of protein necessary for the assay and crystallisation experiments. The large scale cultivation of human tissue is also more difficult and expensive. Our group had successfully expressed 17 β HSD1 in 293-EBNA

mammalian cells but subsequently moved to bacterial systems to more easily produce larger amounts of the protein. The mammalian expression used the gene for 17 β HSD1 cloned into the pCEP4 vector. For the bacterial expression, the gene for 17 β HSD1 was extracted from the pCEP4 vector and cloned into the pET-24a(+) bacterial expression vector. To do this, two restriction enzymes, NheI and XhoI, were used to remove the gene from pCEP4 and to digest the bacterial vector pET-24a(+). The gene and digested pET-24a(+) vector were purified and ligated to form the full vector (Figure 47).

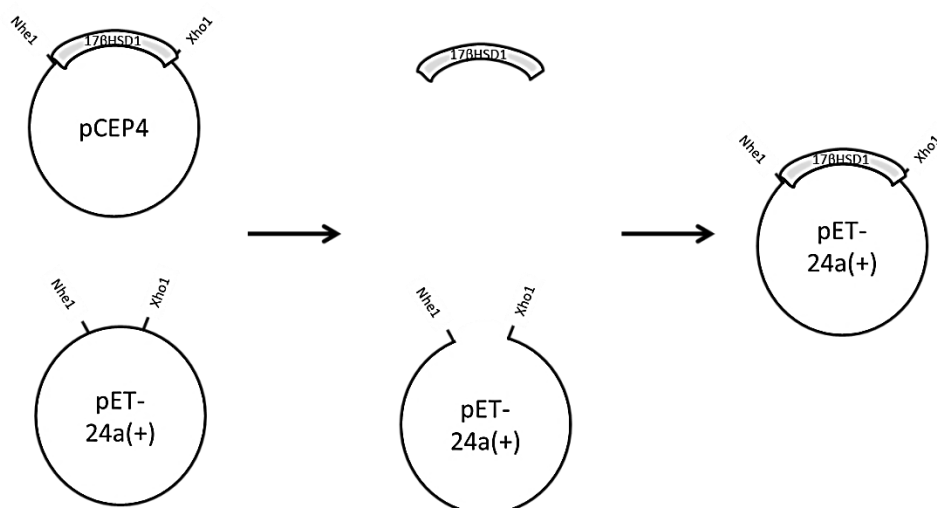


Figure 47. Schematic representation of the insertion of the 17 β HSD1 gene into the pET-24a(+) from the pCEP4 mammalian vector.

The new vector generated was used to transform the *Escherichia coli* (*E. coli*) expression strain Rosetta 2, which is designed for expression of human proteins in bacterial cells. Rosetta 2 is the traditional BL21(DE3)pLysS expression strain but they also contain a vector for the production of rare t-RNAs (codons AGA, AGG, AUA, CUA, GGA, CCC and CGG). These t-RNAs recognise codons that are typical of eukaryotic cells but are rare in bacterial genetic material and for this reason they might become necessary when producing recombinant proteins.

The pET-24a(+) vector is not a mere vehicle and, in addition to the gene for 17 β HSD1 ligated to it, contains other key sections. One is the kanamycin resistance factor, which allows the selection of the cells that are transformed by growing them in kanamycin supplemented media. Another important one is the *lac* operator which is the instrument that enables the control of protein expression (Figure 48).

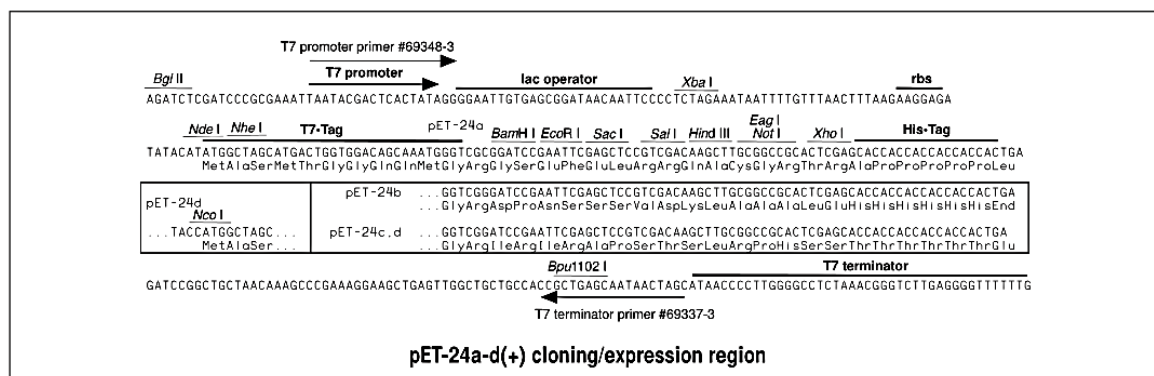


Figure 48. Map of the protein cloning expression region of pET-24a showing the promoter, lac operator, NheI and XhoI restriction enzyme binding sites, His-tag coding region and the terminator sequence.

In *E. coli*, the *lac* operon normally encodes for a series of protein involved in the transport and metabolism of lactose. An operon is a genetic structure containing a promoter, an operator, a series of genes and a terminator sequence. The operator is usually occupied by the *lac* suppressor which prevents transcription in normal conditions. The *lac* suppressor has high affinity for allolactose (Figure 49) and when the repressor binds allolactose, a conformational change displaces the repressor from the operon and the transcription is initiated. This system enable control of the expression of the protein involved in the metabolism of lactose depending on the presence or absence of lactose in the surrounding environment.

The pET-24a(+) vector contains the *lac* operator, which binds the *lac* repressor and consequently the genes on the vector cannot be transcribed. In the experimental conditions, isopropyl β -D-1-thiogalactopyranoside (IPTG), a structural analogue of allolactose, is used to initiate the protein expression. IPTG binds the *lac* repressor displacing it from the operator and thus allows the transcription to start.

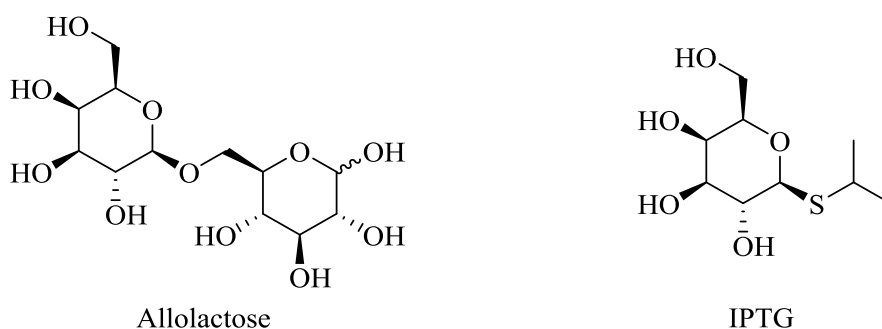


Figure 49. Structure of allolactose and its mimic IPTG.

Two important factors that influence the quality of the protein produced are the speed of production and the total amount produced. If the protein is produced too quickly then it might misfold becoming inactive. Instead, if the amount of protein synthesised is

excessive, the protein might aggregate or precipitate out of the cytosol and become unusable. To control the speed of expression, different concentrations of IPTG were initially screened and 12.5 μ M was found to be the optimal concentration for protein expression. In fact, the speed of expression is proportional to the gene activation induced by IPTG. At the same time, just before the addition of IPTG the cell cultures were cooled to 16 °C to reduce the metabolism of the cells and consequently further reduce the speed of production of the protein.

After the addition of IPTG, the culture was left overnight at 16 °C and then centrifuged to harvest the cells. The pellet was frozen to make the cells more fragile and then mechanically lysed. The lysate was centrifuged and the supernatant collected to give the crude protein which needed to be purified. Thanks to the previous work undertaken by our group, both untagged and His-tagged versions of 17 β HSD1 were available. The tagged 17 β HSD1 (H₆-17 β HSD1) possesses 6 extra histidine residues on the N-terminal that do not interfere with the catalytic capabilities of the enzyme but allow affinity purification. Histidine has high affinity for nickel ions and this affinity can be exploited for column purification. A column loaded with Ni²⁺ binds the histidine tag on the protein and the majority of impurities are washed away. The protein is then eluted with an imidazole gradient. Imidazole shares structural similarities with histidine (Figure 50) and at higher concentrations displaces the tagged protein from the column.

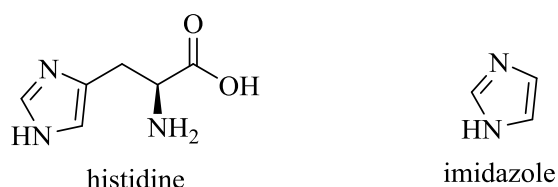


Figure 50. Structure of histidine and imidazole.

Among the fractions obtained, the ones containing the enzyme were identified by SDS PAGE gel, collected and then subjected to dialysis overnight to reduce the high concentration of imidazole and NaCl. Because this technique relies on the specific affinity between the protein tag and the Ni²⁺ ions it usually yields high purity levels. Nevertheless, higher levels of purity are often required especially for protein crystallisation. Hence, the dialysed protein solution was subjected to a second purification step with a Q-sepharose column, which is an ion exchange column. The protein is thus eluted with a gradient of NaCl and again the fractions containing the enzyme are identified by SDS PAGE gel, collected and then subjected to dialysis to

reduce the concentration of NaCl. The dialysed protein solution was concentrated to the desired concentration for use in either biological assays or crystallisation trials.

3.1.2. Protein crystallisation.

Several structures of 17 β HSD1 with different ligands are available in the Protein Data Bank repository and the data obtained from previous work in our group in addition to the already established crystallisation conditions reported in the literature³⁶ were used as the starting point for a new set of crystallisation attempts.

Using the vapour diffusion technique different conditions were selected for crystallisation attempts. The crystallisation buffer containing 0.15 M MgCl₂, 0.1 M Hepes pH 7.5 and 20% glycerol was selected from the literature and a range of PEG4000 concentrations (from 5% to 25%) were screened.

The following conditions were selected, instead, from an automated screening previously undertaken by our group:

- 0.3 mM MgAc₂ and 0.1 M sodium cacodylate with a range of PEG8000 concentrations from 10% to 35%.
- 100 mM Hepes buffer (pH 7.5), 0.16 mM MgCl₂ and 20 % glycerol with a range of PEG6000 concentrations from 10% to 35%.
- Sodium citrate pH 6.5 in a range of concentrations from 1.3 M to 1.8 M.

Four repetitions were set for each condition and the protein was left to crystallise over one to two weeks. Among the conditions tried, 25% PEG4000 was the one that gave the best results and was selected for the investigation of some additives. Two repetitions for each additive were set up but none of the additives gave better results than the original 25% PEG4000 solution.

The composition of the solution that gave the best results was identified as 25% PEG4000, 0.15M MgCl₂, 0.1 M Hepes pH 7.5 and 20% glycerol. Several repetitions were set and to some was added a solution of **170i** (Figure 51) alone or a mixture of **170i** and NADP⁺ when the crystals started to grow.

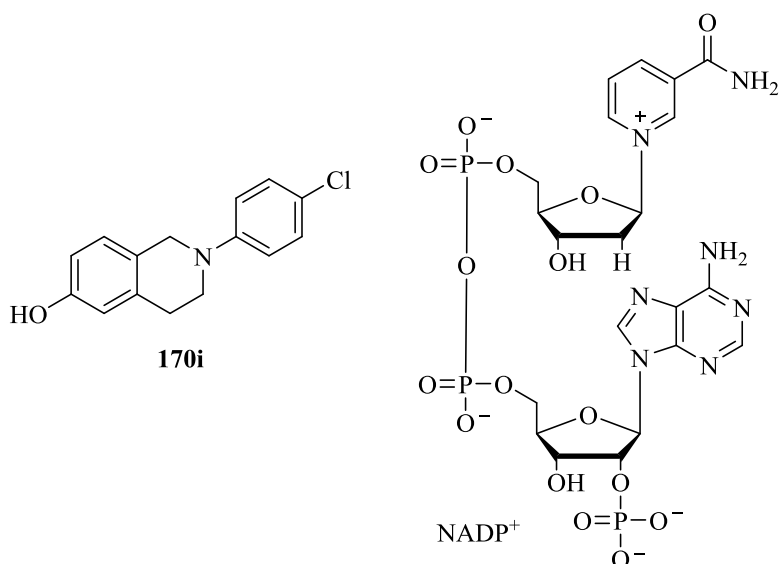


Figure 51. Structure of compound **170i** used for the crystallisation trials.

To estimate if the crystals forming are protein or simply salts from the buffer, the drop is usually watched with a stereoscope and the incident light is polarised in different axis. Proteins usually glow in colours that change with the change of polarisation (Figure 52).

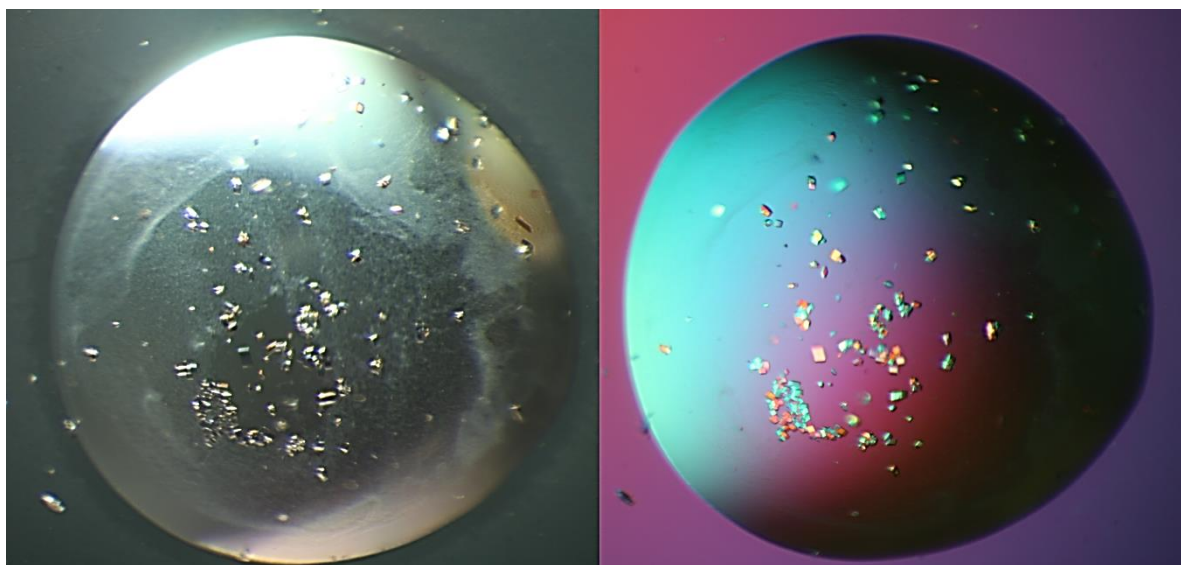


Figure 52. Pictures of a hanging drop of buffer with crystals of apo-17βHSD1. On the left the drop is seen under normal light. On the right the drop is seen under polarised light and the crystals become shiny.

Even if the addition of **170i** did not have any significant effect on the shape of the crystals, when NADP⁺ was added the crystals become clustered needles. Despite the large dimensions of the cluster, the needles were too thin to be suitable for an X-ray diffraction analysis (Figure 53).

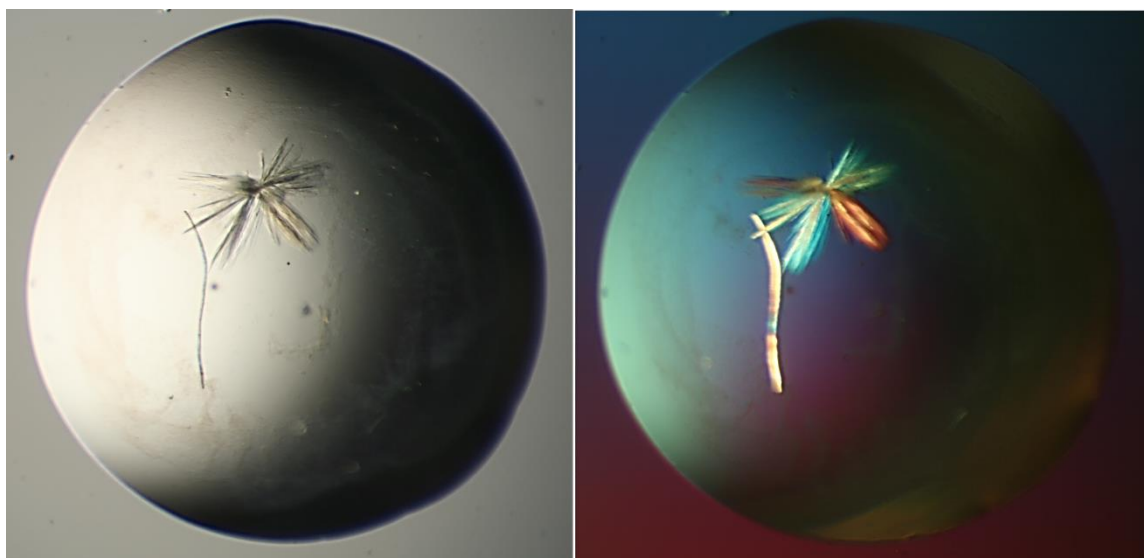


Figure 53. Pictures of a hanging drop of buffer with crystals of 17βHSD1 after the addition of NADP⁺. On the left the drop is seen under normal light. On the right the drop is seen under polarised light.

Disappointingly, only the apo-enzyme (no inhibitor and no cofactor) gave one single crystal big enough to attempt an X-ray diffraction (Figure 54). In addition, when the crystal was analysed it degraded under the X-ray beam and only part of the data was successfully acquired. A reconstruction from the partial data obtained was attempted but the amount and the quality of the data were too low to afford any tangible structure.

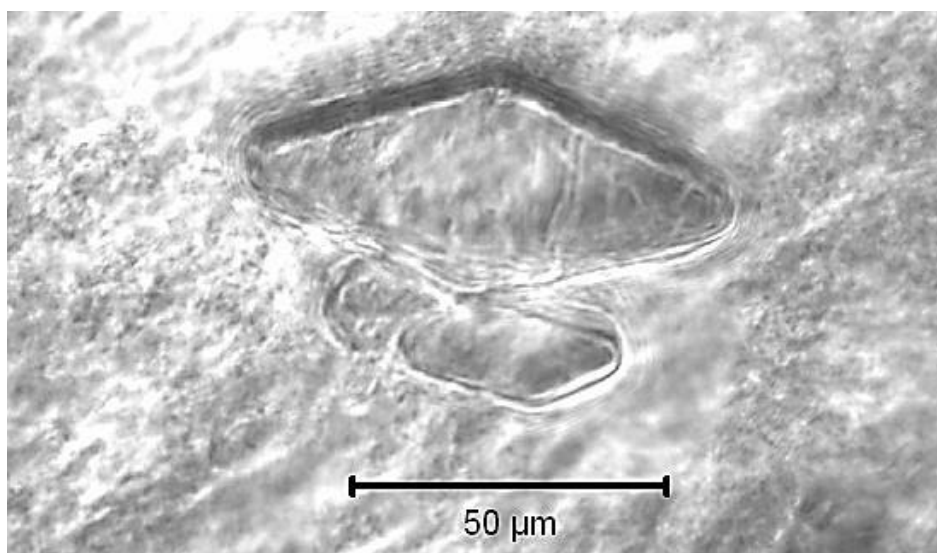


Figure 54. Pictures of a crystal of 17βHSD1 obtained with a SEM. The black bar denotes the scale of the picture and the dimensions of the crystal can be estimated to *ca.* 75 μm of length.

3.1.3. Colourimetric enzymatic assay.

As already described, 17βHSD1 catalyses the conversion of E1 into E2 and uses NADPH as the hydride donor (Figure 55) and though *in vivo* this process proceeds only

towards the formation of E2, the reaction is reversible *in vitro*. In fact, the content of NADPH in living cells is generally high and this pushes the equilibrium towards its conversion to NADP⁺.

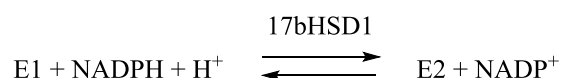


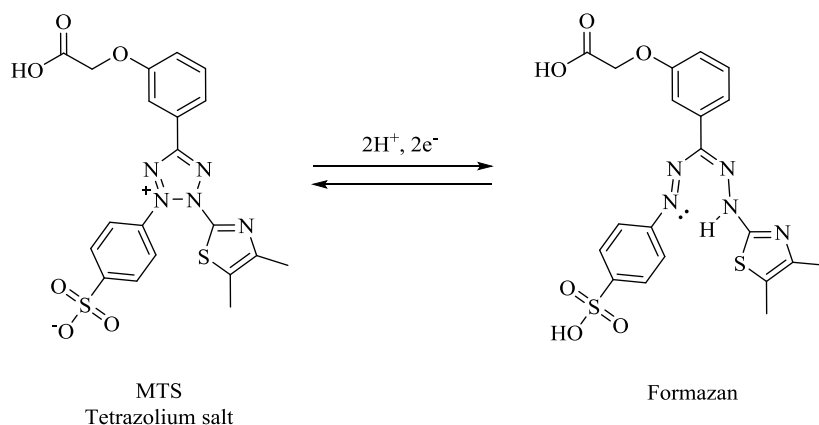
Figure 55. Schematic representation of the conversion of E1 to E2 by 17βHSD1.

Ideally, the assay would either measure the consumption of NADPH or the formation of NADP⁺. NADPH has its maximum point of absorption at 260 nm with a molar extinction coefficient (ε) of 1.69·10⁴ M⁻¹ cm⁻¹ but at the same wavelength NADP⁺ absorbs with a similar ε making it impossible to measure either the formation of NADP⁺ or the consumption of NADPH at 260 nm. In addition, at this wavelength other organic compounds might absorb interfering with the readings. Nevertheless, it is possible to follow the reaction at 340 nm where NADPH still absorbs, though with a lower ε of 6.2·10³ M⁻¹ cm⁻¹, but NADP⁺ does not.

The enzyme inhibition is measured calculating the V₀ (initial rate of reaction) of the enzyme with or without inhibitor and the ratio between the two represent the level of inhibition. To be able to measure V₀ it is necessary to be in steady-state conditions which means that the concentration of the substrate is effectively constant and the rate of product formation is negligible. In fact, when the product concentration becomes significant, the reverse reaction becomes competitive and this is reflected in a variation of the apparent V₀. This also means that the concentration of NADPH, which is a substrate of the enzyme together with E1, would not change significantly over time thus making it impossible to measure its consumption. It is possible to overcome this problem by analysing the reverse reaction and measuring the NADPH formation (Figure 55). Nevertheless, the conditions impose that the amount of product formed must be low in comparison to the substrate and, as stated above, the ε of NADPH at 340 nm is low. These two conditions imply the measurement of signals over a relatively small absorbance range, therefore accurate procedures were needed to prevent large errors. The work previously carried out by our group highlighted that the equipment available was not able to give consistently accurate data using this approach.

A recent piece of literature shows how it is possible to enhance the detection of NADPH by using water soluble dyes used for cell viability assays, namely 3-(4,5-dimethylthiazol-2-yl)-5-(3-carboxymethoxyphenyl)-2-(4-sulfophenyl)-2H-tetrazolium,

internal salt (MTS) and phenazine ethosulfate (PES).¹⁵⁶ The MTS-PES system is usually used for cell viability assays because it is reduced to the formazan form in presence of NADH and NADPH (Scheme 70), which are commonly accepted as general cell viability indicators.

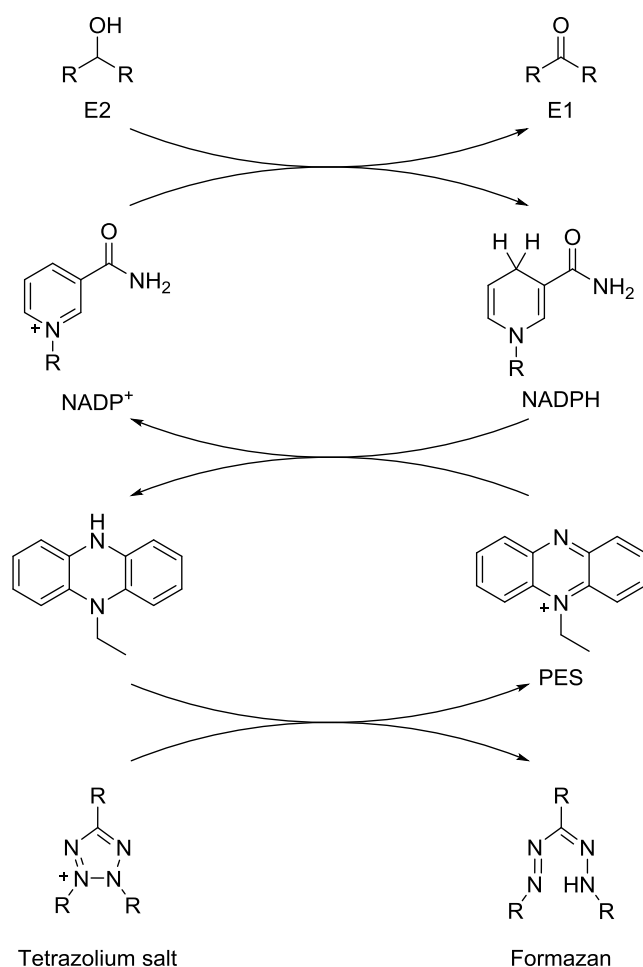


Scheme 70. Conversion of the tetrazolium salt form of MTS into the formazan form.

The reduction of MTS is usually slow and for this reason an electron carrier (PES) is introduced to facilitate the reaction. Using this approach, the NADPH formed by the oxidation of E2 to E1 transfers its electron to PES which then reduces MTS to formazan (Scheme 71, page 110). The latter has a strong absorption at 490 nm where not many common compounds absorb thus both reducing interferences and enhancing the signal of the NADPH formed.

The assay was then set to measure the conversion of E2 to E1 which is the reverse reaction compared to what occurs in living cells. Previous work has shown a reasonable correlation of the steroidal inhibitors between the MTS assay and the radio-assays albeit with ten to fifty fold loss of sensitivity.

The assay was performed incubating enzyme, inhibitor and NADP⁺ for 10 minutes at 37 °C in a 96-well plate and the reaction was started by the addition of a mixture of E2 and MTS/PES. The reaction was monitored reading the plate at 490 nm every 10 seconds for two minutes. The data was plotted using GraphPad to calculate the slope which is a reflection of V_{max}. The percentage of inhibition was calculated as a ratio 100 - (slope_{inhibitor}/slope_{control} x 100).



Scheme 71. Redox cascade that leads to the reduction of the tetrazolium salt MTS to the formazan.

When an initial set of simple THIQs was tested (compounds **163a,e,i,q,s** and **170e,i,o,q,s**, Figure 56, Table 35) it was actually found that there was no correlation between the inhibitory activity of these non-steroidal compounds in the MTS assay and in the whole cell radio-assay. Compounds were initially tested at 10 μ M concentration but they were found inactive at this concentration (Figure 56, Table 35). Notably, the standard deviation (STD) values in the measurements were very high for the THIQ compounds but significantly smaller for the steroidal compound STX1040 (Figure 56, Table 35).

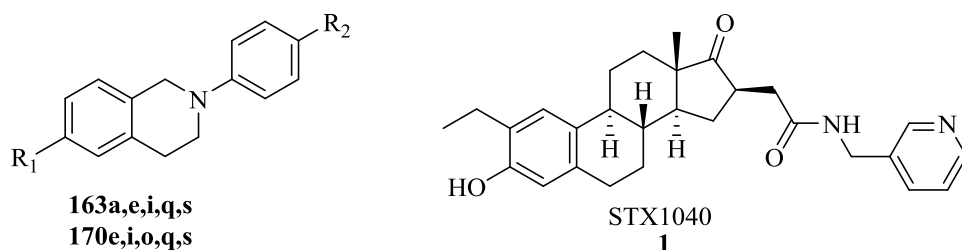


Figure 56. Structure of the initial set of compounds tested against 17 β HSD1 on the colourimetric assay and the control steroidal inhibitor STX1040.

Table 35. Results for the compounds tested against 17 β HSD1 at 10 μ M in the colourimetric assay.

Compound	R ₁	R ₂	% inhib. (10 μ M)
STX1040 1			88.2 \pm 0.5
163a	H	H	-27.5 \pm 3.5
163e	OMe	H	10.2 \pm 19.6
163q	OMe	Me	8.2 \pm 14.7
163i	OMe	Cl	16.8 \pm 13.8
163s	OMe	OMe	2.3 \pm 17.2
170e	OH	H	11.2 \pm 20.5
170q	OH	Me	9.3 \pm 15.9
170i	OH	Cl	6.9 \pm 15.9
163o	OH	OMe	4.3 \pm 18.0
170s	OH	OH	0.4 \pm 16.9

The percentage of inhibition reported were the result of a single experiment in triplicate.

Compounds did not show activity even when the concentration was raised to 200 μ M and this was not in line with the controls used. STX1040 (Figure 56, Table 36) and STX3562 were used as range control, the first is a potent steroidal inhibitor with an IC₅₀ of 27nM (from whole cell radiochemical assay) and the second showed only 28% inhibition at 10 μ M in the same assay. In the same assay the THIQ **170i** (Figure 56, Table 36) showed 78% inhibition at 750 nM and even if the results were not directly comparable it was clear that the activity of **170i** should place itself between the ones of STX1040 and STX3562. Interestingly, when tested in the colourimetric assay the results were different with STX1040 **1** showing 92.4% inhibition, STX3562 showing 46.7% inhibition and **170i** being inactive. It was not clear why the steroidal compounds seemed to follow a similar trend in the two different assays while the THIQ derivative did not.

Table 36. Comparison between the colourimetric assay and the results from Ipsen.

Compound	% inhib. (200 μ M)	Ipsen results
STX1040 1	92.4 \pm 1.0	IC ₅₀ = 27 nM
STX3562	46.7 \pm 1.9	28% @ 10 mM
170i	3.9 \pm 4.7	78% @ 0.75 mM

The percentage of inhibition reported were the result of a single experiment in triplicate.

Being **170i** in theory amphiprotic, it was evaluated if the pH of the buffer would have had any influence on the activity of the compounds. The assay, which was normally

performed at pH 7.5, was repeated at pH 6.5 and 9.2 and the inhibition of **170i** and STX1040 was recorded (Table 37) but no major differences were found.

Table 37. Comparison of the activity of STX1040 and **170i** at three different pHs: 6.5, 7.5, 9.2.

Inhibitor	% inhibition (@ 200 μ M)		
	pH 6.5	pH 7.5	pH 9.2
STX1040	91 \pm 1	92 \pm 1	92 \pm 2
170i	6 \pm 1	4 \pm 5	-3 \pm 5

The percentage of inhibition reported were the result of a single experiment in triplicate.

It was possible for compound **170i** to interfere with some component of the assay even if it should not be able to act as a substrate it could always interfere directly with any redox reaction. For this reason it was evaluated if **170i** had any effect when no E2 was present. The activity of the enzyme was set to 100% when no inhibitor was present and to 0% when no E2 and no inhibitor were present. The addition of **170i** (1 mM in assay) in the presence of E2 reduced the activity of the enzyme to 77% (23% inhibition) while when **170i** was added in the absence of E2 no significant activity was registered (Figure 57). Hence compound **170i** did not react with the dye or NADP⁺ but nevertheless showed only 22.8% \pm 3.2% inhibition at 1 mM.

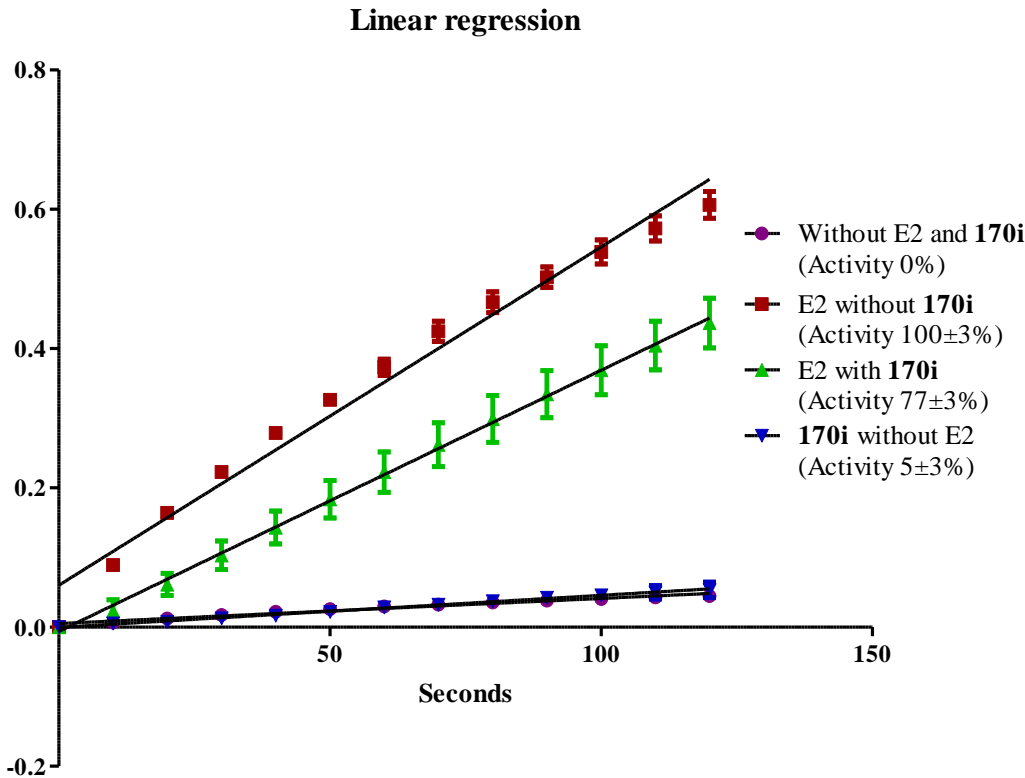


Figure 57. Graph of the measured V_0 of 17 β HSD1 without E2 or **170i**, with E2 but no **170i**, with E2 and **170i** and with **170i** but no E2. The concentration of **170i** was set to 1 mM. Values were normalised for a better reading. The percentage of inhibition reported were the result of a single experiment in triplicate.

It was not clear why compound **170i** which shows a reasonable activity in the whole cell radiochemical assay showed very weak activity on the MTS assay. The reason might lay in the fact the enzyme was tested in opposite directions in the two assays or some biochemical activation might occur *in vivo*.

Another factor that complicated the analysis of the problem was that the enzyme has two substrates and the binding of one or the other might lead to different affinity for the inhibitor. In particular, some docking studies performed by Dr. Mark Thomas have highlighted the possibility of a positive π - π stacking interaction between the N-aryl ring of **170i** and the nicotinamide ring of NADPH (Figure 58). However, docking of the synthesised THIQ into the substrate pocket have proven doubtful. In fact, hydrogen bond donors and acceptors did not point towards any polar residue. In addition, multiple binding modes were found by the software but the scoring was never related to the efficacy of the compound itself. To be able to obtain more information from the docking studies, a crystal structure of the enzyme with a THIQ inhibitor would be necessary.

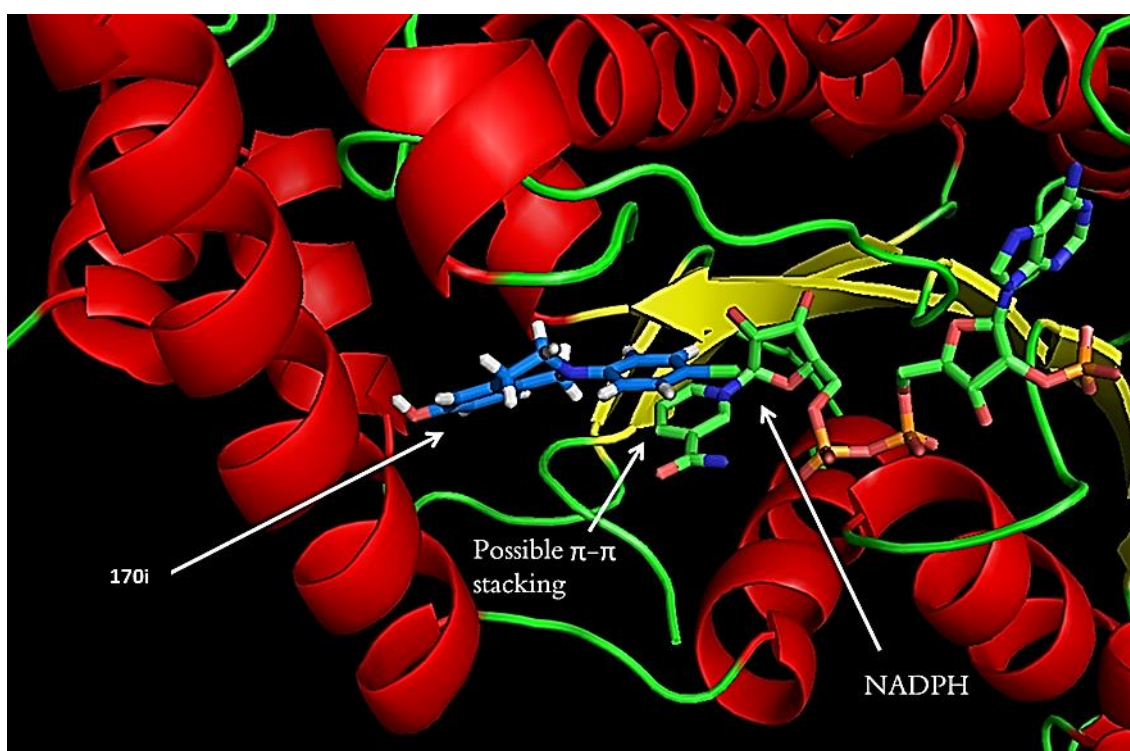


Figure 58. Docking of compound **170i**. Highlighted is the possible interaction between the inhibitor and the cofactor NADPH. Some residues were removed for a clearer view.

3.1.4. Qualitative whole cell assay.

As the results for the assay using purified enzyme showed lower than expected inhibitions by THIQs, a different approach was planned following the literature. 17 β HSD1 is expressed in T47-D breast cancer cells more than in other cell lines.¹⁵⁷ T47-D cells are estrogen dependent breast cancer cells and thus have a direct growth response to E2 levels. Examples are reported in the literature where this cell line has been used to obtain qualitative *in vivo* information about 17 β HSD1 inhibition. The strategic approach consists of measuring the cell growth after treating the cell with the inhibitor alone or with a mixture of inhibitor and E1 or E2. E1 is readily converted to E2 by 17 β HSD1 and inhibition of the enzyme would reduce the stimulating effect of E1. Moreover, by treating the cells with only the inhibitor it is possible to evaluate their estrogenicity. Furthermore, by analysing the effect of the inhibitor against the E2 stimulated growth of cells, it is possible to evaluate the anti-estrogenic properties of the inhibitor. The combination of these data can afford important qualitative information on the properties of the synthesised compounds.

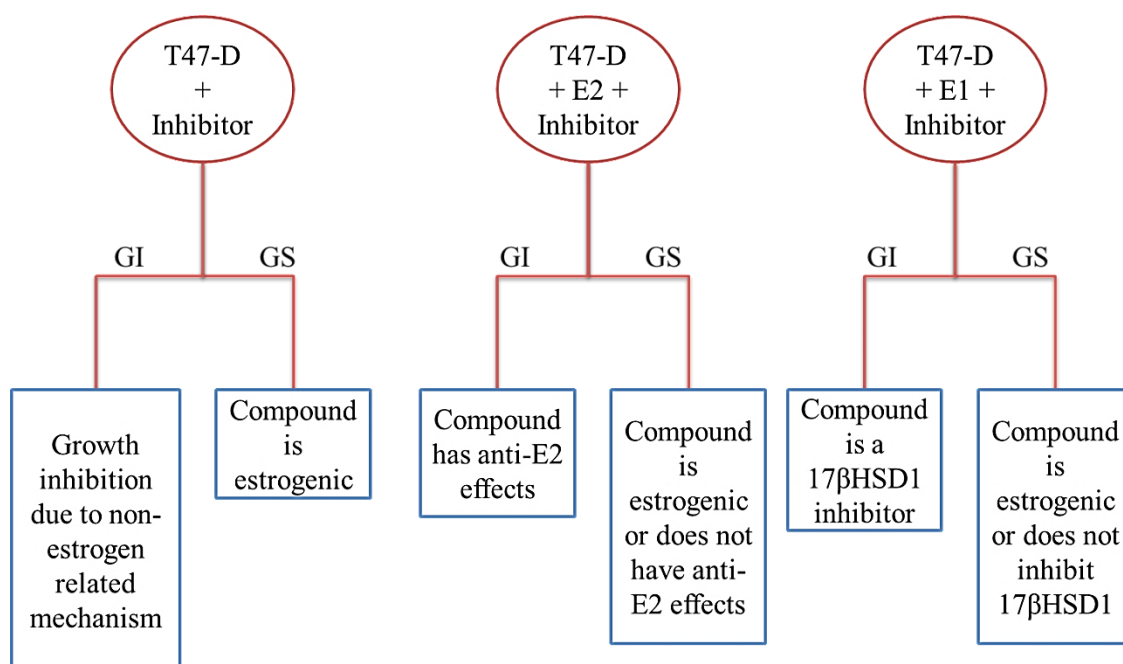


Figure 59. Flow chart depicting the information obtainable by treating T47-D cells with an inhibitor and with or without E1 or E2. GI = growth inhibition; GS = growth stimulation.

T47-D cells, kindly donated by Dr. A. Purohit (Imperial College of London), were grown in the standard conditions reported in the literature⁶⁹ and for the experiments the medium was slightly modified. For the experiment, the medium was supplemented with charcoal stripped serum instead of normal fetal calf serum in order to eliminate the interference from the hormones present in the normal serum. However, to have a better

understanding of the behaviour of the cells, the experiments were repeated in both charcoal stripped serum supplemented medium (CSM) and normal serum supplemented medium (NM). A first experiment was set up and **170e**, **170i**, **170q**, **170s** and **163o** were selected as an initial set of inhibitors (Figure 60). For the experiment the concentration of E1 and E2 were set to 0.1 nM because it is reported in the literature to be the concentration that leads to the maximum effects on growth.¹⁵⁸

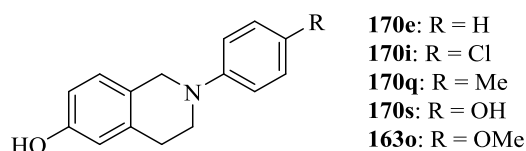


Figure 60. Initial set of compounds used for the screening. Compounds were used as hydrobromide salts except for **163o** which was used as hydrochloride salt.

When the cells were treated with the chosen set of compounds **170s** showed high estrogenicity properties at all concentrations while **163o** was estrogenic only at higher concentrations and the others did not show a significant estrogenic degree (Figure 61).

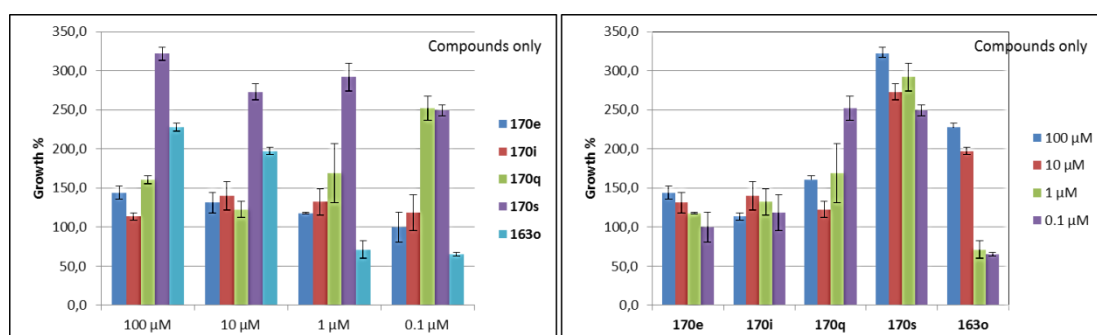


Figure 61. Growth percentage of T47-D cells treated only with the set of THIQs. Growth of cells with the carrier only was arbitrarily set to 100%. On the left graph compounds are grouped by concentration while on the right graph the data are grouped by dose response of each compound. The percentage of inhibition reported were the result of a single experiment in triplicate.

When cells were treated with E2 and the set of compounds, no significant effects were visible. Compounds did not show anti-estrogenic activity and rather show mild estrogenicity at 100 μ M concentration (Figure 62).

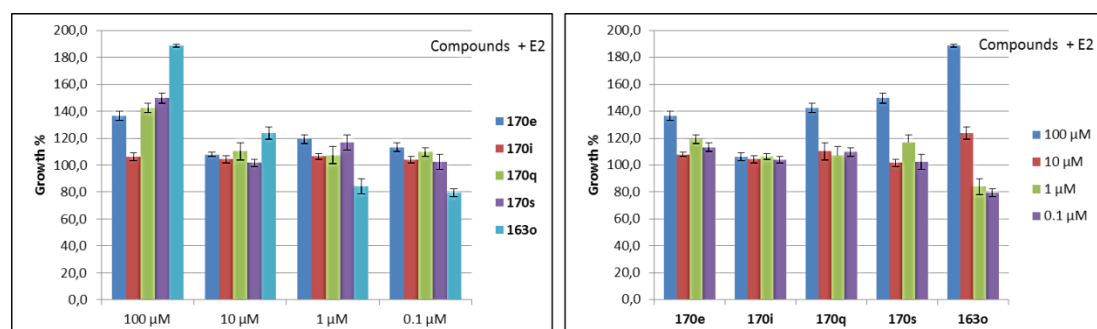


Figure 62. Growth percentage of T47-D cells treated with E2 the set of THIQs. Growth of cells with E2 only was arbitrarily set to 100%. On the left graph compounds are grouped by concentration while on the right graph the data are grouped by dose response of each compound. The percentage of inhibition reported were the result of a single experiment in triplicate.

Similarly, when cells were treated with E1 and the set of compounds no relevant inhibition was observed and only a certain degree of estrogenicity was observed at 100 μM . These results contrasted with the results from the whole cell radiochemical assay which showed for each of them a reasonable percentage of inhibition at 1.0 μM .

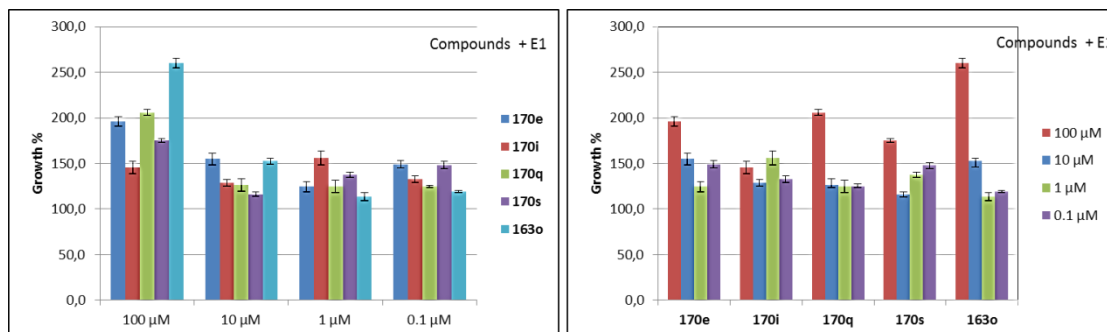


Figure 63. Growth percentage of T47-D cells treated with E1 the set of THIQs. Growth of cells with E1 only was arbitrarily set to 100%. On the left graph compounds are grouped by concentration while on the right graph the data are grouped by dose response of each compound. The percentage of inhibition reported were the result of a single experiment in triplicate.

When the growth of the cells treated with the vehicle only or with E1 or E2 was compared with the growth of untreated cells, a significant discrepancy became visible. In fact, in all the three cases the treated cells had significantly lower growth than the untreated ones albeit the ones treated with E1 or E2 showed higher relative growths than the ones treated with DMSO only (Figure 64). Moreover, comparing the growth of the untreated cells in the three experiment showed a great behavioural variability (Figure 64).

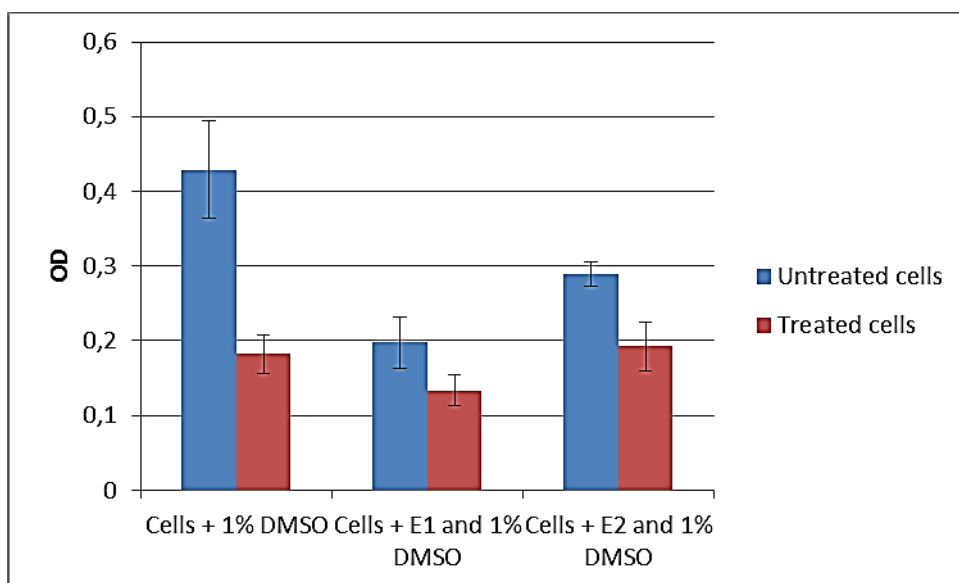


Figure 64. Effect of the vehicle DMSO on the T47-D cell growth. Values are expressed in raw optical density units and are not normalised to emphasise the difference in growth among the three experiments. The percentage of inhibition reported were the result of a single experiment in triplicate. OD = Optical Density

Intrigued by these results the effect of DMSO and the use of ethanol as an alternative vehicle were evaluated. Growth curves of the cells alone or in presence of 1% ethanol with or without E1 or E2 were registered at 2 days intervals. Interestingly, not much difference was visible between the three conditions when NM (graphs C and D, Figure 65) was used while a great stimulation was induced by ethanol when cells were grown in CSM (graphs A and B, Figure 65). It is noteworthy also that no significant stimulation from E1 (graphs A and C, Figure 65) or E2 (graphs B and D, Figure 65) was visible in either media making statistically insignificant the results obtained in the previous experiments about the compounds tested.

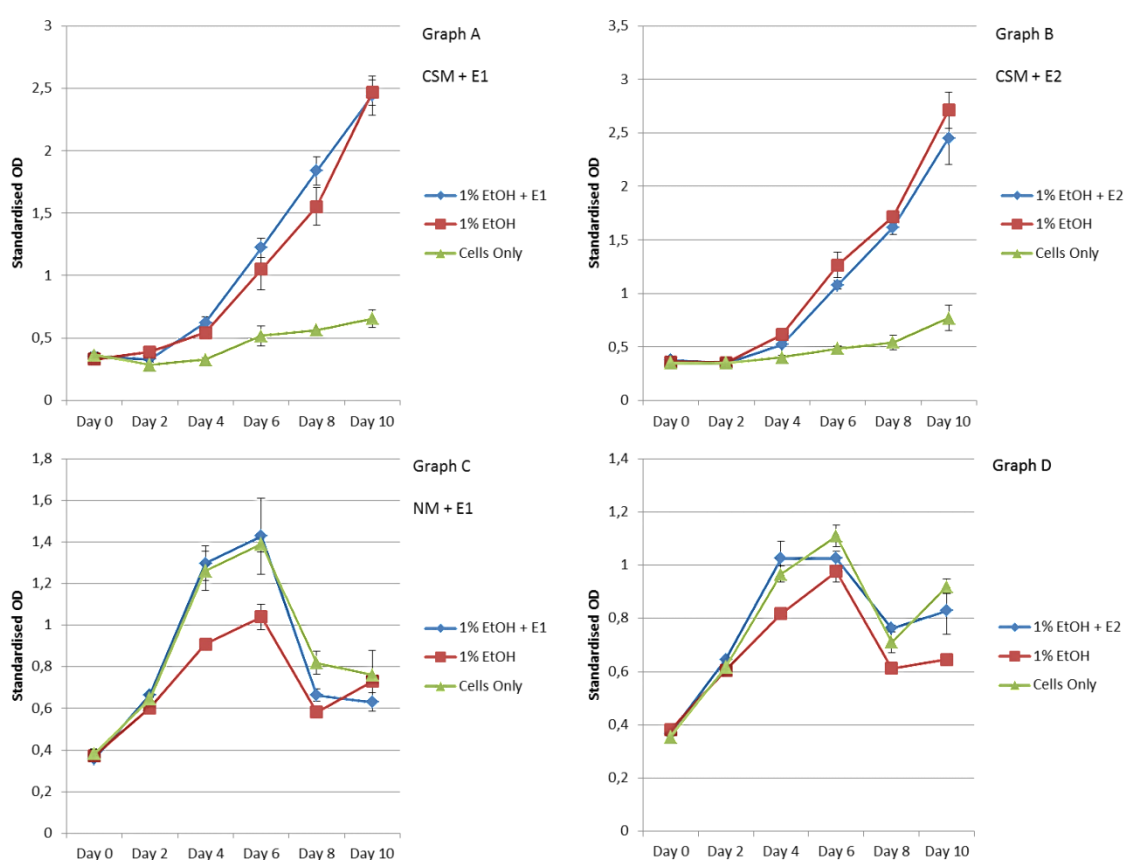


Figure 65. Growth curves of T47-D cells with or without ethanol or either E1 or E2. Graphs A and B refer to cells grown in CSM while graphs C and D refer to cells grown in NM. The percentage of inhibition reported were the result of a single experiment in triplicate. OD = Optical Density

It was not clear why ethanol had such stimulating effect but, after eliminating the possibility of cross contamination repeating the test, the theory that cells were using ethanol as a carbon source became more prominent (1% ethanol correspond to *ca.* 0.17 M). From this point of view, the absence of effect when the NM was used might be explained by the fact that the latter might contain more nutrients than the CSM and then the effect of ethanol became negligible. One problem that could not be addressed was

the exact composition of the CSM. In fact, different batches of serum have different composition and their content is not quantified, but this factor was minimised using the same batch for every experiment.

When the growth of untreated cells was reported in a graph in relation to the passage number it was possible to visualise the change in behaviour over the time (Figure 66). The cells were unsuitable for the purpose of the assay because they did not show any estrogen responsiveness which should be typical of this cell line.

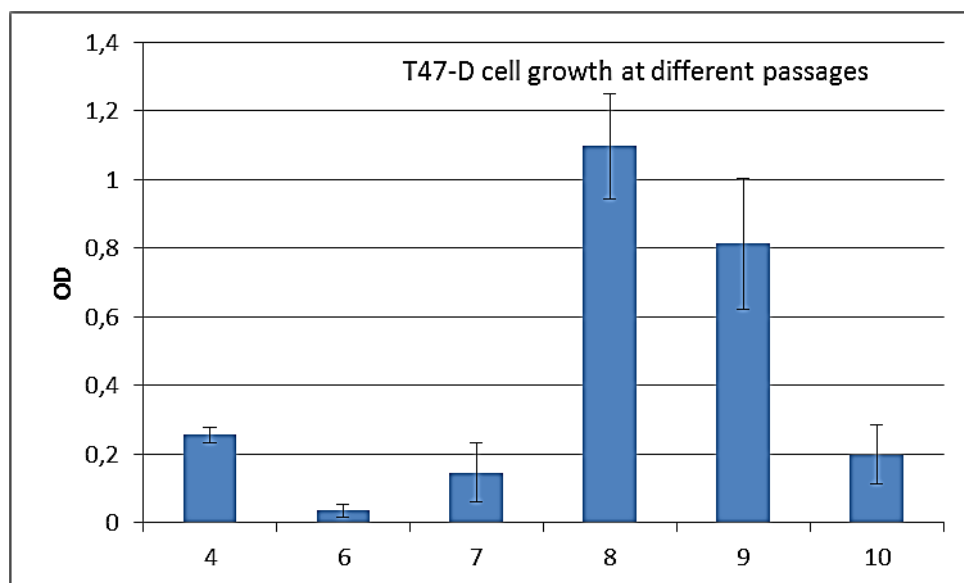


Figure 66. Growth of untreated cells at different passages. On the x axis is reported the number of passages while on the y axis is reported the optical density measured normalised to the reading at day 0. The number of cells seeded was always the same and confirmed by the reading at day 0. The percentage of inhibition reported were the result of a single experiment in triplicate. OD = Optical Density

One last experiment was set up to compare the characteristics of the cells at passage 10 with a new stock of cells at passages 5 and 11 that were taken from the frozen stock. To maximise the information obtained, cells were treated with 1% DMSO or 1% ethanol only or a combination of E1, E2 and 4-hydroxytamoxifen (HO-tam) (graphs A, B and C, Figure 67). HO-Tam is a well-known estrogen receptor (ER) inhibitor¹⁵⁹ and was used in the assay to prove that the growth stimulation from either of the two estrogens, if there was any, was due to ER activation.

In the three cases DMSO had a cytostatic effect while ethanol was stimulating cell growth even though at different degrees among the three experiments. E1 and E2 were not substantially stimulating cell growth compared to the vehicle only. In the late passage of the new stock (graph C, Figure 67) cells were actually showing some inhibitory activities. Similarly, no significant differences were visible between the cells

treated with E1 or E2 only and E1 or E2 with HO-tam, strengthening the hypothesis that cell growth was not stimulated by any ER mediated mechanism.

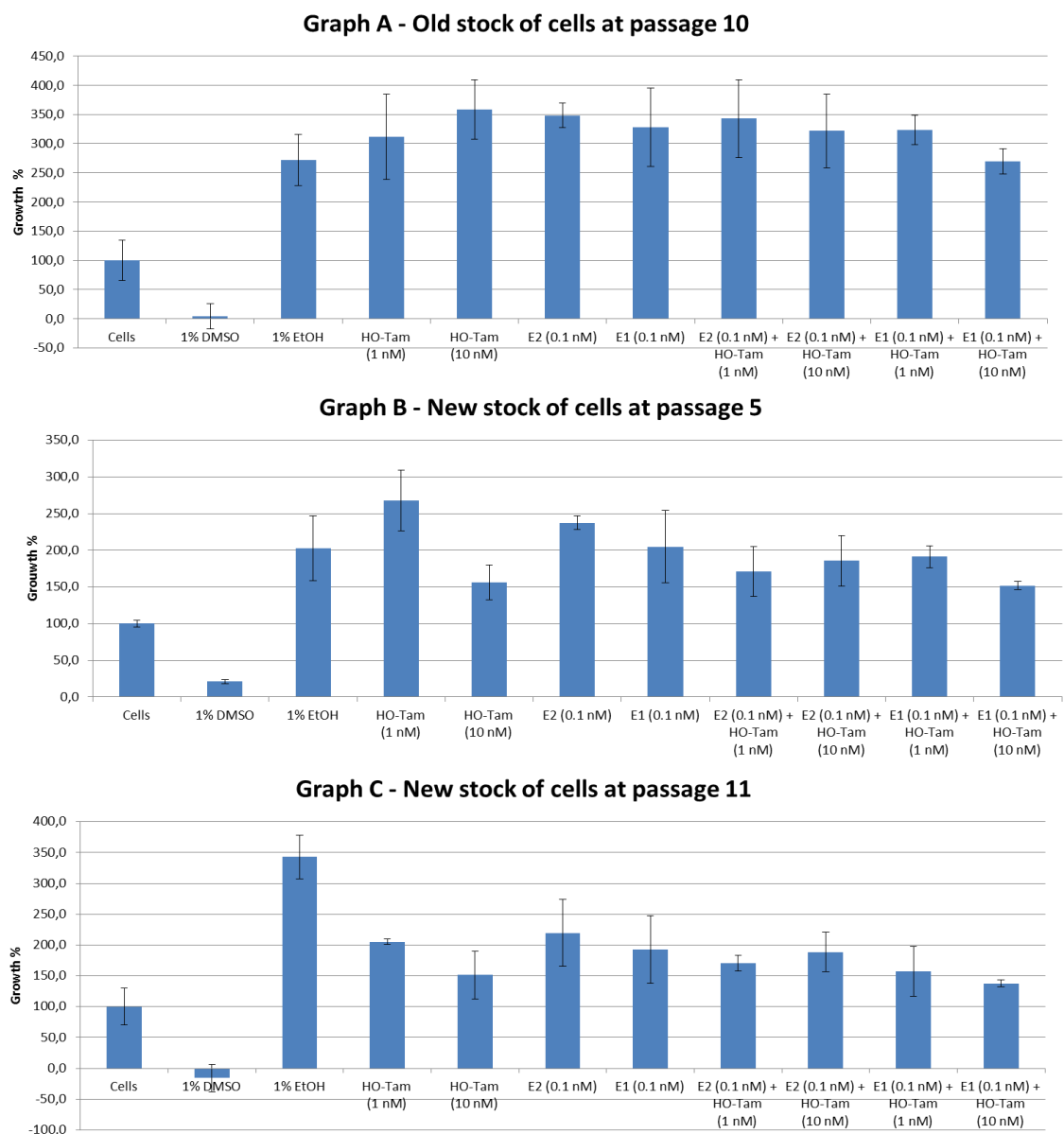


Figure 67. Graph A: cell growth of the original stock of cells used for every experiment previously mentioned. Graph B: early passage of a new stock of cells. Graph C: late passage of the same stock of cells used in graph B. Cells were treated in the same conditions: CSM supplemented with 1% DMSO, 1% ethanol, E1, E2 or HO-tam with or without E1 or E2. The carrier for introducing E1, E2 and HO-tam was ethanol. The growth of untreated cells was arbitrarily set to 100%. The percentage of inhibition reported were the result of a single experiment in triplicate.

A more thorough research in the literature highlighted the fact that T47-D cell line is rather unstable and different phenotypes, if not genotypes, are observed through the time.^{158, 160-162} A paper from Graham *et al.*⁶ even proposed the hypothesis that this cell line could be a good model for the transition from estrogen dependant to estrogen independent status of breast cancer.

It was not possible to carry out a full characterisation of the T47-D cells used but it was concluded that they were unsuitable for the assay proposed and that a fully characterised and guaranteed batch of cells should be used for further experiments.

3.1.5. Structure activity relationship of the synthesised compounds against 17 β HSD1.

Not having access to a reliable in-house screening processes the compounds synthesised were initially tested by our sponsor, Ipsen. When our sponsor could no longer test the compounds it was decided to establish an external collaboration with the group of Prof. Tea Linisnik Rizner. Only a limited selection of compounds (Figure 68, Table 38) could be tested by Prof. Rizner. Compounds were tested at 6.0 μ M for percentage of inhibition against 17 β HSD1 and for the ones showing more than 60% inhibition, the test was repeated at 0.6 μ M. An IC₅₀ value was obtained for the best inhibitor obtained from the tests.

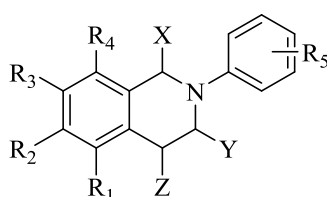


Figure 68. Structure and substitution pattern of the compounds selected and tested against 17 β HSD1. Refer to Table 38 for compound substitution.

Table 38. List of compounds selected for screening against 17 β HSD1. The table reports the substituents and the % inhibition at 6 μ M and 0.6 μ M.

Cmpd.	R ₁	R ₂	R ₃	R ₄	R ₅	X	Y	Z	% Inh. (6 μ M)	% Inh. (0.6 μ M)
163a	H	H	H	H	H	H	H	H	9.3	Nt
163e	H	MeO	H	H	H	H	H	H	27.0	Nt
163q	H	MeO	H	H	4-Me	H	H	H	27.0	Nt
163i	H	MeO	H	H	4-Cl	H	H	H	38.0	Nt
163s	H	MeO	H	H	4-MeO	H	H	H	13.0	Nt
170e	H	OH	H	H	H	H	H	H	45.0	Nt
170q	H	OH	H	H	4-Me	H	H	H	38.0	Nt
170i	H	OH	H	H	4-Cl	H	H	H	64.0	Nt
163o	H	OH	H	H	4-MeO	H	H	H	12.7	Nt
170s	H	OH	H	H	4-OH	H	H	H	42.0	Nt

163t	H	MeO	H	H	3-Cl	H	H	H	33.5	Nt
163v	H	MeO	H	H	2-Cl	H	H	H	25.3	Nt
172	OH	H	H	H	4-Cl	H	H	H	45.4	Nt
171	H	H	OH	H	4-Cl	H	H	H	47.1	Nt
143z	H	H	H	H	4-Cl	H	H	OH	15.7	Nt
163z	H	H	H	H	4-Cl	H	H	H	40.9	Nt
170aa	H	OH	H	H	3,4-Cl ₂	H	H	H	79.8	17.2
170t	H	OH	H	H	3-Cl	H	H	H	65.5	Nt
170u	H	OH	H	H	3-OH	H	H	H	76.2	28.3
167	H	MeO	MeO	H	4-MeO	H	H	H	25.4	Nt
146x	H	MeO	MeO	H	4-MeO	H	H	OH	12.6	Nt
173	H	OH	OH	H	4-OH	H	H	H	0.0	Nt
174	OH	OH	OH	H	4-OH	H	H	H	21.1	Nt
191a	H	OH	H	H	4-Cl	Me	H	H	44.1	Nt
191b	H	OH	H	H	4-Cl	Et	H	H	40.7	Nt
191c	H	OH	H	H	4-Cl	<i>i</i> -Pr	H	H	73.1	10.8
191e	H	OH	H	H	4-Cl	Ph	H	H	90.1	4.7
191f	H	OH	H	H	4-Cl	Bn	H	H	81.0	0.0
143n	H	OH	H	H	4-Cl	H	H	OH	22.3	Nt
145h	Br	H	H	H	H	H	H	OH	47.1	Nt
144h	H	H	Br	H	H	H	H	OH	12.9	Nt
191g	H	OH	H	H	4-Cl	(CH ₂) ₂ Ph	H	H	74.8	11.0
191h	H	OH	H	H	H	Bn	H	H	73.7	10.6
191i	H	OH	H	H	4-OH	Bn	H	H	68.8	24.1
234a	H	OH	H	H	4-Cl	H	Me	H	54.0	Nt
234b	H	OH	H	H	4-Cl	H	Et	H	54.3	Nt
234c	H	OH	H	H	4-Cl	H	H	Me	77.2	19.9
234d	H	OH	H	H	4-Cl	H	H	Et	91.5	45.9
234e	H	OH	H	H	4-Cl	H	H	<i>i</i> -Pr	100.0	60.3
234f	H	OH	H	H	4-Cl	H	H	Bn	84.3	0.0
234h	H	OH	H	H	4-Cl	H	H	Me ₂	80.9	39.6
234i	H	OH	H	H	4-Cl	Bn	H	Me	69.8	23.5
234j	H	OH	H	H	4-Cl	Bn	H	Et	95.1	52.7
234k	H	OH	H	H	4-Cl	Bn	H	Bn	58.6	Nt

Cmpd. = Compound; Nt = not tested; The percentage of inhibition reported were the result of a single experiment in duplicate.

Four non-cyclic compounds were also tested to define the importance of the importance of the THIQ structure (Figure 69, Table 39).

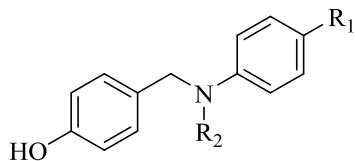


Figure 69. Structure of the non-cyclic compounds tested against 17 β HSD1.

Table 39. Non-cyclic intermediates tested against 17 β HSD1.

Compound	R1	R2	% Inhibition	
			(6 μ M)	(0.6 μ M)
122n	Cl	H	50.2	Nt
122p	OH	H	7.4	Nt
139n	Cl	Pr	70.6	19.1
140n	Cl	<i>i</i> -Bu	86.5	17.3

Nt = not tested; The percentage of inhibition reported were the result of a single experiment in duplicate.

3.1.5.1. Comparison between the assays from Ipsen and Prof. Rizner's group

While the Ipsen assay was a whole cell assay, the one used by Prof. Linisnik Rizner's group used crude cell lysates. In addition, although both were radiochemical assays, Prof. Linisnik Rizner's group used an HPLC combined with a flow radiodetector for the analysis of the samples, while in the assay from Ipsen the E1 and E2 in the assay point were separated by TLC and then quantified separately. Initially the results obtained from Prof. Linisnik Rizner's group were compared with the one previously obtained from Ipsen. The two assay showed to be mostly in line with one another and only compound **163a** laid largely outside the trend (Table 40). Very encouragingly, compounds showed to be significantly active in both whole-cell and cell-lysate assay thus meaning that they could easily penetrate inside the cells.

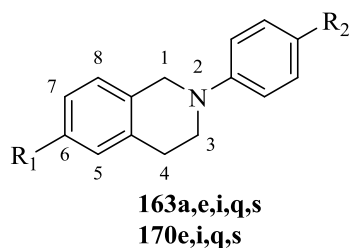


Figure 70. Structure of the compounds tested to evaluate the effect of the nature of groups R₁ and R₂. Refer to Table 40 for R₁ and R₂ descriptions.

Table 40. Comparison of the results from the assays from Ipsen and the assay from Prof. Lanisnik's group.

Compound	R ₁	R ₂	17 β HSD1 (% of inhibition)	
			Ipsen	Lanisnik's group
			@ 1.0 μ M	@ 6.0 μ M
163a	H	H	71.0	9.3
163e	OMe	H	65.5	27.0
163i	OMe	Cl	68.0	38.0
163q	OMe	Me	62.0	27.0
163s	OMe	OMe	32.0	13.0
			@ 750 nM	@ 6.0 μ M
170e	OH	H	52.7	45.0
170i	OH	Cl	77.6	64.0
170q	OH	Me	54.0	38.0
170s	OH	OH	26.7	42.0

The percentage of inhibition reported were the result of a single experiment in duplicate.

3.1.5.2. Effects of the nature of substituents on the *N*-phenyl ring

Considering the R₂ substitution (Figure 70) of the 6-methoxy- series (**163e,i,q,s**), the polar methoxy group showed the least activity (13.0%, **163s**, Table 40). Removing the group increased slightly the activity (27%, **163e**, Table 40) and the introduction of a lipophilic group such as methyl does not vary significantly the activity (27%, **163q**, Table 40) while the lipophilic and electron withdrawing group moderately increased the activity (38%, **163i**, Table 40). Similarly within the 6-hydroxy series (**170e,i,q,s**) the chloro-substituted compound was the most active (64%, **170i**, Table 40) while the other derivatives showed very similar activities (**170e,q,s**, 38%-45%, Table 40). Moreover, the 6-hydroxy (**170e,i,q,s**, Table 40) series was generally more active than the 6-methoxy series (**163e,i,q,s**, Table 40) and as such was selected as standard functionality for further evaluations. This effect could be explained by looking at the structural similarities between E1 and E2 and the two series of compounds (Figure 71).

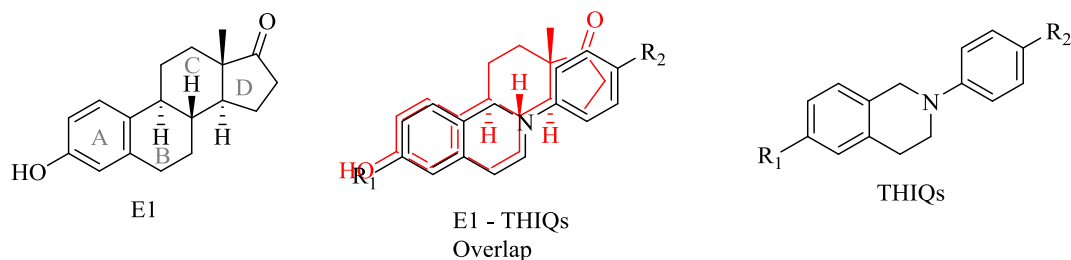


Figure 71. Structures of E1 (on the left) and the tested series of THIQA (on the right). At the centre, the overlap of the two structures highlights the similar spatial disposition of the steroidal phenol and R_1 .

R_1 very likely mimicked the steroidal phenolic group which was fundamental for the activity of estrogens. In fact, androgens and estrogens differ mainly in the structure of the A-ring and the phenolic group is characteristic of all the three estrogens (E1, E2, E3). For this reason, a phenolic group in compounds **170e,i,q,s** might occupy the same region as the phenolic group of E1 and have better affinity for the enzyme.

Other information that it was possible to obtain from the series is the effect of the R_2 substituents with the use of the Craig plot. This graph is obtained by plotting the group lipophilicity (π) against their electronic effects (σ). Hydrogen is considered the reference and sits at the origin of the axis while π and σ are reported along the x axis and y axis, respectively. Apolar groups occupy the right region of the graph while polar groups are on the left side. Groups that are more electron-withdrawing are found in the top region of the graph while groups that are electron donating occupy the bottom part. Looking at the differences among the H, Me and OH substituents one can see how they have rather different π values and σ but all the σ values are lower than or equal to zero. These groups correspond to compounds **170e,q,s** that had very similar activity. Compound **170i** was significantly more active than the other and differed by the presence of a chlorine group. Even though this group had a similar π value to the Me group, it was the only one that had a positive σ value.

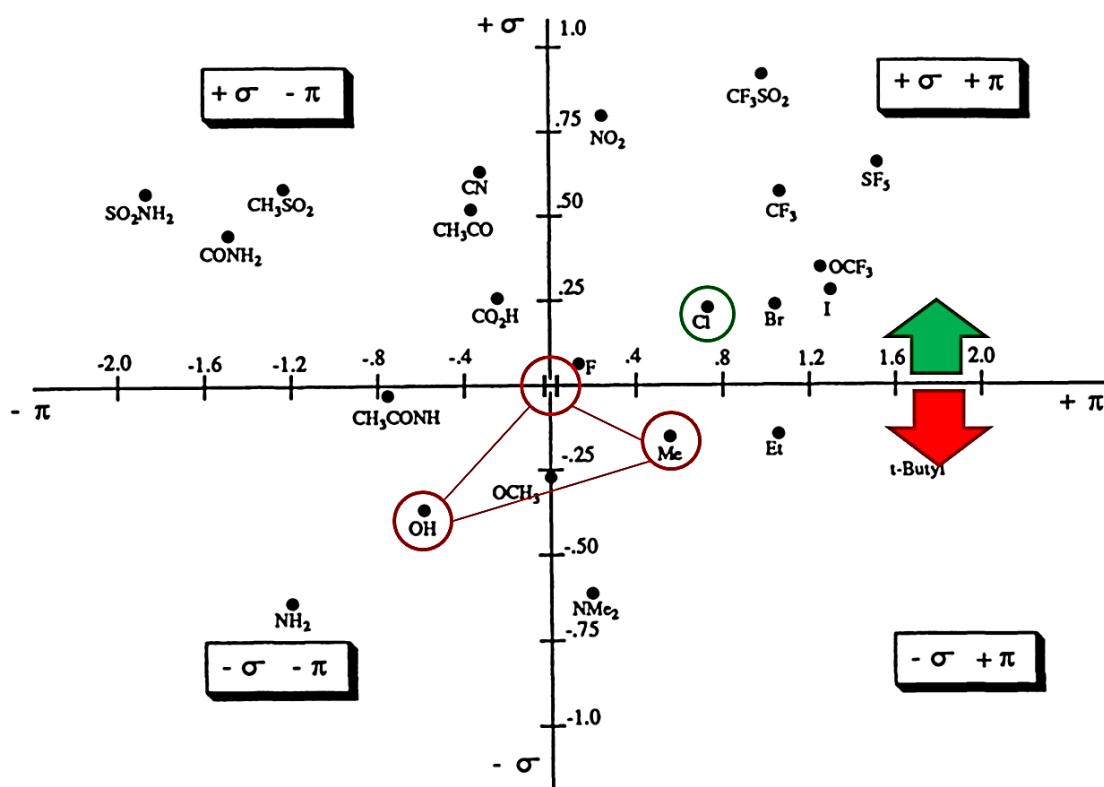


Figure 72. Craig plot with the R_2 substituents (Figure 70) highlighted. In red are circled the groups with minor activity, while in green is circled the Cl which corresponds to the most active substitution. The green and red arrows represent respectively the positive and negative effects of σ on the activity.

The use of the Craig plot made it easy to visualise how the lipophilicity did not influence the activity of the R_2 substituents (Figure 70) while an electron-withdrawing effect enhanced it significantly.

3.1.5.3. Effect of hydroxyl group in position 4, 5, 6 and 7

The effect of the chlorine could be seen by comparing the unsubstituted compound **163a** with **163z** that bore a chlorine group. The latter was *ca.* four times more active and the activity was increased by another 50% by the presence of the hydroxyl group in position 6 (**170i**). If the hydroxyl group was inserted in position 4 (**143n** and **143z**) some activity was lost while the insertion of the same group in position 5 (**172**) or 7 (**171**) led mainly to a retention of activity (Figure 73).

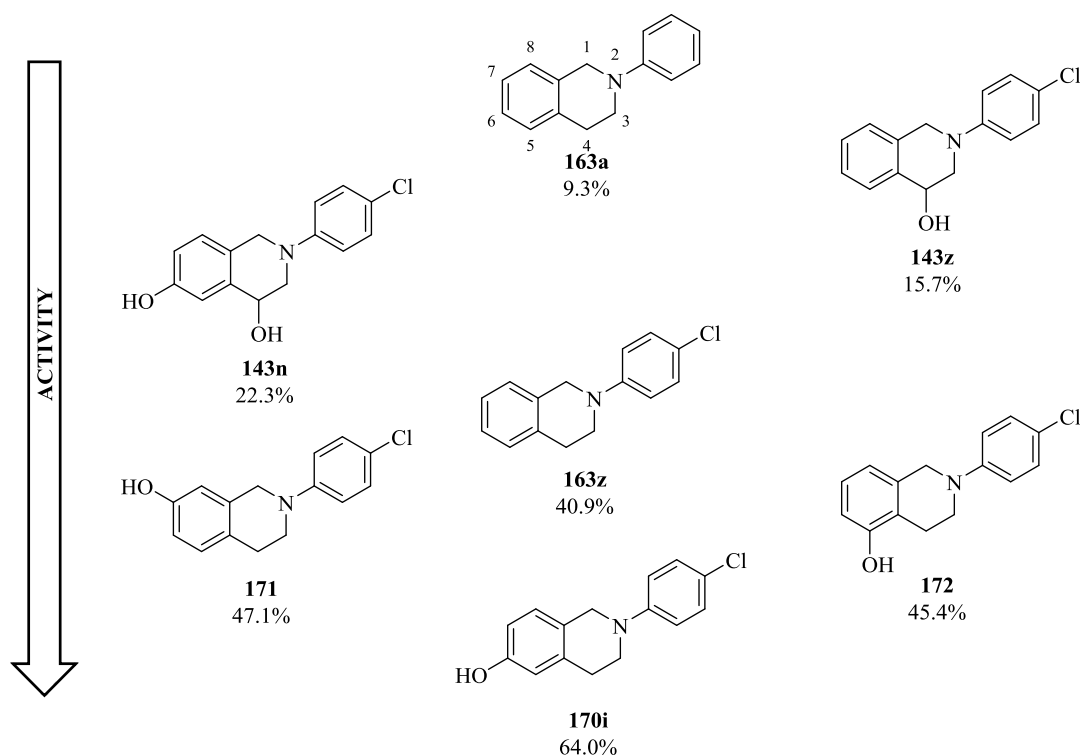


Figure 73. Structure of compounds **143z**, **163a,z**, **170i**, **171** and **172** and relative percentage of inhibition at 6 μ M. Compounds are organised with the weakest inhibitor at the top and the strongest inhibitor at the bottom to better visualise the effect of the different substitution pattern. The percentage of inhibition reported were the result of a single experiment in duplicate.

3.1.5.4. Effect of the position of the substituent on the *N*-phenyl ring

The influence of the position of R_2 was then investigated through compounds **170i,s,t,u,aa** and **163i,t,v** (Figure 74, page 127). Shifting the chlorine from 4' (**170i**, Table 41, page 127) to 3' (**170t**, Table 41, page 127) resulted in a retention of activity which meant that the chlorine in both position had very similar effect. If a chlorine was inserted in both positions (**170aa**, Table 41, page 127), an additive effect was registered even though the resultant effect was smaller than the sum of the two individual effects. Not having access to a 2'-chloro substituted compound in the 6-hydroxy series, the effect of the chlorine in position 2' was evaluated in the 6-methoxy series which had shown lower activities but similar trends. Again, moving the chlorine from 4' (**163i**, Table 41, page 127) to 3' (**163t**, Table 41, page 127) resulted in a retention of activity as seen for compounds **170i** and **170t** but when chlorine was moved to the position 2' (**163v**, Table 41, page 127) the activity registered was lower.

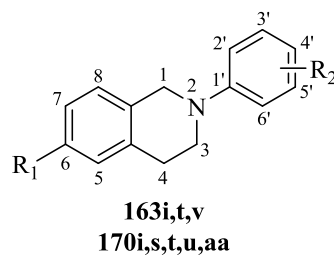


Figure 74. Structure of the compounds tested to evaluate the influence of the position of the group R_2 on the N-phenyl ring. Refer to Table 41 for R_1 and R_2 substitutions.

Table 41. Influence of the position of R_2 on the inhibitory activity against 17 β HSD1.

Compound	R_1	R_2	17 β HSD1 (% of inhibition at 6 μ M)
170i	OH	4-Cl	64.0
170t	OH	3-Cl	65.5
170aa	OH	3,4-Cl ₂	79.8
170s	OH	4-OH	42.0
170u	OH	3-OH	76.2
163i	OMe	4-Cl	38.0
163t	OMe	3-Cl	33.5
163v	OMe	2-Cl	25.3

The percentage of inhibition reported were the result of a single experiment in duplicate.

The loss of activity when a group was introduced in position 2' can be explained considering the effect of such substitution in the 3D structure of the molecule which was substantially flat (image B, Figure 75) but the steric effect introduced by groups in position 2' (image A, Figure 75) would lead to a twisting in the $C_{1'}$ -N bond which would consequently result in a loss of planarity.

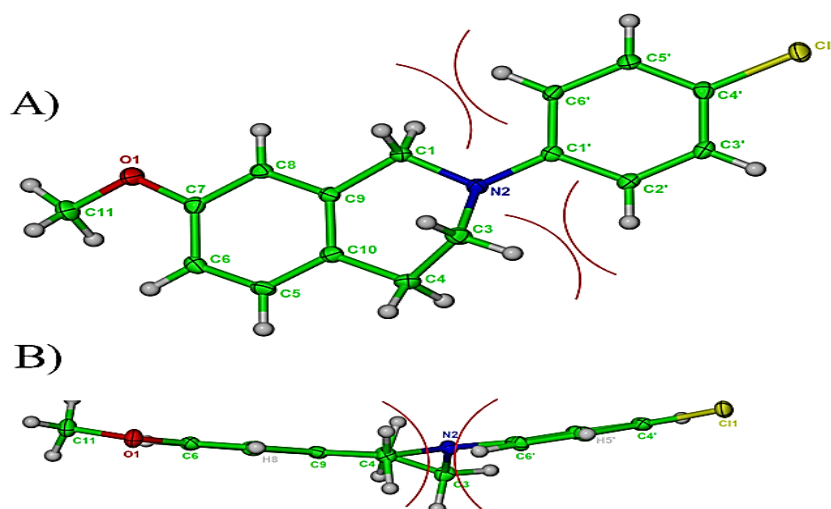


Figure 75. Crystal structure of compound **164j** (Table 17, page 67) which show the planarity of the molecule; A) Top view; B) Side view; In red are marked the negative steric interactions that might arise when a bulky substituent is introduced in position 2' (or 6').

When the effect of the hydroxyl group was considered, shifting it from position 4' to 3' resulted in almost a two-fold increased activity. Superimposition of the minimised 3D model of E2 with the THIQ core showed how closely related the group in position 3' overlapped with the 17 β -hydroxyl group of E2 (Figure 76).

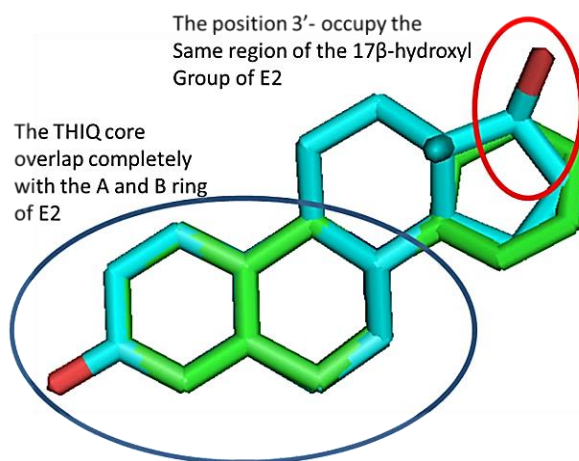


Figure 76. Superimposition of the minimised 3D structure of E2 and the core structure of THIQ. The key points are circled and explained in the picture.

3.1.5.5. Effect of multiple substituents in positions 4, 5, 6 and 7 of the THIQ ring

The effect of multiple polar groups in positions 4, 5, 6, and 7 led to contrasting results. Compound **167** (Figure 77), bearing two methoxy groups in position 6 and 7, was slightly more active than compound **163s** (Figure 77), which only had one methoxy group in position 6. However, the activity was lowered by an additional hydroxyl group in position 4, such as in **146x** (Figure 77).

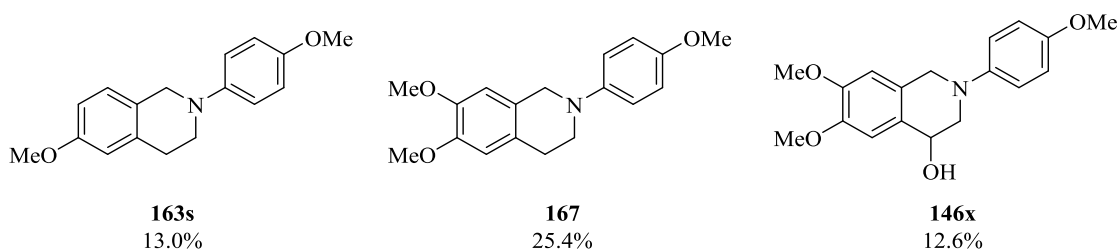


Figure 77. Structure of compounds **163s**, **167** and **146x** with relative percentage of inhibition at 6 μ M. The percentage of inhibition reported were the result of a single experiment in duplicate.

Conversely, when a second hydroxyl group was introduced in position 7, such as in compound **173** (Figure 78), the activity was completely lost compared to compound **170s** (Figure 78) that bore one single hydroxyl group in position 6 and was partially restored by the introduction of a third hydroxyl group in position 5 (compound **174**, Figure 78). It appeared that even if position 6 was the favoured for the hydroxyl group,

the same group in position 5 could still exert a positive effect while position 7 did not tolerate the group at all.

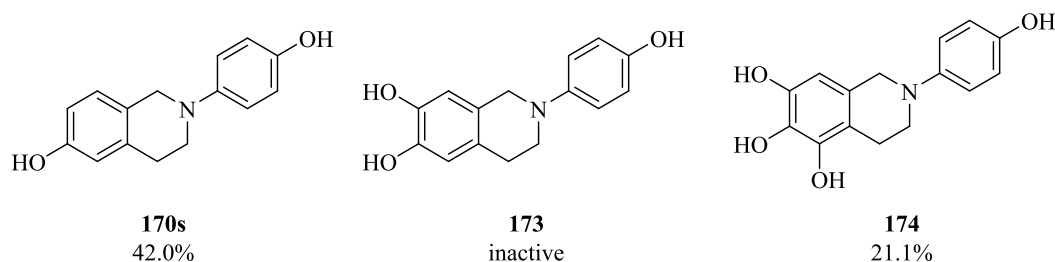


Figure 78. Structure of compounds **170s**, **173** and **174** with relative percentage of inhibition at 6 μ M. The percentage of inhibition reported were the result of a single experiment in duplicate.

This discrepancy might suggest that position 7 did not tolerate hydrogen bond donor but a hydrogen bond acceptor was beneficial. An alternative explanation might be that the hydroxyl derivative **170s** (Figure 78) and the methoxy derivative **163s** (Figure 77) had two different binding modes and thus two different structure activity relationships.

Interesting results were also found when the polar hydroxyl group on the THIQ ring was substituted by the hydrophobic bromine as in compounds **144h** and **145h** (Figure 79). Even if both compounds bore a hydroxyl group in position 4 which should lead to a loss of activity as observed for compounds **143n**, **143z** (Figure 73, page 126) and **146x** (Figure 77, page 128), they were still more active than the parent unsubstituted compound **163a** (Figure 79). Between the two positions, it appeared that position 5 favoured the presence of the lipophilic group more than position 7.

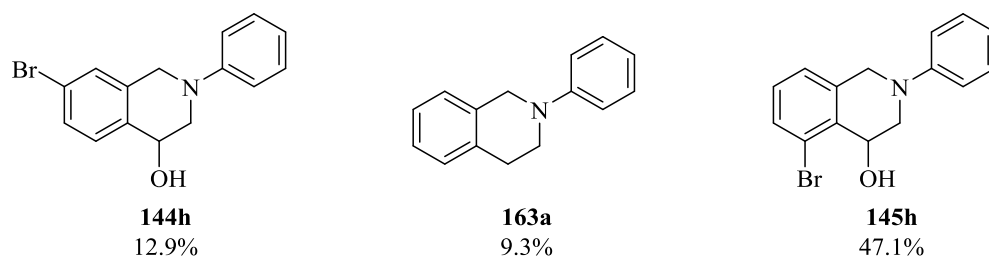


Figure 79. Structure of compounds **144h**, **145h** with relative percentage of inhibition at 6 μ M compared with compound **163a**. The percentage of inhibition reported were the result of a single experiment in duplicate.

3.1.5.6. Effect of substitution in position 1

When a methyl or ethyl group was introduced in position 1 of compound **170i** (Figure 80, Table 42), such as for compounds **181a** and **181b** (Figure 80, Table 42), the activity of the compound was lowered but an isopropyl group (**181c**, Figure 80, Table 42) increased the activity above that for the parent compound **170i** (Figure 80, Table

42). The activity was increased further by the introduction of a phenyl group, as for **181e** (Figure 80, Table 42), reaching 90.1% of inhibition at 6 μ M. While introducing a one or two carbon long linker (**181f** and **181g**, respectively, Figure 80, Table 42) decreased the activity sequentially. Unexpectedly, the trend was reversed when the most potent compounds were tested at 0.6 μ M giving compounds **181g** and **181c** (Figure 80, Table 42) as the most potent with *ca.* 11% of inhibition each while compound **181e** showed only *ca.* 5% inhibition and **181f** was completely inactive.

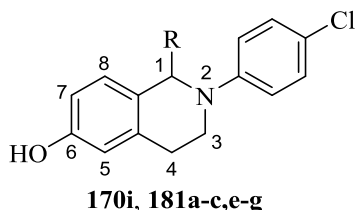


Figure 80. Structure of the compounds tested to evaluate the influence of the substituent R in position 1. Refer to Table 42 for R substitutions.

Table 42. Influence of the substituent in position 1 on the inhibitory activity against 17 β HSD1.

Compound	R	17 β HSD1	
		(% of inhibition at 6 μ M)	(% of inhibition at 0.6 μ M)
170i	H	64.0	Nt
181a	Me	44.1	Nt
181b	Et	40.7	Nt
181c	<i>i</i> -Pr	73.1	10.8
181e	Ph	90.1	4.7
181f	CH ₂ Ph	81.0	Inactive
181g	(CH ₂) ₂ Ph	74.8	11.0

Nt = Not tested at this concentration; The percentage of inhibition reported were the result of a single experiment in duplicate.

3.1.5.7. Effect of substitution on the *N*-phenyl ring for the 1-substituted THIQs

To understand if the binding mode was changed due to the introduction of group with high steric requirement and to be sure that the substitution on the *N*-phenyl ring was still the appropriate one, the activity of compound **181f** (Figure 81, Table 43) was compared to the one of compounds **181h** and **181i** (Figure 81, Table 43) which respectively lack the chlorine group and bore a hydroxyl in place of the chlorine.

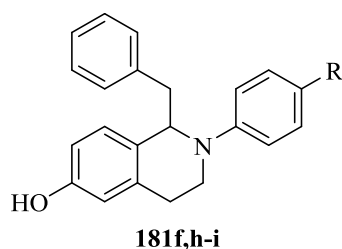


Figure 81. Structure of the 1-benzyl substituted compounds **181f,h-i**. Refer to Table 43 for R substitutions.

Table 43. Influence of the *N*-phenyl substituent on the activity of compounds **181f,h-i**.

Compound	R	17βHSD1	
		(% of inhibition at 6 μM)	(% of inhibition at 0.6 μM)
181f	Cl	81.0	Inactive
181h	H	73.7	10.6
181i	OH	68.9	24.1

The percentage of inhibition reported were the result of a single experiment in duplicate.

3.1.5.8. Effect of substitution in position 3

Substituents in position 3 slightly lowered the activity of the compounds **234a** and **234b** (Figure 82) when compared with the unsubstituted **170i** although this was independent of the size of the substituent.

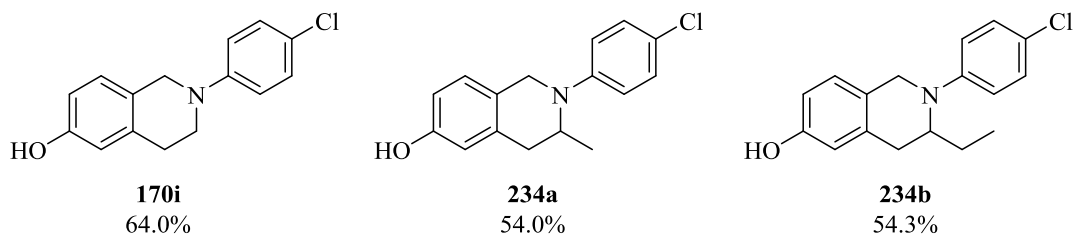


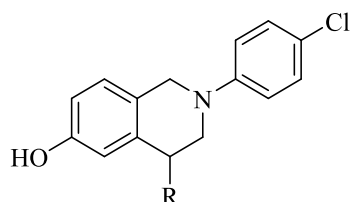
Figure 82. Structure of 3-substituted compounds **234a-b** and their relative percentage of inhibition at 6 μM in comparison with the unsubstituted compound **170i**. The percentage of inhibition reported were the result of a single experiment in duplicate.

3.1.5.9. Effect of substitution in position 4

Very interesting results were obtained investigating the effect of substitution in position 4 with sequentially larger groups. In this position Me, Et and *i*-Pr (**234c**, **234d** and **234e**, respectively, Figure 83, Table 44) increased substantially the activity up to a complete inhibition at 6 μM for compound **234e** (Figure 83, Table 44). Compound **234e** was the most active among the tested compounds and showed an IC₅₀ value of 336 nM.

Compound **234f** (Figure 83, Table 44) bearing a benzyl group was less active than compound **234e** (Figure 83, Table 44) even though it was still more active than the

unsubstituted compound **170i**. When the compounds were tested at 0.6 μM the difference in activity among the compounds was emphasised and moving from Me to *i*-Pr the activity had a three-fold increment and compound **234h** (Figure 83, Table 44), which was only marginally more active than **234c** (Figure 83, Table 44) at 6 μM , was twice as active than it at 0.6 μM .



170i, 234c-f,h

Figure 83. Structure of 4-substituted compounds **234c-f,h** and the parent unsubstituted compound **170i**. Refer to Table 44 for R substitution.

Table 44. Influence of the substituent in position 4 on the activity of compounds **234c-f,h** compared with the activity of the unsubstituted compound **170i**.

Compound	R	17 β HSD1	
		(% of inhibition at 6 μM)	(% of inhibition at 0.6 μM)
170i	H	64.0	Nt
234c	Me	77.2	19.9
234d	Et	91.5	45.9
234e	<i>i</i> -Pr	100	60.3
234f	Bn	84.3	Inactive
234h	(Me) ₂	80.9	39.6

Nt = not tested at this concentration; The percentage of inhibition reported were the result of a single experiment in duplicate.

Another important consideration that has not been done yet is that all the chiral compounds were tested as racemic mixtures and the two enantiomers might have different inhibitory activities one to another. Comparing the activities of **234c** and **234h** (Figure 84) might not be unreasonable to think that one enantiomer of **234c** (Figure 84) might be inactive or significantly less active than the other one. In fact, if that would be the case, the racemate that would obviously contain only 50% of one enantiomer and should be less active than the single enantiomer. Compound **234h** contained the group of both enantiomers (Figure 84) at the same time and thus had 100% content of each enantiomer. However, this was a mere speculation and a chiral resolution of the racemate would be necessary in order to disclose the true activity of each enantiomer.

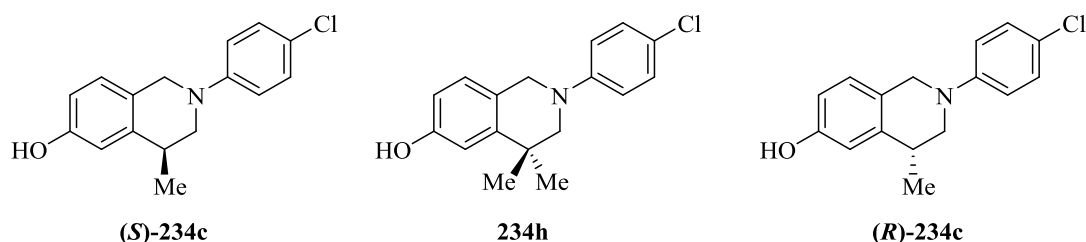


Figure 84. Relationship between **234c** and **234h**. **234h** possess the groups of both enantiomer of **234c** at the same time. The percentage of inhibition reported were the result of a single experiment in duplicate.

3.1.5.10. Effect of disubstitution in position 1 and 4

The effect of the substituent in position 4 could be seen also in the series of 1,4-disubstituted compounds **234i-k** (Table 45). Even if compounds such as **181f** (Table 43, page 131), bearing a benzyl group in position 1 have proved inactive at 0.6 μ M, and the *N*-aryl substitution has proved to be worse than others (**181h-i**, Table 43, page 131), nevertheless compounds **234i-j** (Table 45) have shown good activity even at 0.6 μ M.

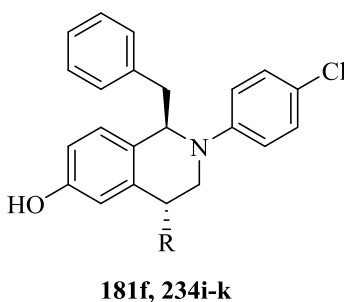


Figure 85. Structure of 1,4-disubstituted compounds **234i-k**. Refer to Table 45 for R substitution. Only one of the two enantiomers has been drawn.

Table 45. Effect of the substituent in position 4 on the activity of compounds **234i-k**.

Compound	R	17 β HSD1 (% inhibition)	
		@ 6 μ M	@ 0.6 μ M
181f	H	81.0	Inactive
234i	Me	69.8	23.5
234j	Et	95.1	52.7
234k	Bn	58.6	Nt

Nt = Not tested at this concentration; The percentage of inhibition reported were the result of a single experiment in duplicate.

3.1.5.11. Comparison between THIQs and the open ring analogues

When comparing the THIQs derivatives **170i,s** (Figure 86) with the respective benzyranilines **122n,p** (Figure 86) it was noteworthy how, when the substituent on the

aniline was a chlorine (**122n**, Figure 86), the THIQ ring was not essential for a good activity even if the rigidity introduced by that ring led to a slight increase in activity. When the aniline ring was substituted with a hydroxyl group (**122p**, Figure 86) the effect of the THIQ ring was even more marked. Furthermore, even though compounds **234c** and **139n** (Figure 86) had the same potency also at 0.6 μ M, the benzyaniline **140n** (Figure 86) was significantly less active than the parent THIQ **234h** (Figure 86). Thus, the presence of the THIQ ring was indeed beneficial and its effect became even more important for the 1-, 2- or 3-substituted derivatives.

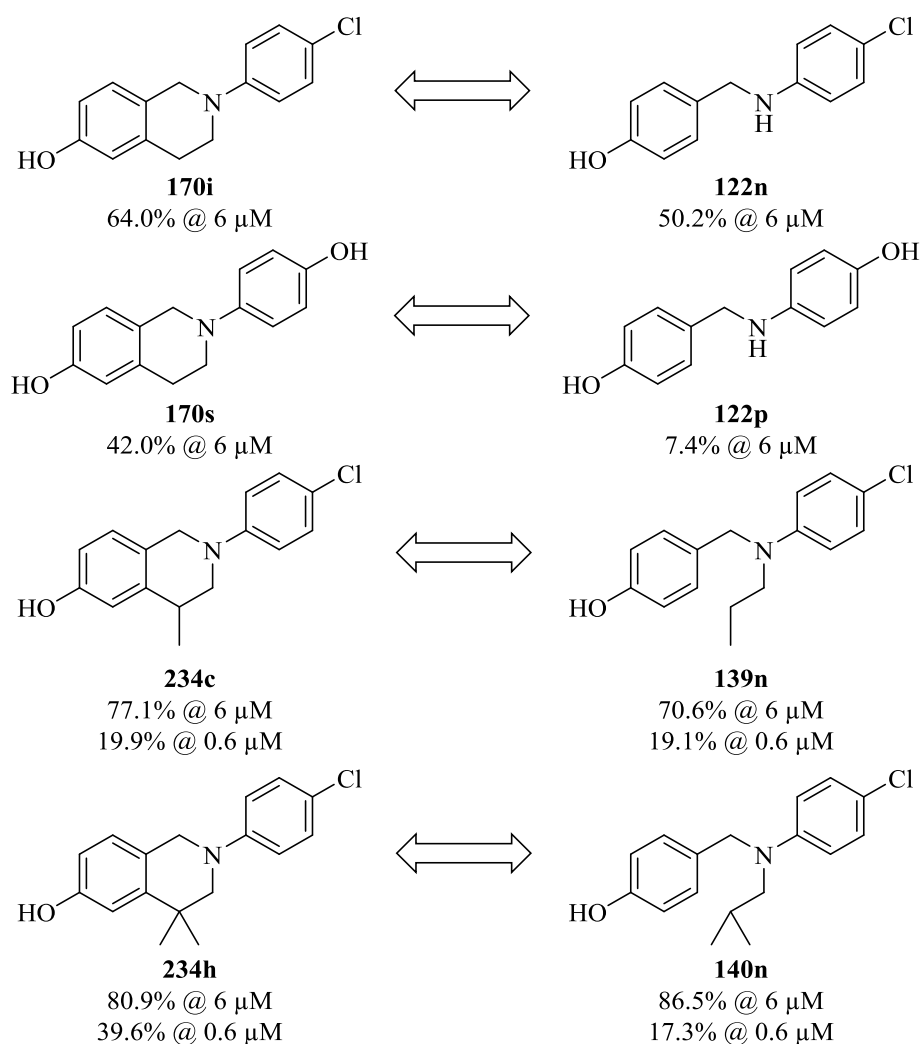


Figure 86. Structure and activity of the THIQs **170i,a** and **234c,h** compared with the open ring analogues **139n** and **140n**. The percentage of inhibition reported were the result of a single experiment in duplicate.

3.1.6. Conclusions

Though the development of a colourimetric assay did not give the desired results further insight is necessary to determine the reason for which steroidal compounds and the synthesised THIQs give different results. The co-crystallisation of the enzyme with

one of the known inhibitors did not give the expected results but additional optimisation of the crystallisation conditions might lead to more successful results. In addition, when a strong enough crystal is obtained, the desired inhibitor can be soaked into the enzyme alone or with the co-factor to give the desired crystal structure.

The reproduction of a qualitative assay for the evaluation of 17 β -HSD1 inhibition, as well as estrogenicity and general cytotoxicity, suffered from the quality of the cell line used. The experiments performed to address the problems encountered during the development of the assay led to the conclusion that the cell line phenotypic or genetic instability was to be considered the most probable issue. Nevertheless, to confirm this hypothesis, the experiments would need to be repeated with a certified batch of cells.

Even if the attempt to develop an in-house assay did not give the desired results, the compounds synthesised could be tested initially by our sponsor and subsequently through a collaboration with Prof. Lanisnik's group. The whole cell assay performed at Ipsen laboratories not only proved that the compounds tested could inhibit the enzyme but also demonstrated that they can penetrate inside the cell where the enzyme resides.

Even though the assay performed by the group of Prof. Lanisnik was less sensitive than the one performed at Ipsen, the two assays largely agreed in the relative rank ordering of the compounds. From the data obtained through the testing it was possible to draw some preliminary conclusions about the structure activity relationship of the compounds.

The hydroxyl group in position 6 was a key feature and position 5 accepted both lipophilic or hydrophilic groups but more examples are needed to clarify if this happened *via* the same binding mode (Figure 87). Position 7 had been shown to accept both lipophilic or hydrophilic groups but a polar group in this position occasionally led to a loss of activity (Figure 87). Position 2' should be free of any substituent probably because the planarity of the molecule plays an important role in the interaction of the compound with the enzyme (Figure 87). Position 4' and 3' benefited from electron withdrawing groups but also a hydroxyl group in position 3' seemed to have a beneficial effect (Figure 87). Small lipophilic groups in position 3 had been tolerated with only a minor loss in activity. Position 1 suffered from small lipophilic substitution but activity was increased again with larger groups (Figure 87). This could probably occur through a change in binding mode because when large lipophilic substituent were present in

position 1, the preference for the substitution in position 4' changed from the chlorine to the hydroxyl group (Figure 87). Position 4 benefited from lipophilic groups and a hydroxyl group in this position was not tolerated (Figure 87). The effect seemed to be size dependant and in the series tested the isopropyl group gave the best results. Geminal disubstitution in this position gave positive results as well as removing the chirality and further examples in this direction should be considered. The introduction of an ethyl group in position 4 was able to restore the activity lost through the insertion of a benzyl group in position 1 (Figure 87). Lastly, though it was not essential for the activity in some cases, the THIQ ring exerted a positive effect on the activity of the compounds probably by both forcing the planarity of the molecule and directing the substituents in positions 1, 3 and 4 (Figure 87).

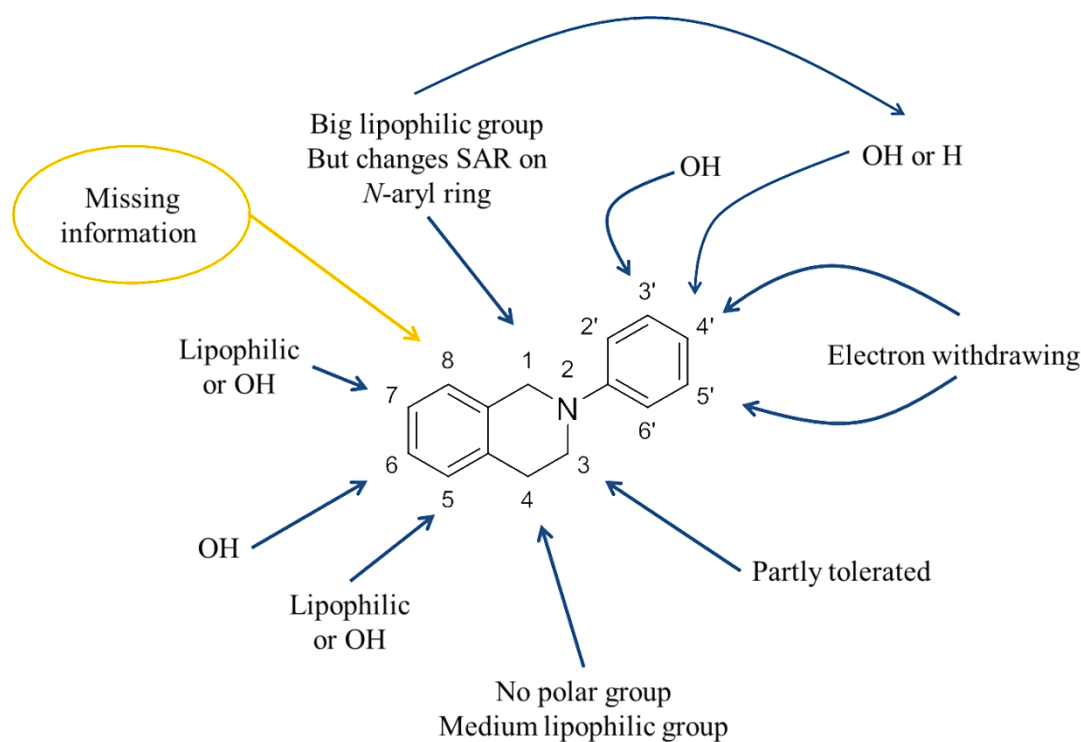


Figure 87. Picture of the SAR conclusions for each position of the THIQ.

The strongest inhibitor was compound **234e** with an IC_{50} of 336 nM and a good chemico-physical profile. Even if the Lipinski's rule of five is probably the most known, there are several rules that attempt to describe the drug-likeness of compounds using different parameters. These rules are not absolute but are useful for the developer to keep under control some important properties that have been too often considered secondary e.g. solubility. Compound **234e** satisfied most of the rules and only slightly exceeded the limits for LogP and LogD (Table 46). This is something important to

consider when the next series of compounds is developed and introduction of polar substituents such as, for instance, a hydroxyl group in position 3' should be evaluated.

Table 46. Chemicophysical descriptors of compound **234e** and relative compliance with some drug-like rules.

Properties	Lipinski's rules	Veber rules	Ghose rules	Lead-likeness	234e
Molecular mass	≤ 500		$160 \leq X \leq 480$	≤ 450	301.81
LogP	≤ 5		$-0.4 \leq X \leq 5.6$		5.24 ¹
H-bond donor	≤ 5			≤ 5	1
H-bond acceptor	≤ 10			≤ 8	2
Number of atoms			$20 \leq X \leq 70$		41
Molecular refractivity			$40 \leq X \leq 130$		89.35 ²
Number of rotatable bonds		≤ 10		≤ 10	2
Polar surface area		≤ 140			23.47
LogD _{7.4}				$-4 \leq X \leq 4$	5.24 ¹
Number of rings				≤ 4	3

In green are highlighted the rules that are being fulfilled while in red are highlighted the rules that are exceeded.

¹CLogP and CLogD, Calculated with MarvinSketch; ²Molecular refractivity, Calculated with ChemBioDraw.

3.2. Estrogen receptor-related receptor α (ERR α)

ERR α is a constitutively active transcription factor and as such, differently from enzymes, does not have substrates and products. ERR α requires the binding of the co-activator PGC1 α to initiate DNA transcription. The commercially available LanthaScreenTM ERR α TR-FRET co-activator assay kit upon this interaction is based. Among the commercially available assays, the kit was chosen for its cost effectiveness and its practicality and was used to measure the activity of the synthesised compounds against ERR α .

3.2.1. LanthaScreen™ TR-FRET assay description

The assay is a Time Resolved Fluorescence Resonance Energy Transfer (TR-FRET) which is an advanced method of FRET. In normal fluorescence, the chromophore absorbs light and an electron passes from a ground state to an excited state at a higher energy level. After vibrational relaxation the electron pass from the ground state of a higher energy level to the ground state of a lower energy level and emits a photon (A, Figure 88). In FRET, two different chromophores are involved and the chromophore that absorbs the light (donor) transfers its energy to a nearby chromophore (acceptor). The excited acceptor subsequently emits a photon when returning to its ground state generating the fluorescence (B, Figure 88).

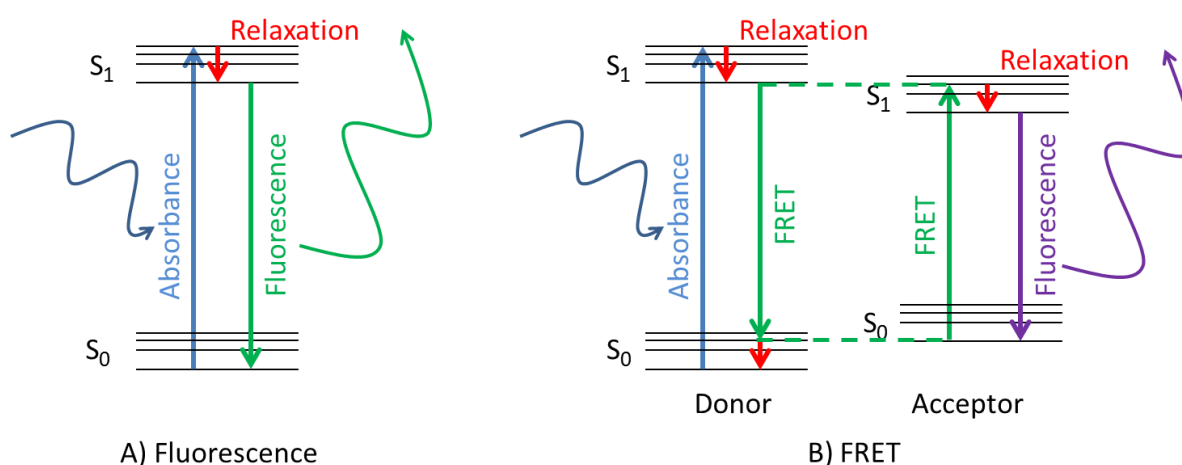


Figure 88. Scheme representing the excitation-relaxation steps coupled with the absorbance and emission of light in normal fluorescence (A) and in FRET (B).

The transfer of energy between the donor and the acceptor occurs without radiation in a range smaller than the wavelength and for this reason FRET phenomena require the two chromophores to be near in space, usually 1-10 nm. Therefore, FRET can be used to determine the proximity of two chromophores, as it can only occur when the donor and acceptor are close to each other.

TR-FRET is an enhancement of a standard FRET, with the main difference that there is a time lapse between the excitation and the reading of the fluorescence generated. In fact, in standard FRET the time between absorption and final emission is on the nanosecond timescale while TR-FRET works on the microsecond timescale. Because interference from auto-fluorescent compounds and scattered light is on the nanosecond timescale, these might generate inaccuracies in a FRET assay. The removal of these interferences in TR-FRET leads to a cleaner background and to more accurate readings.

To be able to measure fluorescence after such a delay, special long-lifetime lanthanide chelates are used as donor species.

The $\text{ERR}\alpha$ assay uses an anti-GST antibody labelled with terbium (Tb) and a GST-labelled $\text{ERR}\alpha$ while the cofactor $\text{PGC-1}\alpha$ is labelled with fluorescein. The antibody binds to GST and $\text{ERR}\alpha$ binds $\text{PGC-1}\alpha$ bringing terbium and fluorescein near enough in space for the energy transfer. Terbium absorbs light at 340 nm and transfers the energy to fluorescein which in return emits light at 520 nm (left side of Figure 89). When an inverse agonist binds to the receptor, it induces a conformational change that displaces $\text{PGC-1}\alpha$. Because the acceptor is no longer in proximity to the terbium, this cannot transfer its energy and as a consequence emits light at 495 nm (right side of Figure 89).

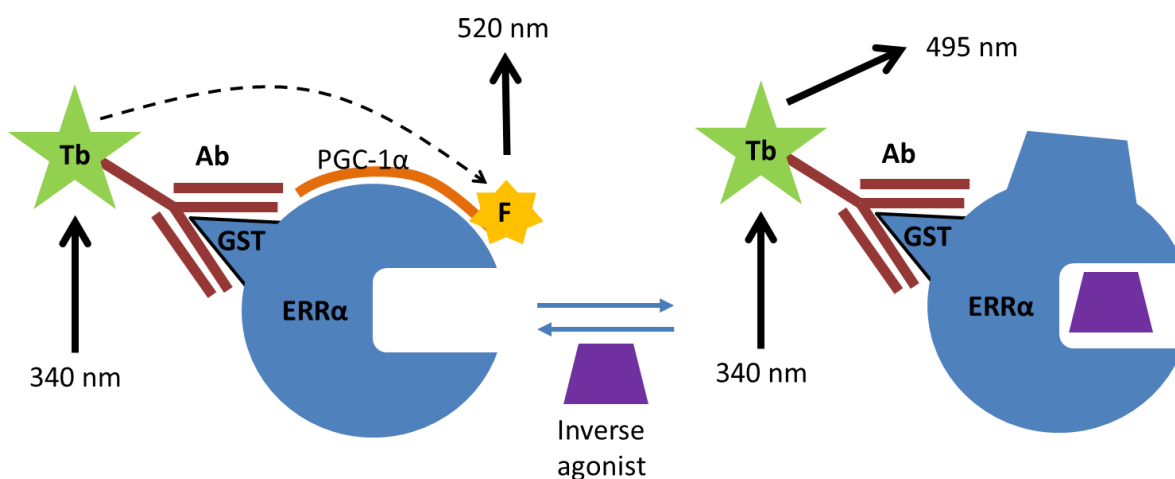


Figure 89. Representation of the $\text{ERR}\alpha$ TR-FRET assay. The binding of the inverse agonist induces a conformational change that displaces $\text{PGC-1}\alpha$ and prevent the energy transfer from Terbium to fluorescein. Tb = Terbium; Ab = Terbium labelled Anti-GST antibody; GST = Glutathione *S*-transferase; F = Fluorescein.

The ratio of the emission at the two wavelengths (520:495) is used to quantify the activity of the inverse agonist.

An initial binding saturation analysis of the known inverse agonist XCT790 **103** (Figure 27, page 36) was performed to decide the concentration of full activity. The assay is carried out in 384 well plates, the total volume per well is 20 μL and no mixing is performed. The same plate was read after 1 h and 2 h since its preparation and both readings resulted in very similar graphs (Figure 90). After two hours the readings were more homogenous leading to smaller error bars and this was probably due to the longer equilibration time. As the equilibration is left to simple diffusion, a longer time might be needed for a more uniform reading from the different wells. It was therefore decided to proceed with reading after two hours to minimise internal errors. The control

compound XCT790 **103** was used at 10 μM which showed to be the binding saturation concentration (Figure 90). The compounds synthesised were initially evaluated at 10 μM but the activity registered was too low (Table 48, page 14). Therefore, it was decided to increase the concentration to 100 μM to be able to deduce some basic SAR information for the set of compounds. The EC_{50} of XCT790 was 242 nM and to have a reference that was in the same range of the tested compounds diethylstilbestrol **97** (DES, Figure 24, page 35) was also evaluated in the same assay. DES resulted in $64.2\% \pm 8.4\%$ efficacy at 100 μM which was closer to the values for the tested compounds.

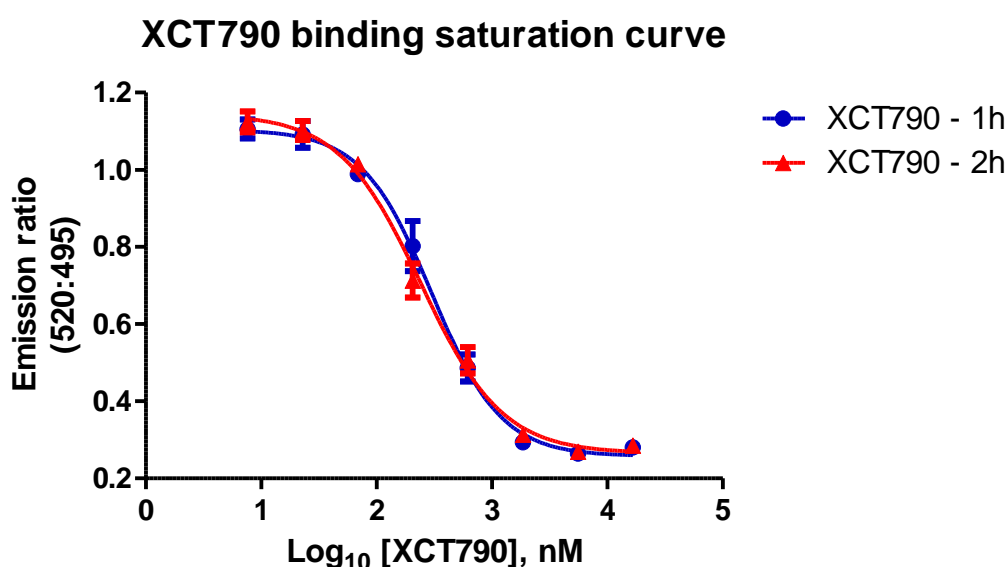


Figure 90. Binding saturation curve of $\text{ERR}\alpha$ for XCT790. In blue are reported the values read after 1 h and in red the values read after 2 h. Complete binding occurred at a Log_{10} value of 4, which corresponds to a concentration of 10^4 nM or 10 μM . The EC_{50} calculated from the curve is 242 nM and was in line with the values reported in the assay protocol. Values reported were obtained with a single experiment in four replicates.

3.2.2. Structure activity relationship of the synthesised compounds against $\text{ERR}\alpha$.

All the compounds that were synthesised and obtained in a sufficient amount were tested for activity against $\text{ERR}\alpha$ (Figure 91, Table 47). Compounds were tested for percentage of inhibition at 100 μM . DES (Figure 24, page 35) was also tested as reference compound for both structural similarities and potency.

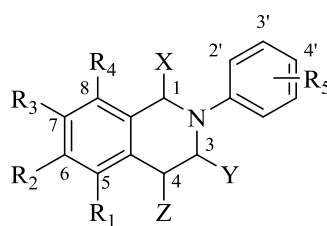


Figure 91. Structure and substitution pattern of the compounds selected and tested against ERR α . Refer to **Table 47** for compound substitution.

Table 47. Full list of compounds tested against ERR α , their relative substitutions and their activity expressed in percentage of inhibition.

Cmpd	R ₁	R ₂	R ₃	R ₄	R ₅	X	Y	Z	% Efficacy (100 μ M)
163a	H	H	H	H	H	H	H	H	-7.8 \pm 3.2
163e	H	MeO	H	H	H	H	H	H	-4.7 \pm 2.7
163q	H	MeO	H	H	4-Me	H	H	H	-5.4 \pm 0.6
163i	H	MeO	H	H	4-Cl	H	H	H	-4.3 \pm 1.6
163s	H	MeO	H	H	4-MeO	H	H	H	30.5 \pm 0.4
170e	H	OH	H	H	H	H	H	H	18.8 \pm 1.3
170q	H	OH	H	H	4-Me	H	H	H	15.1 \pm 3.0
170i	H	OH	H	H	4-Cl	H	H	H	24.8 \pm 1.9
163o	H	OH	H	H	4-MeO	H	H	H	13.9 \pm 3.9
170s	H	OH	H	H	4-OH	H	H	H	33.7 \pm 2.5
163u	H	MeO	H	H	3-MeO	H	H	H	8.9 \pm 2.7
163w	H	MeO	H	H	2-MeO	H	H	H	-9.2 \pm 4.8
163t	H	MeO	H	H	3-Cl	H	H	H	2.5 \pm 5.4
163v	H	MeO	H	H	2-Cl	H	H	H	-1.3 \pm 4.4
165j	MeO	H	H	H	4-Cl	H	H	H	10.9 \pm 3.7
164j	H	H	MeO	H	4-Cl	H	H	H	6.7 \pm 3.0
172	OH	H	H	H	4-Cl	H	H	H	22.7 \pm 3.2
171	H	H	OH	H	4-Cl	H	H	H	6.8 \pm 3.4
163aa	H	MeO	H	H	3,4-Cl ₂	H	H	H	6.7 \pm 4.2
163r	H	MeO	H	H	4-Et	H	H	H	-4.1 \pm 2.8
143z	H	H	H	H	4-Cl	H	H	OH	-8.8 \pm 1.5
163z	H	H	H	H	4-Cl	H	H	H	1.9 \pm 1.9
166i	H	MeO	H	H	4-Cl	H	Me	H	0.3 \pm 4.7
170aa	H	OH	H	H	3,4-Cl ₂	H	H	H	21.6 \pm 1.8
170t	H	OH	H	H	3-Cl	H	H	H	21.6 \pm 2.0

170u	H	OH	H	H	3-OH	H	H	H	-6.6 ± 1.9
167	H	MeO	MeO	H	4-MeO	H	H	H	-1.9 ± 3.0
168	MeO	MeO	MeO	H	4-MeO	H	H	H	11.7 ± 1.1
146x	H	MeO	MeO	H	4-MeO	H	H	OH	10.5 ± 1.1
173	H	OH	OH	H	4-OH	H	H	H	-9.2 ± 0.4
174	OH	OH	OH	H	4-OH	H	H	H	-0.9 ± 2.8
166s	H	MeO	H	H	4-MeO	H	Me	H	-20.5 ± 2.8
176x	H	MeO	MeO	H	4-MeO	H	H	OBn	37.3 ± 1.4
181a	H	MeO	H	H	4-Cl	Me	H	H	12.4 ± 1.2
181b	H	MeO	H	H	4-Cl	Et	H	H	16.8 ± 1.2
181e	H	MeO	H	H	4-Cl	Ph	H	H	12.8 ± 1.0
181f	H	MeO	H	H	4-Cl	Bn	H	H	19.7 ± 4.4
190f	H	H	H	MeO	4-Cl	Bn	H	H	6.5 ± 0.6
191a	H	OH	H	H	4-Cl	Me	H	H	9.6 ± 2.0
191b	H	OH	H	H	4-Cl	Et	H	H	4.5 ± 0.8
191c	H	OH	H	H	4-Cl	<i>i</i> -Pr	H	H	46.7 ± 1.6
191e	H	OH	H	H	4-Cl	Ph	H	H	17.2 ± 1.4
191f	H	OH	H	H	4-Cl	Bn	H	H	53.2 ± 0.7
143n	H	OH	H	H	4-Cl	H	H	OH	18.4 ± 3.7
175n	H	OBn	H	H	4-Cl	H	H	OBn	17.3 ± 3.6
145h	Br	H	H	H	H	H	H	OH	2.6 ± 0.9
144h	H	H	Br	H	H	H	H	OH	9.4 ± 0.4
181g	H	MeO	H	H	4-Cl	(CH ₂) ₂ Ph	H	H	16.0 ± 3.6
190h	H	H	H	MeO	H	Bn	H	H	21.1 ± 2.7
181h	H	MeO	H	H	H	Bn	H	H	19.2 ± 3.6
190i	H	H	H	MeO	4-MeO	Bn	H	H	30.0 ± 1.7
190i	H	MeO	H	H	4-MeO	Bn	H	H	18.2 ± 3.6
166i	H	MeO	H	H	4-Cl	H	Me	H	13.7 ± 2.0
211b	H	MeO	H	H	4-Cl	H	Et	H	20.9 ± 3.5
228a	H	MeO	H	H	4-Cl	H	H	Me	12.9 ± 6.6
228b	H	MeO	H	H	4-Cl	H	H	Et	17.6 ± 1.6
228c	H	MeO	H	H	4-Cl	H	H	<i>i</i> -Pr	23.3 ± 1.3
228e	H	MeO	H	H	4-Cl	H	H	2-(MeO)Et	21.6 ± 2.4
228d	H	MeO	H	H	4-Cl	H	H	Bn	15.8 ± 0.8
228f	H	MeO	H	H	4-Cl	H	H	Me ₂	9.2 ± 1.9

<i>trans</i> - 232a	H	MeO	H	H	4-Cl	Bn	H	Me	8.6 ± 0.7
<i>trans</i> - 232b	H	MeO	H	H	4-Cl	Bn	H	Et	17.3 ± 3.1
<i>trans</i> - 233b	H	H	H	MeO	4-Cl	Bn	H	Et	20.2 ± 3.9
<i>trans</i> - 232d	H	MeO	H	H	4-Cl	Bn	H	Bn	10.7 ± 2.5
191g	H	OH	H	H	4-Cl	(CH ₂) ₂ Ph	H	H	35.5 ± 1.4
191h	H	OH	H	H	H	Bn	H	H	49.1 ± 1.6
191i	H	OH	H	H	4-OH	Bn	H	H	35.8 ± 1.2
234a	H	OH	H	H	4-Cl	H	Me	H	17.8 ± 2.1
234b	H	OH	H	H	4-Cl	H	Et	H	14.8 ± 1.3
234c	H	OH	H	H	4-Cl	H	H	Me	44.8 ± 2.5
234d	H	OH	H	H	4-Cl	H	H	Et	37.3 ± 3.7
234e	H	OH	H	H	4-Cl	H	H	<i>i</i> -Pr	33.5 ± 1.2
234f	H	OH	H	H	4-Cl	H	H	Bn	49.8 ± 1.1
234h	H	OH	H	H	4-Cl	H	H	Me ₂	30.7 ± 1.5
<i>trans</i> - 234i	H	OH	H	H	4-Cl	Bn	H	Me	79.2 ± 0.7
<i>trans</i> - 234j	H	OH	H	H	4-Cl	Bn	H	Et	35.7 ± 4.0
<i>trans</i> - 234k	H	OH	H	H	4-Cl	Bn	H	Bn	14.9 ± 3.0
DES									64.2 ± 8.4

The percentage of efficacy reported were the result of a single experiment in four replicates.

3.2.2.1. Effects of the nature of substituents on the *N*-phenyl ring

Introducing a methoxy group in position 6 of the inactive compound **163a** (Figure 92, Table 48) did not lead to an active compound (**163e**, Figure 92, Table 48). Further addition of lipophilic groups, i.e. methyl, ethyl and chlorine in position 4' (**163q**, **163r** and **63i**, respectively, Figure 92, Table 48), did not increase the activity but the introduction of a second methoxy group in this position (**163s**, Figure 92, Table 48) gave an active compound with an efficacy of 30.5%. With a hydroxyl group in position 6 and no substituent in position 4' (**170e**, Figure 92, Table 48), the efficacy was *ca.*19%. Introducing a methyl or a methoxy group in position 4' (**170q** and **163o**, respectively, Figure 92, Table 48) led to a mild loss in activity. In contrast, a chlorine in the same position 4' (**170i**, Figure 92, Table 48) led to a mild increase in activity compared to

170e (Figure 92, Table 48) and the activity was even higher when a hydroxyl group in position 4' was present instead (**170s**, Figure 92, Table 48).

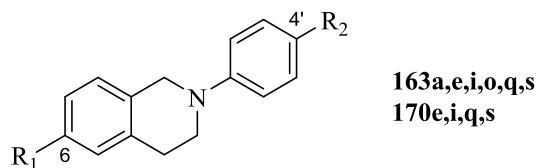


Figure 92. Structure of the compounds tested to evaluate the effect of the nature of groups R_1 and R_2 . Refer to **Table 48** for R_1 and R_2 descriptions.

Table 48. Results of the two series of 4'-substituted compounds tested against $ERR\alpha$.

Compound	R_1	R_2	% of efficacy	
			@ 100 μ M	@ 10 μ M
163a	H	H	Inactive	Inactive
163e	OMe	H	Inactive	Inactive
163q	OMe	Me	Inactive	Inactive
163r	OMe	Et	Inactive	Inactive
163i	OMe	Cl	Inactive	Inactive
163s	OMe	OMe	30.5 ± 0.4	Inactive
170e	OH	H	18.8 ± 1.3	Inactive
170q	OH	Me	15.1 ± 3.0	6.0 ± 2.0
170i	OH	Cl	24.8 ± 1.9	8.1 ± 2.4
163o	OH	OMe	13.9 ± 3.9	Inactive
170s	OH	OH	33.7 ± 2.5	13.5 ± 7.4

The percentage of efficacy reported were the result of a single experiment in four replicates.

Using a Craig plot to visualise the effects of substituents in position 4', it became clear how the 6-methoxy and 6-hydroxy series presented some differences. For the 6-methoxy series, the dimethoxy compound **163s** (Figure 92, Table 48) was the only one active and it appeared from the graph how this could depend on both negative σ and π values.

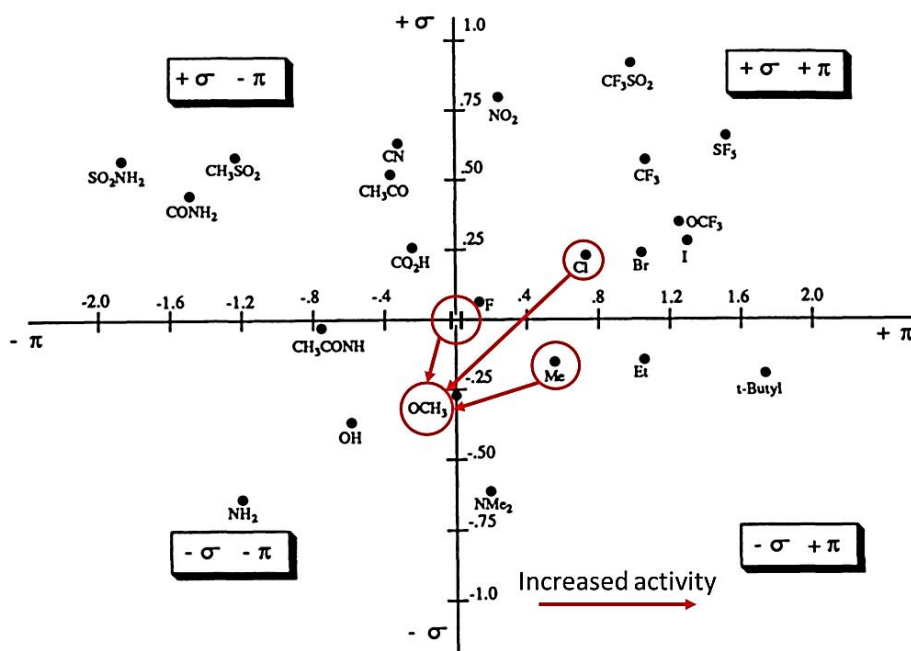


Figure 93. Craig plot graph used to highlight the effects of substitution in position 4' of the 6-methoxy series. Arrows point towards the group with the next higher activity.

When the effects of the substitution on position 4' of the hydroxyl series were visualised on the Craig plot, a complete different trend was observed (Figure 94). The efficacy increased with the increasing values of σ and π effects but the introduction of a hydroxyl group (**170s**, Figure 92, Table 48), which had completely different σ and π values led to a further increase in activity. It is reasonable to assume that the latter compound might have a different binding mode than the others of its series.

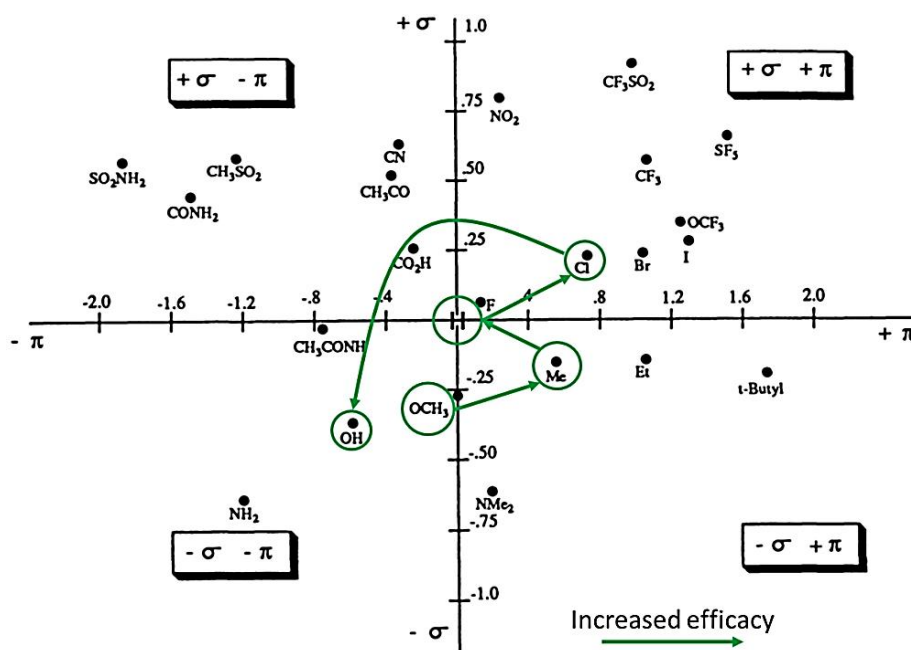


Figure 94. Craig plot graph used to highlight the effects of substitution in position 4' of the 6-hydroxy series. Arrows point towards the group with the next higher activity.

3.2.2.2. Effect of the position of the substituent on the *N*-phenyl ring

For the 6-methoxy series, moving the methoxy group from position 4' (**163s**, Table 49) to 3' (**163u**, Table 49) drastically reduced the activity and, if further shifted to position 2' (**163w**, Table 49), it was completely lost. In addition, for the 6-methoxy series, compounds with a chlorine in position 4', 3' or 2' (**163i**, **163t** and **163v**, Table 49) were inactive and also the introduction of a second chlorine (**163aa**, Table 49) led to an inactive compound. Similarly, for the 6-hydroxy series, moving the hydroxyl group from position 4' (**170s**, Table 49) to position 3' (**170u**, Table 49) made the compound completely inactive. Conversely, in the 6-hydroxy series, when the chlorine was moved from position 4' (**170i**, Table 49) to position 3' (**170t**, Table 49) or if a second chlorine was introduced in position 3' (**170aa**, Table 49) the activity did not vary greatly.

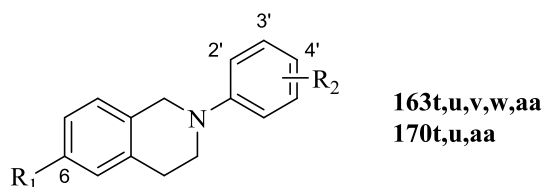


Figure 95. Structure of the compounds tested to evaluate the effect of the position of substituent R_2 on the *N*-phenyl ring. Refer to **Table 49** for R_1 and R_2 descriptions.

Table 49. Effect of the position of substituent R_2 on the activity of the two series of compounds tested.

Compound	R_1	R_2	% of efficacy (@ 100 μ M)
163s	OMe	4-OMe	30.5 \pm 0.4
163u	OMe	3-OMe	8.9 \pm 2.7
163w	OMe	2-OMe	Inactive
163i	OMe	4-Cl	Inactive
163t	OMe	3-Cl	Inactive
163v	OMe	2-Cl	Inactive
163aa	OMe	3,4-Cl ₂	Inactive
170i	OH	4-Cl	24.8 \pm 1.9
170t	OH	3-Cl	21.6 \pm 2.7
170aa	OH	3,4-Cl ₂	21.6 \pm 2.7
170s	OH	4-OH	33.7 \pm 2.5
170u	OH	3-OH	Inactive

The percentage of efficacy reported were the result of a single experiment in four replicates.

3.2.2.3. Effect of substituents in positions 4, 5, 6, 7 and 8 of the THIQ ring

Compound **163i** (Table 50) with a methoxy group in position 6 and a chlorine in position 4' was inactive. If the 6-methoxy group was moved to position 7 (**164j**, Table 50) no activity was gained but if the methoxy group was moved to position 5 (**165j**, Table 50) then a moderate increase in activity was observed. In contrast, compound **170i** (Table 50) with a hydroxyl group in position 6 was active. The activity was retained if the hydroxyl group was moved to position 5 (**172**, Table 50). However, if the hydroxyl group was moved to position 7 (**171**, Table 50) or to position 4 (**143z**, Table 50), the activity was lost. Removing the hydroxyl group led also to an inactive compound (**163z**, Table 50).

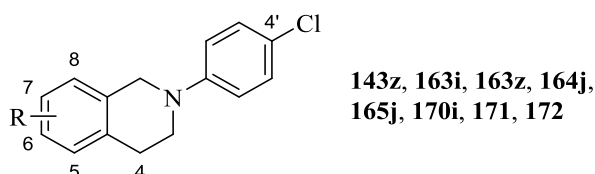


Figure 96. Structure of the compounds used to evaluate the effect of substituents in positions 4, 5, 6 and 7. Refer to **Table 50** for R description.

Table 50. Effect on the activity of the position of the substituent R on the THIQ ring.

Compound	R	% of efficacy (@ 100 μ M)
165j	5-OMe	10.9 \pm 3.7
163i	6-OMe	Inactive
164j	7-OMe	Inactive
143z	4-OH	Inactive
172	5-OH	22.7 \pm 3.2
170i	6-OH	24.8 \pm 1.9
171	7-OH	Inactive
163z	H	Inactive

The percentage of efficacy reported were the result of a single experiment in four replicates.

3.2.2.4. Effect of multiple substituents in positions 4, 5, 6 and 7 of the THIQ ring

The activity of compound **163s** (Table 51), which had a methoxy group in position 4' of the *N*-phenyl ring and a single methoxy on the THIQ ring in position 6, was 30.5%. This activity was completely lost when a second methoxy group was introduced in position 7 of the THIQ ring (**167**, Table 51) and only partly restored when either a third methoxy group in position 5 (**168**, Table 51) or a hydroxyl group in position 4 (**146x**,

Table 51) were introduced. However, the activity was greater than for compound **163s** with the introduction of a benzyloxy group in position 4 (**176x**, Table 51). It seemed that the benzyloxy group in position 4 was able to overcome the negative effect of the methoxy group in position 7 and would have thus been interesting to know the activity of a compound similar to **176x** (Table 51) but lacking the methoxy group in position 7. Conversely, the activity of compound **170s** (Table 51) was again lost when a second hydroxyl group was introduced in position 7 (**173**, Table 51) but it was not restored by the introduction of a third hydroxyl group in position 5 (**174**, Table 51).

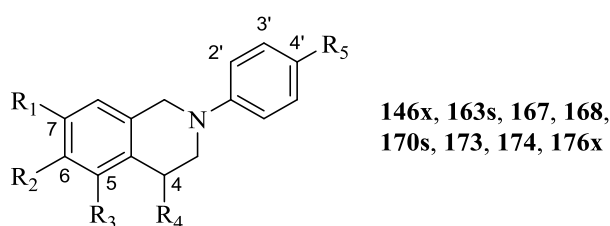


Figure 97. Structure of the compounds used to evaluate the effect of multiple substituents in positions 4, 5, 6 and 7. Refer to **Table 51** for R₁, R₂, R₃, R₄ and R₅ description.

Table 51. Effect of the presence of multiple substituents on the THIQ ring.

Compound	R ₁	R ₂	R ₃	R ₄	R ₅	% of efficacy
163s	H	OMe	H	H	OMe	30.5 ± 0.4
167	OMe	OMe	H	H	OMe	Inactive
168	OMe	OMe	OMe	H	OMe	11.7 ± 1.1
146x	OMe	OMe	H	OH	OMe	10.5 ± 1.1
176x	OMe	OMe	H	OBn	OMe	37.3 ± 1.4
170s	H	OH	H	H	OH	33.7 ± 2.5
173	OH	OH	H	H	OH	Inactive
174	OH	OH	OH	H	OH	Inactive

The percentage of efficacy reported were the result of a single experiment in four replicates.

3.2.2.5. Effect of hydroxyl in position 4

When a second hydroxyl group was introduced in position 4 of compound **170i** (**143n**, Figure 98) the activity was somewhat lower and very interestingly when both hydroxyl group were benzylated (**175n**, Figure 98) no change in activity was observed. Although the activity of compound **175n** was very low, the small amount of activity meant that the binding pocket was large enough to accommodate this compound.

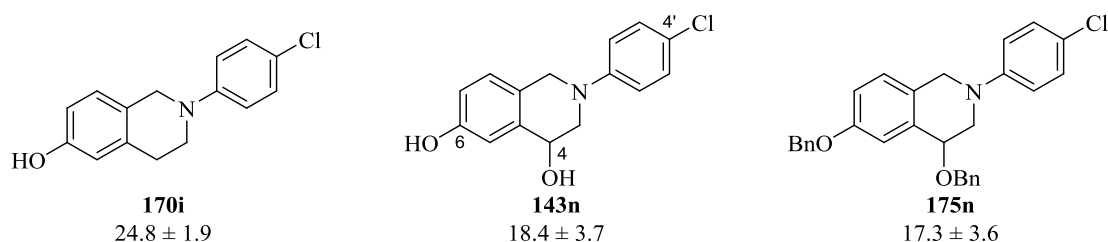


Figure 98. Structure and relative efficacy of compounds **170i**, **143n** and **175n**. Despite the diverse substitution, the three compounds show very similar activities. The percentage of efficacy reported were the result of a single experiment in four replicates.

Compound **145h** (Figure 99) was completely inactive but moving the bromine from position 5 to position 7 led to a slightly active compound (**144h**, Figure 99). Unfortunately, it was not possible to do any direct correlation with the previous compounds because substitution position 4 of the THIQ ring had sometime positive and sometime negative effects (**146x**, Table 51 and **143n**, Figure 98, respectively), depending on the substitution pattern on the rest of the molecule. Thus, it was difficult to anticipate if the hydroxyl in position 4 for compounds **144h** and **145h** (Figure 98) had a positive or negative effect.

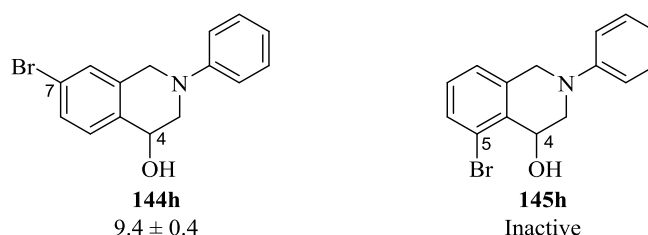


Figure 99. Structure and relative efficacy of compounds **144h** and **145h**. The percentage of efficacy reported were the result of a single experiment in four replicates.

3.2.2.6. Effect of substitution in position 1

Compound **163i** (Table 52), with a methoxy group in position 6 was inactive, whereas compound **171i** (Table 52), with a hydroxyl in the same position had an activity of 24.8%. For the 6-methoxy series, adding a substituent in position 1 (**181a,b,e-g**, Table 52) led to low activity compounds but this might not be size dependent, with every group from the methyl to the phenylethyl having very similar activities. For the 6-hydroxy series, the activity gained by addition of substituents in position 1 (**191a-c,e-g**, Table 52) was significant and appeared to be size dependent as the 1-methyl substituted compound (**191a**, Table 52) was the weakest of the series and the 1-benzyl substituted (**191f**, Table 52) the strongest. The phenethyl group in compound **191g** (Table 52) was probably near the maximum size that could be

accommodated or was spatially not well oriented, leading to a loss in activity compared to compound **191f** (Table 52). The 1-phenyl substituted compound **191e** (Table 52), was the only compound of the series with the substituent in position 1 perpendicularly to the plane of the THIQ. This could lead to steric hindrance or less optimal binding, which might explain the lower activity than the other compounds of the series.

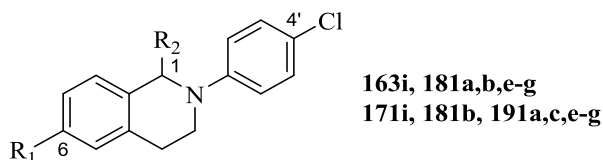


Figure 100. Structure of tested compounds used to evaluate substituents in position 1. Refer to **Table 52** for R_1 and R_2 substitution.

Table 52. Effects of the substituent in position 1 for the two series of compounds tested.

Compound	R_1	R_2	% of efficacy
163i	OMe	H	Inactive
181a	OMe	Me	12.4 ± 1.2
181b	OMe	Et	16.8 ± 1.2
181e	OMe	Ph	12.8 ± 1.0
181f	OMe	Bn	19.7 ± 4.4
181g	OMe	$(CH_2)_2Ph$	16.0 ± 3.6
171i	OH	H	24.8 ± 1.9
191a	OH	Me	9.6 ± 2.0
181b	OH	Et	41.5 ± 0.8
191c	OH	<i>i</i> -Pr	46.7 ± 1.6
191e	OH	Ph	17.2 ± 1.4
191f	OH	Bn	53.2 ± 0.7
191g	OH	$(CH_2)_2Ph$	35.5 ± 1.4

The percentage of efficacy reported were the result of a single experiment in four replicates.

3.2.2.7. Effect of substitution on the *N*-phenyl ring for the 1-substituted THIQs

When there was a chlorine in position 4', for both the 6-methoxy and the 6-hydroxy series, a benzyl group in position 1 gave the highest activity. Retaining the 1-benzyl group, a re-evaluation of the substituent in position 4' of the *N*-phenyl ring of the 6-methoxy substituted **181f** did not lead to any significant change in activity for either no substituent (**181h**, Table 53) or a 4'-hydroxyl group (**181i**, Table 53). This suggested that the effect of the chlorine in **181f** was negligible. When the chlorine of 6-hydroxy compound **191f** was removed (**191h**, Table 53) the activity was retained but the

introduction of a hydroxyl group in the same 4' position (**191i**, Table 53) led to a significant loss in activity. Conversely, when the substituent in position 6 was replaced by a methoxy group in position 8, the 4'-chloro substituted compound (**190f**, Table 53) had the lowest activity and the 4'-methoxy derivative (**190i**, Table 53) the highest. In addition, **190f** was significantly worse than **181f** while **190i** was significantly better than **181i** (Table 53).

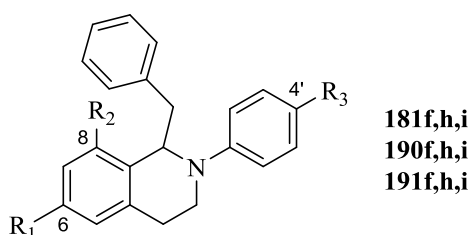


Figure 101. Structure of the compounds used to re-evaluate the influence of the substituent on the *N*-phenyl ring and to evaluate the influence of the substituent in position 8. Refer to **Table 53** for R_1 , R_2 and R_3 substitution.

Table 53. Effect of the substituent in 4' position of the 1-benzyl substituted compounds.

Compound	R_1	R_2	R_3	% of efficacy
181f	OMe	H	Cl	19.7 ± 4.4
181h	OMe	H	H	19.2 ± 3.6
181i	OMe	H	OMe	18.2 ± 3.6
190f	H	OMe	Cl	6.5 ± 0.6
190h	H	OMe	H	21.1 ± 2.7
190i	H	OMe	OMe	30.0 ± 1.7
191f	OH	H	Cl	53.2 ± 0.7
191h	OH	H	H	49.1 ± 1.6
191i	OH	H	OH	35.8 ± 1.2

The percentage of efficacy reported were the result of a single experiment in four replicates.

3.2.2.8. Effect of substitution in position 3

For the 6-methoxy series, the compound with a chlorine in position 4' was inactive with no substituent in position 3 (**163i**, Table 54). However, some activity was obtained by introducing a substituent in position 3 (**166i**, **211b**, Table 54). In the 6-hydroxyl series with a chlorine in position 4', the presence of a substituent in position 3 (**234a**, **234b**, Table 54) led only to a small loss in activity. Very interestingly, when the substituents in 6 and 4' are methoxy groups, the introduction of a methyl group in position 3 (**166s**, Table 54) led to an inversion of activity. In the assay, compounds were

tested as inverse agonists where the signal from the untreated receptor was considered zero. Thus, an increase in activity of the receptor was reported as a negative value.

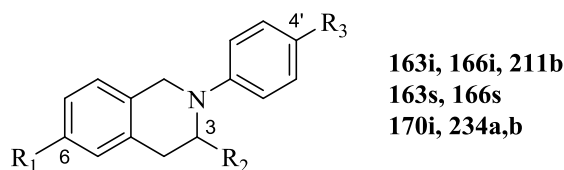


Figure 102. Structure of compounds used to evaluate the effect of substituents in position 3. Refer to **Table 54** for R_1 , R_2 and R_3 substitution.

Table 54. Effect of the substituents in position 3.

Compound	R_1	R_2	R_3	% of efficacy
163i	OMe	H	Cl	Inactive
166i	OMe	Me	Cl	13.7 ± 2.0
211b	OMe	Et	Cl	20.9 ± 3.5
163s	OMe	H	OMe	30.5 ± 0.4
166s	OMe	Me	OMe	-20.5 ± 2.8
170i	OH	H	Cl	24.8 ± 1.9
234a	OH	Me	Cl	17.8 ± 2.1
234b	OH	Et	Cl	14.8 ± 1.3

The percentage of efficacy reported were the result of a single experiment in four replicates.

3.2.2.9. Effect of substitution in position 4

Although every 4-substituted compound of the 6-methoxy-4'-chloro series was more active than the parent compound **163i** (Table 55), the activity was small with a maximum of 23% of efficacy for the 4-isopropyl substituted compound **228c** (Table 55). The type of substitution did not influence the activity significantly but the geminal disubstituted **228f** (Table 55) had the lowest activity of the series. This effect might indicate that one of the two stereoisomers of the 4-substituted compounds could not be accepted well into the binding pocket. More interesting results were found for the 6-hydroxyl-4'-chloro series where the 4-methyl group (**234c**, Table 55) showed a significant increase in activity over the unsubstituted compound **170i** (Table 55). This activity was reduced slightly with a 4-ethyl group (**234d**, Table 55) and a little further with a 4-isopropyl group (**234e**, Table 55). A benzyl group in the same position 4 gave the highest activity for the series of 49.8%. The effect of substitution in position 4 for the 6-hydroxyl-4'-chloro series was not size dependant and did not have a clear explanation. The geminal dimethyl derivative **234h** (Table 55) had a lower activity than

compound **234c** (Table 55) which had a single methyl group. This might implied that one of the two enantiomer of **234c** (Table 55) could not be well accommodated in the binding pocket. As previously discussed (Figure 84, page 133) though, this is just speculation and the two separate enantiomers should be tested individually to evaluate the real effect that each has on the activity.

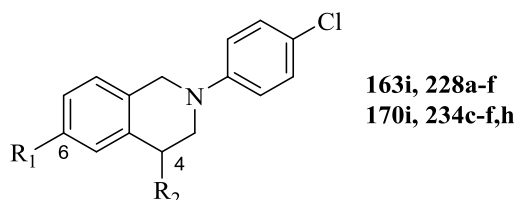


Figure 103. Structure of compounds used to evaluate the effect of substituents in position 4. Refer to **Table 55** for R_1 and R_2 substitution.

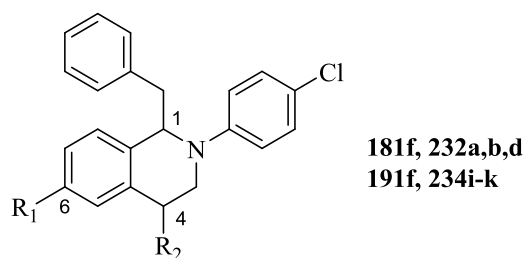
Table 55. Effect of the substituents in position 4.

Compound	R_1	R_2	% of efficacy
163i	OMe	H	Inactive
228a	OMe	Me	12.9 ± 6.6
228b	OMe	Et	17.6 ± 1.6
228c	OMe	<i>i</i> -Pr	23.3 ± 1.3
228e	OMe	(CH ₂) ₂ OMe	21.6 ± 2.4
228d	OMe	Bn	15.8 ± 0.8
228f	OMe	Me ₂	9.2 ± 1.9
170i	OH	H	24.8 ± 1.9
234c	OH	Me	44.8 ± 2.5
234d	OH	Et	37.3 ± 3.7
234e	OH	<i>i</i> -Pr	33.5 ± 1.2
234f	OH	Bn	49.8 ± 1.1
234h	OH	Me ₂	30.7 ± 1.5

The percentage of efficacy reported were the result of a single experiment in four replicates.

3.2.2.10. Effect of disubstitution in position 1 and 4

In the 1-benzyl-6-methoxy series introducing a group in position 4 did not give any positive effect on activity, instead a small loss of activity was observed (**232a**, **232b**, **232d**, Table 56). In contrast, in the 1-benzyl-6-hydroxyl series a methyl group in position 4 (**234i**, Table 56) significantly increased the efficacy to 79.2% but the activity was then sequentially decreased by addition of larger substituents (**234j**, **234k**, Table 56).



Scheme 72. Structure of the 1,4-disubstituted compounds used to evaluate the effects of the substituent in position 4. Refer to **Table 56** for R₁ and R₂ substitutions.

Table 56. Effect of the substituents in position 4 of the 1-benzyl substituted compounds.

Compound	R ₁	R ₂	% of efficacy
181f	OMe	H	19.7 ± 4.4
232a	OMe	Me	8.6 ± 0.7
232b	OMe	Et	17.7 ± 3.1
232d	OMe	Bn	10.7 ± 2.5
191f	OH	H	53.2 ± 0.7
234i	OH	Me	79.2 ± 0.7
234j	OH	Et	35.7 ± 4.0
234k	OH	Bn	14.9 ± 3.0

The percentage of efficacy reported were the result of a single experiment in four replicates.

3.2.2.11. Comparison between THIQs and the open ring analogues

To determine whether the THIQ ring was necessary for the activity, the open ring compounds **122n** and **122p** (Figure 104) were tested and compared with the analogue THIQs, **170i** and **170s**, respectively. Both the open ring derivatives **122n** and **122p** were active, although with a lower efficacy compared to the corresponding THIQs. These results showed that the rigidity introduced by the THIQ ring was not essential for the activity, nevertheless it had a favourable effect on the activity of the compounds.

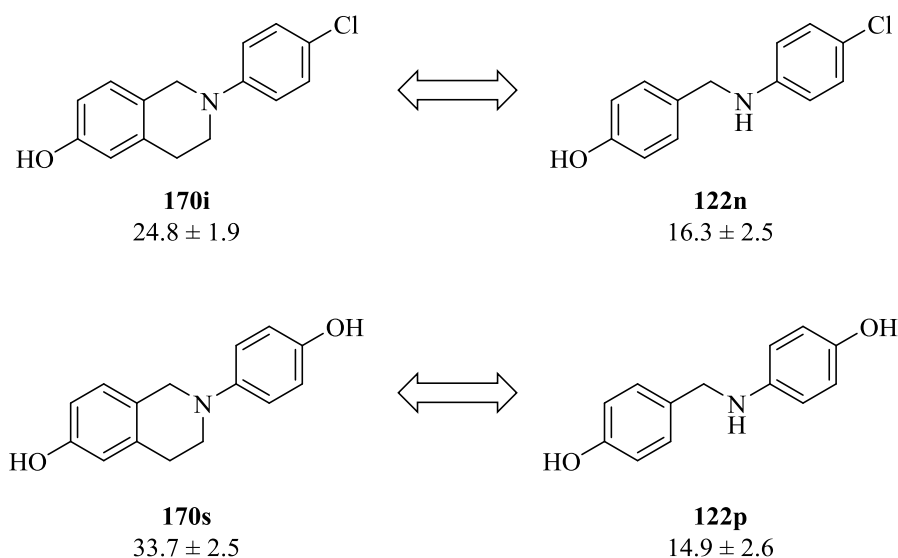


Figure 104. Structure and relative efficacy of the THIQs **170i,s** and the respective open ring derivative **122n,p**. The percentage of efficacy reported were the result of a single experiment in four replicates.

3.2.3. Conclusions

It is difficult to draw specific conclusions on the structure activity relationship of the compounds tested against $ERR\alpha$. A trend was observed, where by altering the substituent at one position the structure activity relationship of substituents at a different position could be modified. For example, this was the case for the substitution in position 4' of the 6-methoxy, 8-methoxy and 6-hydroxy series (Table 53, page 151). Similarly, substitution in position 4 of the 6-methoxy and 6-hydroxy series (Table 55, page 153) had contrasting effect.

From all the compounds synthesised and tested, the best inverse agonist **234i** (Figure 105) had a percentage of efficacy of $79.2\% \pm 0.7\%$ at $100\ \mu\text{M}$. This was moderately higher than that observed for DES at the same concentration, i.e. $64.2\% \pm 8.4\%$. The EC_{50} of DES reported in the literature is *ca.* $10\ \mu\text{M}$, while the EC_{50} of XCT790 is *ca.* $250\ \text{nM}$. Even if more active than DES, compound **234i** (Figure 105) presented already issues of high lipophilicity, which would need to be one of the primary aspects to be addressed in future. In fact, high lipophilicity is inversely correlated with solubility and directly correlated, instead, with aspecific toxicity.

Considering the difference in lipophilicity between **191f** and **191i** (Figure 105), the activity of a compound like **235** (Figure 105) should be investigated. A simplification of the structure as in **236** (Figure 105) should also be considered where no significant loss

of activity is observed. As well as solubility maybe becoming a significant issue when trying to increase the activity of the compounds down to a low nM range, the cellular localisation of the target also needs to be considered. ERR α is located in the nucleus, therefore an active compound needs to penetrate the nucleus to be able to interact with the receptor. Thus, any inverse agonist will have to possess a significant degree of lipophilicity to be able to penetrate the nucleus and exert its activity.

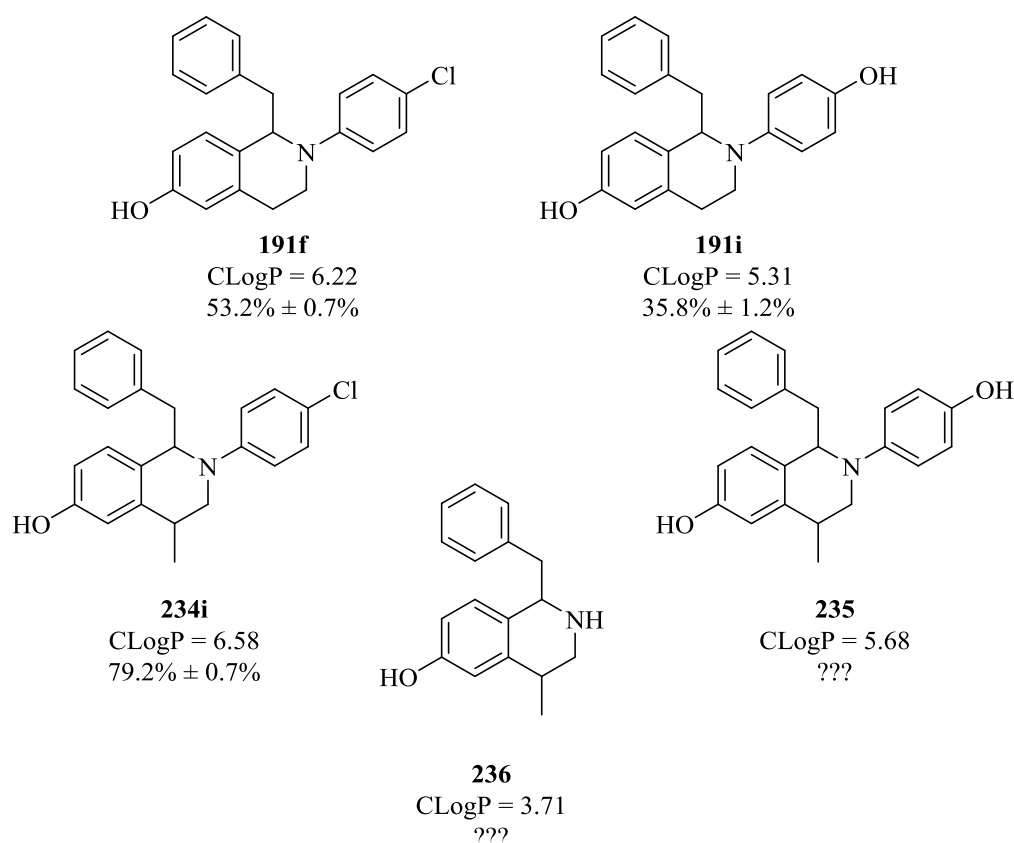


Figure 105. Structure and relative activity and CLogP values of compounds **191f**, **191i** and **234i**, and compounds of possible future interest **235** and **236**. The percentage of efficacy reported were the result of a single experiment in four replicates.

An interesting result was the effect of a methyl group in position 3 of the dimethoxy substituted compound **166s** (Figure 106), which completely inverted the activity of compound **163s** (Figure 106) from an inverse agonist into an agonist. This effect was not encountered in any of the other compounds tested and would be worth future investigation.

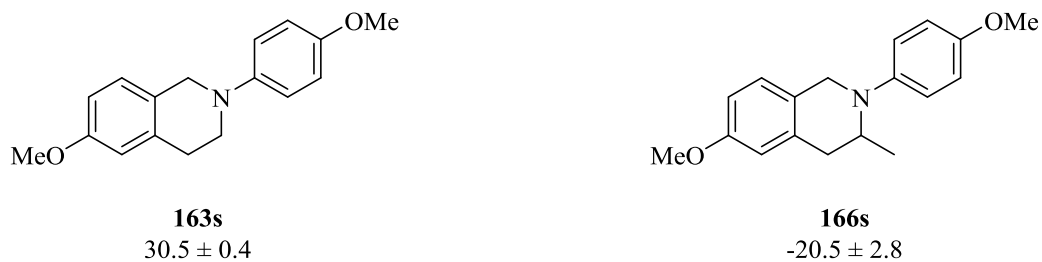


Figure 106. Structure and relative activity of compounds **163s** and **166s**, respectively an inverse agonist and an agonist of $\text{ERR}\alpha$. The percentage of efficacy reported were the result of a single experiment in four replicates.

3.3. Nuclear Hormone Receptors (NHRs) screening.

A panel of 19 NHR was used to prove that the THIQ structure is a good steroidomimetic nucleus and at the same time evaluate possible off-target activity. In addition, through this service, it was possible to evaluate the activity of selected compounds in a whole cell assay against both $\text{ERR}\alpha$ and $\text{ER}\alpha$.

Three selected compounds were tested against a wide range of NHRs to obtain information about their selectivity. The three selected compounds were **170i**, **170s** and **191c** (Figure 107) and they were chosen based on their differences and similarities. In fact, to be able to correlate the data obtained with the structure of the compound it was decided to test compounds that would not differ for more than one substituent.

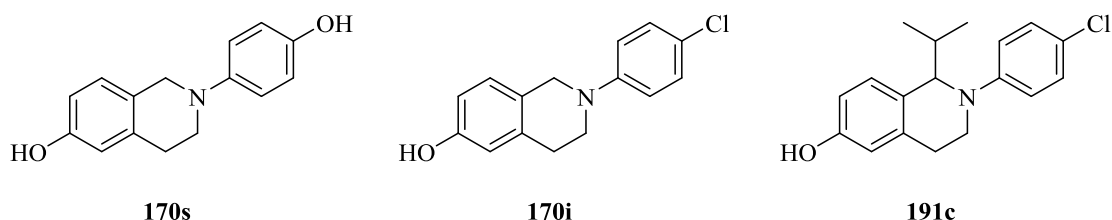


Figure 107. Structure of the three compounds tested against a wide range of NHRs.

The testing was outsourced to DiscoverX which has developed its own whole-cell assay named PathHunter. The principle on which the assay is based is somewhat similar to the LanthaScreenTM TR-FRET. The PathHunter assay uses cells that contain tagged hormone receptor and co-activator peptide, which are both required for signalling transduction and gene expression. Both receptor and co-activator contain half of a β -galactosidase enzyme and when the receptor is activated, it is translocated to the nucleus where it recruits the co-activator peptide in order to initiate gene transcription. In this way, the two parts of the enzyme are put in proximity to one another, the enzyme β -galactosidase becomes active. The active enzyme converts an inactive dye (structural

In antagonist mode, activity values above 100% describe compounds that reduce the activity below the activity of the control vehicle. Thus activity values above 100% describe inverse agonists. Conversely, values below 0% describe compounds that increase the activity of the compounds above the activity of the control agonist. Thus, activity values below 0% describe agonist compounds. Being ERR α constitutively active, values observed for this receptor reflects opposite effects compared to the other receptors in the panel. Hence, negative values describe inverse agonists that deactivate the receptor more than the inverse agonist control. *Vice versa*, values above 100% describe agonist compounds that activate the receptor more than the vehicle control.

The three compounds were tested in agonist and antagonist mode against the following NHRs:

- Androgen receptor (AR)
- Estrogen receptor alpha (ER α)
- Estrogen receptor-related receptor alpha (ERR α)
- Farnesoid X receptor (FXR)
- Glucocorticoid receptor (GR)
- Liver X receptors (LXR α , LXR β)
- Mineralocorticoid receptor (MR)
- Peroxisome proliferator-activated receptors (PPAR α , PPAR β , PPAR γ)
- Progesterone receptors (PR α , PR β)
- Retinoic acid receptors (RAR α , RAR β)
- Retinoid X receptors (RXR α , RXR γ)
- Thyroid hormone receptors (THR α , THR β)

When the compounds were tested in agonist mode **191c** was found to be always a weak inverse agonist against every receptor except ERR α for which it had 115% efficacy as inverse agonist (Table 57). Another important aspect was that **191c** was also non-estrogenic even at 100 μ M showing only 10.7% activity against ER α . This is a basic requirement for a 17 β -HSD1 inhibitor. Conversely, **170i** was the most estrogenic and, in addition, activated also PPAR δ to *ca.* 65% while **170s** did not show any general

agonist activity apart from a significant degree of estrogenicity (Table 57). What is extremely important to consider is that very simple substitutions can change the effect of the compounds, e.g. from ER α agonist (**170i**) to an ERR α inverse agonist (**191c**).

Table 57. Results of the screening against the NHRs panel in agonist mode. Colours are used to visualise the worst (red), the intermediate (yellow) and the best (green) agonist among the three compounds.

	Agonist mode (% of activity)		
	170i	170s	191c
AR	8.9	-0.7	-3.6
ERR α	5.5	27.4	115.4
ER α	114.7	60.7	10.7
FXR	-3.7	-6.6	-8.1
GR	0.9	1.2	0.2
LXR β	10.6	-3.0	-6.9
LXR α	0.5	-1.9	-4.2
MR	-1.4	-0.1	-3.4
PPAR α	0.1	-2.0	-2.4
PPAR γ	-4.6	-3.8	-11.7
PPAR δ	64.8	-5.9	-30.9
PR β	-2.1	-2.2	-5.6
PR α	-0.7	1.9	-13.5
RAR β	-31.3	-0.2	-45.9
RAR α	-2.1	1.3	-15.8
RXR α	30.4	3.8	-12.8
RXR γ	-0.7	0.3	-17.6
THR β	4.6	-2.7	-9.9
THR α	10.1	0.3	-4.0

When tested in antagonist mode **170s** showed only a low to moderate level of competition while **191c** was able to fully inhibit almost every receptor (Table 58). Again, ERR α is an exception because is constitutively active and **191c** was competing against an inverse agonist. At this concentration **191c** was unable to discriminate among the different receptors but **170i**, which was a weaker antagonist, showed different degrees of inhibition against the different targets. Noteworthy is also the activity of **170i**

against RXRs where it acted as a full antagonist against RXR γ (Table 58), but acted as a partial agonist against RXR α (Table 57, Table 58) showing activity as both agonist and antagonist. Moreover, **170i** acted as an antagonist against PPAR γ (Table 58) but as an agonist against PPAR δ (Table 57).

Table 58. Results of the screening against the NHRs panel in Antagonist mode. Colours are used to visualise the worst (red), the intermediate (yellow) and the best (green) agonist among the three compounds.

	Antagonist mode (% of inhibition)		
	170i	170s	191c
AR	77.4	24.3	99.3
ERR α	-8.4	-29.2	-49.7
ER α	-18.1	-53.4	86.5
FXR	95.5	49.0	95.5
GR	76.1	12.3	91.5
LXR β	41.1	17.8	103.3
LXR α	89.1	16.9	102.3
MR	93.9	14.3	100.4
PPAR α	11.2	-28.7	98.2
PPAR γ	91.7	33.2	110.0
PPAR δ	8.9	25.7	127.8
PR β	96.4	40.9	102.5
PR α	80.5	39.4	109.6
RAR β	131.9	-8.1	174.3
RAR α	96.9	36.1	125.3
RXR α	50.0	16.1	115.1
RXR γ	71.8	17.4	115.0
THR β	87.5	16.3	118.0
THR α	72.8	31.6	101.8

The ability to affect all of the NHRs considered in the assay might present major risks in the future development of an inhibitor of 17 β -HSD1 and inverse agonists of ERR α . The data obtained demonstrated that the selectivity against the different NHRs should be continuously evaluated during the different stages of lead optimisation. This awareness would prevent the development of potent compounds which cannot be implemented in therapy due to side effects originating from their lack of selectivity.

From a different point of view, the results prove that the THIQ core is capable of interacting with all the NHRs tested and that simple substitutions have significant effects on the selectivity against the different targets. Hence, even if off-target effects are a risk, selectivity can possibly be achieved with the right substitution pattern. In addition, the THIQ core may prove to be an interesting scaffold for undertaking further studies against the different NHRs.

3.4. National Cancer Institute of America (NCI) – Developmental Therapeutics Program (DTP)

The NCI-DTP 60 cell line panel is a project the development of which started in the late 1980s and finalised in 1990. The project was designed to identify novel antitumoral compounds to treat a wide range of cancer types. The screening service is free of charge and is open to both academic and industrial laboratories. After an electronic submission, compounds are selected based upon structure novelty and diversity and secondly on drug-like properties. When a novel natural product or synthetic compound is accepted, it is initially screened at 10 μ M against every cell line. If the screening results show active compounds, then the test is repeated with a five concentration dose response.

The 60 cell lines are collected from nine different types of cancer and together represent a powerful tool, not only for the discovery of new anticancer drugs, but also for unravelling their mechanism of action. The cell lines are characterised by different responses to the same antitumoural compound and the effect of a compound on the different cell lines is a “fingerprint” of its mechanism of action. Comparing the effect of an unknown compound with the effect of other drugs, which mechanism of action has been previously described, it is possible to determine how the new compound may exert its effects.

Among the compounds synthesised, 54 (Figure 109, Table 59) were selected for the initial screening and three proceeded to the 5 dose assay.

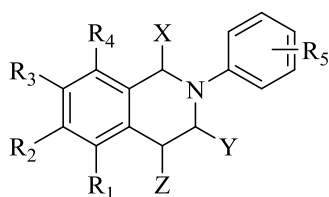


Figure 109. General structure for the compounds tested on the NCI 60 cell line panel. Refer to **Table 59** for compound substitutions.

Table 59. List of the 54 compounds tested on the NCI 60 cell line panel with relative substituents description.

Cmpd	R ₁	R ₂	R ₃	R ₄	R ₅	X	Y	Z
163e	H	OMe	H	H	H	H	H	H
163i	H	OMe	H	H	4-Cl	H	H	H
163q	H	OMe	H	H	4-Me	H	H	H
163s	H	OMe	H	H	4-OMe	H	H	H
170e	H	OH	H	H	H	H	H	H
170i	H	OH	H	H	4-Cl	H	H	H
170q	H	OH	H	H	4-Me	H	H	H
170s	H	OH	H	H	4-OH	H	H	H
163u	H	OMe	H	H	3-OMe	H	H	H
163w	H	OMe	H	H	2-OMe	H	H	H
163t	H	OMe	H	H	3-Cl	H	H	H
163v	H	OMe	H	H	2-Cl	H	H	H
164j	H	H	OMe	H	4-Cl	H	H	H
165j	OMe	H	H	H	4-Cl	H	H	H
163aa	H	OMe	H	H	3,4-Cl ₂	H	H	H
143z	H	H	H	H	4-Cl	H	H	OH
166i	H	OMe	H	H	4-Cl	H	Me	H
170aa	H	OH	H	H	3,4-Cl ₂	H	H	H
170t	H	OH	H	H	3-Cl	H	H	H
170u	H	OH	H	H	3-OH	H	H	H
146x	H	OMe	OMe	H	4-OMe	H	H	OH
167	H	OMe	OMe	H	4-OMe	H	H	H
168	OMe	OMe	OMe	H	4-OMe	H	H	H
166s	H	OMe	H	H	4-OMe	H	Me	H
176x	H	OMe	OMe	H	4-OMe	H	H	OBn
181a	H	OMe	H	H	4-Cl	Me	H	H
181e	H	OMe	H	H	4-Cl	Ph	H	H
181f	H	OMe	H	H	4-Cl	Bn	H	H
191a	H	OH	H	H	4-Cl	Me	H	H
191e	H	OH	H	H	4-Cl	Ph	H	H
190f	H	H	H	OMe	4-Cl	Bn	H	H
181c	H	OMe	H	H	4-Cl	<i>i</i> -Pr	H	H
191b	H	OH	H	H	4-Cl	Et	H	H

191c	H	OH	H	H	4-Cl	<i>i</i> -Pr	H	H
191f	H	OH	H	H	4-Cl	Bn	H	H
173	H	OH	OH	H	4-OH	H	H	H
174	OH	OH	OH	H	4-OH	H	H	H
143n	H	OH	H	H	4-Cl	H	H	OH
175n	H	OBn	H	H	4-Cl	H	H	OBn
145h	Br	H	H	H	H	H	H	OH
144h	H	H	Br	H	H	H	H	OH
181g	H	OMe	H	H	4-Cl	(CH ₂) ₂ Ph	H	H
181i	H	OMe	H	H	4-OMe	Bn	H	H
228a	H	OMe	H	H	4-Cl	H	H	Me
228b	H	OMe	H	H	4-Cl	H	H	Et
228d	H	OMe	H	H	4-Cl	H	H	Bn
234e	H	OH	H	H	4-Cl	H	H	<i>i</i> -Pr
234a	H	OH	H	H	4-Cl	H	Me	H
234c	H	OH	H	H	4-Cl	H	H	Me
234f	H	OH	H	H	4-Cl	H	H	Bn
234h	H	OH	H	H	4-Cl	H	H	Me ₂
191g	H	OH	H	H	4-Cl	(CH ₂) ₂ Ph	H	H
191h	H	OH	H	H	H	Bn	H	H
191i	H	OH	H	H	4-OH	Bn	H	H

The selected compounds were tested for general toxicity against the 60 cell lines. Cytotoxicity is undesirable for an inhibitor of 17 β -HSD1 because such compounds are aimed for long term treatment in recurrence prevention. Nevertheless, compounds with exceptional cytotoxicity might generate unexpected hits for future development.

In general, the compounds tested did not exhibit significant activity at 10 μ M and this is shown by the graph (Figure 110, page 166) where the coloured bars were contained below 50% of growth inhibition and negative values, which practically represent growth stimulation.

The two visual characteristics of the graph (Figure 110) describe the activity of the compounds are the height of the peaks and the density of the peaks. The height of the peaks represents the strength of inhibition, and the density of the peaks represents the number of cell lines affected by the compound. The compounds selected for the 5 doses screening were **164j**, **176x** and **175n**, which correspond to a high density of high peaks

and showed an average growth inhibition of $41.3\% \pm 56.0\%$, $30.2\% \pm 24.5\%$ and $88.1\% \pm 42.1\%$, respectively. The remaining tested compounds showed an average growth inhibition of $3.5\% \pm 13.0\%$.

The five dose curves for compounds **164j** (Figure 111, page 167) and **176x** (Figure 112, page 167) show how the activity of the compounds drops very rapidly with sample dilution and become almost completely inactive at concentrations near 1 μM . Compound **175n** is at present still in the testing queue for the 5 doses assay and for this reason its final results are not yet available.

The COMPARE algorithm is a developmental tool offered by the NCI-DTP to allow the comparison of the pattern of activity of the test compound against the different cell line with the activity of known drugs. This allows the prediction of the most probable mechanism of action for the compound. The algorithm classifies the activity pattern and returns a value which is a reflection of the probability of a matching mechanism between the two compounds considered. The analyses on the results from **164j** and **176x** led to really poor scores and no further investigation of the possible mechanism of action of the two compounds was pursued.

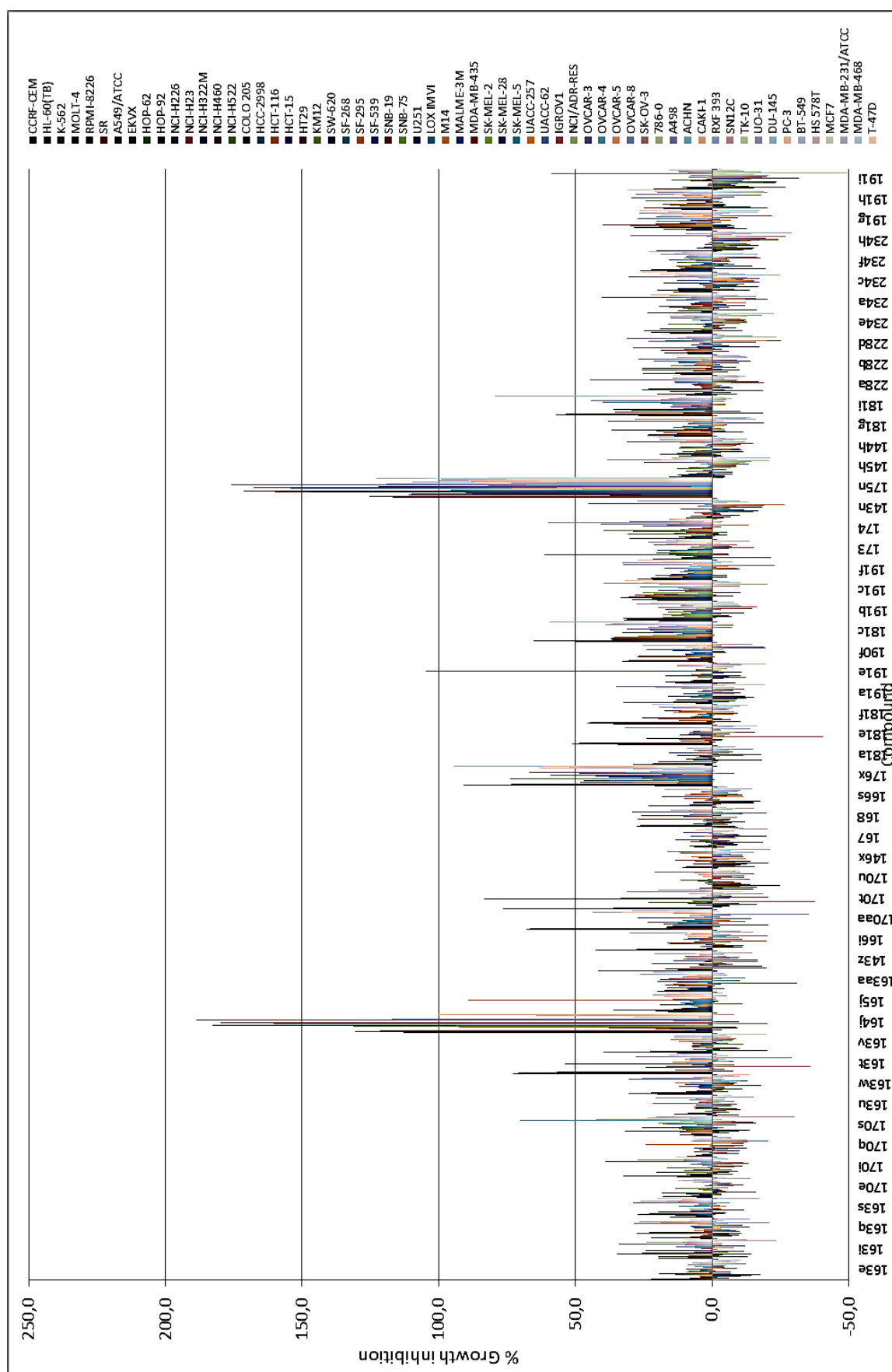


Figure 110. Results from the NCI 60 cell line panel for every compound tested reported in a single graph. Each coloured line represent a cell line. Results are grouped by compound.

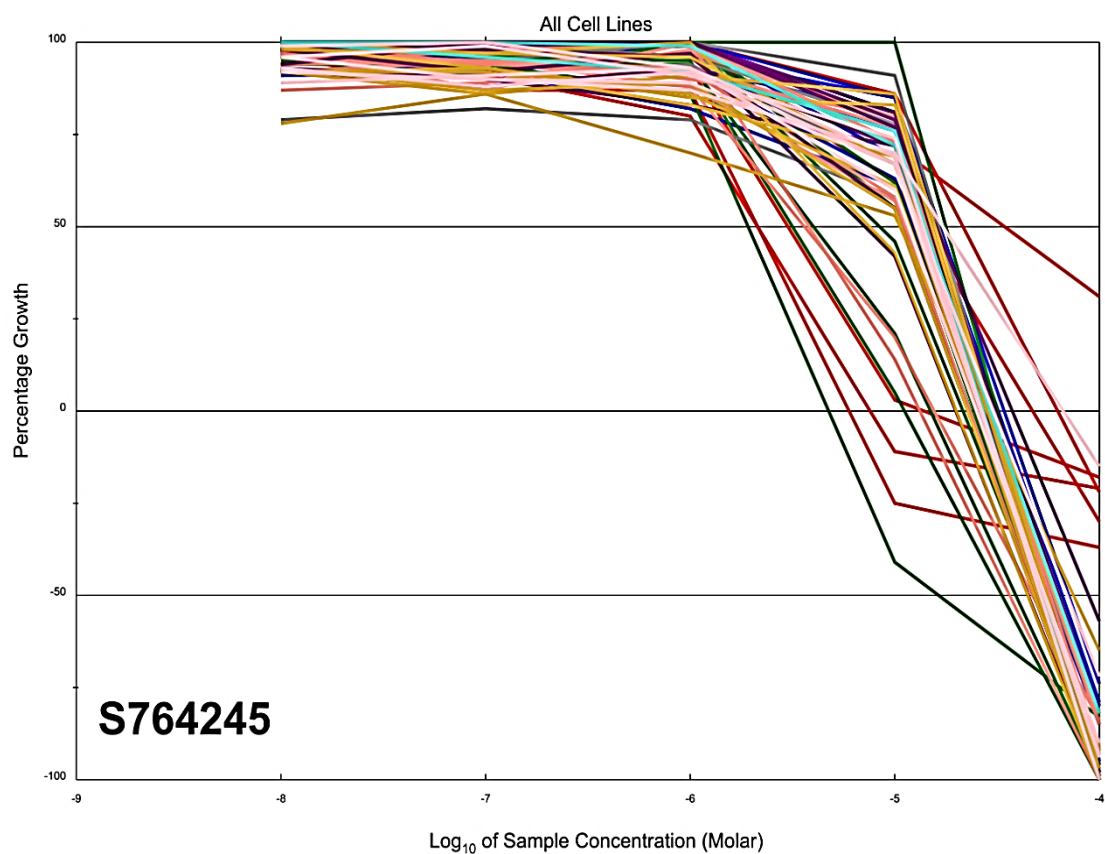


Figure 111. Five dose curve response against the all 60 cell line panel for compound **164j**.

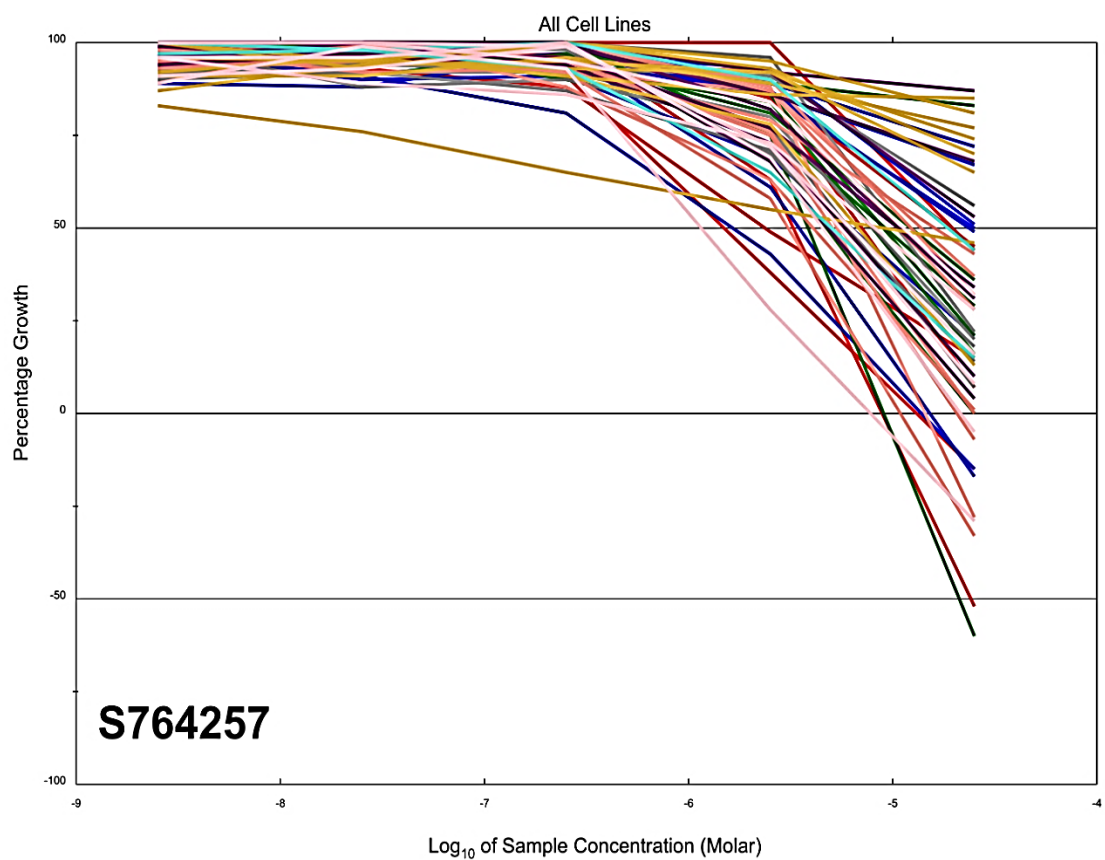


Figure 112. Five dose curve response against the all 60 cell line panel for compound **176x**.

The majority of the compounds tested did not have significant cytotoxic effects and this is a rather positive feature considering the purpose of the compounds as inhibitors of 17 β -HSD1. This kind of therapeutic approach would not aim to a widespread cytotoxic effect but rather induce lower intracellular concentrations of E2 for prevention of rebound. Under this light, cytotoxicity would actually be a major issue rather than a positive aspect.

3.5. Eli Lilly – Open Innovation Drug Discovery (OIDD)

Eli Lilly and company has recently developed a project named Open Innovation Drug Discovery (OIDD) which aims to expand the collaboration between industry and academics. Similar to the NCI DTP, the submitted structures are initially screened before acceptance. In contrast to NCI, the initial screening for the OIDD is performed *in silico*, based on chemicophysical parameters that describes drug-like features and initial structural requirements previously set up in the screening software. Once the structures are accepted, compounds are screened free of charge on two different panels, i.e. Target Drug Discovery (TargetD²) and Phenotypic Drug Discovery (PD²).

TargetD² and PD² are complementary approaches, the first aiming at the development of new therapeutics against already established molecular targets of interest, while the second aiming to discover molecules with multi-target synergic effects and different effective pathways. The attention of both TargetD² and PD² is divided into three main areas: endocrine/cardiovascular, oncology and neuroscience (Table 60).

Table 60. Area of research and relative targets for both TargetD² and PD².*

	Endocrine/Cardiovascular	Oncology	Neuroscience
PD ²	<ul style="list-style-type: none"> • Wnt pathway activator • GLP-1 secretion • PCSK9 synthesis inhibition 	<ul style="list-style-type: none"> • <u>KRas/Wnt synthetic lethal</u> 	
TargetD ²	<ul style="list-style-type: none"> • GPR119 Receptor agonist • <u>Apelin Receptor (APJ) agonist</u> 	<ul style="list-style-type: none"> • Enhancer of Zeste Homolog 2 (EZH2) inhibitor • <u>Hexokinase 2 inhibitor</u> 	<ul style="list-style-type: none"> • mGluR2 receptor allosteric antagonist • CGRP receptor antagonist

*The underlined assays refer to discontinued modules that were only initially implemented.

Amongst the compounds synthesised, 28 compounds (Figure 113, Table 61) were selected for screening and were tested against the different targets of the panel. A brief description of the target and the results are reported in the following sections.

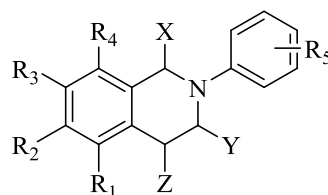


Figure 113. General structure for the compounds tested on the Eli Lilly OIDD screening panel. Refer to **Table 61** for compound substitutions.

Table 61. List of the 28 compounds tested on the Eli Lilly OIDD screening panel with relative substituents description.

Compound	R ₁	R ₂	R ₃	R ₄	R ₅	X	Y	Z
165j	MeO	H	H	H	4-Cl	H	H	H
163aa	H	MeO	H	H	3,4-Cl ₂	H	H	H
143z	H	H	H	H	4-Cl	H	H	OH
166i	H	MeO	H	H	4-Cl	H	Me	H
170aa	H	OH	H	H	3,4-Cl ₂	H	H	H
146x	H	MeO	MeO	H	4-MeO	H	H	OH
166s	H	MeO	H	H	4-MeO	H	Me	H
181b	H	MeO	H	H	4-Cl	Et	H	H
190f	H	H	H	MeO	4-Cl	Bn	H	H
191b	H	OH	H	H	4-Cl	Et	H	H
175n	H	OBn	H	H	4-Cl	H	H	OBn
211b	H	MeO	H	H	4-Cl	H	Et	H
228b	H	MeO	H	H	4-Cl	H	H	Et
228d	H	MeO	H	H	4-Cl	H	H	Bn
181g	H	MeO	H	H	4-Cl	(CH ₂) ₂ Ph	H	H
181i	H	MeO	H	H	H	Bn	H	H
232a	H	MeO	H	H	4-Cl	Bn	H	Me
232b	H	MeO	H	H	4-Cl	Bn	H	Et
191g	H	OH	H	H	4-Cl	(CH ₂) ₂ Ph	H	H
191h	H	OH	H	H	H	Bn	H	H
191i	H	OH	H	H	4-OH	Bn	H	H
234b	H	OH	H	H	4-Cl	H	Et	H
234d	H	OH	H	H	4-Cl	H	H	Et

234e	H	OH	H	H	4-Cl	H	H	<i>i</i> -Pr
234f	H	OH	H	H	4-Cl	H	H	Bn
234i	H	OH	H	H	4-Cl	Bn	H	Me
234j	H	OH	H	H	4-Cl	Bn	H	Et
234k	H	OH	H	H	4-Cl	Bn	H	Bn

3.5.1. PD² – Wnt pathway activator

The Wnt pathway activator assay module tests compounds for their ability to differentiate murine C2C12 cells into an osteoblast-like phenotype through a β -catenin dependant stimulation of alkaline phosphatase activity.¹⁶³

Every compound tested on this assay has proved inactive at 2 μ M and only few compounds showed low activity at 10 μ M with **143z**, **191g** and **191h** (Figure 113, Table 61, page 169) resulting in a maximum stimulation of 15-25% (Table 62).

3.5.2. PD² – GLP1 secretion

Glucagon-like peptide 1 (GLP1) is secreted in response to the presence of nutrients in the lumen of the small intestine and is a potent anti-hyperglycaemic hormone inducing glucose-dependant insulin secretion and suppressing glucagon secretion. The glucose dependency make this mechanism a safer way to control hyper-glycaemia as it does not reduce glucose levels below the safety threshold.^{164, 165} Exentide and liraglutide are already commercially available GLP1-like peptides but as peptides the only administration method possible is by injection.

Every compound tested in this assay proved inactive at both 2 μ M and 20 μ M except compound **143z** (Figure 113, Table 61, page 169), which showed 50% stimulation at 20 μ M. Compound **143z** was therefore assayed in both the human (hNCI-H716) and murine (mSTC-1) systems to obtain EC₅₀ values. The EC₅₀ calculated in the murine system was 12.98 μ M but in the human system it was higher than 40 μ M (Table 62).

3.5.3. PD² – Kras/Wnt synthetic lethal

Most colorectal cancers develop from benign lesions that are initiated by adenomatous polyposis coli (APC). Progression to colorectal cancer requires a second event such as an activating KRAS mutation. The aim of the assay module is to identify

small molecules that are selectively lethal to tumour cells that depend on WNT-KRAS synergy.^{166, 167}

Tested compounds showed a wide range of activity against the different cell lines from being almost completely inactive, to complete inhibition at 20 μ M. The activity was generally lost at 2 μ M and none of the compounds showed significant activity at 0.2 μ M (Table 62). The activity of compounds **143z**, **191g** and **234d** at 0.2 μ M was considered an experimental artefact as the value reported are not dose dependent.

Table 62. Table of the activity of the tested compounds against the PD² assay modules.

Endocrine/cardiovascular											Oncology													
Wnt pathway activator			GLP-1 secretion				Kras- Wnt synthetic lethal																	
WntCondMedia_bc ateninfluor/nucare aC2C12			hNCI-H716		hNCI- H716		mSTC-1		Basal_Viability ATP SW480				Basal_Viability ATP DLD-1				Basal_Viability ATP HCT116				GSK3b inh pretreated_Viability ATP HCT116			
%Stim @ 2uM	%Stim @ 10uM	%Stim @ 20uM	%Stim @ 2uM	%Stim @ 20uM	EC50 (uM)	EC50 (uM)	%Inh @ 0.2uM	%Inh @ 2uM	%Inh @ 20uM	%Inh @ 0.2uM	%Inh @ 2uM	%Inh @ 20uM	%Inh @ 0.2uM	%Inh @ 2uM	%Inh @ 20uM	%Inh @ 0.2uM	%Inh @ 2uM	%Inh @ 20uM	%Inh @ 0.2uM	%Inh @ 2uM	%Inh @ 20uM			
165j	-0.4	0.8	-2.6	3.2			20.8	20.3	74.7	10.8	12.2	49	7.9	-5.7	8.6	2.1	-3.2	8.1						
163aa	1	2.9	-3.1	-2.7			19.6	8	50	12.3	19.9	38.7	10.4	-2.2	6.4	-2.4	6	13.6						
143z	1.3	22.3	1.2	50.2		12.983	40.6	14.2	46.8	7	22.3	48.8	5.9	1.2	2.2	11.2	5.3	9.6						
166i	0.8	2	-1.3	-3.7		≥40.0	17.1	18.9	58.4	13.5	20	41.9	-0.6	7.6	62.7	-8.3	6.9	27.7						
170aa	2.4	9.8	-0.4	16			9	8.8	68	2.8	7.6	73	6.7	-0.4	29.6	20.6	0.6	53.4						
146x	1.8	2	-0.6	3.2			14.6	20.2	6.9	12.6	14.4	10.2	5.7	0.7	-2.9	6.5	0	-3.8						
166s	1.8	2.3	-2.2	-0.1			18.5	5.1	13.6	8.8	13	14.7	-6.3	-3.5	28.9	2.8	3.1	36.8						
181b	-1.3	-1.5	-3.9	-4.9			7.4	8.8	52.1	-1.2	-7.1	62.7	6.3	8.2	53	0.6	-10.1	37.5						
190f	-0.4	-1.4	-1.6	-1.9			13.7	28.2	70	16.5	41.9	50	8.9	13.1	63.5	-0.2	2.7	73.3						
191b	-1.9	7.8	-2.8	-4.6			6.4	7.2	103.1	8.9	-1	102.7	2.7	17.1	99.7	-3.8	-15.4	99.6						
175n	-0.4	2.4	-14	-11.9			5.7	11.9	87.1	2.8	-12.3	102.2	5.4	29.1	79.7	-14	1.8	96.2						
211b	0.7	-2.8	6	-0.1			7.9	6.8	15.6	16	13.4	37.8	10.7	21.7	54.6	-1.6	-7	36						
228b	3.1	-1.5	1.2	3.1			-8.6	6.3	29.6	6.8	16.5	23.1	3	27.7	66.5	-4.6	-10.6	46.9						
228d	-1.5	-2.1	-3.9	-0.7			2.9	3.6	50.8	13.5	10.5	27.8	10.4	21.1	74.9	-13.4	-12	24.9						
181g	-1.4	1	5.8	-0.1			4.3	11.3	49	13.7	17.7	41.2	5.1	23.4	63.7	-1.7	-20.4	63.6						
181i	-0.8	-2	1.8	1.1			0	7.3	47.8	4.3	7.5	68.8	2.8	23.1	71.7	21	-19.7	53.9						
232a	-0.3	0.6	-5.1	-2.4			8.2	9.8	93.1	14.5	-1.4	99	8.9	16.6	81.3	-5.8	-19.6	79.8						
232b	-1.2	1.5	-1.8	-0.3			14.3	17	83.7	13.7	9.5	73.7	4	19.7	70.3	-22.2	-12.1	71.5						
191g	0.6	14.1	-5.7	-6			81.4	10.4	103	7.1	-11.1	102.9	3.6	12.5	100	-2.4	-27.9	100						
191h	0.4	25.3	-2.5	0.1			2.8	6	102.3	6.1	13.1	102.4	9.4	18.9	99.4	0.7	-15.5	98.8						
191i	0.7	-0.5	-4.7	-1.8			-1.5	13.3	35.7	-2.8	-17.7	8.4	4.4	2.2	26.2	-1.9	-6.1	39.6						
234b	0.4	0.9	-3.3	-0.4			4.8	4.3	60.9	1.3	-12.7	-20.2	2.9	2.2	38.2	-4	-3.6	13.8						
234d	-0.8	-0.8	-6.9	-4.3			54.5	-1.7	38.7	0.4	3.7	9.6	0	1.2	31.1	2.5	-3.9	11.7						
234e	-1.6	-0.9	-2.2	-3.4			4.2	6.9	29	13.7	12	3.7	9	12.8	44.8	3.4	-4.4	26.9						
234f	-0.6	-0.7	-2.5	-2.9			4.9	3	43.6	12.4	-8.9	94.5	8.7	8.7	83.6	-9.7	-9.8	98.2						
234i	-1.6	-1.5	-1.1	-2.8			-6.1	-3.2	65.4	-4.1	-2.3	64.5	-7	8.3	48.2	-8.5	-12.4	49.3						
234j	-1.3	0.1	-0.6	-0.5			8.7	10.7	102.8	10.1	18.5	102	14.7	25	99.7	-22.5	-20.2	98.8						
234k	-0.7	-1.2	1.6	1.7			2.5	1	55.7	11.1	21.2	70	10.8	16.2	59.2	-5.9	-7	55.3						

3.5.4. TargetD² – GPR119 receptor antagonist

GPR119 is a G protein coupled receptor with a limited tissue distribution and is expressed only in the pancreas and intestine. In the pancreas, activation of the receptor results in a potentiation of glucose-induced insulin secretion, while in the intestine activation of the receptor increases secretion of incretin peptides, namely GLP1 and gastric inhibitory peptide (GIP). Thus, GPR119 agonists might exert a dual control of glucose homeostasis.^{168, 169}

None of the compounds tested have shown any significant stimulation of the receptor at 10 μ M with the maximum being only 10.5% for **191b** (Table 63).

3.5.5. TargetD² – Apelin Receptor (APJ) agonist

The apelin receptor is a G protein coupled-receptor implicated in a variety of biological processes such as angiogenesis, blood pressure regulation, feeding behaviour and HIV entry.^{170, 171}

None of the compounds tested have shown any significant stimulation of the receptor at 10 μ M, with the maximum stimulation being 15.4% for **191i** (Table 63).

3.5.6. TargetD² – Calcitonin Gene-Related Peptide receptor (CGRP) antagonist

CGRP is a neuropeptide involved in the patho-physiology of migraine. CGRP plasma levels have been reported to increase during a migraine attack and to normalise when the migraine is successfully treated with a triptan. Infusion of CGRP into individuals with past history of migraine can induce an attack and CGRP receptor antagonists have proved to be able to treat migraine attacks.^{172, 173}

Three compounds (**191b**, **234e** and **234f**, Table 63) showed average inhibition at 30 μ M with compound **191b** (Table 63) showing 73.4% of inhibition. The calculated IC₅₀s for compounds **234e** and **234f** were respectively 79.3 μ M and 12.4 μ M (Table 63).

3.5.7. TargetD² – Metabotropic glutamate receptor 2 (mGluR2) allosteric antagonist

Glutamate is the major excitatory neurotransmitter in the mammalian central nervous system, acting at both ligand gated ion channels and G-protein coupled receptors, the

latter known as metabotropic glutamate receptor (mGluR). Antagonists of mGluR2 and mGluR3 are being researched as potential treatments of neurological and neuropsychiatric disorders.^{174, 175}

Among the compounds tested, **165j**, **166i**, **165n**, **191g** and **234f** (Figure 113, Table 61, page 169) have shown strong inhibition of the receptor, with the highest being 305.8% at 50 μ M. Nevertheless, the IC₅₀ values for these compounds were higher than 25 μ M.

3.5.8. TargetD² – Hexokinase 2 (HK2) inhibitor

It is well known that tumour cells often rely on glycolysis for energy production and this phenomenon is known as Warburg effect. Hexokinase 2 catalyses the conversion of glucose into glucose-6-phosphate and this step is essential for both glucose intake and to initiate glycolysis. HK2 is highly expressed in many tumour types and is correlated to tumour aggressiveness and poor survival prognosis.¹⁷⁶

Among the compounds tested, **190f**, **175n**, **181i** and **191g** (Figure 113, Table 61, page 169) have shown enzyme inhibition higher than 50%. The IC₅₀ values for these compounds were though higher than 20 μ M.

3.5.9. TargetD² – Enhancer of Zeste Homolog 2 (EZH2) inhibitor

EZH2 is a histone methyltransferase and EZH2-mediated methylation results in silencing of tumour suppressor gene expression. EZH2 overexpression has been correlated with tumour growth, metastasis and chemo-resistance. Thus, it has been postulated that inhibition of EZH2 may provide a novel approach in the treatment of cancer.^{177, 178}

The tests for the majority of the compounds is still in progress and therefore results for only few of them are currently available. Among the compounds tested, **170aa** (Figure 113, Table 61, page 169) showed 80% inhibition at 100 μ M and might proceed to further screening steps.

Table 63. Table of the activity of the tested compounds against the TargetD² assay modules.*

Compound	Endocrine/cardiovascular		Neuroscience					Oncology		
	GPR 119 Receptor Agonist	Apelin Receptor (APJ) Agonist	CGRP Receptor Antagonist		mGlu2R Allosteric Antagonist			Hexokinase 2 (HK2) Inhibitor		EZH2
	hGPR119 cAMP 384 HEK293 Dxycycl	hApelin cAMP	hCGRP1 cAMP	hCGRP1 cAMP	hMGLUR 2 cAMP DMSO	rMGLUR2 Ca Moblzn	hMGLUR 2 cAMP DMSO	hHK2 ADP-FP	hHK2 ADP-FP	hEZH2_5-mer SPA
	%Stim @ 10uM	%Stim @ 30uM	%Inhib @ 30uM	IC50 (uM)	%Inhib @ 50uM	%Inhib @ 25uM	IC50 (uM)	%Inhib @ 20uM	IC50 (uM)	%Inhib @ 100uM
165j	-2,5	-32,6	4,9		252.7 211.9 305.8	-3		20,4		12,1
163aa	3,9	-21,3	10,7		23.7 30.0			6,3		-3,6
143z	-2,5	-31,4	-53,9		61.3 50.8 96.9	-20,8		18,7		26,7
166i	-2,6	-33,4	-84,4		106.3 86.9 89.7	0	>25.0	-0,7		17,2
170aa	-2,5	-1,5	25,4		66.4 50.8 77.8	9		13,6		81,1
146x	-2,5	-52,1	-37,3		-1.9 4.3			2,2		41,6
166s	0	-70,7	-94,5		19.2 9.2			23		20,1
181b	0	-4,4	-22,2		41,3			-9,1		TIP
190f	-1	-22,3	-16,6		54,2		>25.0	63,4	>20.0	TIP
191b	10,5	3,1	73,4	Fit Error	-14,7			-32,5		TIP
175n	-6,7	14,6	-15,6		153,8		>25.0	67,4	>20.0	TIP
211b	-1,9	-1,2	-51,3		40,4			6,7		TIP
228b	1	-14,3	-79,6		93		>25.0	-20,7		TIP
228d	-4,8	-8,2	16,6		22,8			42,3		TIP
181g	-1	-3,7	-28,1		15,4			39,1		TIP
181i	-5,7	-12,6	-87,8		38			59,4	>20.0	TIP
232a	-6,7	11,9	29,2		47,8			-26		TIP
232b	-1,9	-2	-7,9		36,9			-4,4		TIP
191g	6,7	-16,3	5,2		163,8		>25.0	54,1	>20.0	TIP
191h	-2,9	-58,8	19,4		-3,1			28,7		TIP
191i	2,9	15,4	-17,2		12,6			23,5		TIP
234b	1,9	8,3	5,6		3,2			-17,9		TIP
234d	-1	-12,7	21,7		60,1		>25.0	24,5		TIP
234e	-1,9	-10	44,4	79.32	39,4			-6,7		TIP
234f	-5,7	-17,8	43,4	12.436	205,2		>25.0	27,7		TIP
234i	-4,8	-24,1	19,5		56		>25.0	5,3		TIP
234j	1,9	8	-12,7			>25.0				TIP
234k	3,8	-3,5	-19,7							TIP

*TIP = test in progress

3.5.10. Conclusions

During the screening on the OIDD panel some possible hits have been found against CGRP receptor, Hexokinase 2, GLP1 secretion and maybe EZH2 but mainly against mGlu2R. In fact, concerning GLP1 secretion, one compound (**143z**) has shown higher levels of stimulation than the rest of the tested compounds, which were completely

inactive. Thus, the compound might possess the key functionalisation needed for a good interaction and much space has been left for further investigation and optimisation. For mGlu2R inhibition, a few compounds have shown really high percentage of inhibition and, even though they did not meet the criteria set from Eli Lilly concerning further investigation, they still represent promising examples.

Neuropsychiatric disorders and diabetes are therapeutic areas that are very attractive from an industrial point of view. In fact, they occupy a very wide area of the pharmaceutical market and this is shown also from the interest that Eli Lilly put into the discovery of new therapeutics for these type of diseases.

3.6. Summary

Estrogens play an important role in the development of the majority of breast cancers, which often develop in a hormone-sensitive form. Treatment of hormone-dependent breast cancer (HDBC) is clinically performed with the use of estrogen signalling or biosynthesis disruptors in addition to surgery, radiotherapy and chemotherapy. The use of tamoxifen, a selective estrogen receptor modulator (SERM), and anastrozole, an aromatase inhibitor, is common practice in therapy for the treatment of HDBC. Inhibition of other steroidogenic enzymes like 17β -hydroxysteroid dehydrogenase type 1 (17β -HSD1) is a novel approach for the treatment of HDBC.

Estrogen receptor-related receptor α (ERR α) is an orphan nuclear receptor that shares a high homology with the estrogen receptor α (ER α). Contrarily to ER α , ERR α does not bind estradiol (E2) and is constitutively active. ERR α seems able to take over the functions of ER α in hormone independent breast cancer (HIBC) and is an emerging target for the treatment of HIBC. In addition, ERR α is involved in the metabolic adaptation to hypoxia in cancer cells.

As a route to discovery of new steroidomimetic templates with attractive pharmaceutical properties, that might form the basis for new drug candidates, 1,2,3,4-tetrahydroisoquinoline (THIQ) was chosen as a core structure that would be easy to access and could be broadly substituted. The choice was influenced by the structural similarities between THIQ and both E2 and diethylstilbestrol (DES), the product of 17β HSD1 and a known inhibitor of ERR α , respectively (Figure 114).

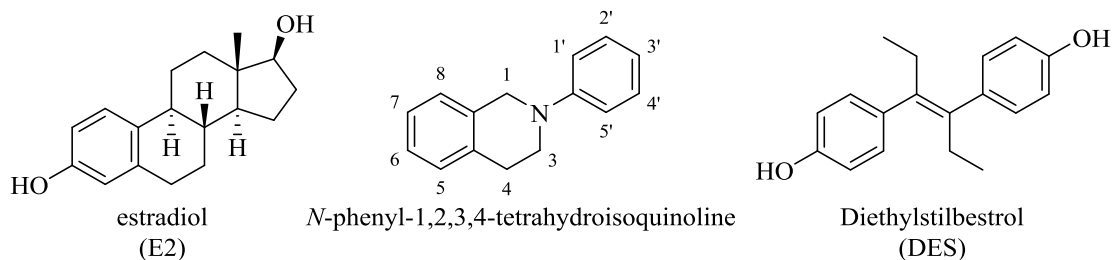


Figure 114. The comparison between the structure of THIQ, E2 and DES gave the rationale for choosing THIQ as core structure.

The synthetic routes were built around three cyclisation methods: Pomeranz-Fritsch (PF), Pictet-Spengler (PS) and Bischler-Napieralski (BN). The synthetic approaches used were specifically chosen to permit simple access to a fairly large number of steroidomimetic compounds, decorated in a fashion that would enhance target interaction and provide clear strategies for optimisation. In this way, 77 final THIQs, substituted in every position, were obtained. Improvements in yield and robustness of the reactions may be achieved with further attention to the reaction conditions, but for the purpose of this work the main emphasis was on creating structural diversity. The use of clean and high-yielding reactions allowed multiple steps to be performed without purification after the workup or to combine two steps in one pot. Where possible, the use of air stable and easy-to-handle reagents generated synthetic processes that may be easily scaled up. Similarly, the use of reactions near to room temperature, will allow for easier future industrial development.

Interestingly, electronic effects were shown to play an important role during the PF reaction and the following reductive dehydroxylation. In fact, compounds lacking a methoxy group *para* to the cyclisation position could only be cyclised using 70% perchloric acid.

Often, it was possible to recover two different regioisomers from one cyclisation step and separate them by flash chromatography. 5- And 7-methoxy THIQs could be obtained from the same PF reaction and similarly it was possible to obtain 6- and 8-methoxy THIQ from a single PS or BN reaction (Figure 115). Further investigation of other factors controlling such cyclisations, such as temperature, may allow greater control over regioisomer formation.

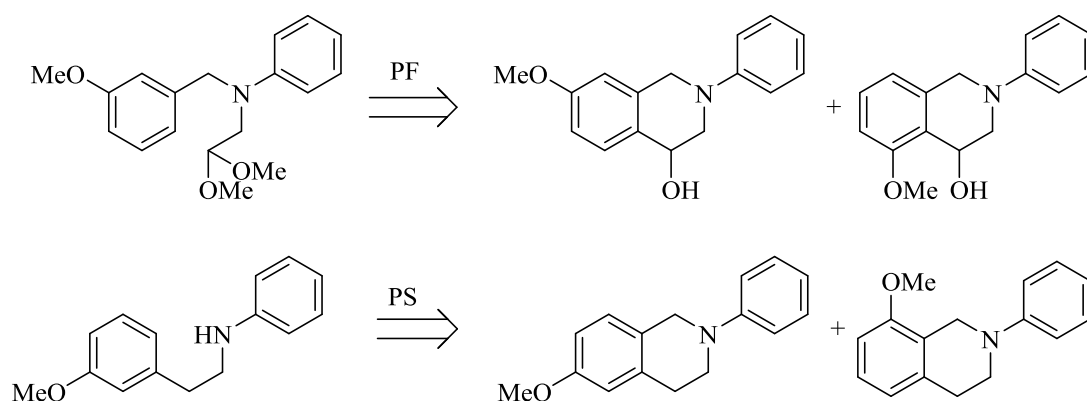


Figure 115. During both the PF and PS reactions, it was sometime possible to isolate two regioisomers in one single cyclisation step. The BN reaction gave results similar to the PS reaction.

The syntheses proceeded with decent overall yields and for one of the most complex compounds (such as the 1,4-disubstituted compound **234a**, Table 34, page 99) the overall yield of the 6 step synthesis was *ca.* 6.8%. For each compound bearing a substituent in position 1, 3 or 4, only the racemic mixture was isolated. Attempts to synthesise enantiomerically pure 1-substituted THIQs failed at the cyclisation step. Furthermore, for compound **234a** (Table 34, page 99), as for some others bearing substituents in both position 1 and 4 (Figure 116), additional stereochemical issues were raised. NOESY analysis confirmed that the relative stereochemistry of the compound was effectively *trans*, while chiral HPLC and a chiral shift NMR experiment confirmed the presence of only two enantiomers, showing that chiral discrimination had occurred.

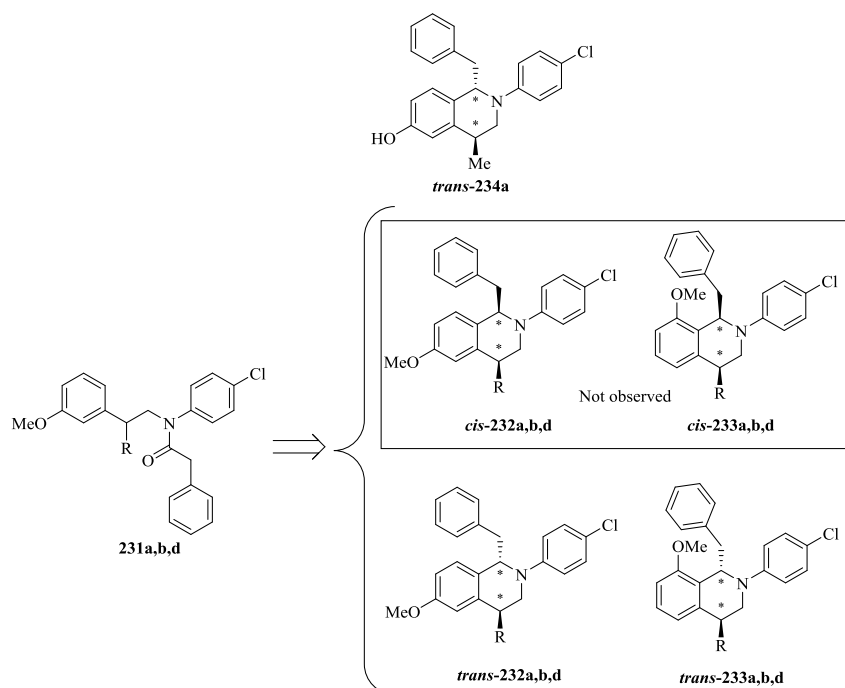


Figure 116. TOP: structure of compound **234a**. BOTTOM: Cyclisation of the amides **231a,b,d** under the BN conditions led to only the *trans* diastereoisomer.

Three THIQs (**170i**, **170s** and **191c**, Figure 117) were selected for their structural differences and screened against a panel of 19 nuclear hormone receptors (NHRs) at 100 μ M. The simple differences in substitution among the three compounds tested showed significant structure-dependent activity and selectivity against NHR subtypes. For instance, **170i** was a strong agonist against ER α , while **191c** was a strong antagonist (Table 57-Table 58, pages 160-161). **170s** showed agonist activity only against ER α and ERR α but only antagonist activity against all the other receptors (Table 57-Table 58, pages 160-161). The same compound 170s was reported in the literature to show K_i of 1000 nM against ER α and of 375 nM against Er β .¹⁸⁷ The differing selectivity obtained with such small substitutions demonstrates that the THIQ core structure may be an effective template for structure-activity relationship (SAR) investigation against many diverse NHRs. Hence, desirable NHR selectivity might in principle be achieved with the appropriate substitution pattern around the THIQ core.

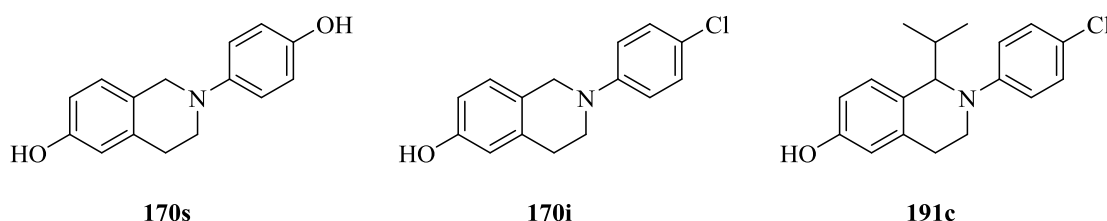


Figure 117. Structure of the three compounds selected for the NHR screening. Compounds **191c** and **170s** differ to **170i** by one single substituent, thus allowing comparison of the results obtained in the screening process,

54 of the synthesised THIQs were selected by the National Cancer Institute of America (NCI) and were evaluated for potential off-target anti-cancer activity against a panel of 60 cell lines. Three compounds, **164j**, **176x** and **175n** (Figure 118) showed a general growth inhibition at 10 μ M against the 60 cell lines of $41.3\% \pm 56.0\%$, $30.2\% \pm 24.5\%$ and $88.1\% \pm 42.1\%$, respectively. The remaining 51 compounds showed only an average of $3.5\% \pm 11.8\%$ inhibition at the same concentration. Cytotoxicity is undesirable for a 17 β -HSD1 inhibitor as the type of targeted clinical approach under consideration is aimed at hormone-dependent tumours, by blocking the availability of active hormone, rather than by exerting tumour cytotoxicity. However, the three compounds that were found to be cytotoxic may be worth pursuing independently, to optimise potency and selectivity, although it is unclear at this stage what their specific targets might be. A single crystal X-ray structure of active compound **164j** (Figure 75, page 127) was successfully obtained.

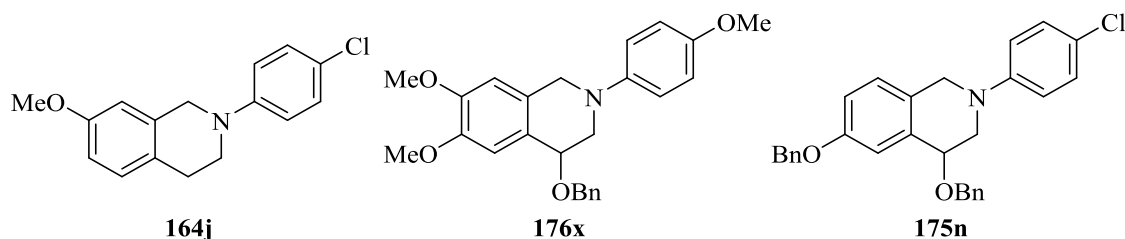


Figure 118. Structure of the three compounds that showed cytotoxic activity in the NCI 60 cell line panel.

Further screening for wider off-target activity through the Eli Lilly Open Innovation in Drug Discovery (OIDD) initiative led to interesting results against some surprising targets. Compound **143z** showed 50% stimulation of glucagon-like peptide 1 (GLP-1) secretion at 20 μM . This compound was the only one of the 28 compounds selected by Lilly to show any activity against this target, probably meaning that the hydroxyl group in position 4 is highly important for activity. Three compounds showed average inhibition of the calcitonin gene-related peptide (CGRP) receptor at 30 μM with **191b** showing 73.4% inhibition and **234e,f** showing an IC_{50} of 79.3 μM and 12.4 μM , respectively. In addition, a few compounds showed high activity against metabotropic glutamate receptor 2 (mGluR2) with allosteric inhibition higher than 100% at 50 μM . However, the relative IC_{50} values were greater than 25 μM . Limited by the number of compounds tested (28 THIQs) and by the lack of direct control in the selection of the compounds, it was not possible to establish an SAR profile for the different targets. However, the hits identified are novel leads and might be worth further optimisation for specific target activity.

The activity of the synthesised THIQs was investigated against $\text{ERR}\alpha$ using a commercially available TR-FRET assay kit. The results obtained were complex and compounds showed only modest to average activity at 100 μM . However, the best inverse agonist, **234i** (Table 56, page 154), showed an efficacy of 79% against $\text{ERR}\alpha$ at 100 μM , where the known inhibitor DES showed only 64% efficacy at the same concentration. A unique SAR profile could not be determined because the SAR of some positions of the THIQs were strictly dependent on the substituent in other positions. For example, this was the case for the substitution in position 4' of the 6-methoxy, 8-methoxy and 6-hydroxy series (Table 53, page 151). Similarly, substitution in position 4 of the 6-methoxy and 6-hydroxy series (Table 55, page 153) had a contrasting effect. Similarly, a methyl group in position 3 of the dimethoxy substituted compound **166s** (Figure 106, page 157) led to completely inverted activity compared to compound **163s** (Figure 106, page 157) from an inverse agonist into an agonist. This effect was not

encountered in any of the other compounds tested and would be worth future investigation. The same substitution on the 4-chloro-6-methoxy or 4-chloro-6-hydroxy compounds (**166i** and **234a**, respectively, Table 54, page 152) did not lead to any similar effect. Compound **234i** (Table 56, page 154) was active at 100 μ M; since this compound possesses significant lipophilicity with a moderate activity, structural simplifications or modifications that reduce lipophilicity should be considered as first priority for future development.

The information that may be obtained from a crystal structure of the target enzyme 17 β -HSD1 with a THIQ would be invaluable in facilitating lead optimization. 17 β -HSD1 was expressed in a bacterial system and the protein was purified in mg amounts. Co-crystals of 17 β -HSD1 bound to compound **170i** were achieved, but attempts to obtain an X-ray crystal structure failed due to the fragility of the crystal obtained, although attempts to obtain a diffraction pattern were made at the Diamond source. Though the conditions used successfully gave crystals, further effort needs to be invested to obtain stronger crystals. This is particularly important for eventual activity correlation and optimisation, since clearly multiple binding modes could be envisaged for a THIQ template.

An in-house cellular assay was devised to obtain general information on toxicity, estrogenicity, anti-estrogenicity, and activity against 17 β -HSD1. T47-D cells were cultured and treated with an initial set of active THIQs, in the presence or absence of estrone (E1) or E2. However, in general this did not give positive results for those evaluated. T47-D is a cell line that naturally expresses a high level of 17 β -HSD1, but has generally proved prone to phenotypic selections or mutations. The cells used were insensitive to estrogenic stimulation and showed anomalies in growth levels over time. In future, the use of certified cells may overcome the problems encountered. Alternatively, the same problem could be overcome using genetically engineered cells that express high levels of 17 β -HSD1 and are hormone-sensitive.

The attempted use of an in-house colourimetric assay did not allow the screening of the synthesised THIQs against 17 β -HSD1, as was hoped. The assay was developed as a colourimetric assay to try to overcome the limitations of the radiochemical assays normally performed. Even though the assay was reliable when testing steroidal derivatives, such as the known potent 17 β -HSD1 inhibitor STX1040 from our group, it proved not sensitive enough for the THIQ lead compounds. The same compounds were

also tested by our industrial colleagues at Ipsen, France in a radiochemical assay and though the steroidal inhibitors showed similar trends in both the colourimetric and radiochemical assays, the THIQ derivatives did not. THIQs were mostly inactive in the colourimetric assay, but generally active in the radiochemical assay. For instance, compound **170i** showed 77% inhibition at 750 nM in the whole-cell radiochemical assay performed by Ipsen and 64% at 6 μ M in a cell lysate radiochemical assay performed by another collaborator, Prof. Tea Lanisnik-Rizner (Table 40, page 123). However, compound **170i** showed only 23% inhibition at 1 mM in the colourimetric assay (Figure 57, page 112). Understanding the reasons that make the assay so insensitive may lead to its optimisation and as a consequence, to simple and quick access to inhibition data, which would be very useful.

Some THIQs synthesised, however, were indeed active in both the whole-cell and cell lysate radiochemical assays. This proved that the compounds can penetrate the cell membrane to inhibit the enzyme and suggested that the THIQs possess a reasonable physicochemical profile, as hoped. Screening of the compounds against the target enzyme in the cell lysate radiochemical assay led to the generation of a SAR profile around the core structure (Figure 119 and chapter 3.1.6, pages 134-137) and to the identification of the best lead compound to date from this work, **234e**, that showed an IC_{50} value of 336 nM against 17 β -HSD1.

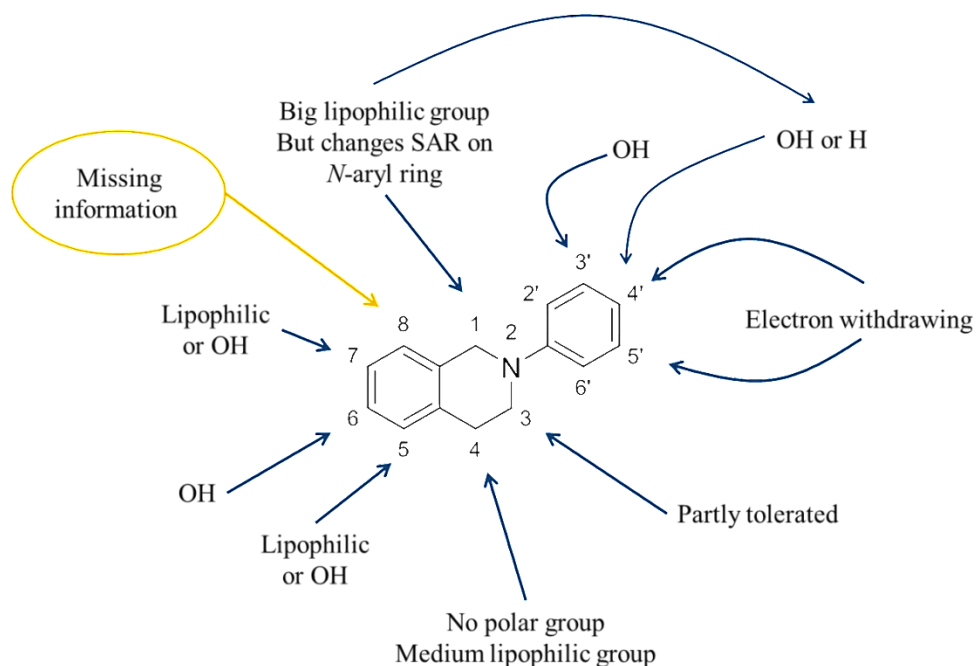


Figure 119. SAR for 17 β -HSD1 of substitutions around the core THIQ structure.

Thus, in this study THIQs have proved to be valuable steroidomimetic core structures against several different targets, even including targets apparently unrelated to steroids. The physicochemical properties of the core structure allowed the introduction of complexity, while maintaining drug-like properties, as described by e.g. the Lipinski rules. This is important for the future development of the compounds prepared, because it decreases the chances for any potential drug to fail at a later stage of clinical testing. It is important that such properties are maintained while further developing these compounds for enhanced target activity. An attractive and potent 17 β -HSD1 inhibitor was successfully designed that, with some further potency optimisation, should exemplify the success of our new THIQ approach and permit essential pre-clinical exploration of the validity of the 17 β -HSD1 enzyme target in hormone dependent malignancies.

CHAPTER 4

Experimental

4.1. Chemistry: materials and methods

All chemicals were purchased from Aldrich Chemical Co. or Alfa Aesar. All organic solvents of A. R. grade were supplied by Fisher Scientific. Thin-layer chromatography (TLC) was performed on precoated plates (Merck TLC aluminium sheets silica gel 60 F254). Product(s) and starting material(s) were detected by either TLC and/or LC-MS. Flash column chromatography was performed on RediSep® prepacked columns (normal phase and reversed phase) with an Isco CombiFlash® Rf. ¹H NMR (400 MHz or 500 MHz) spectra were recorded with a Bruker and chemical shifts are reported in parts per million (ppm). HPLC and low resolution mass spectra analyses were obtained on a Waters Micromass ZQ equipped with a Waters 996 PDA detector using either a Waters Radialpack C18 reversed phase column (8 × 100 mm), or a Symmetry C18 reverse phase column (4.6 × 150 mm) eluting with the solvent system specified at 1.0 mL/min. High-resolution mass spectra were recorded at the Mass Spectrometry Service Centre, University of Bath on a Bruker microTOF. Elemental analyses were performed by the Science Centre at London Metropolitan University. Melting points were determined using an Optimelt block and are uncorrected.

2,2-Dimethoxyacetaldehyde was purchased as aqueous solution and was extracted in CHCl₃ before use. Petroleum ether (pet. ether) used for chromatography was the 40-60 °C distillate. The general procedures were followed unless indicated otherwise. ¹H, ¹³C and 2D NMR analyses of the final THIQ hydrobromide or hydrochloride were performed on the free bases unless specified otherwise.

4.1.1. General reaction procedures

General method for the double reductive amination reaction (Method A):

Benzaldehyde (1.0 mL, 10 mmol) and aniline (1.1 mL, 12 mmol) were dissolved in CHCl₃ (60 mL) then treated with NaBH₄(OAc)₃ (3.3 g, 15 mmol). After stirring for 1 h at rt, 2,2-dimethoxyacetaldehyde (30 mmol) was introduced into the reaction mixture followed by NaBH(OAc)₃ (3.3 g, 15.0 mmol). After stirring for 8 h at rt the mixture was quenched with a saturated aqueous solution of K₂CO₃. The aqueous layer was extracted

with CHCl_3 (30 mL). The combined organics were dried with MgSO_4 , filtered and evaporated to give a pale yellow oil (3.87 g).

General method for the PF cyclisation with HClO_4 (Method B): Compound **123a** (3.0 g, 11.1 mmol) was dissolved in 70% HClO_4 (33 mL) and stirred for 1 h at rt. The mixture was then diluted with water (30 mL) and basified with Na_2CO_3 . The aqueous layer was then extracted with EtOAc (3 x 30 mL). The combined organics were dried with MgSO_4 , filtered and evaporated to give a brown foam (2.97 g).

General method for the PF cyclisation with HCl (Method C): Compound **123f** (500 mg, 1.66 mmol) was dissolved in conc. HCl (2 mL) and stirred at rt for 1 h during which time the mixture turned red. The reaction mixture was cooled to 0 °C and then quenched slowly with aq. 3 N NaOH (10 mL) (a white suspension with a yellow precipitate formed) and extracted with EtOAc (20 mL). The organic layer was dried with MgSO_4 , filtered and evaporated to give a yellow-brown oil (445 mg).

General method for the reductive dehydroxylation (Method D): The crude compound **143a** (2.77 g) was dissolved in DCM (60 mL) and Et_3SiH (6.0 mL, 36.9 mmol) and $\text{BF}_3 \cdot \text{Et}_2\text{O}$ (9.8 mL, 36.9 mmol) were introduced in the order. After refluxing for 18 h, the mixture was cooled to rt and quenched with a saturated aqueous solution of Na_2CO_3 (50 mL). The aqueous layer was then extracted with EtOAc (2 x 50 mL). The combined organics were dried with MgSO_4 , filtered and evaporated to give a green oil (2.03 g).

General method for the reductive dehydroxylation (Method E): NaBH_4 (1.53 g, 39.7 mmol) was added to a stirring solution of **146x** (2.50 g, 7.93 mmol) in DCM (30 mL) followed by the dropwise addition of TFA (3.1 mL) and the mixture was stirred at rt for 3 h. The mixture was then diluted with DCM (30 mL) and washed with a sat. aq. solution of Na_2CO_3 (2 x 60 mL) and dried with MgSO_4 , filtered and evaporated to give a pale yellow solid (2.45 g).

General method for methoxy deprotection (Method F): **163e** (200 mg, 836 μmol) was suspended in 46% HBr (3 mL) and stirred for 3 h at 120 °C. The mixture became a solution upon heating. The mixture was then cooled to rt and filtered to give the product as a white precipitate (230 mg, 90%).

General method for methoxy deprotection (Method G): 1.0 M solution of BBr_3 (6.7 mL, 6.68 mmol) in DCM was added to a stirring solution of **167x** (200 mg, 0.668

mmol) in anhydrous DCM (1 mL) at 0 °C under inert atmosphere. The mixture was stirred for 2 h letting it reach rt then quenched with a minimum amount of ice and stirred for 10 min. The mixture was filtered and the precipitate was washed with DCM then dried to give the product as a yellow solid (168 mg, 74%).

General method for the synthesis of amides 178a-h (Method H): SOCl₂ (14.6 mL, 200 mmol) was added to a stirring solution of 3-methoxyphenylacetic acid (3.39 g, 20.0 mmol) in anhydrous DCM (40 mL) and the mixture was stirred at rt for 4 h. The mixture was then evaporated and the residue was dissolved in anhydrous toluene (40 mL) and *N,N*-diisopropylethylamine (7.0 mL, 40.0 mmol), aniline (2.7 mL, 30.0 mmol) and a catalytic amount of DMAP were introduced in the order. The mixture was refluxed under inert atmosphere overnight and the solvent was then evaporated. The residue was dissolved in EtOAc (150 mL) and washed with 1 N HCl (3 x 100 mL), 1 N NaOH (3 x 100 mL) and brine (2 x 100 mL) then dried with MgSO₄, filtered and evaporated to give a yellow solid (2.73 g).

General method for the reduction of the amides (method I): A solution of **178a** (2.0 g, 8.29 mmol) in anhydrous THF (41 mL) was added to a stirring suspension of LiAlH₄ (521 mg, 12.4 mmol) in THF (10 mL) under inert atmosphere and the mixture was stirred at 80 °C for 4 h during which time the mixture turned green. The mixture was then cooled to 0 °C, diluted with Et₂O (50 mL) and carefully quenched with water (0.6 mL) under inert atmosphere. The mixture was stirred for 15 min, during which time a black precipitate formed. 15% NaOH (0.6 mL) was introduced and the mixture was stirred for 15 min, during which time the precipitate turned white. Water (1.2 mL) was added and after stirring for 15 min the mixture was dried with MgSO₄, filtered and evaporated to give a brown oil (1.7 g).

General method for the PS cyclisation (method J): Compound **179f** (1.0 g, 3.82 mmol) was dissolved in toluene (18 mL) and treated with paraformaldehyde (573 mg, 19.1 mmol) and PTSA (32 mg, 0.191 mmol). After stirring at 90 °C for 18 h, the mixture was cooled to rt and filtered. The solvent was evaporated and the residue was dissolved in DCM (30 mL). The organic layer was washed with 1 N NaOH (20 mL) then dried with MgSO₄, filtered and evaporated to give a yellow oil (996 mg).

General method for the BN cyclisation (Method K): POCl₃ (836 µl, 8.88 mmol) was added to a stirring solution of **180a** (450 mg, 1.48 mmol) in anhydrous toluene (15

mL) and the mixture was stirred at 100 °C overnight. The mixture was then cooled to rt and the solvent was evaporated. The residue was dissolved in MeOH (15 mL) and NaBH₄ (343 mg, 8.88 mmol) was added. The yellow solution started foaming and turned colourless. The mixture was stirred at rt for 1 h then the solvent was evaporated and the residue was dissolved in EtOAc (50 mL). The organic layer was washed with 1 N NaOH (2 x 50 mL) then dried with MgSO₄, filtered and evaporated to give a yellow oil (979 mg).

General method for the Weinreb reaction (Method L): 1.4 M solution of MeMgBr (1.2 mL, 1.67 mmol) in toluene/THF (3:1) was added to a stirring solution of **208** (290 mg, 1.39 mmol) in anhydrous THF (14 mL) under inert atmosphere and the mixture was stirred at rt for 1 h. The mixture was quenched with 1N HCl (3 mL) and extracted with EtOAc (3 x 30 mL). The combined organics were dried with MgSO₄, filtered and evaporated to give the product as a yellow oil (211 mg, 93%).

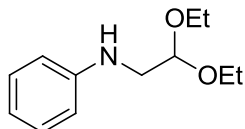
General method for the alkylation of the ester 226 (method M): 2.0 M LDA (3.3 mL, 6.66 mmol) was added to a stirring solution of **226** (1.0 g, 5.55 mmol) in anhydrous THF (50 mL) at -78 °C under inert atmosphere and the mixture was stirred for 1 h. Methyl iodide (384 µL, 6.11 mmol) was added and the mixture was stirred for 1 h at -78 °C then let reach rt and stirred for further 4 h. The mixture was cooled to 0 °C and carefully quenched with 1 N HCl (10 mL) then the organic solvent was evaporated. The aqueous layer was extracted with EtOAc (3 x 50 mL) and the combined organics were washed with 1 N HCl (3 x 50 mL) and brine (3 x 50 mL) then dried with MgSO₄, filtered and evaporated to give a brown oil (1.11 g).

General method for the direct conversion of ester into amide (method N): 4-Chloroaniline (1.10 g, 8.49 mmol) was added to a stirring solution of bis(trimethylaluminum)-1,4-diazabicyclo[2.2.2]octane adduct (2.20 g, 8.49 mmol) in anhydrous THF (15 mL) under inert atmosphere and the mixture was stirred at 40 °C for 1 h. A solution of **227a** (1.10 g, 5.66 mmol) in anhydrous THF (3 mL) was added and the mixture was refluxed overnight. The mixture was then evaporated and the residue was dissolved in EtOAc (50 mL). The organic layer was then washed with 1 N HCl (3 x 50 mL) and brine (50 mL) then dried with MgSO₄, filtered and evaporated to give a brown oil (1.10 g).

4.1.2. Experimental data

***N*-(2,2-Diethoxyethyl)aniline (115a)**

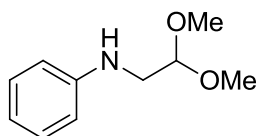
C₁₂H₁₉NO₂, Mol. Wt.: 209.28



Aniline (2.7 mL, 30 mmol) and 2-bromo-1,1-diethoxyethane (3.0 mL, 20 mmol) were dissolved in EtOH 95% (20 ml) and treated with K₂CO₃ (552 mg, 40 mmol). The mixture was refluxed for 18 h. The mixture was filtered and the filtrate was evaporated to give a yellow oil (5.42 g). Part of the crude (1.0 g) was purified by chromatography column in gradient (from 0 % to 5 % EtOAc in pet. ether) to give the product as a yellowish oil (250 mg, 32 % (yield of the purified fraction only)) which showed:^{129, 179} ¹H NMR (400 MHz, CDCl₃) δ 1.26 (6H, t, *J* = 7.2 Hz, CH₃), 3.27 (2H, d, *J* = 5.5 Hz, NCH₂), 3.59 (2H, dq, *J* = 7.2, 14.4 Hz, OCH₂), 3.75 (2H, dq, *J* = 7.2, 14.4 Hz, CH₂), 3.91 (1H, bs, NH), 4.70 (1H, t, *J* = 5.5 Hz, CH(OR)₂), 6.66 (2H, d, *J* = 8.3 Hz, ArH), 6.73 (1H, t, *J* = 7.3 Hz, ArH) and 7.20 (2H, t, *J* = 7.6 Hz, ArH) ppm. ¹³C NMR (101 MHz, CDCl₃) δ 15.5 (CH₃), 46.4 (NCH₂), 62.4 (OCH₂), 101.0 (CH(OR)₂), 113.2 (ArCH), 117.7 (ArCH), 129.3 (ArCH) and 148.0 (ArCN). LC/MS (ES⁺) *t*_r = 1.83 min (97%), *m/z* 210.6 (M⁺+H); (RP, Isocratic, 90% MeOH). HRMS (ES⁺) calcd. for C₁₂H₂₀NO₂ (M⁺+H) 210.1489, found 210.1482.

***N*-(2,2-Dimethoxyethyl)aniline (121)**

C₁₀H₁₅NO₂, Mol. Wt.: 181.23

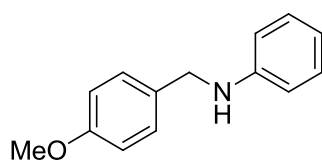


Aniline (456 μL, 5.0 mmol) was dissolved in CHCl₃ (20 mL) and treated in the order with 2,2-dimethoxyacetaldehyde (750 μL, 5.0 mmol) and NaBH(OAc)₃ (3.3 g, 15.0 mmol). After stirring for 18 h at rt, the mixture was quenched with a saturated aqueous solution of K₂CO₃ (20 mL) and the aqueous layer was extracted with CHCl₃ (2 x 20 mL). The combined organics were dried with MgSO₄, filtered and evaporated to give as a yellow oil (834 mg, 92%) which showed:¹⁸⁰ ¹H NMR (500 MHz, CDCl₃) δ

3.26 (2H, d, $J = 5.5$ Hz, NCH_2), 3.42 (6H, s, OCH_3), 3.84 (1H, bs, NH), 4.58 (1H, t, $J = 5.5$ Hz, $\text{CH}(\text{OR})_2$), 6.65 (2H, dd, $J = 1.1, 8.6$ Hz, ArH), 6.73 (1H, tt, $J = 1.1, 7.3$ Hz, ArH) and 7.19 (2H, dd, $J = 7.3, 8.6$ Hz, ArH) ppm. ^{13}C NMR (126 MHz, CDCl_3) δ 45.4 (NCH_2), 53.8 (OCH_3), 102.6 ($\text{CH}(\text{OR})_2$), 113.1 (ArCH), 117.7 (ArCH), 129.3 (ArCH) and 147.9 (ArCN). LC/MS (ES^+) $t_r = 1.57$ min (97%), m/z 182.0 ($\text{M}^+ + \text{H}$); (RP, Isocratic, 90% MeOH) HRMS (ES^+) calcd. for $\text{C}_{10}\text{H}_{16}\text{NO}_2$ ($\text{M}^+ + \text{H}$) 182.1176, found 182.1172.

***N*-(4-Methoxybenzyl)aniline (122a)**

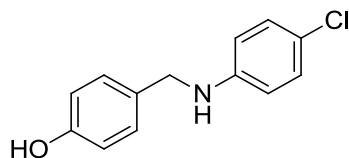
$\text{C}_{14}\text{H}_{15}\text{NO}$, Mol. Wt.: 213.28



4-Methoxybenzaldehyde (1.2 mL, 10.0 mmol) and aniline (1.1 mL, 12.0 mmol) were dissolved in CHCl_3 (60 mL) and treated with sodium triacetoxyborohydride (3.0 g, 14.0 mmol). The reaction mixture was refluxed for 18 h then cooled to rt and quenched with a saturated aqueous solution of NaHCO_3 . The organic layer was washed with brine (20 mL), dried with MgSO_4 , filtered and evaporated to give **153a** as a yellow oil (2.16 g, >99%). ^1H NMR (270 MHz, CDCl_3) δ 3.82 (3H, s), 4.27 (2H, s), 6.60 – 6.82 (3H, m), 6.87 – 6.97 (2H, m), 7.11 – 7.25 (2H, m) and 7.27 – 7.37 (2H, m) ppm.

4-((4-Chlorobenzyl)amino)phenol (122n)

$\text{C}_{13}\text{H}_{12}\text{ClNO}$, Mol. Wt.: 233.69

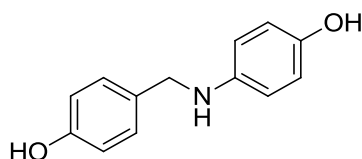


$\text{NaBH}(\text{OAc})_3$ (549 mg, 2.46 mmol) was added to a stirring solution of *p*-hydroxybenzaldehyde (204 mg, 1.64 mmol) and *p*-chloroaniline (182 mg, 1.64 mmol) in CHCl_3 (5 mL) and the mixture was stirred at rt for 1 h. The mixture was washed with a sat. aq. sol. of NaHCO_3 (2 x 5 mL) and the organic layer was dried with MgSO_4 ,

filtered and evaporated to give a pale yellow oil (450 mg). The product was precipitate as hydrochloride from MeOH/DCM to give a pale yellow solid (234 mg, 53%) which showed:¹⁸¹ ¹H NMR (500 MHz, D₆-DMSO) δ 4.09 (2H, d, *J* = 5.9 Hz, CH₂), 6.27 (1H, t, *J* = 5.8 Hz, NH), 6.55 (2H, d, *J* = 8.9 Hz, 2 x ArCH, aniline), 6.70 (2H, d, *J* = 8.5 Hz, 2 x ArCH, benzyl), 7.03 (2H, d, *J* = 8.9 Hz, 2 x ArCH, aniline), 7.12 (2H, d, *J* = 8.5 Hz, 2 x ArCH, benzyl) and 9.28 (1H, bs, OH) ppm. ¹³C NMR (126 MHz, D₆-DMSO) δ 46.0 (CH₂), 113.6 (2 x ArCH, aniline), 115.0 (2 x ArCH, benzyl), 118.7 (ArCCl), 128.4 (2 x ArCH, aniline), 128.4 (2 x ArCH, benzyl), 129.6 (ArCCH₂), 147.7 (ArCN) and 156.2 (ArCO) ppm. HRMS (ES⁺) calcd. C₁₇H₁₉³⁵ClNO (M⁺+H) 234.0680, found 234.0669; calcd. C₁₇H₁₉³⁷ClNO (M⁺+H) 236.0651, found 236.0639. Mp 206-209 °C (as hydrochloride from Et₂O).

4-((4-Hydroxybenzyl)amino)phenol (122p)

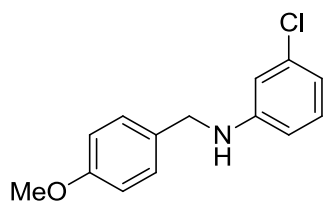
C₁₃H₁₃NO₂, Mol. Wt.: 215.25



NaBH(OAc)₃ (549 mg, 2.46 mmol) was added to a stirring solution of *p*-hydroxybenzaldehyde (204 mg, 1.64 mmol) and *p*-aminophenol (183 mg, 1.64 mmol) in CHCl₃ (5 mL) and the mixture was stirred at rt for 1 h. The mixture was washed with a sat. aq. sol. of NaHCO₃ (2 x 5 mL) and the organic layer was dried with MgSO₄, filtered and evaporated to give a black oil (489 mg). The product was precipitate as hydrochloride from MeOH/DCM to give a black solid (198 mg, 56%) which showed:¹⁸² ¹H NMR (400 MHz, D₆-DMSO) δ 4.07 (2H, s), 6.48 (2H, d, *J* = 8.6 Hz), 6.56 (2H, d, *J* = 8.6 Hz), 6.74 (2H, d, *J* = 8.0 Hz), 7.18 (2H, d, *J* = 8.0 Hz), 8.40 (1H, s) and 9.26 (1H, s) ppm. HRMS (ES⁺) calcd. C₁₃H₁₄NO₂ (M⁺+H) 216.1019, found 216.1011. Degraded before melting (as hydrochloride from DCM).

3-Chloro-*N*-(4-methoxybenzyl)aniline (122t)

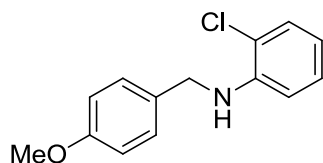
C₁₄H₁₄ClNO, Mol. Wt.: 247.72



4-Methoxybenzaldehyde (2.5 mL, 20.0 mmol) and 3-chloroaniline (2.1 mL, 20.0 mmol) were dissolved in CHCl_3 (40 mL) then treated with $\text{NaBH}_4(\text{OAc})_3$ (6.0 g, 30.0 mmol). After stirring for 18 h at rt, the mixture was quenched with a saturated aqueous solution of Na_2CO_3 (50 mL). The aqueous layer was extracted with CHCl_3 (50 mL). The combined organics were dried with MgSO_4 , filtered and evaporated to give a yellow oil (4.88 g, 98%) which showed: ^1H NMR (500 MHz, CDCl_3) δ 3.81 (3H, s, CH_3), 4.03 (1H, bs, NH), 4.23 (2H, s, CH_2), 6.49 (1H, ddd, $J = 0.8, 2.1, 8.0$ Hz, ArCH, aniline), 6.61 (1H, t, $J = 2.1$ Hz, ArCH, aniline), 6.67 (1H, ddd, $J = 0.8, 2.1, 8.0$ Hz, ArCH, aniline), 6.89 (2H, d, $J = 8.7$ Hz, ArCH, benzyl), 7.07 (1H, t, $J = 8.0$ Hz, ArCH, aniline) and 7.27 (2H, d, $J = 8.7$ Hz, ArCH, benzyl) ppm. ^{13}C NMR (126 MHz, CDCl_3) δ 47.5 (CH_2), 55.3 (CH_3), 111.1 (ArCH, aniline), 112.4 (ArCH, aniline), 114.1 (2 x ArCH, benzyl), 117.3 (ArCH, aniline), 128.8 (2 x ArCH, benzyl), 130.1 (ArCH, aniline), 130.7 (ArCCH_2), 135.0 (ArCCl), 149.2 (ArCN) and 159.0 (ArCO) ppm. LC/MS (ES^+) $t_r = 2.22$ min (89 %), m/z 248.0 ($\text{M}^+ + \text{H}$); (RP, Isocratic, 90% MeOH)

2-Chloro-*N*-(4-methoxybenzyl)aniline (122v)

$\text{C}_{14}\text{H}_{14}\text{ClNO}$, Mol. Wt.: 247.72

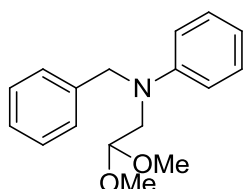


4-Methoxybenzaldehyde (2.5 mL, 20.0 mmol) and 2-chloroaniline (2.1 mL, 20.0 mmol) were dissolved in CHCl_3 (40 mL) then treated with $\text{NaBH}_4(\text{OAc})_3$ (6.0 g, 30.0 mmol). After stirring for 18 h at rt, the mixture was quenched with a saturated aqueous solution of Na_2CO_3 (50 mL). The aqueous layer was extracted with CHCl_3 (50 mL). The combined organics were dried with MgSO_4 , filtered and evaporated to give white solid which was recrystallised from EtOH (5.16 g, >99%) and showed: ^1H NMR (400 MHz, CDCl_3) δ 3.85 (3H, s, CH_3O), 4.37 (2H, s, CH_2N), 4.75 (1H, bs, NH), 6.71 (1H, ddd, $J = 1.5, 7.3, 7.9$ Hz, ArH, aniline), 6.72 (1H, dd, $J = 1.5, 8.2$ Hz, ArH,

aniline), 6.97 (2H, d, $J = 8.7$ Hz, ArH, benzyl), 7.18 (1H, ddd, $J = 1.5, 7.3, 8.2$ Hz, ArH, aniline), 7.34 (1H, dd, $J = 1.5, 7.9$ Hz, ArH, aniline) and 7.36 (2H, d, $J = 8.8$ Hz, ArH, benzyl) ppm. ^{13}C NMR (126 MHz, CDCl_3) δ 47.3 (CH_2), 55.2 (CH_3), 64.9, 111.5 (ArCH, aniline), 114.1 (2 x ArCH, benzyl), 117.3 (ArCH, aniline), 119.1 (ArCCl), 127.8 (ArCH, aniline), 128.6 (2 x ArCH, benzyl), 129.1 (ArCH, aniline), 130.7 (ArCCH₂), 143.9 (ArCN) and 158.9 (ArCO) ppm. LC/MS (ES^+) $t_r = 2.74$ min (94 %), m/z 248.0 ($\text{M}^+ + \text{H}$); (RP, Isocratic, 90% MeOH). HRMS (ES^+) calcd. $\text{C}_{14}\text{H}_{15}^{35}\text{ClNO}$ ($\text{M}^+ + \text{H}$) 248.0837, found 248.0842. calcd. $\text{C}_{14}\text{H}_{15}^{37}\text{ClNO}$ ($\text{M}^+ + \text{H}$) 250.0807, found 250.0820.

***N*-Benzyl-*N*-(2,2-dimethoxyethyl)aniline (123a)**

$\text{C}_{17}\text{H}_{21}\text{NO}_2$, Mol. Wt.: 271.35

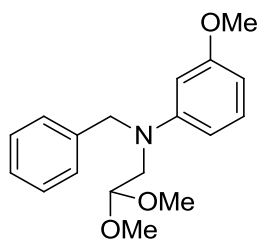


(Method A)

The crude compound was purified by column chromatography (eluent: from 0% to 30% EtOAc in pet. ether) to give **123a** as a colourless oil (2.92 g, 99%) which showed: ^1H NMR (500 MHz, CDCl_3) δ 3.41 (6H, s, OCH_3), 3.58 (2H, d, $J = 5.1$ Hz, NCH_2CH), 4.63 (1H, t, $J = 5.1$ Hz, $\text{CH}(\text{OR})_2$), 4.67 (2H, s, CH_2Ar), 6.70 (1H, tt, $J = 0.9, 7.4$ Hz, ArH), 6.74 (2H, dd, $J = 0.9, 8.9$ Hz, ArH), 7.16 - 7.25 (5H, m, ArH) and 7.27 - 7.34 (2H, m, ArH) ppm. ^{13}C NMR (126 MHz, CDCl_3) δ 53.9 (CH_2CH), 54.6 (CH_3), 54.9 (ArCH₂), 103.5 ($\text{CH}(\text{OR})_2$), 112.3 (ArCH), 116.7 (ArCH), 126.6 (ArCH), 126.8 (ArCH), 128.7 (ArCH), 129.4 (ArCH), 138.9 (ArCCH₂) and 148.7 (ArCN) ppm. LC/MS (ES^+) $t_r = 1.81$ min (87%), m/z 226.0 ($\text{M}^+ + \text{H}$); HRMS (ES^+) calcd. for $\text{C}_{17}\text{H}_{22}\text{NO}_2$ ($\text{M}^+ + \text{H}$) 272.16451, found 272.1651.

***N*-Benzyl-*N*-(2,2-dimethoxyethyl)-3-methoxyaniline (123b)**

$\text{C}_{18}\text{H}_{23}\text{NO}_3$, Mol. Wt.: 301.38

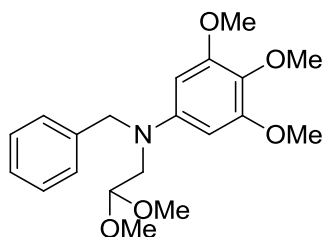


(Method A)

The crude compound was purified by column chromatography (eluent: from 0% to 10% EtOAc in pet. ether) to give a colourless oil (2.21 g, 73%) which showed: ^1H NMR (500 MHz, CDCl_3) δ 3.40 (6H, s, $\text{CH}(\text{OCH}_3)_2$), 3.55 (2H, d, $J = 5.1$ Hz, CH_2CH), 3.74 (3H, s, ArOCH_3), 4.62 (1H, t, $J = 5.1$ Hz, $\text{CH}(\text{OR})_2$), 4.65 (2H, s, ArCH_2), 6.28 (1H, ddd, $J = 0.6, 2.5, 8.2$ Hz, ArH), 6.30 (1H, t, $J = 2.5$ Hz, ArH), 6.36 (1H, ddd, $J = 0.6, 2.5, 8.2$ Hz, ArH), 7.10 (1H, t, $J = 8.2$ Hz, ArH), 7.19 - 7.23 (3H, m, ArH) and 7.27 - 7.32 (2H, m, ArH) ppm. ^{13}C NMR (126 MHz, CDCl_3) δ 53.9 (CH_2CH), 54.7 ($\text{CH}(\text{OCH}_3)_2$), 55.0 (ArCH_2), 55.2 (ArOCH_3), 99.0 (ArCH), 101.5 (ArCH), 103.5 ($\text{CH}(\text{OR})_2$), 105.5 (ArCH), 126.6 (ArCH), 126.8 (ArCH), 128.7 (ArCH), 130.1 (ArCH), 138.8 (ArCCH_2), 150.2 (ArCN) and 160.9 (ArCOCH_3) ppm. LC/MS (ES^+) $t_r = 2.48$ min (96 %), m/z 301.5 (M^+); (RP, Isocratic, 90% MeOH). HRMS (ES^+) calcd. for $\text{C}_{18}\text{H}_{24}\text{NO}_3$ ($\text{M}^+ + \text{H}$) 302.1751, found 302.1738.

***N*-Benzyl-*N*-(2,2-dimethoxyethyl)-3,4,5-trimethoxyaniline (123d)**

$\text{C}_{20}\text{H}_{27}\text{NO}_5$, Mol. Wt.: 361.43



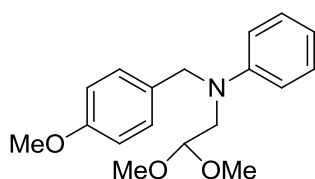
(Method A)

The crude compound was purified by column chromatography (eluent 0% to 30% EtOAc in pet. ether) to give the product as a colourless oil (3.08 g, 85%) which showed: ^1H NMR (500 MHz, CDCl_3) δ 3.41 (6H, s, $\text{CH}(\text{OCH}_3)_2$), 3.54 (2H, d, $J = 5.0$ Hz, CH_2CH), 3.74 (6H, s, ArOCH_3), 3.76 (3H, s, ArOCH_3), 4.59 (1H, t, $J = 5.0$ Hz, $\text{CH}(\text{OR})_2$), 4.60 (2H, s, ArCH_2), 5.97 (2H, s, ArH), 7.21 - 7.24 (3H, m, ArH) and 7.28 -

7.33 (2H, m, ArH) ppm. ^{13}C NMR (126 MHz, CDCl_3) δ 54.66 ($\text{CH}(\text{OCH}_3)_2$), 54.69 (CH_2CH), 55.73 (ArCH_2), 56.07 (ArOCH_3), 61.21 (ArOCH_3), 91.0 (ArCH), 103.8 ($\text{CH}(\text{OR})_2$), 126.8 (ArCH), 127.0 (ArCH), 128.7 (ArCH), 129.9 (ArCOCH_3), 139.1 (ArCCH_2), 145.8 (ArCN) and 153.8 (ArCOCH_3) ppm. LC/MS (ES^+) t_r = 1.93 min (89 %), m/z 361.3 (M^+); (RP, Isocratic, 90% MeOH). HRMS (ES^+) calcd. for $\text{C}_{20}\text{H}_{28}\text{NO}_5$ (M^++H) 362.1962, found 362.1948.

***N*-(2,2-Dimethoxyethyl)-*N*-(4-methoxybenzyl)aniline (123e)**

$\text{C}_{18}\text{H}_{23}\text{NO}_3$, Mol. Wt.: 301.38

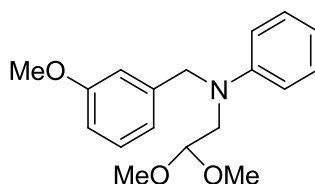


(Method A)

The crude compound was purified by column chromatography (from 0% to 10% EtOAc in pet. ether) to give the product as a yellowish oil (2.09 g, 69%). ^1H NMR (400 MHz, CDCl_3) δ 3.41 (6H, s, CHOCH_3), 3.56 (2H, d, J = 5.0 Hz, NCH_2CH), 3.79 (3H, s, ArOCH_3), 4.60 - 4.65 (3H, m, $\text{CH}(\text{OR})_2$, ArCH_2), 6.61 - 6.73 (1H, m, ArH), 6.76 (2H, d, J = 8.3 Hz, ArH), 6.85 (2H, d, J = 8.3 Hz, ArH), 7.14 (2H, d, J = 8.4 Hz, ArH) and 7.20 (2H, t, J = 7.8 Hz, ArH) ppm. ^{13}C NMR (101 MHz, CDCl_3) δ 53.7 (NCH_2CH), 54.3 (ArOCH_3), 54.6 ($\text{CH}(\text{OCH}_3)_2$), 55.4 (ArCH_2), 103.4 ($\text{CH}(\text{OR})_2$), 112.4 (ArCH), 114.1 (ArCH), 116.6 (ArCH), 127.8 (ArCH), 129.3 (ArCH), 130.7 (ArCCH_2), 148.7 (ArCN) and 158.6 (ArCOCH_3) ppm. LC/MS (ES^+) t_r = 2.46 min (70%), m/z 302.2 (M^++H); HRMS (ES^+) calcd. for $\text{C}_{18}\text{H}_{24}\text{NO}_3$ (M^++H) 302.1751, found 302.1761.

***N*-(2,2-Dimethoxyethyl)-*N*-(3-methoxybenzyl)aniline (123f)**

$\text{C}_{18}\text{H}_{23}\text{NO}_3$, Mol. Wt.: 301.38

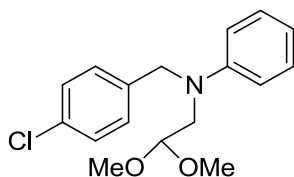


(Method A)

The crude product was purified by column chromatography (from 0% to 10% EtOAc in pet. ether 40-60 °C) to give the product as a pale yellow oil (3.56 g, 79 %) which showed: ^1H NMR (400 MHz, CDCl_3) δ 3.48 (6H, s, CHOCH_3), 3.65 (2H, d, $J = 5.1$ Hz, NCH_2CH), 3.84 (3H, s, ArOCH_3), 4.66 - 4.75 (3H, m, ArCH_2 , $\text{CH}(\text{OR})_2$), 6.67 - 6.92 (6H, m, ArH) and 7.21 - 7.35 (3H, m, ArH) ppm. ^{13}C NMR (101 MHz, CDCl_3) δ 53.86 (NCH_2CH), 54.60 ($\text{CH}(\text{OCH}_3)_2$), 54.93 (ArOCH_3), 55.27 (ArCH_2N), 103.38 ($\text{CH}(\text{OR})_2$), 112.0 (ArCH), 112.3 (ArCH), 112.4 (ArCH), 116.7 (ArCH), 118.9 (ArCH), 129.3 (ArCH), 129.7 (ArCH), 140.8 (ArCCH_2), 148.6 (ArCN) and 160.0 (ArCOCH_3) ppm. LC/MS (ES^+) $t_r = 2.51$ min (98 %), m/z 302.2 ($\text{M}^+ + \text{H}$); (RP, Isocratic, 90% MeOH). HRMS (ES^+) calcd. for $\text{C}_{18}\text{H}_{24}\text{NO}_3$ ($\text{M}^+ + \text{H}$) 302.1751, found 302.1739.

***N*-(4-Chlorobenzyl)-*N*-(2,2-dimethoxyethyl)aniline (123g)**

$\text{C}_{17}\text{H}_{20}\text{ClNO}_2$, Mol. Wt.: 305.80

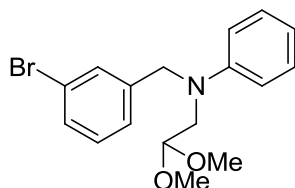


(Method A)

The crude compound was purified by column chromatography (eluent: pet. ether) to give a colourless oil (2.73 g, 88%) which showed: ^1H NMR (500 MHz, CDCl_3) δ 3.40 (6H, s) (2 x OCH_3), 3.55 (2H, d, $J = 5.1$ Hz) (CHCH_2), 4.61 (1H, t, $J = 5.0$ Hz) (OCH), 4.62 (2H, s) (ArCH_2N), 6.70 (2H, d, $J = 8.9$ Hz) (2 x ArCH , aniline), 6.71 (1H, t, $J = 7.3$ Hz) (ArCH , aniline), 7.14 (2H, d, $J = 8.6$ Hz) (2 x ArCH , benzyl), 7.19 (2H, dd, $J = 7.3$, 8.9 Hz) (2 x ArCH , aniline) and 7.26 (2H, d, $J = 8.6$ Hz) (2 x ArCH , benzyl) ppm. ^{13}C NMR (126 MHz, CDCl_3) δ 53.9 (CHCH_2), 54.5 (ArCH_2), 54.7 (2 x OCH_3), 103.4 (OCH), 112.4 (2 x ArCH , aniline), 117.0 (ArCH , aniline), 128.0 (ArCH , benzyl), 128.8 (ArCH , benzyl), 129.5 (ArCH , aniline), 132.5 (ArCCl), 137.5 (ArCCH_2) and 148.4 (ArCN) ppm. LC/MS (ES^+) $t_r = 3.18$ min (97 %), m/z 306.2 (M^+); (RP, Isocratic, 90% MeOH). HRMS (ES^+) calcd. for $\text{C}_{17}\text{H}_{20}^{35}\text{ClNO}_2$ ($\text{M}^+ + \text{H}$) 306.1255, found 306.1245; calcd. for $\text{C}_{17}\text{H}_{20}^{37}\text{ClNO}_2$ ($\text{M}^+ + \text{H}$) 308.1226, found 308.1245.

***N*-(3-Bromobenzyl)-*N*-(2,2-dimethoxyethyl)aniline (123h)**

C₁₇H₂₀BrNO₂, Mol. Wt.: 350.25

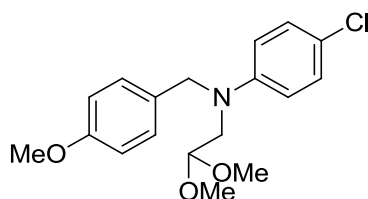


(Method A)

The crude compound was purified by column chromatography (eluent: 0% to 10% EtOAc in pet. ether) to give the product as a colourless oil (1.9 g, 54%) which showed: ¹H NMR (400 MHz, CDCl₃) δ 3.48 (6H, s, CH(OCH₃)₂), 3.65 (2H, d, *J* = 5.1 Hz, NCH₂CH), 3.84 (3H, s, ArOCH₃), 4.66 - 4.75 (3H, m, ArCH₂, CH(OR)₂), 6.67 - 6.92 (6H, m, ArH) and 7.21 - 7.35 (3H, m, ArH) ppm. ¹³C NMR (101 MHz, CDCl₃) δ 53.9 (NCH₂CH), 54.6 (CH(OCH₃)₂), 54.9 (ArOCH₃), 55.3 (ArCH₂N), 103.4 (CH(OR)₂), 112.0 (ArCH), 112.3 (ArCH), 112.4 (ArCH), 116.7 (ArCH), 118.9 (ArCH), 129.3 (ArCH), 129.7 (ArCH), 140.8 (ArCCH₂), 148.6 (ArCN) and 160.0 (ArCOCH₃) ppm. LC/MS (ES⁺) t_r = 2.51 min (98 %), m/z 302.2 (M⁺+H); (RP, Isocratic, 90% MeOH). HRMS (ES⁺) calcd. for C₁₈H₂₄NO₃ (M⁺+H) 302.1751, found 302.1739.

***4*-Chloro-*N*-(2,2-dimethoxyethyl)-*N*-(4-methoxybenzyl)aniline (123i)**

C₁₈H₂₂ClNO₃, Mol. Wt.: 335.83



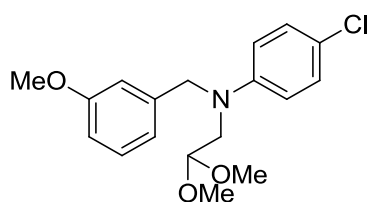
(Method A)

The crude compound was purified by column chromatography (eluent: from 0% to 20% EtOAc in pet. ether) to give the product as a yellow oil (9.16 g, 91%) which showed: ¹H NMR (500 MHz, CDCl₃) δ 3.39 (6H, s, CH(OCH₃)₂), 3.52 (2H, d, *J* = 5.1 Hz, CHCH₂), 3.78 (3H, s, ArOCH₃), 4.55 (1H, t, *J* = 5.1 Hz, CH₂CH), 4.56 (2H, s, ArCH₂N), 6.65 (2H, d, *J* = 9.2 Hz, ArH, aniline), 6.84 (2H, d, *J* = 8.7 Hz, ArH, benzyl), 7.09 (2H, d, *J* = 8.7 Hz, ArH, benzyl) and 7.11 (2H, d, *J* = 9.2 Hz, ArH, aniline) ppm.

^{13}C NMR (126 MHz, CDCl_3) δ 54.0 (CHCH_2), 54.5 (ArCH_2), 54.7 ($\text{CH}(\text{OCH}_3)_2$), 55.4 (ArOCH_3), 103.3 (CH_2CH), 113.7 (2 x ArCH , aniline), 114.2 (2 x ArCH , benzyl), 121.5 (ArCCl), 127.8 (ArCH , benzyl), 129.1 (ArCH , aniline), 130.1 (ArCCH_2), 147.4 (ArCN) and 158.7 (ArCO) ppm. LC/MS (ES^+) t_r = 2.98 min (85 %), m/z 336.1 ($\text{M}^+ + \text{H}$). HRMS (ES^+) calcd. for $\text{C}_{18}\text{H}_{23}^{35}\text{ClNO}_3$ ($\text{M}^+ + \text{H}$) 336.1361, found 336.1346; calcd. for $\text{C}_{18}\text{H}_{23}^{37}\text{ClNO}_3$ ($\text{M}^+ + \text{H}$) 338.1331, found 338.1346.

4-Chloro-*N*-(2,2-dimethoxyethyl)-*N*-(3-methoxybenzyl)aniline (123j)

$\text{C}_{18}\text{H}_{22}\text{ClNO}_3$, Mol. Wt.: 335.83

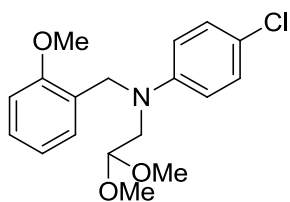


(Method A)

The crude compound was purified by column chromatography (eluent: from 0% to 20% EtOAc in pet. ether) to give the product as a pale yellow oil (9.08 g, 90%) which showed: ^1H NMR (500 MHz, CDCl_3) δ 3.40 (6H, s, $\text{CH}(\text{OCH}_3)_2$), 3.54 (2H, d, J = 5.1 Hz, CHCH_2), 3.76 (3H, s, ArOCH_3), 4.58 (1H, t, J = 5.1 Hz, CHCH_2), 4.60 (2H, s, ArCH_2N), 6.63 (2H, d, J = 9.2 Hz, ArH , aniline), 6.71 – 6.74 (1H, m, ArH , benzyl), 6.74 – 6.80 (2H, m, ArH , benzyl), 7.10 (2H, d, J = 9.2 Hz, ArH , aniline) and 7.22 (1H, t, J = 7.9 Hz, ArH , benzyl) ppm. ^{13}C NMR (126 MHz, CDCl_3) δ 54.2 (CHCH_2), 54.7 ($\text{CH}(\text{OCH}_3)_2$), 55.1 (ArCH_2N), 55.3 (ArOCH_3), 103.3 ($\text{CH}(\text{OCH}_3)_2$), 112.0 (ArCH , benzyl), 112.4 (ArCH , benzyl), 113.6 (ArCH , aniline), 118.8 (ArCH , benzyl), 121.6 (ArCCl), 129.1 (ArCH , aniline), 129.8 (ArCH , benzyl), 140.2 (ArCCH_2), 147.2 (ArCN) and 160.1 (ArCO) ppm. LC/MS (ES^+) t_r = 2.91 min (98 %), m/z 336.0 ($\text{M}^+ + \text{H}$); (RP, Isocratic, 90% MeOH). HRMS (ES^+) calcd. $\text{C}_{18}\text{H}_{23}^{35}\text{ClNO}_3$ ($\text{M}^+ + \text{H}$) 336.1361, found 336.1353; calcd. $\text{C}_{18}\text{H}_{23}^{37}\text{ClNO}_3$ ($\text{M}^+ + \text{H}$) 338.1331, found 338.1353

4-Chloro-*N*-(2,2-dimethoxyethyl)-*N*-(2-methoxybenzyl)aniline (123k)

$\text{C}_{18}\text{H}_{22}\text{ClNO}_3$, Mol. Wt.: 335.83

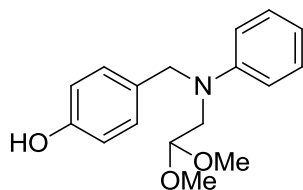


(Method A)

The crude compound was purified by column chromatography (from 0% to 30% EtOAc in pet. ether) to give the product as a yellow oil (4.84 g, 96%) which showed: ^1H NMR (500 MHz, CDCl_3) δ 3.40 (6H, s, $\text{CH}(\text{OCH}_3)_2$), 3.54 (2H, d, $J = 5.1$ Hz, NCH_2CH), 3.86 (3H, s, ArOCH_3), 4.59 (2H, s, ArCH_2N), 4.62 (1H, t, $J = 5.1$ Hz, $\text{CH}(\text{OCH}_3)_2$), 6.66 (2H, d, $J = 9.1$ Hz, ArCH , aniline), 6.84 (1H, td, $J = 1.3, 7.2$ Hz, ArCH , benzyl), 6.88 (1H, d, $J = 8.2$ Hz, ArCH , benzyl), 6.98 (1H, d, $J = 7.2$ Hz, ArCH , benzyl), 7.10 (2H, d, $J = 9.1$ Hz, ArCH , aniline) and 7.22 (1H, td, $J = 1.3, 8.2$ Hz, ArCH , benzyl) ppm. ^{13}C NMR (126 MHz, CDCl_3) δ 50.6 (ArCH_2), 54.2 (NCH_2CH), 54.7 ($\text{CH}(\text{OCH}_3)_2$), 55.1 (ArOCH_3), 103.1 ($\text{CH}(\text{OCH}_3)_2$), 110.0 (ArCH , benzyl), 113.7 (2 x ArCH , aniline), 120.3 (ArCH , benzyl), 121.8 (ArCCl), 124.9 (ArCCH_2), 127.2 (ArCH , benzyl), 127.9 (ArCH , benzyl), 128.9 (2 x ArCH , aniline), 146.7 (ArCN) and 157.1 (ArCO) ppm. HRMS (ES^+) calc. for $\text{C}_{18}\text{H}_{23}^{35}\text{ClNO}_3$ ($\text{M}^+ + \text{H}$) 336.1361, found 336.1355. Calc. for $\text{C}_{18}\text{H}_{23}^{37}\text{ClNO}_3$ ($\text{M}^+ + \text{H}$) 338.1331, found 338.1306.

4-(((2,2-Dimethoxyethyl)(phenyl)amino)methyl)phenol (123I)

$\text{C}_{17}\text{H}_{21}\text{NO}_3$, Mol. Wt.: 287.35



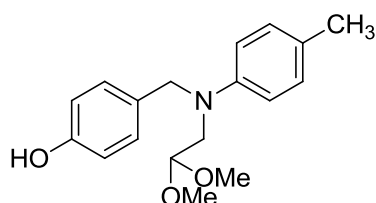
(Method A)

The crude compound was purified by column chromatography (eluent: from 0% to 30% of EtOAc in pet. ether) to give the product as a colourless oil (2.5 g, 90%) which showed: ^1H NMR (500 MHz, CDCl_3) δ 3.40 (6H, s, CH_3), 3.54 (2H, d, $J = 5.1$ Hz, CH_2CH), 4.58 (2H, s, ArCH_2), 4.61 (1H, t, $J = 5.1$ Hz, $\text{CH}(\text{OR})_2$), 5.01 (1H, bs, OH), 6.70 (1H, t, $J = 7.2$ Hz, ArH), 6.74 (2H, d, $J = 8.7$ Hz, ArH) 6.74 (2H, d, $J = 8.6$ Hz,

ArH), 7.06 (2H, d, $J = 8.6$ Hz, ArH) and 7.19 (2H, dd, $J = 7.2, 8.7$ Hz, ArH) ppm. ^{13}C NMR (126 MHz, CDCl_3) δ 53.6 (CH_2CH), 54.3 (ArCH_2), 54.7 (CH_3), 103.5 ($\text{CH}(\text{OR})_2$), 112.4 (ArCH), 115.5 (ArCH), 116.7 (ArCH), 128.0 (ArCH), 129.4 (ArCCH_2), 148.7 (ArCN) and 154.5 (ArCOH) ppm. LC/MS (ES^+) $t_r = 2.91$ min (65 %), m/z 287.5 (M^+); (RP, Isocratic, 80% MeOH). HRMS (ES^+) calcd. for $\text{C}_{17}\text{H}_{22}\text{NO}_3$ ($\text{M}^+ + \text{H}$) 288.1600, found 288.1595; calcd. for $\text{C}_{17}\text{H}_{21}\text{NNaO}_3$ ($\text{M}^+ + \text{Na}$) 310.1419, found 310.1421.

4-(((2,2-Dimethoxyethyl)(*p*-tolyl)amino)methyl)phenol (123m)

$\text{C}_{18}\text{H}_{23}\text{NO}_3$, Mol. Wt.: 301.38

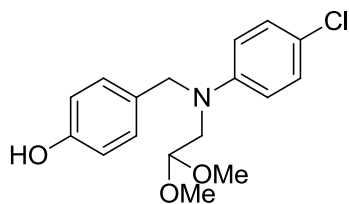


(Method A)

The crude compound was purified by column chromatography (eluent: from 0% to 30% EtOAc in pet. ether) to give the product as a colourless oil (2.83 g, 94%) which showed: ^1H NMR (500 MHz, CDCl_3) δ 2.24 (3H, s, ArCH_3), 3.40 (6H, s, $\text{CH}(\text{OCH}_3)_2$), 3.51 (2H, d, $J = 5.1$ Hz, CH_2CH), 4.54 (2H, s, ArCH_2), 4.59 (1H, t, $J = 5.1$ Hz, $\text{CH}(\text{OR})_2$), 5.10 (1H, bs, OH), 6.66 (2H, d, $J = 8.6$ Hz, ArH), 6.74 (2H, d, $J = 8.7$ Hz, ArH), 7.00 (2H, d, $J = 8.6$ Hz, ArH) and 7.06 (2H, d, $J = 8.7$ Hz, ArH) ppm. ^{13}C NMR (126 MHz, CDCl_3) δ 20.1 (ArCH_3), 53.7 (CH_2CH), 54.4 (ArCH_2), 54.5 ($\text{CH}(\text{OCH}_3)_2$), 103.4 ($\text{CH}(\text{OR})_2$), 112.5 (ArCH), 115.3 (ArCH), 125.7 (ArCCH_3), 127.9 (ArCH), 129.7 (ArCH), 130.8 (ArCCH_2), 146.5 (ArCN) and 154.4 (ArCOH) ppm. LC/MS (ES^+) $t_r = 1.92$ min (>99 %), m/z 301.5 (M^+); (RP, Isocratic, 90% MeOH). HRMS (ES^+) calcd. for $\text{C}_{18}\text{H}_{24}\text{NO}_3$ ($\text{M}^+ + \text{H}$) 302.1751, found 302.1757.

4-(((4-Chlorophenyl)(2,2-dimethoxyethyl)amino)methyl)phenol (123n)

$\text{C}_{17}\text{H}_{20}\text{ClNO}_3$, Mol. Wt.: 321.80

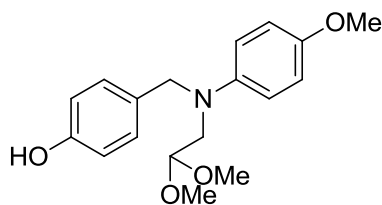


(Method A)

The crude compound was purified by column chromatography (eluent: from 0% to 30% EtOAc in pet. ether) to give the product as a colourless oil (2.12 g, 66%) which showed: ^1H NMR (500 MHz, CDCl_3) δ 3.39 (6H, s, CH_3), 3.51 (2H, d, $J = 5.1$ Hz, CH_2CH), 4.54 (2H, s, ArCH_2), 4.56 (1H, t, $J = 5.1$ Hz, $\text{CH}(\text{OR})_2$), 5.02 (1H, bs, OH), 6.64 (2H, d, $J = 9.2$ Hz, ArH), 6.76 (2H, d, $J = 8.6$ Hz, ArH), 7.03 (2H, d, $J = 8.6$ Hz, ArH) and 7.10 (2H, d, $J = 9.1$ Hz, ArH) ppm. ^{13}C NMR (126 MHz, CDCl_3) δ 53.8 (CH_2CH), 54.4 (ArCH_2), 54.6 (CH_3), 103.2 ($\text{CH}(\text{OR})_2$), 113.6 (ArCH), 115.4 (ArCH), 121.4 (ArCCl), 127.8 (ArCH), 128.9 (ArCH), 129.1 (ArCCH_2), 147.2 (ArCN) and 154.5 (ArCOH) ppm. LC/MS (ES^+) $t_r = 4.19$ min (74 %), m/z 321.6 (M^+); (RP, Isocratic, 80% MeOH). HRMS (ES^+) calcd. for $\text{C}_{17}\text{H}_{21}\text{ClNO}_3$ ($\text{M}^+ + \text{H}$) 322.1210, found 322.1201; calcd. for $\text{C}_{17}\text{H}_{20}\text{ClNNaO}_3$ ($\text{M}^+ + \text{Na}$) 344.1029, found 344.1043.

4-(((2,2-dimethoxyethyl)(4-methoxyphenyl)amino)methyl)phenol (123o)

$\text{C}_{18}\text{H}_{23}\text{NO}_4$, Mol. Wt.: 317.38



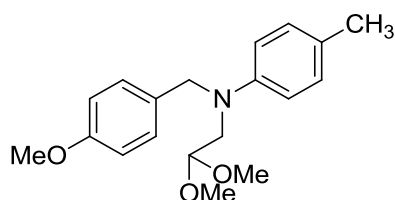
(Method A)

The crude compound was purified by column chromatography (eluent 0% to 40% EtOAc in pet. ether) to give the product as a colourless oil (2.87 g, 90%) which showed: ^1H NMR (500 MHz, CDCl_3) δ 3.38 (6H, s, $\text{CH}(\text{OCH}_3)_2$), 3.46 (2H, d, $J = 5.1$ Hz, CH_2CH), 3.74 (3H, s, ArOCH_3), 4.48 (2H, s, ArCH_2), 4.55 (1H, t, $J = 5.1$ Hz, $\text{CH}(\text{OR})_2$), 5.12 (1H, bs, OH), 6.71 (2H, d, $J = 9.1$ Hz, ArH), 6.74 (2H, d, $J = 8.6$ Hz, ArH), 6.79 (2H, d, $J = 9.1$ Hz, ArH) and 7.07 (2H, d, $J = 8.6$ Hz, ArH) ppm. ^{13}C NMR (126 MHz, CDCl_3) δ 54.4 (CH_2CH), 54.5 ($\text{CH}(\text{OCH}_3)_2$), 55.3 (ArCH_2), 55.9 (ArOCH_3),

103.6 (CH(OR)₂), 114.6 (ArCH), 114.9 (ArCH), 115.4 (ArCH), 128.3 (ArCH), 131.0 (ArCCH₂), 143.5 (ArCN), 151.7 (ArCOCH₃) and 154.6 (ArCOH) ppm. LC/MS (ES⁺) t_r = 1.56 min (97 %), m/z 317.5 (M⁺); (RP, Isocratic, 90% MeOH). HRMS (ES⁺) calcd. for C₁₈H₂₄NO₄ (M⁺+H) 318.1700, found 318.1698.

***N*-(2,2-Dimethoxyethyl)-*N*-(4-methoxybenzyl)-4-methylaniline (123q)**

C₁₉H₂₅NO₃, Mol. Wt.: 315.41

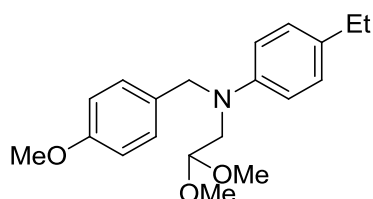


(Method A)

The crude compound was purified by column chromatography (eluent: from 0% to 20% EtOAc in pet. ether) to give the product as a yellow oil (8.6 g, 91%) which showed: ¹H NMR (500 MHz, CDCl₃) δ 2.23 (3H, s, ArCH₃), 3.39 (6H, s, CH(OCH₃)₂), 3.51 (2H, d, *J* = 5.1 Hz, CH₂CH), 3.78 (3H, s, ArOCH₃), 4.56 (2H, s, ArCH₂), 4.58 (1H, t, *J* = 5.1 Hz, CHCH₂), 6.66 (2H, d, *J* = 8.7 Hz, ArH, aniline), 6.83 (2H, d, *J* = 8.7 Hz, ArH, benzyl), 7.00 (2H, d, *J* = 8.7 Hz, ArH, aniline) and 7.12 (2H, d, *J* = 8.7 Hz, ArH, benzyl) ppm. ¹³C NMR (126 MHz, CDCl₃) δ 20.3 (ArCH₃), 53.9 (CHCH₂), 54.5 (ArCH₂), 54.6 (CH(OCH₃)₂), 55.4 (ArOCH₃), 103.5 (CHCH₂), 112.6 (ArCH, aniline), 114.2 (ArCH, benzyl), 125.9 (ArCCH₃), 128.0 (ArCH, benzyl), 130.0 (ArCH, aniline), 131.0 (ArCCH₂), 146.7 (ArCN) and 158.6 (ArCO) ppm. LC/MS (ES⁺) t_r = 2.83 min (92 %), m/z 316.2 (M⁺+H). HRMS (ES⁺) calcd. for C₁₉H₂₆NO₃ (M⁺+H) 316.1907, found 316.1916.

***N*-(2,2-Dimethoxyethyl)-4-ethyl-*N*-(4-methoxybenzyl)aniline (123r)**

C₂₀H₂₇NO₃, Mol. Wt.: 329.43

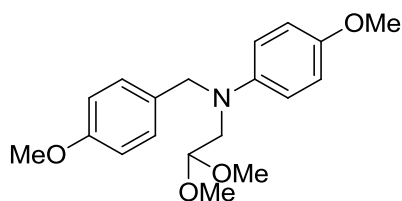


(Method A)

The crude compound was purified by column chromatography (eluent: from 0% to 10% EtOAc in pet. ether) to give the product as a yellow oil (3.42 g, 52%) which showed: ^1H NMR (500 MHz, CDCl_3) δ 1.19 (3H, t, $J = 7.6$ Hz, CH_2CH_3), 2.54 (2H, q, $J = 7.6$ Hz, CH_2CH_3), 3.39 (6H, s, $\text{CH}(\text{OCH}_3)_2$), 3.52 (2H, d, $J = 5.1$ Hz, CHCH_2), 3.78 (3H, s, ArOCH_3), 4.56 (2H, s, ArCH_2N), 4.59 (1H, t, $J = 5.1$ Hz, CHCH_2), 6.68 (2H, d, $J = 8.7$ Hz, ArH, aniline), 6.83 (2H, d, $J = 8.7$ Hz, ArH, benzyl), 7.02 (2H, d, $J = 8.7$ Hz, ArH, aniline) and 7.13 (2H, d, $J = 8.7$ Hz, ArH, benzyl) ppm. ^{13}C NMR (126 MHz, CDCl_3) δ 15.9 (CH_2CH_3), 27.8 (CH_2CH_3), 53.9 (CHCH_2), 54.5 (ArCH_2N), 54.6 ($\text{CH}(\text{OCH}_3)_2$), 55.4 (ArOCH_3), 103.5 (CHCH_2), 112.5 (ArCH, aniline), 114.0 (ArCH, benzyl), 127.9 (ArCH, benzyl), 128.7 (ArCH, aniline), 131.0 (ArCCH_2N), 132.3 (ArCEt), 146.9 (ArCN) and 158.6 (ArCO) ppm. LC/MS (ES^+) $t_r = 3.42$ min (85 %), m/z 330.2 ($\text{M}^+ + \text{H}$); (RP, Isocratic, 90% MeOH). HRMS (ES^+) calcd. $\text{C}_{20}\text{H}_{28}\text{NO}_3$ ($\text{M}^+ + \text{H}$) 330.2064, found 330.2053.

***N*-(2,2-Dimethoxyethyl)-4-methoxy-*N*-(4-methoxybenzyl)aniline (123s)**

$\text{C}_{19}\text{H}_{25}\text{NO}_4$, Mol. Wt.: 331.41



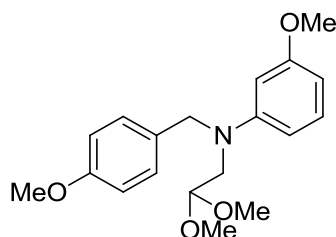
(Method A)

The crude compound was purified by column chromatography (eluent: from 0% to 20% EtOAc in pet. ether) to give the product as a yellow oil (9.65 g, 97%) which showed: ^1H NMR (500 MHz, CDCl_3) δ 3.38 (6H, s, $\text{CH}(\text{OCH}_3)_2$), 3.47 (2H, d, $J = 5.1$ Hz, CH_2CH), 3.74 (3H, s, ArOCH_3), 3.78 (3H, s, ArOCH_3), 4.51 (2H, s, ArCH_2), 4.55 (1H, t, $J = 5.1$ Hz, CHCH_2), 6.72 (2H, d, $J = 9.2$ Hz, ArH, aniline), 6.79 (2H, d, $J = 9.2$ Hz, ArH, aniline), 6.83 (2H, d, $J = 8.7$ Hz, ArH, benzyl) and 7.13 (2H, d, $J = 8.7$ Hz, ArH, benzyl) ppm. ^{13}C NMR (126 MHz, CDCl_3) δ 54.4 (CHCH_2), 54.5 ($\text{CH}(\text{OCH}_3)_2$), 55.2 (ArCH_2), 55.4 (ArOCH_3), 55.9 (ArOCH_3), 103.6 (CHCH_2), 114.0 (ArCH, benzyl), 114.5 (ArCH, aniline), 114.9 (ArCH, aniline), 128.1 (ArCH, benzyl), 131.1 (ArCCH_2), 143.5 (ArCN), 151.7 (ArCO, aniline) and 158.6 (ArCO, benzyl) ppm. LC/MS (ES^+) t_r

= 1.99 min (92 %), m/z 332.2 ($M^+ + H$). HRMS (ES⁺) calcd. for $C_{19}H_{26}NO_4$ ($M^+ + H$) 332.1856, found 332.1859.

***N*-(2,2-Dimethoxyethyl)-3-methoxy-*N*-(4-methoxybenzyl)aniline (123u)**

$C_{19}H_{25}NO_4$, Mol. Wt.: 331.41

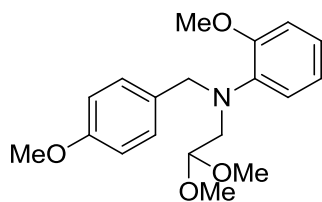


(Method A)

As described in the general method A except that after stirring for 12 h at rt the mixture was concentrated *in vacuo* into a slurry and stirred for further 6 h. The crude compound was purified by column chromatography (eluent: from 0% to 10% EtOAc in pet. ether) to give the product as an orange oil (5.93 g, 89%) which showed: 1H NMR (500 MHz, $CDCl_3$) δ 3.39 (6H, s, $CH(OCH_3)_2$), 3.52 (2H, d, $J = 5.1$ Hz, $CHCH_2$), 3.74 (3H, s, OCH_3 , benzyl), 3.78 (3H, s, OCH_3 , aniline), 4.58 (2H, s, $ArCH_2N$), 4.60 (1H, t, $J = 5.1$ Hz, $CHCH_2$), 6.27 (1H, ddd, $J = 0.9, 2.5, 8.2$ Hz, ArH, aniline), 6.30 (1H, t, $J = 2.5$ Hz, ArH, aniline), 6.36 (1H, ddd, $J = 0.9, 2.5, 8.2$ Hz, ArH aniline), 6.83 (2H, d, $J = 8.9$ Hz, ArH, benzyl), 7.09 (1H, t, $J = 8.2$ Hz, ArH, aniline) and 7.11 (2H, d, $J = 8.9$ Hz, ArH, benzyl) ppm. ^{13}C NMR (126 MHz, $CDCl_3$) δ 53.8 ($CHCH_2$), 54.4 ($ArCH_2N$), 54.7 ($CH(OCH_3)_2$), 55.2 ($ArOCH_3$, benzyl), 55.4 ($ArOCH_3$, aniline), 99.1 ($ArCH$, aniline), 101.5 ($ArCH$, aniline), 103.5 ($CH(OCH_3)_2$), 105.6 ($ArCH$, aniline), 114.1 ($ArCH$, benzyl), 127.8 ($ArCH$, benzyl), 130.0 ($ArCH$, aniline), 130.7 ($ArCCH_2$), 150.2 ($ArCN$), 158.6 ($ArCO$, aniline) and 160.9 ($ArCO$, benzyl) ppm. LC/MS (ES⁺) $t_r = 2.30$ min (96 %), m/z 332.1 ($M^+ + H$); (RP, Isocratic, 90% MeOH). HRMS (ES⁺) calcd. $C_{19}H_{26}NO_4$ ($M^+ + H$) 332.1856, found 332.1840.

***N*-(2,2-Dimethoxyethyl)-2-methoxy-*N*-(4-methoxybenzyl)aniline (123w)**

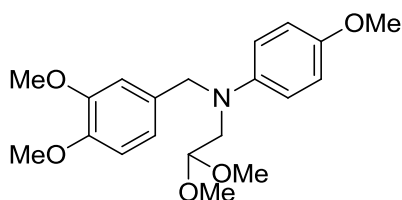
$C_{19}H_{25}NO_4$, Mol. Wt.: 331.41



As described in the general method A except that after stirring for 12 h at rt the mixture was concentrated *in vacuo* into a slurry and stirred for further 6 h. The crude compound was purified by column chromatography (eluent: from 0% to 10% EtOAc in pet. ether) to give the product as a yellow oil (5.34 g, 81%) which showed: ^1H NMR (500 MHz, CDCl_3) δ 3.25 (6H, s, $\text{CH}(\text{OCH}_3)_2$), 3.26 (2H, d, $J = 5.2$ Hz, CHCH_2), 3.77 (3H, s, OCH_3 , benzyl), 3.88 (3H, s, OCH_3 , aniline), 4.33 (2H, s, ArCH_2N), 4.44 (1H, t, $J = 5.2$ Hz, CHCH_2), 6.80 (2H, d, $J = 8.8$ Hz, ArH, benzyl), 6.83 (1H, dd, $J = 1.6, 8.0$ Hz, ArH, aniline), 6.87 (1H, dd, $J = 1.4, 7.9$ Hz, ArH, aniline), 6.91 – 6.96 (2H, m, ArH, aniline) and 7.21 (2H, d, $J = 8.8$ Hz, ArH, benzyl) ppm. ^{13}C NMR (126 MHz, CDCl_3) δ 53.2 (CHCH_2), 53.7 ($\text{CH}(\text{OCH}_3)_2$), 55.4 (ArOCH_3 , aniline), 55.7 (ArOCH_3 , benzyl), 56.9 (ArCH_2N), 103.8 ($\text{CH}(\text{OCH}_3)_2$), 112.2 (ArCH, aniline), 113.6 (ArCH, benzyl), 120.9 (ArCH, aniline), 122.1 (ArCH, aniline), 122.6 (ArCH, aniline), 129.7 (ArCH, benzyl), 131.4 (ArCCH_2), 140.0 (ArCN), 153.4 (ArCO, benzyl) and 158.6 (ArCO, aniline) ppm. LC/MS (ES^+) $t_r = 1.87$ min (99 %), m/z 332.1 ($\text{M}^+ + \text{H}$); (RP, Isocratic, 90% MeOH). HRMS (ES^+) calcd. $\text{C}_{19}\text{H}_{26}\text{NO}_4$ ($\text{M}^+ + \text{H}$) 332.1856, found 332.1863.

***N*-(3,4-Dimethoxybenzyl)-*N*-(2,2-dimethoxyethyl)-4-methoxyaniline (123x)**

$\text{C}_{20}\text{H}_{27}\text{NO}_5$, Mol. Wt.: 361.43

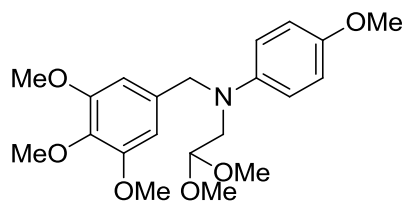


(Method A)

The crude compound was purified by column chromatography (eluent: from 0% to 40% EtOAc in pet. ether) to give the product as an orange oil (6.58 g, 91%) which showed: ^1H NMR (400 MHz, CDCl_3) δ 3.37 (6H, s), 3.45 (2H, t, $J = 4.7$ Hz), 3.73 (3H, s), 3.81 (3H, s), 3.84 (3H, s), 4.48 (2H, s), 4.56 (1H, bs) and 6.69 – 6.82 (7H, m) ppm. HRMS (ES^+) calcd. $\text{C}_{20}\text{H}_{28}\text{NO}_5$ ($\text{M}^+ + \text{H}$) 362.1962, found 362.1976.

***N*-(2,2-Dimethoxyethyl)-4-methoxy-*N*-(3,4,5-trimethoxybenzyl)aniline (123y)**

C₂₁H₂₉NO₆, Mol. Wt.: 391.46

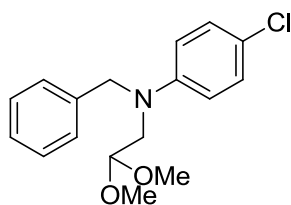


(Method A)

The crude compound was purified by column chromatography (eluent: from 0% to 50% EtOAc in pet. ether) to give the product as an orange oil (7.71 g, 98%) which showed: ¹H NMR (400 MHz, CDCl₃) δ 3.37 (6H, s), 3.47 (2H, d, *J* = 5.1 Hz), 3.74 (3H, s), 3.78 (6H, s), 3.81 (3H, s), 4.47 (2H, s), 4.56 (1H, t, *J* = 5.1 Hz), 6.46 (2H, s), 6.72 (2H, d, *J* = 9.2 Hz) and 6.79 (2H, d, *J* = 9.2 Hz) ppm. HRMS (ES⁺) calcd. C₂₁H₃₀NO₆ (M⁺+H) 392.2068, found 392.2081.

4-Chloro-*N*-(2,2-dimethoxyethyl)-*N*-benzyl-aniline (123z)

C₁₇H₂₀ClNO₂, Mol. Wt.: 305.80

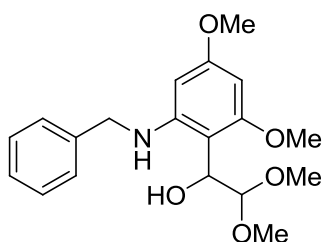


The crude compound was purified by column chromatography (eluent: from 0% to 20% EtOAc in pet. ether) to give the product as a colourless oil (3.74 g, 82%) which solidified upon standing and showed: ¹H NMR (500 MHz, CDCl₃) δ 3.40 (6H, s, CH(OCH₃)₂), 3.55 (2H, d, *J* = 5.1 Hz, CHCH₂), 4.58 (1H, t, *J* = 5.1 Hz, CHCH₂), 4.63 (2H, s, ArCH₂N), 6.64 (2H, d, *J* = 9.2 Hz, ArH, aniline), 7.11 (2H, d, *J* = 9.2 Hz, ArH, aniline), 7.17 (2H, d, *J* = 7.0 Hz, ArH, benzyl), 7.23 (1H, t, *J* = 7.3 Hz, ArH, benzyl) and 7.30 (1H, t, *J* = 7.4 Hz, ArH, benzyl) ppm. ¹³C NMR (126 MHz, CDCl₃) δ 54.2 (CHCH₂), 54.7 (CH(OCH₃)₂), 55.1 (ArCH₂N), 103.3 (CHCH₂), 113.6 (ArCH, aniline), 121.5 (ArCCl), 126.5 (ArCH, benzyl), 127.0 (ArCH, benzyl), 128.8 (ArCH, benzyl), 129.1 (ArCH, aniline), 138.3 (ArCCH₂) and 147.3 (ArCN) ppm. LC/MS (ES⁺) t_r =

3.08 min (96 %), m/z 305.9 ($M^+ + H$); (RP, Isocratic, 90% MeOH). HRMS (ES^+) calcd. $C_{17}H_{21}^{35}ClNO_2$ ($M^+ + H$) 306.1255, found 306.1244; calcd. $C_{17}H_{21}^{37}ClNO_2$ ($M^+ + H$) 308.1226, found 308.1244. Mp 61-63 °C (pet. ether). Anal. calcd. for $C_{17}H_{20}ClNO_2$: C 66.8, H 6.59, N 4.58% found C 66.3, H 6.52, N 4.52%.

1-(2-(Benzylamino)-4,6-dimethoxyphenyl)-2,2-dimethoxyethan-1-ol (124)

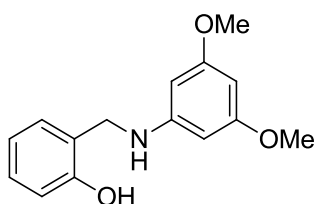
$C_{19}H_{25}NO_5$, Mol. Wt.: 347.41



The crude compound was purified by chromatography (eluent 0% to 40% EtOAc in pet. ether) to give the product as a pale yellow oil (1.94 g, 56%). 1H NMR (400 MHz, $CDCl_3$) δ 3.28 (3H, s, $CHOCH_3$), 3.47 (3H, s, $CHOCH_3$), 3.70 (3H, s, $ArOCH_3$), 3.78 (3H, s, $ArOCH_3$), 4.32 (2H, d, $J = 2.8$ Hz, $ArCH_2$), 4.75 (1H, d, $J = 6.9$ Hz, $CH(OR)_2$), 5.24 (1H, d, $J = 6.9$ Hz, $ArCH$), 5.88 (1H, d, $J = 2.2$ Hz, ArH), 5.94 (1H, d, $J = 2.2$ Hz, ArH), 7.23 - 7.26 (1H, m, ArH) and 7.31 - 7.37 (4H, m, ArH) ppm. ^{13}C NMR (101 MHz, $CDCl_3$) δ 48.0 ($ArCH_2$), 54.9 ($ArOCH_3$), 55.0 ($CHOCH_3$), 55.7 ($ArOCH_3$), 55.9 ($CHOCH_3$), 68.2 ($ArCHOH$), 88.2 ($ArCH$), 91.3 ($ArCH$), 103.7 ($ArCCH$), 105.2 ($CH(OR)_2$), 127.0 ($ArCH$), 127.3 ($ArCH$), 128.6 ($ArCH$), 139.7 ($ArCCH_2$), 149.4 ($ArCN$), 159.3 ($ArCOCH_3$) and 161.1 ($ArCOCH_3$) ppm. LC/MS (ES^+) $t_r = 1.27$ min (95%), m/z 348.0 ($M^+ + H$); HRMS (ES^+) calcd. for $C_{19}H_{26}NO_5$ ($M^+ + H$) 348.1805, found 348.1793.

2-((3,5-Dimethoxyphenylamino)methyl)phenol (125)

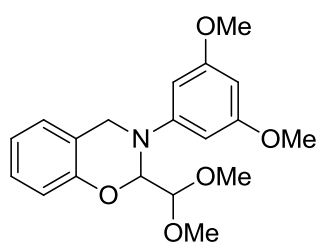
$C_{15}H_{17}NO_3$, Mol. Wt.: 259.30



2-Hydroxybenzaldehyde (320 μ L, 3.00 mmol) and 3,5-dimethoxyaniline (469 mg, 3.00 mmol) were dissolved in CHCl_3 (20 mL) and treated with $\text{NaBH}(\text{OAc})_3$ (870 mg, 3.90 mmol). The mixture was stirred for 4 h at rt, during which time it turned from pale yellow to bright yellow. $\text{NaBH}(\text{OAc})_3$ (870 mg, 3.90 mmol) was introduced and, after stirring for 1 h at rt, the mixture was quenched with a saturated aqueous solution of K_2CO_3 . The aqueous layer was then extracted with CHCl_3 (2 x 20 mL). The combined organics were dried with MgSO_4 , filtered and evaporated to give a bright yellow oil (966 mg) which showed: ^1H NMR (500 MHz, CDCl_3) δ 3.74 (6H, s, CH_3), 3.95 (1H, bs, NH), 4.38 (2H, s, ArCH_2), 6.01 (2H, d, $J = 2.1$ Hz, ArH), 6.04 (1H, t, $J = 2.1$ Hz, ArH), 6.87 (1H, td, $J = 1.2, 7.4$ Hz, ArH), 6.89 (2H, dd, $J = 1.2, 7.4$ Hz, ArH), 7.15 (1H, dd, $J = 1.6, 7.4$ Hz, ArH), 7.22 (1H, td, $J = 1.6, 7.4$ Hz, ArH) and 8.06 (1H, bs, ArOH) ppm. ^{13}C NMR (126 MHz, CDCl_3) δ 48.5 (ArCH_2), 55.4 (CH_3), 92.8 (ArCH), 94.7 (ArCH), 116.8 (ArCH), 120.3 (ArCH), 123.0 (ArCCH_2), 128.9 (ArCH), 129.4 (ArCH), 149.4 (ArCN), 156.7 (ArCOH) and 161.8 (ArCOCH_3) ppm. LC/MS (ES^+) $t_r = 1.21$ min (99 %), m/z 260.0 (M^+); (RP, Isocratic, 90% MeOH). HRMS (ES^+) calcd. for $\text{C}_{15}\text{H}_{18}\text{NO}_3$ ($\text{M}^+ + \text{H}$) 260.1281, found 260.1274.

2-(Dimethoxymethyl)-3-(3,5-dimethoxyphenyl)-3,4-dihydro-2H-benzo[e][1,3]oxazine (126)

$\text{C}_{19}\text{H}_{23}\text{NO}_5$, Mol. Wt.: 345.39

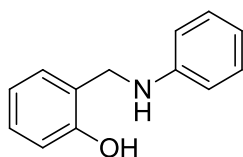


Compound **125** (780 mg, 3.00 mmol) was dissolved in CHCl_3 (5 mL) and 2,2-dimethoxyacetaldehyde (1.0 mL, 6.7 mmol) was introduced. After stirring overnight, the mixture was extracted with water and the organic layer was dried with MgSO_4 , filtered and evaporated to give a pale green oil. The crude compound was purified by chromatography (eluent: from 0% to 30% EtOAc in pet. ether) to give the product as a pale green oil (55 mg, 5%) which showed: ^1H NMR (500 MHz, CDCl_3) δ 3.39 (3H, s,

CHOCH₃), 3.47 (3H, s, CHOCH₃), 3.74 (6H, s, ArOCH₃), 4.44 (1H, d, *J* = 16.6 Hz, ArCH₂), 4.66 (1H, d, *J* = 16.6 Hz, ArCH₂), 4.67 (1H, d, *J* = 6.7 Hz, CH(OR)₂), 5.48 (1H, dd, *J* = 1.5, 6.7 Hz, NCH), 6.09 (1H, t, *J* = 2.2 Hz, ArH), 6.28 (2H, d, *J* = 2.2 Hz, ArH), 6.89 (1H, td, *J* = 1.3, 7.5 Hz, ArH), 6.91 (1H, dd, *J* = 1.3, 8.4 Hz, ArH), 7.01 (1H, dd, *J* = 1.7, 7.5 Hz, ArH) and 7.14 (1H, td, *J* = 1.7, 8.4 Hz, ArH) ppm. ¹³C NMR (126 MHz, CDCl₃) δ 46.8 (ArCH₂), 53.5 (CHOCH₃), 55.3 (ArOCH₃), 55.6 (CHOCH₃), 87.0 (NCH), 93.8 (ArCH), 98.0 (ArCH), 101.2 (CH(OR)₂), 117.2 (ArCH), 120.1 (ArCCH₂), 120.9 (ArCH), 126.6 (ArCH), 128.2 (ArCH), 151.3 (ArCN), 152.5 (ArCOCH) and 161.4 (ArCOCH₃) ppm. LC/MS (ES⁺) t_r = 2.03 min (4%), m/z 346.1 (M⁺+H); (RP, Isocratic, 90% MeOH).

2-((Phenylamino)methyl)phenol (128)

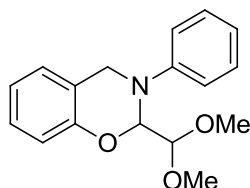
C₁₃H₁₃NO, Mol. Wt.: 199.25



Salicylaldehyde (1.1 mL, 10.0 mmol) and aniline (0.9 mL, 10.0 mmol) were dissolved in CHCl₃ (40 mL) and treated with NaBH(OAc)₃ (3.3 g, 15.0 mmol). After stirring for 3 h at rt, the mixture was quenched with a saturated aqueous solution of NaHCO₃ and the aqueous layer was extracted with EtOAc (1 x 40 mL). The combined organics were dried with MgSO₄, filtered and evaporated to give a yellow-green solid which showed: ¹H NMR (500 MHz, CDCl₃) δ 3.94 (1H, bs) (OH or NH), 4.42 (2H, s) (CH₂), 6.86 (2H, dd, *J* = 1.0, 8.5 Hz) (ArH, Aniline), 6.87 – 6.91 (2H, m) (2 x ArH, benzyl), 6.92 (1H, tt, *J* = 1.0, 7.4 Hz) (ArH, aniline), 7.16 (1H, dd, *J* = 1.6, 7.4 Hz) (ArH, benzyl), 7.21 – 7.25 (1H, m) (ArH, benzyl), 7.25 (2H, dd, *J* = 7.4, 8.5 Hz) (2 x ArH, aniline) and 8.37 (1H, bs) (OH or NH) ppm. ¹³C NMR (126 MHz, CDCl₃) δ 48.9 (CH₂), 116.1, 116.8, 120.2, 121.0 (ArCH, Aniline), 123.0 (ArCCH₂), 128.9 (ArCH, benzyl), 129.4 (ArCH, benzyl), 129.5 (ArCH, aniline), 147.3 (ArCN) and 156.9 (ArCO) ppm. LC/MS (ES⁺) t_r = min 1.40 (%), m/z 199.3 (M⁺); (RP, Isocratic, 90% MeOH). HRMS (ES⁺) calcd. for C₁₃H₁₄NO (M⁺+H) 200.1070, found 200.1063.

2-(Dimethoxymethyl)-3-phenyl-3,4-dihydro-2H-benzo[e][1,3]oxazine (129a)

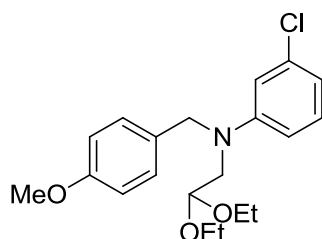
C₁₇H₁₉NO₃, Mol. Wt.: 285.34



Compound **128** (598 mg, 3.0 mmol) was dissolved in CHCl₃ (20 mL) and treated with 2,2-dimethoxyacetaldehyde (452 μ L, 3.0 mmol) and K₂CO₃ (828 mg, 6.0 mmol). After stirring for 24 h at rt, the mixture was filtered and the filtrate was evaporated to give the a yellow oil (782 mg). The crude compound was purified by column chromatography (eluent: from 0% to 20% EtOAc in pet. ether) to give the product as a pale yellow oil (638 mg, 75%) which showed: ¹H NMR (400 MHz, CDCl₃) δ 3.39 (3H, s), 3.46 (3H, s), 4.45 (1H, d, *J* = 16.8 Hz), 4.65 (1H, d, *J* = 6.6 Hz), 4.66 (1H, d, *J* = 16.8 Hz), 5.46 (1H, dd, *J* = 1.2, 6.6 Hz), 6.90 (2H, d, *J* = 7.8 Hz), 6.94 (1H, t, *J* = 7.0 Hz), 7.00 (1H, d, *J* = 7.9 Hz), 7.10 (2H, d, *J* = 7.9 Hz), 7.15 (1H, d, *J* = 7.9 Hz) and 7.24 (2H, dd, *J* = 7.0, 7.8 Hz) ppm.

3-Chloro-*N*-(2,2-diethoxyethyl)-*N*-(4-methoxybenzyl)aniline (131t)

C₂₀H₂₆ClNO₃, Mol. Wt.: 363.88

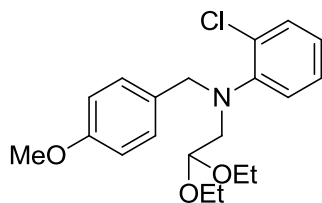


The crude compound **122t** (4.9 g) was dissolved in anhydrous DMF (20 mL) under inert atmosphere and treated with NaH (2.4 g, 60.0 mmol). The mixture was stirred for 30 min at rt and then 2-bromo-1,1-diethoxyethane (6.2 mL, 40.0 mmol) was introduced. After stirring for 6 h at 60 °C, the mixture was cooled to rt, quenched with ice, and extracted with EtOAc (3 x 50 mL). The combined organics were washed with brine (3 x 15 mL) then dried with MgSO₄, filtered and evaporated to give a dark yellow oil (9.3 g).

The crude compound was purified twice by column chromatography (eluent: pet. ether) to give the product as a pale yellow oil (1.5 g, 21%) which showed: ^1H NMR (500 MHz, CDCl_3) δ 1.20 (6H, t, $J = 7.0$ Hz, CH_2CH_3), 3.49 – 3.56 (4H, m, CH_2CH_3 , NCH_2CH), 3.72 (2H, dq, $J = 7.0, 9.3$ Hz, CH_2CH_3), 3.78 (3H, s, ArOCH_3), 4.58 (2H, s, ArCH_2N), 4.69 (1H, t, $J = 5.2$ Hz, CH_2CH), 6.59 (1H, ddd, $J = 0.5, 2.2, 8.6$ Hz, ArCH, aniline), 6.64 (1H, ddd, $J = 0.5, 2.2, 7.8$ Hz, ArCH, aniline), 6.74 (1H, t, $J = 0.5$ Hz, ArCH, aniline), 6.84 (2H, d, $J = 8.7$ Hz, ArCH, benzyl), 7.06 (1H, t, $J = 8.2$ Hz, ArCH, aniline) and 7.09 (2H, d, $J = 8.7$ Hz, ArCH, benzyl) ppm. ^{13}C NMR (126 MHz, CDCl_3) δ 15.4 (CH_2CH_3), 54.1(ArCH_2), 54.3(NCH_2CH), 55.3(ArOCH_3), 63.2(CH_2CH_3), 101.2(CH_2CH), 110.4 (ArCH, aniline), 112.1 (ArCH, aniline), 114.0 (ArCH, benzyl), 116.2 (ArCH, aniline), 127.6 (ArCH, benzyl), 129.8 (ArCCH_2), 130.0 (ArCH, aniline), 135.1 (ArCCl), 149.8 (ArCN) and 158.6 (ArCOCH_3) ppm. LC/MS (ES^+) $t_r = 4.13$ min (88 %), m/z 364.0 ($\text{M}^+ + \text{H}$); (RP, Isocratic, 90% MeOH). HRMS (ES^+) calcd. $\text{C}_{20}\text{H}_{27}^{35}\text{ClNO}_3$ ($\text{M}^+ + \text{H}$) 364.1674, found 364.1662; calcd. $\text{C}_{20}\text{H}_{27}^{37}\text{ClNO}_3$ ($\text{M}^+ + \text{H}$) 366.1644, found 366.1649.

2-Chloro-*N*-(2,2-diethoxyethyl)-*N*-(4-methoxybenzyl)aniline (**131v**)

$\text{C}_{20}\text{H}_{26}\text{ClNO}_3$, Mol. Wt.: 363.88

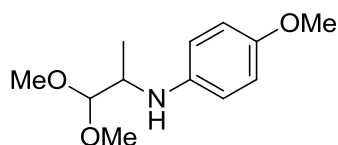


Compound **122v** (5.2 g) was dissolved in anhydrous DMF (20 mL) under inert atmosphere and treated with NaH (2.4 g, 60.0 mmol). The mixture was stirred for 30 min at 80 °C and then 2-bromo-1,1-diethoxyethane (6.2 mL, 40.0 mmol) was introduced. After stirring for 6 h at 60 °C, the mixture was cooled to rt, quenched with ice, and extracted with EtOAc (3 x 50 mL). The combined organics were washed with brine (3 x 15 mL) then dried with MgSO_4 , filtered and evaporated to give a yellow oil (12.2 g). The crude compound was dissolved in pet. ether and the remaining starting material was crystallised out. The recovered organic solvent was evaporated and the residue was purified by column chromatography (eluent: from 0% to 10% EtOAc in pet. ether) to give the product as a pale yellow oil (2.45 g, 34%) which showed: ^1H NMR

(500 MHz, CDCl₃) δ 1.12 (6H, t, J = 7.1 Hz, CH₂CH₃), 3.24 (2H, d, J = 5.4 Hz, NCH₂CH), 3.41 (2H, dq, J = 7.1, 9.3 Hz, CH₂CH₃), 3.55 (2H, dq, J = 7.1, 9.1 Hz, CH₂CH₃), 3.78 (3H, s, OCH₃), 4.31 (2H, s, ArCH₂N), 4.53 (1H, t, J = 5.4 Hz, NCH₂CH), 6.81 (2H, d, J = 8.7 Hz, 2 x ArCH, benzyl), 6.94 (1H, ddd, J = 1.8, 7.2, 7.9 Hz, ArCH, aniline), 7.09 (1H, dd, J = 1.8, 8.0 Hz, ArCH, aniline), 7.11 – 7.16 (1H, m, ArCH, aniline), 7.23 (2H, d, J = 8.7 Hz, 2 x ArCH, benzyl) and 7.35 (1H, dd, J = 1.5, 7.9 Hz, ArCH, aniline) ppm. ¹³C NMR (126 MHz, CDCl₃) δ 15.3 (2 x CH₂CH₃), 53.5 (NCH₂CH), 55.2 (OCH₃), 57.3 (NCH₂CH), 62.0 (2 x CH₂CH₃), 101.3 (NCH₂CH), 113.5 (2 x ArCH, benzyl), 123.8 (ArCH, aniline), 124.4 (ArCH, aniline), 126.9 (ArCH, aniline), 129.7 (2 x ArCH, benzyl), 130.0 (ArCCH₂), 130.5 (ArCCl), 130.6 (ArCH, aniline), 147.9 (ArCN) and 158.6 (ArCO) ppm. LC/MS (ES⁺) t_r = 3.61 min (99 %), m/z 364.0 (M⁺+H); (RP, Isocratic, 90% MeOH). HRMS (ES⁺) calcd. C₂₀H₂₇³⁵ClNO₃ (M⁺+H) 364.1674, found 364.1662. calcd. C₂₀H₂₇³⁷ClNO₃ (M⁺+H) 366.1644, found 366.1648.

***N*-(1,1-Dimethoxypropan-2-yl)-4-methoxyaniline (136s)**

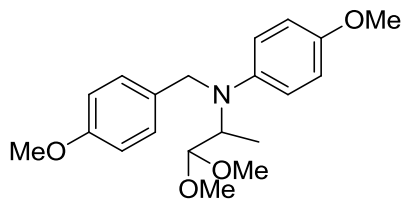
C₁₂H₁₉NO₃, Mol. Wt.: 225.28



NaBH(OAc)₃ (6.69g, 30.0 mmol) was added to a stirring solution of *p*-methoxyaniline (2.46 g, 20.0 mmol) and 2,2-dimethoxyacetone (5.0 mL, 40.0 mmol) in CHCl₃ (40 mL) and the mixture was stirred at rt for 1 h. The mixture was washed with a sat. aq. solution of NaHCO₃ (2 x 40 mL) and the organic layer was dried with MgSO₄, filtered and evaporated to give a dark yellow oil (4.45 g, 99 %) which showed: ¹⁸³ ¹H NMR (500 MHz, CDCl₃) δ 1.16 (3H, d, J = 6.5 Hz, CH₃CH), 3.44 (3H, s, CHOCH₃), 3.47 (3H, s, CHOCH₃), 3.50 – 3.57 (1H, m, CH₂CH), 3.75 (3H, s, ArOCH₃), 4.29 (1H, d, J = 4.0 Hz, CHCHCH₃), 6.65 (2H, d, J = 9.0 Hz, 2 x ArCH) and 6.77 (2H, d, J = 9.0 Hz, 2 x ArCH) ppm. ¹³C NMR (126 MHz, CDCl₃) δ 14.4 (CH₃CH), 52.0 (CH₃CH), 55.6 (CHOCH₃), 55.7 (ArOCH₃), 56.5 (CHOCH₃), 106.9 (CH₃CHCH), 114.9 (2 x ArCH), 115.7 (2 x ArCH), 140.7 (ArCN) and 152.6 (ArCO) ppm. HRMS (ES⁺) calcd. C₁₂H₂₀NO₃ (M⁺+H) 226.1438, found 226.1437.

***N*-(1,1-Dimethoxypropan-2-yl)-4-methoxy-*N*-(4-methoxybenzyl)aniline (138s)**

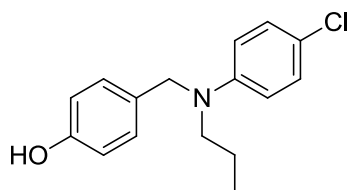
C₂₀H₂₇NO₄, Mol. Wt.: 345.43



NaH (1.2g, 30.0 mmol) was added to a stirring solution of **136s** (4.8g, 20.0 mmol) in anhydrous THF (40 mL) and stirred at rt for 1 h. 4-Methoxybenzyl chloride (4.2 ml, 30.0 mmol) was added to the reaction mixture and the mixture was then refluxed overnight. The mixture was quenched with water and the THF was evaporated. The residue was dissolved in EtOAc (150 mL) and washed with sat. aq. NaHCO₃ (3 x 100 mL) then dried with MgSO₄, filtered and evaporated to give a brown oil (1.97 g). The crude compound was purified by column chromatography (from 0% to 10% EtOAc in pet. ether) to give the pure compound as a yellow oil (1.67 g, 24%) which showed: ¹H NMR (500 MHz, CDCl₃) δ 1.23 (3H, d, *J* = 6.3 Hz, CH₃CH), 3.34 (3H, s, CHOCH₃), 3.37 (3H, s, CHOCH₃), 3.72 (3H, s, ArOCH₃), 3.76 (3H, s, ArOCH₃), 3.92 – 4.05 (1H, m, CH₃CH), 4.29 – 4.45 (3H, m, CH₃CHCH, ArCH₂), 6.74 (4H, s, 4 x ArCH, aniline), 6.81 (2H, d, *J* = 8.4 Hz, 2 x ArCH, benzyl) and 7.20 (2H, d, *J* = 7.8 Hz, 2 x ArCH, benzyl) ppm. ¹³C NMR (126 MHz, CDCl₃) δ 12.7, 49.3, 54.3, 55.2, 55.4, 55.6, 56.3, 106.6, 113.7, 114.4, 116.4, 127.7, 129.3, 132.3, 143.4, 151.8 and 158.1 ppm. HRMS (ES⁺) calcd. C₂₀H₂₈NO₄ (M⁺+H) 346.2018, found 346.2031; calcd. C₂₀H₂₇NNaO₄ (M⁺+H) 368.1838, found 368.1836.

4-(((4-Chlorophenyl)(propyl)amino)methyl)phenol (139n)

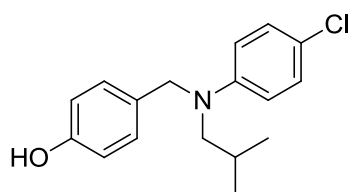
C₁₆H₁₈ClNO, Mol. Wt.: 275.77



NaBH(OAc)₃ (1.34 g, 6.00 mmol) was added to a stirring solution of 4-hydroxybenzaldehyde (498 mg, 4.00 mmol) and 4-chloroaniline (525 mg, 4.00 mmol) in CHCl₃ (20 mL) and the mixture was stirred at rt for 2 h. Propanal (351 µL, 4.80 mmol) was introduced followed by NaBH(OAc)₃ (1.34 g, 6.00 mmol) and the mixture was stirred at rt overnight. The mixture was washed with 1 N NaOH (3 x 20 mL) and the dried with MgSO₄, filtered and evaporated to give an orange oil (773 mg). The crude compound was purified by column chromatography (eluent: from 0% to 30% EtOAc in pet. ether) to give the product as a yellow oil (655 mg, 59%) which showed: ¹H NMR (500 MHz, D₆-DMSO) δ 0.86 (3H, t, *J* = 7.4 Hz, CH₂CH₃), 1.47 – 1.62 (2H, m, CH₂CH₃), 3.26 – 3.33 (2H, m, NCH₂CH₂), 4.39 (2H, s, ArCH₂N), 6.61 (2H, d, *J* = 9.2 Hz, 2 x ArCH, aniline), 6.71 (2H, d, *J* = 8.5 Hz, 2 x ArCH, benzyl), 6.97 (2H, d, *J* = 8.5 Hz, 2 x ArCH, benzyl), 7.09 (2H, d, *J* = 9.1 Hz, 2 x ArCH, aniline) and 9.42 (1H, bs, OH) ppm. ¹³C NMR (126 MHz, D₆-DMSO) δ 11.2 (CH₂CH₃), 19.8 (CH₂CH₃), 52.5 (NCH₂CH₂), 53.2 (ArCH₂N), 113.3 (2 x ArCH, aniline), 115.3 (2 x ArCH, benzyl), 118.7 (ArCCl), 127.6 (2 x ArCH, benzyl), 128.5 (2 x ArCH, aniline), 128.6 (ArCCH₂), 147.0 (ArCN) and 156.3 (ArCO) ppm. HRMS (ES⁺) calcd. C₁₆H₁₉³⁵ClNO (M⁺+H) 276.1150, found 276.1147; calcd. C₁₆H₁₉³⁷ClNO (M⁺+H) 278.1120, found 278.1120. Mp 143-146 °C (aqueous HBr).

4-(((4-Chlorophenyl)(isobutyl)amino)methyl)phenol (140n)

C₁₇H₂₀ClNO, Mol. Wt.: 289.80

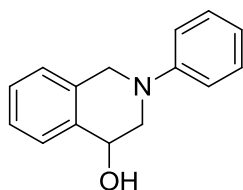


NaBH(OAc)₃ (1.34 g, 6.00 mmol) was added to a stirring solution of 4-hydroxybenzaldehyde (498 mg, 4.00 mmol) and 4-chloroaniline (525 mg, 4.00 mmol) in CHCl₃ (20 mL) and the mixture was stirred at rt for 2 h. Isobutyraldehyde (447 µL, 4.80 mmol) was introduced followed by NaBH(OAc)₃ (1.34 g, 6.00 mmol) and the mixture was stirred at rt overnight. The mixture was washed with 1 N NaOH (3 x 20 mL) and the dried with MgSO₄, filtered and evaporated to give an orange oil (1.43 g). The crude compound was purified by column chromatography (eluent: from 0% to 30%

EtOAc in pet. ether) to give the product as a yellow oil (598 mg, 52%) which showed: ^1H NMR (500 MHz, $\text{D}_6\text{-DMSO}$) δ 0.87 (6H, d, $J = 6.7$ Hz, $\text{CH}(\text{CH}_3)_2$), 1.91 – 2.06 (1H, m, $\text{CH}(\text{CH}_3)_2$), 3.18 (2H, d, $J = 7.3$ Hz, NCH_2CH), 4.44 (2H, s, ArCH_2N), 6.61 (2H, d, $J = 9.2$ Hz, 2 x ArCH, aniline), 6.71 (2H, d, $J = 8.5$ Hz, 2 x ArCH, benzyl), 6.93 (2H, d, $J = 8.5$ Hz, 2 x ArCH, benzyl), 7.07 (2H, d, $J = 9.1$ Hz, 2 x ArCH, aniline) and 9.58 (1H, bs, OH) ppm. ^{13}C NMR (126 MHz, $\text{D}_6\text{-DMSO}$) δ 20.1 ($\text{CH}(\text{CH}_3)_2$), 26.7 ($\text{CH}(\text{CH}_3)_2$), 54.1 (ArCH_2N), 58.7 (NCH_2CH), 113.7 (2 x ArCH, aniline), 115.3 (2 x ArCH, benzyl), 118.8 (ArCCl), 127.5 (2 x ArCH, benzyl), 128.1 (ArCCH_2), 128.5 (2 x ArCH, aniline), 147.2 (ArCN) and 156.3 (ArCO) ppm. HRMS (ES^+) calcd. $\text{C}_{17}\text{H}_{21}^{35}\text{ClNO}$ ($\text{M}^+ + \text{H}$) 290.1306, found 290.1303; calcd. $\text{C}_{17}\text{H}_{21}^{37}\text{ClNO}$ ($\text{M}^+ + \text{H}$) 292.1277, found 292.1281. Mp 135-137 °C (aqueous HBr).

2-Phenyl-1,2,3,4-tetrahydroisoquinolin-4-ol (143a)

$\text{C}_{15}\text{H}_{15}\text{NO}$, Mol. Wt.: 225.29

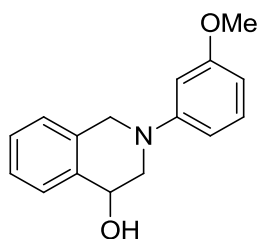


(Method B)

A sample of crude compound was purified by column chromatography (eluent: from 0% to 10% EtOAc in pet. ether) to give a yellow oil which showed: ^1H NMR (500 MHz, CDCl_3) δ 2.65 (1H, bs, OH), 3.39 (1H, dd, $J = 2.6, 12.6$ Hz, $\text{H}_3\text{-THIQ}$), 3.86 (1H, ddd, $J = 1.1, 3.8, 12.6$ Hz, $\text{H}_3\text{-THIQ}$), 4.20 (1H, d, $J = 15.4$ Hz, $\text{H}_1\text{-THIQ}$), 4.49 (1H, d, $J = 15.4$ Hz, $\text{H}_1\text{-THIQ}$), 4.79 (1H, bs, $\text{H}_4\text{-THIQ}$), 6.94 (1H, tt, $J = 1.1, 7.4$ Hz, ArH, phenyl), 7.09 (2H, dd, $J = 1.0, 8.8$ Hz, ArH, phenyl), 7.17 – 7.23 (1H, m), 7.29 – 7.32 (2H, m, $\text{H}_6, \text{H}_7\text{-THIQ}$), 7.34 (2H, dd, $J = 7.3, 8.8$ Hz, ArH, phenyl) and 7.47 – 7.51 (1H, m) ppm. ^{13}C NMR (126 MHz, CDCl_3) δ 51.4 ($\text{C}_1\text{-THIQ}$), 55.6 ($\text{C}_3\text{-THIQ}$), 67.3 ($\text{C}_4\text{-THIQ}$), 116.6 (ArCH, phenyl), 120.2 (ArCH, phenyl), 126.5, 127.2, 128.2, 129.3, 129.4 (ArCH, phenyl), 136.7, 134.3 and 151.1 (ArCN) ppm. LC/MS (ES^+) $t_r = 1.75$ min (66 %), m/z 226.0 ($\text{M}^+ + \text{H}$); (RP, Isocratic, 90% MeOH). HRMS (ES^+) calcd. for $\text{C}_{15}\text{H}_{16}\text{NO}$ ($\text{M}^+ + \text{H}$) 226.1226, found 226.1234.

2-(3-Methoxyphenyl)-1,2,3,4-tetrahydroisoquinolin-4-ol (143b)

C₁₆H₁₇NO₂, Mol. Wt.: 255.31

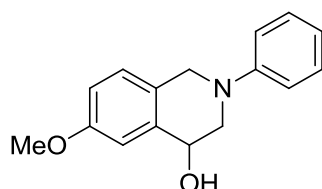


(Method B)

The crude compound was obtained as a yellow oil (1.73 g) which showed: ¹H NMR (400 MHz, CDCl₃) δ 2.46 (1H, bs), 3.40 (1H, dd, *J* = 2.7, 12.6 Hz), 3.83 (3H, s), 3.85 (1H, ddd, *J* = 0.7, 3.9, 12.6 Hz), 4.21 (1H, d, *J* = 15.5 Hz), 4.50 (1H, d, *J* = 15.5 Hz), 4.79 (1H, s), 6.47 (1H, dd, *J* = 2.3, 8.2 Hz), 6.61 (1H, t, *J* = 2.3 Hz), 6.69 (1H, dd, *J* = 2.3, 8.2 Hz), 7.17 - 7.20 (1H, m), 7.23 (1H, t, *J* = 8.2 Hz), 7.28 - 7.32 (2H, m) and 7.45 - 7.53 (1H, m) ppm. LC/MS (ES⁺) *t*_r = 1.78 min (87 %), *m/z* 256.1 (M⁺+H); (RP, Isocratic, 90% MeOH).

6-Methoxy-2-phenyl-1,2,3,4-tetrahydroisoquinolin-4-ol (143e)

C₁₆H₁₇NO₂, Mol. Wt.: 255.31



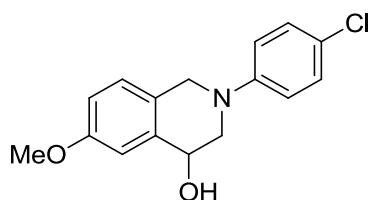
(Method B)

A sample of crude compound was purified by column chromatography (eluent: from 0% to 30% EtOAc in pet. ether) to give a yellow oil which showed: ¹H NMR (500 MHz, CDCl₃) δ 2.54 (1H, bs, OH), 3.37 (1H, dd, *J* = 2.6, 12.6 Hz, H₃-THIQ), 3.83 (3H, s, ArOCH₃), 3.84 (4H, ddd, *J* = 1.1, 3.8, 12.6 Hz, H₃-THIQ), 4.14 (1H, d, *J* = 14.9 Hz, H₁-THIQ), 4.43 (1H, d, *J* = 14.9 Hz, H₁-THIQ), 4.74 (1H, bs, H₄-THIQ), 6.88 (1H, dd, *J* = 2.7, 8.4 Hz, H₇-THIQ), 6.91 (1H, tt, *J* = 0.8, 7.4 Hz, ArH, phenyl), 7.01 (1H, d, *J* = 2.7 Hz, H₅-THIQ), 7.07 (2H, dd, *J* = 0.8, 8.7 Hz, ArH, phenyl), 7.10 (1H, d, *J* = 8.4 Hz, H₈-THIQ) and 7.32 (2H, dd, *J* = 7.3, 8.7 Hz, ArH, phenyl) ppm. ¹³C NMR (126 MHz,

CDCl₃) δ 50.9 (C₁-THIQ), 55.5 (ArOCH₃), 55.5 (C₃-THIQ), 67.6 (C₄-THIQ), 113.1 (C₅-THIQ), 115.3 (C₇-THIQ), 116.6 (ArCH, phenyl), 120.2 (ArCH, phenyl), 126.4 (C₁CC₈-THIQ), 127.6 (C₈-THIQ), 129.4 (ArCH, phenyl), 137.8 (C₄CC₅-THIQ), 151.2 (ArCN) and 158.7 (C₆-THIQ) ppm. LC/MS (ES⁺) t_r = 1.77 min (56%), m/z 255.9 (M⁺+H). HRMS (ES⁺) calcd. for C₁₆H₁₈NO₂ (M⁺+H) 256.1332, found 256.1326.

2-(4-Chlorophenyl)-6-methoxy-1,2,3,4-tetrahydroisoquinolin-4-ol (143i)

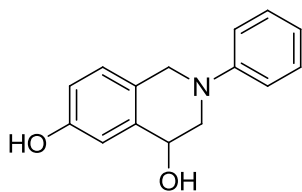
C₁₆H₁₆ClNO₂, Mol. Wt.: 289.76



A sample of crude compound was purified by column chromatography (eluent: from 0% to 30% EtOAc in pet. ether) to give a yellow oil which showed: ¹H NMR (500 MHz, CDCl₃) δ 2.45 (1H, bs, OH), 3.36 (1H, dd, J = 2.7, 12.6 Hz, H₃-THIQ), 3.77 (1H, ddd, J = 0.9, 3.9, 12.6 Hz, H₃-THIQ), 3.83 (3H, s, ArOCH₃), 4.11 (1H, d, J = 14.8 Hz, H₁-THIQ), 4.38 (1H, d, J = 14.8 Hz, H₁-THIQ), 4.74 (1H, bs, H₄-THIQ), 6.88 (1H, dd, J = 2.7, 8.5 Hz, H₇-THIQ), 6.97 (2H, d, J = 9.0 Hz, ArH, phenyl), 7.00 (1H, d, J = 2.6 Hz, H₅-THIQ), 7.09 (1H, d, J = 8.5 Hz, H₈-THIQ) and 7.25 (2H, d, J = 9.0 Hz, ArH, phenyl) ppm. ¹³C NMR (126 MHz, CDCl₃) δ 50.8 (C₁-THIQ), 55.5 (C₃-THIQ), 55.5 (ArOCH₃), 67.5 (C₄-THIQ), 113.15 (C₅-THIQ), 115.45 (C₇-THIQ), 117.7 (ArCH, phenyl), 125.0 (ArCCl), 126.0 (C₁CC₈), 127.65 (C₈-THIQ), 129.2 (ArCH, phenyl), 137.6 (C₄CC₅), 149.8 (ArCN) and 158.85 (C₆-THIQ) ppm. LC/MS (ES⁺) t_r = 2.08 min (58 %), m/z 290.1 (M⁺+H); (RP, Isocratic, 90% MeOH). HRMS (ES⁺) calcd. for C₁₆H₁₅NO₂³⁵Cl (M⁺+H) 288.0786, found 288.0776. calcd. for C₁₆H₁₅NO₂³⁷Cl (M⁺+H) 290.0756, found 290.0769

2-Phenyl-1,2,3,4-tetrahydroisoquinoline-4,6-diol (143l)

C₁₅H₁₅NO₂, Mol. Wt.: 241.29

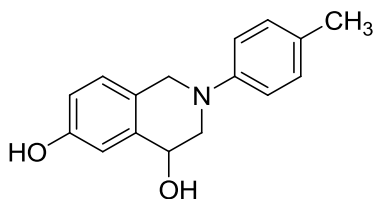


(Method B)

The crude compound was obtained as a brown-yellow solid (2.15 g) which showed: ^1H NMR (400 MHz, CDCl_3) δ 3.42 (1H, ddd, $J = 0.6, 2.9, 12.7$ Hz), 3.85 (1H, ddd, $J = 1.0, 4.0, 12.7$ Hz), 4.17 (1H, d, $J = 14.3$ Hz), 4.46 (1H, d, $J = 14.2$ Hz), 4.76 (1H, s), 6.84 (1H, dd, $J = 2.7, 8.4$ Hz), 6.92 - 7.05 (2H, m), 7.08 - 7.13 (3H, m) and 7.31 - 7.39 (3H, m) ppm. LC/MS (ES^+) $t_r = 1.22$ min (81 %), m/z 242.1 ($\text{M}^+ + \text{H}$); (RP, Isocratic, 90% MeOH).

2-*p*-Tolyl-1,2,3,4-tetrahydroisoquinoline-4,6-diol (143m)

$\text{C}_{16}\text{H}_{17}\text{NO}_2$, Mol. Wt.: 255.31

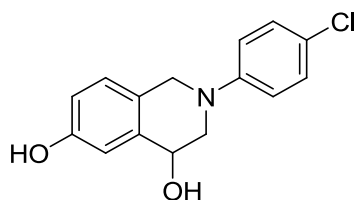


(Method B)

The crude compound was obtained as a brown-yellow solid (2.05 g) which showed: ^1H NMR (400 MHz, CDCl_3) δ 3.31 (1H, dd, $J = 2.5, 12.2$ Hz), 3.76 (1H, dd, $J = 3.5, 12.2$ Hz), 4.07 (1H, d, $J = 14.9$ Hz), 4.36 (1H, d, $J = 14.9$ Hz), 4.69 (1H, s), 6.64 (1H, d, $J = 8.7$ Hz), 6.71 - 6.83 (2H, m) and 6.89 - 7.17 (4H, m) ppm. LC/MS (ES^+) $t_r = 1.52$ min (70 %), m/z 256.1 ($\text{M}^+ + \text{H}$); (RP, Isocratic, 90% MeOH).

2-(4-Chlorophenyl)-1,2,3,4-tetrahydroisoquinoline-4,6-diol (143n)

$\text{C}_{15}\text{H}_{14}\text{ClNO}_2$, Mol. Wt.: 275.73

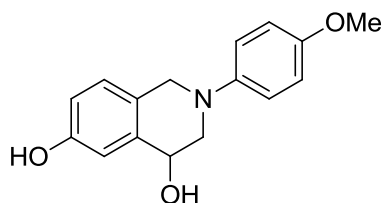


(Method B)

The crude compound was purified by column chromatography (eluent: 10% MeOH in DCM) to give a yellow-brown solid (1.88g, 95%) which showed: ^1H NMR (500 MHz, CDCl_3) δ 2.63 (1H, bs, C_4OH), 3.37 (1H, dd, $J = 2.2, 12.6$ Hz, $\text{H}_3\text{-THIQ}$), 3.76 (1H, dd, $J = 3.6, 12.6$ Hz, $\text{H}_3\text{-THIQ}$), 4.11 (1H, d, $J = 14.8$ Hz, $\text{H}_1\text{-THIQ}$), 4.38 (1H, d, $J = 14.8$ Hz, $\text{H}_1\text{-THIQ}$), 4.72 (1H, s, $\text{H}_4\text{-THIQ}$), 5.30 (1H, bs, C_6OH), 6.81 (1H, dd, $J = 2.3, 8.3$ Hz, $\text{H}_7\text{-THIQ}$), 6.96 (1H, d, $J = 2.2$ Hz, $\text{H}_5\text{-THIQ}$), 6.99 (2H, d, $J = 8.7$ Hz, 2 x ArCH, phenyl), 7.05 (1H, d, $J = 8.3$ Hz, $\text{H}_7\text{-THIQ}$) and 7.27 (2H, d, $J = 8.7$ Hz, 2 x ArCH, phenyl) ppm. ^{13}C NMR (126 MHz, CDCl_3) δ 50.8 ($\text{C}_1\text{-THIQ}$), 55.3 ($\text{C}_3\text{-THIQ}$), 67.1 ($\text{C}_4\text{-THIQ}$), 115.1 ($\text{C}_5\text{-THIQ}$), 115.9 ($\text{C}_7\text{-THIQ}$), 117.6 (2 x ArCH, phenyl), 125.0 (ArCCl), 125.9 ($\text{C}_1\text{CC}_8\text{-THIQ}$), 127.7 ($\text{C}_8\text{-THIQ}$), 129.1 (2 x ArCH, phenyl), 137.6 ($\text{C}_4\text{CC}_5\text{-THIQ}$), 149.6 (ArCN) and 154.6 ($\text{C}_6\text{-THIQ}$) ppm. LC/MS (ES^+) $t_r = 1.65$ min (72 %), m/z 276.1 ($\text{M}^+ + \text{H}$); (RP, Isocratic, 90% MeOH). HRMS (ES^-) calcd. for $\text{C}_{15}\text{H}_{13}\text{ClNO}_2$ ($\text{M}^- - \text{H}$) 274.0640, found 274.0629. Mp 168-171 $^\circ\text{C}$

2-(4-methoxyphenyl)-1,2,3,4-tetrahydroisoquinoline-4,6-diol (143o)

$\text{C}_{16}\text{H}_{17}\text{NO}_3$, Mol. Wt.: 271.31



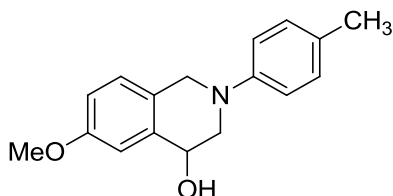
(Method B)

The crude compound was obtained as a brown-yellow solid (2.17 g) which showed: ^1H NMR (400 MHz, CDCl_3) δ 3.26 (1H, dd, $J = 2.5, 12.4$ Hz), 3.62 (1H, ddd, $J = 1.1, 3.7, 12.2$ Hz), 3.78 (3H, s), 4.00 (1H, d, $J = 14.6$ Hz), 4.25 (1H, d, $J = 14.6$ Hz), 4.66 (1H, t, $J = 3.0$ Hz), 6.77 (1H, dd, $J = 2.7, 8.3$ Hz), 6.87 (2H, d, $J = 9.0$ Hz), 6.90 (1H, d,

$J = 2.7$ Hz), 6.99 (1H, d, $J = 8.3$ Hz) and 7.02 (2H, d, $J = 9.0$ Hz) ppm. LC/MS (ES^+) $t_r = 1.35$ min (98 %), m/z 271.8 ($\text{M}^+ + \text{H}$); (RP, Isocratic, 90% MeOH).

6-Methoxy-2-(*p*-tolyl)-1,2,3,4-tetrahydroisoquinolin-4-ol (143q)

$\text{C}_{17}\text{H}_{19}\text{NO}_2$, Mol. Wt.: 269.34

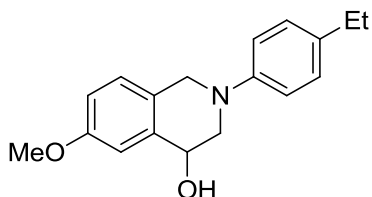


(Method B)

A sample of crude compound was purified by column chromatography (eluent: from 0% to 30% EtOAc in pet. ether) to give a yellow oil which showed: ^1H NMR (500 MHz, CDCl_3) δ 2.30 (3H, s, ArCH_3), 2.64 (1H, bs, OH), 3.31 (1H, dd, $J = 2.6, 12.5$ Hz, $\text{H}_3\text{-THIQ}$), 3.77 (1H, ddd, $J = 1.1, 3.8, 12.5$ Hz, $\text{H}_3\text{-THIQ}$), 3.83 (3H, s, ArOCH_3), 4.08 (1H, d, $J = 14.9$ Hz, $\text{H}_1\text{-THIQ}$), 4.37 (1H, d, $J = 14.8$ Hz, $\text{H}_1\text{-THIQ}$), 4.72 (1H, bs, $\text{H}_4\text{-THIQ}$), 6.87 (1H, dd, $J = 2.7, 8.5$ Hz, $\text{H}_7\text{-THIQ}$), 6.98 (2H, d, $J = 8.6$ Hz, ArH, phenyl), 7.00 (1H, d, $J = 2.7$ Hz, $\text{H}_5\text{-THIQ}$), 7.09 (1H, d, $J = 8.5$ Hz, $\text{H}_8\text{-THIQ}$) and 7.13 (2H, d, $J = 8.6$ Hz, ArH, phenyl) ppm. ^{13}C NMR (126 MHz, CDCl_3) δ 20.6 (ArCH_3), 51.6 ($\text{C}_1\text{-THIQ}$), 55.5 (ArOCH_3), 56.2 ($\text{C}_3\text{-THIQ}$), 67.6 ($\text{C}_4\text{-THIQ}$), 113.1 ($\text{C}_5\text{-THIQ}$), 115.3 ($\text{C}_7\text{-THIQ}$), 117.1 (ArCH, phenyl), 126.6 (C_1CC_8), 127.6 ($\text{C}_8\text{-THIQ}$), 129.9 (ArCH, ArCCH_3 , phenyl), 137.9 (C_4CC_5), 149.1 (ArCN) and 158.7 ($\text{C}_6\text{-THIQ}$) ppm. LC/MS (ES^+) $t_r = 1.82$ min (70 %), m/z 270.2 ($\text{M}^+ + \text{H}$); (RP, Isocratic, 90% MeOH).

6-Methoxy-2-(4-ethylphenyl)-1,2,3,4-tetrahydroisoquinolin-4-ol (143r)

$\text{C}_{18}\text{H}_{21}\text{NO}_2$, Mol. Wt.: 283.37

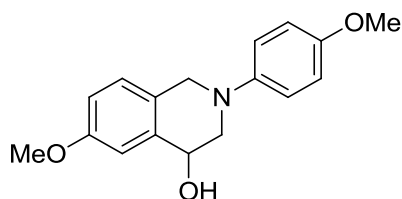


(Method B)

The crude compound was purified by column chromatography (eluent: from 0% to 20% EtOAc in pet. ether) to give the product as an orange wax (900 mg, 31%) which showed: ^1H NMR (500 MHz, CDCl_3) δ 1.23 (1H, t, $J = 7.6$ Hz, CH_2CH_3), 2.56 (1H, d, $J = 10.8$ Hz, OH), 2.61 (1H, q, $J = 7.6$ Hz, CH_2CH_3), 3.32 (1H, dd, $J = 2.5, 12.5$ Hz, H_3 -THIQ), 3.81 (1H, ddd, $J = 1.0, 3.7, 12.5$ Hz, H_3 -THIQ), 3.83 (1H, s, OCH_3), 4.09 (1H, d, $J = 14.8$ Hz, H_1 -THIQ), 4.40 (1H, d, $J = 14.8$ Hz, H_1 -THIQ), 4.73 (1H, dt, $J = 3.1, 10.8$ Hz, H_4 -THIQ), 6.87 (1H, dd, $J = 2.7, 8.5$ Hz, H_7 -THIQ), 7.00 (1H, d, $J = 2.4$ Hz, H_5 -THIQ), 7.02 (1H, d, $J = 8.8$ Hz), 7.10 (1H, d, $J = 8.5$ Hz, H_8 -THIQ) and 7.16 (1H, d, $J = 8.6$ Hz) ppm. ^{13}C NMR (126 MHz, CDCl_3) δ 15.8 (CH_2CH_3), 28.0 (CH_2CH_3), 51.3 (C_1 -THIQ), 55.4 (OCH_3), 55.9 (C_3 -THIQ), 67.5 (C_4 -THIQ), 113.0 (C_5 -THIQ), 115.1 (C_7 -THIQ), 116.9 (ArCH, phenyl), 126.4 (C_1CC_8 -THIQ), 127.5 (C_8 -THIQ), 128.6 (ArCH, phenyl), 136.3 (ArCEt), 137.7 (C_4CC_6 -THIQ), 149.1 (ArCN) and 158.5 (C_6 -THIQ) ppm. LC/MS (ES^+) $t_r = 2.19$ min (48 %), m/z 284.2 ($\text{M}^+ + \text{H}$); (RP, Isocratic, 90% MeOH). HRMS (ES^+) calcd. $\text{C}_{18}\text{H}_{22}\text{NO}_2$ ($\text{M}^+ + \text{H}$) 284.1645, found 284.1636.

6-Methoxy-2-(4-methoxyphenyl)-1,2,3,4-tetrahydroisoquinolin-4-ol (143s)

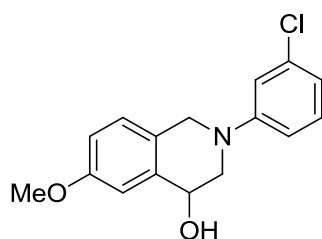
$\text{C}_{17}\text{H}_{19}\text{NO}_3$, Mol. Wt.: 285.34



A sample of crude compound was purified by column chromatography (eluent: from 0% to 30% EtOAc in pet. ether) to give a yellow oil which showed: ^1H NMR (400 MHz, CDCl_3) δ 3.28 (1H, dd, $J = 2.6, 12.2$ Hz, H_3 -THIQ), 3.75 (1H, dd, $J = 4.5, 12.2$ Hz), 3.79 (3H, s, OMe), 3.83 (3H, s, OMe), 4.04 (1H, d, $J = 14.7$ Hz, H_1 -THIQ), 4.29 (1H, d, $J = 14.7$ Hz, H_1 -THIQ), 4.71 (1H, m, H_4 -THIQ), 6.86 (1H, dd, $J = 2.5, 8.4$ Hz, H_7 -THIQ), 6.89 (2H, d, $J = 9.0$ Hz, 2 x ArH, phenyl), 7.01 (1H, d, $J = 2.5$ Hz, H_5 -THIQ), 7.03 (2H, d, $J = 9.0$ Hz, 2 x ArH, phenyl) and 7.07 (1H, d, $J = 8.4$ Hz, H_8 -THIQ) ppm. LC/MS (ES^+) $t_r = 1.52$ min (83 %), m/z 286.0 ($\text{M}^+ + \text{H}$); (RP, Isocratic, 90% MeOH). HRMS (ES^+) calcd. for $\text{C}_{17}\text{H}_{20}\text{NO}_3$ ($\text{M}^+ + \text{H}$) 286.1438, found 286.1445.

6-Methoxy-2-(3-chlorophenyl)-1,2,3,4-tetrahydroisoquinolin-4-ol (143t)

C₁₆H₁₆ClNO₂, Mol. Wt.: 289.76

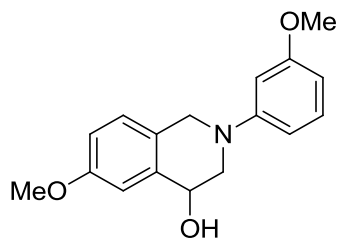


(Method B)

The crude compound was purified by column chromatography (eluent: from 0% to 40% EtOAc in pet. ether) to give a yellow oil (504 mg, 41%) which showed: ¹H NMR (500 MHz, CDCl₃) δ 2.38 (1H, bs, OH), 3.41 (1H, dd, *J* = 2.4, 12.9 Hz, H₃-THIQ), 3.81 (2H, ddd, *J* = 1.7, 4.0, 12.9 Hz, H₃-THIQ), 3.83 (3H, s, OCH₃), 4.16 (1H, d, *J* = 14.9 Hz, H₁-THIQ), 4.42 (1H, d, *J* = 14.9 Hz, H₁-THIQ), 4.76 (1H, bs, H₄-THIQ), 6.86 (1H, ddd, *J* = 0.8, 2.0, 8.1 Hz, ArH, phenyl), 6.89 (1H, dd, *J* = 2.8, 8.5 Hz, H₇-THIQ), 6.92 (1H, ddd, *J* = 0.8, 2.0, 8.1 Hz, ArH, phenyl), 7.01 (1H, d, *J* = 2.8 Hz, H₅-THIQ), 7.01 (1H, t, *J* = 2.0 Hz, ArH, phenyl), 7.11 (1H, d, *J* = 8.5 Hz, H₈-THIQ) and 7.21 (1H, t, *J* = 8.1 Hz, ArH, phenyl) ppm. ¹³C NMR (126 MHz, CDCl₃) δ 50.3 (C₁-THIQ), 54.9 (C₃-THIQ), 55.6 (OCH₃), 67.5 (C₄-THIQ), 113.0 (ArCH, phenyl), 114.2 (ArCH, phenyl), 115.4 (C₇-THIQ), 116.0 (C₅-THIQ), 119.7 (ArCH, phenyl), 125.8 (C₁CC₈-THIQ), 127.7 (C₈-THIQ), 130.3 (ArCH, phenyl), 135.2 (ArCCl), 137.6 (C₄CC₅-THIQ), 152.2 (ArCN) and 158.8 (C₆-THIQ) ppm. LC/MS (ES⁺) *t*_r = 2.10 min (96 %), *m/z* 290.0 (M⁺+H); (RP, Isocratic, 90% MeOH). HRMS (ES⁺) calcd. C₁₆H₁₇³⁵ClNO₂ (M⁺+H) 290.0942, found 290.0952; calcd. C₁₆H₁₇³⁷ClNO₂ (M⁺+H) 292.0913, found 292.0952.

6-Methoxy-2-(3-methoxyphenyl)-1,2,3,4-tetrahydroisoquinolin-4-ol (143u)

C₁₇H₁₉NO₃, Mol. Wt.: 285.34

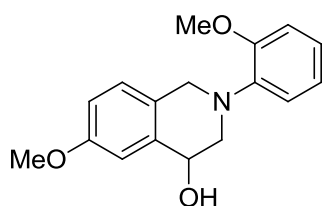


(Method B)

The crude compound was purified by column chromatography (eluent: from 0% to 50% EtOAc in pet. ether) to give a yellow oil (1.9 g, 36%) which showed: ^1H NMR (500 MHz, CDCl_3) δ 2.48 (1H, d, $J = 10.5$ Hz, OH), 3.38 (1H, dd, $J = 2.6, 12.6$ Hz, $\text{H}_3\text{-THIQ}$), 3.83 (3H, s, OCH_3 , THIQ), 3.83 (1H, ddd, $J = 1.0, 3.9, 12.6$ Hz, $\text{H}_3\text{-THIQ}$), 3.83 (3H, s, OCH_3 , phenyl), 4.14 (1H, d, $J = 14.9$ Hz, $\text{H}_1\text{-THIQ}$), 4.43 (1H, d, $J = 14.9$ Hz, $\text{H}_1\text{-THIQ}$), 4.74 (1H, dt, $J = 3.1, 10.5$ Hz, $\text{H}_4\text{-THIQ}$), 6.47 (1H, ddd, $J = 0.5, 2.3, 8.2$ Hz, ArH, phenyl), 6.60 (1H, t, $J = 2.3$ Hz, ArH, phenyl), 6.68 (1H, ddd, $J = 0.5, 2.3, 8.2$ Hz, ArH, phenyl), 6.88 (1H, dd, $J = 2.7, 8.5$ Hz, $\text{H}_7\text{-THIQ}$), 7.01 (1H, d, $J = 2.6$ Hz, $\text{H}_5\text{-THIQ}$), 7.10 (1H, d, $J = 8.5$ Hz, $\text{H}_8\text{-THIQ}$) and 7.23 (1H, t, $J = 8.2$ Hz, ArH, phenyl) ppm. ^{13}C NMR (126 MHz, CDCl_3) δ 50.8 ($\text{C}_1\text{-THIQ}$), 55.3 ($\text{C}_3\text{-THIQ}$), 55.4 (OCH_3 , THIQ), 55.5 (OCH_3 , phenyl), 67.6 ($\text{C}_4\text{-THIQ}$), 102.9 (ArCH, phenyl), 104.9 (ArCH, phenyl), 109.2 (ArCH, phenyl), 113.0 ($\text{C}_5\text{-THIQ}$), 115.3 ($\text{C}_7\text{-THIQ}$), 126.3 ($\text{C}_1\text{CC}_8\text{-THIQ}$), 127.6 ($\text{C}_8\text{-THIQ}$), 130.1 (ArCH, phenyl), 137.8 ($\text{C}_4\text{CC}_5\text{-THIQ}$), 152.6 (ArCN), 158.7 (ArCO) and 160.8 ($\text{C}_6\text{-THIQ}$) ppm. LC/MS (ES^+) $t_r = 1.75$ min (94 %), m/z 286.0 ($\text{M}^+ + \text{H}$); (RP, Isocratic, 90% MeOH). HRMS (ES^+) calcd. $\text{C}_{17}\text{H}_{20}\text{NO}_3$ ($\text{M}^+ + \text{H}$) 286.1438, found 286.1428.

6-Methoxy-2-(2-methoxyphenyl)-1,2,3,4-tetrahydroisoquinolin-4-ol (143w)

$\text{C}_{17}\text{H}_{19}\text{NO}_3$, Mol. Wt.: 285.34



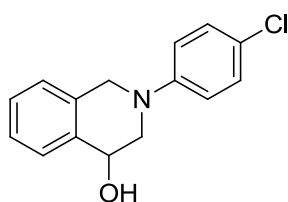
(Method B)

The crude compound was purified by column chromatography (eluent: from 0% to 50% EtOAc in pet. ether) to give a yellow oil (1.4 g, 26%) which showed: ^1H NMR (500 MHz, CDCl_3) δ 3.17 (1H, dd, $J = 2.5, 12.3$ Hz, $\text{H}_3\text{-THIQ}$), 3.49 (1H, d, $J = 10.1$ Hz, OH), 3.68 (1H, dd, $J = 2.9, 12.1$ Hz, $\text{H}_3\text{-THIQ}$), 3.83 (3H, s, OCH_3 , THIQ), 3.88 (3H, s, OCH_3 , phenyl), 4.12 – 4.25 (2H, m, $\text{H}_1\text{-THIQ}$), 4.67 (1H, dt, $J = 2.7, 9.9$ Hz, $\text{H}_4\text{-THIQ}$), 6.85 (1H, dd, $J = 2.8, 8.4$ Hz, $\text{H}_7\text{-THIQ}$), 6.91 (1H, dd, $J = 1.3, 8.0$ Hz, ArH, phenyl), 6.97 (1H, td, $J = 1.4, 7.6$ Hz, ArH, phenyl), 7.01 (1H, d, $J = 2.7$ Hz, $\text{H}_5\text{-THIQ}$) and 7.04 – 7.11 (3H, m, $\text{H}_8\text{-THIQ}$, 2 x ArH, phenyl) ppm. ^{13}C NMR (126 MHz, CDCl_3)

δ 52.4 (C₁-THIQ), 55.5 (OCH₃, THIQ), 55.5 (OCH₃, phenyl), 57.1 (C₃-THIQ), 67.9 (C₄-THIQ), 111.3 (ArCH, phenyl), 113.5 (C₅-THIQ), 114.9 (C₇-THIQ), 119.4 (ArCH, phenyl), 121.1 (ArCH, phenyl), 123.6 (ArCH, phenyl), 127.1 (C₁CC₈-THIQ), 127.4 (C₈-THIQ), 138.2 (C₄CC₅-THIQ), 140.9 (ArCN), 152.7 (ArCO, phenyl) and 158.6 (C₆-THIQ) ppm. LC/MS (ES⁺) t_r = 1.59 min (68 %), m/z 285.9 (M⁺+H); (RP, Isocratic, 90% MeOH). HRMS (ES⁺) calcd. C₁₇H₂₀NO₃ (M⁺+H) 286.1438, found 286.1443.

2-(4-Chlorophenyl)-1,2,3,4-tetrahydroisoquinolin-4-ol (143z)

C₁₅H₁₄ClNO, Mol. Wt.: 259.73

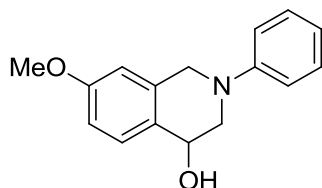


(Method B)

The crude compound was purified by column chromatography (eluent: from 0% to 30% EtOAc in pet. ether) to give a white solid (1.9 g, 61%). The compound was recrystallised from Et₂O/pet. ether to give a white solid which showed: ¹H NMR (500 MHz, CDCl₃) δ 2.43 (1H, d, J = 9.9 Hz, OH), 3.37 (1H, dd, J = 2.4, 12.6 Hz, H₃-THIQ), 3.81 (1H, ddd, J = 1.2, 3.7, 12.6 Hz, H₃-THIQ), 4.18 (1H, d, J = 15.3 Hz, H₁-THIQ), 4.45 (1H, d, J = 15.3 Hz, H₁-THIQ), 4.75 – 4.84 (1H, m, H₄-THIQ), 6.99 (2H, d, J = 9.0 Hz, ArH, phenyl), 7.17 – 7.21 (1H, m, H₅-THIQ), 7.26 (2H, d, J = 9.0 Hz, ArH, phenyl), 7.31 (2H, t, J = 3.5 Hz, H₆,H₇-THIQ) and 7.46 – 7.50 (1H, m, H₈-THIQ) ppm. ¹³C NMR (126 MHz, CDCl₃) δ 51.3 (C₁-THIQ), 55.6 (C₃-THIQ), 67.3 (C₄-THIQ), 117.7 (ArCH, phenyl), 125.1 (ArCCl), 126.5 (C-THIQ), 127.3 (C-THIQ), 128.4 (C-THIQ), 129.3 (ArCH, phenyl), 129.3 (C₇,C₆-THIQ), 134.0 (C₁CC₈-THIQ), 136.5 (C₄CC₅-THIQ) and 149.7 (ArCN) ppm. LC/MS (ES⁺) t_r = 2.01 min (99 %), m/z 259.9 (M⁺+H); (RP, Isocratic, 90% MeOH). HRMS (ES⁺) calcd. C₁₅H₁₅ClNO (M⁺+H) (³⁵Cl) 260.0837, found 260.0830; calcd. C₁₅H₁₅ClNO (M⁺+H) (³⁷Cl) 262.0807, found 262.0830. Mp 98-100 °C (Et₂O/Pet). Anal. calcd. for C₁₅H₁₄ClNO: C 69.4, H 5.43, N 5.39% found C 69.4, H 5.43, N 5.28%.

7-Methoxy-2-phenyl-1,2,3,4-tetrahydroisoquinolin-4-ol (144f)

C₁₆H₁₇NO₂, Mol. Wt.: 255.31

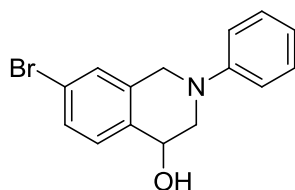


(Method C)

The crude compound was purified with chromatography (eluent: from 0% to 25% EtOAc in pet. ether) to give the product as a yellow oil (302 mg, 71 %) which showed: ¹H NMR (400 MHz, CDCl₃) δ 2.54 (1H, bs), 3.33 (2H, dd, *J* = 2.3, 12.6 Hz), 3.81 (4H, s), 3.87 (2H, dd, *J* = 3.0, 12.6 Hz), 4.14 (2H, d, *J* = 15.4 Hz), 4.45 (2H, d, *J* = 15.4 Hz), 4.73 (1H, s), 6.69 (1H, d, *J* = 2.3 Hz), 6.84 (1H, dd, *J* = 2.3, 8.4 Hz), 6.92 (1H, t, *J* = 7.3 Hz), 7.07 (2H, d, *J* = 8.1 Hz), 7.32 (2H, t, *J* = 7.8 Hz) and 7.39 (2H, d, *J* = 8.4 Hz) ppm. LC/MS (ES⁺) *t_r* = 1.71 min (75 %), *m/z* 255.9 (M⁺+H); (RP, Isocratic, 90% MeOH). HRMS (ES⁺) calcd. C₁₆H₁₇NNaO₂ (M⁺+Na) 278.1151, found 278.1153.

7-Bromo-2-phenyl-1,2,3,4-tetrahydroisoquinolin-4-ol (144h)

C₁₅H₁₄BrNO, Mol. Wt.: 304.18



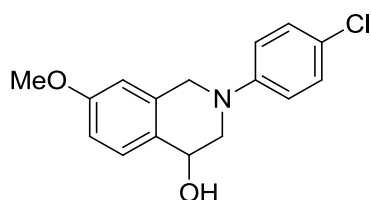
(Method B)

The crude compound was obtained as a pale yellow oil (250 mg, 48%) which showed: ¹H NMR (500 MHz, CDCl₃) δ 3.19 (1H, dd, *J* = 2.1, 12.9 Hz, CH₂CH), 4.07 (1H, ddd, *J* = 1.6, 2.4, 12.9 Hz, CH₂CH), 4.11 (1H, d, *J* = 15.2 Hz, ArCH₂), 4.54 (1H, d, *J* = 15.5 Hz, ArCH₂), 5.03 (1H, t, *J* = 2.3 Hz, CHOH), 6.95 (1H, tt, *J* = 0.9, 7.4 Hz, ArH), 7.10 (2H, dd, *J* = 0.9, 8.7 Hz, ArH), 7.16 (1H, d, *J* = 2.0 Hz, ArH), 7.17 (1H, d, *J* = 7.2 Hz, ArH), 7.34 (2H, dd, *J* = 7.4, 8.7 Hz, ArH) and 7.52 (1H, dd, *J* = 2.0, 7.2 Hz, ArH) ppm. ¹³C NMR (126 MHz, CDCl₃) δ 51.5 (ArCH₂), 55.7 (CH₂CH), 66.7 (CHOH), 116.8 (ArCH), 117.0 (ArCH), 120.8 (ArCH), 125.8 (ArCBr), 126.0 (ArCH), 129.4

(ArCH), 131.4 (ArCH), 135.6 (ArCCH), 137.1 (ArCCH₂) and 150.9 (ArCN) ppm. LC/MS (ES⁺) t_r = 1.97 min (61 %), m/z 303.4 (M⁺+H) (⁷⁹Br), 305.4 (M⁺+H) (⁸¹Br); (RP, Isocratic, 90% MeOH). HRMS (ES⁺) calcd. for C₁₅H₁₅BrNO (M⁺+H) (⁷⁹Br) 304.0332, found 304.0335; calcd. for C₁₅H₁₅BrNO (M⁺+H) (⁸¹Br) 306.0311, found 306.0323.

2-(4-Chlorophenyl)-7-methoxy-1,2,3,4-tetrahydroisoquinolin-4-ol (144j)

C₁₆H₁₆ClNO₂, Mol. Wt.: 289.76

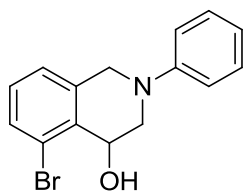


(Method C)

The crude compound was purified by column chromatography (eluent: from 0% to 40% EtOAc in pet. ether) to give a dark yellow wax (2.39 g, 31%) which showed: ¹H NMR (500 MHz, CDCl₃) δ 2.36 (1H, d, *J* = 8.6 Hz, OH), 3.32 (2H, dd, *J* = 2.5, 12.6 Hz, H₃-THIQ), 3.82 (3H, s, OCH₃), 3.82 (5H, ddd, *J* = 1.3, 3.5, 12.8 Hz, H₃-THIQ), 4.13 (2H, d, *J* = 15.3 Hz, H₁-THIQ), 4.42 (2H, d, *J* = 15.3 Hz, H₁-THIQ), 4.74 (1H, bs, H₄-THIQ), 6.69 (1H, d, *J* = 2.6 Hz, H₈-THIQ), 6.85 (1H, dd, *J* = 2.6, 8.5 Hz, H₆-THIQ), 6.98 (3H, d, *J* = 9.0 Hz, ArH, phenyl), 7.25 (4H, d, *J* = 9.0 Hz, ArH, phenyl) and 7.39 (1H, d, *J* = 8.5 Hz, H₅-THIQ) ppm. ¹³C NMR (126 MHz, CDCl₃) δ 51.3 (C₁-THIQ), 55.3 (OCH₃), 55.7 (C₃-THIQ), 66.7 (C₄-THIQ), 110.9 (C₈-THIQ), 113.4 (C₆-THIQ), 117.6 (ArCH, phenyl), 124.9 (ArCCl), 129.0 (C₅CC₆-THIQ), 129.1 (ArCH, phenyl), 130.5 (C₅-THIQ), 135.3 (C₁CC₈-THIQ), 149.6 (ArCN) and 159.4 (C₇-THIQ) ppm. LC/MS (ES⁺) t_r = 1.95 min (92 %), m/z 290.0 (M⁺+H); (RP, Isocratic, 90% MeOH). HRMS (ES⁺) calcd. for C₁₆H₁₇³⁵ClNO₂ (M⁺+H) 290.0942, found 290.0935; calcd. C₁₆H₁₇³⁷ClNO₂ (M⁺+H) 292.0913, found 292.0935.

5-Bromo-2-phenyl-1,2,3,4-tetrahydroisoquinolin-4-ol (145h)

C₁₅H₁₄BrNO, Mol. Wt.: 304.18

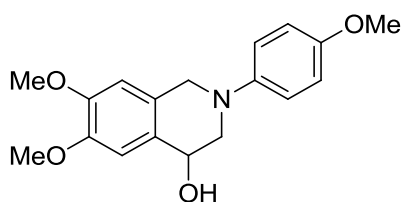


(Method B)

The crude compound was obtained as a pale yellow oil (50 mg, 10%) which showed: ^1H NMR (500 MHz, CDCl_3) δ 3.35 (1H, dd, $J = 2.7, 12.7$ Hz, CH_2CH), 3.77 (1H, ddd, $J = 1.0, 3.9, 12.7$ Hz, CH_2CH), 3.89 (1H, bs, OH), 4.13 (1H, d, $J = 15.6$ Hz, ArCH_2), 4.37 (1H, d, $J = 15.6$ Hz, ArCH_2), 4.72 (1H, t, $J = 3.3$ Hz, CHOH), 6.93 (1H, tt, $J = 0.9, 7.2$ Hz, ArH), 7.03 (2H, dd, $J = 0.9, 8.7$ Hz, ArH), 7.29 - 7.35 (4H, m, ArH) and 7.39 (1H, dd, $J = 2.0, 8.2$ Hz, ArH) ppm. ^{13}C NMR (126 MHz, CDCl_3) δ 51.0 (ArCH_2), 55.5 (CH_2CH), 66.6 (CHOH), 116.7 (ArCH), 120.6 (ArCH), 121.9 (ArCBr), 129.3 (ArCH), 129.4 (ArCH), 130.3 (ArCH), 131.0 (ArCH), 135.7 (ArCCH), 136.5 (ArCCH_2) and 150.7 (ArCN) ppm. LC/MS (ES^+) $t_r = 2.20$ min (86 %), m/z 303.4 ($\text{M}^+ + \text{H}$) (^{79}Br), 305.4 ($\text{M}^+ + \text{H}$) (^{81}Br); (RP, Isocratic, 90% MeOH). HRMS (ES^+) calcd. for $\text{C}_{15}\text{H}_{15}^{79}\text{BrNO}$ ($\text{M}^+ + \text{H}$) 304.0332, found 304.0321; calcd. for $\text{C}_{15}\text{H}_{15}^{81}\text{BrNO}$ ($\text{M}^+ + \text{H}$) 306.0311, found 306.0320.

6,7-Dimethoxy-2-(4-methoxyphenyl)-1,2,3,4-tetrahydroisoquinolin-4-ol (146x)

$\text{C}_{18}\text{H}_{21}\text{NO}_4$, Mol. Wt.: 315.36



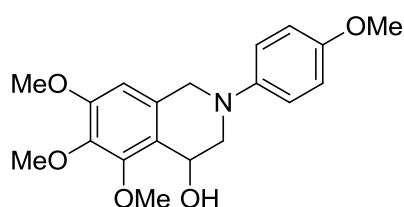
(Method B)

The crude compound was purified by column chromatography (eluent: from 0% to 50% EtOAc in pet. ether) to give the product as a white solid (3.54 g, 62%) which showed: ^1H NMR (500 MHz, CDCl_3) δ 2.67 (1H, bs, OH), 3.23 (1H, dd, $J = 2.3, 12.3$ Hz, $\text{H}_3\text{-THIQ}$), 3.71 (1H, dd, $J = 3.1, 12.3$ Hz, $\text{H}_3\text{-THIQ}$), 3.79 (3H, s, OCH_3 , phenyl), 3.88 (3H, s, $\text{C}_6\text{OCH}_3\text{-THIQ}$), 3.90 (3H, s, $\text{C}_7\text{OCH}_3\text{-THIQ}$), 4.01 (1H, d, $J = 14.8$ Hz, $\text{H}_1\text{-THIQ}$), 4.27 (1H, d, $J = 14.8$ Hz, $\text{H}_1\text{-THIQ}$), 4.67 (1H, bs, $\text{H}_4\text{-THIQ}$), 6.62 (1H, s,

H₈-THIQ), 6.89 (2H, d, *J* = 9.0 Hz, 2 x ArCH, phenyl), 6.96 (1H, s, H₅-THIQ) and 7.03 (2H, d, *J* = 8.9 Hz, 2 x ArCH, phenyl) ppm. ¹³C NMR (126 MHz, CDCl₃) δ 52.7 (C₁-THIQ), 55.6 (OCH₃, phenyl), 55.9 (2 x OCH₃, THIQ), 57.2 (C₃-THIQ), 67.2 (C₄-THIQ), 108.6 (C₈-THIQ), 111.6 (C₅-THIQ), 114.5 (2 x ArCH, phenyl), 118.9 (2 x ArCH, phenyl), 126.8 (C₁CC₈-THIQ), 128.6 (C₄CC₅-THIQ), 145.3 (ArCN), 148.1 (C₇-THIQ), 148.9 (C₆-THIQ) and 154.2 (ArCO, phenyl) ppm. HRMS (ES⁺) calcd. C₁₈H₂₂NO₄ (M⁺+H) 316.1543, found 316.1543. Mp 136-137 °C (DCM/Et₂O).

5,6,7-Trimethoxy-2-(4-methoxyphenyl)-1,2,3,4-tetrahydroisoquinolin-4-ol (148y)

C₁₉H₂₃NO₅, Mol. Wt.: 345.39

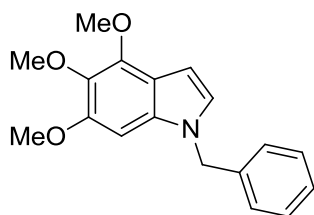


(Method B)

The crude compound was purified by column chromatography (eluent: from 0% to 100% EtOAc in pet. ether) to give the product as a dark brown solid (5.49 g, 82%) which showed: ¹H NMR (500 MHz, CDCl₃) δ 2.90 (1H, bs, OH), 3.18 (1H, dd, *J* = 2.7, 12.4 Hz, H₃-THIQ), 3.70 (1H, dd, *J* = 3.5, 12.6 Hz, H₃-THIQ), 3.79 (3H, s, OCH₃, phenyl), 3.86 (3H, s, C₆OCH₃-THIQ), 3.87 (3H, s, C₇OCH₃-THIQ), 3.98 (1H, d, *J* = 15.1 Hz, H₁-THIQ), 4.02 (3H, s, C₅OCH₃-THIQ), 4.29 (1H, d, *J* = 15.0 Hz, H₁-THIQ), 4.98 (1H, bs, H₄-THIQ), 6.45 (1H, s, H₈-THIQ), 6.88 (2H, d, *J* = 9.0 Hz, 2 x ArCH, phenyl) and 7.04 (2H, d, *J* = 9.0 Hz, 2 x ArCH, phenyl) ppm. ¹³C NMR (126 MHz, CDCl₃) δ 53.2 (C₁-THIQ), 55.6 (OCH₃, phenyl), 56.0 (C₆OCH₃-THIQ), 56.9 (C₃-THIQ), 60.9 (C₇OCH₃-THIQ), 61.5 (C₅OCH₃-THIQ), 62.7 (C₄-THIQ), 104.6 (C₈-THIQ), 114.5 (2 x ArCH, phenyl), 119.1 (2 x ArCH, phenyl), 123.0 (C₁CC₈-THIQ), 130.5 (C₄CC₅-THIQ), 140.6 (C₇-THIQ), 145.3 (ArCN), 152.2 (C₅-THIQ), 153.5 (C₆-THIQ) and 154.3 (ArCO, phenyl) ppm. HRMS (ES⁺) calcd. C₁₉H₂₄NO₅ (M⁺+H) 346.1649, found 346.1638.

1-Benzyl-4,5,6-trimethoxy-1*H*-indole (154d)

C₁₈H₁₉NO₃, Mol. Wt.: 297.35

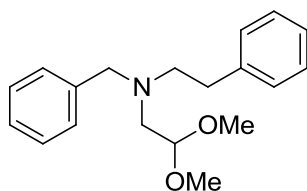


(Method B)

The crude compound was purified by chromatography (eluent from 0% to 30% EtOAc in pet. ether) to yield the product as a pale yellow oil (71 mg, 22%) which showed: ¹H NMR (500 MHz, CDCl₃) δ 3.82 (3H, s, CH₃), 3.87 (3H, s, CH₃), 4.13 (3H, s, CH₃), 5.23 (2H, s, ArCH₂), 6.47 (1H, s, ArH), 6.59 (1H, dd, *J* = 0.8, 3.2 Hz, ArH), 6.94 - 6.97 (1H, m, ArH), 7.11 - 7.15 (2H, m, ArH) and 7.25 - 7.34 (3H, m, ArH) ppm. ¹³C NMR (126 MHz, CDCl₃) δ 50.2 (ArCH₂), 56.3 (CH₃), 60.7 (CH₃), 61.4 (CH₃), 88.2 (ArCH), 99.2 (ArCH), 115.6 (ArCCH), 126.2 (ArCH), 126.8 (ArCH), 127.6 (ArCH), 128.7 (ArCH), 133.4 (ArCN), 135.5 (ArCOCH₃), 137.3 (ArCCH₂), 145.9 (ArCOCH₃) and 151.0 (ArCOCH₃) ppm. LC/MS (ES⁺) *t*_r = 1.02 min (76 %), *m/z* 298.1 (M⁺+H); (RP, Isocratic, 90% MeOH); HRMS (ES⁺) calcd. for C₁₈H₂₀NO₃ (M⁺+H) 298.1438, found 298.1448.

***N*-Benzyl-2,2-dimethoxy-*N*-phenylethanamine (155)**

C₁₉H₂₅NO₂, Mol. Wt.: 299.41

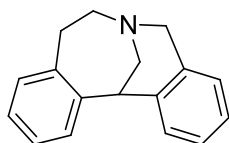


2-Phenylethylamine (1.3 mL, 10.0 mmol) and benzaldehyde (1.0 mL, 10.0 mmol) were dissolved in CHCl₃ (50 mL) and treated with NaBH(OAc)₃ (3.3 g, 15.0 mmol). After stirring for 2 h at rt, 2,2-dimethoxyacetaldehyde (1.5 mL, 10.0 mmol) was introduced followed by NaBH(OAc)₃ (3.30 g, 15.0 mmol). After stirring for 6 h, the mixture was quenched with a saturated aqueous solution of NaHCO₃ and the aqueous layer was extracted with EtOAc (2 x 50 mL). The combine organics were dried with MgSO₄, filtered and evaporated to give a pale green oil (2.52 g) which showed:¹⁸⁴ ¹H

NMR (500 MHz, CDCl₃) δ 2.74 (2H, d, J = 5.2 Hz, CHCH₂), 2.83 (4H, s, CH₂CH₂), 3.34 (6H, s, CH₃), 3.77 (2H, s, ArCH₂N), 4.43 (1H, t, J = 5.2 Hz, ArH), 7.15 - 7.23 (3H, m, ArH) and 7.24 - 7.37 (7H, m, ArH) ppm. ¹³C NMR (126 MHz, CDCl₃) δ 33.6 (ArCH₂CH₂), 53.9 (CH₃), 55.9 (CHCH₂N), 56.7 (CH₂CH₂N), 59.4 (ArCH₂N), 104.2 (CH(OR)₂), 126.0 (ArCH), 127.0 (ArCH), 128.3 (ArCH), 128.4 (ArCH), 129.0 (ArCH), 129.0 (ArCH), 139.7 (ArCCH₂N) and 140.7 (ArCCH₂CH₂) ppm. LC/MS (ES⁺) t_r = 1.08 min (98 %), m/z 300.2 (M⁺+H); (RP, Isocratic, 90% MeOH). HRMS (ES⁺) calcd. for C₁₉H₂₆NO₂ (M⁺+H) 300.1958, found 300.1967.

5,7,8,13-tetrahydro-6,13-methanodibenzo[c,f]azonine (158)

C₁₇H₁₇N, Mol. Wt.: 235.32

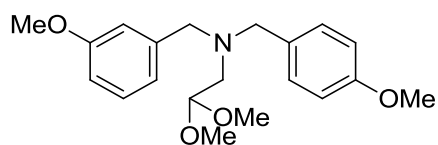


(Method B)

The crude compound was obtained as a yellow oil (856 mg, 83%) which showed: ¹H NMR (500 MHz, CDCl₃) δ 2.35 (1H, ddd, J = 1.3, 4.4, 15.7 Hz, ArCH₂CH₂N), 3.10 (1H, ddd, J = 2.2, 12.9, 15.7 Hz, ArCH₂CH₂N), 3.31 (1H, ddd, J = 2.2, 12.9, 15.0 Hz, ArCH₂CH₂N), 3.46 (1H, ddd, J = 1.3, 4.4, 15.0 Hz, ArCH₂CH₂N), 3.56 (1H, dd, J = 0.8, 13.9 Hz, NCH₂CH), 3.67 (1H, ddd, J = 1.0, 5.2, 13.9 Hz, NCH₂CH), 3.88 (1H, d, J = 5.2 Hz, CH₂CH), 4.09 (1H, dd, J = 1.5, 17.1 Hz, ArCH₂N), 4.61 (1H, d, J = 17.3 Hz, ArCH₂N), 6.96 (1H, d, J = 7.4 Hz, ArH), 7.03 (1H, d, J = 8.6 Hz, ArH), 7.06 - 7.13 (3H, m, ArH), 7.13 - 7.22 (2H, m, ArH) and 7.32 (1H, dd, J = 1.2, 7.4 Hz, ArH) ppm. ¹³C NMR (126 MHz, CDCl₃) δ 34.7 (ArCH₂CH₂N), 44.5 (CH₂CH), 52.5 (NCH₂CH), 53.6 (ArCH₂N), 56.2 (ArCH₂CH₂N), 125.1 (ArCH), 126.7 (ArCH), 126.8 (ArCH), 126.9 (ArCH), 126.9 (ArCH), 129.0 (ArCH), 130.4 (ArCH), 130.9 (ArCH), 134.6 (ArCCH₂N), 135.2 (ArCCH), 140.8 (ArCCH₂CH₂) and 145.0 (ArCCH) ppm. LC/MS (ES⁺) t_r = 0.95 min (99 %), m/z 236.0 (M⁺+H); (RP, Isocratic, 90% MeOH). HRMS (ES⁺) calcd. for C₁₇H₁₈N (M⁺+H) 236.1434, found 236.1441.

2,2-Dimethoxy-N-(3-methoxybenzyl)-N-(4-methoxybenzyl)ethanamine (159)

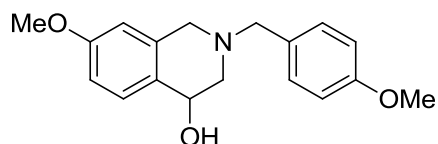
C₂₀H₂₇NO₄, Mol. Wt.: 345.43



m-Anisaldehyde (1.2 mL, 10.0 mmol) and 2,2-dimethoxyethylamine (1.1 mL, 10.0 mmol) were dissolved in CHCl₃ (50 mL) and treated with NaBH(OAc)₃ (3.3 g, 15.0 mmol). After stirring for 2 h at rt, *p*-anisaldehyde (1.2 mL, 10.0 mmol) was introduced followed by NaBH(OAc)₃ (3.30 g, 15.0 mmol). After stirring for 6 h at rt, the mixture was quenched with a saturated aqueous solution of NaHCO₃ and the aqueous layer was extracted with EtOAc (2 x 50 mL). The combined organics were dried with MgSO₄, filtered and evaporated to give a pale green oil (3.49 g). The crude compound was purified by column chromatography to give the product as a colourless oil (2.78 g, 80%) which showed: ¹H NMR (500 MHz, CDCl₃) δ 2.63 (2H, d, *J* = 5.2 Hz, CH₂CH), 3.27 (6H, s, CH(OCH₃)), 3.56 - 3.66 (4H, m, ArCH₂), 3.80 (3H, s, ArOCH₃), 3.81 (3H, s, ArOCH₃), 4.46 (1H, t, *J* = 5.2 Hz, CH(OR)₂), 6.78 (1H, dd, *J* = 2.1, 7.8 Hz, ArH), 6.85 (2H, d, *J* = 8.7 Hz, ArH), 6.95 (2H, d, *J* = 7.8 Hz, ArH), 6.97 - 6.98 (1H, m, ArH), 7.22 (1H, t, *J* = 7.8 Hz, ArH) and 7.28 (2H, d, *J* = 8.7 Hz, ArH) ppm. ¹³C NMR (126 MHz, CDCl₃) δ 53.6 CH(OCH₃)₂, 55.0 (CH₂CH), 55.3 (ArOCH₃), 55.4 (ArOCH₃), 58.5 (ArCH₂), 58.9 (ArCH₂), 104.0 (ArCH), 112.4 (ArCH), 113.7 (ArCH), 114.5 (ArCH), 121.3 (ArCH), 129.2 (ArCH), 130.2 (ArCH), 131.6 (ArCCH₂), 141.6 (ArCCH₂), 158.8 (ArCOCH₃) and 159.7 (ArCOCH₃) ppm. LC/MS (ES⁺) *t*_r = 1.03 min (96 %), *m/z* 346.3 (M⁺+H); (RP, Isocratic, 90% MeOH). HRMS (ES⁺) calcd. for C₂₀H₂₈NO₄ (M⁺+H) 346.2013, found 346.2025.

7-Methoxy-2-(4-methoxybenzyl)-1,2,3,4-tetrahydroisoquinolin-4-ol (160)

C₁₈H₂₁NO₃, Mol. Wt.: 299.36

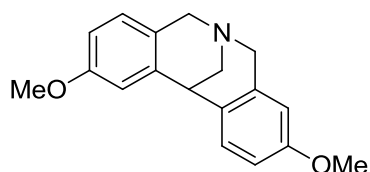


(Method C)

The crude compound was purified by column chromatography (eluent: from 0% to 100% EtOAc in pet. ether) to give the product as a yellow oil (223 mg, 34%) which showed: ^1H NMR (500 MHz, CDCl_3) δ 2.61 (1H, dd, $J = 2.6, 11.6$ Hz CHCH_2), 2.81 (1H, bs, OH), 3.05 (1H, ddd, $J = 1.2, 3.1, 11.6$ Hz, CHCH_2), 3.33 (1H, d, $J = 15.1$ Hz, ArCH_2 (THIQ)), 3.66 (2H, d, $J = 5.1$ Hz, ArCH_2 (benzylic)), 3.76 (3H, s, CH_3), 3.76 (1H, d, $J = 15.1$ Hz, ArCH_2 (THIQ)), 3.81 (3H, s, CH_3), 4.56 (1H, bs), 6.53 (1H, d, $J = 2.5$ Hz, ArH (THIQ)), 6.79 (1H, dd, $J = 2.5, 8.4$ Hz, ArH (THIQ)), 6.88 (3H, d, $J = 8.7$ Hz, ArH (benzyl)), 7.28 (2H, d, $J = 8.7$ Hz, ArH (benzyl)) and 7.32 (1H, d, $J = 8.4$ Hz, ArH (THIQ)) ppm. ^{13}C NMR (126 MHz, CDCl_3) δ 55.4 (CH_3), 55.4 (CH_3), 56.0 (ArCH_2 (THIQ)), 58.5 (CHCH_2), 62.1 (ArCH_2 (benzyl)), 66.9 (CHCH_2), 110.8 (ArCH (THIQ)), 113.3 (ArCH (THIQ)), 113.9 (ArCH (benzyl)), 129.5 (CHCH_2), 129.9 (ArCH_2 (benzyl)), 130.3 (ArCH (benzyl)), 130.7 (ArCH (THIQ)), 136.5 (ArCH_2 (THIQ)), 159.0 (CH_3) and 159.1 (CH_3) ppm. LC/MS (ES^+) $t_r = 0.88$ min (69 %), m/z 300.0 ($\text{M}^+ + \text{H}$); (RP, Isocratic, 90% MeOH). HRMS (ES^+) calcd. for $\text{C}_{18}\text{H}_{22}\text{NO}_3$ ($\text{M}^+ + \text{H}$) 300.1594, found 300.1587.

2,9-Dimethoxy-7,12-dihydro-5H-6,12-methanodibenzo[c,f]azocine (161)

$\text{C}_{18}\text{H}_{19}\text{NO}_2$, Mol. Wt.: 281.35



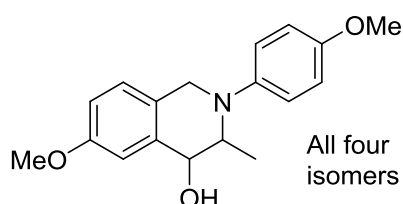
(Method B)

The crude compound was purified by column chromatography (eluent: from 0% to 30% EtOAc in pet. ether) to give the product as a brown gum (181 mg, 15%) which showed: ^1H NMR (500 MHz, CDCl_3) δ 3.35 (1H, d, $J = 7.0$ Hz, CHCH_2), 3.62 (1H, s, ArCH), 3.72 (3H, s, CH_3), 3.77 (3H, s, CH_3), 3.87 (1H, d, $J = 14.0$ Hz, ArCH_2), 3.90 (1H, d, $J = 7.0$ Hz, CHCH_2), 3.90 (1H, d, $J = 14.5$ Hz, ArCH_2), 4.52 (1H, d, $J = 14.5$ Hz, ArCH_2), 4.55 (1H, d, $J = 14.0$ Hz, ArCH_2), 6.52 (1H, d, $J = 2.6$ Hz, ArH), 6.63 (1H, dd, $J = 2.6, 8.4$ Hz, ArH), 6.66 (1H, dd, $J = 2.6, 8.4$ Hz, ArH), 6.75 (1H, d, $J = 2.6$ Hz, ArH), 6.89 (1H, d, $J = 8.4$ Hz, ArH) and 7.15 (1H, d, $J = 8.4$ Hz, ArH) ppm. ^{13}C NMR (126 MHz, CDCl_3) δ 35.9 (CHCH_2), 49.4 (CHCH_2), 55.2 (CH_3), 55.3 (CH_3),

56.9 (ArCH₂), 57.7 (ArCH₂), 110.8 (ArCH), 111.9 (ArCH), 112.4 (ArCH), 112.5 (ArCH), 126.0 (ArCCH₂), 127.1 (ArCH), 128.4 (ArCH), 132.8 (ArCCH), 135.5 (ArCCH₂), 142.1 (ArCCH), 157.8 (ArCOCH₃) and 157.9 (ArCOCH₃) ppm. LC/MS (ES⁺) t_r = 0.90 min (94 %), m/z 282.2 (M⁺+H); (RP, Isocratic, 90% MeOH). HRMS (ES⁺) calcd. for C₁₈H₂₀NO₂ (M⁺+H) 282.1489, found 282.1482.

6-Methoxy-2-(4-methoxyphenyl)-3-methyl-1,2,3,4-tetrahydroisoquinolin-4-ol (162s)

C₁₈H₂₁NO₃, Mol. Wt.: 299.36

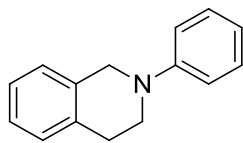


(Method B)

The crude compound was not purified and showed: HRMS (ES⁺) calcd. C₁₈H₂₂NO₃ (M⁺+H) 300.1594, found 300.1595.

2-Phenyl-1,2,3,4-tetrahydroisoquinoline (163a)

C₁₅H₁₅N, Mol. Wt.: 209.29



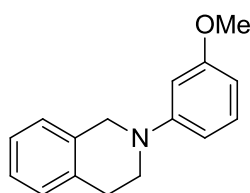
(Method D)

The crude product was purified by column chromatography (eluent: pet. ether) to yield the product as a pale yellow oil (1.72 g, 67%) which solidified upon standing and which showed:¹⁸⁵ ¹H NMR (500 MHz, CDCl₃) δ 3.00 (2H, t, *J* = 5.8 Hz, H₄-THIQ), 3.57 (2H, t, *J* = 5.8 Hz, H₃-THIQ), 4.42 (2H, s, H₁-THIQ), 6.83 (1H, t, *J* = 7.3 Hz, ArH, phenyl), 6.99 (2H, d, *J* = 8.7 Hz, ArH, phenyl), 7.14 – 7.21 (4H, m, H₅,H₆,H₇,H₈-THIQ) and 7.30 (2H, dd, *J* = 7.3, 8.7 Hz, ArH, phenyl) ppm. ¹³C NMR (126 MHz, CDCl₃) δ 29.27 (C₄-THIQ), 46.67 (C₃-THIQ), 50.89 (C₁-THIQ), 115.29 (ArCH, phenyl), 118.8

(ArCH, phenyl), 126.2 (ArCH, THIQ), 126.5 (ArCH, THIQ), 126.7 (ArCH, THIQ), 128.7 (ArCH, THIQ), 129.4 (ArCH, phenyl), 134.6 (C₁CC₈-THIQ), 135.0 (C₅CC₆-THIQ) and 150.7 (ArCN) ppm. LC/MS (ES⁺) t_r = 2.79 min (97 %), m/z 209.9 (M⁺+H); (RP, Isocratic, 90% MeOH). HRMS (ES⁺) calcd. for C₁₅H₁₆N (M⁺+H) 210.1277, found 210.1284. Mp 44-45 °C (pet. ether). Anal. calcd. for C₁₅H₁₅N: C 86.1, H 7.22, N 6.69. Found: C 85.3, H 7.11, N 6.59%.

2-(3-Methoxyphenyl)-1,2,3,4-tetrahydroisoquinoline (163b)

C₁₆H₁₇NO, Mol. Wt.: 239.31

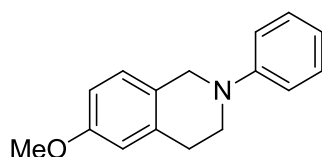


(Method D)

The crude product was purified by column chromatography (eluent 0% to 30% EtOAc in pet. ether) to yield the product as a dark yellow oil (152 mg, 11%) which showed: ¹⁸⁵ ¹H NMR (500 MHz, CDCl₃) δ 2.99 (2H, t, *J* = 5.9 Hz, ArCH₂CH₂), 3.56 (2H, t, *J* = 5.9 Hz, NCH₂CH₂), 3.82 (3H, s, ArOCH₃), 4.41 (2H, s, ArCH₂N), 6.39 (1H, dd, *J* = 2.4, 8.1 Hz, ArH), 6.52 (1H, t, *J* = 2.4 Hz, ArH), 6.60 (1H, dd, *J* = 2.4, 8.1 Hz, ArH) and 7.14 - 7.22 (5H, m, ArH) ppm. ¹³C NMR (126 MHz, CDCl₃) δ 29.3 (ArCH₂CH₂), 46.5 (NCH₂CH₂), 50.8 (ArCH₂N), 55.3 (ArOCH₃), 101.6 (ArCH), 103.4 (ArCH), 108.0 (ArCH), 126.2 (ArCH), 126.5 (ArCH), 126.7 (ArCH), 128.6 (ArCH), 130.0 (ArCH), 134.6 (ArCCH₂N), 135.1 (ArCCH₂CH₂), 152.0 (ArCN) and 160.9 (ArCOCH₃) ppm. LC/MS (ES⁺) t_r = 2.84 min (84%), m/z 240.0 (M⁺+H); (RP, Isocratic, 90% MeOH). HRMS (ES⁺) calcd. for C₁₆H₁₈NO (M⁺+H) 240.1383, found 240.1373.

6-Methoxy-2-phenyl-1,2,3,4-tetrahydroisoquinoline (163e)

C₁₆H₁₇NO, Mol. Wt.: 239.31

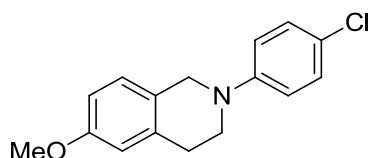


(Method D)

The crude product was purified by column chromatography (eluent: from 0% to 0.5% EtOAc in pet. ether) to yield the product as a colourless oil (1.3 g, 25%) which showed: ^1H NMR (500 MHz, CDCl_3) δ 2.96 (2H, t, $J = 5.8$ Hz, $\text{H}_4\text{-THIQ}$), 3.55 (2H, t, $J = 5.8$ Hz, $\text{H}_3\text{-THIQ}$), 3.80 (3H, s, ArOCH_3), 4.36 (2H, s, $\text{H}_1\text{-THIQ}$), 6.70 (1H, d, $J = 2.6$ Hz, $\text{H}_5\text{-THIQ}$), 6.77 (1H, dd, $J = 2.6, 8.4$ Hz, $\text{H}_7\text{-THIQ}$), 6.83 (1H, tt, $J = 1.0, 7.3$ Hz, ArH, phenyl), 6.98 (2H, dd, $J = 1.0, 8.8$ Hz, ArH, phenyl), 7.08 (1H, d, $J = 8.4$ Hz, $\text{H}_8\text{-THIQ}$) and 7.29 (2H, dd, $J = 7.3, 8.8$ Hz, ArH, phenyl) ppm. ^{13}C NMR (126 MHz, CDCl_3) δ 29.6 ($\text{C}_4\text{-THIQ}$), 46.6 ($\text{C}_3\text{-THIQ}$), 50.3 ($\text{C}_1\text{-THIQ}$), 55.4 (ArOCH_3), 112.5 ($\text{C}_7\text{-THIQ}$), 113.4 ($\text{C}_5\text{-THIQ}$), 115.3 (ArCH, phenyl), 118.8 (ArCH, phenyl), 126.8 ($\text{C}_1\text{CC}_8\text{-THIQ}$), 127.6 ($\text{C}_8\text{-THIQ}$), 129.3 (ArCH, phenyl), 136.2 ($\text{C}_5\text{CC}_6\text{-THIQ}$), 150.7 (ArCN) and 158.2 ($\text{C}_6\text{-THIQ}$) ppm. LC/MS (ES^+) $t_r = 2.48$ min (97 %), m/z 239.9 ($\text{M}^+ + \text{H}$); (RP, Isocratic, 90% MeOH). HRMS (ES^+) calcd. for $\text{C}_{16}\text{H}_{18}\text{NO}$ ($\text{M}^+ + \text{H}$) 240.1383, found 240.1372. Mp 72-73 °C (pet. ether). Anal. calcd. for $\text{C}_{16}\text{H}_{17}\text{NO}$: C 80.3, H 7.16, N 5.85. Found: C 80.2, H 7.16, N 5.73%.

2-(4-Chlorophenyl)-6-methoxy-1,2,3,4-tetrahydroisoquinoline (163i)

$\text{C}_{16}\text{H}_{16}\text{ClNO}$, Mol. Wt.: 273.76



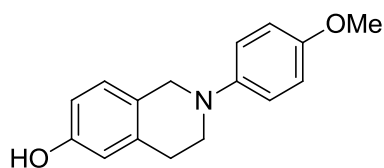
(Method D)

The crude product was purified by column chromatography (eluent: from 0% to 30% EtOAc in pet. ether) to yield the product as a white solid (1.41 g, 20%) which showed: ^{186}H NMR (500 MHz, CDCl_3) δ 2.95 (2H, t, $J = 5.8$ Hz, $\text{H}_4\text{-THIQ}$), 3.51 (2H, t, $J = 5.9$ Hz, $\text{H}_3\text{-THIQ}$), 3.80 (3H, s, ArOCH_3), 4.31 (2H, s, $\text{H}_1\text{-THIQ}$), 6.70 (1H, d, $J = 2.6$ Hz, $\text{H}_5\text{-THIQ}$), 6.77 (1H, dd, $J = 2.7, 8.4$ Hz, $\text{H}_7\text{-THIQ}$), 6.87 (2H, d, $J = 9.1$ Hz, ArH, phenyl), 7.06 (1H, d, $J = 8.4$ Hz, $\text{H}_8\text{-THIQ}$) and 7.21 (2H, d, $J = 9.1$ Hz, ArH, phenyl) ppm. ^{13}C NMR (126 MHz, CDCl_3) δ 29.4 ($\text{C}_4\text{-THIQ}$), 46.6 ($\text{C}_3\text{-THIQ}$), 50.3 ($\text{C}_1\text{-THIQ}$), 55.5 (ArOCH_3), 112.6 ($\text{C}_7\text{-THIQ}$), 113.4 ($\text{C}_5\text{-THIQ}$), 116.3 (ArCH, phenyl), 123.4 (ArCCl), 126.4 ($\text{C}_1\text{CC}_8\text{-THIQ}$), 127.6 ($\text{C}_8\text{-THIQ}$), 129.1 (ArCH, phenyl), 136.0

(C₅CC₆-THIQ), 149.3 (ArCN) and 158.3 (C₆-THIQ) ppm. LC/MS (ES⁺) t_r = 3.56 min (96 %), m/z 274.0 (M⁺+H) (³⁵Cl), 276.0 (M⁺+H) (³⁷Cl); (RP, Isocratic, 90% MeOH). HRMS (ES⁺) calcd. for C₁₆H₁₇³⁵ClNO (M⁺+H) 274.0993, found 274.0980; calcd. for C₁₆H₁₇³⁷ClNO (M⁺+H) 276.0964, found 274.0980. Mp 99-100 °C (pet. ether). Anal. calcd. for C₁₆H₁₆ClNO: C 70.2, H 5.89, N 5.12. Found: C 69.3, H 5.83, N 5.14 %.

2-(4-Methoxyphenyl)-1,2,3,4-tetrahydroisoquinolin-6-ol (163o)

C₁₆H₁₇NO₂, Mol. Wt.: 255.31

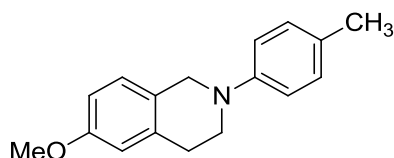


(Method D)

The crude compound was purified by reversed phase column chromatography (eluent: from 5% to 100% MeOH in water) to get the compound as a yellow oil (503 mg, 20%) which showed: ¹H NMR (500 MHz, CDCl₃) δ 2.93 (2H, t, *J* = 5.9 Hz, ArCH₂CH₂), 3.42 (2H, t, *J* = 5.9 Hz, ArCH₂CH₂), 3.78 (3H, s, ArOCH₃), 4.22 (2H, s, ArCH₂N), 6.62 (1H, d, *J* = 2.5 Hz, ArH), 6.67 (1H, dd, *J* = 2.5, 8.2 Hz, ArH), 6.86 (2H, d, *J* = 9.1 Hz, ArH), 6.97 (2H, d, *J* = 9.1 Hz, ArH) and 7.00 (1H, d, *J* = 8.2 Hz, ArH) ppm. ¹³C NMR (126 MHz, CDCl₃) δ 29.1 (ArCH₂CH₂), 48.4 (NCH₂CH₂), 52.2 (ArCH₂N), 55.6 (ArOCH₃), 113.4 (ArCH), 114.6 (ArCH), 114.9 (ArCH), 118.1 (ArCH), 126.7 (ArCCH₂N), 127.6 (ArCH), 131.0 (Ar CCH₂CH₂), 145.5 (ArCN), 153.5 (ArCOCH₃) and 154.0 (ArCOH) ppm. LC/MS (ES⁺) t_r = 1.17 min (96%), m/z 255.7 (M⁺+H); (RP, Isocratic, 90% MeOH). HRMS (ES⁺) calcd. for C₁₆H₁₈NO₂ (M⁺+H) 256.1332, found 256.1336. Mp 192-194 °C (Hydrochloride from MeOH/Et₂O). Anal. calcd. for C₁₆H₁₈ClNO₂: C 65.9, H 6.22, N 4.80% found C 64.4, H 6.09, N 4.57%.

6-Methoxy-2-(*p*-tolyl)-1,2,3,4-tetrahydroisoquinoline (163q)

C₁₇H₁₉NO, Mol. Wt.: 253.34

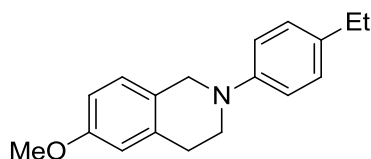


(Method D)

The crude product was purified by column chromatography (eluent: from 0% to 10% EtOAc in pet. ether) to yield the product as a white solid (1.65 g, 25%) which showed: ^1H NMR (500 MHz, CDCl_3) δ 2.28 (3H, s, ArCH_3), 2.95 (2H, t, $J = 5.8$ Hz, $\text{H}_4\text{-THIQ}$), 3.49 (2H, t, $J = 5.8$ Hz, $\text{H}_3\text{-THIQ}$), 3.79 (3H, s, ArOCH_3), 4.30 (2H, s, $\text{H}_1\text{-THIQ}$), 6.69 (1H, d, $J = 2.6$ Hz, $\text{H}_5\text{-THIQ}$), 6.76 (1H, dd, $J = 2.6, 8.4$ Hz, $\text{H}_7\text{-THIQ}$), 6.91 (2H, d, $J = 8.6$ Hz, ArH, phenyl), 7.06 (1H, d, $J = 8.4$ Hz, $\text{H}_8\text{-THIQ}$) and 7.09 (2H, d, $J = 8.6$ Hz, ArH, phenyl) ppm. ^{13}C NMR (126 MHz, CDCl_3) δ 20.5 (ArCH_3), 29.5 ($\text{C}_4\text{-THIQ}$), 47.4 ($\text{C}_3\text{-THIQ}$), 51.1 ($\text{C}_1\text{-THIQ}$), 55.4 (ArOCH_3), 112.5 ($\text{C}_7\text{-THIQ}$), 113.4 ($\text{C}_5\text{-THIQ}$), 116.0 (ArCH, phenyl), 126.9 ($\text{C}_1\text{CC}_8\text{-THIQ}$), 127.6 ($\text{C}_8\text{-THIQ}$), 128.5 (ArCCH_3), 129.8 (ArCH, phenyl), 136.1 ($\text{C}_5\text{CC}_6\text{-THIQ}$), 148.8 (ArCN) and 158.2 ($\text{C}_6\text{-THIQ}$) ppm. LC/MS (ES^+) $t_r = 2.62$ min (97 %), m/z 254.0 ($\text{M}^+ + \text{H}$); (RP, Isocratic, 90% MeOH). HRMS (ES^+) calcd. for $\text{C}_{17}\text{H}_{20}\text{NO}$ ($\text{M}^+ + \text{H}$) 254.1539, found 254.1535. Mp 69-70 °C (pet. ether). Anal. calcd. for $\text{C}_{17}\text{H}_{19}\text{NO}$: C 80.6, H 7.56, N 5.53. Found: C 80.4, H 7.55, N 5.44 %.

2-(4-Ethylphenyl)-6-methoxy-1,2,3,4-tetrahydroisoquinoline (163r)

$\text{C}_{18}\text{H}_{21}\text{NO}$, Mol. Wt.: 267.36



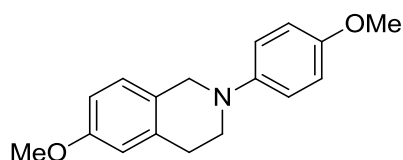
(Method D)

The crude compound was purified by column chromatography (eluent: from 0% to 20% EtOAc in pet. ether) to get the product as a yellow solid (409 mg, 51%) which was recrystallised from pet. ether and showed: ^1H NMR (500 MHz, CDCl_3) δ 1.22 (3H, t, $J = 7.6$ Hz, CH_2CH_3), 2.59 (2H, q, $J = 7.6$ Hz, CH_2CH_3), 2.97 (2H, t, $J = 5.8$ Hz, $\text{H}_4\text{-THIQ}$), 3.51 (2H, t, $J = 5.8$ Hz, $\text{H}_3\text{-THIQ}$), 3.80 (3H, s, OCH_3), 4.32 (2H, s, $\text{H}_1\text{-THIQ}$), 6.70 (1H, d, $J = 2.5$ Hz, $\text{H}_5\text{-THIQ}$), 6.77 (1H, dd, $J = 2.5, 8.4$ Hz, $\text{H}_7\text{-THIQ}$),

6.96 (2H, d, $J = 8.3$ Hz, 2 x ArCH, phenyl), 7.07 (1H, d, $J = 8.4$ Hz, H₈-THIQ) and 7.13 (2H, d, $J = 8.6$ Hz, 2 x ArCH, phenyl) ppm. ^{13}C NMR (126 MHz, CDCl_3) δ 15.8 (CH_2CH_3), 27.9 (CH_2CH_3), 29.3 (C₄-THIQ), 47.2 (C₃-THIQ), 50.9 (C₁-THIQ), 55.3 (OCH_3), 112.3 (C₇-THIQ), 113.2 (C₅-THIQ), 115.8 (2 x ArCH, phenyl), 126.6 (C₁CC₈-THIQ), 127.5 (C₈-THIQ), 128.5 (2 x ArCH, phenyl), 135.0 ($\text{ArCCH}_2\text{CH}_3$), 135.8 (C₄CC₅-THIQ), 148.6 (ArCN), 158.0 (C₆-THIQ) ppm. HRMS (ES^+) calcd. $\text{C}_{18}\text{H}_{22}\text{NO}$ ($\text{M}^+ + \text{H}$) 268.1696, found 268.1694. Mp 78-80 °C (pet. ether). Anal. calcd. for $\text{C}_{18}\text{H}_{21}\text{NO}$: C 80.86, H 7.92, N 5.24 %. Found: C 80.91, H 8.00, N 5.14 %.

6-Methoxy-2-(4-methoxyphenyl)-1,2,3,4-tetrahydroisoquinoline (163s)

$\text{C}_{17}\text{H}_{19}\text{NO}_2$, Mol. Wt.: 269.34

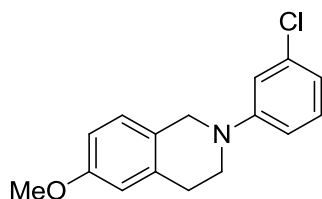


(Method D)

The crude product was purified by column chromatography (eluent: from 0% to 15% EtOAc in pet. ether) to yield the product as a white solid (1.395 g, 21%) which showed: ^{187}H NMR (500 MHz, CDCl_3) δ 2.96 (2H, t, $J = 5.8$ Hz, H₄-THIQ), 3.43 (2H, t, $J = 5.8$ Hz, H₃-THIQ), 3.78 (3H, s, ArOCH_3), 3.79 (3H, s, ArOCH_3), 4.24 (2H, s, H₁-THIQ), 6.68 (1H, d, $J = 2.6$ Hz, H₅-THIQ), 6.75 (1H, dd, $J = 2.6, 8.4$ Hz, H₇-THIQ), 6.86 (2H, d, $J = 9.1$ Hz, ArH, phenyl), 6.97 (2H, d, $J = 9.1$ Hz, ArH, phenyl) and 7.04 (1H, d, $J = 8.4$ Hz, H₈-THIQ) ppm. ^{13}C NMR (126 MHz, CDCl_3) δ 29.5 (C₄-THIQ), 48.5 (C₃-THIQ), 52.3 (C₁-THIQ), 55.4 (ArOCH_3), 55.8 (ArOCH_3), 112.5 (C₇-THIQ), 113.4 (C₅-THIQ), 114.7 (ArCH, phenyl), 118.2 (ArCH, phenyl), 127.0 (C₁CC₈-THIQ), 127.6 (C₈-THIQ), 135.9 (C₅CC₆-THIQ), 145.6 (ArCN), 153.6 (ArCO, phenyl) and 158.2 (C₆-THIQ) ppm. LC/MS (ES^+) $t_r = 1.47$ min (90 %), m/z 270.0 ($\text{M}^+ + \text{H}$); (RP, Isocratic, 90% MeOH). HRMS (ES^+) calcd. for $\text{C}_{17}\text{H}_{20}\text{NO}_2$ ($\text{M}^+ + \text{H}$) 270.1489, found 270.1477. Mp 124-125 °C (pet. ether). Anal. calcd. for $\text{C}_{17}\text{H}_{19}\text{NO}$: C 75.81, H 7.11, N 5.20. Found: C 75.5, H 7.16, N 5.10 %.

2-(3-Chlorophenyl)-6-methoxy-1,2,3,4-tetrahydroisoquinoline (163t)

C₁₆H₁₆ClNO, Mol. Wt.: 273.76

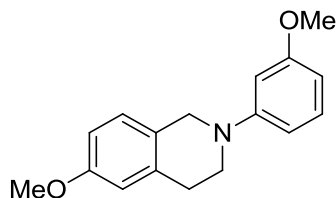


(Method D)

The crude compound was purified by column chromatography (eluent: from 0% to 20% EtOAc in pet. ether) to get the product as a colourless oil (247 mg, 52%) which showed: ¹H NMR (500 MHz, CDCl₃) δ 2.95 (1H, t, *J* = 5.8 Hz, H₄-THIQ), 3.54 (1H, t, *J* = 5.8 Hz, H₃-THIQ), 3.80 (1H, s, OCH₃), 4.35 (1H, s, H₁-THIQ), 6.71 (1H, d, *J* = 2.5 Hz, H₅-THIQ), 6.76 (1H, ddd, *J* = 0.9, 2.2, 8.1 Hz, ArH, phenyl), 6.77 (1H, dd, *J* = 2.5, 8.4 Hz, H₇-THIQ), 6.81 (1H, ddd, *J* = 0.9, 2.2, 8.1 Hz, ArH, phenyl), 6.90 (1H, t, *J* = 2.2 Hz, ArH, phenyl), 7.08 (1H, d, *J* = 8.4 Hz, H₈-THIQ) and 7.17 (1H, t, *J* = 8.1 Hz, ArH, phenyl) ppm. ¹³C NMR (126 MHz, CDCl₃) δ 29.4 (C₄-THIQ), 46.0 (C₃-THIQ), 49.7 (C₁-THIQ), 55.5 (OCH₃), 112.6 (C₇-THIQ), 112.7 (ArCH, phenyl), 113.3 (C₅-THIQ), 114.5 (ArCH, phenyl), 118.1 (ArCH, phenyl), 126.3 (C₁CC₈-THIQ), 127.6 (C₈-THIQ), 130.2 (ArCH, phenyl), 135.2 (ArCCl), 136.1 (C₅CC₆-THIQ), 151.5 (ArCN) and 158.4 (C₆-THIQ). LC/MS (ES⁺) *t*_r = 3.84 min (95 %), *m/z* 273.9 (M⁺+H); (RP, Isocratic, 90% MeOH). HRMS (ES⁺) calcd. C₁₆H₁₇³⁵ClNO (M⁺+H) 274.0993, found 274.0981; calcd. C₁₆H₁₇³⁷ClNO (M⁺+H) 276.0964, found 276.0974. Mp 112-114 °C (as hydrochloride from Et₂O).

6-Methoxy-2-(3-methoxyphenyl)-1,2,3,4-tetrahydroisoquinoline (163u)

C₁₇H₁₉NO₂, Mol. Wt.: 269.34



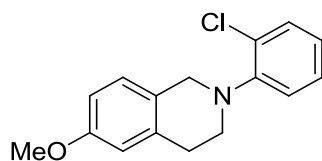
(Method D)

The crude compound was purified by column chromatography (eluent: from 0% to 20% EtOAc in pet. ether) to get the compound as a yellow oil (761 mg, 44%) which

showed: ^1H NMR (500 MHz, CDCl_3) δ 2.95 (2H, t, $J = 5.9$ Hz, $\text{H}_4\text{-THIQ}$), 3.54 (2H, t, $J = 5.9$ Hz, $\text{H}_3\text{-THIQ}$), 3.80 (3H, s, ArOCH_3 , THIQ), 3.81 (3H, s, ArOCH_3 , phenyl), 4.35 (2H, s, $\text{H}_1\text{-THIQ}$), 6.39 (1H, ddd, $J = 0.9, 2.5, 8.4$ Hz, ArH, phenyl), 6.50 (1H, t, $J = 2.5$ Hz, ArH, phenyl), 6.59 (1H, ddd, $J = 0.9, 2.5, 8.4$ Hz, ArH, phenyl), 6.70 (1H, d, $J = 2.6$ Hz, $\text{H}_5\text{-THIQ}$), 6.76 (1H, dd, $J = 2.7, 8.4$ Hz, $\text{H}_7\text{-THIQ}$), 7.07 (1H, d, $J = 8.4$ Hz, $\text{H}_8\text{-THIQ}$) and 7.19 (1H, t, $J = 8.4$ Hz, ArH, phenyl) ppm. ^{13}C NMR (126 MHz, CDCl_3) δ 29.5 ($\text{C}_4\text{-THIQ}$), 46.4 ($\text{C}_3\text{-THIQ}$), 50.2 ($\text{C}_1\text{-THIQ}$), 55.3 (OCH_3 , phenyl), 55.4 (OCH_3 , THIQ), 101.6 (ArCH, phenyl), 103.4 (ArCH, phenyl), 108.0 (ArCH, phenyl), 112.5 ($\text{C}_7\text{-THIQ}$), 113.3 ($\text{C}_5\text{-THIQ}$), 126.7 ($\text{C}_1\text{CC}_8\text{-THIQ}$), 127.6 ($\text{C}_8\text{-THIQ}$), 130.0 (ArCH, phenyl), 136.2 ($\text{C}_4\text{CC}_5\text{-THIQ}$), 152.0 (ArCN), 158.2 ($\text{C}_6\text{-THIQ}$) and 160.8 (ArCO, phenyl) ppm. HRMS (ES^+) calcd. $\text{C}_{17}\text{H}_{20}\text{NO}_2$ ($\text{M}^+ + \text{H}$) 270.1489, found 270.1479. Mp 119-120 $^\circ\text{C}$ (pet. ether).

2-(2-Chlorophenyl)-6-methoxy-1,2,3,4-tetrahydroisoquinoline (163v)

$\text{C}_{16}\text{H}_{16}\text{ClNO}$, Mol. Wt.: 273.76



(Method J)

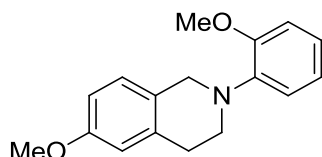
The crude compound was purified by column chromatography (eluent: from 0% to 10% EtOAc in pet. ether) to give a colourless oil (600 mg, 57%) which was crystallised as hydrochloride from Et_2O and showed (^1H and ^{13}C NMR data refer to the free base):

^1H NMR (500 MHz, CDCl_3) δ 3.00 (2H, t, $J = 5.8$ Hz, $\text{H}_4\text{-THIQ}$), 3.38 (2H, t, $J = 5.8$ Hz, $\text{H}_3\text{-THIQ}$), 3.80 (3H, s, OCH_3), 4.22 (2H, s, $\text{H}_1\text{-THIQ}$), 6.71 (1H, d, $J = 2.6$ Hz, $\text{H}_5\text{-THIQ}$), 6.75 (1H, dd, $J = 2.6, 8.4$ Hz, $\text{H}_7\text{-THIQ}$), 6.98 (1H, ddd, $J = 1.5, 7.4, 7.8$ Hz, ArH, phenyl), 7.02 (1H, d, $J = 8.4$ Hz, $\text{H}_8\text{-THIQ}$), 7.12 (1H, dd, $J = 1.5, 8.0$ Hz, ArH, phenyl), 7.22 (1H, ddd, $J = 1.5, 7.4, 8.0$ Hz, ArH, phenyl) and 7.39 (1H, dd, $J = 1.5, 7.8$ Hz, ArH, phenyl) ppm. ^{13}C NMR (126 MHz, CDCl_3) δ 29.4 ($\text{C}_4\text{-THIQ}$), 49.8 ($\text{C}_3\text{-THIQ}$), 52.7 ($\text{C}_2\text{-THIQ}$), 55.3 (CH_3O), 112.2 ($\text{C}_7\text{-THIQ}$), 113.5 ($\text{C}_5\text{-THIQ}$), 120.6, 123.5, 126.9 ($\text{C}_1\text{CC}_8\text{-THIQ}$), 127.3, 127.5, 128.8 (ArCCl), 130.7, 135.7 ($\text{C}_4\text{CC}_5\text{-THIQ}$), 149.1 (ArCN), 158.1 ($\text{C}_6\text{-THIQ}$) ppm. HRMS (ES^+) calc. for $\text{C}_{16}\text{H}_{17}^{35}\text{ClNO}$ ($\text{M}^+ + \text{H}$)

274.0993, found 274.0980; Calc. for $C_{16}H_{17}^{37}ClNO$ ($M^+ + H$) 276.0964, found 276.0974.
Mp 59-61 °C (pet. ether).

6-Methoxy-2-(2-methoxyphenyl)-1,2,3,4-tetrahydroisoquinoline (163w)

$C_{17}H_{19}NO_2$, Mol. Wt.: 269.34

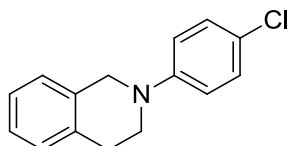


(Method D)

The crude compound was purified by column chromatography (eluent: from 0% to 20% EtOAc in pet. ether) to get the product as a colourless oil (143 mg, 38%) which showed: 1H NMR (500 MHz, $CDCl_3$) δ 2.95 (2H, t, J = 5.8 Hz, H_4 -THIQ), 3.39 (2H, t, J = 5.9 Hz, H_3 -THIQ), 3.79 (3H, s, H_1 -THIQ), 3.89 (3H, s, OCH_3), 4.23 (2H, s, OCH_3), 6.67 (1H, d, J = 2.3 Hz, H_5 -THIQ), 6.74 (1H, dd, J = 2.6, 8.4 Hz, H_7 -THIQ), 6.88 – 6.94 (2H, m, 2 x ArH, phenyl) and 6.98 – 7.05 (3H, m, H_8 -THIQ and 2 x ArH, phenyl) ppm. ^{13}C NMR (126 MHz, $CDCl_3$) δ 29.1 (C_4 -THIQ), 48.8 (C_3 -THIQ), 52.5 (C_1 -THIQ), 55.2 (CH_3O -), 55.4 (CH_3O -), 111.2 (ArCH, phenyl), 112.1 (C_7 -THIQ), 113.4 (C_5 -THIQ), 118.9 (ArCH, phenyl), 120.9 (ArCH, phenyl), 122.9 (ArCH, phenyl), 127.3 (C_6 -THIQ), 127.4 (C_1CC_8 -THIQ), 135.7 (C_4CC_5 -THIQ), 141.1 (ArCN), 152.5 ($COCH_3$) and 157.9 ($COCH_3$) ppm. HRMS (ES^+) calcd. $C_{17}H_{20}NO_2$ ($M^+ + H$) 270.1489, found 270.1499. Mp 199-200 °C (as hydrochloride from Et_2O).

2-(4-Chlorophenyl)-1,2,3,4-tetrahydroisoquinoline (163z)

$C_{15}H_{14}ClN$, Mol. Wt.: 243.73

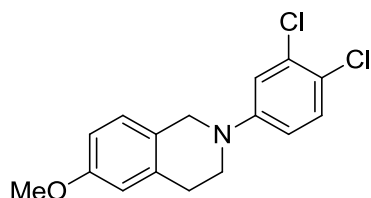


The crude compound was purified by column chromatography (eluent: from 0% to 20% EtOAc in pet. ether) to get the product as a white solid which was recrystallised from pet. ether (1.14 g, 76%) and showed: ^{188}H NMR (500 MHz, $CDCl_3$) δ 2.98 (2H, t,

$J = 5.9$ Hz, H₄-THIQ), 3.53 (2H, t, $J = 5.9$ Hz, H₃-THIQ), 4.38 (2H, s, H₁-THIQ), 6.89 (2H, d, $J = 9.1$ Hz, ArH, phenyl), 7.12 – 7.21 (4H, m, H₅,H₆,H₇,H₈ -THIQ) and 7.22 (2H, d, $J = 9.1$ Hz, ArH, phenyl) ppm. ¹³C NMR (126 MHz, CDCl₃) δ 29.1 (C₄-THIQ), 46.7 (C₃-THIQ), 50.8 (C₁-THIQ), 116.3 (ArCH, phenyl), 123.5, 126.3 (C₈-THIQ), 126.6 (ArCH-THIQ), 126.7 (ArCH-THIQ), 128.7 (C₅-THIQ), 129.2 (ArCH, phenyl), 134.2 (C₁CC₈-THIQ), 134.8 (C₄CC₅-THIQ) and 149.2 (ArCN) ppm. HRMS (ES⁺) calcd. C₁₅H₁₅³⁵ClN (M⁺+H) 244.0888, found 244.0896; calcd. C₁₅H₁₅³⁷ClN (M⁺+H) 246.0858, found 246.0866.

2-(3,4-Dichlorophenyl)-6-methoxy-1,2,3,4-tetrahydroisoquinoline (163aa)

C₁₆H₁₅Cl₂NO, Mol. Wt.: 308.20

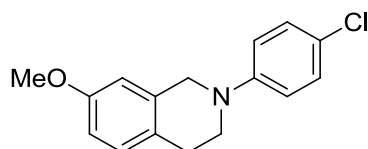


(Method J)

The crude compound was purified by column chromatography (eluent: from 0% to 20% EtOAc in pet. ether) to give yellow solid (631 mg, 55%) which showed: ¹H NMR (500 MHz, CDCl₃) δ 2.94 (2H, t, $J = 5.9$ Hz, H₄-THIQ), 3.51 (2H, t, $J = 5.9$ Hz, H₃-THIQ), 3.80 (3H, s, OCH₃), 4.32 (2H, s, H₁-THIQ), 6.70 (1H, d, $J = 2.5$ Hz), 6.75 (1H, dd, $J = 2.9, 8.9$ Hz), 6.77 (1H, dd, $J = 2.3, 8.1$ Hz), 6.97 (1H, d, $J = 2.9$ Hz), 7.07 (1H, d, $J = 8.4$ Hz) and 7.27 (1H, d, $J = 8.9$ Hz) ppm. ¹³C NMR (126 MHz, CDCl₃) δ 29.1, 45.8, 49.5, 55.3, 112.5, 113.2, 113.9, 115.7, 120.6, 125.8, 127.5, 130.4, 132.8, 135.8 and 158.3 ppm. HRMS (ES⁺) calc. for C₁₆H₁₇³⁵Cl₂NO (M⁺+H) 306.0447, found 306.0406. Calc. for C₁₆H₁₇³⁷Cl₂NO (M⁺+H) 310.0388, found 310.0394. Calc. for C₁₆H₁₇³⁵Cl³⁷ClNO (M⁺+H) 308.0417, found 308.0390. Mp 81-82 °C (pet. ether). Anal. calcd. for C₁₆H₁₅Cl₂NO: C 62.35, H 4.91, N 4.54%. Found: C 62.18, H 4.83, N 4.42%.

2-(4-Chlorophenyl)-7-methoxy-1,2,3,4-tetrahydroisoquinoline (164j)

C₁₆H₁₆ClNO, Mol. Wt.: 273.76

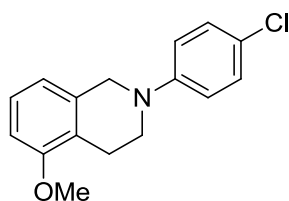


(Method E)

The crude compound was purified by column chromatography (eluent: from 0% to 30% EtOAc in pet. ether) to get the product as a white solid (1.1 g, 51%) which was recrystallised from pet. ether and showed: ^1H NMR (500 MHz, CDCl_3) δ 2.90 (2H, t, J = 5.9 Hz, $\text{H}_4\text{-THIQ}$), 3.52 (2H, t, J = 5.9 Hz, $\text{H}_3\text{-THIQ}$), 3.80 (3H, s, OCH_3), 4.35 (2H, s, $\text{H}_1\text{-THIQ}$), 6.70 (1H, d, J = 2.6 Hz, $\text{H}_8\text{-THIQ}$), 6.76 (1H, dd, J = 2.6, 8.4 Hz, $\text{H}_7\text{-THIQ}$), 6.88 (2H, d, J = 9.1 Hz, ArH, phenyl), 7.07 (1H, d, J = 8.4 Hz, $\text{H}_5\text{-THIQ}$) and 7.22 (2H, d, J = 9.1 Hz, ArH, phenyl) ppm. ^{13}C NMR (126 MHz, CDCl_3) δ 28.1 ($\text{C}_4\text{-THIQ}$), 47.0 ($\text{C}_3\text{-THIQ}$), 51.0 ($\text{C}_1\text{-THIQ}$), 55.5 (OCH_3), 111.4 ($\text{C}_8\text{-THIQ}$), 112.8 ($\text{C}_6\text{-THIQ}$), 116.4 (ArCH, phenyl), 123.5 (ArCCl), 126.9 ($\text{C}_5\text{CC}_6\text{-THIQ}$), 129.1 (ArCH, phenyl), 129.6 ($\text{C}_5\text{-THIQ}$), 135.2 ($\text{C}_1\text{CC}_8\text{-THIQ}$), 149.2 (ArCN) and 158.1 ($\text{C}_7\text{-THIQ}$) ppm. LC/MS (ES^+) t_r = 3.49 min (99 %), m/z 273.9 ($\text{M}^+\text{+H}$); (RP, Isocratic, 90% MeOH). HRMS (ES^+) calcd. $\text{C}_{16}\text{H}_{17}^{35}\text{ClNO}$ ($\text{M}^+\text{+H}$) 274.0993, found 274.0987; calcd. $\text{C}_{16}\text{H}_{17}^{37}\text{ClNO}$ ($\text{M}^+\text{+H}$) 276.0964, found 276.0987. Mp 79-80 °C (pet. ether).

2-(4-Chlorophenyl)-5-methoxy-1,2,3,4-tetrahydroisoquinoline (165j)

$\text{C}_{16}\text{H}_{16}\text{ClNO}$, Mol. Wt.: 273.76



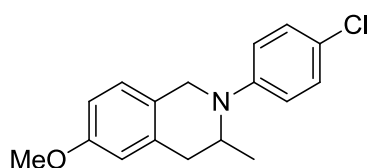
(Method E)

The crude compound was purified by column chromatography (eluent: from 0% to 30% EtOAc in pet. ether) to get the product as a white solid (230 mg, 11%) which was recrystallised from pet. ether and showed: ^1H NMR (500 MHz, CDCl_3) δ 2.87 (2H, t, J = 6.0 Hz, $\text{H}_4\text{-THIQ}$), 3.52 (2H, t, J = 6.0 Hz, $\text{H}_3\text{-THIQ}$), 3.83 (3H, s, OCH_3), 4.35 (2H, s, $\text{H}_1\text{-THIQ}$), 6.72 (1H, d, J = 8.1 Hz, $\text{H}_6\text{-THIQ}$), 6.77 (1H, d, J = 7.7 Hz, $\text{H}_8\text{-THIQ}$), 6.91 (2H, d, J = 9.0 Hz, ArH, phenyl), 7.17 (1H, t, J = 8.0 Hz, $\text{H}_7\text{-THIQ}$) and 7.21 (2H,

d, $J = 9.0$ Hz, ArH, phenyl) ppm. ^{13}C NMR (126 MHz, CDCl_3) δ 23.0 (C_4 -THIQ), 46.8 (C_3 -THIQ), 51.0 (C_1 -THIQ), 55.5 (OCH_3), 107.8 (C_6 -THIQ), 116.8 (ArCH, phenyl), 118.8 (C_8 -THIQ), 123.6 (C_5CC_6 -THIQ), 123.7 (ArCCl), 126.8 (C_7 -THIQ), 129.1 (ArCH, phenyl), 135.5 (C_1CC_8 -THIQ), 149.4 (ArCN) and 157.2 (C_5 -THIQ) ppm. HRMS (ES^+) calcd. $\text{C}_{16}\text{H}_{17}^{35}\text{ClNO}$ ($\text{M}^+\text{+H}$) 274.0993, found 274.1015; Mp 75-78 °C (pet. ether).

2-(4-Chlorophenyl)-6-methoxy-3-methyl-1,2,3,4-tetrahydroisoquinoline (166i)

$\text{C}_{17}\text{H}_{18}\text{ClNO}$, Mol. Wt.: 287.78

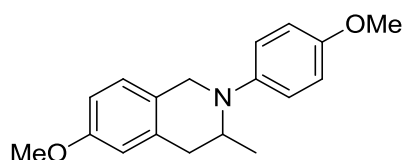


(method E)

The crude compound was purified by column chromatography (eluent: from 0% to 20% EtOAc in pet. ether) to give the product as a white solid (120 mg, 28%) which showed: ^1H NMR (500 MHz, CDCl_3) δ 1.04 (3H, d, $J = 6.6$ Hz, CHCH_3), 2.66 (1H, dd, $J = 2.0, 15.6$ Hz, H_4 -THIQ), 3.23 (1H, dd, $J = 5.4, 15.6$ Hz, H_4 -THIQ), 3.81 (3H, s, OCH_3), 4.17 (1H, d, $J = 15.0$ Hz, H_1 -THIQ), 4.24 – 4.32 (1H, m, H_3 -THIQ), 4.35 (1H, d, $J = 15.0$ Hz, H_1 -THIQ), 6.72 (1H, d, $J = 2.6$ Hz, H_5 -THIQ), 6.79 (1H, dd, $J = 2.6, 8.4$ Hz, H_7 -THIQ), 6.85 (2H, d, $J = 9.0$ Hz, 2 x ArCH, phenyl), 7.09 (1H, d, $J = 8.4$ Hz, H_8 -THIQ) and 7.23 (2H, d, $J = 9.0$ Hz, 2 x ArCH, phenyl) ppm. ^{13}C NMR (126 MHz, CDCl_3) δ 15.5 (CHCH_3), 35.7 (C_4 -THIQ), 45.7 (C_1 -THIQ), 48.8 (C_3 -THIQ), 55.2 (OCH_3), 112.2 (C_7 -THIQ), 113.8 (C_5 -THIQ), 115.4 (2 x ArCH, phenyl), 122.4 (ArCCl), 125.3 (C_1CC_8 -THIQ), 127.3 (C_8 -THIQ), 129.0 (2 x ArCH, phenyl), 134.3 (C_4CC_5 -THIQ), 147.9 (ArCN) and 158.3 (C_6 -THIQ) ppm. HRMS (ES^+) calcd. $\text{C}_{17}\text{H}_{19}^{35}\text{ClNO}$ ($\text{M}^+\text{+H}$) 288.1150, found 288.1156. Mp 86-90 °C (pet. ether).

6-Methoxy-2-(4-methoxyphenyl)-3-methyl-1,2,3,4-tetrahydroisoquinoline (166s)

$\text{C}_{18}\text{H}_{21}\text{NO}_2$, Mol. Wt.: 283.36

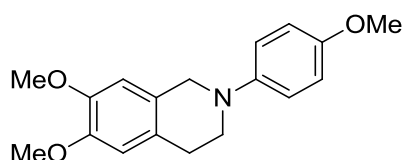


(Method E)

The crude compound was purified by column chromatography (eluent: from 0% to 20% EtOAc in pet. ether) to give the product as a yellow solid (170 mg, 6%, yield of the last two steps) which showed: ^1H NMR (500 MHz, CDCl_3) δ 1.02 (3H, d, $J = 6.6$ Hz, CHCH_3), 2.63 (1H, dd, $J = 3.0, 15.9$ Hz, $\text{H}_4\text{-THIQ}$), 3.21 (1H, dd, $J = 5.3, 15.9$ Hz, $\text{H}_4\text{-THIQ}$), 3.78 (3H, s, OCH_3 , phenyl), 3.80 (3H, s, $\text{C}_6\text{OCH}_3\text{-THIQ}$), 4.04 – 4.13 (1H, m, $\text{H}_3\text{-THIQ}$), 4.16 (1H, d, $J = 15.1$ Hz, $\text{H}_1\text{-THIQ}$), 4.26 (1H, d, $J = 15.1$ Hz, $\text{H}_1\text{-THIQ}$), 6.68 (1H, d, $J = 2.4$ Hz, $\text{H}_5\text{-THIQ}$), 6.76 (1H, dd, $J = 2.6, 8.3$ Hz, $\text{H}_7\text{-THIQ}$), 6.86 (2H, d, $J = 9.1$ Hz, 2 x ArCH, phenyl), 6.95 (2H, d, $J = 9.1$ Hz, 2 x ArCH, phenyl) and 7.06 (1H, d, $J = 8.4$ Hz, $\text{H}_8\text{-THIQ}$) ppm. ^{13}C NMR (126 MHz, CDCl_3) δ 15.3 (CHCH_3), 35.8 ($\text{C}_4\text{-THIQ}$), 47.2 ($\text{C}_1\text{-THIQ}$), 50.6 ($\text{C}_3\text{-THIQ}$), 55.2 (OCH_3), 55.6 (OCH_3), 112.1 ($\text{C}_6\text{-THIQ}$), 113.8 ($\text{C}_5\text{-THIQ}$), 114.5 (2 x ArCH, phenyl), 118.2 (2 x ArCH, phenyl), 126.1 ($\text{C}_1\text{CC}_8\text{-THIQ}$), 127.2 ($\text{H}_8\text{-THIQ}$), 134.6 ($\text{C}_4\text{CC}_5\text{-THIQ}$), 144.1 (ArCN), 153.1 (ArCO, phenyl) and 158.1 ($\text{C}_6\text{-THIQ}$) ppm. HRMS (ES^+) calcd. $\text{C}_{18}\text{H}_{22}\text{NO}_2$ ($\text{M}^+ + \text{H}$) 284.1645, found 284.1647; calcd. $\text{C}_{18}\text{H}_{21}\text{NNaO}_2$ ($\text{M}^+ + \text{Na}$) 306.1465, found 306.1470. Mp 108-110 $^\circ\text{C}$ (pet. ether). Anal. calcd. for $\text{C}_{18}\text{H}_{21}\text{NO}_2$: C 76.30, H 7.47, N 4.94. Found: C 76.25, H 7.36, N 4.85%.

6,7-Dimethoxy-2-(4-methoxyphenyl)-1,2,3,4-tetrahydroisoquinoline (167x)

$\text{C}_{18}\text{H}_{21}\text{NO}_3$, Mol. Wt.: 299.36



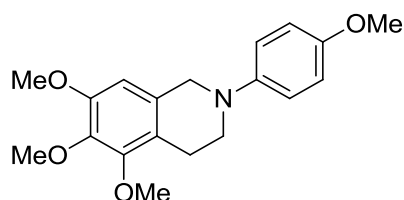
(Method E)

The crude compound was purified by column chromatography (eluent: from 0% to 60% EtOAc in pet. ether) to give the product as a yellow solid (698 mg, 29%) which showed:¹⁸⁹ ^1H NMR (500 MHz, CDCl_3) δ 2.89 (2H, t, $J = 5.7$ Hz, $\text{H}_4\text{-THIQ}$), 3.43 (2H, t, $J = 5.7$ Hz, $\text{H}_3\text{-THIQ}$), 3.78 (3H, s, OCH_3 , phenyl), 3.86 (3H, s, $\text{OCH}_3\text{-THIQ}$), 3.87

(3H, s, OCH₃-THIQ), 4.22 (2H, s, H₁-THIQ), 6.62 (1H, s), 6.63 (1H, s), 6.86 (2H, d, *J* = 9.0 Hz, 2 x ArCH, phenyl) and 6.98 (2H, d, *J* = 9.0 Hz, 2 x ArCH, phenyl) ppm. ¹³C NMR (126 MHz, CDCl₃) δ 28.5 (C₄-THIQ), 48.6 (C₃-THIQ), 52.4 (C₁-THIQ), 55.6 (OCH₃, phenyl), 55.9 (OCH₃-THIQ), 56.0 (OCH₃-THIQ), 109.3 (C_y-THIQ), 111.4 (C_y-THIQ), 114.5 (2 x ArCH, phenyl), 118.1 (2 x ArCH, phenyl), 126.3 (C₁CC₈-THIQ), 126.4 (C₄CC₅-THIQ), 145.3 (ArCN), 147.4 (C-THIQ), 147.6 (C-THIQ) and 153.5 (ArCO, phenyl) ppm. HRMS (ES⁺) calcd. C₁₈H₂₂NO₃ (M⁺+H) 300.1594, found 300.1581. Mp 138-140 °C (DCM/Et₂O).

5,6,7-Trimethoxy-2-(4-methoxyphenyl)-1,2,3,4-tetrahydroisoquinoline (168y)

C₁₉H₂₃NO₄, Mol. Wt.: 329.39

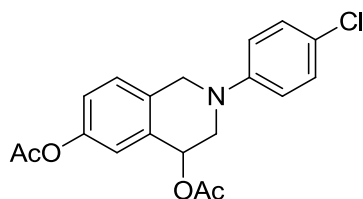


(Method E)

The crude compound was purified by column chromatography (eluent: from 0% to 70% EtOAc in pet. ether) to give the product as a white solid (1.13 g, 49%) which showed: ¹H NMR (500 MHz, CDCl₃) δ 2.86 (2H, t, *J* = 5.9 Hz, H₄-THIQ), 3.39 (2H, t, *J* = 5.9 Hz, H₃-THIQ), 3.78 (3H, s, OCH₃, phenyl), 3.85 (3H, s, C₅OCH₃), 3.86 (3H, s, C₇OCH₃), 3.87 (3H, s, C₆OCH₃), 4.20 (2H, s, H₁-THIQ), 6.45 (1H, s, H₈-THIQ), 6.86 (2H, d, *J* = 9.1 Hz, 2 x ArCH, phenyl) and 6.98 (2H, d, *J* = 9.0 Hz, 2 x ArCH, phenyl) ppm. ¹³C NMR (126 MHz, CDCl₃) δ 23.3 (C₄-THIQ), 48.5 (C₃-THIQ), 52.9 (C₁-THIQ), 55.6 (OCH₃, phenyl), 56.0 (C₅OCH₃), 60.5 (C₇OCH₃), 60.9 (C₆OCH₃), 105.2 (C₈-THIQ), 114.5 (2 x ArCH, phenyl), 118.4 (2 x ArCH, phenyl), 120.7 (C₄CC₅-THIQ), 130.1 (C₁CC₈-THIQ), 140.5 (C₇-THIQ), 145.4 (ArCN), 151.2 (C₆-THIQ), 151.9 (C₅-THIQ) and 153.7 (ArCO, phenyl) ppm. HRMS (ES⁺) calcd. C₁₉H₂₄NO₄ (M⁺+H) 330.1700, found 330.1697. Mp 103-104 °C (DCM/Et₂O). Anal. calcd. for C₁₉H₂₃NO₄: C 69.28, H 7.04, N 4.25. Found: C 69.36, H 6.95, N 4.13 %.

2-(4-Chlorophenyl)-1,2,3,4-tetrahydroisoquinoline-4,6-diyl diacetate (169)

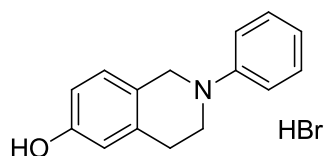
C₁₉H₁₈ClNO₄, Mol. Wt.: 359.80



A solution of acetyl chloride (39 μ L, 0.544 mmol) in EtOAc (1 mL) was added to a stirring solution of **143l** (150 mg, 0.544 mmol) and Et₃N (76 μ L, 0.544 mmol) in EtOAc (1 mL) at 0 °C and the mixture was stirred for 1 h. The mixture was then let reach rt, filtered and the filtrate was evaporated to give a brown oil (166 mg). The crude compound was purified by column chromatography (eluent: from 0% to 40% EtOAc in pet. ether) to give a yellow oil (54 mg, 28%) which showed: ¹H NMR (500 MHz, CDCl₃) δ 2.11 (3H, s, C₆OCOCH₃), 2.30 (3H, s, C₄OCOCH₃), 3.59 (1H, dd, J = 3.8, 13.1 Hz, H₃-THIQ), 3.70 (1H, dd, J = 3.8, 13.2 Hz, H₃-THIQ), 4.25 (1H, d, J = 15.5 Hz, H₁-THIQ), 4.47 (1H, d, J = 15.5 Hz, H₁-THIQ), 6.00 (1H, t, J = 3.8 Hz, H₄-THIQ), 6.88 (2H, d, J = 8.8 Hz, 2 x ArCH, phenyl), 7.07 (1H, dd, J = 1.9, 8.3 Hz, H₇-THIQ), 7.14 (1H, d, J = 2.4 Hz, H₅-THIQ), 7.21 (1H, d, J = 8.3 Hz, H₈-THIQ) and 7.23 (2H, d, J = 8.8 Hz, 2 x ArCH, phenyl) ppm. ¹³C NMR (126 MHz, CDCl₃) δ 21.0 (C₄OCOCH₃), 21.2 (C₆OCOCH₃), 50.2 (C₁-THIQ), 51.1 (C₃-THIQ), 68.1 (C₄-THIQ), 116.7 (2 x ArCH, phenyl), 121.7 (C₅-THIQ), 122.1 (C₇-THIQ), 124.4 (ArCCl), 127.4 (C₈-THIQ), 129.1 (2 x ArCH, phenyl), 132.5 (C₄CC₅-THIQ), 133.7 (C₁CC₈-THIQ), 148.6 (ArCN), 149.3 (C₆-THIQ), 169.4 (C₄OCOCH₃) and 170.9 (C₆OCOCH₃) ppm.

2-Phenyl-1,2,3,4-tetrahydroisoquinolin-6-ol hydrobromide (170e)

C₁₅H₁₆BrNO, Mol. Wt.: 306.20



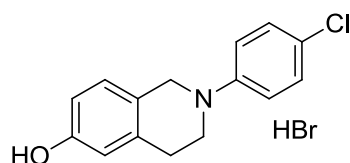
(Method F)

The product was obtained as a white precipitate (230 mg, 90%) which showed (¹H and ¹³C NMR data refer to the free base): ¹H NMR (500 MHz, CDCl₃) δ 2.93 (2H, t, J = 5.8 Hz, H₄-THIQ), 3.54 (2H, t, J = 5.8 Hz, H₃-THIQ), 4.34 (2H, s, H₁-THIQ), 4.75 (1H,

bs, OH), 6.63 (1H, d, $J = 2.6$ Hz, H₅-THIQ), 6.68 (1H, dd, $J = 2.6, 8.2$ Hz, H₇-THIQ), 6.83 (1H, t, $J = 7.3$ Hz, ArH, phenyl), 6.97 (2H, d, $J = 8.8$ Hz, ArH, phenyl), 7.03 (1H, d, $J = 8.2$ Hz, H₈-THIQ) and 7.29 (2H, dd, $J = 7.3, 8.8$ Hz, ArH, phenyl) ppm. ¹³C NMR (126 MHz, CDCl₃) δ 29.3 (C₄-THIQ), 46.6 (C₃-THIQ), 50.4 (C₁-THIQ), 113.6 (C₇-THIQ), 115.0 (C₅-THIQ), 115.4 (ArCH, phenyl), 118.9 (ArCH, phenyl), 126.9 (C₁CC₈-THIQ), 127.9 (C₈-THIQ), 129.3 (ArCH, phenyl), 136.5 (C₅CC₆-THIQ), 150.7 (ArCN) and 154.1 (C₆-THIQ) ppm. LC/MS (ES⁺) $t_r = 2.14$ min (98 %), m/z 225.9 (M⁺+H); (RP, Isocratic, 80% MeOH). HRMS (ES⁺) calcd. for C₁₅H₁₆NO (M⁺+H) 226.1226, found 226.1258. Mp 220-221 °C (aqueous HBr). Anal. calcd. for C₁₅H₁₆BrNO: C 58.54, H 5.27, N 4.57. Found: C 58.6, H 5.25, N 4.44 %.

2-(4-Chlorophenyl)-1,2,3,4-tetrahydroisoquinolin-6-ol hydrobromide (170i)

C₁₅H₁₅BrClNO, Mol. Wt.: 340.64

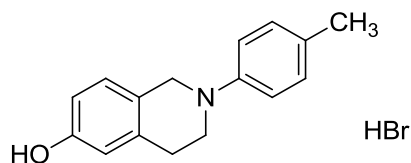


(Method F)

The product was obtained as a yellow precipitate (196 mg, 79%) which showed: ¹H NMR (500 MHz, CDCl₃) δ 2.92 (2H, t, $J = 5.9$ Hz, H₄-THIQ), 3.50 (2H, t, $J = 5.9$ Hz, H₃-THIQ), 4.30 (2H, s, H₁-THIQ), 4.79 (1H, bs, OH), 6.64 (1H, d, $J = 2.6$ Hz, H₅-THIQ), 6.68 (1H, dd, $J = 2.6, 8.2$ Hz, H₇-THIQ), 6.87 (2H, d, $J = 9.1$ Hz, ArH, phenyl), 7.02 (1H, d, $J = 8.2$ Hz, H₈-THIQ) and 7.21 (2H, d, $J = 9.1$ Hz, ArH, phenyl) ppm. ¹³C NMR (126 MHz, CDCl₃) δ 29.2 (C₄-THIQ), 46.6 (C₃-THIQ), 50.3 (C₁-THIQ), 113.7 (C₇-THIQ), 115.0 (C₅-THIQ), 116.3 (ArCH, phenyl), 123.5 (ArCCl), 126.5 (C₁CC₈-THIQ), 127.8 (C₈-THIQ), 129.1 (ArCH, phenyl), 136.3 (C₅CC₆-THIQ), 149.2 (ArCN) and 154.2 (C₆-THIQ) ppm. LC/MS (ES⁺) $t_r = 4.39$ min (97 %), m/z 259.8 (M⁺+H); (RP, Isocratic, 80% MeOH). HRMS (ES⁺) calcd. C₁₅H₁₅³⁵ClNO (M⁺+H) 260.0837, found 260.0845, calcd. C₁₅H₁₅³⁷ClNO (M⁺+H) 262.0807, found 262.0845. Mp 196-197 °C (aqueous HBr). Anal. calcd. for C₁₅H₁₅BrClNO: C 52.89, H 4.44, N 5.39. Found: C 51.6, H 4.33, N 3.96 %.

2-(*p*-Tolyl)-1,2,3,4-tetrahydroisoquinolin-6-ol hydrobromide (170q)

C₁₆H₁₈BrNO, Mol. Wt.: 320.22

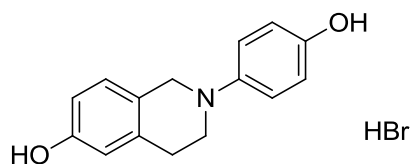


(Method F)

The product was obtained as a yellow precipitate (240 mg, 95%) which showed: ¹H NMR (500 MHz, CDCl₃) δ 2.28 (3H, s, CH₃), 2.92 (2H, t, *J* = 5.8 Hz, H₄-THIQ), 3.48 (2H, t, *J* = 5.9 Hz, H₃-THIQ), 4.28 (2H, s, H₁-THIQ), 4.77 (1H, bs), 6.62 (1H, d, *J* = 2.5 Hz, H₅-THIQ), 6.67 (1H, dd, *J* = 2.5, 8.2 Hz, H₇-THIQ), 6.91 (2H, d, *J* = 8.6 Hz, ArH, phenyl), 7.01 (1H, d, *J* = 8.2 Hz, H₈-THIQ) and 7.09 (2H, d, *J* = 8.6 Hz, ArH, phenyl) ppm. ¹³C NMR (126 MHz, CDCl₃) δ 20.5 (CH₃), 29.3 (C₄-THIQ), 47.4 (C₃-THIQ), 51.2 (C₁-THIQ), 113.5 (C₇-THIQ), 115.0 (C₅-THIQ), 116.1 (ArCH, phenyl), 127.0 (C₁CC₈-THIQ), 127.8 (C₈-THIQ), 128.6 (ArCCH₃), 129.8 (ArCH, phenyl), 136.4 (C₅CC₆-THIQ), 148.8 (ArCN) and 154.0 (C₆-THIQ) ppm. LC/MS (ES⁺) t_r = 1.73 min (97 %), m/z 239.9 (M⁺+H); (RP, Isocratic, 80% MeOH). HRMS (ES⁺) calcd. C₁₆H₁₇NO (M⁺+H) 240.1383, found 240.1380. Mp 224-225 °C (aqueous HBr). Anal. calcd. for C₁₆H₁₈BrClNO: C 60.0, H 5.67, N 4.37. Found: C 59.5, H 5.69, N 4.32 %.

2-(4-Hydroxyphenyl)-1,2,3,4-tetrahydroisoquinolin-6-ol hydrobromide (170s)

C₁₅H₁₆BrNO₂, Mol. Wt.: 322.20



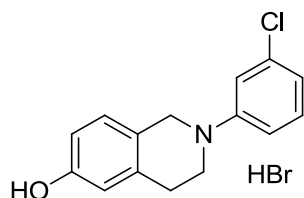
(Method F)

The product was obtained as a yellow precipitate (217 mg, 91%) which showed:¹⁸⁷ ¹H NMR (500 MHz, D₆-DMSO) δ 2.78 (2H, t, *J* = 5.7 Hz, H₄-THIQ), 3.27 (2H, t, *J* = 5.9 Hz, H₃-THIQ), 4.05 (2H, s, H₁-THIQ), 6.52 (1H, d, *J* = 2.5 Hz, H₅-THIQ), 6.56 (1H, dd, *J* = 2.5, 8.2 Hz, H₇-THIQ), 6.66 (2H, d, *J* = 8.9 Hz, ArH, phenyl), 6.84 (2H, d, *J* = 8.9 Hz, ArH, phenyl), 6.94 (1H, d, *J* = 8.2 Hz, H₈-THIQ), 8.80 (1H, bs, OH, phenyl)

and 9.15 (1H, bs, OH-THIQ) ppm. ^{13}C NMR (126 MHz, $\text{D}_6\text{-DMSO}$) δ 28.6 ($\text{C}_4\text{-THIQ}$), 47.8 ($\text{C}_3\text{-THIQ}$), 51.7 ($\text{C}_1\text{-THIQ}$), 113.3 ($\text{C}_7\text{-THIQ}$), 114.6 ($\text{C}_5\text{-THIQ}$), 115.6 (ArCH, phenyl), 117.7 (ArCH, phenyl), 125.0 ($\text{C}_1\text{CC}_8\text{-THIQ}$), 127.4 ($\text{C}_8\text{-THIQ}$), 135.3 ($\text{C}_5\text{CC}_6\text{-THIQ}$), 143.9 (ArCN), 150.6 (ArCO, phenyl) and 155.5 ($\text{C}_6\text{-THIQ}$) ppm. LC/MS (ES^+) t_r = 1.96 min (95 %), m/z 241.8 (M^++H); (RP, Isocratic, 70% MeOH). HRMS (ES^+) calcd. $\text{C}_{15}\text{H}_{15}\text{NO}_2$ (M^++H) 242.1176, found 242.1178. Mp 245-246 °C (aqueous HBr). Anal. calcd. for $\text{C}_{15}\text{H}_{16}\text{BrNO}_2$: C 55.9, H 5.01, N 4.35. Found: C 55.7, H 4.99, N 4.17 %.

2-(3-Chlorophenyl)-1,2,3,4-tetrahydroisoquinolin-6-ol hydrobromide (170t)

$\text{C}_{15}\text{H}_{15}\text{BrClNO}$, Mol. Wt.: 340.64

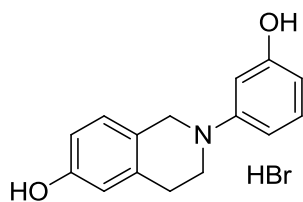


(Method F)

The product was obtained as a yellow solid (35 mg, 64%) which showed: ^1H NMR (500 MHz, $\text{D}_6\text{-DMSO}$) δ 2.79 (2H, t, J = 5.7 Hz, $\text{H}_4\text{-THIQ}$), 3.48 (9H, t, J = 5.7 Hz, $\text{H}_3\text{-THIQ}$), 4.27 (2H, s, $\text{H}_1\text{-THIQ}$), 6.57 (1H, s, $\text{H}_5\text{-THIQ}$), 6.60 (1H, dd, J = 2.3, 8.2 Hz, $\text{H}_7\text{-THIQ}$), 6.70 (1H, d, J = 7.8 Hz, ArCH, phenyl), 6.89 (1H, dd, J = 2.2, 8.4 Hz, ArCH, phenyl), 6.92 (1H, s, ArCH, phenyl), 7.01 (1H, d, J = 8.2 Hz, $\text{H}_8\text{-THIQ}$), 7.20 (1H, t, J = 8.1 Hz, ArCH, phenyl) and 9.29 (1H, bs, OH) ppm. ^{13}C NMR (126 MHz, $\text{D}_6\text{-DMSO}$) δ 28.2 ($\text{C}_4\text{-THIQ}$), 45.1 ($\text{C}_3\text{-THIQ}$), 48.7 ($\text{C}_1\text{-THIQ}$), 112.6 (ArCH, phenyl), 113.4 (ArCH, phenyl), 113.5 ($\text{C}_7\text{-THIQ}$), 114.5 ($\text{C}_5\text{-THIQ}$), 116.8 (ArCH, phenyl), 124.4 ($\text{C}_1\text{CC}_8\text{-THIQ}$), 127.5 ($\text{C}_8\text{-THIQ}$), 130.5 (ArCH, phenyl), 134.0 (ArCCl), 135.7 ($\text{C}_4\text{CC}_5\text{-THIQ}$), 151.3 (ArCN) and 155.8 ($\text{C}_6\text{-THIQ}$) ppm. HRMS (ES^+) calcd. $\text{C}_{15}\text{H}_{15}^{35}\text{ClNO}$ (M^++H) 260.0837, found 260.0825; calcd. $\text{C}_{15}\text{H}_{15}^{37}\text{ClNO}$ (M^++H) 262.0807, found 262.0805. Mp 211-215 °C.

2-(3-Hydroxyphenyl)-1,2,3,4-tetrahydroisoquinolin-6-ol hydrobromide (170u)

$\text{C}_{15}\text{H}_{16}\text{BrNO}_2$, Mol. Wt.: 322.20

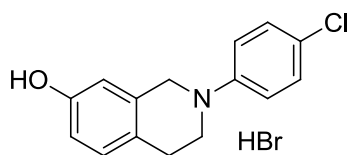


(Method F)

The product was obtained as a black solid (20 mg, 67%) which showed: ^1H NMR (400 MHz, CDCl_3) δ 2.90 (2H, t, $J = 5.8$ Hz), 3.51 (2H, t, $J = 5.9$ Hz), 4.32 (2H, s), 4.66 (2H, bs), 6.27 (1H, ddd, $J = 0.7, 2.3, 8.0$ Hz), 6.42 (1H, t, $J = 2.3$ Hz), 6.54 (1H, dd, $J = 2.1, 8.0$ Hz), 6.63 (1H, d, $J = 2.6$ Hz), 6.67 (1H, dd, $J = 2.7, 8.2$ Hz), 7.01 (1H, d, $J = 8.3$ Hz) and 7.12 (1H, t, $J = 8.1$ Hz) ppm. HRMS (ES^+) calcd. $\text{C}_{15}\text{H}_{16}\text{NO}_2$ ($\text{M}^+ + \text{H}$) 242.1176, found 242.1187;

2-(4-Chlorophenyl)-1,2,3,4-tetrahydroisoquinolin-7-ol hydrobromide (171)

$\text{C}_{15}\text{H}_{15}\text{BrClNO}$, Mol. Wt.: 340.64

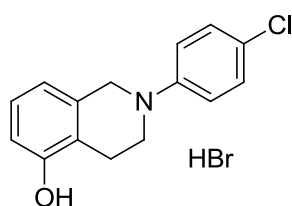


(Method F)

The product was obtained as a yellow precipitate (92 mg, 74%) which showed: ^1H NMR (500 MHz, $\text{D}_6\text{-DMSO}$) δ 2.75 (2H, t, $J = 5.9$ Hz, $\text{H}_4\text{-THIQ}$), 3.48 (2H, t, $J = 5.9$ Hz, $\text{H}_3\text{-THIQ}$), 4.27 (2H, s, $\text{H}_1\text{-THIQ}$), 6.58 (1H, dd, $J = 2.4, 8.2$ Hz, $\text{H}_6\text{-THIQ}$), 6.60 (1H, d, $J = 2.4$ Hz, $\text{H}_8\text{-THIQ}$), 6.94 (1H, d, $J = 8.2$ Hz, $\text{H}_5\text{-THIQ}$), 6.97 (2H, d, $J = 9.1$ Hz, ArH, phenyl), 7.22 (2H, d, $J = 9.1$ Hz, ArH, phenyl) and 9.20 (1H, bs, OH) ppm. ^{13}C NMR (126 MHz, $\text{D}_6\text{-DMSO}$) δ 27.0 ($\text{C}_4\text{-THIQ}$), 45.9 ($\text{C}_3\text{-THIQ}$), 49.7 ($\text{C}_1\text{-THIQ}$), 112.8 ($\text{C}_8\text{-THIQ}$), 113.8 ($\text{C}_6\text{-THIQ}$), 116.0 (ArCH, phenyl), 121.2 (ArCCl), 124.6 ($\text{C}_4\text{CC}_5\text{-THIQ}$), 128.7 (ArCH, phenyl), 129.2 ($\text{C}_5\text{-THIQ}$), 135.0 ($\text{C}_1\text{CC}_8\text{-THIQ}$), 148.9 (ArCN) and 155.4 ($\text{C}_7\text{-THIQ}$) ppm. HRMS (ES^+) calcd. $\text{C}_{15}\text{H}_{15}^{35}\text{ClNO}$ ($\text{M}^+ + \text{H}$) 260.0837, found 260.0827; calcd. $\text{C}_{15}\text{H}_{15}^{37}\text{ClNO}$ ($\text{M}^+ + \text{H}$) 262.0807, found 262.0831. Mp 225-228 °C.

2-(4-Chlorophenyl)-1,2,3,4-tetrahydroisoquinolin-5-ol hydrobromide (172)

C₁₅H₁₅BrClNO, Mol. Wt.: 340.64



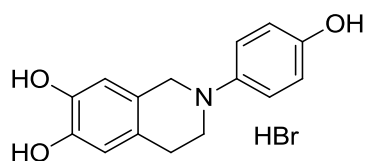
(Method F)

The product was obtained as a brown precipitate (47 mg, 75%) which showed: ¹H NMR (500 MHz, D₆-DMSO) δ 2.69 (2H, t, *J* = 5.9 Hz, H₄-THIQ), 3.51 (2H, t, *J* = 5.9 Hz, H₃-THIQ), 4.31 (2H, s, H₁-THIQ), 6.64 (1H, d, *J* = 7.9 Hz, H₆-THIQ), 6.65 (1H, d, *J* = 7.9 Hz, H₈-THIQ), 6.97 (1H, t, *J* = 7.9 Hz, H₇-THIQ), 7.00 (2H, d, *J* = 9.1 Hz, ArH, phenyl), 7.22 (2H, d, *J* = 9.1 Hz, ArH, phenyl) and 9.37 (1H, bs, OH) ppm. ¹³C NMR (126 MHz, D₆-DMSO) δ 22.2 (C₄-THIQ), 45.6 (C₃-THIQ), 49.9 (C₁-THIQ), 112.2 (C₆-THIQ), 116.4 (ArCH, phenyl), 117.1 (C₈-THIQ), 121.3 (C₄CC₅-THIQ), 121.4 (ArCCl), 126.3 (C₇-THIQ), 128.7 (ArCH, phenyl), 135.4 (C₁CC₈-THIQ), 149.0 (ArCN) and 154.7 (C₅-THIQ) ppm. HRMS (ES⁺) calcd. C₁₅H₁₅³⁵ClNO (M⁺+H) 260.0837, found 260.0826; calcd. C₁₅H₁₅³⁷ClNO (M⁺+H) 262.0807, found 262.0830. Mp 271-274 °C (as hydrobromide).

2-(4-Hydroxyphenyl)-1,2,3,4-tetrahydroisoquinoline-6,7-diol hydrobromide

(173)

C₁₅H₁₆BrNO₃, Mol. Wt.: 338.20



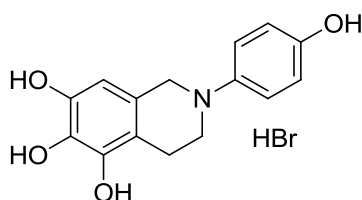
(Method G)

The product was obtained as a yellow solid (168 mg, 74%) which showed: ¹H NMR (500 MHz, D₂O) δ 3.18 (2H, t, *J* = 6.0 Hz, H₄-THIQ), 3.93 (2H, t, *J* = 6.0 Hz, H₃-THIQ), 4.63 (2H, s, H₁-THIQ), 6.74 (1H, s, H₈-THIQ), 6.84 (1H, s, H₅-THIQ), 7.06 (2H, d, *J* = 8.3 Hz, 2 x ArCH, phenyl) and 7.50 (2H, d, *J* = 8.3 Hz, 2 x ArCH, phenyl) ppm. ¹³C NMR (126 MHz, D₂O) δ 24.9 (C₄-THIQ), 53.4 (C₃-THIQ), 56.5 (C₁-THIQ), 113.4 (C₈-THIQ), 115.7 (C₅-THIQ), 116.8 (2 x ArCH, phenyl), 120.0 (C₁CC₈-THIQ),

122.5 (2 x ArCH, phenyl), 122.9 (C₄CC₅-THIQ), 133.5 (ArCN), 143.2 (C₆-THIQ), 144.2 (C₇-THIQ) and 156.9 (ArCO, phenyl) ppm. HRMS (ES⁺) calcd. C₁₅H₁₆NO₃ (M⁺+H) 258.1125, found 258.1127. Compound degraded before melting.

2-(4-Hydroxyphenyl)-1,2,3,4-tetrahydroisoquinoline-5,6,7-triol hydrobromide (174)

C₁₅H₁₆BrNO₄, Mol. Wt.: 354.20

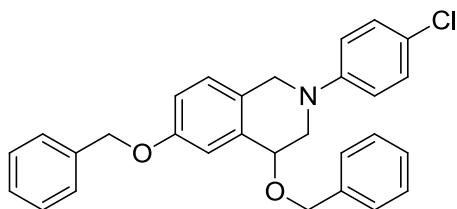


(Method G)

The product was obtained as a yellow solid (245 mg, 99%) which showed: ¹H NMR (500 MHz, D₂O) δ 3.10 (2H, t, *J* = 6.3 Hz, H₄-THIQ), 3.94 (2H, t, *J* = 6.4 Hz, H₃-THIQ), 4.61 (2H, s, H₁-THIQ), 6.40 (1H, s, H₈-THIQ), 7.07 (2H, d, *J* = 9.1 Hz, 2 x ArCH, phenyl) and 7.49 (2H, d, *J* = 9.1 Hz, 2 x ArCH, phenyl) ppm. ¹³C NMR (126 MHz, D₂O) δ 20.6 (C₄-THIQ), 53.1 (C₃-THIQ), 56.4 (C₁-THIQ), 105.5 (C₈-THIQ), 111.4 (C₄CC₅-THIQ), 116.8 (2 x ArCH, phenyl), 120.4 (C₁CC₈-THIQ), 122.4 (2 x ArCH, phenyl), 132.3 (C₆-THIQ), 133.6 (ArCN), 143.0 (C₅-THIQ), 144.5 (C₇-THIQ) and 156.8 (ArCO, phenyl) ppm. Mp 178-181 °C.

4,6-Bis(benzyloxy)-2-(4-chlorophenyl)-1,2,3,4-tetrahydroisoquinoline (175n)

C₂₉H₂₆ClNO₂, Mol. Wt.: 455.98

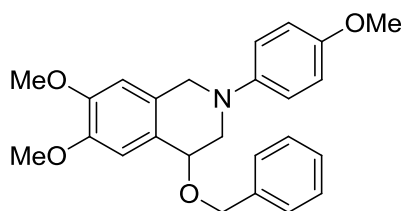


NaH (54 mg, 1.36 mmol) was added to a stirring solution of **143n** (150 mg, 0.544 mmol) in anhydrous THF (2 mL) under inert atmosphere followed by 15-crown-5 (216 μL, 1.09 mmol) and the mixture was stirred for 30 min at rt during which time the

mixture turned dark brown. Benzyl bromide (139 μ L, 1.14 mmol) was introduced and the mixture was stirred for 2 h at rt. The mixture was then quenched with water then dried with MgSO_4 , filtered and evaporated to give a brown oil (154 mg). The crude compound was purified by column chromatography (eluent: from 0% to 10% EtOAc in pet. ether) to give the product as a pale yellow oil (49 mg, 20%) which solidified upon standing and showed: ^1H NMR (500 MHz, CDCl_3) δ 3.55 – 3.66 (2H, m, H_3 -THIQ), 4.25 (1H, d, J = 14.6 Hz, H_1 -THIQ), 4.40 (1H, d, J = 14.6 Hz, H_1 -THIQ), 4.65 (1H, t, J = 4.5 Hz, H_4 -THIQ), 4.69 (2H, s, C_4OCH_2), 5.07 (2H, d, J = 2.4 Hz, C_6OCH_2), 6.83 (2H, d, J = 8.8 Hz, 2 x ArCH, phenyl), 6.93 (1H, dd, J = 2.2, 8.4 Hz, H_7 -THIQ), 7.03 (1H, d, J = 2.2 Hz, H_5 -THIQ), 7.11 (1H, d, J = 8.4 Hz, H_8 -THIQ), 7.22 (2H, d, J = 8.8 Hz, 2 x ArCH, phenyl) and 7.29 – 7.48 (10H, m, 10 x ArCH, benzyl) ppm. ^{13}C NMR (126 MHz, CDCl_3) δ 49.6 (C_1 -THIQ), 50.8 (C_3 -THIQ), 70.1 (C_6OCH_3), 71.0 (C_4OCH_3), 73.3 (C_1 -THIQ), 113.8 (C_5 -THIQ), 115.2 (C_7 -THIQ), 115.7 (2 x ArCH, phenyl), 123.3 (ArCCl), 126.9 (C_1CC_8 -THIQ), 127.5, 127.8, 127.9, 128.0, 128.5, 128.6, 128.7, 129.0, 135.8 (C_4CC_5 -THIQ), 136.9 (ArCCH₂OC₆), 138.3 (ArCCH₂OC₄), 148.9 (ArCN) and 157.6 (C_6 -THIQ) ppm. Mp 138-138 (as hydrochloride from Et_2O) $^\circ\text{C}$

4-(Benzyloxy)-6,7-dimethoxy-2-(4-methoxyphenyl)-1,2,3,4-tetrahydroisoquinoline (176x)

$\text{C}_{25}\text{H}_{27}\text{NO}_4$, Mol. Wt.: 405.49

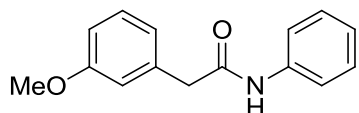


NaH (23 mg, 0.580 mmol) was added to a stirring solution of **146x** (100 mg, 0.290 mmol) in anhydrous THF (3 mL) under inert atmosphere. After stirring at rt for 30 min benzyl bromide (51 μ L, 0.435 mmol) was added and the mixture was stirred at rt for further 6 h. The mixture was then quenched with water and the organic solvent was evaporated. The aqueous layer was extracted with EtOAc (3 x 10 mL) and the combined organics were then dried with MgSO_4 , filtered and evaporated to give a yellow oil (238 mg). The crude compound was purified by column chromatography (eluent: from 0% to 20% EtOAc in pet. ether) to give the product as a yellow solid (34 mg, 29%)

which showed: ^1H NMR (500 MHz, CDCl_3) δ 3.50 (1H, dd, $J = 4.5, 12.3$ Hz, $\text{H}_3\text{-THIQ}$), 3.57 (1H, dd, $J = 4.5, 12.3$ Hz, $\text{H}_3\text{-THIQ}$), 3.79 (3H, s, C_7OCH_3 , phenyl), 3.85 (3H, s, $\text{C}_6\text{OCH}_3\text{-THIQ}$), 3.88 (3H, s, $\text{OCH}_3\text{-THIQ}$), 4.12 (1H, d, $J = 14.8$ Hz, $\text{H}_1\text{-THIQ}$), 4.29 (1H, d, $J = 14.8$ Hz, $\text{H}_1\text{-THIQ}$), 4.67 (1H, t, $J = 4.5$ Hz, $\text{H}_4\text{-THIQ}$), 4.72 (1H, d, $J = 12.1$ Hz, CH_2O), 4.77 (1H, d, $J = 12.1$ Hz, CH_2O), 6.63 (1H, s, $\text{H}_8\text{-THIQ}$), 6.86 (1H, s, $\text{H}_5\text{-THIQ}$), 6.88 (2H, d, $J = 9.1$ Hz, 2 x ArCH, phenyl), 6.98 (2H, d, $J = 9.1$ Hz, 2 x ArCH, phenyl), 7.31 (1H, t, $J = 7.3$ Hz, ArCH, benzyl), 7.37 (2H, t, $J = 7.3$ Hz, 2 x ArCH, benzyl) and 7.43 (2H, d, $J = 7.3$ Hz, 2 x ArCH, benzyl) ppm. ^{13}C NMR (126 MHz, CDCl_3) δ 52.2 ($\text{C}_1\text{-THIQ}$), 53.0 ($\text{C}_3\text{-THIQ}$), 55.6 (OCH_3 , phenyl), 55.8 ($\text{OCH}_3\text{-THIQ}$), 55.9 ($\text{OCH}_3\text{-THIQ}$), 70.7 (CH_2O), 73.2 ($\text{C}_4\text{-THIQ}$), 108.5 ($\text{C}_8\text{-THIQ}$), 110.9 ($\text{C}_5\text{-THIQ}$), 114.5 (2 x ArCH, phenyl), 118.1 (2 x ArCH, phenyl), 126.5 ($\text{C}_1\text{CC}_8\text{-THIQ}$), 127.5 ($\text{C}_4\text{CC}_5\text{-THIQ}$), 127.6 (ArCH, benzyl), 127.9 (2 x ArCH, benzyl), 128.4 (2 x ArCH, benzyl), 138.7 (ArCCH_2O), 145.2 (ArCN), 147.7 ($\text{C}_7\text{-THIQ}$), 148.7 ($\text{C}_6\text{-THIQ}$) and 153.6 (ArCO, phenyl) ppm. HRMS (ES^+) calcd. $\text{C}_{25}\text{H}_{28}\text{NO}_4$ ($\text{M}^+ + \text{Na}$) 406.2013, found 406.2024.

2-(3-Methoxyphenyl)-*N*-phenylacetamide (178a)

$\text{C}_{15}\text{H}_{15}\text{NO}_2$, Mol. Wt.: 241.29

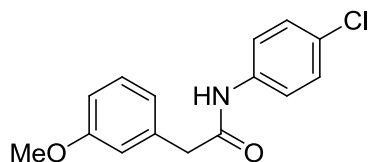


(Method H)

The crude compound was purified by column chromatography (eluent: from 0% to 80% EtOAc in pet. ether) to give the product as a pale yellow solid (2.20 g, 46 %) which showed: ^{190}H NMR (400 MHz, CDCl_3) δ 3.71 (2H, s), 3.82 (3H, s), 6.81 – 6.89 (2H, m), 6.91 (1H, d, $J = 7.5$ Hz), 7.08 (1H, dd, $J = 4.2, 10.5$ Hz), 7.14 (1H, bs), 7.26 – 7.35 (2H, m) and 7.41 (2H, dd, $J = 1.0, 8.5$ Hz) ppm. HRMS (ES^+) calcd. $\text{C}_{15}\text{H}_{16}\text{NO}_2$ ($\text{M}^+ + \text{H}$) 242.1176, found 242.1184. Mp 109-110 °C (as hydrochloride from Et_2O).

N-(4-Chlorophenyl)-2-(3-methoxyphenyl)acetamide (178b)

$\text{C}_{15}\text{H}_{14}\text{ClNO}_2$, Mol. Wt.: 275.73

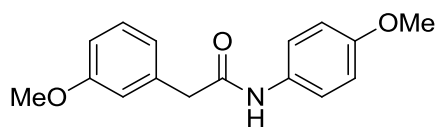


(Method H)

The crude compound was recrystallised from EtOAc/pet. ether to give a white solid (2.51 g, 46%) showed:¹⁸⁶ ¹H NMR (500 MHz, CDCl₃) δ 3.77 (2H, s, CH₂CO), 3.83 (3H, s, CH₃O), 6.88 – 6.92 (2H, m, phenyl), 6.95 (1H, d, *J* = 7.5 Hz, ArCH, phenyl), 7.00 (1H, td, *J* = 1.5, 7.9 Hz, aniline), 7.24 (1H, dd, *J* = 0.9, 8.2 Hz, aniline), 7.28 (1H, dd, *J* = 1.4, 8.0 Hz, aniline), 7.34 (1H, dd, *J* = 7.5, 9.0 Hz, ArCH, phenyl), 7.72 (1H, bs, NH) and 8.36 (1H, d, *J* = 7.5 Hz, ArCH, aniline) ppm. ¹³C NMR (126 MHz, CDCl₃) δ 45.4 (CCO), 55.4 (CH₃O), 113.7 (ArCH, phenyl), 115.2 (ArCH, phenyl), 121.4 (ArCH, aniline), 122.0 (ArCH, phenyl), 122.9 (ArCCl), 124.8 (ArCH, aniline), 127.8 (ArCH, aniline), 129.1 (ArCH, aniline), 130.6 (ArCH, phenyl), 134.6 (ArCN), 135.5 (ArCCH₂), 160.4 (COCH₃) and 169.1 (NCO) ppm. LC/MS (ES⁺) *t*_r = 1.66 min (95 %), *m/z* 276.1 (M⁺+H); (RP, Isocratic, 90% MeOH). HRMS (ES⁺) calc. for C₁₅H₁₄³⁵ClNaNO₂ (M⁺+Na) 298.0605, found 298.0599. Calc. for C₁₅H₁₄³⁷ClNaNO₂ (M⁺+Na) 300.0575, found 300.0590. Mp 224-225 °C (EtOAc/pet. ether).

2-(3-methoxyphenyl)-*N*-(4-methoxyphenyl)acetamide (178c)

C₁₆H₁₇NO₃, Mol. Wt.: 271.31

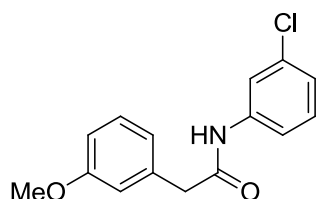


(Method H)

The crude compound was purified by column chromatography (eluent: from 0% to 80% EtOAc in pet. ether) to give the product as a pale yellow solid (2.77 g, 51 %) which showed:¹⁹¹ ¹H NMR (400 MHz, CDCl₃) δ 3.69 (2H, s), 3.76 (3H, s), 3.81 (3H, s), 6.81 (2H, d, *J* = 9.0 Hz), 6.84 – 6.89 (2H, m), 6.91 (1H, d, *J* = 7.5 Hz), 7.07 (1H, bs) and 7.27 – 7.35 (3H, m) ppm. HRMS (ES⁺) calcd. C₁₆H₁₈NO₃ (M⁺+H) 272.1281, found 272.1277. Mp 102-103 °C (as hydrochloride from Et₂O).

***N*-(3-chlorophenyl)-2-(3-methoxyphenyl)acetamide (178d)**

C₁₅H₁₄ClNO₂, Mol. Wt.: 275.73

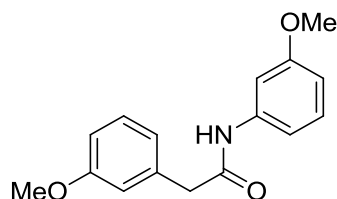


(Method H)

A sample of the crude compound (100 mg) was recrystallised from EtOAc/pet. ether and showed:¹⁹² ¹H NMR (500 MHz, CDCl₃) δ 3.70 (2H, s, ArCH₂), 3.82 (3H, s, ArOCH₃), 6.84 – 6.86 (1H, m, ArCH, benzyl), 6.87 – 6.93 (2H, m, 2 x ArCH, benzyl), 7.05 (1H, dd, *J* = 1.7, 8.1 Hz, ArCH, aniline), 7.16 (1H, bs, NH), 7.19 (1H, t, *J* = 8.1 Hz, ArCH, aniline), 7.27 (1H, dd, *J* = 1.7, 8.1 Hz, ArCH, aniline), 7.32 (1H, t, *J* = 8.0 Hz, ArCH, benzyl) and 7.52 (1H, t, *J* = 1.7 Hz, ArCH, aniline) ppm. ¹³C NMR (126 MHz, CDCl₃) δ 44.9 (ArCH₂), 55.3 (ArOCH₃), 113.2 (ArCH, benzyl), 115.2 (ArCH, benzyl), 117.7 (ArCH, aniline), 119.8 (ArCH, aniline), 121.6 (ArCH, benzyl), 124.4 (ArCH, benzyl), 129.9 (ArCH, aniline), 130.4 (ArCH, aniline), 134.6 (ArCCl), 135.5 (ArCCH₂), 138.7 (ArCN), 160.2 (ArCO) and 168.9 (CH₂CONH) ppm. HRMS (ES⁺) calc. for C₁₅H₁₄³⁵ClNNaO₂ (M⁺+Na) 298.0605, found 298.0600. Calc. for C₁₅H₁₄³⁷ClNNaO₂ (M⁺+Na) 300.0576, found 300.0589. Mp 93-94 °C (EtOAc/pet. ether).

***N*-(3-Methoxyphenyl)-2-(3-methoxyphenyl)acetamide (178e)**

C₁₆H₁₇NO₃, Mol. Wt.: 271.31



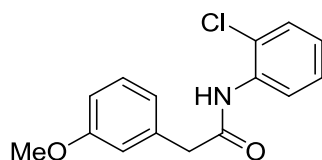
(Method H)

A sample of the crude compound (100 mg) was recrystallised from EtOAc/pet. ether and showed:¹⁹⁰ ¹H NMR (500 MHz, CDCl₃) δ 3.71 (2H, s, ArCH₂), 3.78 (3H, s, ArOCH₃, aniline), 3.82 (3H, s, ArOCH₃, benzyl), 6.64 (1H, dd, *J* = 2.4, 8.2 Hz, ArCH,

aniline), 6.84 (1H, dd, $J = 2.4, 8.2$ Hz, ArCH, aniline), 6.87 (1H, m, ArCH, benzyl), 6.88 – 6.93 (2H, m, ArCH, benzyl), 7.07 (1H, bs, NH), 7.16 (1H, t, $J = 8.2$ Hz, ArCH, aniline), 7.22 (1H, t, $J = 2.4$ Hz, ArCH, aniline) and 7.32 (1H, t, $J = 7.8$ Hz, ArCH, benzyl) ppm. ^{13}C NMR (126 MHz, CDCl_3) δ 45.0 (ArCH₂), 55.2 (ArOCH₃, aniline), 55.3 (ArOCH₃, benzyl), 105.5 (ArCH, aniline), 110.3 (ArCH, aniline), 111.8 (ArCH, aniline), 113.2 (ArCH, benzyl), 115.1 (ArCH, benzyl), 121.7 (ArCH, benzyl), 129.6 (ArCH, aniline), 130.3 (ArCH, benzyl), 135.7 (ArCCH₂), 138.8 (ArCN, aniline), 160.1 (ArCO, aniline), 160.2 (ArCO, benzyl) and 168.8 (CH₂CONH) ppm. HRMS (ES^+) calc. for $\text{C}_{16}\text{H}_{18}\text{NO}_3$ ($\text{M}^+ + \text{H}$) 272.1281, found 272.1288. Mp 79-81 °C (EtOAc/pet. ether).

***N*-(2-Chlorophenyl)-2-(3-methoxyphenyl)acetamide (178f)**

$\text{C}_{15}\text{H}_{14}\text{ClNO}_2$, Mol. Wt.: 275.73

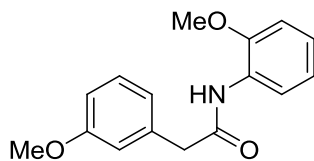


(Method H)

The crude compound was obtained as a white solid (3.65 g, 66%) which showed:¹⁹³ ^1H NMR (500 MHz, CDCl_3) δ 3.77 (2H, s, CH₂CO), 3.83 (3H, s, CH₃O), 6.88 – 6.92 (2H, m, phenyl), 6.95 (1H, d, $J = 7.5$ Hz, ArCH, phenyl), 7.00 (1H, td, $J = 1.5, 7.9$ Hz, aniline), 7.24 (1H, dd, $J = 0.9, 8.2$ Hz, aniline), 7.28 (1H, dd, $J = 1.4, 8.0$ Hz, aniline), 7.34 (1H, dd, $J = 7.5, 9.0$ Hz, ArCH, phenyl), 7.72 (1H, bs, NH), 8.36 (1H, d, $J = 7.5$ Hz, ArCH, aniline) ppm. ^{13}C NMR (126 MHz, CDCl_3) δ 45.4 (CCO), 55.4 (CH₃O), 113.7 (ArCH, phenyl), 115.2 (ArCH, phenyl), 121.4 (ArCH, aniline), 122.0 (ArCH, phenyl), 122.9 (ArCCl), 124.8 (ArCH, aniline), 127.8 (ArCH, aniline), 129.1 (ArCH, aniline), 130.6 (ArCH, phenyl), 134.6 (ArCN), 135.5 (ArCCH₂), 160.4 (COCH₃) and 169.1 (NCO) ppm. LC/MS (ES^+) $t_r = 1.66$ min (95 %), m/z 276.1 ($\text{M}^+ + \text{H}$); (RP, Isocratic, 90% MeOH) HRMS (ES^+) calc. for $\text{C}_{15}\text{H}_{14}^{35}\text{ClNaNO}_2$ ($\text{M}^+ + \text{Na}$) 298.0605, found 298.0599. Calc. for $\text{C}_{15}\text{H}_{14}^{37}\text{ClNaNO}_2$ ($\text{M}^+ + \text{Na}$) 300.0575, found 300.0590. Mp 109-110 °C (EtOAc/pet. ether).

***N*-(2-Methoxyphenyl)-2-(3-methoxyphenyl)acetamide (178g)**

C₁₆H₁₇NO₃, Mol. Wt.: 271.31

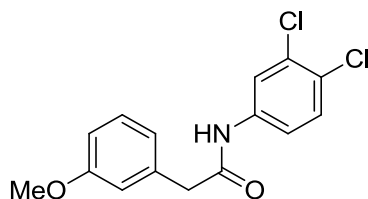


(Method H)

The crude compounds was obtained as a pale brown oil which solidified upon standing (2.52 g, 93%) which showed: ¹H NMR (500 MHz, CDCl₃) δ 3.73 (2H, s, ArCH₂), 3.73 (3H, s, ArOCH₃, aniline), 3.83 (3H, s, ArOCH₃, benzyl), 6.80 (1H, dd, *J* = 1.2, 8.1 Hz, ArCH, aniline), 6.85 – 6.91 (2H, m, ArCH, benzyl), 6.91 – 6.97 (2H, m, ArCH, aniline, ArCH, benzyl), 7.01 (1H, td, *J* = 1.6, 7.8 Hz, ArCH, aniline), 7.31 (1H, t, *J* = 7.8 Hz, ArCH, benzyl), 7.84 (1H, bs, CONH) and 8.34 (1H, dd, *J* = 1.5, 8.0 Hz, ArCH, aniline) ppm. ¹³C NMR (126 MHz, CDCl₃) δ 45.2 (ArCH₂), 55.2 (ArOCH₃, benzyl), 55.6 (ArOCH₃, aniline), 109.9 (ArCH, aniline), 113.2 (ArCH, benzyl), 114.9 (ArCH, benzyl), 119.5 (ArCH, aniline), 121.1 (ArCH, benzyl), 121.8 (ArCH, aniline), 123.7 (ArCH, aniline), 127.5 (ArCN), 130.0 (ArCH, benzyl), 136.0 (ArCCH₂), 147.9 (ArCO), 160.1 (ArCO) and 168.7 (CH₂CONH) ppm. HRMS (ES⁺) calc. for C₁₆H₁₈NO₃ (M⁺+H) 272.1281, found 272.1292. Mp 52-54 °C (EtOAc/pet. ether).

***N*-(3,4-Dichlorophenyl)-2-(3-methoxyphenyl)acetamide (178h)**

C₁₅H₁₃Cl₂NO₂, Mol. Wt.: 310.18



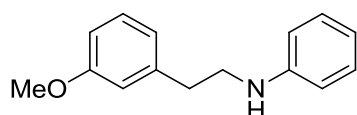
(Method H)

The crude compound was obtained as a white solid (4.7 g, 76%) which showed: ¹H NMR (500 MHz, CDCl₃) δ 3.71 (2H, s, CH₂CO), 3.83 (3H, s, CH₃O), 6.85 (1H, t, *J* = 2.1 Hz, ArH, phenyl), 6.89 (2H, dd, *J* = 2.1, 8.0 Hz, ArH, phenyl), 7.08 (1H, bs, NH), 7.25 (1H, dd, *J* = 2.4, 9.0 Hz, ArH, aniline), 7.32 (1H, d, *J* = 9.0 Hz, ArH, Aniline), 7.33 (1H, t, *J* = 8.0 Hz, ArH, phenyl) and 7.64 (1H, d, *J* = 2.4 Hz, ArH, aniline) ppm. ¹³C NMR (126 MHz, CDCl₃) δ 44.8 (CH₂CO), 55.3 (CH₃O), 113.3 (ArCH, phenyl), 115.2

(ArCH, phenyl), 118.9 (ArCH, aniline), 121.4 (ArCH, aniline), 121.6 (ArCH, phenyl), 127.6 (ArCN), 130.4 (ArCH, phenyl), 130.5 (ArCH, aniline), 132.7 (ArCCl), 135.3 (ArCCH₂), 137.0 (ArCCl), 160.3 (ArCO) and 168.9 (NCO) ppm. LC/MS (ES⁺) t_r = 2.10 min (92 %), m/z (not ionised) (M⁺+H); (RP, Isocratic, 90% MeOH). HRMS (ES⁺) calc. for C₁₅H₁₃³⁵Cl₂NaNO₂ (M⁺+Na) 332.0216, found 332.0219. Calc. for C₁₅H₁₃³⁵Cl³⁷ClNaNO₂ (M⁺+Na) 334.0238, found 334.0235. Mp 121-122 °C (EtOAc/pet. ether).

***N*-(3-Methoxyphenethyl)aniline (179a)**

C₁₅H₁₇NO, Mol. Wt.: 227.30

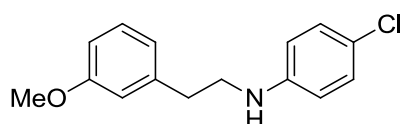


(Method I)

The crude compound was purified by column chromatography (eluent: from 0% to 40% EtOAc in pet. ether) to give the product as a colourless oil (1.21 g, 64%) which showed: ¹⁰ ¹H NMR (500 MHz, CDCl₃) δ 2.91 (2H, t, *J* = 7.1 Hz, CH₂CH₂N), 3.41 (2H, t, *J* = 7.1 Hz, CH₂CH₂N), 3.80 (3H, s, ArOCH₃), 6.67 (2H, d, *J* = 7.8 Hz, 2 x ArCH, aniline), 6.74 (1H, t, *J* = 7.8 Hz, ArCH, aniline), 6.76 – 6.80 (2H, m, 2 x ArCH, phenethyl), 6.82 (1H, d, *J* = 7.5 Hz, ArCH, phenethyl), 7.20 (2H, t, *J* = 7.8 Hz, 2 x ArCH, aniline) and 7.24 (1H, t, *J* = 7.9 Hz, ArCH, phenethyl) ppm. ¹³C NMR (126 MHz, CDCl₃) δ 35.3 (CH₂CH₂N), 45.3 (CH₂CH₂N), 55.2 (ArOCH₃), 111.7 (ArCH, phenethyl), 113.4 (2 x ArCH, aniline), 114.5 (ArCH, phenethyl), 118.0 (ArCH, aniline), 121.1 (ArCH, phenethyl), 129.3 (2 x ArCH, aniline), 129.6 (ArCH, phenethyl), 140.7 (ArCCH₂), 147.4 (ArCN) and 159.7 (ArCO) ppm. HRMS (ES⁺) calcd. C₁₅H₁₇NNaO (M⁺+Na) 250.1208, found 250.1201. Mp 98-100 °C (as hydrochloride from Et₂O).

4-Chloro-*N*-(3-methoxyphenethyl)aniline (179b)

C₁₅H₁₆ClNO, Mol. Wt.: 261.75

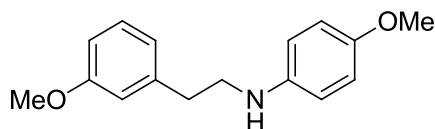


(Method I)

The compound was precipitate as hydrochloride from Et₂O to give a pale yellow solid (1.38 g, 64%) which showed: ¹⁸⁶ ¹H NMR (400 MHz, CDCl₃) δ 2.87 (2H, t, *J* = 6.9 Hz), 3.36 (2H, t, *J* = 6.9 Hz), 3.79 (3H, s), 6.52 (2H, d, *J* = 8.8 Hz), 6.74 (1H, s), 6.76 – 6.82 (2H, m), 7.11 (2H, d, *J* = 8.8 Hz) and 7.23 (3H, t, *J* = 7.9 Hz) ppm. HRMS (ES⁺) calcd. C₁₅H₁₇ClNO (*M*⁺+H) 262.0993, found 262.1000. Mp 149-151 °C (EtOAc/pet. ether).

4-Methoxy-*N*-(3-methoxyphenethyl)aniline (179c)

C₁₆H₁₉NO₂, Mol. Wt.: 257.33

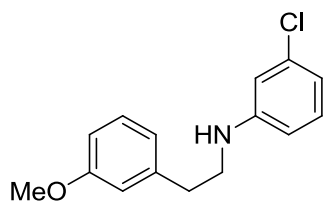


(Method I)

The crude compound was purified by column chromatography (eluent: from 0% to 40% EtOAc in pet. ether) to give the product as a yellow oil (1.39 g, 59%) which showed: ¹⁹⁴ ¹H NMR (500 MHz, CDCl₃) δ 2.89 (2H, t, *J* = 7.0 Hz, CH₂CH₂N), 3.36 (2H, t, *J* = 7.0 Hz, CH₂CH₂N), 3.75 (3H, s, ArOCH₃, aniline), 3.80 (3H, s, ArOCH₃, phenethyl), 6.63 (2H, d, *J* = 8.8 Hz, 2 x ArCH, aniline), 6.74 – 6.83 (5H, m, 3 x ArCH, phenethyl, 2 x ArCH, aniline) and 7.23 (1H, t, *J* = 7.8 Hz, ArCH, phenethyl) ppm. ¹³C NMR (126 MHz, CDCl₃) δ 35.4 (CH₂CH₂N), 46.2 (CH₂CH₂N), 55.2 (ArOCH₃, phenethyl), 55.8 (ArOCH₃, aniline), 111.7 (ArCH, phenethyl), 114.5 (ArCH, phenethyl), 114.8 (2 x ArCH, aniline), 114.9 (2 x ArCH, aniline), 121.1 (ArCH, phenethyl), 129.6 (ArCH, phenethyl), 140.8 (ArCCH₂), 141.6 (ArCN), 152.4 (ArCO, aniline) and 159.7 (ArCO, phenethyl) ppm. HRMS (ES⁺) calcd. C₁₆H₁₉NNaO₂ (*M*⁺+Na) 280.1308, found 280.1312. Mp 108-111 °C (as hydrochloride from Et₂O).

3-Chloro-*N*-(3-methoxyphenethyl)aniline (179d)

C₁₅H₁₆ClNO, Mol. Wt.: 261.75

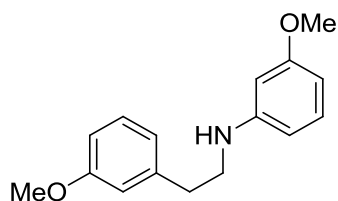


(Method I)

The crude compound was purified by column chromatography (from 0% to 20% EtOAc in pet. ether) to give the product as a yellow oil (1.32 g, 66%) which showed: ^1H NMR (500 MHz, CDCl_3) δ 2.89 (2H, t, $J = 6.9$ Hz, ArCH_2CH_2), 3.38 (2H, t, $J = 6.9$ Hz, $\text{CH}_2\text{CH}_2\text{N}$), 3.76 (1H, bs, NH), 3.80 (3H, s, ArOCH_3), 6.46 (1H, ddd, $J = 0.8, 2.1, 8.0$ Hz, ArCH, aniline), 6.58 (1H, t, $J = 2.1$ Hz, ArCH, aniline), 6.66 (1H, ddd, $J = 0.8, 2.1, 8.0$ Hz, ArCH, aniline), 6.73 – 6.77 (1H, m, ArCH, phenethyl), 6.77 – 6.83 (2H, m, ArCH, phenethyl), 7.07 (1H, t, $J = 8.0$ Hz, ArCH, aniline) and 7.24 (1H, t, $J = 7.9$ Hz, ArCH, phenethyl) ppm. ^{13}C NMR (126 MHz, CDCl_3) δ 35.3 (ArCH_2CH_2), 44.6 (ArCH_2CH_2), 55.2 (ArOCH_3), 111.3 (ArCH, aniline), 111.8 (ArCH, phenethyl), 112.5 (ArCH, aniline), 114.6 (ArCH, phenethyl), 117.2 (ArCH, aniline), 121.1 (ArCH, phenethyl), 129.7 (ArCH, phenethyl), 130.2 (ArCH, aniline), 135.0 (ArCCl), 140.5 (ArCCH_2), 149.1 (ArCN) and 159.8 (ArCO) ppm. HRMS (ES^+) calc. for $\text{C}_{15}\text{H}_{17}^{35}\text{ClNO}$ ($\text{M}^+ + \text{H}$) 262.0993, found 262.0988. Calc. for $\text{C}_{15}\text{H}_{17}^{37}\text{ClNO}$ ($\text{M}^+ + \text{H}$) 264.0964, found 264.0966. Mp 136-138 °C (as hydrochloride from Et_2O).

3-Methoxy-*N*-(3-methoxyphenethyl)aniline (179e)

$\text{C}_{16}\text{H}_{19}\text{NO}_2$, Mol. Wt.: 257.33



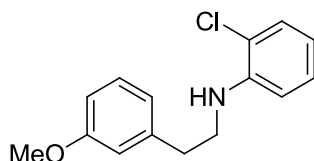
(Method I)

The crude compound was purified by column chromatography (from 0% to 20% EtOAc in pet. ether) to give the product as a yellow oil (1.28g, 64%) which showed: 187 ^1H NMR (500 MHz, CDCl_3) δ 2.89 (2H, t, $J = 7.0$ Hz, ArCH_2CH_2), 3.39 (2H, t, $J = 7.0$ Hz, $\text{CH}_2\text{CH}_2\text{N}$), 3.72 (1H, bs, NH), 3.77 (3H, s, ArOCH_3 , aniline), 3.80 (3H, s,

ArOCH₃, phenethyl), 6.18 (1H, t, $J = 2.3$ Hz, ArCH, aniline), 6.23 (1H, ddd, $J = 0.7, 2.3, 8.1$ Hz, ArCH, aniline), 6.28 (1H, ddd, $J = 0.7, 2.3, 8.1$ Hz, ArCH, aniline), 6.76 – 6.80 (2H, m, ArCH, phenethyl), 6.80 – 6.84 (1H, m, ArCH, phenethyl), 7.08 (1H, t, $J = 8.1$ Hz, ArCH, aniline) and 7.24 (1H, t, $J = 7.8$ Hz, ArCH, phenethyl) ppm. ¹³C NMR (126 MHz, CDCl₃) δ 35.5 (ArCH₂CH₂), 44.9 (CH₂CH₂N), 55.1 (ArOCH₃, aniline), 55.2 (ArOCH₃, phenethyl), 98.9 (ArCH, aniline), 102.6 (ArCH, aniline), 106.2 (ArCH, aniline), 111.7 (ArCH, phenethyl), 114.5 (ArCH, phenethyl), 121.1 (ArCH, phenethyl), 129.6 (ArCH, phenethyl), 130.0 (ArCH, aniline), 140.9 (ArCCH₂), 149.4 (ArCN), 159.8 (ArCO, phenethyl) and 160.9 (ArCO, aniline) ppm. HRMS (ES⁺) calc. for C₁₆H₂₀NO₂ (M⁺+H) 258.1489, found 258.1490. Mp 99-101 °C (as hydrochloride from Et₂O).

2-Chloro-*N*-(3-methoxyphenethyl)aniline (179f)

C₁₅H₁₆ClNO, Mol. Wt.: 261.75

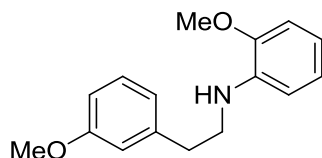


(Method I)

The filtrate was evaporated to give a yellow oil (1.5 g, 93%) which showed:¹⁹³ ¹H NMR (500 MHz, CDCl₃) δ 2.93 (2H, t, $J = 7.1$ Hz, ArCH₂), 3.44 (2H, t, $J = 7.1$ Hz, CH₂N), 3.81 (3H, s), 4.38 (1H, bs, NH), 6.63 (1H, td, $J = 1.5, 7.6$ Hz, ArH, aniline), 6.70 (1H, dd, $J = 1.3, 8.2$ Hz, ArH, aniline), 6.76 – 6.78 (1H, m, ArH, benzyl), 6.80 (1H, ddd, $J = 0.7, 2.5, 8.2$ Hz, ArH, benzyl), 6.81 – 6.85 (1H, m, ArH, benzyl), 7.12 – 7.18 (1H, m, ArH, aniline) and 7.25 (2H, td, $J = 1.3, 7.8$ Hz, ArH, aniline and ArH, benzyl) ppm. ¹³C NMR (126 MHz, CDCl₃) δ 35.4 (ArCH₂), 44.8 (CH₂N), 55.2 (OCH₃), 111.2 (ArCH, aniline), 111.9 (ArCH, benzyl), 114.4 (ArCH, benzyl), 117.2 (ArCH, aniline), 119.3 (ArCCl), 121.1 (ArCH, benzyl), 127.8 (ArCH, aniline), 129.2 (ArCH, aniline), 129.6 (ArCH, benzyl), 140.6 (ArCCH₂), 143.7 (ArCN) and 159.8 (ArCO) ppm. LC/MS (ES⁺) $t_r = 3.12$ min (85 %), m/z 262.1 (M⁺+H); (RP, Isocratic, 90% MeOH). HRMS (ES⁺) calc. for C₁₅H₁₇³⁵ClNO (M⁺+H) 262.0993, found 262.0990. Calc. for C₁₅H₁₇³⁷Cl NO (M⁺+H) 264.0964, found 264.0976. Mp 127-129 °C (as hydrochloride from Et₂O).

2-Methoxy-N-(3-methoxyphenethyl)aniline (179g)

C₁₆H₁₉NO₂, Mol. Wt.: 257.33

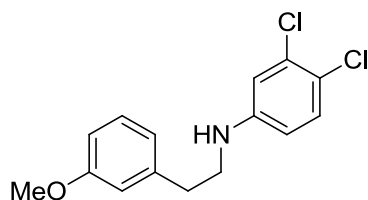


(Method I)

The crude compound was purified by column chromatography (from 0% to 20% EtOAc in pet. ether) to give the product as a yellow oil (721 mg, 31%) which showed: ¹H NMR (500 MHz, CDCl₃) δ 2.93 (2H, t, *J* = 7.3 Hz, ArCH₂CH₂), 3.41 (2H, t, *J* = 7.3 Hz, CH₂CH₂N), 3.80 (1H, s, ArOCH₃, phenethyl), 3.82 (3H, s, ArOCH₃, aniline), 4.35 (1H, bs, NH), 6.67 (1H, d, *J* = 7.7 Hz, ArCH, aniline), 6.69 (1H, dd, *J* = 1.5, 7.4 Hz, ArCH, aniline), 6.75 – 6.80 (3H, m, 3 x ArCH, phenethyl), 6.83 (1H, d, *J* = 7.4 Hz, ArCH, aniline), 6.89 (1H, td, *J* = 1.5, 7.7 Hz, ArCH, aniline) and 7.24 (1H, dd, *J* = 7.5, 8.9 Hz, ArCH, phenethyl) ppm. ¹³C NMR (126 MHz, CDCl₃) δ 35.7 (ArCH₂CH₂), 44.9 (CH₂CH₂N), 55.1 (ArOCH₃, phenethyl), 55.4 (ArOCH₃, phenethyl), 109.5 (ArCH, phenethyl), 110.0 (ArCH, aniline), 111.7 (ArCH, phenethyl), 114.4 (ArCH, phenethyl), 116.5 (ArCH, aniline), 121.1 (ArCH, aniline), 121.3 (ArCH, aniline), 129.5 (ArCH, phenethyl), 137.9 (ArCN), 141.1 (ArCCH₂), 146.9 (ArOCH₃, aniline) and 159.7 (ArOCH₃, phenethyl) ppm. HRMS (ES⁺) calc. for C₁₆H₂₀NO₂ (M⁺+H) 258.1489, found 258.1499. Mp 132-134 °C (as hydrochloride from Et₂O).

3,4-Dichloro-N-(3-methoxyphenethyl)aniline (179h)

C₁₅H₁₅Cl₂NO, Mol. Wt.: 296.19

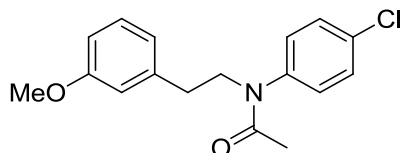


(Method I)

The crude compound was purified by column chromatography (eluent: from 0% to 30% EtOAc in pet. ether) to get the product as a yellow oil (1.6 g, 75%) which showed: ^1H NMR (500 MHz, CDCl_3) δ 2.88 (2H, t, $J = 6.9$ Hz, ArCH_2CH_2), 3.36 (2H, t, $J = 6.9$ Hz, $\text{CH}_2\text{CH}_2\text{N}$), 3.80 (3H, s, OCH_3), 6.42 (1H, dd, $J = 2.7, 8.7$ Hz, ArCH, aniline), 6.66 (1H, d, $J = 2.7$ Hz, ArCH, aniline), 6.75 (1H, t, $J = 2.1$, ArCH, phenethyl), 6.80 (2H, dd, $J = 2.1, 7.9$ Hz, 2 x ArCH, phenethyl), 7.17 (1H, d, $J = 8.7$ Hz, ArCH, aniline) and 7.25 (1H, t, $J = 7.9$ Hz, ArCH, phenethyl) ppm. ^{13}C NMR (126 MHz, CDCl_3) δ 35.2 (ArCH_2CH_2), 44.7 ($\text{CH}_2\text{CH}_2\text{N}$), 55.2 (OCH_3), 111.8 (ArCH, phenethyl), 112.7 (ArCH, aniline), 113.9 (ArCH, aniline), 114.6 (ArCH, phenethyl), 119.8 (ArCCl), 121.0 (ArCH, phenethyl), 129.7 (ArCH, phenethyl), 130.6 (ArCH, aniline), 132.8 (ArCCl), 140.3 (ArCCH_2), 147.4 (ArCN) and 159.9 (ArCO) ppm. LC/MS (ES^+) $t_r = 3.09$ min (89 %), m/z 296.1 ($\text{M}^+ + \text{H}$) (^{35}Cl), m/z 298.0 ($\text{M}^+ + \text{H}$) (^{37}Cl); (RP, Isocratic, 90% MeOH) HRMS (ES^+) calc. for $\text{C}_{15}\text{H}_{16}^{35}\text{Cl}_2\text{NO}$ ($\text{M}^+ + \text{H}$) 296.0609, found 296.0597; calc. for $\text{C}_{15}\text{H}_{16}^{35}\text{Cl}^{37}\text{ClNO}$ ($\text{M}^+ + \text{H}$) 298.0580, found 298.0592. Mp 134-136 °C (as hydrochloride from Et_2O).

***N*-(4-Chlorophenyl)-*N*-(3-methoxyphenethyl)acetamide (180a)**

$\text{C}_{17}\text{H}_{18}\text{ClNO}_2$, Mol. Wt.: 303.78

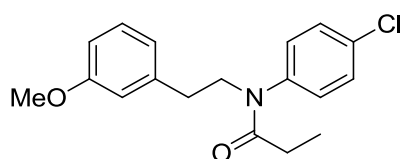


Compound **179b** (150 mg, 0.503 mmol) was dissolved in a mixture of EtOAc (2 mL) and Pyridine (123 μL , 1.51 mmol) and Acetylchloride (13.3 μL , 1.01 mmol) was added dropwise. The mixture was stirred for 1 h at rt during which time a white precipitate formed. The mixture was filtered and the filtrate was diluted with EtOAc (5 mL) washed with 1N HCl (5 mL) and 1N NaOH (5 mL). The organic layer was then dried with MgSO_4 , filtered and evaporated to give a white solid (132 mg, 86%) which showed: ^1H NMR (500 MHz, CDCl_3) δ 1.83 (3H, s, COCH_3), 2.83 (2H, t, $J = 7.8$ Hz, ArCH_2CH_2), 3.77 (3H, s, ArOCH_3), 3.90 (2H, t, $J = 7.8$ Hz, $\text{CH}_2\text{CH}_2\text{N}$), 6.70 (1H, s, ArCH, phenethyl), 6.74 (2H, d, $J = 8.3$ Hz, 2 x ArCH, phenethyl), 6.98 (2H, d, $J = 8.5$ Hz, 2 x ArCH, aniline), 7.17 (1H, t, $J = 7.8$ Hz, ArCH, phenethyl) and 7.36 (2H, d, $J = 8.5$ Hz, 2 x ArCH, aniline) ppm. ^{13}C NMR (126 MHz, CDCl_3) δ 22.9 (NCOCH_3), 34.0

(ArCH₂CH₂), 50.6 (CH₂CH₂N), 55.2 (ArOCH₃), 112.0 (ArCH, phenethyl), 114.3 (ArCH, phenethyl), 121.2 (ArCH, phenethyl), 129.4 (ArCH, aniline), 129.4 (ArCH, phenethyl), 129.9 (ArCH, aniline), 133.7 (ArCCl), 140.2 (ArCCH₂), 141.8 (ArCN), 159.7 (ArCO) and 170.1 (NCO) ppm. HRMS (ES⁺) calcd. C₁₇H₁₈³⁵ClNNaO₂ (M⁺+Na) 326.0918, found 326.0924; calcd. C₁₇H₁₈³⁷ClNNaO₂ (M⁺+Na) 328.0889, found 328.0890.

***N*-(4-Chlorophenyl)-*N*-(3-methoxyphenethyl)propionamide (180b)**

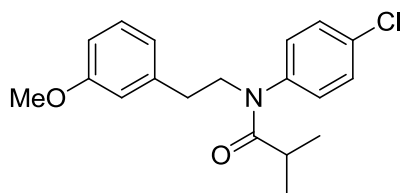
C₁₈H₂₀ClNO₂, Mol. Wt.: 317.81



Propanoyl chloride (90 μ L, 1.01 mmol) was added to a stirring solution of **179b** (150 mg, 0.503 mmol) and pyridine (123 μ L, 1.51 mmol) in DCM (2 mL) and the mixture was stirred at rt for 10 h. A white precipitate formed after the first ten minutes. The mixture was then diluted with DCM (10 mL) washed with a sat. aq. solution of NaHCO₃ (2 x 10 mL) and 1N HCl (2 x 10 mL) and the organic layer was dried with MgSO₄, filtered and evaporated to give the product as a pale yellow oil (114 mg, 71%) which showed: ¹H NMR (500 MHz, CDCl₃) δ 1.05 (3H, t, *J* = 7.4 Hz, CH₂CH₃), 2.02 (2H, q, *J* = 7.4 Hz, CH₂CH₃), 2.78 – 2.91 (2H, m, CH₂CH₂N), 3.77 (3H, s, OCH₃), 3.82 – 3.96 (2H, m, CH₂CH₂N), 6.69 – 6.72 (1H, m, ArCH, benzyl), 6.72 – 6.79 (2H, m, 2 x ArCH, benzyl), 6.97 (2H, d, *J* = 8.4 Hz, 2 x ArCH, aniline), 7.17 (1H, t, *J* = 7.9 Hz, ArCH, benzyl) and 7.36 (2H, d, *J* = 8.6 Hz, ArCH, aniline) ppm. ¹³C NMR (126 MHz, CDCl₃) δ 9.5 (CH₂CH₃), 27.9 (CH₂CH₃), 34.1 (CH₂CH₂N), 50.9 (CH₂CH₂N), 55.2 (OCH₃), 112.0 (ArCH, phenethyl), 114.3 (ArCH, phenethyl), 121.2 (ArCH, phenethyl), 129.4 (ArCH, phenethyl), 129.6 (ArCH, aniline), 129.9 (ArCH, aniline), 133.7 (ArCCl), 140.2 (ArCCH₂), 141.5 (ArCN), 159.7 (ArCO) and 173.5 (NCO) ppm. HRMS (ES⁺) calcd. C₁₈H₂₁³⁵ClNO₂ (M⁺+H) 318.1255, found 318.1255; calcd. C₁₈H₂₁³⁷ClNO₂ (M⁺+H) 320.1226, found 320.1237.

***N*-(4-Chlorophenyl)-*N*-(3-methoxyphenethyl)isobutyramide (180c)**

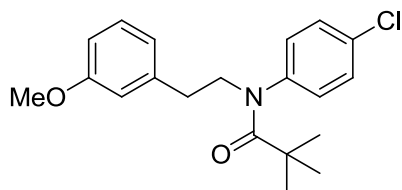
C₁₉H₂₂ClNO₂, Mol. Wt.: 331.84



Isobutyryl chloride (108 μ L, 1.01 mmol) was added to a stirring solution of **179b** (150 mg, 0.503 mmol) and pyridine (123 μ L, 1.51 mmol) in DCM (2 mL) and the mixture was stirred at rt for 10 h. A white precipitate formed after the first ten minutes. The mixture was then diluted with DCM (10 mL) washed with a sat. aq. solution of NaHCO₃ (2 x 10 mL) and 1N HCl (2 x 10 mL) and the organic layer was dried with MgSO₄, filtered and evaporated to give the product as a pale yellow solid (113 mg, 68%) which showed: ¹H NMR (500 MHz, CDCl₃) δ 1.01 (6H, d, J = 6.7 Hz, (CH₃)₂CH), 2.38 (1H, septet, J = 6.7 Hz, (CH₃)₂CH), 2.85 (2H, t, J = 7.8 Hz, CH₂CH₂N), 3.77 (3H, s, OCH₃), 3.86 (2H, t, J = 7.8 Hz, CH₂CH₂N), 6.71 (1H, s, ArCH, phenethyl), 6.74 (2H, d, J = 8.0 Hz, 2 x ArCH, phenethyl), 6.95 (2H, d, J = 8.4 Hz, 2 x ArCH, aniline), 7.17 (1H, t, J = 7.8 Hz, ArCH, phenethyl) and 7.35 (2H, d, J = 8.6 Hz, 2 x ArCH, aniline) ppm. ¹³C NMR (126 MHz, CDCl₃) δ 19.6 ((CH₃)₂CH), 31.3 ((CH₃)₂CH), 34.0 (CH₂CH₂N), 51.0 (CH₂CH₂N), 55.2 (CH₃O), 112.1 (ArCH, phenethyl), 114.3 (ArCH, phenethyl), 121.2 (ArCH, phenethyl), 129.4 (ArCH, phenethyl), 129.5 (2 x ArCH, aniline), 129.8 (2 x ArCH, aniline), 133.7 (ArCCl), 140.3 (ArCCH₂), 141.6 (ArCN), 159.7 (ArCO) and 177.0 (NCO) ppm. HRMS (ES⁺) calcd. C₁₉H₂₃³⁵ClNO₂ (M⁺+H) 332.1412, found 332.1399; calcd. C₁₉H₂₃³⁷ClNO₂ (M⁺+H) 334.1382, found 334.1394.

N-(4-Chlorophenyl)-N-(3-methoxyphenethyl)pivalamide (180d)

C₂₀H₂₄ClNO₂, Mol. Wt.: 345.86

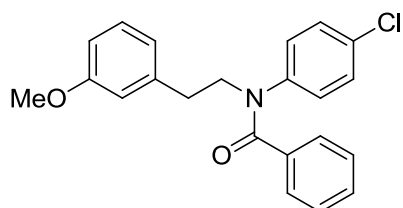


Pivaloyl chloride (126 μ L, 1.01 mmol) was added to a stirring solution of **179b** (150 mg, 0.503 mmol) and pyridine (123 μ L, 1.51 mmol) in DCM (2 mL) and the mixture

was stirred at rt for 10 h. A white precipitate formed after the first ten minutes. The mixture was then diluted with DCM (10 mL) washed with a sat. aq. solution of NaHCO₃ (2 x 10 mL) and 1N HCl (2 x 10 mL) and the organic layer was dried with MgSO₄, filtered and evaporated to give the product as a yellow solid (122 mg, 70%) which showed: ¹H NMR (500 MHz, CDCl₃) δ 1.03 (9H, s, C(CH₃)₃), 2.79 – 2.92 (1H, m, CH₂CH₂N), 3.68 – 3.83 (2H, m, CH₂CH₂N), 3.77 (3H, s, CH₃O), 6.69 – 6.72 (1H, m, ArCH, phenethyl), 6.74 (1H, dd, *J* = 2.0, 8.0 Hz, 2 x ArCH, phenethyl), 6.99 (2H, d, *J* = 8.6 Hz, ArCH, aniline), 7.17 (1H, t, *J* = 7.9 Hz, ArCH, aniline) and 7.33 (2H, d, *J* = 8.6 Hz, ArCH, aniline) ppm. ¹³C NMR (126 MHz, CDCl₃) δ 29.5 (C(CH₃)₃), 33.7 (CH₂CH₂N), 41.0 (C(CH₃)₃), 55.0 (CH₂CH₂N), 55.2 (OCH₃), 112.0 (ArCH, phenethyl), 114.4 (ArCH, phenethyl), 121.3 (ArCH, phenethyl), 129.3 (2 x ArCH, aniline), 129.4 (ArCH, phenethyl), 130.9 (2 x ArCH, aniline), 133.7 (ArCCl), 140.5 (ArCCH₂), 142.5 (ArCN), 159.7 (ArCO) and 177.6 (NCO) ppm. HRMS (ES⁺) calcd. C₂₀H₂₅³⁵ClNO₂ (M⁺+H) 346.1568, found 346.1566; calcd. C₂₀H₂₅³⁷ClNO₂ (M⁺+H) 348.1539, found 348.1537.

***N*-(4-Chlorophenyl)-*N*-(3-methoxyphenethyl)benzamide (180e)**

C₂₂H₂₀ClNO₂, Mol. Wt.: 365.85

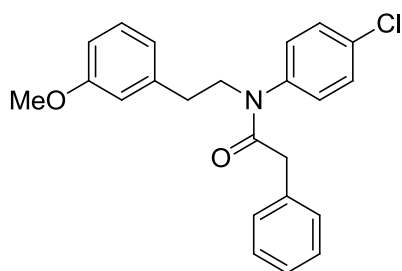


Benzoyl chloride (118 μL, 1.01 mmol) was added to a stirring solution of **179b** (150 mg, 0.503 mmol) and pyridine (123 μL, 1.51 mmol) in DCM (2 mL) and the mixture was stirred at rt for 10 h. A white precipitate was formed after the first ten minutes. The mixture was then diluted with DCM (10 mL) washed with a sat. aq. solution of NaHCO₃ (2 x 10 mL) and 1N HCl (2 x 10 mL) and the organic layer was dried with MgSO₄, filtered and evaporated to give a yellow oil (263 mg). The crude compound was purified by column chromatography (from 0% to 30% EtOAc in pet. ether) to give the product as a pale yellow oil (89 mg, 48%) which showed: ¹H NMR (500 MHz, CDCl₃) δ 2.98 (2H, t, *J* = 6.8 Hz, CH₂CH₂N), 3.77 (3H, s, OCH₃), 4.10 (2H, t, *J* = 6.8 Hz, CH₂CH₂N), 6.70 – 6.85 (5H, m), 7.14 (2H, d, *J* = 8.6 Hz), 7.20 (3H, td, *J* = 7.0,

14.4 Hz) and 7.25 – 7.31 (3H, m) ppm. ^{13}C NMR (126 MHz, CDCl_3) δ 33.8 ($\text{CH}_2\text{CH}_2\text{N}$), 52.4 ($\text{CH}_2\text{CH}_2\text{N}$), 55.1 (OCH_3), 112.1, 114.4, 121.3, 127.9, 128.6, 128.7, 129.2, 129.5, 129.8, 132.1 (ArCCl), 135.7 (ArCCO), 140.3 (ArCCH_2), 142.3 (ArCN), 159.7 (ArCO) and 170.3 (NCO) ppm. HRMS (ES^+) calcd. $\text{C}_{22}\text{H}_{21}^{35}\text{ClNO}_2$ ($\text{M}^+ + \text{H}$) 366.1255, found 366.1257; calcd. $\text{C}_{22}\text{H}_{21}^{37}\text{ClNO}_2$ ($\text{M}^+ + \text{H}$) 368.1226, found 368.1250.

***N*-(4-Chlorophenyl)-*N*-(3-methoxyphenethyl)-2-phenylacetamide (180f)**

$\text{C}_{23}\text{H}_{22}\text{ClNO}_2$, Mol. Wt.: 379.88

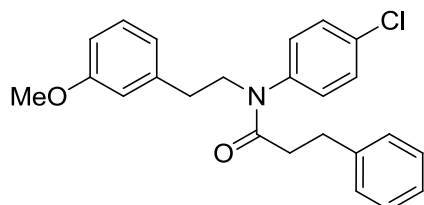


Phenacetyl chloride (136 μL , 1.01 mmol) was added to a stirring solution of **179b** (150 mg, 0.503 mmol) and pyridine (123 μL , 1.51 mmol) in DCM (2 mL) and the mixture was stirred at rt for 10 h. A white precipitate was formed after the first ten minutes. The mixture was then diluted with DCM (10 mL) washed with a sat. aq. solution of NaHCO_3 (2 x 10 mL) and 1N HCl (2 x 10 mL) and the organic layer was dried with MgSO_4 , filtered and evaporated to give a yellow oil (140 mg). The crude compound was purified by column chromatography (from 0% to 30% EtOAc in pet. ether) to give the product as a pale yellow oil (34 mg, 18%) which showed: ^1H NMR (500 MHz, CDCl_3) δ 2.84 (2H, t, $J = 7.7$ Hz, $\text{CH}_2\text{CH}_2\text{N}$), 3.41 (2H, s, ArCH_2CO), 3.75 (3H, s, OCH_3), 3.90 (2H, t, $J = 7.7$ Hz, $\text{CH}_2\text{CH}_2\text{N}$), 6.65 – 6.80 (3H, m, 3 x ArCH, phenethyl), 6.88 (2H, d, $J = 8.5$ Hz, 2 x ArCH, aniline), 7.02 (2H, d, $J = 7.0$ Hz, 2 x ArCH, phenacetyl), 7.15 (1H, t, $J = 7.8$ Hz, ArCH, phenethyl), 7.18 – 7.27 (3H, m, 3 x ArCH, phenacetyl) and 7.32 (2H, d, $J = 8.5$ Hz, 2 x ArCH, aniline) ppm. ^{13}C NMR (126 MHz, CDCl_3) δ 33.9 ($\text{CH}_2\text{CH}_2\text{N}$), 41.3 (ArCH_2CO), 51.1 ($\text{CH}_2\text{CH}_2\text{N}$), 55.1 (OCH_3), 112.0 (ArCH, phenethyl), 114.2 (ArCH, phenethyl), 121.2 (ArCH, phenethyl), 126.6 (ArCH, phenacetyl), 128.4 (2 x ArCH, phenacetyl), 128.9 (2 x ArCH, phenacetyl), 129.4 (ArCH, phenethyl), 129.7 (2 x ArCH, aniline), 129.8 (2 x ArCH, aniline), 133.8 (ArCCl), 135.0 (ArCCH_2CO), 140.0 ($\text{ArCCH}_2\text{CH}_2$), 141.1 (ArCN), 159.7 (ArCO) and

170.6 (NCO) ppm. HRMS (ES^+) calcd. $\text{C}_{23}\text{H}_{23}^{35}\text{ClNO}_2$ ($\text{M}^+ + \text{H}$) 380.1412, found 380.1408; calcd. $\text{C}_{23}\text{H}_{23}^{37}\text{ClNO}_2$ ($\text{M}^+ + \text{H}$) 382.1382, found 382.1383.

***N*-(4-Chlorophenyl)-*N*-(3-methoxyphenethyl)-3-phenylpropanamide (180g)**

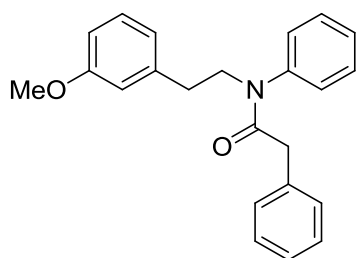
$\text{C}_{24}\text{H}_{24}\text{ClNO}_2$, Mol. Wt.: 393.91



3-Phenylpropanoyl chloride (153 μL , 1.01 mmol) was added to a stirring solution of **179b** (300 mg, 1.01 mmol) and Et_3N (353 μL , 2.53 mmol) in DCM (3 mL) and the mixture was stirred at rt overnight. The mixture was then diluted with DCM (10 mL) and washed with 1 N HCl (3 x 10 mL), 1 N NaOH (3 x 10 mL) and brine (3 x 10 mL) then dried with MgSO_4 , filtered and evaporated to give a yellow oil (364 mg) which partly solidify upon standing. The crude compound was purified by column chromatography (eluent: from 0% to 30% EtOAc in pet. ether) to give the product as a pale yellow solid (301 mg, 76%) which showed: ^1H NMR (500 MHz, CDCl_3) δ 2.31 (1H, t, $J = 6.5$ Hz, $\text{CH}_2\text{CH}_2\text{CO}$), 2.81 (1H, t, $J = 7.8$ Hz, $\text{CH}_2\text{CH}_2\text{N}$), 2.91 (1H, t, $J = 6.5$ Hz, $\text{CH}_2\text{CH}_2\text{CO}$), 3.77 (1H, s, ArOCH_3), 3.87 (1H, t, $J = 7.6$ Hz, $\text{CH}_2\text{CH}_2\text{N}$), 6.66 – 6.79 (2H, m), 7.04 – 7.10 (1H, m), 7.14 – 7.21 (1H, m), 7.21 – 7.25 (1H, m) and 7.26 – 7.33 (1H, m) ppm. ^{13}C NMR (126 MHz, CDCl_3) δ 31.7 ($\text{CH}_2\text{CH}_2\text{CO}$), 34.0 ($\text{CH}_2\text{CH}_2\text{N}$), 36.3 ($\text{CH}_2\text{CH}_2\text{CO}$), 51.0 ($\text{CH}_2\text{CH}_2\text{N}$), 55.2 (ArOCH_3), 112.0 (2 x ArCH), 114.3 (ArCH), 121.2 (ArCH), 126.1 (ArCH), 128.4 (2 x ArCH), 128.5 (2 x ArCH), 129.4 (ArCH), 129.6 (ArCH), 129.8 (2 x ArCH), 133.7 (ArCCl), 140.1 ($\text{ArCCH}_2\text{CH}_2\text{N}$), 141.0 ($\text{ArCCH}_2\text{CH}_2\text{CO}$), 141.1 (ArCN), 159.7 (ArCO) and 171.8 (CON) ppm. HRMS (ES^+) calcd. $\text{C}_{24}\text{H}_{25}^{35}\text{ClNO}_2$ ($\text{M}^+ + \text{H}$) 394.1568, found 394.1571; calcd. $\text{C}_{24}\text{H}_{25}^{37}\text{ClNO}_2$ ($\text{M}^+ + \text{H}$) 396.1539, found 396.1549.

***N*-(3-Methoxyphenethyl)-*N*,2-diphenylacetamide (180h)**

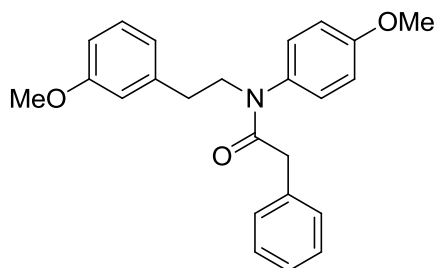
$\text{C}_{23}\text{H}_{23}\text{NO}_2$, Mol. Wt.: 345.43



Phenacetyl chloride (154 μ L, 1.14 mmol) was added to a stirring solution of **179a** (300 mg, 1.14 mmol) and Et₃N (398 μ L, 2.85 mmol) in DCM (3 mL) and the mixture was stirred at rt overnight. The mixture was then diluted with DCM (10 mL) and washed with 1 N HCl (3 x 10 mL), 1 N NaOH (3 x 10 mL) and brine (3 x 10 mL) then dried with MgSO₄, filtered and evaporated to give a yellow oil (336 mg) which partly solidify upon standing. The crude compound was purified by column chromatography (eluent: from 0% to 30% EtOAc in pet. ether) to give the product as a pale yellow-brown oil (289 mg, 73%) which showed: ¹⁹⁵ ¹H NMR (500 MHz, CDCl₃) δ 2.87 (2H, t, J = 6.7 Hz, CH₂CH₂N), 3.42 (2H, s, CH₂CO), 3.75 (3H, s, ArOCH₃), 3.93 (2H, t, J = 6.7 Hz, CH₂CH₂N), 6.69 – 6.79 (3H, m, 3 x ArCH), 6.97 – 7.09 (3H, m, 3 x ArCH), 7.11 – 7.25 (5H, m, 5 x ArCH) and 7.33 – 7.42 (3H, m, 3 x ArCH) ppm. ¹³C NMR (126 MHz, CDCl₃) δ 34.0 (CH₂CH₂N), 41.4 (CH₂CO), 51.2 (CH₂CH₂N), 55.2 (ArOCH₃), 112.0 (ArCH), 114.2 (ArCH), 121.2 (ArCH), 126.5 (ArCH), 128.0 (ArCH), 128.3 (2 x ArCH), 128.6 (2 x ArCH), 129.1 (2 x ArCH), 129.4 (ArCH), 129.6 (2 x ArCH), 135.4 (ArCCH₂CO), 140.3 (ArCCH₂CH₂), 142.6 (ArCN), 159.7 (ArCO) and 170.8 (CON) ppm. HRMS (ES⁺) calcd. C₂₃H₂₄NO₂ (M⁺+H) 346.1835, found 346.1832; C₂₃H₂₃NNaO₂ (M⁺+Na) 368.1621, found 368.1639.

***N*-(3-Methoxyphenethyl)-*N*-(4-methoxyphenyl)-2-phenylacetamide (180i)**

C₂₄H₂₅NO₃, Mol. Wt.: 375.46

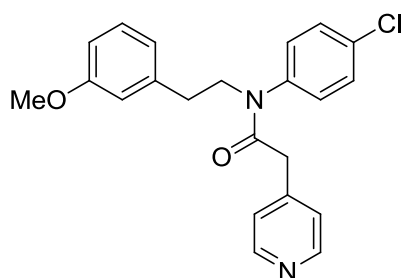


Phenacetyl chloride (138 μ L, 1.02 mmol) was added to a stirring solution of **179c** (300 mg, 1.02 mmol) and Et₃N (356 μ L, 2.55 mmol) in DCM (3 mL) and the mixture

was stirred at rt overnight. The mixture was then diluted with DCM (10 mL) and washed with 1 N HCl (3 x 10 mL), 1 N NaOH (3 x 10 mL) and brine (3 x 10 mL) then dried with MgSO₄, filtered and evaporated to give a yellow oil (379 mg) which partly solidify upon standing. The crude compound was purified by column chromatography (eluent: from 0% to 30% EtOAc in pet. ether) to give the product as a pale yellow oil (320 mg, 87%) which showed: ¹H NMR (500 MHz, CDCl₃) δ 2.85 (2H, t, *J* = 7.9 Hz, CH₂CH₂N), 3.42 (2H, s, CH₂CO), 3.75 (3H, s, ArOCH₃, phenethyl), 3.84 (3H, s, ArOCH₃, aniline), 3.89 (2H, t, *J* = 7.9 Hz, CH₂CH₂N), 6.68 - 6.79 (3H, m, 3 x ArCH, phenethyl), 6.88 (2H, d, *J* = 17.4 Hz, 2 x ArCH, aniline), 6.90 (2H, d, *J* = 17.4 Hz, 2 x ArCH, aniline), 7.04 (2H, d, *J* = 7.2 Hz, 2 x ArCH, phenacetyl), 7.15 (1H, t, *J* = 7.8 Hz, ArCH, phenethyl), 7.21 (1H, t, *J* = 6.9 Hz, ArCH, phenacetyl) and 7.23 (2H, t, *J* = 6.9 Hz, 2 x ArCH, phenacetyl) ppm. ¹³C NMR (126 MHz, CDCl₃) δ 33.9 (CH₂CH₂N), 41.1 (CH₂CO), 51.1 (CH₂CH₂N), 55.1 (ArOCH₃, phenethyl), 55.5 (ArOCH₃, aniline), 112.0 (ArCH, phenethyl), 114.2 (ArCH, phenethyl), 114.6 (2 x ArCH, aniline), 121.2 (ArCH, phenethyl), 126.5 (ArCH, phenacetyl), 128.3 (2 x ArCH, phenacetyl), 129.0 (2 x ArCH, phenacetyl), 129.3 (ArCH, phenethyl), 129.5 (2 x ArCH, aniline), 135.3 (ArCN), 135.5 (ArCCH₂CO), 140.3 (ArCCH₂CH₂), 159.0 (ArCO, aniline), 159.6 (ArCO, phenethyl) and 171.2 (CON) ppm. HRMS (ES⁺) calcd. C₂₄H₂₆NO₃ (M⁺+H) 376.1907, found 376.1918.

***N*-(4-Chlorophenyl)-*N*-(3-methoxyphenethyl)-2-(pyridin-4-yl)acetamide (180j)**

C₂₂H₂₁ClN₂O₂, Mol. Wt.: 380.87

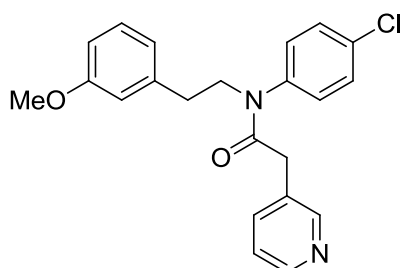


A solution of **179b** (500 mg, 1.91 mmol) in DCM (3 mL) was added to a stirring solution of 2-(pyridin-4-yl)acetic acid hydrochloride (372 mg, 2.10 mmol), EDCI (935 mg, 4.78 mmol) and Et₃N (533 μL, 3.82 mmol) in DCM (6 mL) and the mixture was stirred overnight at rt. The mixture was diluted with DCM (20 mL) and washed with 1 N NaOH (3 x 25 mL) and brine (25 mL) then dried with MgSO₄, filtered and

evaporated to give a yellow oil (825 mg). The crude compound was purified by column chromatography (eluent: from 0% to 10% MeOH in DCM) to give the product as a yellow oil (463 mg, 64%) which showed: ^1H NMR (500 MHz, CDCl_3) δ 2.86 (2H, t, J = 7.5 Hz, $\text{CH}_2\text{CH}_2\text{N}$), 3.45 (2H, s, CH_2CO), 3.77 (3H, s, OCH_3), 3.95 (2H, t, J = 7.5 Hz, $\text{CH}_2\text{CH}_2\text{N}$), 6.70 (1H, s, ArCH, phenyl), 6.74 (1H, d, J = 7.7 Hz, ArCH, phenyl), 6.77 (1H, d, J = 7.7 Hz, ArCH, phenyl), 6.92 (2H, d, J = 7.8 Hz, 2 x ArCH, aniline), 7.14 (2H, d, J = 4.6 Hz, 2 x ArCH, pyridine), 7.18 (1H, t, J = 7.7 Hz, ArCH, phenyl), 7.38 (2H, d, J = 7.8 Hz, 2 x ArCH, aniline) and 8.52 (2H, d, J = 4.6 Hz, 2 x ArCH, pyridine) ppm. ^{13}C NMR (126 MHz, CDCl_3) δ 33.8 ($\text{CH}_2\text{CH}_2\text{N}$), 40.8 (CH_2CO), 51.0 ($\text{CH}_2\text{CH}_2\text{N}$), 55.2 (OCH_3), 112.0 (ArCH, phenyl), 114.5 (ArCH, phenyl), 121.2 (ArCH, phenyl), 125.1 (2 x ArCH, pyridine), 129.5 (ArCH, phenyl), 129.6 (2 x ArCH, aniline), 130.2 (2 x ArCH, aniline), 134.5 (ArCCl), 139.7 (ArCCH₂, phenyl), 140.6 (ArCN), 146.7 (ArCCH₂, pyridine), 147.6 (2 x ArCH, pyridine), 159.8 (ArCO) and 168.4 (CON) ppm.

***N*-(4-Chlorophenyl)-*N*-(3-methoxyphenethyl)-2-(pyridin-3-yl)acetamide (180k)**

$\text{C}_{22}\text{H}_{21}\text{ClN}_2\text{O}_2$, Mol. Wt.: 380.87

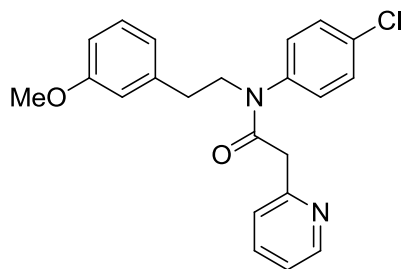


A solution of **179b** (500 mg, 1.91 mmol) in DCM (3 mL) was added to a stirring solution of 2-(pyridin-3-yl)acetic acid hydrochloride (372 mg, 2.10 mmol), EDCI (935 mg, 4.78 mmol) and Et_3N (533 μL , 3.82 mmol) in DCM (6 mL) and the mixture was stirred overnight at rt. The mixture was diluted with DCM (20 mL) and washed with 1 N NaOH (3 x 25 mL) and brine (25 mL) then dried with MgSO_4 , filtered and evaporated to give a yellow oil (763 mg). The crude compound was purified by column chromatography (eluent: from 0% to 10% MeOH in DCM) to give the product as a yellow oil (437 mg, 60%) which showed: ^1H NMR (500 MHz, CDCl_3) δ 2.86 (2H, t, J = 7.7 Hz, $\text{CH}_2\text{CH}_2\text{N}$), 3.43 (2H, s, CH_2CO), 3.77 (3H, s, OCH_3), 3.93 (2H, t, J = 7.7 Hz, $\text{CH}_2\text{CH}_2\text{N}$), 6.70 (1H, d, J = 2.1 Hz, ArCH, phenyl), 6.73 (1H, d, J = 7.9 Hz, ArCH,

phenyl), 6.77 (1H, dd, $J = 2.1, 7.9$ Hz, ArCH, phenyl), 6.96 (2H, d, $J = 8.5$ Hz, 2 x ArCH, aniline), 7.18 (1H, t, $J = 7.9$ Hz, ArCH, phenyl), 7.34 (1H, dd, $J = 5.0, 7.8$ Hz, ArCH, pyridine), 7.41 (2H, d, $J = 8.5$ Hz, 2 x ArCH, aniline), 7.68 (1H, d, $J = 7.8$ Hz, ArCH, pyridine), 8.26 (1H, s, ArCH, pyridine) and 8.52 (1H, d, $J = 5.0$ Hz, ArCH, pyridine) ppm. ^{13}C NMR (126 MHz, CDCl_3) δ 33.9 ($\text{CH}_2\text{CH}_2\text{N}$), 38.3 (CH_2CO), 51.2 ($\text{CH}_2\text{CH}_2\text{N}$), 55.2 (OCH_3), 112.0 (ArCH, phenyl), 114.4 (ArCH, phenyl), 121.2 (ArCH, phenyl), 123.9 (ArCH, pyridine), 129.5 (ArCH, phenyl), 129.7 (2 x ArCH, aniline), 130.2 (2 x ArCH, aniline), 131.8 (ArCCH_2 , pyridine), 134.5 (ArCCl), 138.6 (ArCH, pyridine), 139.8 (ArCCH_2 , phenyl), 140.7 (ArCN), 146.5 (ArCH, pyridine), 148.5 (ArCH, pyridine), 159.8 (ArCO) and 169.1 (CON) ppm.

***N*-(4-Chlorophenyl)-*N*-(3-methoxyphenethyl)-2-(pyridin-2-yl)acetamide (180l)**

$\text{C}_{22}\text{H}_{21}\text{ClN}_2\text{O}_2$, Mol. Wt.: 380.87

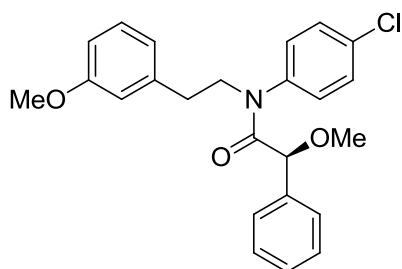


A solution of **179b** (500 mg, 1.91 mmol) in DCM (3 mL) was added to a stirring solution of 2-(pyridin-2-yl)acetic acid hydrochloride (372 mg, 2.10 mmol), EDCI (935 mg, 4.78 mmol) and Et_3N (533 μL , 3.82 mmol) in DCM (6 mL) and the mixture was stirred overnight at rt. The mixture was diluted with DCM (20 mL) and washed with 1 N NaOH (3 x 25 mL) and brine (25 mL) then dried with MgSO_4 , filtered and evaporated to give a yellow oil (869 mg). The crude compound was purified by column chromatography (eluent: from 0% to 10% MeOH in DCM) to give the product as a yellow oil (485 mg, 67%) which showed: ^1H NMR (500 MHz, CDCl_3) δ 2.81 – 2.97 (2H, m, $\text{CH}_2\text{CH}_2\text{N}$), 3.69 (2H, s, CH_2CO), 3.77 (3H, s, OCH_3), 3.90 – 4.00 (2H, m, $\text{CH}_2\text{CH}_2\text{N}$), 6.73 (1H, s, ArCH, phenyl), 6.76 (1H, d, $J = 7.9$ Hz, ArCH, phenyl), 6.77 (1H, d, $J = 7.9$ Hz, ArCH, phenyl), 7.07 (2H, d, $J = 8.5$ Hz, 2 x ArCH, aniline), 7.18 (1H, t, $J = 7.9$ Hz, ArCH, phenyl), 7.20 – 7.26 (2H, m, 2 x ArCH, pyridine), 7.36 (2H, d, $J = 8.5$ Hz, 2 x ArCH, aniline), 7.63 – 7.73 (1H, m, ArCH, pyridine) and 8.51 (1H, d, $J = 4.5$ Hz, ArCH, pyridine) ppm. ^{13}C NMR (126 MHz, CDCl_3) δ 34.0 ($\text{CH}_2\text{CH}_2\text{N}$),

43.5 (CH₂N), 51.2 (CH₂CH₂N), 55.2 (OCH₃), 112.1 (ArCH, phenyl), 114.3 (ArCH, phenyl), 121.2 (ArCH, phenyl), 122.1 (ArCH, pyridine), 124.5 (ArCH, pyridine), 129.5 (ArCH, phenyl), 129.8 (2 x ArCH, aniline), 129.9 (2 x ArCH, aniline), 134.1 (ArCCl), 137.3 (ArCH, pyridine), 140.1 (ArCCH₂), 140.9 (ArCN), 148.3 (ArCH, pyridine), 155.2 (ArCCH₂, pyridine), 159.7 (ArCO) and 169.3 (CON) ppm.

(*S*)-*N*-(4-Chlorophenyl)-2-methoxy-*N*-(3-methoxyphenethyl)-2-phenylacetamide (180m)

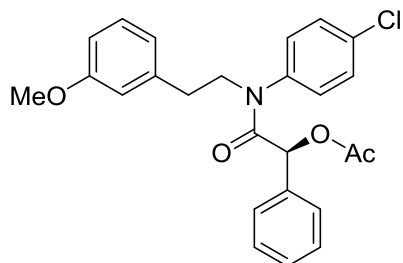
C₂₄H₂₄ClNO₃, Mol. Wt.: 409.91



A solution of **179b** (500 mg, 1.91 mmol) in DCM (3 mL) was added to a stirring solution of (*S*)-2-methoxy-2-phenylacetic acid (352 mg, 2.10 mmol), EDCI (935 mg, 4.78 mmol) and Et₃N (533 µL, 3.82 mmol) in DCM (6 mL) and the mixture was stirred overnight at rt. The mixture was diluted with DCM (20 mL) and washed with 1 N NaOH (3 x 25 mL) and brine (25 mL) then dried with MgSO₄, filtered and evaporated to give a yellow oil (668 mg). The crude compound was purified by column chromatography (eluent: from 0% to 40% EtOAc in pet. ether) to give the product as a yellow oil (422 mg, 54%) which showed: ¹H NMR (500 MHz, CDCl₃) δ 2.77 – 2.94 (2H, m, CH₂CH₂N), 3.23 (3H, s, CHOCH₃), 3.78 (3H, s, ArOCH₃), 3.81 – 3.92 (1H, m, CH₂CH₂N), 3.92 – 4.05 (1H, m, CH₂CH₂N), 4.57 (1H, s, CHOCH₃), 6.65 – 6.73 (2H, m, 2 x ArCH, methoxyphenyl), 6.73 – 6.85 (2H, m, ArCH, methoxyphenyl, ArCH), 7.10 (2H, d, *J* = 6.8 Hz, 2 x ArCH), 7.16 (1H, t, *J* = 8.1 Hz, ArCH, methoxyphenyl) and 7.31 (6H, dd, *J* = 2.2, 6.8 Hz, 6 x ArCH) ppm. ¹³C NMR (126 MHz, CDCl₃) δ 33.8 (CH₂CH₂N), 51.5 (CH₂CH₂N), 55.2 (ArOCH₃), 56.8 (CHOCH₃), 80.9 (CHOCH₃), 112.1 (ArCH, methoxyphenyl), 114.3 (ArCH, methoxyphenyl), 121.3 (ArCH, methoxyphenyl), 128.2 (2 x ArCH), 128.4 (2 x ArCH), 128.7 (ArCH), 129.4 (ArCH, methoxyphenyl), 129.7 (2 x ArCH), 130.3 (2 x ArCH), 134.2 (ArCCl), 136.1 (ArCCH), 139.9 (ArCN), 140.0 (ArCCH₂), 159.7 (ArCO) and 169.5 (CON) ppm.

(*S*)-2-((4-Chlorophenyl)(3-methoxyphenethyl)amino)-2-oxo-1-phenylethyl acetate (180n**)**

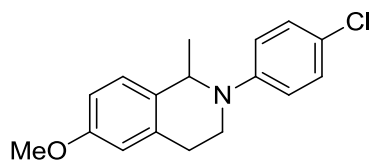
C₂₅H₂₄ClNO₄, Mol. Wt.: 437.92



A solution of **179b** (100 mg, 0.335 mmol) in DCM (2 mL) was added to a stirring solution of (*S*)-2-methoxy-2-phenylacetic acid (66 mg, 0.335 mmol), EDCI (131 mg, 0.670 mmol) and Et₃N (106 μ L, 0.764 mmol) in DCM (2 mL) and the mixture was stirred overnight at rt. The mixture was diluted with DCM (20 mL) and washed with 1 N NaOH (3 x 25 mL) and brine (25 mL) then dried with MgSO₄, filtered and evaporated to give a yellow oil (115 mg) which showed: ¹H NMR (400 MHz, CDCl₃) δ 2.14 (3H, s), 2.72 – 2.90 (2H, m), 3.74 (3H, s), 3.85 (2H, t, *J* = 7.8 Hz), 5.66 (1H, s), 6.63 – 6.69 (2H, m), 6.69 – 6.75 (1H, m), 7.04 (2H, d, *J* = 7.1 Hz), 7.11 (1H, t, *J* = 8.0 Hz) and 7.24 – 7.36 (7H, m) ppm. HRMS (ES⁺) calcd. C₂₅H₂₄³⁵ClNNaO₄ (M⁺+H) 460.1286, found 460.1311.

2-(4-Chlorophenyl)-6-methoxy-1-methyl-1,2,3,4-tetrahydroisoquinoline (181a**)**

C₁₇H₁₈ClNO, Mol. Wt.: 287.78



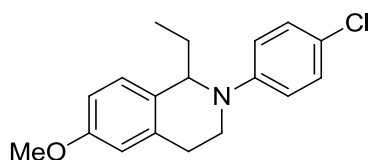
(Method K)

The crude compound was purified by column chromatography (eluent: 100% pet. ether) to give white solid (292 mg, 69%) which showed: ¹H NMR (500 MHz, CDCl₃) δ 1.39 (3H, d, *J* = 6.6 Hz, CHCH₃), 2.77 – 2.93 (1H, m, H₄-THIQ), 2.93 – 3.06 (1H, m, H₄-THIQ), 3.41 – 3.50 (1H, m, H₃-THIQ), 3.50 – 3.62 (1H, m, H₃-THIQ), 3.79 (3H, s,

OCH₃), 4.81 (1H, q, J = 6.6 Hz, CHCH₃), 6.68 (1H, d, J = 2.6 Hz, H₅-THIQ), 6.76 (1H, dd, J = 2.6, 8.4 Hz, H₇-THIQ), 6.84 (2H, bs, 2 x ArCH, phenyl), 7.04 (1H, d, J = 8.4 Hz, H₈-THIQ) and 7.19 (2H, d, J = 8.9 Hz, 2 x ArCH, phenyl) ppm. ¹³C NMR (126 MHz, CDCl₃) δ 20.8 (C₁CH₃), 28.6 (C₄-THIQ), 41.2 (C₃-THIQ), 54.0 (C₁-THIQ), 55.3 (OCH₃), 112.4 (C₇-THIQ), 113.2 (C₅-THIQ), 115.8 (2 x ArCH, phenyl), 122.2 (ArCCl), 127.7 (C₈-THIQ), 129.0 (2 x ArCH, phenyl), 131.9 (C₈CC₁), 135.4 (C₅CC₄), 147.9 (ArCN) and 158.0 (C₆-THIQ) ppm. HRMS (ES⁺) calcd. C₁₇H₁₉³⁵ClNO (M⁺+H) 288.1150, found 288.1157; calcd. C₁₇H₁₉³⁷ClNO (M⁺+H) 290.1120, found 290.1142. Mp 186-189 °C (as a hydrochloride from Et₂O).

2-(4-Chlorophenyl)-1-ethyl-6-methoxy-1,2,3,4-tetrahydroisoquinoline (181b)

C₁₈H₂₀ClNO, Mol. Wt.: 301.81



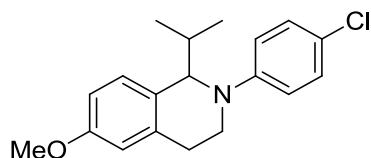
(Method K)

The crude compound was purified by column chromatography (eluent: 100 % pet. ether) to give the product as a colourless oil (335 mg, 71%) which showed: ¹H NMR (500 MHz, CDCl₃) δ 0.99 (3H, t, J = 7.4 Hz, CH₃CH₂), 1.71 (1H, ddq, J = 7.0, 7.4, 14.2 Hz, CH₃CH₂), 1.94 (1H, ddq, J = 7.0, 7.4, 14.2 Hz, CH₃CH₂), 2.86 (1H, dd, J = 5.7, 15.8 Hz, H₄-THIQ), 2.97 (1H, ddd, J = 5.3, 7.8, 15.8 Hz, H₄-THIQ), 3.43 - 3.55 (1H, m, H₃-THIQ), 3.58 (1H, ddd, J = 5.0, 7.8, 12.6 Hz, H₄-THIQ), 3.80 (3H, s, OCH₃), 4.45 (1H, t, J = 7.0 Hz, H₁-THIQ), 6.71 (1H, d, J = 2.6 Hz, H₅-THIQ), 6.75 (1H, dd, J = 2.6, 8.4 Hz, H₇-THIQ), 6.78 (2H, d, J = 9.1 Hz, 2 x ArCH, phenyl), 7.04 (1H, d, J = 8.4 Hz, H₈-THIQ) and 7.18 (2H, d, J = 9.1 Hz, 2 x ArCH, phenyl) ppm. ¹³C NMR (126 MHz, CDCl₃) δ 11.3 (CH₃CH₂), 27.5 (C₄-THIQ), 29.5 (CH₃CH₂), 42.1 (C₃-THIQ), 55.2 (OCH₃), 60.2 (C₁-THIQ), 111.7 (C₇-THIQ), 113.3 (C₅-THIQ), 114.6 (2 x ArCH, phenyl), 121.4 (ArCCl), 128.3 (C₈-THIQ), 128.9 (2 x ArCH, phenyl), 130.7 (C₁CC₈-THIQ), 136.0 (C₄CC₅-THIQ), 148.3 (ArCN) and 158.1 (C₆-THIQ) ppm. HRMS (ES⁺) calcd. C₁₈H₂₁³⁵ClNO (M⁺+H) 302.1306, found 302.1292; calcd. C₁₈H₂₁³⁷ClNO (M⁺+H) 304.1277, found 304.1287. Mp 142-144 °C (pet. ether).

2-(4-Chlorophenyl)-1-isopropyl-6-methoxy-1,2,3,4-tetrahydroisoquinoline

(181c)

C₁₉H₂₂ClNO, Mol. Wt.: 315.84

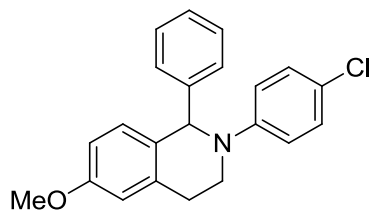


(Method K)

The crude compound was purified by column chromatography (eluent: 100% pet. ether) to give a colourless oil (267 mg, 56%) which showed: ¹H NMR (500 MHz, CDCl₃) δ 0.92 (3H, d, *J* = 6.6 Hz, (CH₃)₂CH), 1.03 (3H, d, *J* = 6.9 Hz, (CH₃)₂CH), 2.03 – 2.13 (1H, m, (CH₃)₂CH), 2.92 – 3.01 (2H, m, H₄-THIQ), 3.36 – 3.46 (1H, m, H₃-THIQ), 3.68 (1H, dt, *J* = 6.1, 12.2 Hz, H₃-THIQ), 3.79 (3H, s, OCH₃), 4.26 (1H, d, *J* = 8.1 Hz, H₁-THIQ), 6.68 – 6.72 (2H, m, H₅,H₇-THIQ), 6.76 (2H, d, *J* = 9.1 Hz, 2 x ArCH, phenyl), 7.02 (1H, d, *J* = 7.9 Hz, H₈-THIQ) and 7.14 (2H, d, *J* = 9.1 Hz, 2 x ArCH, phenyl) ppm. ¹³C NMR (126 MHz, CDCl₃) δ 20.0 ((CH₃)₂CH), 20.5 ((CH₃)₂CH), 27.5 (C₄-THIQ), 34.4 ((CH₃)₂CH), 42.9 (C₃-THIQ), 55.2 (OCH₃), 64.2 (C₁-THIQ), 111.0 (C₇-THIQ), 113.4 (C₅-THIQ), 114.3 (2 x ArCH, phenyl), 121.1 (ArCCl), 128.8 (2 x ArCH, phenyl), 129.2 (C₈-THIQ), 129.6 (C₁CC₈-THIQ), 136.3 (C₅CC₄-THIQ), 148.6 (ArCN) and 158.3 (C₆-THIQ) ppm. HRMS (ES⁺) calcd. C₁₉H₂₃³⁵ClNO (M⁺+H) 316.1463, found 316.1460; calcd. C₁₉H₂₃³⁷ClNO (M⁺+H) 318.1433, found 318.1448.

2-(4-Chlorophenyl)-6-methoxy-1-phenyl-1,2,3,4-tetrahydroisoquinoline (181e)

C₂₂H₂₀ClNO, Mol. Wt.: 349.85

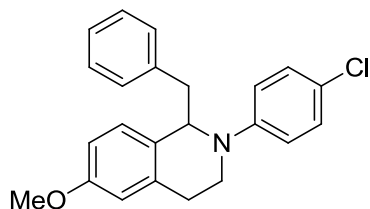


(Method K)

The crude compound was purified by column chromatography (eluent: 100% pet. ether) to give a colourless oil (342 mg, 68%) which showed: ^1H NMR (400 MHz, CDCl_3) δ 2.80 – 2.97 (2H, m, $\text{H}_4\text{-THIQ}$), 3.45 (1H, ddd, $J = 5.7, 8.0, 11.4$ Hz, $\text{H}_3\text{-THIQ}$), 3.66 (1H, dt, $J = 5.5, 11.2$ Hz, $\text{H}_3\text{-THIQ}$), 3.79 (3H, s, OCH_3), 5.71 (1H, s, $\text{H}_1\text{-THIQ}$), 6.71 (1H, d, $J = 2.6$ Hz, $\text{H}_5\text{-THIQ}$), 6.74 (2H, d, $J = 9.1$ Hz, 2 x ArCH, *N*-phenyl), 6.77 (2H, dd, $J = 2.5, 8.3$ Hz, $\text{H}_7\text{-THIQ}$), 7.14 (2H, d, $J = 9.1$ Hz, 2 x ArCH, *N*-phenyl) and 7.16 – 7.25 (6H, m, $\text{H}_8\text{-THIQ}$, 5 x ArCH, $\text{C}_1\text{-phenyl}$) ppm. ^{13}C NMR (101 MHz, CDCl_3) δ 28.2 ($\text{C}_4\text{-THIQ}$), 43.8 ($\text{C}_3\text{-THIQ}$), 55.2 (OCH_3), 62.3 ($\text{C}_1\text{-THIQ}$), 111.9 ($\text{C}_7\text{-THIQ}$), 113.2 ($\text{C}_5\text{-THIQ}$), 115.1 (2 x ArCH, *N*-phenyl), 122.2 (ArCCl), 126.8 (ArCH), 127.1 (2 x ArCH, $\text{C}_1\text{-phenyl}$), 128.2 (2 x ArCH, $\text{C}_1\text{-phenyl}$), 128.7 (ArCH), 128.9 (2 x ArCH, *N*-phenyl), 129.9 ($\text{C}_1\text{CC}_8\text{-THIQ}$), 136.7 ($\text{C}_4\text{CC}_5\text{-THIQ}$), 143.0 (ArCC $_1$, $\text{C}_1\text{-phenyl}$), 148.1 (ArCN) and 158.6 ($\text{C}_6\text{-THIQ}$) ppm. Mp 188-191 °C (pet. ether)

1-Benzyl-2-(4-chlorophenyl)-6-methoxy-1,2,3,4-tetrahydroisoquinoline (181f)

$\text{C}_{23}\text{H}_{22}\text{ClNO}$, Mol. Wt.: 363.88



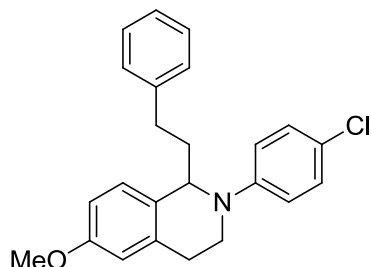
(Method K)

The crude compound was purified by column chromatography (eluent: 100% pet. ether) to give a yellow oil (437 mg, 78%) which showed: ^1H NMR (500 MHz, CDCl_3) δ 2.92 – 3.05 (1H, m), 3.05 – 3.19 (1H, m), 3.29 – 3.43 (1H, m), 3.67 – 3.78 (1H, m), 3.80 (3H, s), 3.83 – 3.92 (1H, m), 3.92 – 4.03 (1H, m), 4.86 – 4.96 (1H, m), 6.57 (1H, d, $J = 7.8$ Hz), 6.66 (1H, dd, $J = 2.6, 8.6$ Hz), 6.74 (1H, d, $J = 2.5$ Hz), 7.03 – 7.12 (2H, m), 7.19 – 7.25 (3H, m), 7.32 – 7.40 (2H, m) and 7.61 (2H, d, $J = 8.4$ Hz) ppm. ^{13}C NMR (126 MHz, CDCl_3) δ 25.2, 40.1, 51.4, 55.3, 66.2, 107.0, 113.2, 113.5, 123.5, 123.9, 127.1, 128.4, 128.7, 129.6, 130.1, 134.8, 136.0, 140.4, 142.2 and 159.5 ppm. Mp 149-151 °C (pet. ether).

2-(4-Chlorophenyl)-6-methoxy-1-phenethyl-1,2,3,4-tetrahydroisoquinoline

(181g)

C₂₄H₂₄ClNO, Mol. Wt.: 377.91

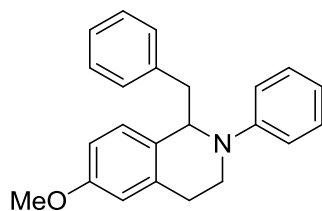


(Method K)

The crude compound was purified by column chromatography (eluent: from 0% to 20% EtOAc in pet. ether) to give a yellow oil (194 mg, 67%) which showed: ¹H NMR (500 MHz, CDCl₃) δ 1.94 - 2.05 (1H, m, CHH₂CH₂), 2.17 - 2.34 (1H, m, CHCH₂CH₂), 2.66 - 2.79 (2H, m, CHCH₂CH₂), 2.80 - 2.90 (1H, m, H₄-THIQ), 2.90 - 3.03 (1H, m H₄-THIQ), 3.52 - 3.68 (2H, m H₃-THIQ), 3.79 (3H, s, OCH₃), 4.55 (1H, t, *J* = 6.9 Hz, H₁-THIQ), 6.68 (1H, d, *J* = 2.4 Hz, H₅-THIQ), 6.71 - 6.83 (3H, m, H₇-THIQ, 2 x ArCH, *N*-phenyl), 7.05 (1H, d, *J* = 8.4 Hz, H₈-THIQ), 7.10 - 7.22 (5H, m, 3 x ArCH, phenethyl, 2 x ArCH, *N*-phenyl) and 7.25 - 7.31 (2H, m, 2 x ArCH, phenethyl) ppm. ¹³C NMR (126 MHz, CDCl₃) δ 26.9 (C₄-THIQ), 32.7 (CHCH₂CH₂), 38.0 (CHCH₂CH₂), 43.2 (C₃-THIQ), 55.3 (OCH₃), 59.0 (C₁-THIQ), 112.1, 113.5 (C₅-THIQ), 121.0, 125.9, 128.2 (C₈-THIQ), 128.4 (2 x ArCH), 128.5 (2 x ArCH), 129.0, 135.9 (C₁CC₈-THIQ), 141.6 (ArCCH₂, phenethyl), 147.7 (ArCN) and 158.3 (C₆-THIQ) ppm. HRMS (ES⁺) calcd. C₂₄H₂₅³⁷ClNO (M⁺+H) 380.1590, found 380.1615.

1-Benzyl-6-methoxy-2-phenyl-1,2,3,4-tetrahydroisoquinoline (181h)

C₂₃H₂₃NO, Mol. Wt.: 329.43

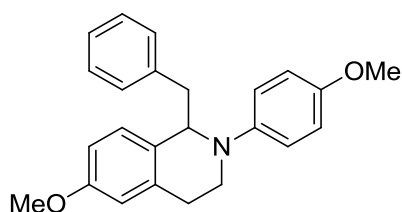


(Method K)

The crude compound was purified by column chromatography (eluent: from 0% to 20% EtOAc in pet. ether) to give a yellow oil (155 mg, 58%) which showed:¹⁹⁵ ¹H NMR (500 MHz, CDCl₃) δ 2.64 – 2.83 (1H, m, 1 x H₄-THIQ), 2.87 – 3.06 (2H, m, 1 x H₄-THIQ, 1 x CHCH₂), 3.11 – 3.34 (1H, m, 1 x CHCH₂), 3.44 – 3.58 (1H, m, H₃-THIQ), 3.58 – 3.70 (1H, m, H₃-THIQ), 3.78 (3H, s, OCH₃), 4.86 (1H, t, *J* = 6.5 Hz, H₁-THIQ), 6.60 (1H, dd, *J* = 2.4, 8.4 Hz, H₇-THIQ), 6.63 (1H, d, *J* = 8.4 Hz, H₈-THIQ), 6.67 (1H, d, *J* = 1.8 Hz, H₅-THIQ), 6.70 – 6.79 (1H, m), 6.79 – 6.94 (2H, m), 7.02 (2H, d, *J* = 6.5 Hz) and 7.15 – 7.25 (5H, m) ppm. ¹³C NMR (126 MHz, CDCl₃) δ 27.8 (C₄-THIQ), 42.1 (C₃-THIQ), 42.4 (CHCH₂), 55.2 (OCH₃), 61.0 (C₁-THIQ), 111.5 (C₇-THIQ), 113.0 (C₅-THIQ), 113.7 (2 x ArCH), 117.3 (ArCH), 126.2 (ArCH), 128.1 (2 x ArCH), 128.6 (C₈-THIQ), 129.2 (2 x ArCH), 129.6 (C₁CC₈-THIQ), 129.8 (2 x ArCH), 136.2 (C₄CC₅-THIQ), 138.7 (ArCCH₂CH), 149.1 (ArCN) and 158.1 (C₆-THIQ) ppm.

1-Benzyl-6-methoxy-2-(4-methoxyphenyl)-1,2,3,4-tetrahydroisoquinoline (181i)

C₂₄H₂₅NO₂, Mol. Wt.: 359.46



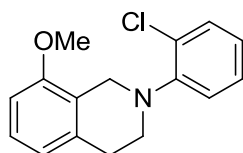
(Method K)

The crude compound was purified by column chromatography (eluent: from 0% to 20% EtOAc in pet. ether) to give a yellow oil (182 mg, 61%) which showed:¹⁸⁷ ¹H NMR (500 MHz, CDCl₃) δ 2.62 – 2.79 (1H, m, 1 x H₄-THIQ), 2.86 – 3.05 (2H, m, 1 x H₄-THIQ, 1 x CHCH₂), 3.20 (1H, dd, *J* = 5.4, 13.5 Hz, 1 x CHCH₂), 3.43 – 3.55 (1H, m, H₃-THIQ), 3.60 (1H, ddd, *J* = 4.5, 9.0, 13.5 Hz, H₃-THIQ), 3.77 (3H, s, OCH₃), 3.79 (3H, s, OCH₃), 4.76 (1H, t, *J* = 6.5 Hz, H₁-THIQ), 6.59 – 6.66 (2H, m, H₇-THIQ, H₈-THIQ), 6.67 (1H, d, *J* = 1.7 Hz, H₅-THIQ), 6.78 – 6.92 (4H, m), 7.04 (2H, d, *J* = 6.8 Hz) and 7.15 – 7.29 (3H, m) ppm. ¹³C NMR (126 MHz, CDCl₃) δ 27.5 (C₄-THIQ), 42.0 (CHCH₂), 42.4 (C₃-THIQ), 55.1 (OCH₃), 55.6 (OCH₃), 61.8 (C₁-THIQ), 111.5 (C₇-THIQ), 113.1 (C₅-THIQ), 114.6 (2 x ArCH), 116.8 (2 x ArCH), 126.0 (ArCH), 128.0 (2 x ArCH), 128.6 (C₈-THIQ), 129.7 (2 x ArCH), 130.0 (C₁CC₈-THIQ), 136.0 (C₄CC₅-

THIQ), 139.3 (ArCCH₂CH), 144.2 (ArCN), 152.4 (ArCO, phenyl) and 158.0 (C₆-THIQ) ppm.

2-(2-Chlorophenyl)-8-methoxy-1,2,3,4-tetrahydroisoquinoline (185v)

C₁₆H₁₆ClNO, Mol. Wt.: 273.76

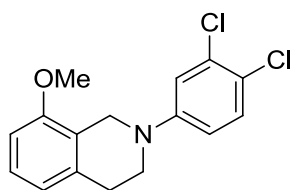


(Method J)

The crude compound was purified by column chromatography (eluent: from 0% to 10% EtOAc in pet. ether) to give a pale yellow oil (46 mg, 4%) which showed: ¹H NMR (400 MHz, CDCl₃) δ 3.01 (2H, t, *J* = 5.7 Hz), 3.36 (2H, t, *J* = 5.7 Hz), 3.82 (3H, s), 4.21 (2H, s), 6.70 (1H, d, *J* = 8.1 Hz), 6.78 (1H, d, *J* = 7.6 Hz), 6.94 – 7.00 (1H, m), 7.15 (1H, t, *J* = 7.9 Hz), 7.18 – 7.23 (2H, m) and 7.38 (1H, dd, *J* = 1.5, 7.9 Hz) ppm. LC/MS (ES⁺) *t*_r = 4.13 min (82 %), *m/z* 274.1 (M⁺+H); (RP, Isocratic, 90% MeOH)

2-(3,4-Dichlorophenyl)-8-methoxy-1,2,3,4-tetrahydroisoquinoline (185aa)

C₁₆H₁₅Cl₂NO, Mol. Wt.: 308.20



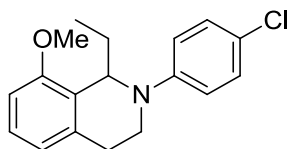
(Method J)

The crude compound was purified by column chromatography (eluent: from 0% to 20% EtOAc in pet. ether) to give pale yellow oil (36 mg, 4%) which showed: ¹H NMR (500 MHz, CDCl₃) δ 2.95 (2H, t, *J* = 5.8 Hz, H₄-THIQ), 3.50 (2H, t, *J* = 5.8 Hz, H₃-THIQ), 3.87 (3H, s, OCH₃), 4.28 (2H, s, H₁-THIQ), 6.73 (1H, d, *J* = 8.1 Hz, H₇-THIQ), 6.78 (1H, d, *J* = 7.6 Hz, H₅-THIQ), 6.82 (1H, dd, *J* = 2.9, 9.0 Hz, ArCH, phenyl), 7.04 (1H, d, *J* = 2.9 Hz, ArCH, phenyl), 7.17 (1H, t, *J* = 7.9 Hz, H₆-THIQ) and 7.28 (1H, d, *J* = 9.0 Hz, ArCH, phenyl) ppm. ¹³C NMR (126 MHz, CDCl₃) δ 29.1, 45.6, 45.7, 55.4,

107.5, 114.3, 116.1, 120.8, 122.5, 127.2, 130.6, 132.9, 135.9, 150.2 and 156.2 ppm.
LC/MS (ES⁺) t_r = 6.12 min (12 %), m/z 308.1 (M⁺+H); (RP, Isocratic, 90% MeOH)

2-(4-Chlorophenyl)-1-ethyl-8-methoxy-1,2,3,4-tetrahydroisoquinoline (190b)

C₁₈H₂₀ClNO, Mol. Wt.: 301.81

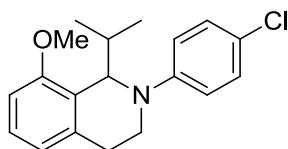


(Method K)

The crude compound was purified by column chromatography (eluent: 100% pet. ether) to give a colourless oil (24 mg, 5%) which showed: ¹H NMR (400 MHz, CDCl₃) δ 0.97 (3H, t, *J* = 7.4 Hz, CH₃CH₂), 1.74 – 1.91 (2H, m, CH₃CH₂), 2.78 (1H, dt, *J* = 5.1, 16.2 Hz, H₄-THIQ), 2.97 (1H, ddd, *J* = 5.9, 8.8, 15.0 Hz, H₄-THIQ), 3.49 – 3.68 (2H, m, H₃-THIQ), 3.83 (3H, s, OCH₃), 4.87 (1H, dd, *J* = 5.7, 8.0 Hz, H₁-THIQ), 6.71 (1H, d, *J* = 7.9 Hz, H₅ or H₇-THIQ), 6.72 (1H, d, *J* = 7.9 Hz, H₅ or H₇-THIQ), 6.80 (2H, d, *J* = 9.1 Hz, 2 x ArCH, phenyl), 7.11 (1H, t, *J* = 7.9 Hz, H₆-THIQ) and 7.13 (2H, d, *J* = 9.2 Hz, 2 x ArCH, phenyl) ppm. ¹³C NMR (101 MHz, CDCl₃) δ 11.3 (CH₃CH₂), 26.3 (C₄-THIQ), 27.6 (CH₃CH₂), 41.1 (C₃-THIQ), 54.6 (C₁-THIQ), 55.2 (OCH₃), 107.8 (C₅ or C₇-THIQ), 115.0 (2 x ArCH, phenyl), 120.8 (C₅ or C₇-THIQ), 121.3 (ArCCl), 126.9 (C₆-THIQ), 127.7 (C₁CC₈-THIQ), 128.8 (2 x ArCH, phenyl), 135.9 (C₄CC₅-THIQ), 148.7 (ArCN) and 155.7 (C₈-THIQ) ppm.

2-(4-Chlorophenyl)-1-isopropyl-8-methoxy-1,2,3,4-tetrahydroisoquinoline (190c)

C₁₉H₂₂ClNO, Mol. Wt.: 315.84

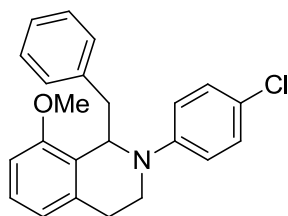


(Method K)

The crude compound was purified by column chromatography (eluent: 100% pet. ether) to give a white solid (57 mg, 12%) which showed: ^1H NMR (400 MHz, CDCl_3) δ 0.86 (3H, d, $J = 6.7$ Hz, $(\text{CH}_3)_2\text{CH}$), 1.02 (3H, d, $J = 6.8$ Hz, $(\text{CH}_3)_2\text{CH}$), 2.08 (1H, ddt, $J = 6.8, 9.4, 13.6$ Hz, $(\text{CH}_3)_2\text{CH}$), 2.92 (1H, ddd, $J = 4.5, 6.3, 15.8$ Hz, $\text{H}_4\text{-THIQ}$), 3.02 – 3.18 (1H, m, $\text{H}_4\text{-THIQ}$), 3.31 (1H, ddd, $J = 6.3, 9.3, 11.4$ Hz, $\text{H}_3\text{-THIQ}$), 3.68 (1H, ddd, $J = 4.5, 6.8, 11.4$ Hz, $\text{H}_4\text{-THIQ}$), 3.81 (3H, s, OCH_3), 4.95 (1H, d, $J = 9.3$ Hz, $\text{H}_1\text{-THIQ}$), 6.72 (1H, d, $J = 7.4$ Hz, H_5 or $\text{H}_7\text{-THIQ}$), 6.75 (1H, d, $J = 7.4$ Hz, H_5 or $\text{H}_7\text{-THIQ}$), 6.76 (2H, d, $J = 9.2$ Hz, 2 x ArCH, phenyl), 7.12 (2H, d, $J = 9.2$ Hz, 2 x ArCH, phenyl) and 7.13 (1H, t, $J = 7.4$ Hz, $\text{H}_6\text{-THIQ}$) ppm. ^{13}C NMR (101 MHz, CDCl_3) δ 19.8 ($(\text{CH}_3)_2\text{CH}$), 20.9 ($(\text{CH}_3)_2\text{CH}$), 27.2 ($\text{C}_4\text{-THIQ}$), 34.9 ($(\text{CH}_3)_2\text{CH}$), 43.3 ($\text{C}_3\text{-THIQ}$), 55.1 (OCH_3), 56.5 ($\text{C}_1\text{-THIQ}$), 108.0 (C_5 or $\text{C}_7\text{-THIQ}$), 113.8 (2 x ArCH, phenyl), 120.3 (C_5 or $\text{C}_7\text{-THIQ}$), 120.5 (ArCCl), 127.2 ($\text{C}_6\text{-THIQ}$), 127.6 ($\text{C}_1\text{CC}_8\text{-THIQ}$), 128.6 (2 x ArCH, phenyl), 136.3 ($\text{C}_4\text{CC}_5\text{-THIQ}$), 148.8 (ArCN) and 155.6 ($\text{C}_8\text{-THIQ}$) ppm. HRMS (ES^+) calcd. $\text{C}_{19}\text{H}_{23}\text{ClNO}$ ($\text{M}^+ + \text{H}$) 316.1463, found 316.1475.

1-Benzyl-2-(4-chlorophenyl)-8-methoxy-1,2,3,4-tetrahydroisoquinoline (190f)

$\text{C}_{23}\text{H}_{22}\text{ClNO}$, Mol. Wt.: 363.88

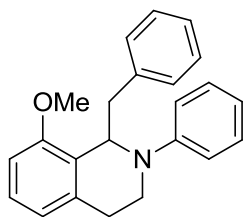


(Method K)

The crude compound was purified by column chromatography (eluent: 100% pet. ether) to give a colourless oil (62 mg, 11%) which showed: ^1H NMR (400 MHz, CDCl_3) δ 2.55 (1H, dt, $J = 5.1, 16.2$ Hz), 2.87 – 2.99 (1H, m), 3.04 (1H, dd, $J = 7.8, 13.5$ Hz), 3.15 (1H, dd, $J = 4.5, 13.5$ Hz), 3.51 – 3.60 (1H, m), 3.66 – 3.74 (1H, m), 3.78 (3H, s), 5.15 (1H, dd, $J = 4.5, 7.7$ Hz), 6.60 (2H, d, $J = 9.1$ Hz), 6.66 – 6.75 (2H, m), 7.04 (2H, d, $J = 9.1$ Hz) and 7.09 – 7.24 (6H, m) ppm.

1-Benzyl-8-methoxy-2-phenyl-1,2,3,4-tetrahydroisoquinoline (190h)

$\text{C}_{23}\text{H}_{23}\text{NO}$, Mol. Wt.: 329.43

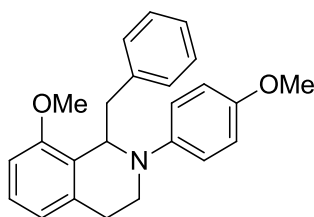


(Method K)

The crude compound was purified by column chromatography (eluent: from 0% to 20% EtOAc in pet. ether) to give a white solid (16 mg, 6%) which showed: ^1H NMR (500 MHz, CDCl_3) δ 2.46 - 2.73 (1H, m, H_4 -THIQ), 2.89 - 3.03 (1H, m, H_4 -THIQ), 3.03 - 3.24 (2H, m, CHCH_2), 3.53 - 3.64 (1H, m, H_3 -THIQ), 3.67 - 3.82 (4H, m, OCH_3 , H_3 -THIQ), 5.23 (1H, t, $J = 6.1$ Hz, H_1 -THIQ), 6.69 (2H, d, $J = 8.1$ Hz), 6.72 (1H, d, $J = 7.6$ Hz), 6.74 - 6.85 (2H, m), 7.09 - 7.17 (6H, m) and 7.17 - 7.23 (2H, m) ppm. ^{13}C NMR (126 MHz, CDCl_3) δ 26.3 (C_4 -THIQ), 40.2 (CHCH_2), 41.1 (C_3 -THIQ), 55.1 (OCH_3), 56.5 (C_1 -THIQ), 107.7 (ArCH), 114.1 (2 x ArCH), 120.7 (2 x ArCH), 125.9 (ArCH), 126.8 (C_q), 127.9 (2 x ArCH), 129.0 (ArCH), 129.5 (2 x ArCH), 129.7 (ArCH), 130.9 (ArCH), 136.1 (C_4CC_5 -THIQ), 139.8 (C_q), 149.4 (C_q) and 155.6 (C_8 -THIQ) ppm. HRMS (ES^+) calcd. $\text{C}_{23}\text{H}_{24}\text{NO}$ ($\text{M}^+ + \text{H}$) 330.1858, found 330.1842. Mp 126-128 $^\circ\text{C}$ (pet. ether).

1-Benzyl-8-methoxy-2-(4-methoxyphenyl)-1,2,3,4-tetrahydroisoquinoline (190i)

$\text{C}_{24}\text{H}_{25}\text{NO}_2$, Mol. Wt.: 359.46



(Method K)

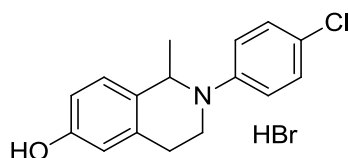
The crude compound was purified by column chromatography (eluent: from 0% to 20% EtOAc in pet. ether) to give a yellow oil (25 mg, 8%) which showed: ^1H NMR (500 MHz, CDCl_3) δ 2.41 - 2.65 (1H, m, H_4 -THIQ), 2.84 - 2.99 (1H, m, H_4 -THIQ), 2.99 - 3.23 (2H, m, CHCH_2), 3.44 - 3.63 (1H, m, H_3 -THIQ), 3.70 (3H, s, OCH_3), 3.71 - 3.75 (1H, m, H_3 -THIQ), 3.78 (3H, s, $J = 30.7$ Hz, OCH_3), 5.05 (1H, bs, H_1 -THIQ), 6.61 - 6.77 (6H, m), 7.09 - 7.18 (4H, m) and 7.18 - 7.25 (2H, m) ppm. ^{13}C NMR (126

MHz, CDCl₃) δ 25.8 (C₄-THIQ), 40.2 (CHCH₂), 41.6 (C₃-THIQ), 55.1 (OCH₃), 55.7 (OCH₃), 57.1 (H₁-THIQ), 107.5 (ArCH), 114.4 (2 x ArCH), 116.5 (ArCH), 120.9 (2 x ArCH), 125.8 (ArCH), 127.0 (ArCH), 127.9 (2 x ArCH), 129.6 (2 x ArCH), 136.2 (C_q), 140.5 (C_q), 144.5 (C_q), 146.9 (ArCN), 151.9 (ArCO) and 155.7 (ArCO) ppm. HRMS (ES⁺) calcd. C₂₄H₂₆NO₂ (M⁺+H) 360.1964, found 360.1973. Mp 114-118 °C (pet. ether).

2-(4-Chlorophenyl)-1-methyl-1,2,3,4-tetrahydroisoquinolin-6-ol hydrobromide

(191a)

C₁₆H₁₇BrClNO, Mol. Wt.: 354.67



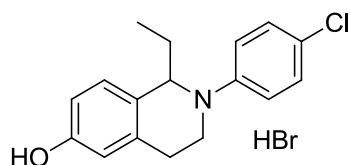
(Method G)

The product was obtained as a white solid (130 mg, 41%) which showed: ¹H NMR (500 MHz, CDCl₃) δ 1.37 (3H, d, *J* = 6.7 Hz, CH₃), 2.81 (1H, dt, *J* = 4.6, 16.0 Hz, H₄-THIQ), 2.88 – 3.05 (1H, m, H₄-THIQ), 3.35 – 3.49 (1H, m, H₃-THIQ), 3.54 (1H, dt, *J* = 5.2, 12.2 Hz, H₃-THIQ), 4.79 (1H, q, *J* = 6.7 Hz, H₁-THIQ), 6.63 (1H, d, *J* = 2.5 Hz, H₅-THIQ), 6.68 (1H, dd, *J* = 2.6, 8.3 Hz, H₇-THIQ), 6.81 (2H, d, *J* = 9.1 Hz, 2 x ArCH, phenyl), 6.99 (1H, d, *J* = 8.3 Hz, H₈-THIQ) and 7.19 (2H, d, *J* = 9.1 Hz, 2 x ArCH, phenyl) ppm. ¹³C NMR (126 MHz, CDCl₃) δ 20.8 (CH₃), 28.4 (C₄-THIQ), 41.0 (C₃-THIQ), 54.0 (C₁-THIQ), 113.5 (C₇-THIQ), 114.8 (C₅-THIQ), 115.8 (2 x ArCH, phenyl), 122.3 (ArCCl), 128.0 (C₈-THIQ), 129.0 (2 x ArCH, phenyl), 132.0 (C₁CC₈-THIQ), 135.8 (C₄CC₅-THIQ), 148.1 (ArCN) and 153.9 (C₆-THIQ) ppm. HRMS (ES⁺) calcd. C₁₆H₁₇³⁵ClNO (M⁺+H) 274.0993, found 274.0979; calcd. C₁₆H₁₇³⁷ClNO (M⁺+H) 276.0964, found 276.0981. Mp 210-213 °C.

2-(4-Chlorophenyl)-1-ethyl-1,2,3,4-tetrahydroisoquinolin-6-ol hydrobromide

(191b)

C₁₇H₁₉BrClNO, Mol. Wt.: 368.70

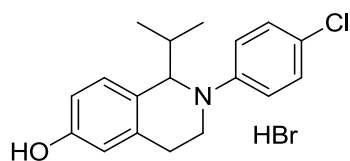


(Method G)

The product was obtained as a white solid (57 mg, 61%) which showed: ^1H NMR (500 MHz, $\text{D}_6\text{-DMSO}$) δ 0.88 (3H, t, $J = 7.3$ Hz, CH_3), 1.52 – 1.68 (1H, m, CH_3CH_2), 1.72 – 1.87 (1H, m, CH_3CH_2), 2.73 (1H, dt, $J = 5.5, 16.0$ Hz, $\text{H}_4\text{-THIQ}$), 2.83 (1H, dt, $J = 6.5, 13.3$ Hz, $\text{H}_4\text{-THIQ}$), 3.43 – 3.50 (2H, m, $\text{H}_3\text{-THIQ}$), 4.49 (1H, t, $J = 7.0$ Hz, $\text{H}_1\text{-THIQ}$), 6.48 – 6.63 (2H, m, $\text{H}_5, \text{H}_7\text{-THIQ}$), 6.84 (2H, d, $J = 8.8$ Hz, 2 x ArCH, phenyl), 6.96 (1H, d, $J = 8.0$ Hz, $\text{H}_8\text{-THIQ}$), 7.17 (2H, d, $J = 8.8$ Hz, 2 x ArCH, phenyl) and 9.33 (1H, bs, OH) ppm. ^{13}C NMR (126 MHz, $\text{D}_6\text{-DMSO}$) δ 11.1 (CH_3), 26.4 ($\text{C}_4\text{-THIQ}$), 28.9 (CH_3CH_2), 41.0 ($\text{C}_3\text{-THIQ}$), 58.9 ($\text{C}_1\text{-THIQ}$), 112.9 (C_5 or $\text{C}_7\text{-THIQ}$), 114.4 (2 x ArCH, phenyl), 114.6 (C_5 or $\text{C}_7\text{-THIQ}$), 119.5 (ArCCl), 128.3 ($\text{C}_8\text{-THIQ}$), 128.6 ($\text{C}_1\text{CC}_8\text{-THIQ}$), 128.7 (2 x ArCH, phenyl), 135.6 ($\text{C}_4\text{CC}_5\text{-THIQ}$), 148.1 (ArCN) and 155.8 ($\text{C}_6\text{-THIQ}$) ppm. HRMS (ES^+) calcd. $\text{C}_{17}\text{H}_{19}^{35}\text{ClNO}$ ($\text{M}^+ + \text{H}$) 290.1120, found 290.1107. Mp 184–187 °C.

2-(4-Chlorophenyl)-1-isopropyl-1,2,3,4-tetrahydroisoquinolin-6-ol hydrobromide (191c)

$\text{C}_{18}\text{H}_{21}\text{BrClNO}$, Mol. Wt.: 382.72



(Method G)

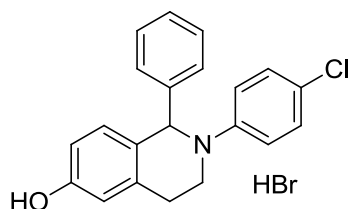
The product was obtained as a pale grey solid (37 mg, 58%) which showed: ^1H NMR (500 MHz, $\text{D}_6\text{-DMSO}$) δ 0.86 (3H, d, $J = 6.3$ Hz, $(\text{CH}_3)_2\text{CH}$), 0.93 (3H, d, $J = 6.9$ Hz, $(\text{CH}_3)_2\text{CH}$), 1.98 (1H, td, $J = 6.8, 13.8$ Hz, $(\text{CH}_3)_2\text{CH}$), 2.76 – 2.94 (2H, m, $\text{H}_4\text{-THIQ}$), 3.37 – 3.40 (1H, m, $\text{H}_3\text{-THIQ}$), 3.58 (1H, dt, $J = 6.1, 12.4$ Hz, $\text{H}_3\text{-THIQ}$), 4.31 (1H, d, $J = 8.6$ Hz, $\text{H}_1\text{-THIQ}$), 6.54 (1H, d, $J = 8.2$ Hz, $\text{H}_7\text{-THIQ}$), 6.56 (1H, s, $\text{H}_5\text{-THIQ}$), 6.86 (2H, d, $J = 8.6$ Hz, 2 x ArCH, phenyl), 6.95 (1H, d, $J = 8.2$ Hz, $\text{H}_8\text{-THIQ}$), 7.14 (2H, d, $J = 8.0$ Hz, 2 x ArCH, phenyl) and 9.30 (1H, bs, OH) ppm. ^{13}C NMR (126 MHz, $\text{D}_6\text{-DMSO}$) δ 11.1 (CH_3), 26.4 ($\text{C}_4\text{-THIQ}$), 28.9 (CH_3CH_2), 41.0 ($\text{C}_3\text{-THIQ}$), 58.9 ($\text{C}_1\text{-THIQ}$), 112.9 (C_5 or $\text{C}_7\text{-THIQ}$), 114.4 (2 x ArCH, phenyl), 114.6 (C_5 or $\text{C}_7\text{-THIQ}$), 119.5 (ArCCl), 128.3 ($\text{C}_8\text{-THIQ}$), 128.6 ($\text{C}_1\text{CC}_8\text{-THIQ}$), 128.7 (2 x ArCH, phenyl), 135.6 ($\text{C}_4\text{CC}_5\text{-THIQ}$), 148.1 (ArCN) and 155.8 ($\text{C}_6\text{-THIQ}$) ppm.

DMSO) δ 19.9 ((CH₃)₂CH), 20.3 ((CH₃)₂CH), 26.4 (C₄-THIQ), 33.6 ((CH₃)₂CH), 41.9 (C₃-THIQ), 62.9 (C₁-THIQ), 112.2 (C₇-THIQ), 114.2 (2 x ArCH, phenyl), 114.7 (C₅-THIQ), 119.2 (ArCCl), 127.7 (C₁CC₈-THIQ), 128.5 (2 x ArCH, phenyl), 129.1 (C₈-THIQ), 135.8 (C₄CC₅-THIQ), 148.5 (ArCN) and 156.0 (C₆-THIQ) ppm. HRMS (ES⁻) calcd. C₁₈H₁₉³⁵ClNO (M⁻-H) 300.1155, found 300.1151; calcd. C₁₈H₁₉³⁷ClNO (M⁻-H) 302.1131, found 302.1135. Mp 111-115 °C.

2-(4-Chlorophenyl)-1-phenyl-1,2,3,4-tetrahydroisoquinolin-6-ol hydrobromide

(191e)

C₂₁H₁₉BrClNO, Mol. Wt.: 416.74



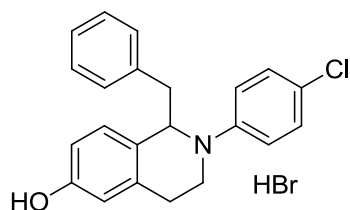
(Method G)

The product was obtained as a white solid (247 mg, 79%) which showed: ¹H NMR (500 MHz, CDCl₃) δ 2.80 – 2.94 (2H, m, H₄-THIQ), 3.44 (1H, ddd, *J* = 5.7, 8.1, 11.4 Hz, H₃-THIQ), 3.65 (1H, dt, *J* = 5.5, 11.2 Hz, H₃-THIQ), 4.69 (1H, bs, OH), 5.70 (1H, s, H₁-THIQ), 6.65 (1H, d, *J* = 2.5 Hz, H₅-THIQ), 6.70 (1H, dd, *J* = 2.5, 8.2 Hz, H₇-THIQ), 6.74 (2H, d, *J* = 9.0 Hz, 2 x ArCH, *N*-phenyl), 7.14 (1H, d, *J* = 8.2 Hz, H₈-THIQ), 7.15 (2H, d, *J* = 9.0 Hz, 2 x ArCH, *N*-phenyl), 7.19 (2H, d, *J* = 6.9 Hz, 2 x ArCH, C₁-phenyl) and 7.22 – 7.27 (3H, m, 3 x ArCH, C₁-phenyl) ppm. ¹³C NMR (126 MHz, CDCl₃) δ 28.0 (C₄-THIQ), 43.8 (C₃-THIQ), 62.3 (C₁-THIQ), 113.3 (C₇-THIQ), 114.7 (C₅-THIQ), 115.1 (2 x ArCH, *N*-phenyl), 122.3 (ArCCl), 126.9 (ArCH, C₁-phenyl), 127.2 (2 x ArCH, C₁-phenyl), 128.3 (2 x ArCH, C₁-phenyl), 128.9 (2 x ArCH, *N*-phenyl), 129.0 (C₈-THIQ), 130.1 (C₁CC₈-THIQ), 137.1 (C₄CC₅-THIQ), 142.9 (ArCCH₂, C₁-phenyl), 148.1 (ArCN) and 154.5 (C₆-THIQ) ppm. HRMS (ES⁺) calcd. C₂₁H₁₉³⁵ClNO (M⁺+H) 336.1150, found 336.1133; calcd. C₂₁H₁₉³⁷ClNO (M⁺+H) 338.1120, found 338.1140. Mp 227-228 °C.

1-Benzyl-2-(4-chlorophenyl)-1,2,3,4-tetrahydroisoquinolin-6-ol hydrobromide

(191f)

C₂₂H₂₁BrClNO, Mol. Wt.: 430.77

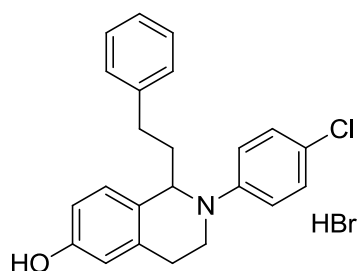


(Method G)

The product was obtained as a yellow precipitate (62 mg, 44%) which showed: ¹⁹⁶ ¹H NMR (400 MHz, CDCl₃) δ 2.64 (1H, dt, *J* = 5.7, 15.9 Hz), 2.80 – 2.91 (1H, m), 2.94 (1H, dd, *J* = 7.1, 13.3 Hz), 3.15 (1H, dd, *J* = 6.0, 13.3 Hz), 3.38 – 3.49 (1H, m), 3.50 – 3.61 (1H, m), 4.75 (1H, t, *J* = 6.5 Hz), 6.53 – 6.62 (2H, m), 6.64 (1H, d, *J* = 2.1 Hz), 6.69 (2H, d, *J* = 9.1 Hz), 6.99 (2H, dd, *J* = 1.8, 7.5 Hz), 7.13 (2H, d, *J* = 9.1 Hz) and 7.16 – 7.23 (3H, m) ppm. HRMS (ES⁺) calcd. C₂₂H₂₁³⁵ClNO (M⁺+H) 350.1306, found 350.1296; calcd. C₂₁H₁₉³⁷ClNO (M⁺+H) 352.1277, found 352.1331. Mp 143-147 °C.

2-(4-Chlorophenyl)-1-phenethyl-1,2,3,4-tetrahydroisoquinolin-6-ol hydrobromide (191g)

C₂₃H₂₃BrClNO, Mol. Wt.: 444.79



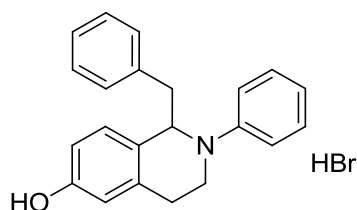
(Method G)

The product was obtained as a white precipitate (98 mg, 61%) which showed: ¹H NMR (500 MHz, D₆-DMSO) δ 1.85 – 2.01 (1H, m, ArCH₂CH₂CH), 2.01 – 2.13 (1H, m, ArCH₂CH₂CH), 2.58 – 2.70 (2H, m, ArCH₂CH₂CH), 2.74 (1H, dt, *J* = 6.1, 14.0 Hz, H₄-THIQ), 2.85 (1H, dt, *J* = 6.1, 14.0 Hz, H₄-THIQ), 3.53 (2H, t, *J* = 6.1 Hz, H₃-THIQ), 4.62 (1H, t, *J* = 7.0 Hz, H₁-THIQ), 6.56 (1H, d, *J* = 2.3 Hz, H₅-THIQ), 6.59 (1H, dd, *J* =

2.3, 8.3 Hz, H₅-THIQ), 6.82 (2H, d, $J = 9.1$ Hz, 2 x ArCH, *N*-phenyl), 7.02 (1H, d, $J = 8.3$ Hz, H₈-THIQ), 7.12 – 7.18 (3H, m, 2 x ArCH, *N*-phenyl, ArCH, phenyl), 7.19 (2H, d, $J = 7.4$ Hz, 2 x ArCH, phenyl), 7.27 (2H, t, $J = 7.5$ Hz, 2 x ArCH, phenyl) and 9.27 (1H, bs, OH) ppm. ¹³C NMR (126 MHz, D₆-DMSO) δ 26.1 (C₄-THIQ), 32.2 (ArCH₂CH₂CH), 37.9 (ArCH₂CH₂CH), 40.8 (C₃-THIQ), 57.1 (C₁-THIQ), 113.0 (C₇-THIQ), 114.6 (C₅-THIQ), 114.7 (2 x ArCH, *N*-phenyl), 119.8 (ArCCl), 125.7 (ArCH, phenyl), 128.1 (C₈-THIQ), 128.2 (2 x ArCH, phenyl), 128.3 (2 x ArCH, phenyl), 128.6 (C₁CC₈-THIQ), 128.7 (2 x ArCH, *N*-phenyl), 135.7 (C₄CC₅-THIQ), 141.7 (ArCCH₂, phenyl), 148.0 (ArCN) and 155.8 (C₆-THIQ) ppm. HRMS (ES⁺) calcd. C₂₃H₂₃³⁵ClNO (M⁺+H) 364.1463, found 364.1456; calcd. C₂₃H₂₃³⁷ClNO (M⁺+H) 366.1433, found 366.1465. Mp 190-192 °C.

1-Benzyl-2-phenyl-1,2,3,4-tetrahydroisoquinolin-6-ol hydrobromide (191h)

C₂₂H₂₂BrNO, Mol. Wt.: 396.32

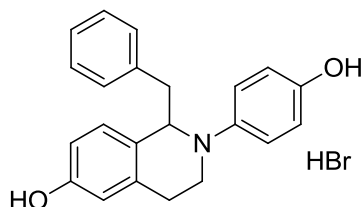


(Method G)

The product was obtained as a dark green precipitate (118 mg, 87%) which showed: ¹⁰ ¹H NMR (500 MHz, D₆-DMSO) δ 2.62 (1H, dt, $J = 4.7, 16.2$ Hz, H₄-THIQ), 2.78 – 2.90 (1H, m, H₄-THIQ), 2.95 (1H, dd, $J = 6.8, 13.4$ Hz, CH₂CH), 3.11 (1H, dd, $J = 6.8, 13.4$ Hz, CH₂CH), 3.49 – 3.64 (2H, m, H₃-THIQ), 4.87 (1H, t, $J = 6.8$ Hz, H₁-THIQ), 6.48 (1H, dd, $J = 2.2, 8.2$ Hz, H₇-THIQ), 6.53 (1H, d, $J = 2.2$ Hz, H₅-THIQ), 6.59 (1H, t, $J = 7.2$ Hz, ArCH), 6.72 – 6.81 (3H, m, 2 x ArCH, H₈-THIQ), 7.11 (2H, t, $J = 7.9$ Hz, 2 x ArCH), 7.13 – 7.19 (3H, m, 3 x ArCH), 7.23 (2H, t, $J = 7.3$ Hz, 2 x ArCH) and 9.21 (1H, bs, OH) ppm. ¹³C NMR (126 MHz, D₆-DMSO) δ 26.1 (C₄-THIQ), 40.3 (C₃-THIQ), 41.7 (CH₂CH), 59.8 (C₁-THIQ), 112.7 (C₇-THIQ), 113.3 (2 x ArCH), 114.5 (C₅-THIQ), 116.5 (ArCH), 125.9 (ArCH), 127.9 (2 x ArCH), 128.1 (C₁CC₈-THIQ), 128.3 (C₈-THIQ), 129.0 (2 x ArCH), 129.5 (2 x ArCH), 135.8 (C₄CC₅-THIQ), 139.1 (ArCCH₂CH), 149.1 (ArCN) and 155.6 (C₆-THIQ) ppm. Mp 137-141 °C.

**1-benzyl-2-(4-hydroxyphenyl)-1,2,3,4-tetrahydroisoquinolin-6-ol hydrobromide
(191i)**

C₂₂H₂₂BrNO₂, Mol. Wt.: 412.32

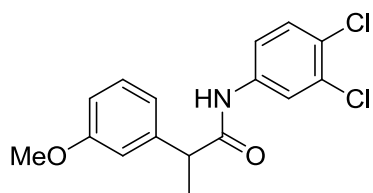


(Method G)

The product was obtained as a pale yellow precipitate (104 mg, 96%) which showed:¹⁸⁷ ¹H NMR (500 MHz, D₆-DMSO) δ 2.51 – 2.57 (1H, m, H₄-THIQ), 2.79 (1H, ddd, *J* = 6.0, 10.0, 16.0 Hz, H₄-THIQ), 2.86 (1H, dd, *J* = 6.1, 13.5 Hz, CH₂CH), 3.04 (1H, dd, *J* = 7.6, 13.5 Hz, CH₂CH), 3.39 – 3.47 (1H, m, H₃-THIQ), 3.47 – 3.56 (1H, m, H₃-THIQ), 4.66 (1H, t, *J* = 6.7 Hz, H₁-THIQ), 6.47 (1H, dd, *J* = 2.2, 8.3 Hz, H₇-THIQ), 6.49 (1H, d, *J* = 2.2 Hz, H₅-THIQ), 6.57 (2H, d, *J* = 8.9 Hz, 2 x ArCH, *N*-phenyl), 6.64 (2H, d, *J* = 8.9 Hz, 2 x ArCH, *N*-phenyl), 6.71 (1H, d, *J* = 8.3 Hz, H₈-THIQ), 7.12 (2H, d, *J* = 7.3 Hz, 2 x ArCH, phenyl), 7.15 (1H, t, *J* = 7.3 Hz, 2 x ArCH, phenyl), 7.22 (2H, t, *J* = 7.3 Hz, ArCH, phenyl), 8.66 (1H, bs, OH) and 9.16 (1H, bs, OH) ppm. ¹³C NMR (126 MHz, D₆-DMSO) δ 25.9 (C₄-THIQ), 41.1 (C₃-THIQ), 41.5 (CH₂CH), 60.7 (C₁-THIQ), 112.7 (C₇-THIQ), 114.6 (C₅-THIQ), 115.5 (2 x ArCH, *N*-phenyl), 116.7 (2 x ArCH, *N*-phenyl), 125.8 (ArCH, phenyl), 127.8 (2 x ArCH, phenyl), 128.3 (C₈-THIQ), 128.4 (C₁CC₈-THIQ), 129.4 (2 x ArCH, phenyl), 135.6 (C₄CC₅-THIQ), 139.6 (ArCCH₂CH), 142.7 (ArCN), 149.5 (ArCO, *N*-phenyl) and 155.4 (C₆-THIQ) ppm. HRMS (ES⁺) calcd. C₂₂H₂₁³⁵ClNNaO (M⁺+Na) 354.1465, found 354.1481. Degraded before melting.

***N*-(3,4-Dichlorophenyl)-2-(3-methoxyphenyl)propanamide (196)**

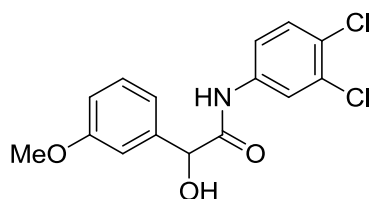
C₁₆H₁₅Cl₂NO₂, Mol. Wt.: 324.20



POCl₃ (304 μ L, 3.22 mmol) was added to a stirring suspension of **178h** (100 mg, 0.322 mmol) in toluene (6 mL) and stirred at 100 °C overnight. The solvent and the excess of POCl₃ were evaporated under reduced pressure and the residue was dissolved in toluene (6 mL) and treated with a 3.0 M solution of MeMgBr (161 μ L, 0.483 mmol) in THF. The mixture was stirred at rt overnight and then refluxed for one further day. The mixture was then cooled to rt, quenched with water and extracted with EtOAc (3 x 15 mL). The combined organics were dried with MgSO₄, filtered and evaporated to give a yellow oil (186 mg). The crude compound was purified by column chromatography (eluent: from 0% to 20% EtOAc in pet. ether) to give the product as a yellow oil (21 mg, 20%) which showed: ¹H NMR (400 MHz, CDCl₃) δ 1.58 (3H, d, J = 7.2 Hz), 3.67 (1H, q, J = 7.2 Hz), 3.81 (3H, s), 6.83 – 6.88 (2H, m), 6.88 – 6.95 (1H, m), 7.03 (1H, bs), 7.22 (1H, dd, J = 2.5, 8.7 Hz), 7.30 (1H, d, J = 8.7 Hz), 7.31 (1H, dt, J = 1.6, 7.5 Hz) and 7.65 (1H, d, J = 2.4 Hz) ppm. HRMS (ES⁺) calcd. C₁₆H₁₅³⁵Cl₂NNaO₂ (M⁺+Na) 346.0372, found 346.0360.

N-(3,4-Dichlorophenyl)-2-hydroxy-2-(3-methoxyphenyl)acetamide (**197**)

C₁₅H₁₃Cl₂NO₃, Mol. Wt.: 326.17

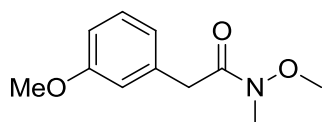


POCl₃ (304 μ L, 3.22 mmol) was added to a stirring suspension of **178h** (100 mg, 0.322 mmol) in toluene (6 mL) and stirred at 100 °C overnight. The solvent and the excess of POCl₃ were evaporated under reduced pressure and the residue was dissolved in toluene (6 mL) and treated with a 3.0 M solution of MeMgBr (161 μ L, 0.483 mmol) in THF. The mixture was stirred at rt overnight and then refluxed for one further day. The mixture was then cooled to rt, quenched with water and extracted with EtOAc (3 x 15 mL). The combined organics were dried with MgSO₄, filtered and evaporated to give

a yellow oil (186 mg). The crude compound was purified by column chromatography (eluent: from 0% to 20% EtOAc in pet. ether) to give the product as a yellow oil (28 mg, 27%) which showed: ^1H NMR (400 MHz, CDCl_3) δ 3.80 (3H, s), 5.16 (1H, s), 6.64 – 6.70 (1H, m), 6.89 (1H, ddd, $J = 0.9, 2.6, 8.3$ Hz), 6.98 – 7.01 (1H, m), 7.02 – 7.05 (1H, m), 7.28 – 7.33 (1H, m), 7.35 (1H, d, $J = 1.3$ Hz), 7.74 – 7.79 (1H, m) and 8.28 (1H, s) ppm. HRMS (ES^+) calcd. $\text{C}_{15}\text{H}_{13}^{35}\text{Cl}_2\text{NNaO}_3$ ($\text{M}^+ + \text{Na}$) 348.0165, found 348.0159; calcd. $\text{C}_{15}\text{H}_{13}^{35}\text{Cl}^{37}\text{ClNNaO}_3$ ($\text{M}^+ + \text{Na}$) 350.0135, found 350.0146.

***N*-Methoxy-2-(3-methoxyphenyl)-*N*-methylacetamide (208)**

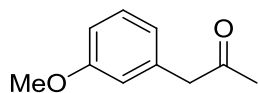
$\text{C}_{11}\text{H}_{15}\text{NO}_3$, Mol. Wt.: 209.24



A solution of PCl_3 (3.5 mL, 40.0 mmol) in anhydrous toluene (50 mL) was added to a stirring suspension of *N,O*-dimethylhydroxylamine hydrochloride (12.3 g, 124.0 mmol) and Et_3N (39 mL, 280 mmol) at 0 °C under inert atmosphere and the mixture was stirred at rt overnight. 3-Methoxyphenylacetic acid (13.7 g, 80.0 mmol) was added and the mixture was stirred overnight at 120 °C under inert atmosphere. The mixture was evaporated and the residue was dissolved with EtOAc (150 mL). The organic layer was washed with 1 N HCl (3 x 100 mL) and brine (3 x 100 mL), then dried with MgSO_4 , filtered and evaporated to give a brown oil (6.40 g). The crude compound was purified by column chromatography (eluent: from 0% to 40% EtOAc in pet. ether) to give the product as a yellow oil (5.50 g, 21%) which showed: ^{197}H NMR (400 MHz, CDCl_3) δ 3.19 (3H, s), 3.60 (3H, s), 3.74 (2H, s), 3.79 (3H, s), 6.78 (1H, dd, $J = 2.3, 8.2$ Hz), 6.83 – 6.91 (2H, m) and 7.22 (1H, t, $J = 7.8$ Hz) ppm. HRMS (ES^+) calcd. $\text{C}_{11}\text{H}_{16}\text{NO}_3$ ($\text{M}^+ + \text{H}$) 210.1125, found 210.1125.

1-(3-Methoxyphenyl)propan-2-one (209a)

$\text{C}_{10}\text{H}_{12}\text{O}_2$, Mol. Wt.: 164.20

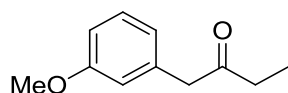


(Method L)

The product was obtained as a yellow oil (211 mg, 93%) which showed:¹⁹⁸ ¹H NMR (500 MHz, CDCl₃) δ 2.15 (3H, s, CH₃CO), 3.66 (2H, s, CH₂CO), 3.80 (3H, s, ArOCH₃), 6.73 – 6.76 (1H, m, ArCH), 6.77 – 6.80 (1H, m, ArCH), 6.80 – 6.84 (1H, m, ArCH) and 7.25 (1H, t, *J* = 7.9 Hz, ArCH) ppm. ¹³C NMR (126 MHz, CDCl₃) δ 29.2 (CH₃CO), 51.1 (CH₂CO), 55.2 (ArOCH₃), 112.5 (ArCH), 115.0 (ArCH), 121.7 (ArCH), 129.8 (ArCH), 135.7 (ArCCH₂), 159.8 (ArCO) and 206.3 (CH₂CO) ppm. HRMS (ES⁺) calcd. C₁₀H₁₃O₂ (M⁺+H) 165.0910, found 165.0923; calcd. C₁₀H₁₂NaO₂ (M⁺+Na) 187.0730, found 187.0737.

1-(3-Methoxyphenyl)butan-2-one (209b)

C₁₁H₁₄O₂, Mol. Wt.: 178.23

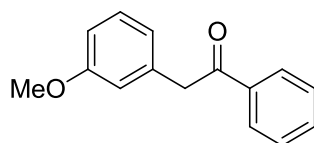


(Method L)

The crude compound was purified by column chromatography (eluent: from 0% to 15% EtOAc in pet. ether) to give a colourless oil (257 mg, 50%) which showed:¹⁹⁹ ¹H NMR (500 MHz, CDCl₃) δ 1.02 (3H, t, *J* = 7.3 Hz, CH₂CH₃), 2.47 (2H, q, *J* = 7.3 Hz, CH₂CH₃), 3.65 (2H, s, ArCH₂), 3.80 (3H, s, OCH₃), 6.73 – 6.77 (1H, m, ArCH), 6.77 – 6.84 (2H, m, 2 x ArCH) and 7.24 (1H, t, *J* = 8.0 Hz, ArCH) ppm. ¹³C NMR (126 MHz, CDCl₃) δ 7.8 (CH₂CH₃), 35.1 (CH₂CH₃), 49.9 (ArCH₂), 55.2 (OCH₃), 112.4 (ArCH), 115.0 (ArCH), 121.7 (ArCH), 129.7 (ArCH), 135.9 (ArCCH₂), 159.8 (ArCO) and 208.9 (CH₂CO) ppm. HRMS (ES⁺) calcd. C₁₁H₁₅O₂ (M⁺+H) 179.1067, found 179.1075.

2-(3-Methoxyphenyl)-1-phenylethanone (209d)

C₁₅H₁₄O₂, Mol. Wt.: 226.27

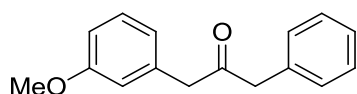


(Method L)

The crude compound was purified by column chromatography (eluent: pet. ether) to give the product as a yellow oil (356 mg, 66%) which showed: ^1H NMR (500 MHz, CDCl_3) δ 3.79 (3H, s, ArOCH_3), 4.26 (2H, s, CH_2), 6.80 (1H, d, $J = 8.2$ Hz, ArCH, methoxyphenyl), 6.82 (1H, s, ArCH, methoxyphenyl), 6.86 (1H, d, $J = 7.5$ Hz, ArCH, methoxyphenyl), 7.24 (1H, t, $J = 8.0$ Hz, ArCH, methoxyphenyl), 7.46 (2H, t, $J = 7.7$ Hz, 2 x ArCH, phenyl), 7.56 (1H, t, $J = 7.7$ Hz, ArCH, phenyl) and 8.01 (2H, d, $J = 7.7$ Hz, 2 x ArCH, phenyl) ppm. ^{13}C NMR (126 MHz, CDCl_3) δ 45.6 (CH_2), 55.2 (ArOCH_3), 112.4 (ArCH, methoxyphenyl), 115.1 (ArCH, methoxyphenyl), 121.8 (ArCH, methoxyphenyl), 128.6 (4 x ArCH, phenyl), 129.6 (ArCH, methoxyphenyl), 133.2 (ArCH, phenyl), 136.0 (ArCCH_2), 136.6 (ArCCO), 159.8 (ArCO) and 197.5 (CH_2CO) ppm. HRMS (ES^+) calcd. $\text{C}_{15}\text{H}_{15}\text{O}_2$ ($\text{M}^+ + \text{H}$) 227.1072, found 227.1082; calcd. $\text{C}_{15}\text{H}_{14}\text{NaO}_2$ ($\text{M}^+ + \text{Na}$) 249.0891, found 249.0901.

1-(3-Methoxyphenyl)-3-phenylpropan-2-one (209e)

$\text{C}_{16}\text{H}_{16}\text{O}_2$, Mol. Wt.: 240.30

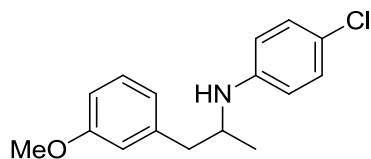


(Method L)

The crude compound was purified by column chromatography (eluent: pet. ether) to give the product as a colourless oil (160 mg, 28%) which showed:²⁰⁰ ^1H NMR (500 MHz, CDCl_3) δ 3.69 (2H, s, CH_2 , methoxyphenyl), 3.72 (2H, s, CH_2 , phenyl), 3.78 (3H, s, ArOCH_3), 6.69 (1H, s, ArCH, methoxyphenyl), 6.75 (1H, d, $J = 7.5$ Hz, ArCH, methoxyphenyl), 6.81 (1H, dd, $J = 1.9, 7.9$ Hz, ArCH, methoxyphenyl), 7.15 (2H, d, $J = 7.4$ Hz, 2 x ArCH, phenyl), 7.24 (1H, t, $J = 7.9$ Hz, ArCH, methoxyphenyl), 7.26 – 7.29 (1H, m, ArCH, phenyl) and 7.32 (2H, t, $J = 7.4$ Hz, 2 x ArCH, phenyl) ppm. ^{13}C NMR (126 MHz, CDCl_3) δ 49.0 (CH_2 , phenyl), 49.2 (CH_2 , methoxyphenyl), 55.2 (ArOCH_3), 112.7 (ArCH, methoxyphenyl), 115.0 (ArCH, methoxyphenyl), 121.8 (ArCH, methoxyphenyl), 127.0 (ArCH, phenyl), 128.7 (2 x ArCH, phenyl), 129.5 (2 x ArCH, phenyl), 129.7 (ArCH, methoxyphenyl), 134.0 (ArCCH_2 , phenyl), 135.4 (ArCCH_2 , methoxyphenyl), 159.8 (ArCO) and 205.6 (CH_2CO) ppm.

4-Chloro-*N*-(1-(3-methoxyphenyl)propan-2-yl)aniline (**210a**)

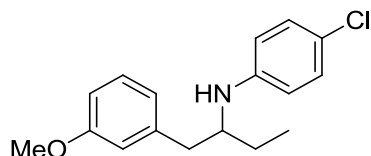
C₁₆H₁₈ClNO, Mol. Wt.: 275.77



NaBH(OAc)₃ (306 mg, 1.37 mmol) was added to a stirring solution of **209a** (105 mg, 0.914 mmol) and 4-chloroaniline (117 mg, 0.914 mmol) in CHCl₃ (5 mL) and the mixture was stirred at rt for 6 h. The mixture was diluted with CHCl₃ (15 mL) and washed with sat. aq. Na₂CO₃ (3 x 10 mL), then dried with MgSO₄, filtered and evaporated to give a yellow oil (205 mg). The crude compound was purified by column chromatography (eluent: from 0% to 30 % EtOAc in pet. ether) to get the product as a yellow oil (53 mg, 21%) which showed: ¹H NMR (500 MHz, CDCl₃) δ 1.16 (3H, d, *J* = 6.4 Hz, CHCH₃), 2.70 (1H, dd, *J* = 7.4, 13.4 Hz, CH₂CH), 2.91 (1H, dd, *J* = 4.7, 13.4 Hz, CH₂CH), 3.67 – 3.75 (1H, m, CHCH₃), 3.79 (3H, s, OCH₃), 6.61 (2H, d, *J* = 8.5 Hz, 2 x ArCH, aniline), 6.70 (1H, s, ArCH, phenyl), 6.73 – 6.81 (2H, m, 2 x ArCH, phenyl), 7.14 (2H, d, *J* = 8.7 Hz, 2 x ArCH, aniline) and 7.22 (1H, t, *J* = 7.9 Hz, ArCH, phenyl) ppm. ¹³C NMR (126 MHz, CDCl₃) δ 19.8 (CHCH₃), 41.9 (CH₂CH), 50.2 (CHCH₃), 55.1 (OCH₃), 111.5 (ArCH, phenyl), 115.2 (2 x ArCH, aniline), 115.3 (ArCH, phenyl), 121.8 (ArCH, phenyl), 122.5 (ArCCl), 129.2 (2 x ArCH, aniline), 129.3 (ArCH, phenyl), 139.6 (ArCCH₂), 144.9 (ArCN) and 159.6 (ArCO) ppm.

4-Chloro-*N*-(1-(3-methoxyphenyl)butan-2-yl)aniline (**210b**)

C₁₇H₂₀ClNO, Mol. Wt.: 289.80

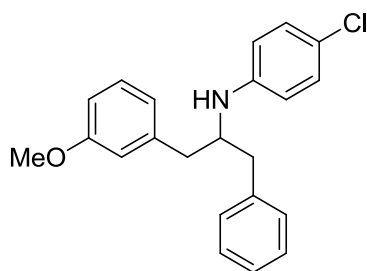


NaBH(OAc)₃ (445 mg, 2.10 mmol) was added to a stirring solution of **209b** (250 mg, 1.40 mmol) and 4-chloroaniline (268 mg, 2.10 mmol) in CHCl₃ (15 mL) and the mixture was stirred at rt overnight. The mixture was diluted with CHCl₃ (15 mL) and washed with sat. aq. Na₂CO₃ (2 x 30 mL) then dried with MgSO₄, filtered and evaporated to give a yellow oil (383 mg). the crude compound was purified by column

chromatography (eluent: from 0% to 20% EtOAc in pet. ether) to give the product as a colourless oil (67 mg, 19%) which showed: ^1H NMR (500 MHz, CDCl_3) δ 0.99 (3H, t, J = 7.4 Hz, CH_2CH_3), 1.35 – 1.51 (1H, m, CH_2CH_3), 1.57 – 1.71 (1H, m, CH_2CH_3), 2.74 – 2.90 (2H, m, ArCH_2), 3.47 – 3.60 (1H, m, CHN), 3.80 (3H, s, OCH_3), 6.57 (2H, d, J = 8.7 Hz, 2 x ArCH , aniline), 6.72 (1H, s, ArCH , phenyl), 6.77 (1H, d, J = 8.7 Hz, ArCH , phenyl), 6.79 (1H, d, J = 8.7 Hz, ArCH , phenyl), 7.14 (2H, d, J = 8.7 Hz, ArCH , phenyl) and 7.23 (1H, t, J = 7.9 Hz) ppm. ^{13}C NMR (126 MHz, CDCl_3) δ 10.4 (CH_2CH_3), 26.6 (CH_2CH_3), 39.6 (ArCH_2), 55.1 (OCH_3), 55.5 (CHN), 111.4 (ArCH , phenyl), 114.5 (2 x ArCH , aniline), 115.4 (ArCH , phenyl), 121.8 (ArCCl), 121.9 (ArCH , phenyl), 129.2 (2 x ArCH , aniline), 129.3 (ArCH , phenyl), 139.8 (ArCCH_2), 145.9 (ArCN) and 159.6 (ArCO) ppm. HRMS (ES^-) calcd. $\text{C}_{17}\text{H}_{19}^{35}\text{ClNO}$ (M^- -H) 288.1161, found 288.1159; calcd. $\text{C}_{17}\text{H}_{19}^{37}\text{ClNO}$ (M^- -H) 290.1131, found 290.1119.

4-Chloro-*N*-(1-(3-methoxyphenyl)-3-phenylpropan-2-yl)aniline (210e)

$\text{C}_{22}\text{H}_{22}\text{ClNO}$, Mol. Wt.: 351.87

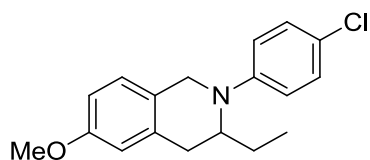


$\text{NaBH}(\text{OAc})_3$ (393 mg, 1.76 mmol) was added to a stirring solution of **209e** (280 mg, 1.17 mmol) and 4-chloroaniline (149 mg, 1.17 mmol) in dichloroethane (3.0 mL). Glacial acetic acid (67 μL , 1.17 mmol) was introduced and the mixture was stirred at rt overnight during which time the suspension turned into a solution. The mixture was diluted with DCM (10 mL) and washed with 1 N NaOH (1 x 10 mL) then dried with MgSO_4 , filtered and evaporated to give a yellow oil (305 mg). The crude compound was purified by column chromatography (eluent: from 0% to 40 % EtOAc in pet. ether) to give the product as a yellow oil (116 mg, 28%) which showed: ^1H NMR (400 MHz, CDCl_3) δ 2.64 – 2.95 (4H, z m), 3.77 (3H, m), 3.85 – 4.01 (1H, m), 6.51 (2H, d, J = 8.9 Hz), 6.69 – 6.72 (1H, m), 6.73 – 6.79 (2H, m), 7.09 (2H, d, J = 8.9 Hz), 7.15 – 7.19 (2H, m), 7.22 (2H, dd, J = 2.1, 7.7 Hz) and 7.26 – 7.30 (2H, m) ppm. HRMS (ES^+)

calcd. C₂₂H₂₁³⁵ClNO (M⁻H) 350.1317, found 350.1328; calcd. C₂₂H₂₁³⁷ClNO (M⁻H) 352.1288, found 352.1301;

2-(4-Chlorophenyl)-3-ethyl-6-methoxy-1,2,3,4-tetrahydroisoquinoline (211b)

C₁₈H₂₀ClNO, Mol. Wt.: 301.81

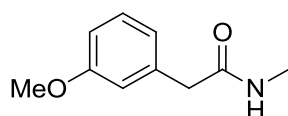


(Method J)

The crude compound was purified by column chromatography (eluent: from 0% to 20% EtOAc in pet. ether) to give the product as a colourless oil (92 mg, 44%) which showed: ¹H NMR (500 MHz, CDCl₃) δ 0.87 (3H, t, *J* = 7.4 Hz, CH₂CH₃), 1.27 – 1.37 (1H, m, CH₂CH₃), 1.49 – 1.60 (1H, m, CH₂CH₃), 2.78 (1H, dd, *J* = 1.5, 15.8 Hz, H₄-THIQ), 3.11 (1H, dd, *J* = 5.4, 15.7 Hz, H₄-THIQ), 3.81 (3H, s, OCH₃), 3.95 – 4.03 (1H, m, H₃-THIQ), 4.20 (1H, d, *J* = 15.2 Hz, H₁-THIQ), 4.35 (1H, d, *J* = 15.1 Hz, H₁-THIQ), 6.70 (1H, d, *J* = 2.2 Hz, H₅-THIQ), 6.78 (1H, dd, *J* = 2.5, 8.4 Hz, H₇-THIQ), 6.81 (2H, d, *J* = 9.0 Hz, 2 x ArCH, phenyl), 7.08 (1H, d, *J* = 8.4 Hz, H₈-THIQ) and 7.20 (2H, d, *J* = 9.0 Hz, 2 x ArCH, phenyl) ppm. ¹³C NMR (126 MHz, CDCl₃) δ 11.4 (CH₂CH₃), 23.2 (CH₂CH₃), 32.3 (C₄-THIQ), 45.7 (C₁-THIQ), 55.1 (C₃-THIQ), 55.2 (OCH₃), 112.1 (C₇-THIQ), 113.9 (C₅-THIQ), 115.0 (2 x ArCH, phenyl), 121.9 (ArCCl), 125.6 (C₁CC₈-THIQ), 127.2 (C₈-THIQ), 129.0 (2 x ArCH, phenyl), 134.5 (C₄CC₅-THIQ), 148.3 (ArCN) and 158.2 (C₆-THIQ) ppm.

2-(3-Methoxyphenyl)-*N*-methylacetamide (218)

C₁₀H₁₃NO₂, Mol. Wt.: 179.22

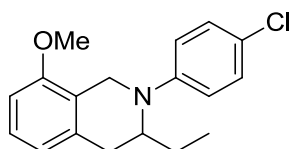


2.0 M solution of isopropylmagnesium chloride (1.72 mL, 3.44 mmol) in THF was added to a stirring solution of **208** (600 mg, 2.87 mmol) in anhydrous THF (29 mL) under inert atmosphere and the mixture was stirred at rt for 1 h. The mixture was

quenched with 1N HCl (6 mL) and extracted with EtOAc (3 x 50 mL). The combined organics were dried with MgSO₄, filtered and evaporated to give a yellow oil (486 mg). The crude compound was purified by column chromatography (eluent: from 0% to 50% EtOAc in pet. ether) to give the product as yellow oil (323 mg, 62%) which showed:²⁰¹ ¹H NMR (500 MHz, CDCl₃) δ 2.75 (3H, d, *J* = 4.8 Hz, NCH₃), 3.55 (2H, s, ArCH₂), 3.81 (3H, s, OCH₃), 5.40 (1H, bs, NH), 6.77 – 6.81 (1H, m, ArCH), 6.81 – 6.86 (2H, m, 2 x ArCH) and 7.25 – 7.31 (1H, m, ArCH) ppm. ¹³C NMR (126 MHz, CDCl₃) δ 26.5 (NCH₃), 43.8 (ArCH₂), 55.2 (OCH₃), 112.8 (ArCH), 115.2 (ArCH), 121.8 (ArCH), 130.1 (ArCH), 136.4 (ArCCH₂), 160.1 (ArCO) and 171.4 (CON) ppm. HRMS (ES⁺) calcd. C₁₀H₁₄NO₂ (M⁺+H) 180.1019, found 180.1016.

2-(4-Chlorophenyl)-3-ethyl-8-methoxy-1,2,3,4-tetrahydroisoquinoline (219b)

C₁₈H₂₀ClNO, Mol. Wt.: 301.81

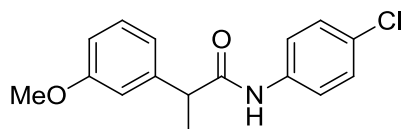


(Method J)

The crude compound was purified by column chromatography (eluent: from 0% to 20% EtOAc in pet. ether) to give the product as a colourless oil (8 mg, 4%) which showed: ¹H NMR (500 MHz, CDCl₃) δ 0.85 (3H, t, *J* = 7.4 Hz, CH₂CH₃), 1.27 – 1.42 (1H, m, CH₂CH₃), 1.47 – 1.59 (1H, m, CH₂CH₃), 2.79 (1H, d, *J* = 15.9 Hz, H₄-THIQ), 3.13 (1H, dd, *J* = 5.4, 15.9 Hz, H₄-THIQ), 3.87 (3H, s, OCH₃), 3.99 – 4.06 (1H, m, H₃-THIQ), 4.09 (1H, d, *J* = 17.4 Hz, H₁-THIQ), 4.37 (1H, d, *J* = 16.8 Hz, H₁-THIQ), 6.73 (1H, d, *J* = 7.9 Hz, H₇-THIQ), 6.76 (1H, d, *J* = 7.9 Hz, H₅-THIQ), 6.88 (2H, d, *J* = 9.1 Hz, 2 x ArCH, phenyl), 7.17 (1H, t, *J* = 7.9 Hz, H₆-THIQ) and 7.20 (2H, d, *J* = 9.1 Hz, 2 x ArCH, phenyl) ppm. ¹³C NMR (126 MHz, CDCl₃) δ 11.5 (CH₂CH₃), 22.6 (CH₂CH₃), 32.0 (C₄-THIQ), 41.5 (C₁-THIQ), 54.5 (C₃-THIQ), 55.2 (OCH₃), 107.2 (C₇-THIQ), 115.3 (2 x ArCH, phenyl), 121.3 (C₅-THIQ), 121.9 (ArCCl), 122.0 (C₁CC₈-THIQ), 126.9 (C₆-THIQ), 128.9 (2 x ArCH, phenyl), 134.2 (C₄CC₅-THIQ), 148.6 (ArCN) and 155.7 (C₈-THIQ) ppm.

***N*-(4-Chlorophenyl)-2-(3-methoxyphenyl)propanamide (224a)**

C₁₆H₁₆ClNO₂, Mol. Wt.: 289.76

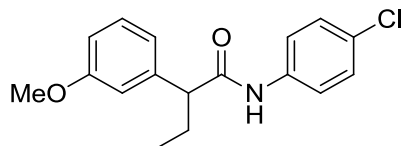


(Method N)

The crude compound was purified by column chromatography (eluent: from 0% to 40% EtOAc in pet. ether) to give the product as a yellow oil (418 mg, 25%) which showed: ¹H NMR (500 MHz, CDCl₃) δ 1.58 (3H, d, *J* = 7.1 Hz, CHCH₃), 3.68 (1H, q, *J* = 7.1 Hz, CHCH₃), 3.81 (3H, s, OCH₃), 6.85 (1H, dd, *J* = 2.3, 7.9 Hz, ArCH, phenacetyl), 6.87 – 6.90 (1H, m, ArCH, phenacetyl), 6.93 (1H, d, *J* = 7.9 Hz, ArCH, phenacetyl), 7.08 (1H, bs, NH), 7.22 (2H, d, *J* = 8.8 Hz, ArCH, aniline), 7.30 (1H, t, *J* = 7.9 Hz, ArCH, phenacetyl) and 7.36 (2H, d, *J* = 8.8 Hz, ArCH, aniline) ppm. ¹³C NMR (126 MHz, CDCl₃) δ 18.3 (CHCH₃), 48.1 (CHCH₃), 55.3 (OCH₃), 112.9 (ArCH, phenacetyl), 113.5 (ArCH, phenacetyl), 119.9 (ArCH, phenacetyl), 120.9 (2 x ArCH, aniline), 128.9 (2 x ArCH, aniline), 129.2 (ArCCl), 130.3 (ArCH, phenacetyl), 136.4 (ArCN), 142.2 (ArCCH), 160.2 (ArCO) and 172.1 (CON) ppm. HRMS (ES⁺) calcd. C₁₆H₁₇³⁵ClNO₂ (M⁺+H) 290.0942, found 290.0954; calcd. C₁₆H₁₇³⁷ClNO₂ (M⁺+H) 292.0913, found 292.0961.

***N*-(4-Chlorophenyl)-2-(3-methoxyphenyl)butanamide (224b)**

C₁₇H₁₈ClNO₂, Mol. Wt.: 303.78



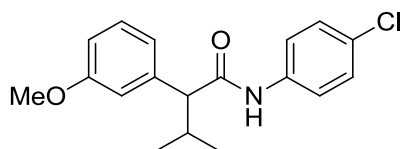
(Method N)

The crude compound was purified by column chromatography (eluent: from 0% to 40% EtOAc in pet. ether) to give the product as a yellow solid (400 mg, 24%) which showed: ¹H NMR (500 MHz, CDCl₃) δ 0.92 (3H, t, *J* = 7.4 Hz, CH₂CH₃), 1.77 – 1.96 (1H, m, CHCH₂), 2.16 – 2.35 (1H, m, CHCH₂), 3.35 (1H, t, *J* = 7.5 Hz, CHCH₂), 3.81 (3H, s, OCH₃), 6.84 (1H, dd, *J* = 2.1, 8.2 Hz, ArCH, phenacetyl), 6.87 – 6.90 (1H, m,

ArCH, phenacetyl), 6.92 (1H, d, $J = 7.6$ Hz, ArCH, phenacetyl), 7.08 (1H, bs, NH), 7.23 (2H, d, $J = 8.8$ Hz, ArCH, aniline), 7.29 (1H, t, $J = 7.9$ Hz, ArCH, phenacetyl) and 7.38 (2H, d, $J = 8.8$ Hz, ArCH, aniline) ppm. ^{13}C NMR (126 MHz, CDCl_3) δ 12.3 (CH_2CH_3), 26.2 (CHCH_2), 55.2 (OCH_3), 56.1 (CHCH_2), 112.8 (ArCH, phenacetyl), 113.8 (ArCH, phenacetyl), 120.3 (ArCH, phenacetyl), 120.9 (2 x ArCH, aniline), 128.9 (2 x ArCH, aniline), 129.2 (ArCCl), 130.1 (ArCH, phenacetyl), 136.4 (ArCN), 140.8 (ArCCH), 160.1 (ArCO) and 171.5 (CON) ppm. HRMS (ES^+) calcd. $\text{C}_{17}\text{H}_{19}^{35}\text{ClNO}_2$ ($\text{M}^+ + \text{H}$) 304.1099, found 304.1116; calcd. $\text{C}_{17}\text{H}_{19}^{37}\text{ClNO}_2$ ($\text{M}^+ + \text{H}$) 306.1069, found 306.1098.

***N*-(4-Chlorophenyl)-2-(3-methoxyphenyl)-3-methylbutanamide (224c)**

$\text{C}_{18}\text{H}_{20}\text{ClNO}_2$, Mol. Wt.: 317.81

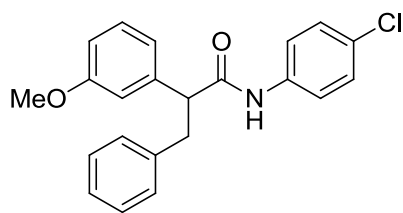


(Method N)

The crude compound was purified by column chromatography (eluent: from 0% to 20 % EtOAc in pet. ether) to give the product as a yellow oil (212 mg, 42%) which showed: ^1H NMR (500 MHz, CDCl_3) δ 0.76 (3H, d, $J = 6.6$ Hz, $(\text{CH}_3)_2\text{CH}$), 1.09 (3H, d, $J = 6.5$ Hz, $(\text{CH}_3)_2\text{CH}$), 2.40 – 2.56 (1H, m, $(\text{CH}_3)_2\text{CH}$), 2.95 (1H, d, $J = 10.0$ Hz, $(\text{CH}_3)_2\text{CHCH}$), 3.80 (3H, s, OCH_3), 6.81 (1H, dd, $J = 1.9, 8.2$ Hz, ArCH, phenacetyl), 6.87 – 6.96 (2H, m, 2 x ArCH, phenacetyl), 7.18 (1H, bs, NH), 7.20 – 7.25 (3H, m, 2 x ArCH, aniline, ArCH, phenacetyl) and 7.42 (2H, d, $J = 8.7$ Hz, 2 x ArCH, aniline) ppm. ^{13}C NMR (126 MHz, CDCl_3) δ 20.3 ($(\text{CH}_3)_2\text{CH}$), 21.7 ($(\text{CH}_3)_2\text{CH}$), 31.5 ($(\text{CH}_3)_2\text{CH}$), 55.2 (OCH_3), 62.8 ($(\text{CH}_3)_2\text{CHCH}$), 112.7 (ArCH, phenacetyl), 113.9 (ArCH, phenacetyl), 120.7 (ArCH, phenacetyl), 121.0 (2 x ArCH, aniline), 128.9 (2 x ArCH, aniline), 129.2 (ArCCl), 129.7 (ArCH, phenacetyl), 136.4 (ArCN), 140.2 (ArCCH), 159.8 (ArCO) and 171.4 (CON) ppm.

***N*-(4-Chlorophenyl)-2-(3-methoxyphenyl)-3-phenylpropanamide (224d)**

$\text{C}_{22}\text{H}_{20}\text{ClNO}_2$, Mol. Wt.: 365.85

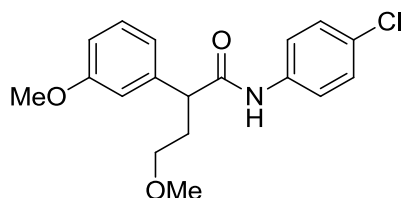


(Method N)

The crude compound was purified by column chromatography (eluent: from 0% to 40% EtOAc in pet. ether) to give the product as a yellow oil (145 mg, 9%) which showed: ^1H NMR (500 MHz, CDCl_3) δ 3.04 (1H, dd, $J = 7.4, 13.6$ Hz, CHCH_2), 3.60 (1H, dd, $J = 7.4, 13.6$ Hz, CHCH_2), 3.69 (1H, t, $J = 7.4$ Hz, CHCH_2), 3.78 (3H, s, OCH_3), 6.82 (1H, dd, $J = 2.2, 8.2$ Hz, ArCH, methoxyphenyl), 6.84 – 6.88 (1H, m, ArCH, methoxyphenyl), 6.90 (1H, d, $J = 7.6$ Hz, ArCH, methoxyphenyl) 6.98 (1H, bs, NH), 7.13 (2H, d, $J = 7.3$ Hz, 2 x ArCH, phenyl), 7.17 (1H, t, $J = 7.3$ Hz, ArCH, phenyl), 7.21 (3H, d, $J = 8.8$ Hz, 2 x ArCH, aniline), 7.23 (2H, d, $J = 7.3$ Hz, ArCH, phenyl), 7.26 (1H, d, $J = 7.8$ Hz, ArCH, methoxyphenyl) and 7.32 (2H, d, $J = 8.7$ Hz, ArCH, aniline) ppm. ^{13}C NMR (126 MHz, CDCl_3) δ 39.5 (CHCH_2), 55.3 (OCH_3), 56.5 (CHCH_2), 113.1 (ArCH, methoxyphenyl), 113.8 (ArCH, methoxyphenyl), 120.4 (ArCH, methoxyphenyl), 121.1 (2 x ArCH, aniline), 126.4 (ArCH, phenyl), 128.4 (2 x ArCH, aniline), 128.9 (2 x ArCH, phenyl), 129.0 (2 x ArCH, aniline), 129.3 (ArCCl), 130.0 (ArCH, methoxyphenyl), 136.2 (ArCN), 139.3 (ArCCH₂), 140.4 (ArCCH), 160.0 (ArCO) and 170.7 (CON) ppm. HRMS (ES^+) calcd. $\text{C}_{22}\text{H}_{21}^{35}\text{ClNO}_2$ ($\text{M}^+ + \text{H}$) 366.1255, found 366.1274; calcd. $\text{C}_{22}\text{H}_{21}^{37}\text{ClNO}_2$ ($\text{M}^+ + \text{H}$) 368.1226, found 368.1250.

***N*-(4-Chlorophenyl)-4-methoxy-2-(3-methoxyphenyl)butanamide (224e)**

$\text{C}_{18}\text{H}_{20}\text{ClNO}_3$, Mol. Wt.: 333.81



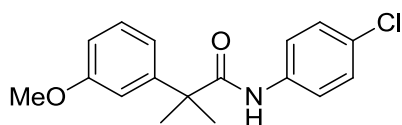
(Method N)

The crude compound was purified by column chromatography (eluent: from 0% to 40% EtOAc in pet. ether) to give the product as a yellow oil (44 mg, 3%) which

showed: ^1H NMR (500 MHz, CDCl_3) δ 1.98 – 2.10 (1H, m, CHCH_2), 2.39 – 2.52 (1H, m, CHCH_2), 3.25 – 3.31 (1H, m, CH_2O), 3.31 (3H, s, CH_2OCH_3), 3.40 – 3.49 (1H, m, CHCH_2), 3.72 (1H, t, $J = 7.4$ Hz, CHCH_2), 3.80 (3H, s, ArOCH_3), 6.83 (1H, dd, $J = 2.1$, 8.2 Hz, ArCH, phenacetyl), 6.88 – 6.92 (1H, m, ArCH, phenacetyl), 6.94 (1H, d, $J = 7.6$ Hz, ArCH, phenacetyl), 7.23 (2H, d, $J = 8.8$ Hz, 2 x ArCH, aniline), 7.27 (2H, t, $J = 8.0$ Hz, ArCH, phenacetyl), 7.35 (1H, bs, NH) and 7.40 (2H, d, $J = 8.8$ Hz, 2 x ArCH, aniline) ppm. ^{13}C NMR (126 MHz, CDCl_3) δ 33.1 (CHCH_2), 50.3 (CHCH_2), 55.2 (ArOCH_3), 58.6 (CH_2OCH_3), 69.8 (CH_2OCH_3), 112.9 (ArCH, phenacetyl), 113.8 (ArCH, phenacetyl), 120.4 (ArCH, phenacetyl), 120.9 (2 x ArCH, aniline), 128.9 (2 x ArCH, aniline), 129.1, 130.0 (ArCH, phenacetyl), 136.5 (ArCN), 140.6 (ArCCH), 160.0 (ArCO) and 171.3 (CON) ppm. HRMS (ES^+) calcd. $\text{C}_{18}\text{H}_{21}^{35}\text{ClNO}_2$ ($\text{M}^+ + \text{H}$) 334.1204, found 334.1215; calcd. $\text{C}_{18}\text{H}_{21}^{37}\text{ClNO}_2$ ($\text{M}^+ + \text{H}$) 336.1175, found 336.1190.

***N*-(4-Chlorophenyl)-2-(3-methoxyphenyl)-2-methylpropanamide (224f)**

$\text{C}_{17}\text{H}_{18}\text{ClNO}_2$, Mol. Wt.: 303.78

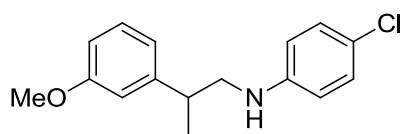


(Method N)

The crude compound was not purified and showed: ^1H NMR (500 MHz, CDCl_3) δ 1.64 (6H, s, $(\text{CH}_3)_2\text{C}$), 3.82 (3H, s, OCH_3), 6.81 (1H, bs, NH), 6.86 (1H, dd, $J = 2.1$, 7.9 Hz, ArCH, phenacetyl), 6.96 (1H, t, $J = 2.1$ Hz, ArCH, phenacetyl), 7.01 (1H, dd, $J = 2.1$, 7.9 Hz, ArCH, phenacetyl), 7.21 (2H, d, $J = 8.8$ Hz, 2 x ArCH, aniline), 7.31 (2H, d, $J = 8.8$ Hz, 2 x ArCH, aniline) and 7.33 (2H, t, $J = 7.9$ Hz, ArCH, phenacetyl) ppm. ^{13}C NMR (126 MHz, CDCl_3) δ 26.9 ($(\text{CH}_3)_2\text{C}$), 48.1 ($(\text{CH}_3)_2\text{C}$), 55.3 (OCH_3), 112.2 (ArCH, phenacetyl), 112.9 (ArCH, phenacetyl), 118.8 (ArCH, phenacetyl), 120.9 (2 x ArCH, aniline), 128.8 (2 x ArCH, aniline), 129.1 (ArCCl), 130.1 (ArCH, phenacetyl), 136.5 (ArCN), 146.0 ($\text{ArC}(\text{CH}_3)_2$), 160.0 (ArCO) and 175.5 (CON) ppm. HRMS (ES^+) calcd. $\text{C}_{18}\text{H}_{21}^{35}\text{ClNO}_2$ ($\text{M}^+ + \text{H}$) 334.1204, found 334.1215; calcd. $\text{C}_{18}\text{H}_{21}^{37}\text{ClNO}_2$ ($\text{M}^+ + \text{H}$) 336.1175, found 336.1190.

4-Chloro-*N*-(2-(3-methoxyphenyl)propyl)aniline (225a)

C₁₆H₁₈ClNO, Mol. Wt.: 275.77

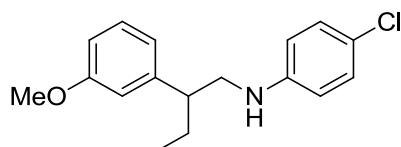


(Method I)

The crude compound was not purified and showed: ¹H NMR (500 MHz, CDCl₃) δ 1.33 (3H, d, *J* = 6.9 Hz, CHCH₃), 2.97 – 3.11 (1H, m, CHCH₃), 3.20 (1H, dd, *J* = 8.3, 12.4 Hz, CHCH₂), 3.31 (1H, dd, *J* = 6.2, 12.4 Hz, CHCH₂), 3.80 (3H, s, OCH₃), 6.57 (2H, d, *J* = 8.8 Hz, 2 x ArCH, aniline), 6.74 – 6.76 (1H, m, ArCH, phenyl), 6.76 – 6.83 (2H, m, 2 x ArCH, phenyl), 7.11 (2H, d, *J* = 8.8 Hz, 2 x ArCH, aniline) and 7.25 (2H, t, *J* = 7.9 Hz, ArCH, phenyl) ppm. ¹³C NMR (126 MHz, CDCl₃) δ 19.7 (CHCH₃), 39.0 (CHCH₃), 51.6 (CHCH₂), 55.2 (OCH₃), 111.7 (ArCH, phenyl), 113.2 (ArCH, phenyl), 115.0 (2 x ArCH, aniline), 119.5 (ArCH, phenyl), 123.0 (ArCCl), 129.1 (2 x ArCH, aniline), 129.7 (ArCH, phenyl), 145.5 (ArCN), 145.7 (ArCCH) and 159.9 (ArCO) ppm.

4-Chloro-*N*-(2-(3-methoxyphenyl)butyl)aniline (225b)

C₁₇H₂₀ClNO, Mol. Wt.: 289.80



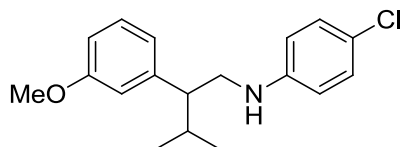
(Method I)

The crude compound was not purified and showed: ¹H NMR (500 MHz, CDCl₃) δ 0.83 (3H, t, *J* = 7.4 Hz, CH₂CH₃), 1.56 – 1.67 (1H, m, CH₂CH₃), 1.73 – 1.85 (1H, m, CH₂CH₃), 2.70 – 2.83 (1H, m, CHCH₂CH₃), 3.18 (1H, dd, *J* = 9.1, 12.3 Hz, CH₂N), 3.41 (1H, dd, *J* = 5.6, 12.4 Hz, CH₂N), 3.80 (3H, s, OCH₃), 6.56 (2H, d, *J* = 8.8 Hz, 2 x ArCH, aniline), 6.69 – 6.72 (1H, m, ArCH, phenyl), 6.76 (1H, d, *J* = 8.0 Hz, ArCH, phenyl), 6.78 (1H, dd, *J* = 2.4, 8.0 Hz, ArCH, phenyl), 7.10 (2H, d, *J* = 8.8 Hz, 2 x ArCH, aniline) and 7.24 (1H, t, *J* = 8.0 Hz, ArCH, phenyl) ppm. ¹³C NMR (126 MHz, CDCl₃) δ 12.0 (CH₂CH₃), 27.0 (CH₂CH₃), 46.8 (CHCH₂CH₃), 50.4 (CH₂N), 55.2 (OCH₃), 111.7 (ArCH, phenyl), 113.9 (ArCH, phenyl), 115.2 (2 x ArCH, aniline), 120.2 (ArCH, phenyl), 123.2 (ArCCl), 129.1 (2 x ArCH, aniline), 129.7 (ArCH, phenyl),

144.1 (ArCCH), 145.2 (ArCN) and 159.9 (ArCO) ppm. HRMS (ES^+) calcd. $\text{C}_{17}\text{H}_{21}^{35}\text{ClNO}_2$ (M^++H) 290.1306, found 290.1322; calcd. $\text{C}_{17}\text{H}_{21}^{37}\text{ClNO}_2$ (M^++H) 292.1277, found 292.1268.

4-Chloro-*N*-(2-(3-methoxyphenyl)-3-methylbutyl)aniline (225c)

$\text{C}_{18}\text{H}_{22}\text{ClNO}$, Mol. Wt.: 303.83

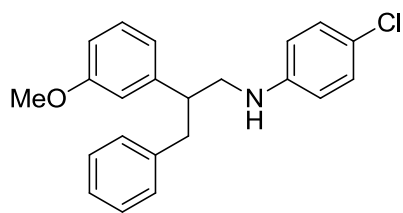


(Method I)

The crude compound was not purified and showed: ^1H NMR (500 MHz, CDCl_3) δ 0.77 (3H, d, $J = 6.7$ Hz, $\text{CH}(\text{CH}_3)_2$), 1.05 (3H, d, $J = 6.6$ Hz, $\text{CH}(\text{CH}_3)_2$), 1.84 – 1.99 (1H, m, $\text{CH}(\text{CH}_3)_2$), 2.55 (1H, ddd, $J = 4.4, 8.4, 10.5$ Hz, CHCH_2), 3.16 (1H, dd, $J = 10.7, 11.8$ Hz, CHCH_2), 3.37 (1H, bs, NH), 3.56 (1H, dd, $J = 4.2, 11.9$ Hz, CHCH_2), 3.79 (3H, s, OCH_3), 6.44 (2H, d, $J = 8.9$ Hz, 2 x ArCH, aniline), 6.68 – 6.70 (1H, m, ArCH, phenethyl), 6.72 – 6.76 (1H, m, ArCH, phenethyl), 6.79 (1H, ddd, $J = 0.8, 2.6, 8.2$ Hz, ArCH, phenethyl), 7.07 (2H, d, $J = 8.9$ Hz, 2 x ArCH, aniline) and 7.20 – 7.26 (1H, m, ArCH, phenethyl) ppm. ^{13}C NMR (126 MHz, CDCl_3) δ 21.1($\text{CH}(\text{CH}_3)_2$), 21.2($\text{CH}(\text{CH}_3)_2$), 31.9 ($\text{CH}(\text{CH}_3)_2$), 47.0 (CHCH_2), 52.6 (CHCH_2), 55.3 (OCH_3), 111.8 (ArCH, phenethyl), 114.3 (2 x ArCH, aniline), 114.7 (ArCH, phenethyl), 121.0 (ArCH, phenethyl), 121.9 (ArCCl), 129.1 (2 x ArCH, aniline), 129.6 (ArCH, phenethyl), 143.8 (ArCCH₂), 147.0 (ArCN) and 159.9 (ArCO) ppm. HRMS (ES^+) calcd. $\text{C}_{18}\text{H}_{23}^{35}\text{ClNO}_2$ (M^++H) 304.1463, found 304.1465; calcd. $\text{C}_{18}\text{H}_{23}^{37}\text{ClNO}_2$ (M^++H) 306.1433, found 306.1465.

4-Chloro-*N*-(2-(3-methoxyphenyl)-3-phenylpropyl)aniline (225d)

$\text{C}_{22}\text{H}_{22}\text{ClNO}$, Mol. Wt.: 351.87

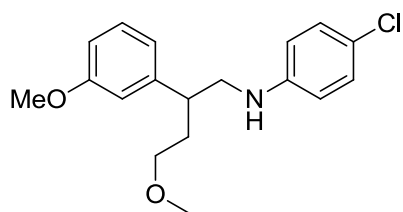


(Method I)

The crude compound was not purified and showed: ^1H NMR (500 MHz, CDCl_3) δ 2.97 (2H, d, $J = 7.3$ Hz, ArCH_2 , phenyl), 3.13 – 3.20 (1H, m, CHCH_2), 3.23 (1H, dd, $J = 8.9, 12.2$ Hz, CH_2N), 3.41 (1H, dd, $J = 4.9, 12.2$ Hz, CH_2N), 3.77 (3H, s, OCH_3), 6.43 (2H, d, $J = 8.8$ Hz, 2 x ArCH , aniline), 6.67 – 6.71 (1H, m, ArCH , methoxyphenyl), 6.74 – 6.80 (2H, m, 2 x ArCH , methoxyphenyl), 7.06 (2H, d, $J = 8.8$ Hz, 2 x ArCH , aniline), 7.09 (2H, d, $J = 7.1$ Hz, 2 x ArCH , phenyl) and 7.18 – 7.26 (4H, m, 3 x ArCH , phenyl, ArCH , methoxyphenyl) ppm. ^{13}C NMR (126 MHz, CDCl_3) δ 40.8 (ArCH_2 , phenyl), 46.6 (CHCH_2), 49.3 (CH_2N), 55.2 (OCH_3), 112.0 (ArCH , methoxyphenyl), 113.8 (ArCH , methoxyphenyl), 115.0 (2 x ArCH , aniline), 120.0 (ArCH , methoxyphenyl), 123.1 (ArCCl), 126.3 (ArCH , phenyl), 127.7, 128.3 (2 x ArCH , phenyl), 129.0 (2 x ArCH , phenyl), 129.1 (2 x ArCH , aniline), 129.7 (ArCH , methoxyphenyl), 139.5 (ArCCH_2), 143.8 (ArCCH), 145.3 (ArCN) and 159.8 (ArCO) ppm. HRMS (ES^+) calcd. $\text{C}_{22}\text{H}_{22}^{35}\text{ClNO}$ ($\text{M}^+\text{-H}$) 350.1317, found 350.1330; calcd. $\text{C}_{22}\text{H}_{23}^{37}\text{ClNO}$ ($\text{M}^+\text{-H}$) 352.1288, found 352.1275.

4-Chloro-N-(4-methoxy-2-(3-methoxyphenyl)butyl)aniline (225e)

$\text{C}_{18}\text{H}_{22}\text{ClNO}_2$, Mol. Wt.: 319.83

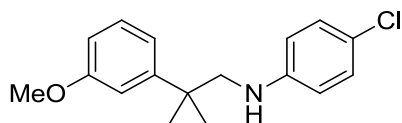


(Method I)

The crude compound was not purified and showed: HRMS (ES^+) calcd. $\text{C}_{18}\text{H}_{23}^{35}\text{ClNO}_2$ ($\text{M}^+\text{+H}$) 320.1412, found 320.1414; calcd. $\text{C}_{18}\text{H}_{23}^{37}\text{ClNO}_2$ ($\text{M}^+\text{+H}$) 322.1382, found 322.1399.

4-Chloro-*N*-(2-(3-methoxyphenyl)-2-methylpropyl)aniline (225f)

C₁₇H₂₀ClNO, Mol. Wt.: 289.80

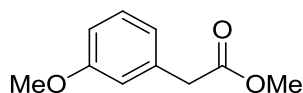


(Method I)

The crude compound was not purified and showed: ¹H NMR (500 MHz, CDCl₃) δ 1.32 (6H, s, (CH₃)₂C), 3.15 (2H, s, CH₂N), 3.74 (3H, s, OCH₃), 6.40 (2H, d, *J* = 8.7 Hz, 2 x ArCH, aniline), 6.71 (1H, dd, *J* = 2.4, 8.0 Hz, ArCH, phenyl), 6.83 – 6.87 (1H, m, ArCH, phenyl), 6.89 (1H, d, *J* = 8.0 Hz, ArCH, phenyl), 6.99 (2H, d, *J* = 8.7 Hz, 2 x ArCH, aniline) and 7.20 (1H, t, *J* = 8.0 Hz, ArCH, phenyl) ppm. ¹³C NMR (126 MHz, CDCl₃) δ 27.2 ((CH₃)₂C), 38.8 ((CH₃)₂C), 55.2 (OCH₃), 57.9 (CH₂N), 111.0 (ArCH, phenyl), 112.9 (ArCH, phenyl), 116.3 (2 x ArCH, aniline), 118.4 (ArCH, phenyl), 124.2 (ArCCl), 129.1 (2 x ArCH, aniline), 129.6 (ArCH, phenyl), 147.4 (ArCN), 147.7 (ArCC(CH₃)₂) and 159.8 (ArCO). HRMS (ES⁺) calcd. C₁₇H₂₁³⁵ClNO (M⁺+H) 290.1306, found 290.1320.

Methyl 2-(3-methoxyphenyl)acetate (226)

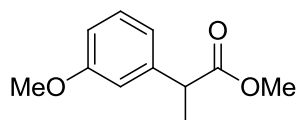
C₁₀H₁₂O₃, Mol. Wt.: 180.20



Conc. H₂SO₄ (1.2 mL) was added dropwise to a stirring solution of 3-methoxyphenylacetic acid (6.78 g, 40.0 mmol) in MeOH (80 mL) and the mixture was refluxed for 3 days. Product did not form according to TLC. The mixture was then stirred for 3 h under reflux and inert atmosphere using a Soxhlet extractor containing CaH₂ as dehydrating agent. The mixture was then neutralised with Na₂CO₃, filtered and evaporated. The residue was dissolved in EtOAc (100 mL) and washed with 1 N NaOH (3 x 100 mL) and brine (100 mL) then dried with MgSO₄, filtered and evaporated to give the product as a colourless oil (6.36 g, 88%) which showed: ¹H NMR (400 MHz, CDCl₃) δ 3.60 (2H, s), 3.69 (3H, s), 3.80 (3H, s), 6.79 – 6.84 (2H, m), 6.86 (1H, d, *J* = 7.6 Hz) and 7.24 (1H, t, *J* = 7.8 Hz) ppm.

Methyl 2-(3-methoxyphenyl)propanoate (227a)

C₁₁H₁₄O₃, Mol. Wt.: 194.23

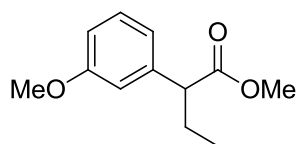


(Method M)

The crude compound was not purified and showed: ¹H NMR (500 MHz, CDCl₃) δ 1.49 (3H, d, *J* = 7.1 Hz, CHCH₃), 3.66 (3H, s, COOCH₃), 3.70 (1H, q, *J* = 7.1 Hz, CHCH₃), 3.80 (3H, s, ArOCH₃), 6.80 (1H, dd, *J* = 2.3, 8.2 Hz, ArCH), 6.84 (1H, t, *J* = 2.3 Hz, ArCH), 6.88 (1H, dd, *J* = 2.3, 8.2 Hz, ArCH) and 7.24 (1H, t, *J* = 8.0 Hz, ArCH) ppm. ¹³C NMR (126 MHz, CDCl₃) δ 18.5 (CHCH₃), 45.4 (CHCH₃), 52.0 (COOCH₃), 55.2 (ArOCH₃), 112.4 (ArCH), 113.2 (ArCH), 119.8 (ArCH), 129.6 (ArCH), 142.0 (ArCCH), 159.7 (ArCO) and 174.8 (COO) ppm. HRMS (ES⁺) calcd. C₁₁H₁₅O₃ (M⁺+H) 195.1021, found 195.1014; calcd. C₁₁H₁₄NaO₃ (M⁺+H) 217.0841, found 217.0831.

Methyl 2-(3-methoxyphenyl)butanoate (227b)

C₁₂H₁₆O₃, Mol. Wt.: 208.25

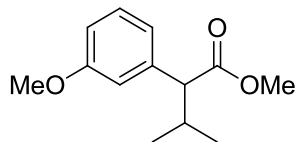


(Method M)

The crude compound was not purified and showed: ¹H NMR (500 MHz, CDCl₃) δ 0.89 (3H, t, *J* = 7.4 Hz, CH₂CH₃), 1.72 – 1.86 (1H, m, CHCH₂), 2.03 – 2.14 (1H, m, CHCH₂), 3.42 (1H, t, *J* = 7.7 Hz, CHCH₂), 3.66 (3H, s, COOCH₃), 3.80 (3H, s, ArOCH₃), 6.80 (1H, ddd, *J* = 0.6, 2.5, 7.9 Hz, ArCH), 6.83 – 6.86 (1H, m, ArCH), 6.88 (1H, d, *J* = 7.9 Hz, ArCH) and 7.23 (1H, t, *J* = 7.9 Hz, ArCH) ppm. ¹³C NMR (126 MHz, CDCl₃) δ 12.1 (CH₂CH₃), 26.7 (CHCH₂), 51.9 (COOCH₃), 53.4 (CHCH₂), 55.2 (ArOCH₃), 112.5 (ArCH), 113.6 (ArCH), 120.4 (ArCH), 129.5 (ArCH), 140.6 (ArCCH), 159.7 (ArCO) and 174.4 (COO) ppm. HRMS (ES⁺) calcd. C₁₂H₁₇O₃ (M⁺+H) 209.1178, found 209.1163; calcd. C₁₂H₁₆NaO₃ (M⁺+H) 231.0997, found 231.0980.

Methyl 2-(3-methoxyphenyl)-3-methylbutanoate (227c)

C₁₃H₁₈O₃, Mol. Wt.: 222.28

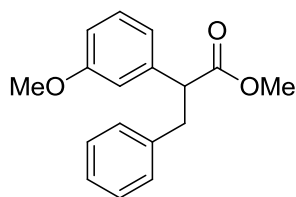


(Method M)

The crude compound was purified by column chromatography (eluent: from 0% to 20% EtOAc in pet. ether) to give the product as a yellow oil (243mg, 20%) which showed: ¹H NMR (500 MHz, CDCl₃) δ 0.71 (3H, d, *J* = 6.7 Hz, (CH₃)₂CH), 1.02 (3H, d, *J* = 6.5 Hz, (CH₃)₂CH), 2.24 – 2.41 (1H, m, (CH₃)₂CH), 3.12 (1H, d, *J* = 10.6 Hz, (CH₃)₂CHCH), 3.65 (3H, s, COOCH₃), 3.80 (3H, s, ArOCH₃), 6.80 (1H, dd, *J* = 1.7, 8.2 Hz, ArCH), 6.90 (2H, d, *J* = 7.8 Hz, 2 x ArCH) and 7.22 (1H, t, *J* = 7.8 Hz, ArCH) ppm. ¹³C NMR (126 MHz, CDCl₃) δ 20.2 ((CH₃)₂CH), 21.5 ((CH₃)₂CH), 31.9 ((CH₃)₂CH), 51.7 (COOCH₃), 55.2 (ArOCH₃), 60.0 ((CH₃)₂CHCH), 112.5 (ArCH), 114.1 (ArCH), 121.0 (ArCH), 129.3 (ArCH), 139.9 (ArCCH), 159.6 (ArCO) and 174.3 (COO) ppm. HRMS (ES⁺) calcd. C₁₃H₁₉O₃ (M⁺+H) 223.1334, found 223.1325; calcd. C₁₃H₁₈NaO₃ (M⁺+H) 245.1153, found 245.1133.

Methyl 2-(3-methoxyphenyl)-3-phenylpropanoate (227d)

C₁₇H₁₈O₃, Mol. Wt.: 270.32



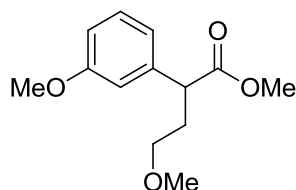
(Method M)

The crude compound was purified by column chromatography (eluent: from 0% to 10% EtOAc in pet. ether) to give the product as a colourless oil (1.29 g, 86 %) which showed: ¹H NMR (500 MHz, CDCl₃) δ 3.02 (1H, dd, *J* = 6.7, 13.7 Hz, CH₂CH), 3.41 (1H, dd, *J* = 8.8, 13.7 Hz, CH₂CH), 3.61 (3H, s, COOCH₃), 3.79 (3H, s, ArOCH₃), 3.83

(1H, dd, $J = 6.7, 8.8$ Hz, CH_2CH), 6.81 (1H, dd, $J = 2.4, 8.2$ Hz, ArCH, methoxyphenyl), 6.84 – 6.88 (1H, m, ArCH, methoxyphenyl), 6.89 (1H, d, $J = 7.7$ Hz, ArCH, methoxyphenyl), 7.13 (2H, d, $J = 7.1$ Hz, 2 x ArCH, phenyl) and 7.16 – 7.26 (4H, m, 3 x ArCH, phenyl, ArCH, methoxyphenyl) ppm. ^{13}C NMR (126 MHz, CDCl_3) δ 39.7 (CH_2CH), 52.0 (COOCH_3), 53.6 (CH_2CH), 55.2 (ArOCH_3), 112.8 (ArCH, methoxyphenyl), 113.6 (ArCH, methoxyphenyl), 120.3 (ArCH, methoxyphenyl), 126.4 (ArCH, phenyl), 128.3 (2 x ArCH, phenyl), 128.9 (2 x ArCH, phenyl), 129.6 (ArCH, methoxyphenyl), 139.0 (ArCCH_2), 140.1 (ArCCH), 159.7 (ArCO) and 173.7 (COO) ppm. HRMS (ES^+) calcd. $\text{C}_{17}\text{H}_{19}\text{O}_3$ ($\text{M}^+ + \text{H}$) 271.1334, found 271.1320; calcd. $\text{C}_{17}\text{H}_{18}\text{NaO}_3$ ($\text{M}^+ + \text{H}$) 293.1154, found 293.1149.

Methyl 4-methoxy-2-(3-methoxyphenyl)butanoate (227e)

$\text{C}_{13}\text{H}_{18}\text{O}_4$, Mol. Wt.: 238.28

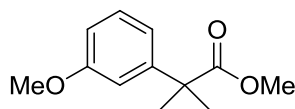


(Method M)

The crude compound was purified by column chromatography (eluent: from 0% to 10% EtOAc in pet. ether) to give the product as a yellow oil (430 mg, 33%) which showed: ^1H NMR (500 MHz, CDCl_3) δ 1.91 – 2.05 (1H, m, CHCH_2), 2.29 – 2.42 (1H, m, CHCH_2), 3.22 – 3.28 (1H, m, CH_2O), 3.29 (3H, s, CH_2OCH_3), 3.36 (1H, dt, $J = 5.8, 11.3$ Hz, CH_2O), 3.66 (3H, s, COOCH_3), 3.71 – 3.76 (1H, m, CHCH_2), 3.80 (3H, s, ArOCH_3), 6.78 – 6.83 (1H, m, ArCH), 6.85 (1H, s, ArCH), 6.89 (1H, d, $J = 8.0$ Hz, ArCH) and 7.23 (1H, t, $J = 8.0$ Hz, ArCH) ppm. ^{13}C NMR (126 MHz, CDCl_3) δ 33.2 (CHCH_2), 47.9 (CHCH_2), 52.0 (COOCH_3), 55.2 (ArOCH_3), 58.6 (CH_2OCH_3), 69.9 (CH_2OCH_3), 112.7 (ArCH), 113.6 (ArCH), 120.4 (ArCH), 129.6 (ArCH), 140.2 (ArCCH), 159.8 (ArCO) and 174.2 (COO) ppm. HRMS (ES^+) calcd. $\text{C}_{13}\text{H}_{18}\text{NaO}_4$ ($\text{M}^+ + \text{H}$) 261.1103, found 261.1116.

Methyl 2-(3-methoxyphenyl)-2-methylpropanoate (227f)

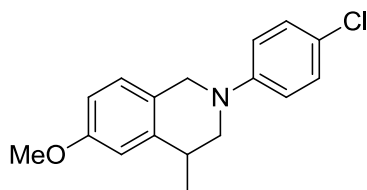
C₁₂H₁₆O₃, Mol. Wt.: 208.25



(Method M)

The crude compound was not purified and showed: ²⁰⁰ ¹H NMR (500 MHz, CDCl₃) δ 1.57 (6H, s, C(CH₃)₂), 3.65 (3H, s, COOCH₃), 3.80 (3H, s, ArOCH₃), 6.78 (1H, dd, *J* = 2.2, 7.9 Hz, ArCH), 6.88 (1H, t, *J* = 2.2 Hz, ArCH), 6.92 (1H, dd, *J* = 2.2, 7.9 Hz, ArCH) and 7.25 (1H, t, *J* = 7.9 Hz, ArCH) ppm. ¹³C NMR (126 MHz, CDCl₃) δ 26.5 (C(CH₃)₂), 46.5 (C(CH₃)₂), 52.2 (COOCH₃), 55.2 (ArOCH₃), 111.4 (ArCH), 112.1 (ArCH), 118.0 (ArCH), 129.3 (ArCH), 146.3 (ArCC(CH₃)₂), 159.5 (ArCO) and 177.1 (COO) ppm. HRMS (ES⁺) calcd. C₁₂H₁₆NaO₃ (M⁺+H) 231.0997, found 231.0990.

2-(4-Chlorophenyl)-6-methoxy-4-methyl-1,2,3,4-tetrahydroisoquinoline (228a)

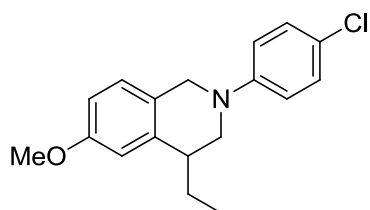


(Method J)

The crude compound was purified by column chromatography (eluent: from 0% to 20% EtOAc in pet. ether) to give the product as a white solid (302 mg, 58%) which showed: ¹H NMR (500 MHz, CDCl₃) δ 1.29 (3H, d, *J* = 6.9 Hz, CHCH₃), 2.96 – 3.06 (1H, m, H₄-THIQ), 3.19 (1H, dd, *J* = 6.2, 12.0 Hz, H₃-THIQ), 3.40 (1H, dd, *J* = 4.3, 12.0 Hz, H₃-THIQ), 3.74 (3H, s, OCH₃), 4.18 (1H, d, *J* = 14.7 Hz, H₁-THIQ), 4.27 (1H, d, *J* = 14.7 Hz, H₁-THIQ), 6.69 (1H, dd, *J* = 2.6, 8.3 Hz, H₇-THIQ), 6.72 (1H, d, *J* = 2.6 Hz, H₅-THIQ), 6.78 (2H, d, *J* = 9.0 Hz, 2 x ArCH, phenyl), 7.00 (1H, d, *J* = 8.3 Hz, H₈-THIQ) and 7.14 (2H, d, *J* = 9.0 Hz, 2 x ArCH, phenyl) ppm. ¹³C NMR (126 MHz, CDCl₃) δ 19.6 (CHCH₃), 33.5 (C₄-THIQ), 50.0 (C₁-THIQ), 53.4 (C₃-THIQ), 55.3 (OCH₃), 112.0 (C₅-THIQ), 112.3 (C₇-THIQ), 115.7 (2 x ArCH, phenyl), 122.9 (ArCCl), 125.8 (C₁CC₈-THIQ), 127.4 (C₈-THIQ), 129.0 (2 x ArCH, phenyl), 141.2 (C₄CC₅-THIQ), 149.3 (ArCN) and 158.4 (C₆-THIQ) ppm. Mp 72-75 °C (pet. ether).

2-(4-Chlorophenyl)-4-ethyl-6-methoxy-1,2,3,4-tetrahydroisoquinoline (228b)

C₁₈H₂₀ClNO, Mol. Wt.: 301.81



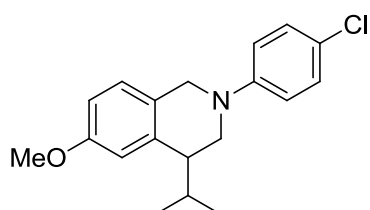
(Method J)

The crude compound was purified by column chromatography (eluent: from 0% to 20% EtOAc in pet. ether) to give the product as a yellow oil (384 mg, 74%) which showed: ¹H NMR (500 MHz, CDCl₃) δ 0.97 (3H, t, *J* = 7.4 Hz, CH₂CH₃), 1.59 – 1.72 (2H, m, CH₂CH₃), 2.67 – 2.75 (1H, m, H₄-THIQ), 3.24 (1H, dd, *J* = 3.8, 12.1 Hz, H₃-THIQ), 3.53 (1H, dd, *J* = 4.1, 12.1 Hz, H₃-THIQ), 3.74 (3H, s, OCH₃), 4.10 (1H, d, *J* = 14.6 Hz, H₁-THIQ), 4.32 (1H, d, *J* = 14.7 Hz, H₁-THIQ), 6.68 (1H, d, *J* = 2.4 Hz, H₅-THIQ), 6.70 (1H, dd, *J* = 2.6, 8.3 Hz, H₇-THIQ), 6.77 (2H, d, *J* = 9.0 Hz, 2 x ArCH, phenyl), 7.00 (1H, d, *J* = 8.3 Hz, H₈-THIQ) and 7.15 (2H, d, *J* = 9.0 Hz, 2 x ArCH, phenyl) ppm. ¹³C NMR (126 MHz, CDCl₃) δ 12.3 (CH₂CH₃), 27.2 (CH₂CH₃), 41.0 (C₄-THIQ), 49.5 (C₃-THIQ), 49.7 (C₁-THIQ), 55.3 (OCH₃), 112.2 (C₇-THIQ), 113.1 (C₅-THIQ), 115.2 (2 x ArCH, phenyl), 122.6 (ArCCl), 125.7 (C₁CC₈-THIQ), 127.5 (C₈-THIQ), 129.0 (2 x ArCH, phenyl), 140.3 (C₄CC₅-THIQ), 149.4 (ArCN) and 158.1 (C₆-THIQ) ppm.

2-(4-Chlorophenyl)-4-isopropyl-6-methoxy-1,2,3,4-tetrahydroisoquinoline

(228c)

C₁₉H₂₂ClNO, Mol. Wt.: 315.84

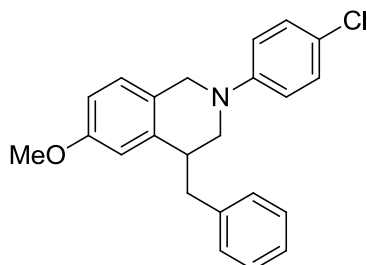


(Method J)

The crude compound was purified by column chromatography (eluent: from 0% to 20% EtOAc in pet. ether) to give the product as a colourless oil (53 mg, 36%) which showed: ^1H NMR (500 MHz, CDCl_3) δ 0.94 (3H, d, $J = 6.8$ Hz, $(\text{CH}_3)_2\text{CH}$), 0.98 (3H, d, $J = 6.8$ Hz, $(\text{CH}_3)_2\text{CH}$), 1.93 – 2.04 (1H, m, $(\text{CH}_3)_2\text{CH}$), 2.61 (1H, dt, $J = 3.6, 7.2$ Hz, $\text{H}_4\text{-THIQ}$), 3.23 (1H, dd, $J = 3.6, 12.1$ Hz, $\text{H}_3\text{-THIQ}$), 3.79 (1H, dd, $J = 3.6, 12.1$ Hz, $\text{H}_3\text{-THIQ}$), 3.81 (3H, s, OCH_3), 4.16 (1H, d, $J = 14.6$ Hz, $\text{H}_1\text{-THIQ}$), 4.44 (1H, d, $J = 14.6$ Hz, $\text{H}_1\text{-THIQ}$), 6.73 (1H, d, $J = 2.6$ Hz, $\text{H}_5\text{-THIQ}$), 6.79 (1H, dd, $J = 2.6, 8.4$ Hz, $\text{H}_7\text{-THIQ}$), 6.81 (2H, d, $J = 9.1$ Hz, 2 x ArCH, phenyl), 7.08 (1H, d, $J = 8.4$ Hz, $\text{H}_8\text{-THIQ}$) and 7.22 (2H, d, $J = 9.0$ Hz, 2 x ArCH, phenyl) ppm. ^{13}C NMR (126 MHz, CDCl_3) δ 20.1 ($(\text{CH}_3)_2\text{CH}$), 21.5 ($(\text{CH}_3)_2\text{CH}$), 30.7 ($(\text{CH}_3)_2\text{CH}$), 46.2 ($\text{C}_4\text{-THIQ}$), 46.4 ($\text{C}_3\text{-THIQ}$), 49.4 ($\text{C}_1\text{-THIQ}$), 55.3 (OCH_3), 112.1 ($\text{C}_7\text{-THIQ}$), 114.0 ($\text{C}_5\text{-THIQ}$), 114.3 (2 x ArCH, phenyl), 122.0 (ArCCL), 125.9 ($\text{C}_1\text{CC}_8\text{-THIQ}$), 127.6 ($\text{C}_8\text{-THIQ}$), 128.8, 129.0 (2 x ArCH, phenyl), 139.5 ($\text{C}_4\text{CC}_5\text{-THIQ}$), 148.7 (ArCN) and 157.8 ($\text{C}_6\text{-THIQ}$) ppm.

4-Benzyl-2-(4-chlorophenyl)-6-methoxy-1,2,3,4-tetrahydroisoquinoline (228d)

$\text{C}_{23}\text{H}_{22}\text{ClNO}$, Mol. Wt.: 363.88



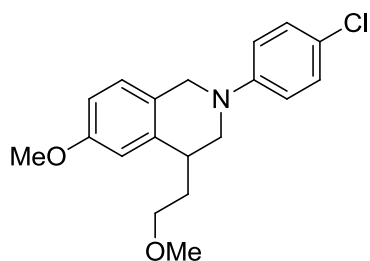
(Method J)

The crude compound was purified by column chromatography (eluent: from 0% to 20% EtOAc in pet. ether) to give the product as a white solid (327 mg, 63%) which showed: ^1H NMR (500 MHz, CDCl_3) δ 2.86 (1H, dd, $J = 10.1, 13.7$ Hz, ArCH_2CH), 2.97 (1H, dd, $J = 5.3, 13.7$ Hz, ArCH_2CH), 3.03 (1H, dd, $J = 3.4, 12.2$ Hz, $\text{H}_3\text{-THIQ}$), 3.06 - 3.12 (1H, m, $\text{H}_4\text{-THIQ}$), 3.48 (1H, dd, $J = 3.0, 12.2$ Hz, $\text{H}_3\text{-THIQ}$), 3.68 (3H, s, OCH_3), 4.07 (1H, d, $J = 14.8$ Hz, $\text{H}_1\text{-THIQ}$), 4.44 (1H, d, $J = 14.7$ Hz, $\text{H}_1\text{-THIQ}$), 6.57 (1H, d, $J = 2.5$ Hz, $\text{H}_5\text{-THIQ}$), 6.70 (2H, d, $J = 9.0$ Hz, 2 x ArCH, *N*-phenyl), 6.73 (1H, dd, $J = 2.6, 8.5$ Hz, $\text{H}_7\text{-THIQ}$), 7.03 (1H, d, $J = 8.4$ Hz, $\text{H}_8\text{-THIQ}$), 7.08 - 7.15 (4H, m, 2 x ArCH, *N*-phenyl, 2 x ArCH, $\text{C}_4\text{-phenyl}$), 7.17 – 7.19 (1H, m, ArCH, $\text{C}_4\text{-phenyl}$) and

7.25 (2H, t, $J = 7.3$ Hz, 2 x ArCH, C₄-phenyl) ppm. ¹³C NMR (126 MHz, CDCl₃) δ 41.3 (ArCH₂CH), 41.6 (C₄-THIQ), 48.5 (C₃-THIQ), 49.9 (C₁-THIQ), 55.3 (OCH₃), 112.9 (C₇-THIQ), 113.0 (C₅-THIQ), 115.4 (2 x ArCH, *N*-phenyl), 122.9 (ArCCl), 125.5 (C₁CC₈-THIQ), 126.4 (ArCH, C₄-phenyl), 127.6 (C₈-THIQ), 128.5 (2 x ArCH, C₄-phenyl), 128.9 (2 x ArCH), 129.4 (2 x ArCH), 139.4 (C₄CC₅-THIQ), 140.1 (ArCCH₂, C₄-phenyl), 149.3 (ArCN) and 158.1 (C₆-THIQ) ppm. Mp 84-87 °C (pet. ether).

2-(4-Chlorophenyl)-6-methoxy-4-(2-methoxyethyl)-1,2,3,4-tetrahydroisoquinoline (228e)

C₁₉H₂₂ClNO₂, Mol. Wt.: 331.84



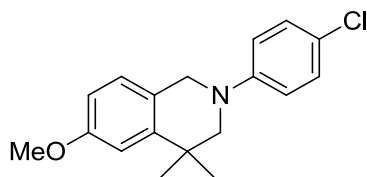
(Method J)

The crude compound was purified by column chromatography (eluent: from 0% to 20% EtOAc in pet. ether) to give the product as a yellow oil (76 mg, 37%) which showed: ¹H NMR (500 MHz, CDCl₃) δ 1.88 – 2.03 (2H, m, CHCH₂), 3.06 – 3.13 (1H, m, H₄-THIQ), 3.28 (1H, dd, $J = 3.5, 12.1$ Hz, H₃-THIQ), 3.39 (3H, s, CH₂OCH₃), 3.42 - 3.55 (2H, m, CH₂O), 3.67 (1H, dd, $J = 3.3, 12.1$ Hz, H₃-THIQ), 3.81 (3H, s, ArOCH₃), 4.15 (1H, d, $J = 14.7$ Hz, H₁-THIQ), 4.43 (1H, d, $J = 14.7$ Hz, H₁-THIQ), 6.76 (1H, d, $J = 2.6$ Hz, H₅-THIQ), 6.79 (1H, dd, $J = 2.6, 8.3$ Hz, H₇-THIQ), 6.85 (2H, d, $J = 9.0$ Hz, 2 x ArCH, phenyl), 7.08 (1H, d, $J = 8.3$ Hz, H₈-THIQ) and 7.22 (2H, d, $J = 9.0$ Hz, 2 x ArCH, phenyl) ppm. ¹³C NMR (126 MHz, CDCl₃) δ 34.3 (CHCH₂), 36.4 (C₄-THIQ), 49.6 (C₁-THIQ), 50.0 (C₃-THIQ), 55.3 (ArOCH₃), 58.7 (CH₂OCH₃), 70.6 (CH₂O), 112.6 (C₇-THIQ), 113.1 (C₅-THIQ), 115.2 (2 x ArCH, phenyl), 122.7 (ArCCl), 125.6 (C₁CC₈-THIQ), 127.6 (C₈-THIQ), 128.9 (2 x ArCH, phenyl), 139.6 (C₄CC₅-THIQ), 149.3 (ArCN) and 158.1 (C₆-THIQ) ppm.

2-(4-Chlorophenyl)-6-methoxy-4,4-dimethyl-1,2,3,4-tetrahydroisoquinoline

(228f)

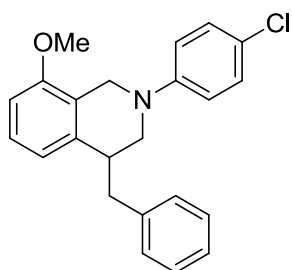
C₁₈H₂₀ClNO, Mol. Wt.: 301.81



(Method J)

The crude compound was purified by column chromatography (eluent: from 0% to 20% EtOAc in pet. ether) to give the product as a white solid (94 mg, 23%) which showed: ¹H NMR (500 MHz, CDCl₃) δ 1.28 (6H, s, (CH₃)₂C), 3.14 (2H, s, H₃-THIQ), 3.74 (3H, s, OCH₃), 4.22 (2H, s, H₁-THIQ), 6.68 (1H, dd, *J* = 2.6, 8.4 Hz, H₇-THIQ), 6.79 (2H, d, *J* = 9.0 Hz, 2 x ArCH, phenyl), 6.83 (1H, d, *J* = 2.6 Hz, H₅-THIQ), 6.98 (1H, d, *J* = 8.4 Hz, H₈-THIQ) and 7.15 (2H, d, *J* = 9.0 Hz, 2 x ArCH, phenyl) ppm. ¹³C NMR (126 MHz, CDCl₃) δ 28.1 ((CH₃)₂C), 35.8 (C₄-THIQ), 50.5 (C₁-THIQ), 55.3 (OCH₃), 59.9 (C₃-THIQ), 110.9 (C₅-THIQ), 111.6 (C₇-THIQ), 115.7 (2 x ArCH, phenyl), 123.0 (ArCCl), 125.1 (C₁CC₈-THIQ), 127.4 (C₈-THIQ), 129.0 (2 x ArCH, phenyl), 145.0 (C₄CC₅-THIQ), 149.5 (ArCN) and 158.4 (C₆-THIQ). Mp 90-93 °C (pet. ether) ppm.

4-Benzyl-2-(4-chlorophenyl)-8-methoxy-1,2,3,4-tetrahydroisoquinoline (230d)



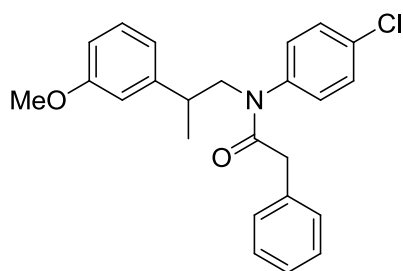
(Method J)

The crude compound was purified by column chromatography (eluent: from 0% to 20% EtOAc in pet. ether) to give the product as a colourless oil (19 mg, 4%) which showed: ¹H NMR (500 MHz, CDCl₃) δ 2.81 – 2.88 (1H, m, ArCH₂CH), 2.93 – 2.99 (2H, m, ArCH₂CH, H₃-THIQ), 3.08 – 3.16 (1H, m, H₄-THIQ), 3.49 (1H, dd, *J* = 2.6, 12.3 Hz, H₃-THIQ), 3.81 (3H, s, OCH₃), 3.97 (1H, d, *J* = 16.4 Hz, H₁-THIQ), 4.44 (1H,

d, $J = 16.4$ Hz, H₁-THIQ), 6.69 (1H, d, $J = 8.1$ Hz, H₅ or H₇-THIQ), 6.76 (3H, d, $J = 8.9$ Hz, 2 x ArCH, *N*-phenyl, H₅ or H₇-THIQ), 7.10 – 7.16 (5H, m, 2 x ArCH, *N*-phenyl, 2 x ArCH, C₄-phenyl, H₆-THIQ), 7.18 (1H, t, $J = 7.2$ Hz, ArCH, C₄-phenyl) and 7.25 (2H, t, $J = 7.3$ Hz, 2 x ArCH, C₄-phenyl) ppm. ¹³C NMR (126 MHz, CDCl₃) δ 41.4 (C₃-THIQ), 41.5 (ArCH₂CH), 46.0 (C₁-THIQ), 47.7 (C₄-THIQ), 55.3 (OCH₃), 107.4 (C₇ or C₅-THIQ), 115.5 (2 x ArCH, *N*-phenyl), 120.4 (C₇ or C₅-THIQ), 122.3 (C₁CC₈-THIQ), 122.8 (ArCCl), 126.3 (ArCH), 126.9 (ArCH, C₄-phenyl), 128.5 (2 x ArCH), 128.9 (2 x ArCH), 129.4 (2 x ArCH), 139.7 (C₄CC₅-THIQ), 140.3 (ArCCH₂, C₄-phenyl), 149.5 (ArCN) and 156.0 (C₈-THIQ) ppm.

***N*-(4-Chlorophenyl)-*N*-(2-(3-methoxyphenyl)propyl)-2-phenylacetamide (231a)**

C₂₄H₂₄ClNO₂, Mol. Wt.: 393.91

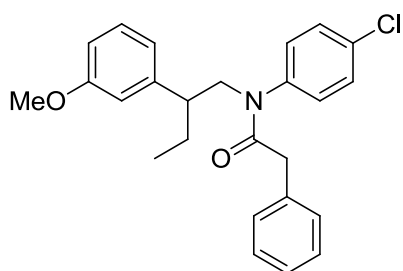


Phenacetyl chloride (162 μ L, 1.20 mmol) was added to a stirring solution of **225a** (300 mg, 1.09 mmol) and Et₃N (229 μ L, 1.64 mmol) in DCM (3 mL) and the mixture was stirred overnight at rt under inert atmosphere. The mixture was then diluted with DCM (25 mL) washed with 1 N NaOH (3 x 25 mL), 1 N HCl (3 x 25 mL) and brine (25 mL), then dried with MgSO₄, filtered and evaporated to give a yellow oil (403 mg). The crude compound was purified by column chromatography (eluent: from 0% to 40% EtOAc in pet. ether) to give the product as a colourless oil (223 mg, 52%) which showed: ¹H NMR (500 MHz, CDCl₃) δ 1.14 (3H, d, $J = 7.0$ Hz, CHCH₃), 2.89 – 3.01 (1H, m, CHCH₃), 3.27 (2H, s, CH₂CO), 3.67 (3H, s, OCH₃), 3.68 – 3.73 (1H, m, CH₂N), 3.93 (1H, dd, $J = 6.9, 13.5$ Hz, CH₂N), 6.58 (2H, d, $J = 7.4$ Hz, 2 x ArCH, aniline), 6.59 – 6.61 (1H, m, ArCH, methoxyphenyl), 6.63 (1H, d, $J = 7.9$ Hz, ArCH, methoxyphenyl), 6.67 (1H, dd, $J = 2.0, 7.9$ Hz, ArCH, methoxyphenyl), 6.85 (2H, d, $J = 7.4$ Hz, 2 x ArCH, aniline), 7.08 (1H, t, $J = 7.9$ Hz, ArCH, methoxyphenyl) and 7.10 – 7.17 (5H, m, 5 x ArCH, phenyl) ppm. ¹³C NMR (126 MHz, CDCl₃) δ 19.9 (CHCH₃), 38.3 (CHCH₃), 41.4 (CH₂CO), 55.2 (OCH₃), 55.9 (CH₂N), 112.1 (ArCH,

methoxyphenyl), 113.1 (ArCH, methoxyphenyl), 120.0 (ArCH, methoxyphenyl), 126.6 (ArCH, phenyl), 128.4 (2 x ArCH, phenyl), 128.8 (2 x ArCH, aniline), 129.4 (ArCH, methoxyphenyl), 129.5 (ArCH, phenyl), 129.7 (2 x ArCH, aniline), 133.6 (ArCCl), 135.2 (ArCCH₂), 141.3 (ArCN), 145.7 (ArCCH), 159.7 (ArCO) and 170.9 (CON) ppm.

***N*-(4-Chlorophenyl)-*N*-(2-(3-methoxyphenyl)butyl)-2-phenylacetamide (231b)**

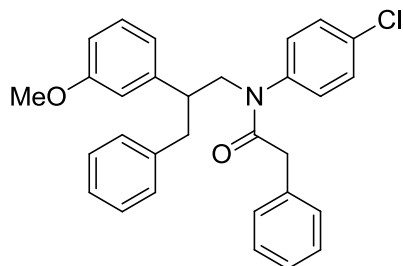
C₂₅H₂₆ClNO₂, Mol. Wt.: 407.93



Phenacetyl chloride (154 μ L, 1.14 mmol) was added to a stirring solution of **225b** (300 mg, 1.04 mmol) and Et₃N (218 μ L, 1.56 mmol) in DCM (3 mL) and the mixture was stirred overnight at rt under inert atmosphere. The mixture was then diluted with DCM (25 mL) washed with 1 N NaOH (3 x 25 mL), 1 N HCl (3 x 25 mL) and brine (25 mL), then dried with MgSO₄, filtered and evaporated to give a yellow oil (426 mg). The crude compound was purified by column chromatography (eluent: from 0% to 40% EtOAc in pet. ether) to give the product as a colourless oil (361 mg, 85%) which showed: ¹H NMR (500 MHz, CDCl₃) δ 0.68 (3H, t, *J* = 7.4 Hz, CH₂CH₃), 1.36 – 1.48 (1H, m, CH₂CH₃), 1.54 – 1.63 (1H, m, CH₂CH₃), 2.64 – 2.79 (1H, m, CHCH₂), 3.24 (2H, s, CH₂CO), 3.66 (3H, s, OCH₃), 3.72 (1H, dd, *J* = 9.9, 13.5 Hz, CH₂N), 3.98 (1H, dd, *J* = 6.1, 13.5 Hz, CH₂N), 6.44 - 6.53 (2H, m, 2 x ArCH, aniline), 6.53 – 6.57 (1H, m, ArCH, methoxyphenyl), 6.58 (1H, d, *J* = 7.8 Hz, ArCH, methoxyphenyl), 6.68 (1H, dd, *J* = 2.1, 7.8 Hz, ArCH, methoxyphenyl), 6.80 – 6.85 (2H, m, 2 x ArCH, phenyl), 7.07 (2H, t, *J* = 7.8 Hz, ArCH, methoxyphenyl) and 7.09 – 7.15 (5H, m, 3 x ArCH, phenyl, 2 x ArCH, aniline) ppm. ¹³C NMR (126 MHz, CDCl₃) δ 11.8 (CH₂CH₃), 27.1 (CH₂CH₃), 41.4 (CH₂CO), 45.8 (CHCH₂), 54.8 (CH₂N), 55.2 (OCH₃), 112.1 (ArCH, methoxyphenyl), 113.8 (ArCH, methoxyphenyl), 120.9 (ArCH, methoxyphenyl), 126.5 (ArCH, phenyl), 128.3 (2 x ArCH), 128.8 (2 x ArCH), 129.2 (ArCH, methoxyphenyl), 129.4 (2 x ArCH), 129.7 (2 x ArCH), 133.5 (ArCCl), 135.2 (ArCCH₂), 141.4 (ArCN), 144.0 (ArCCH), 159.6 (ArCO) and 170.8 (CON) ppm.

***N*-(4-Chlorophenyl)-*N*-(2-(3-methoxyphenyl)-3-phenylpropyl)-2-phenylacetamide (231d)**

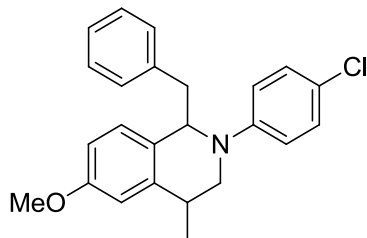
C₃₀H₂₈ClNO₂, Mol. Wt.: 470.00



Phenacetyl chloride (127 μ L, 0.938 mmol) was added to a stirring solution of **225c** (300 mg, 0.853 mmol) and Et₃N (179 μ L, 1.28 mmol) in DCM (3 mL) and the mixture was stirred overnight at rt under inert atmosphere. The mixture was then diluted with DCM (25 mL) washed with 1 N NaOH (3 x 25 mL), 1 N HCl (3 x 25 mL) and brine (25 mL), then dried with MgSO₄, filtered and evaporated to give a yellow oil (387 mg). The crude compound was purified by column chromatography (eluent: from 0% to 40% EtOAc in pet. ether) to give the product as a colourless oil (153 mg, 38%) which showed: ¹H NMR (500 MHz, CDCl₃) δ 2.77 (2H, dd, J = 8.4, 13.8 Hz, ArCH₂CH), 2.83 (2H, dd, J = 6.5, 13.8 Hz, ArCH₂CH), 3.07 – 3.17 (1H, m, ArCH₂CH), 3.23 (2H, s, ArCH₂CO), 3.62 (3H, s, OCH₃), 3.86 (1H, dd, J = 9.9, 13.6 Hz, CH₂N), 4.00 (1H, dd, J = 6.1, 13.6 Hz, CH₂N), 6.48 (2H, d, J = 7.4 Hz, 2 x ArCH, aniline), 6.49 – 6.52 (1H, m, ArCH, methoxyphenyl), 6.54 (1H, d, J = 7.8 Hz, ArCH, methoxyphenyl), 6.66 (1H, dd, J = 2.1, 7.8 Hz, ArCH, methoxyphenyl), 6.78 – 6.84 (2H, m, 2 x ArCH), 6.88 (2H, d, J = 7.0 Hz, 2 x ArCH), 7.03 (1H, t, J = 7.8 Hz, ArCH, methoxyphenyl) and 7.05 - 7.15 (8H, m, 8 x ArCH) ppm. ¹³C NMR (126 MHz, CDCl₃) δ 41.0 (ArCH₂CH), 41.4 (ArCH₂CO), 45.6 (ArCH₂CH), 54.0 (CH₂N), 55.2 (OCH₃), 112.4 (ArCH, methoxyphenyl), 113.7 (ArCH, methoxyphenyl), 120.8 (ArCH, methoxyphenyl), 126.0 (ArCH), 126.6 (ArCH), 128.1 (2 x ArCH), 128.3 (2 x ArCH), 128.8 (2 x ArCH), 129.0 (2 x ArCH), 129.3 (ArCH, methoxyphenyl), 129.4 (2 x ArCH), 129.7 (2 x ArCH), 133.6 (ArCCl), 135.1 (ArCCH₂CO), 139.4 (ArCCH₂CH), 141.1 (ArCN), 143.3 (ArCCH), 159.6 (ArCO) and 170.9 (CON) ppm.

***trans*-1-Benzyl-2-(4-chlorophenyl)-6-methoxy-4-methyl-1,2,3,4-tetrahydroisoquinoline (*trans*-232a)**

C₂₄H₂₄ClNO, Mol. Wt.: 377.91

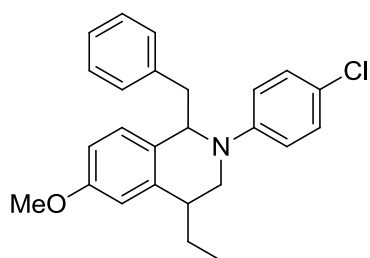


(Method K)

The crude compound was purified by column chromatography (eluent: from 0% to 10% EtOAc in pet. ether) to give the product as a yellow oil (22 mg, 36%) which showed: ¹H NMR (500 MHz, CDCl₃) δ 1.32 (3H, d, *J* = 6.8 Hz, CHCH₃), 3.02 (1H, dd, *J* = 5.5, 13.7 Hz, ArCH₂CH), 3.04 – 3.14 (1H, m, H₄-THIQ), 3.14 – 3.26 (2H, m, 1 x ArCH₂CH, 1 x H₃-THIQ), 3.66 – 3.74 (1H, m, 1 x H₃-THIQ), 3.79 (3H, s, OCH₃), 4.78 – 4.87 (1H, m, H₁-THIQ), 6.61 (2H, d, *J* = 9.1 Hz, 2 x ArCH, *N*-phenyl), 6.68 (1H, dd, *J* = 2.6, 8.5 Hz, H₇-THIQ), 6.82 (H, d, *J* = 2.6 Hz, H₅-THIQ), 6.86 (H, d, *J* = 8.5 Hz, H₈-THIQ), 7.05 (2H, d, *J* = 9.1 Hz, 2 x ArCH, *N*-phenyl), 7.10 – 7.15 (2H, m, 2 x ArCH, benzyl), 7.18 – 7.22 (2H, m, 2 x ArCH, benzyl) and 7.22 – 7.25 (1H, m, ArCH, benzyl) ppm. ¹³C NMR (126 MHz, CDCl₃) δ 18.0 (CHCH₃), 29.5 (C₄-THIQ), 41.9 (ArCH₂CH), 48.0 (C₃-THIQ), 55.2 (OCH₃), 61.9 (C₁-THIQ), 111.4 (C₇-THIQ), 112.1 (C₅-THIQ), 116.5 (2 x ArCH, *N*-phenyl), 122.5 (ArCCl), 126.3(2 x ArCH, benzyl), 128.3(ArCH, benzyl), 128.4(2 x ArCH, *N*-phenyl), 128.8(C₈-THIQ), 129.0 (C₁CC₈-THIQ), 129.6 (2 x ArCH, benzyl), 139.2 (ArCCH₂), 140.9 (C₄CC₅-THIQ), 148.6 (ArCN) and 158.3 (C₆-THIQ) ppm.

***trans*-1-Benzyl-2-(4-chlorophenyl)-4-ethyl-6-methoxy-1,2,3,4-tetrahydroisoquinoline (*trans*-232b)**

C₂₅H₂₆ClNO, Mol. Wt.: 391.93

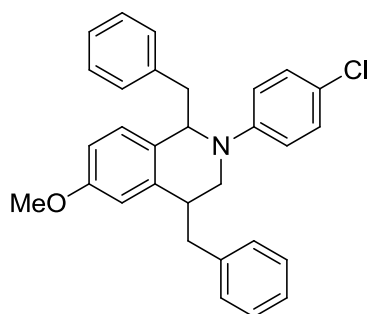


(Method K)

The crude compound was purified by column chromatography (eluent: from 0% to 10% EtOAc in pet. ether) to give the product as a yellow oil (87 mg, 46%) which showed: ^1H NMR (500 MHz, CDCl_3) δ 1.03 (3H, t, $J = 7.4$ Hz, CH_2CH_3), 1.59 – 1.78 (1H, m, CH_2CH_3), 1.90 – 2.04 (1H, m, CH_2CH_3), 2.92 – 3.05 (2H, m, H_4 -THIQ, ArCH_2CH), 3.19 (1H, dd, $J = 7.2, 13.4$ Hz, ArCH_2CH), 3.32 (1H, dd, $J = 10.5, 13.6$ Hz, H_3 -THIQ), 3.73 (1H, dd, $J = 5.8, 13.6$ Hz, H_3 -THIQ), 3.78 (3H, s, OCH_3), 4.80 (1H, t, $J = 6.5$ Hz, H_1 -THIQ), 6.65 (1H, dd, $J = 2.6, 8.6$ Hz, H_7 -THIQ), 6.67 (2H, d, $J = 8.8$ Hz, 2 x ArCH , N -phenyl), 6.77 (1H, d, $J = 8.5$ Hz, H_8 -THIQ), 6.81 (1H, d, $J = 2.2$ Hz, H_5 -THIQ), 7.02 – 7.14 (4H, m, 2 x ArCH , N -phenyl, 2 x ArCH , phenyl), 7.15 – 7.21 (1H, m, ArCH , phenyl) and 7.21 – 7.25 (2H, m, 2 x ArCH , phenyl) ppm. ^{13}C NMR (126 MHz, CDCl_3) δ 10.9 (CH_2CH_3), 25.8 (CH_2CH_3), 35.9 (C_4 -THIQ), 41.7 (ArCH_2CH), 45.8 (C_3 -THIQ), 55.2 (OCH_3), 61.8 (C_1 -THIQ), 111.3 (C_7 -THIQ), 112.3 (C_5 -THIQ), 116.9 (2 x ArCH , N -phenyl), 120.9 (ArCCl), 126.3 (ArCH , phenyl), 128.3 (2 x ArCH , phenyl), 128.6 (C_8 -THIQ), 128.9 (2 x ArCH , N -phenyl), 129.3 (C_1CC_8 -THIQ), 129.7 (2 x ArCH , phenyl), 138.9 (ArCCH_2CH), 139.4 (C_4CC_5 -THIQ), 148.5 (ArCN) and 158.3 (C_6 -THIQ) ppm.

***trans*-1,4-Dibenzyl-2-(4-chlorophenyl)-6-methoxy-1,2,3,4-tetrahydroisoquinoline
(*trans*-232d)**

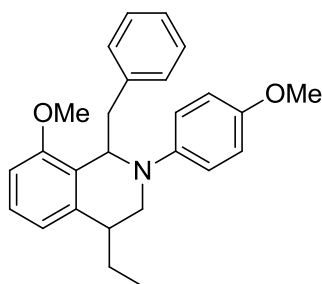
$\text{C}_{30}\text{H}_{28}\text{ClNO}$, Mol. Wt.: 454.00



(Method K)

The crude compound was purified by column chromatography (eluent: from 0% to 10% EtOAc in pet. ether) to give the product as a colourless oil (11 mg, 46%) which showed: ^1H NMR (400 MHz, CDCl_3) δ 2.68 (1H, dd, $J = 8.5, 13.5$ Hz), 2.94 (1H, dd, $J = 6.6, 13.6$ Hz), 3.29 (4H, t, $J = 10.7$ Hz), 3.47 (1H, d, $J = 7.6$ Hz), 3.76 (3H, s), 4.80 (1H, t, $J = 6.3$ Hz), 6.63 – 6.73 (3H, m), 6.78 (1H, d, $J = 8.6$ Hz), 6.85 (1H, d, $J = 2.5$ Hz), 7.01 (2H, d, $J = 6.4$ Hz), 7.07 (2H, d, $J = 8.9$ Hz), 7.14 – 7.24 (6H, m) and 7.29 – 7.37 (2H, m) ppm.

***trans*-1-Benzyl-4-ethyl-8-methoxy-2-(4-methoxyphenyl)-1,2,3,4-tetrahydroisoquinoline (*trans*-233b)**



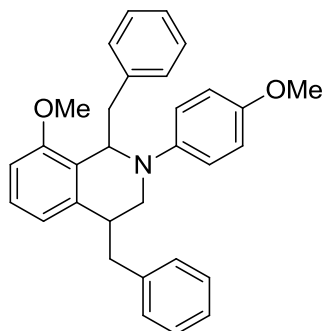
(Method K)

The crude compound was purified by column chromatography (eluent: from 0% to 10% EtOAc in pet. ether) to give the product as a white solid (22mg, 12%) which showed: ^1H NMR (500 MHz, CDCl_3) δ 1.04 (3H, t, $J = 7.4$ Hz, CH_2CH_3), 1.60 – 1.74 (1H, m, CH_2CH_3), 1.97 – 2.13 (1H, m, CH_2CH_3), 2.99 – 3.12 (2H, m, ArCH_2CH , $\text{H}_4\text{-THIQ}$), 3.19 (1H, dd, $J = 3.0, 13.8$ Hz, ArCH_2CH), 3.51 (1H, dd, $J = 11.5, 14.3$ Hz, $\text{H}_3\text{-THIQ}$), 3.82 (1H, dd, $J = 6.6, 14.3$ Hz, $\text{H}_3\text{-THIQ}$), 3.89 (3H, s, OCH_3), 5.05 (1H, d, $J = 8.1$ Hz, $\text{H}_1\text{-THIQ}$), 6.50 (2H, d, $J = 9.0$ Hz, 2 x ArCH , $N\text{-phenyl}$), 6.72 (1H, d, $J = 8.1$ Hz, $\text{H}_7\text{-THIQ}$), 6.92 (1H, d, $J = 7.8$ Hz, $\text{H}_5\text{-THIQ}$), 6.95 (2H, d, $J = 9.0$ Hz, 2 x ArCH , $N\text{-phenyl}$), 7.15 – 7.22 (2H, m, 1 x ArCH , phenyl, $\text{H}_6\text{-THIQ}$) and 7.22 - 7.29 (4H, m, 4 x ArCH , phenyl) ppm. ^{13}C NMR (126 MHz, CDCl_3) δ 10.8 (CH_2CH_3), 25.9 (CH_2CH_3), 34.1 ($\text{C}_4\text{-THIQ}$), 39.4 (ArCH_2CH), 44.5 ($\text{C}_3\text{-THIQ}$), 55.3 (OCH_3), 58.0 ($\text{C}_1\text{-THIQ}$), 107.3 ($\text{C}_7\text{-THIQ}$), 116.2 (2 x ArCH , $N\text{-phenyl}$), 119.5 ($\text{C}_5\text{-THIQ}$), 122.0 (ArCCl), 126.0 (ArCH , phenyl), 127.3 ($\text{C}_6\text{-THIQ}$), 127.5 ($\text{C}_1\text{CC}_8\text{-THIQ}$), 128.2 (2 x ArCH , phenyl),

128.6 (2 x ArCH, *N*-phenyl), 129.4 (2 x ArCH, phenyl), 139.5 (C₄CC₅-THIQ), 140.5 (ArCCH₂CH), 148.9 (ArCN) and 155.6 (C₈-THIQ) ppm.

***trans*-1,4-Dibenzyl-8-methoxy-2-(4-methoxyphenyl)-1,2,3,4-tetrahydroisoquinoline (*trans*-233d)**

C₃₀H₂₈ClNO, Mol. Wt.: 454.00

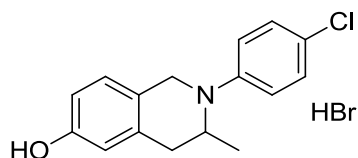


(Method K)

The crude compound was purified by column chromatography (eluent: from 0% to 10% EtOAc in pet. ether) to give the product as a colourless oil (2 mg, 8%) which showed: ¹H NMR (500 MHz, CDCl₃) δ 2.64 (1H, dd, *J* = 9.5, 13.8 Hz), 2.96 (1H, dd, *J* = 9.5, 13.7 Hz), 3.15 (1H, dd, *J* = 3.1, 13.8 Hz), 3.34 – 3.54 (3H, m), 3.90 (3H, s), 5.03 (1H, d, *J* = 7.5 Hz), 6.25 – 6.34 (2H, m), 6.76 (1H, d, *J* = 8.1 Hz), 6.86 – 6.91 (2H, m), 7.05 (1H, d, *J* = 7.4 Hz), 7.24 (6H, s), 7.24 – 7.29 (3H, m) and 7.35 (2H, dd, *J* = 6.4, 13.9 Hz) ppm.

2-(4-Chlorophenyl)-3-methyl-1,2,3,4-tetrahydroisoquinolin-6-ol hydrobromide (234a)

C₁₆H₁₇BrClNO, Mol. Wt.: 354.67

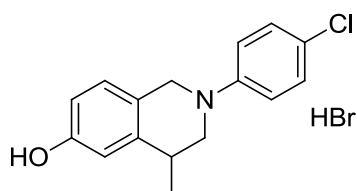


(Method G)

Filtration afforded the product as a white precipitate (429 mg, 87%) which showed: ^1H NMR (500 MHz, $\text{D}_6\text{-DMSO}$) δ 0.91 (3H, d, $J = 6.5$ Hz, CHCH_3), 2.59 (1H, dd, $J = 1.6, 15.7$ Hz, $\text{H}_4\text{-THIQ}$), 3.06 (1H, dd, $J = 5.3, 15.7$ Hz, $\text{H}_4\text{-THIQ}$), 4.03 (1H, d, $J = 15.3$ Hz, $\text{H}_1\text{-THIQ}$), 4.29 – 4.31 (1H, m, $\text{H}_3\text{-THIQ}$), 4.32 (1H, d, $J = 15.3$ Hz, $\text{H}_1\text{-THIQ}$), 6.60 (1H, d, $J = 2.2$ Hz, $\text{H}_5\text{-THIQ}$), 6.63 (1H, dd, $J = 2.2, 8.2$ Hz, $\text{H}_7\text{-THIQ}$), 6.93 (2H, d, $J = 9.1$ Hz, 2 x ArCH, phenyl), 7.04 (1H, d, $J = 8.2$ Hz, $\text{H}_8\text{-THIQ}$), 7.23 (2H, d, $J = 9.0$ Hz, 2 x ArCH, phenyl) and 9.26 (1H, bs, OH) ppm. ^{13}C NMR (126 MHz, $\text{D}_6\text{-DMSO}$) δ 15.3 (CHCH_3), 34.9 ($\text{C}_4\text{-THIQ}$), 44.9 ($\text{C}_1\text{-THIQ}$), 47.5 ($\text{C}_3\text{-THIQ}$), 113.3 ($\text{C}_7\text{-THIQ}$), 115.0 ($\text{C}_5\text{-THIQ}$), 115.1 (2 x ArCH, phenyl), 120.4 (ArCCl), 123.3 ($\text{C}_1\text{CC}_8\text{-THIQ}$), 127.2 ($\text{C}_8\text{-THIQ}$), 128.7 (2 x ArCH, phenyl), 133.8 ($\text{C}_1\text{CC}_4\text{-THI}$), 147.8 (ArCN) and 155.8 ($\text{C}_6\text{-THIQ}$) ppm. Mp 240-242 °C.

2-(4-Chlorophenyl)-4-methyl-1,2,3,4-tetrahydroisoquinolin-6-ol hydrobromide (234c)

$\text{C}_{16}\text{H}_{17}\text{BrClNO}$, Mol. Wt.: 354.67



(Method G)

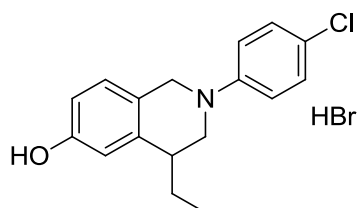
Filtration afforded the product as a yellow precipitate (178 mg, 58%) which showed: ^1H NMR (500 MHz, $\text{D}_6\text{-DMSO}$) δ 1.25 (3H, d, $J = 6.9$ Hz, CHCH_3), 2.92 – 3.04 (1H, m, $\text{H}_4\text{-THIQ}$), 3.21 (1H, dd, $J = 6.6, 12.2$ Hz, $\text{H}_3\text{-THIQ}$), 3.47 (1H, dd, $J = 4.4, 12.2$ Hz, $\text{H}_3\text{-THIQ}$), 4.20 (1H, d, $J = 15.0$ Hz, $\text{H}_1\text{-THIQ}$), 4.28 (1H, d, $J = 15.0$ Hz, $\text{H}_1\text{-THIQ}$), 6.61 (1H, dd, $J = 2.3, 8.3$ Hz, $\text{H}_7\text{-THIQ}$), 6.66 (1H, d, $J = 2.3$ Hz, $\text{H}_5\text{-THIQ}$), 6.95 (2H, d, $J = 9.0$ Hz, 2 x ArCH, phenyl), 7.00 (1H, d, $J = 8.3$ Hz, $\text{H}_8\text{-THIQ}$), 7.23 (2H, d, $J = 9.0$ Hz, 2 x ArCH, phenyl) and 9.25 (1H, bs, OH) ppm. ^{13}C NMR (126 MHz, $\text{D}_6\text{-DMSO}$) δ 19.3 (CHCH_3), 32.3 ($\text{C}_4\text{-THIQ}$), 49.0 ($\text{C}_1\text{-THIQ}$), 52.2 ($\text{C}_3\text{-THIQ}$), 113.2 ($\text{C}_5\text{-THIQ}$), 113.3 ($\text{C}_7\text{-THIQ}$), 115.5 (2 x ArCH, phenyl), 120.8 (ArCCl), 123.7 ($\text{C}_1\text{CC}_8\text{-THIQ}$), 127.3 ($\text{C}_8\text{-THIQ}$), 128.6 (2 x Arch, phenyl), 140.7 ($\text{C}_4\text{CC}_5\text{-THIQ}$), 149.1 (ArCN) and 155.8 ($\text{C}_6\text{-THIQ}$) ppm. HRMS (ES^+) calcd. $\text{C}_{16}\text{H}_{17}^{35}\text{ClNO}$ ($\text{M}^+ + \text{H}$)

274.0993, found 274.0956; calcd. $C_{16}H_{17}^{37}ClNO$ ($M^+ + H$) 276.0965, found 276.0967.
Mp 205-209 °C.

2-(4-Chlorophenyl)-4-ethyl-1,2,3,4-tetrahydroisoquinolin-6-ol hydrobromide

(234d)

$C_{17}H_{19}BrClNO$, Mol. Wt.: 368.70

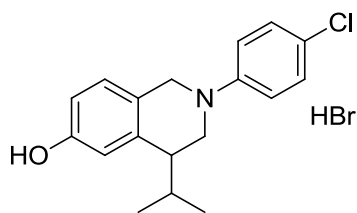


(Method G)

Filtration afforded the product as a yellow precipitate (161 mg, 47%) which showed: 1H NMR (500 MHz, D_6 -DMSO) δ 0.97 (3H, t, $J = 7.4$ Hz, CH_2CH_3), 1.50 – 1.70 (2H, m, CH_2CH_3), 2.66 – 2.78 (1H, m, H_4 -THIQ), 3.27 (1H, dd, $J = 3.9, 12.3$ Hz, H_3 -THIQ), 3.56 (1H, dd, $J = 4.4, 12.3$ Hz, H_3 -THIQ), 4.11 (1H, d, $J = 15.0$ Hz, H_1 -THIQ), 4.35 (1H, d, $J = 15.0$ Hz, H_1 -THIQ), 6.58 – 6.67 (2H, m, H_5, H_7 -THIQ), 6.94 (2H, d, $J = 9.0$ Hz, 2 x ArCH, phenyl), 7.01 (1H, d, $J = 8.9$ Hz, H_8 -THIQ), 7.24 (2H, d, $J = 9.0$ Hz, 2 x ArCH, phenyl) and 9.25 (1H, bs, OH) ppm. ^{13}C NMR (126 MHz, D_6 -DMSO) δ 11.8 (CH_2CH_3), 26.6 (CH_2CH_3), 39.6 (C_4 -THIQ), 48.7 (C_3 -THIQ), 48.8 (C_1 -THIQ), 113.4 (C_5 or C_7 -THIQ), 114.0 (C_5 or C_7 -THIQ), 115.1 (2 x ArCH, phenyl), 120.6 (ArCCl), 123.7 (C_1CC_8 -THIQ), 127.4 (C_8 -THIQ), 128.6 (2 x ArCH, phenyl), 139.6 (C_4CC_5 -THIQ), 149.1 (ArCN) and 155.6 (C_6 -THIQ) ppm. HRMS (ES^+) calcd. $C_{17}H_{19}^{35}ClNO$ ($M^+ + H$) 288.1150, found 288.1148; calcd. $C_{17}H_{19}^{37}ClNO$ ($M^+ + H$) 290.1120, found 290.1150. Mp 119-123 °C.

2-(4-Chlorophenyl)-4-isopropyl-1,2,3,4-tetrahydroisoquinolin-6-ol hydrobromide (234e)

$C_{18}H_{21}BrClNO$, Mol. Wt.: 382.72

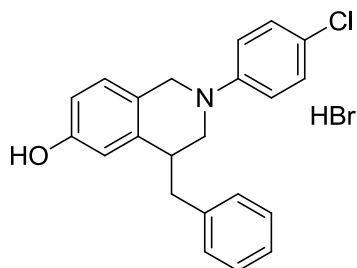


(Method G)

Filtration afforded the product as a pale yellow precipitate (12 mg, 31%) which showed: ^1H NMR (500 MHz, $\text{D}_6\text{-DMSO}$) δ 0.86 (3H, d, $J = 6.7$ Hz, $(\text{CH}_3)_2\text{CH}$), 0.92 (3H, d, $J = 6.8$ Hz, $(\text{CH}_3)_2\text{CH}$), 1.80 – 1.97 (1H, m, $(\text{CH}_3)_2\text{CH}$), 2.57 (1H, dt, $J = 3.6, 7.1$ Hz, $\text{H}_4\text{-THIQ}$), 3.15 (1H, dd, $J = 3.7, 12.4$ Hz, $\text{H}_3\text{-THIQ}$), 3.75 (1H, dd, $J = 3.9, 12.4$ Hz, $\text{H}_3\text{-THIQ}$), 4.11 (1H, d, $J = 15.1$ Hz, $\text{H}_1\text{-THIQ}$), 4.37 (1H, d, $J = 15.0$ Hz, $\text{H}_1\text{-THIQ}$), 6.62 (1H, d, $J = 2.1$ Hz, $\text{H}_5\text{-THIQ}$), 6.64 (1H, dd, $J = 2.4, 8.2$ Hz, $\text{H}_7\text{-THIQ}$), 6.91 (2H, d, $J = 9.0$ Hz, 2 x ArCH, phenyl), 7.03 (1H, d, $J = 8.2$ Hz, $\text{H}_8\text{-THIQ}$), 7.23 (2H, d, $J = 9.0$ Hz, 2 x ArCH, phenyl) and 9.27 (1H, bs, OH) ppm. ^{13}C NMR (126 MHz, $\text{D}_6\text{-DMSO}$) δ 19.7 ($(\text{CH}_3)_2\text{CH}$), 21.1 ($(\text{CH}_3)_2\text{CH}$), 30.1 ($(\text{CH}_3)_2\text{CH}$), 44.8 ($\text{C}_4\text{-THIQ}$), 45.7 ($\text{C}_3\text{-THIQ}$), 48.6 ($\text{C}_{14}\text{-THIQ}$), 113.5 ($\text{C}_7\text{-THIQ}$), 114.3 (2 x ArCH, phenyl), 114.8 ($\text{C}_5\text{-THIQ}$), 120.1 (ArCCl), 123.9 ($\text{C}_1\text{CC}_8\text{-THIQ}$), 127.5 ($\text{C}_8\text{-THIQ}$), 128.6 (2 x ArCH, phenyl), 138.9 ($\text{C}_1\text{CC}_4\text{-THIQ}$), 148.5 (ArCN) and 155.3 ($\text{C}_6\text{-THIQ}$) ppm. Mp 190-193 $^\circ\text{C}$.

4-Benzyl-2-(4-chlorophenyl)-1,2,3,4-tetrahydroisoquinolin-6-ol hydrobromide (234f)

$\text{C}_{22}\text{H}_{21}\text{BrClNO}$, Mol. Wt.: 430.77



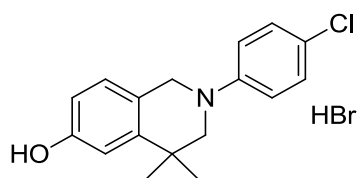
(Method G)

The crude compound was purified by reversed phase column chromatography (eluent: from 10% to 100% MeOH in water) to give the desired product as a yellow solid (201 mg, 66%) which showed: ^1H NMR (500 MHz, $\text{D}_6\text{-DMSO}$) δ 2.78 (1H, dd, J

= 10.2, 13.3 Hz, ArCH₂, benzyl), 2.96 (1H, dd, J = 4.9, 13.5 Hz, ArCH₂, benzyl), 3.05 (1H, dd, J = 3.2, 12.1 Hz, H₃-THIQ), 3.11 – 3.20 (1H, m, H₄-THIQ), 3.38 (3H, dd, J = 4.3, 12.1 Hz, H₃-THIQ), 4.08 (1H, d, J = 15.0 Hz, H₁-THIQ), 4.45 (1H, d, J = 15.0 Hz, H₄-THIQ), 6.60 – 6.69 (2H, m, H₅, H₇-THIQ), 6.80 (2H, d, J = 8.9 Hz, 2 x ArCH, phenyl), 7.04 (1H, d, J = 8.9 Hz, H₈-THIQ), 7.18 – 7.28 (5H, m, 3 x ArCH, benzyl, 2 x ArCH, phenyl), 7.32 (2H, t, J = 7.4 Hz, 2 x ArCH, benzyl) and 9.30 (1H, bs, OH) ppm. Mp 172-175 °C.

2-(4-Chlorophenyl)-4,4-dimethyl-1,2,3,4-tetrahydroisoquinolin-6-ol hydrobromide (234h)

C₁₇H₁₉BrClNO, Mol. Wt.: 368.70

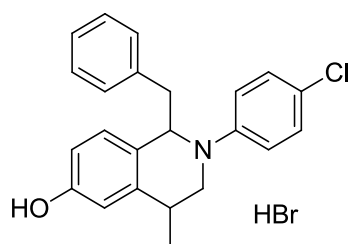


(Method G)

Filtration afforded the product as a white precipitate (81 mg, 85%) which showed: ¹H NMR (500 MHz, D₆-DMSO) δ 1.26 (6H, s, (CH₃)₂C), 3.22 (2H, s, H₃-THIQ), 4.23 (2H, s, H₁-THIQ), 6.61 (1H, dd, J = 2.3, 8.3 Hz, H₇-THIQ), 6.77 (1H, d, J = 2.3 Hz, H₅-THIQ), 6.98 (1H, d, J = 8.3 Hz), 6.98 (2H, d, J = 9.1 Hz, 2 x ArCH, phenyl), 7.25 (2H, d, J = 9.1 Hz, 2 x ArCH, phenyl) and 9.20 (1H, bs, OH) ppm. ¹³C NMR (126 MHz, D₆-DMSO) δ 27.7 ((CH₃)₂C), 35.2 (C₄-THIQ), 49.6 (C₁-THIQ), 58.5 (C₃-THIQ), 111.4 (C₅-THIQ), 113.4 (C₇-THIQ), 115.6 (2 x ArCH, phenyl), 121.0 (ArCCl), 122.8 (C₁CC₈-THIQ), 127.3 (C₈-THIQ), 128.6 (2 x ArCH, phenyl), 144.5 (C₄CC₅-THIQ), 149.3 (ArCN) and 155.9 (C₆-THIQ) ppm. HRMS (ES⁺) calcd. C₁₇H₁₉³⁵ClNO (M⁺+H) 288.1150, found 288.1137; calcd. C₁₇H₁₉³⁷ClNO (M⁺+H) 290.1120, found 290.1141. Mp 207-211 °C.

1-Benzyl-2-(4-methoxyphenyl)-4-methyl-1,2,3,4-tetrahydroisoquinolin-6-ol hydrobromide (234i)

C₂₃H₂₃ClBrNO, Mol. Wt.: 444.79

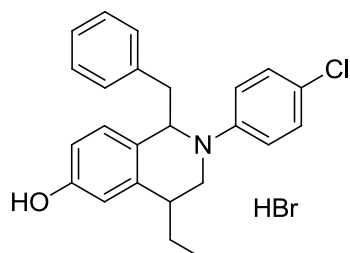


(Method G)

Filtration afforded the product as a pale yellow precipitate (19 mg, 63%) which showed: ^1H NMR (500 MHz, D_6 -DMSO) δ 1.15 (3H, d, $J = 6.6$ Hz, CHCH_3), 2.74 – 2.88 (1H, m, H_4 -THIQ), 2.91 (1H, dd, $J = 4.5, 13.7$ Hz, CH_2CH), 3.03 (1H, dd, $J = 9.4, 13.7$ Hz, CH_2CH), 3.08 – 3.18 (1H, m, H_3 -THIQ), 3.65 (1H, dd, $J = 5.5, 14.4$ Hz, H_3 -THIQ), 4.77 – 4.90 (1H, m, H_1 -THIQ), 6.44 – 6.53 (3H, m), 6.59 (2H, d, $J = 8.9$ Hz), 6.88 – 6.96 (2H, m), 7.08 (2H, dd, $J = 4.6, 10.9$ Hz), 7.16 (3H, q, $J = 7.3$ Hz) and 9.19 (2H, bs, OH) ppm. ^{13}C NMR (126 MHz, D_6 -DMSO) δ 17.8 (CHCH_3), 28.2 (C_4 -THIQ), 41.5 (CH_2CH), 46.2 (C_3 -THIQ), 60.4 (C_1 -THIQ), 113.0 (ArCH), 115.5 (2 x ArCH), 120.1 (ArCCl), 126.0 (ArCH), 127.9 (C_1CC_8 -THIQ), 128.0 (2 x ArCH), 128.3 (ArCH), 128.5 (2 x ArCH), 128.6 (ArCH), 129.4 (2 x ArCH), 139.4 (ArCH_2CH), 140.4 (C_4CC_5 -THIQ), 148.4 (ArCN) and 155.9 (C_6 -THIQ) ppm. HRMS (ES^+) calcd. $\text{C}_{23}\text{H}_{21}^{35}\text{ClNO}$ ($\text{M}^+ + \text{H}$) 362.1317, found 362.1335. Mp 133-137 °C.

1-Benzyl-4-ethyl-2-(4-methoxyphenyl)-1,2,3,4-tetrahydroisoquinolin-6-ol hydrobromide (234j)

$\text{C}_{24}\text{H}_{25}\text{ClBrNO}$, Mol. Wt.: 458.82



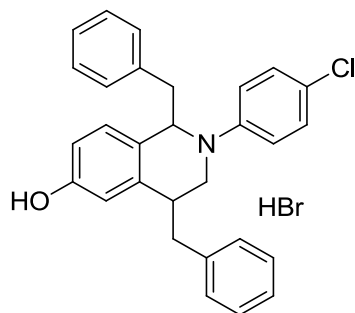
(Method G)

Filtration afforded the product as a pale yellow precipitate (88 mg, 86%) which showed: ^1H NMR (500 MHz, D_6 -DMSO) δ 0.97 (3H, t, $J = 7.4$ Hz, CH_2CH_3), 1.47 – 1.72 (1H, m, CH_2CH_3), 1.82 – 2.01 (1H, m, CH_2CH_3), 2.80 – 2.93 (1H, m, H_4 -THIQ),

2.99 (1H, dd, $J = 5.0, 13.7$ Hz, ArCH₂CH), 3.10 (1H, dd, $J = 9.2, 13.7$ Hz, ArCH₂CH), 3.32 (1H, dd, $J = 11.6, 14.2$ Hz, H₃-THIQ), 3.76 (1H, dd, $J = 5.8, 14.2$ Hz, H₃-THIQ), 4.91 (1H, dd, $J = 5.0, 8.6$ Hz, H₁-THIQ), 6.54 (1H, dd, $J = 1.9, 8.3$ Hz, H₇-THIQ), 6.68 (1H, d, $J = 1.9$ Hz, H₅-THIQ), 6.71 (2H, d, $J = 9.0$ Hz, 2 x ArCH, *N*-phenyl), 6.95 (1H, d, $J = 8.4$ Hz, H₈-THIQ), 7.05 (2H, d, $J = 9.0$ Hz, 2 x ArCH, *N*-phenyl), 7.12 - 7.19 (1H, m, ArCH, phenyl), 7.20 - 7.28 (4H, m, 4 x ArCH, phenyl) and 9.22 (1H, bs, OH) ppm. ¹³C NMR (126 MHz, D₆-DMSO) δ 10.4 (CH₂CH₃), 25.0 (CH₂CH₃), 34.0 (C₄-THIQ), 41.3 (ArCH₂CH), 43.6 (C₃-THIQ), 60.2 (C₁-THIQ), 112.8 (C₇-THIQ), 113.0 (C₅-THIQ), 115.8 (2 x ArCH, *N*-phenyl), 120.2 (ArCCl), 126.0 (ArCH), 128.0 (2 x ArCH, phenyl), 128.3 (C₁CC₈-THIQ), 128.4 (C₈-THIQ), 128.5 (2 x ArCH, *N*-phenyl), 129.4 (2 x ArCH, phenyl), 138.8 (C₄CC₅-THIQ), 139.2 (ArCCH₂CH), 148.5 (ArCN) and 155.8 (C₆-THIQ) ppm. HRMS (ES⁺) calcd. C₂₄H₂₅³⁵ClNO (M⁺+H) 378.1619, found 378.1632; calcd. C₂₄H₂₅³⁷ClNO (M⁺+H) 380.1590, found 380.1616; calcd. C₂₄H₂₄³⁵ClNNaO (M⁺+H) 400.1439, found 400.1466. Mp 179-181 °C.

1,4-Dibenzyl-2-(4-methoxyphenyl)-1,2,3,4-tetrahydroisoquinolin-6-ol hydrobromide (234k)

C₂₉H₂₇ClBrNO, Mol. Wt.: 520.89



(Method G)

Filtration afforded the product as a white precipitate (12 mg, 45%) which showed: ¹H NMR (500 MHz, D₆-DMSO) δ 2.60 - 2.77 (1H, m, H₃-THIQ), 2.95 (2H, ddd, $J = 7.2, 13.7, 18.8$ Hz, CH₂C₁), 3.15 - 3.32 (4H, m, H₃, H₄-THIQ, CH₂C₄), 4.84 - 4.95 (1H, m, H₁-THIQ), 6.50 (2H, d, $J = 8.9$ Hz, 2 x ArCH, *N*-phenyl), 6.57 (1H, d, $J = 8.4$ Hz, H₇-THIQ), 6.85 (1H, s, H₅-THIQ), 6.96 (1H, d, $J = 8.4$ Hz, H₈-THIQ), 7.01 (2H, d, $J = 8.9$ Hz, 2 x ArCH, *N*-phenyl), 7.12 - 7.17 (3H, d, $J = 7.5$ Hz), 7.22 (2H, t, $J = 7.4$ Hz), 7.26 (1H, dd, $J = 6.0, 13.5$ Hz), 7.32 (2H, d, $J = 7.2$ Hz), 7.36 (2H, t, $J = 7.4$ Hz) and 9.28

(1H, bs, OH) ppm. ^{13}C NMR (126 MHz, $\text{D}_6\text{-DMSO}$) δ 34.6 ($\text{C}_4\text{-THIQ}$), 38.8 ($\text{C}_3\text{-THIQ}$), 41.1 (CH_2C_4), 44.2 (CH_2C_1), 60.2 ($\text{C}_1\text{-THIQ}$), 113.1 ($\text{C}_7\text{-THIQ}$), 113.4 ($\text{C}_5\text{-THIQ}$), 115.7 (2 x ArCH), 120.4 (ArCCl), 126.0 (ArCH), 126.2 (ArCH), 127.9 (2 x ArCH), 128.2 ($\text{C}_1\text{CC}_8\text{-THIQ}$), 128.3 (2 x ArCH), 128.4 ($\text{C}_8\text{-THIQ}$), 128.5 (2 x ArCH), 129.1 (2 x ArCH), 129.4 (2 x ArCH), 138.7 ($\text{C}_4\text{CC}_5\text{-THIQ}$), 139.0 (ArCCH₂CH), 139.6 (ArCCH₂CH), 148.4 (ArCN) and 155.8 ($\text{C}_6\text{-THIQ}$) ppm. HRMS (ES^+) calcd. $\text{C}_{29}\text{H}_{27}^{35}\text{ClNO}$ ($\text{M}^+ + \text{H}$) 440.1776, found 440.1768; calcd. $\text{C}_{24}\text{H}_{25}^{37}\text{ClNO}$ ($\text{M}^+ + \text{H}$) 442.1746, found 442.1762; calcd. $\text{C}_{24}\text{H}_{24}^{35}\text{ClNNaO}$ ($\text{M}^+ + \text{H}$) 400.1439, found 400.1466. Mp 148-151 °C.

4.2. Biology: materials and methods

All chemicals were purchased from Aldrich Chemical Co. (Gillingham, UK), or Fischer Scientific (Loughborough, UK). For purification of the His-17 β -HSD1 protein an AKTA FPLC from Amersham Biosciences (GE Healthcare), HisTrap chelating HP column from Pharmacia (GE Healthcare) loaded with Ni²⁺, and a Q-sepharose column Amersham Biosciences (GE Healthcare) were used. For enzyme and inhibitor assays Cell Titer 96 ® AQueous One solution was purchased from Promega (Southampton, UK).

For the ERR α screening, the LanthaScreen™ Estrogen Related Receptor alpha TR-FRET Co-activator assay kit was purchased from Invitrogen (catalogue number PV4663) and contained all the necessary components for the assay. As indicated by the protocol, the plates used were 384 well microplates Non-Binding Surface low volume, low flange, round bottom non-sterile black and were purchased from Fisher Scientific (Loughborough, UK) (product code HTS-120-040L).

T47-D cells were kindly supplied by Dr. Atul Purohit, Imperial College of London, while the MCF-7 cells were kindly supplied by Prof. Rex Tyrell, University of Bath and all the media and additives were purchased from Aldrich Chemical Co. (Gillingham, UK).

4.2.1. Glycerol stock

Cells were inoculated into 5 mL of LB medium with the appropriate antibiotic (Kanamycin and chloramphenicol; final conc. 30 mg/L and 34 mg/L, respectively) and incubated at 37 °C. Cell density was checked by a monochromator until OD₆₀₀ *ca.* 0.8 and then 1 mL of cell culture was mixed with 0.2 mL of sterile glycerol, and stored at – 80 °C.

4.2.2. Expression of His-17- β HSD1

Cells were inoculated into 10 mL of LB medium with the appropriate antibiotic (Kanamycin and chloramphenicol; final conc. 30 mg/L and 34 mg/L, respectively) and incubated at 37 °C for 6 h. The 10 mL culture was transferred into 100 mL of fresh LB medium containing the same antibiotics and the cell were incubated overnight at 37 °C and shaken at 250 rpm. 10 mL of the overnight culture was transferred into 1 L of fresh

LB medium containing the same antibiotics and incubated at 37 °C until an $OD_{600} = 0.6$ was measured. The culture was then cooled to 16 °C and IPTG was added to a final concentration of 12.5 μ M. The culture was incubated overnight at 16 °C and shaken at 250 rpm then harvested by centrifuging at 5000 rpm (2740 g) for 10 min. The supernatant was discarded and the pellet was suspended in *ca.* 30 mL of low imidazole Buffer A (buffer composition is described below) and frozen for four days.

4.2.3. Purification of His-17- β HSD1

Buffer A (low imidazole): 40 mM Tris·HCl pH 8.0, 20% glycerol, 0.2 mM DTT, 0.4 mM PMSF, 500 mM NaCl, 20 mM imidazole.

Buffer B (High imidazole): 40 mM Tris·HCl pH 8.0, 20% glycerol, 0.2 mM DTT, 0.4 mM PMSF, 500 mM NaCl, 500 mM imidazole.

Buffer C (Low salt): 40 mM Tris·HCl pH 8.0, 20% glycerol, 0.2 mM DTT, 0.4 mM PMSF, 20 mM NaCl.

Buffer D (High salt): 40 mM Tris·HCl pH 8.0, 20% glycerol, 0.2 mM DTT, 0.4 mM PMSF, 500 mM NaCl.

4.2.3.1. HisTrap column purification

The pellet was defrosted and benzonase (5 units/mL of cells) was added prior to treatment with a One Shot Constant Cell Disruption System. The cell lysate was centrifuged at 10000 rpm (9600 g) for 30 min at 4 °C and the supernatant was steri-filtered prior to further purification. The filtered supernatant was loaded onto an AKTA FPLC with a HisTrap chelating HP column that was previously activated by loading it with Nickel ions. The protein was loaded with 100% Buffer A and after rinsing with 5% Buffer B for 5 min at 3 mL/min the protein was eluted with a gradient of Buffer B from 5% to 100% in 30 min, then 100% Buffer B for 10 min. The fractions containing the purified protein were identified by using SDS-PAGE gel electrophoresis and were subsequently dialysed at 5 °C for 3-4 h in low salt Buffer C (buffer composition described below) before leaving the dialysis cell in fresh Buffer C overnight.

4.2.3.2. Q-sepharose column purification

The dialysed protein was loaded onto an AKTA FPLC with a Q-sepharose column previously equilibrated with 100% Buffer C. The protein was loaded with 100% Buffer C and after rinsing with 5% Buffer D for 5 min at 3 mL/min the protein was eluted with a gradient of Buffer B from 5% to 100% in 30 min, then 100% Buffer B for 10 min. The fractions containing the purified protein were identified by using SDS-PAGE gel electrophoresis and were subsequently dialysed at 5 °C for 3-4 h in low salt Buffer E (40 mM Tris·HCl pH 7.5, 20% glycerol, 0.2 mM DTT, 1.0 mM EDTA) before leaving the dialysis cell in fresh Buffer E overnight.

4.2.4. SDS polyacrylamide gel electrophoresis (SDS-PAGE)

SDS-PAGE was carried out using a Mini Protean II TM apparatus (Bio-Rad). A 3% stacking gel and 10%, 12.5% or 15% running gel were used along with gel running buffer containing 25 mM Tris, 0.2 M glycine and 0.5% (w/v) SDS.

- Stacking gel: 30% (w/v) acrylamide and 0.8% (w/v) bisacrylamide solution (320 µL), Tris-HCl (1 M, pH 6.8, 400 µL), 10% (w/v) SDS (32 µL), 1% (w/v) ammonium persulphate (160 µL), water (2.32 mL), TEMED (5 µL).
- Running gel: 30% (w/v) acrylamide and 0.8% (w/v) bisacrylamide solution (2 mL for 10%, 2.5 mL for 12.5%, 3 mL for 15%), Tris-HCl (0.75 M, pH 8.8, 3 mL), 10% Pr(w/v) SDS (60 µL), 1% (w/v) ammonium persulphate (300 µL), water (750 µL for 10%, 200 µL for 12.5% and no water in 15%), TEMED (5 µL).
- Sample loading buffer (2x): Tris-HCl (0.625 M, pH 6.8, 2.5 mL), glycerol (2.0 mL), 10% (w/v) SDS solution (5.0 mL), β-mercaptoethanol (1.0 mL), water (9.5 mL), 0.01% (w/v) bromophenol blue.
- Gel staining solution: Coomassie Brilliant Blue R-250 [0.25% (w/v)] with water in methanol [30% (v/v)] in water and acetic acid [10% (v/v)] in water.
- Gel destaining solution: methanol [30% (v/v)] in water, acetic acid [10% (v/v)] in water.
- Gel storing solution: methanol [30% (v/v)] in water, glycerol [3% (v/v)] in water.

The protein sample (10 µL) and 5X SDS sample loading buffer (2 µL) were transferred into an Eppendorf tube. The sample was loaded onto a SDS-PAGE with a

3% stacking gel. The power supply was set at 40 mA per gel, 90V until the samples stacked, then 250 V until the end of the gel electrophoresis. Gels were stained and destained after electrophoresis using the above mentioned solutions. Standard molecular weight markers were used to calibrate the SDS-PAGE containing: 250 kDa, 148 kDa, 98 kDa, 64 kDa, 50 kDa, 36 kDa, 22 kDa, 16 kDa and 4 kDa marker proteins.

4.2.5. Protein concentration determination

Protein concentrations were determined by the method of Bradford and the test was performed in triplicates. The Bradford reagent was gently mixed and brought to room temperature. Protein standards in buffer ranging from 0.1-1.4 mg/ml were prepared using a bovine serum albumin (BSA) standard. 5 μ L of the protein standard were added to separate wells in a 96 well plate. For the blank wells 5 μ L of buffer were added. The unknown protein sample was prepared with approximate concentrations between 0.1-1.4 mg/ml. To each well, 250 μ L of the Bradford reagent was added and mixed on a shaker for approximately 30 s. The samples were left to incubate at room temperature for 5 to 45 min to construct a standard curve at 595 nm. The protein concentration was determined by comparing the absorbance values of the protein samples against the standard curve at 595 nm.

4.2.6. 17 β -HSD1 inhibition: MTS assay

N-Octyl- β -D-glucopyranoside (to a final concentration of 0.6 mg/mL) was added to the purified protein solution prior to concentrating to approximately 1 mg/mL using a size filter falcon tube centrifuging at 5,500 rpm for 15 min.

The 17 β -HSD1 inhibition assay was performed measuring the oxidation of E2 to E1 and using the MTS/PMS reagents (3-(4,5-dimethylthiazol-2-yl)-5-(3-carboxymethoxyphenyl)-2-(4-sulfophenyl)-2H-tetrazolium and phenazine methosulfate, respectively) as visual enhancer. The reaction was performed in triplicates and run in 100 μ L of solution made of 10 mM Tris·HCl pH 7.5, 25 μ M NADP⁺, 10 μ L of 17 β -HSD1 solution (1 mg/mL) 10% DMSO (or a solution of inhibitor in DMSO) and Milli-Q water. The reaction was started by addition of a solution containing 10 μ L of MTS/PES and 10 μ L of E2 solution in DMSO (10 μ M final concentration in assay). The reaction was followed using a Molecular Devices Versamax plate reader and reading the

absorbance at 490 nm at 10 seconds intervals for 2 min. The V_{\max} was extrapolated from the data using Graphpad and the inhibition was measured as ratio $V_{\max\text{inhib}}/V_{\max0}$ and the results were given as percentage of inhibition $100 - (V_{\max\text{inhib}}/V_{\max0} \times 100)$.

4.2.7. Crystallisation

N-Octyl- β -D-glucopyranoside (to a final concentration of 0.6 mg/mL) was added to the purified protein solution prior to concentrating to approximately 10 mg/mL using a size filter falcon tube centrifuging at 5,500 rpm (g equivalence) for 15 min. Crystals of the enzyme were obtained using the vapour-diffusion method in a hanging-drop set-up. In a 24 well plate, 1 ml of the solutions described below was added into each well. A 1 μ L drop of enzyme solution was positioned on a glass lid and added of 1 μ L of solution from the respective well, with or without mixing. Alternatively, 1 μ L of solution containing NADP^+ , an inhibitor or both, was added to the drop on the glass lid. The lid was sealed on top of the respective well with the drop hanging on the top and the system was let to equilibrate. Apoenzyme crystals appeared in 3-4 days and were then soaked by slowly adding inhibitor to the drop.

Crystallisation solution tested:

- 100 mM Hepes buffer (pH 7.5), 0.16 mM MgCl_2 and 20 % glycerol with: 5%, 10%, 15%, 20%, 22%, 24%, 25%, 26%, 28% or 30% PEG 4000.
- 0.3 mM MgAc_2 and 0.1 M Sodium Cacodylate with: 10%, 15%, 20%, 25%, 30% or 35% PEG 8000.
- 100 mM Hepes buffer (pH 7.5), 0.16 mM MgCl_2 and 20 % glycerol with: 10%, 15%, 20%, 25%, 30% or 35% PEG 6000.
- 1.3 M, 1.4 M, 1.5 M, 1.6 M, 1.7 M or 1.8 M Sodium Citrate pH 6.5.
- 25% PEG 4000, 100 mM Hepes buffer (pH 7.5), 0.16 mM MgCl_2 and 20 % glycerol with: 0.1 M ammonium sulphate, 30% DMSO, 0.1 M glycine, 0.1 M guanidine hydrochloride, 30% glycerol, 7% 1-butanol, 30% MMD, 50% PEG 400, 30% ethanol, 30% isopropanol, 30% methanol or 40% acetone.

4.2.8. T-47D and MCF-7 cell culture

The T-47D cells were cultured in RPMI-1640 medium supplemented with 10% (v/v) fetal bovine serum, 2mM L-glutamine, insulin, sodium pyruvate, 100 U/mL penicillin and 100 g/mL streptomycin, and incubated in a humidified atmosphere of 5% CO₂ in air, at 37 °C.

The MCF-7 cells supplied by Prof. R. Tyrell, University of Bath, were cultured in Dulbecco's modified Eagle's medium (DMEM) high glucose (4.5 g/L), supplemented with 10% (v/v) fetal bovine serum, 100 U/mL penicillin, 100 g/mL streptomycin, sodium pyruvate, L-glutamine, NaHCO₃, and incubated in a humidified atmosphere of 5% CO₂ in air, at 37 °C.

Cells were grown in T75 flasks and subcultured approximately when 90% confluent.

4.2.9. T47D and MCF-7 growth inhibition assay

The assay was performed to test the effect of the compounds on the cell growth stimulated by estrogens. After removing the medium the cells were rinsed with PBS and trypsinized at 37 °C for 5-10 min. The enzyme was stopped with the addition of fresh culture medium and the cell suspension was centrifuged at 1500 rpm for 10 min. The pellet was resuspended in PBS and centrifuged again at 1500 rpm for 10 min. The pellet was resuspended in the same growth medium supplemented with 10% charcoal-stripped serum (CSS) or 10% normal fetal bovine serum (FBS) according to the experiment. The cells were counted and opportunistically diluted and then 50 µL of cell suspension were transferred into each well of a 96 well plate. The seed density was 10⁴ cells per well for T-47D and 500 cells per well for MCF-7. To each well were added 50 µL of the same medium used for the seeding modified with the following additives accordingly to the experiment:

Using T-47D cell line

- E1 stimulated growth inhibition: E1 at 0.1 nM and the tested compound at 100 µM, 10 µM, 1.0 µM or 0.1 µM in DMSO (1% in assay). The medium used supplemented with 10% CSS.
- E2 stimulated growth inhibition: E2 at 0.1 nM and the tested compound at 100 µM, 10 µM, 1.0 µM or 0.1 µM in DMSO (1% in assay). The medium used supplemented with 10% CSS.

- Testing compound growth stimulation: tested compound at 100 μ M, 10 μ M, 1.0 μ M or 0.1 μ M in DMSO (1% in assay). The medium used supplemented with 10% CSS.
- Vehicle dependence growth curve: No vehicle, 1% DMSO or 1% EtOH in medium supplemented with 10% CSS. Cell density was analysed at day 0, 2, 4, 6, 8 and 10.
- Vehicle dependence growth curve: No vehicle, 1% DMSO or 1% EtOH in medium supplemented with 10% FBS. Cell density was analysed at day 0, 2, 4, 6, 8 and 10.
- E1 stimulated growth curve with EtOH as vehicle: with or without E1 at 0.1 nM in EtOH (1% in assay) in medium supplemented with 10% CSS. Cell density was analysed at day 0, 2, 4, 6, 8 and 10.
- E2 stimulated growth curve with EtOH as vehicle: with or without E2 at 0.1 nM in EtOH (1% in assay) in medium supplemented with 10% CSS. Cell density was analysed at day 0, 2, 4, 6, 8 and 10.
- E1 stimulated growth curve with EtOH as vehicle: with or without E1 at 0.1 nM in EtOH (1% in assay) in medium supplemented with 10% FBS. Cell density was analysed at day 0, 2, 4, 6, 8 and 10.
- E2 stimulated growth curve with EtOH as vehicle: with or without E2 at 0.1 nM in EtOH (1% in assay) in medium supplemented with 10% FBS. Cell density was analysed at day 0, 2, 4, 6, 8 and 10.
- Vehicle dependant growth inhibition or stimulation: 0.01%, 0.05, 0.1% 0.5, 1% of DMSO or EtOH in medium supplemented with 10% CSS.
- Vehicle dependant growth inhibition or stimulation: 0.01%, 0.05, 0.1% 0.5, 1% of DMSO or EtOH in medium supplemented with 10% FBS.
- E2 growth stimulation at different vehicle concentrations: E2 at 0.1, 1.0 or 10 nM in EtOH at final concentrations of 0.01%, 0.05, 0.1% 0.5 or 1% in medium supplemented with 10% CSS.
- 4-Hydroxytamoxifen inhibition of E2 stimulated growth inhibition: 4-Hydroxytamoxifen at 1 nM or 10 nM with or without E2 at 0.1 nM in EtOH (1% in assay). The medium used supplemented with 10% CSS.

- 4-Hydroxytamoxifen inhibition of E1 stimulated growth inhibition: 4-Hydroxytamoxifen at 1 nM or 10 nM with or without E1 at 0.1 nM in EtOH (1% in assay). The medium used supplemented with 10% CSS.

Using MCF-7 cell line

- 4-Hydroxytamoxifen inhibition of E2 stimulated growth inhibition: 4-Hydroxytamoxifen at 1 nM or 10 nM with or without E2 at 0.1 nM in EtOH (1% in assay). The medium used supplemented with 10% CSS.
- 4-Hydroxytamoxifen inhibition of E1 stimulated growth inhibition: 4-Hydroxytamoxifen at 1 nM or 10 nM with or without E1 at 0.1 nM in EtOH (1% in assay). The medium used supplemented with 10% CSS.
- Vehicle dose response: no vehicle, 0.1% or 1% of DMSO or EtOH in medium used supplemented with 10% CSS.
- E2 dose response: 0.01 nM, 0.1 nM, 1.0 nM, 10 nM, 100 nM, 1.0 μ M of E2 in EtOH (1% final concentration in assay) in medium supplemented with 10% CSS.
- E2 dose response: 0.01 nM, 0.1 nM, 1.0 nM, 10 nM, 100 nM, 1.0 μ M of E2 in EtOH (1% final concentration in assay) in medium supplemented with 10% FBS.

Cells were incubated in a humidified atmosphere of 5% CO₂ in air, at 37 °C for 2-3 h prior to the Day 0 reading. Cell density evaluation was performed by addition of 20 μ L of MTS/PES reagent and the plate was incubated at 37 °C for 2 h before the reading. For the T47-D cells the reading was repeated after further 2 h. Values are expressed as mean OD_{490nm} of four replicates. Percentage of inhibitions are calculated arbitrarily setting to 100% growth the control with no inhibitor and expressing the percentage of inhibition as $(\text{mean OD}_{\text{inhib}})/(\text{mean OD}_{\text{no-inhib}}) \times 100 \%$.

4.2.10. Inhibition of ERR α

The inhibition of ERR α was measured using a kit commercially available from Invitrogen. The standard protocol supplied with the kit was modified only to obtain percentage of inhibition instead of curves of inhibition. The complete TR-FRET co-regulator Buffer G (complete Buffer G) was prepared by addition of a 1 M DTT

solution to TR-FRET co-regulator Buffer G to a final concentration of 5 mM. One quarter of the complete Buffer G was stored on ice while the rest was stored at rt.

Step 1: in a 96 well plate was prepared a solution of 1 μ L inverse agonist (10 mM stock solution), XCT790 (inhibitor control, 1 mM stock solution) or DMSO (no inhibitor control) and 49 μ L of complete Buffer G. The solution from each well of the 96 well plate, was transferred into four wells of a 384 well plate in 10- μ L aliquots (Figure 120).

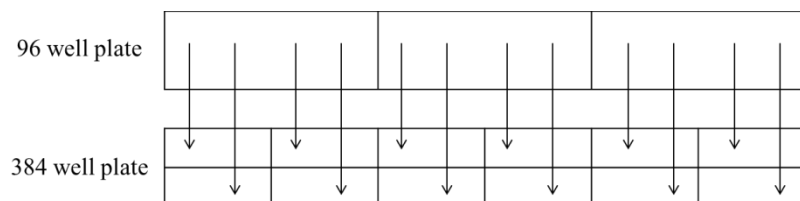


Figure 120. Scheme of the transfer of aliquots from the 96 well plate to the 384 well plate.

Step 2: in a 96 well plate, 25 μ L of a solution of ERR α -LBD in ice cold complete Buffer G was prepared at 4X the final concentration recommended in the Certificate of Analysis. 5 μ L aliquots were transferred from the 96 well plate into each well of the 384 well plate (Figure 120).

Step 3: in a 96 well plate, 25 μ L of a solution of 2 μ M Fluorescein-PDC1a and 20 nM Tb anti-GST antibody in complete buffer G were prepared and 5 μ L aliquots were transferred from the 96 well plate into each well of the 384 well plate (Figure 120).

The plate was incubated at rt and read after 1 h and 2 h. Every point is reported as ratio of the emissions 520:495 nm and the percentage of activity (inverse agonism) is calculated as a ratio $(520:495)_{\text{inverse agonist}} / (520:495)_{\text{XCT790}} \times 100$.

4.2.11. OUTSOURCED ASSAYS

4.2.11.1. 17 β -HSD1 inhibition: whole cell radio-assay

The assay was performed by the Ipsen laboratories. T-47D human breast cancer cells were incubated with ^3H -E1 at a concentration of 2 nM per well, in a 24 well tissue culture plate, in the absence or presence of the inhibitor (0.1 nM – 10 μ M). After incubation of the substrate with or without the inhibitor for 30 min at 37 $^{\circ}\text{C}$, the products were isolated from the mixture by extraction with diethyl ether (4 ml), using ^{14}C -E2 (5000 dpm) to monitor procedural losses. Separation of ^3H -E2 from the mixture

was achieved using TLC (DCM/EtOAc, 4:1 v/v) and the mass of ^3H -E2 produced was calculated from the ^3H counts detected and recovery of ^{14}C -E2.

4.2.11.2. 17β -HSD1 inhibition: cell homogenate radio-assay

The assay was performed by Prof. Lanisnik laboratories. Inhibition assays were carried out in 100 mM phosphate buffer (pH 6.5) in the presence of 1% acetonitrile as the cosolvent. The inhibitor stock solutions were prepared in DMSO, and diluted with acetonitrile prior to the assays. The concentration of the substrate (^3H]-labelled E1 [2,4,6,7- ^3H (N)] and unlabelled E1) in the reaction solution was 62 nM, and the concentration of NADPH was 100 μM . The reactions were carried out at 37 °C and stopped with EtOAc after the time needed to convert approximately 30% of the substrate in a control assay (in the absence of inhibitor). Substrate and product were extracted from the reaction mixture in ethyl acetate. The organic phase was removed, the residue was dissolved in acetonitrile and separated on a reverse-phase (C18) HPLC column with a mobile phase of acetonitrile and water (45:55, v/v) at 1 mL/min. The assays were performed in duplicates and the results are expressed as the mean values. Detection and quantification of the radioactive steroids were performed using a radioflow detector.

4.2.11.3. Nuclear receptors screening from DiscoverX

Cell Handling

1. PathHunter NHRPro cell lines were expanded from freezer stocks in T25 flasks according to standard procedures and maintained in selective growth media prior to the assay.
2. Once it was established that the cells were healthy and growing normally, cells were passaged from flasks using cell dissociation reagent and seeded into white-walled, clear-bottom 384-well micro-plates for compound profiling.
3. For profiling, cells were seeded at a density of 10,000 cells per well in a total volume of 20 μL and were allowed to adhere and recover overnight prior to compound addition. Media contained charcoal-dextran filtered serum to reduce the level of hormones present.

Agonist Format

1. Intermediate dilution of compound stocks were generated such that 5 μ L of 5X compound could be added to each well with a final vehicle concentration of 1% of the total volume.

2. For profiling compound in agonist mode, the cells were incubated in the presence of the compound at 37°C for 5 hours.

Inverse Agonist Format

1. Intermediate dilution of the compound stocks were generated such that 5 μ L of 5X compound could be added to each well with a final vehicle concentration of 1% of the total volume.

2. For profiling compound in inverse agonist mode, the cells were incubated in the presence of compound at 37°C for 5 hours.

Antagonist Format

1. For antagonist determination, cells were pre-incubated with antagonist followed by agonist challenge at the EC 80 concentration: 2.5 μ L of 5X compound was added to the cells and incubated at 37°C for 1 hour.

3. 5 μ L of 6X EC 80 agonist was added to the cells and incubated at 37°C for 5 hours.

Signal Detection

1. After appropriate compound incubation, assay signal was generated through a single addition of 12.5 or 15 μ L (50% v/v) of PathHunter Detection reagent cocktail for agonist and antagonist assays, respectively, followed by a one hour incubation at room temperature.

2. Microplates were read following signal generation with a PerkinElmer EnvisionTM instrument for chemiluminescent signal detection.

Data Analysis

1. Compound activity was analysed using CBIS data analysis suite (ChemInnovation, CA).

2. For agonist mode assays, percentage activity was calculated using the following formula: % Activity = $100\% \times (\text{Mean RLU of test sample} - \text{mean RLU of vehicle control}) / (\text{mean MAX RLU control ligand} - \text{mean RLU of vehicle control})$.

3. For antagonist mode assays, percentage inhibition was calculated using the following formula: % Inhibition = $100\% \times (1 - (\text{Mean RLU of test sample} - \text{mean RLU of vehicle control}) / (\text{mean RLU of EC 80 control} - \text{mean RLU of vehicle control}))$.

4.2.11.4. Eli Lilly

OIDD screening data supplied courtesy of Eli Lilly and Company - used with Lilly's permission.

TargetD²

CGRP Receptor Antagonist

Primary Assays: - hCGRP cAMP antagonist SK-N-MC cells SP (% Inhibition)

- hCGRP cAMP antagonist SK-N-MC cells CRC (IC₅₀)

Secondary Assays: - hCGRP Arrestin CHO cells CRC (IC₅₀)

- hCGRP Bndg CRC SK-N-MC cells SP/CRC (%Efficacy) / (IC₅₀)

- Main peak confirmation HPLC

Confirmatory Assay: - Profiling Biochemical Activity rCGRP (spleen homo), hCT, hAMY, hADM Bndg SPA CHO CRC (Ki)

mGlu2 Receptor Allosteric Antagonist

Primary Assays: - hmGlu2R cAMP/FLIPR antagonist AV12 cells SP (% Inhibition)

- rMGluR2 Calcium Mobilzn Antag SP (% Inhibition)

- hmGlu2R cAMP antagonist AV12 cells CRC (IC₅₀)

- hmGlu3R cAMP antagonist AV12 cells CRC (IC₅₀)

Secondary Assay: - hmGlu6R cAMP antagonist AV12 cells CRC (IC₅₀)

Confirmatory Assay: - mGlu2R Binding CRC (K_i)

GPR 119 Receptor Agonist

Primary Assays: - hGPR119 cAMP agonist HEK293 cells SP (% Efficacy)

- hGPR119 cAMP agonist HEK293 cells CRC (EC₅₀)

- Parental cAMP agonist HEK293 cells CRC (EC₅₀)

Secondary Assays: - Profiling Biochemical Activity Kinase Panel (Ki, % Efficacy)

- PDE profiling (IC₅₀)

- mGPR119 cAMP agonist HEK293 cells CRC (EC₅₀)

Confirmatory Assays: - mGPR119 cAMP agonist HEK293 cells CRC (EC₅₀)

- GLP-1 Secretion Glutag cells (EC₅₀)

- GLP-1 Secretion STC-1 cells (EC₅₀)

EZH2 Inhibitor (Enhancer of Zeste Homolog 2)

Primary Assays: - hPRC2 (EZH2) H3 SPA (% Inhibition)

- hPRC2 (EZH2) H3 SPA CRC (IC₅₀)

Secondary assays: - hPRC2 MS MOA CRC (IC₅₀)

- Main peak confirmation HPLC

Confirmatory Assays: - EZH2 H3K27Me3 Cell Based CRC (IC₅₀)

- Profiling Biochemical Activity CRC (IC₅₀)

PD²

GLP – 1 Secretion

Primary Assays: - GLP-1 Secretion NCI SP / CRC (% Efficacy) / (EC₅₀)

- GLP-1 Secretion STC-1 CRC (EC₅₀)

- GLP-1 Secretion Glu-Tag CRC (EC₅₀)

Secondary assays: - Growth Hormone Secretion Primary Rat Hepatocyte SP / CRC
(% Efficacy / EC₅₀)

- Profiling Biochemical Activity - CSR Panel (K_i , % Efficacy)
- PDE Profiling (IC_{50})
- cAMP NCI (EC_{50})
- Calcium Mobilization NCI (EC_{50})

Confirmatory Assays: - GPCR Profiling (EC_{50})

PCSK9 Synthesis Inhibition

Primary assays: - HepG2 PCSK9 Secretion SP / CRC (% Efficacy / IC_{50})

Secondary assays: - mLuciferase PCSK9 Reporter CRC (IC_{50})

- Nuclear Hormone Receptor Assays (PPAR α , LXR α /b, FXR) CRC (% Efficacy / EC_{50})
- Profiling Biochemical Activity - Kinase panel (% Efficacy)
- Cytotoxicity Primary Rat Hepatocyte CRC (IC_{50})

Confirmatory assays: - HepG2 PCSK9 transcription CRC (EC_{50})

Wnt Pathway Activator

Primary Assays: - β -Catenin Levels C2C12 cells SP / CRC (% Efficacy / EC_{50})

- Alkaline Phosphatase C2C12 cells CRC (EC_{50})

Secondary assays: - G2/M Counterscreen – DNA Content HeLa cells (IC_{50})

- Profiling Biochemical Activity - GSK-3 (% Efficacy)
- Cytotoxicity Primary Rat Hepatocyte CRC (IC_{50})

Confirmatory assays: - β -Catenin Levels hADSC cells CRC (EC_{50})

- Alkaline Phosphatase hADSC cells CRC (EC_{50})

4.2.11.5. National Cancer Institute of America (NCI) – Developmental Therapeutics Program (DTP)

The screening is a two-stage process, beginning with the evaluation of all compounds against the 60 cell lines at a single dose of 10 μ M. The output from the single dose screen is reported as a mean graph and is available for analysis by the COMPARE

program. Compounds which exhibit significant growth inhibition are evaluated against the 60 cell panel at five concentration levels.

The human tumour cell lines of the cancer screening panel are grown in RPMI 1640 medium containing 5% fetal bovine serum and 2 mM L-glutamine. For a typical screening experiment, cells are inoculated into 96 well microtiter plates in 100 µL at plating densities ranging from 5,000 to 40,000 cells/well depending on the doubling time of individual cell lines. After cell inoculation, the microtiter plates are incubated at 37 °C, 5% CO₂, 95% air and 100% relative humidity for 24 h prior to addition of experimental drugs.

After 24 h, two plates of each cell line are fixed *in situ* with TCA, to represent a measurement of the cell population for each cell line at the time of drug addition (T_z). Experimental drugs are solubilised in dimethyl sulfoxide at 400-fold the desired final maximum test concentration and stored frozen prior to use. At the time of drug addition, an aliquot of frozen concentrate is thawed and diluted to twice the desired final maximum test concentration with complete medium containing 50 µg/ml gentamicin. Additional four, 10-fold or ½ log serial dilutions are made to provide a total of five drug concentrations plus control. Aliquots of 100 µl of these different drug dilutions are added to the appropriate microtiter wells already containing 100 µl of medium, resulting in the required final drug concentrations.

Following drug addition, the plates are incubated for an additional 48 h at 37 °C, 5% CO₂, 95% air, and 100% relative humidity. For adherent cells, the assay is terminated by the addition of cold TCA. Cells are fixed *in situ* by the gentle addition of 50 µl of cold 50% (w/v) TCA (final concentration, 10% TCA) and incubated for 60 minutes at 4°C. The supernatant is discarded, and the plates are washed five times with tap water and air dried. Sulforhodamine B (SRB) solution (100 µl) at 0.4% (w/v) in 1% acetic acid is added to each well, and plates are incubated for 10 minutes at room temperature. After staining, unbound dye is removed by washing five times with 1% acetic acid and the plates are air dried. Bound stain is subsequently solubilised with 10 mM trizma base, and the absorbance is read on an automated plate reader at a wavelength of 515 nm. For suspension cells, the methodology is the same except that the assay is terminated by fixing settled cells at the bottom of the wells by gently adding 50 µl of 80 % TCA (final concentration, 16 % TCA). Using the seven absorbance measurements [time zero, (T_z), control growth, (C), and test growth in the presence of drug at the five

concentration levels (T_i), the percentage growth is calculated at each of the drug concentrations levels. Percentage growth inhibition is calculated as:

$$[(T_i - T_z)/(C - T_z)] \times 100 \text{ for concentrations for which } T_i \geq T_z$$

$$[(T_i - T_z)/T_z] \times 100 \text{ for concentrations for which } T_i < T_z.$$

Three dose response parameters are calculated for each experimental agent. Growth inhibition of 50% (GI50) is calculated from $[(T_i - T_z)/(C - T_z)] \times 100 = 50$, which is the drug concentration resulting in a 50% reduction in the net protein increase (as measured by SRB staining) in control cells during the drug incubation. The drug concentration resulting in total growth inhibition (TGI) is calculated from $T_i = T_z$. The LC_{50} (concentration of drug resulting in a 50% reduction in the measured protein at the end of the drug treatment as compared to that at the beginning) indicating a net loss of cells following treatment is calculated from $[(T_i - T_z)/T_z] \times 100 = -50$. Values are calculated for each of these three parameters if the level of activity is reached; however, if the effect is not reached or is exceeded, the value for that parameter is expressed as greater or less than the maximum or minimum concentration tested.

Bibliography

1. Various. Cancer in the UK: April 2011. <http://www.cancerresearchuk.org/cancer-info/cancerstats/> **2011**.
2. Easton, D. F. How many more breast cancer predisposition genes are there? *Breast Cancer Res.* **1999**, *1*, 14 - 17.
3. Various. BRCA1 and BRCA2: cancer risk and genetic testing. <http://www.cancer.gov/cancertopics/factsheet/Risk/BRCA> **2013**.
4. Various. Treating breast cancer. http://www.cancerresearchuk.org/prod_consump/groups/cr_common/@cah/@gen/documents/generalcontent/treating-breast-cancer.pdf **2013**.
5. Hudis, C. A.; Gianni, L. Triple-negative breast cancer: an unmet medical need. *Oncologist* **2011**, *16*, 1-11.
6. Graham, M. L., 2nd; Krett, N. L.; Miller, L. A.; Leslie, K. K.; Gordon, D. F.; Wood, W. M.; Wei, L. L.; Horwitz, K. B. T47DCO cells, genetically unstable and containing estrogen receptor mutations, are a model for the progression of breast cancers to hormone resistance. *Cancer Res.* **1990**, *50*, 6208-6217.
7. Wang, L.; Wang, Z. Y. The Wilms' tumor suppressor WT1 induces estrogen-independent growth and anti-estrogen insensitivity in ER-positive breast cancer MCF7 cells. *Oncol. Rep.* **2010**, *23*, 1109-1117.
8. Untch, M.; Thomssen, C. Clinical practice decisions in endocrine therapy. *Cancer Invest.* **2010**, *28*, 4-13.
9. Long, X.; Nephew, K. P. Fulvestrant (ICI 182,780)-dependent interacting proteins mediate immobilization and degradation of estrogen receptor- α . *J. Biol. Chem.* **2006**, *281*, 9607-9615.
10. Chesworth, R.; Zawistoski, M. P.; Lefker, B. A.; Cameron, K. O.; Day, R. F.; Mangano, F. M.; Rosati, R. L.; Colella, S.; Petersen, D. N.; Brault, A.; Lu, B.; Pan, L. C.; Perry, P.; Ng, O.; Castleberry, T. A.; Owen, T. A.; Brown, T. A.; Thompson, D. D.; DaSilva-Jardine, P. Tetrahydroisoquinolines as subtype selective estrogen agonists/antagonists. *Bioorg. Med. Chem. Lett.* **2004**, *14*, 2729-2733.
11. Payne, A. H.; Abbaszade, I. G.; Clarke, T. R.; Bain, P. A.; Park, C.-H. J. The multiple murine 3 β -hydroxysteroid dehydrogenase isoforms: Structure, function, and tissue- and developmentally specific expression. *Steroids* **1997**, *62*, 169-175.
12. Group, A. T. Results of the ATAC (Arimidex, Tamoxifen, Alone or in Combination) trial after completion of 5 years' adjuvant treatment for breast cancer. *Lancet* **2005**, *365*, 60-62.
13. Jakesz, R.; Jonat, W.; Gnant, M.; Mittlboeck, M.; Greil, R.; Tausch, C.; Hilfrich, J.; Kwasny, W.; Menzel, C.; Samonigg, H.; Seifert, M.; Gademann, G.; Kaufmann, M. Switching of postmenopausal women with endocrine-responsive early breast cancer to anastrozole after 2 years' adjuvant tamoxifen: combined results of ABCSG trial 8 and ARNO 95 trial. *Lancet* **2005**, *366*, 455-462.
14. Miller, W. L.; Auchus, R. J. The molecular biology, biochemistry, and physiology of human steroidogenesis and its disorders. *Endocr. Rev.* **2011**, *32*, 81-151.
15. Purohit, A.; Woo, L. W. L.; Chander, S. K.; Newman, S. P.; Ireson, C.; Ho, Y.; Grasso, A.; Leese, M. P.; Potter, B. V. L.; Reed, M. J. Steroid sulphatase inhibitors for breast cancer therapy. *J. Steroid Biochem. Mol. Biol.* **2003**, *86*, 423-432.

16. Stanway, S. J.; Delavault, P.; Purohit, A.; Woo, L. W. L.; Thurieau, C.; Potter, B. V. L.; Reed, M. J. Steroid sulfatase: A new target for the endocrine therapy of breast cancer. *Oncologist* **2007**, *12*, 370-374.
17. Adamski, J.; Normand, T.; Leenders, F.; Monté, D.; Begue, A.; Stéhelin, D.; Jungblut, P. W.; de Launoit, Y. Molecular cloning of a novel widely expressed human 80 kDa 17 beta-hydroxysteroid dehydrogenase IV. *Biochem. J.* **1995**, *311*, 437-440.
18. Dufort, I.; Rheault, P.; Huang, X.-F.; Soucy, P.; Luu-The, V. Characteristics of a highly labile human type 5 17 β -hydroxysteroid dehydrogenase. *Endocrinology* **1999**, *140*, 568-574.
19. Fomitcheva, J.; Baker, M. E.; Anderson, E.; Lee, G. Y.; Aziz, N. Characterization of Ke 6, a new 17 β -hydroxysteroid dehydrogenase, and its expression in gonadal tissues. *J. Biol. Chem.* **1998**, *273*, 22664-22671.
20. Geissler, W. M.; Davis, D. L.; Wu, L.; Bradshaw, K. D.; Patel, S.; Mendonca, B. B.; Elliston, K. O.; Wilson, J. D.; Russell, D. W.; Andersson, S. Male pseudohermaphroditism caused by mutations of testicular 17beta-hydroxysteroid dehydrogenase 3. *Nat. Genet.* **1994**, *7*, 34-39.
21. Lukacik, P.; Keller, B.; Bunkoczi, G.; Kavanagh, K.; Hwa lee, W.; Adamski, J.; Oppermann, U. Structural and biochemical characterization of human orphan DHRS10 reveals a novel cytosolic enzyme with steroid dehydrogenase activity. *Biochem. J.* **2007**, *402*, 419-427.
22. Luu-The, V.; Bélanger, A.; Labrie, F. Androgen biosynthetic pathways in the human prostate. *Best Pract. Res. Cl. En.* **2008**, *22*, 207-221.
23. Luu-The, V.; Tremblay, P.; Labrie, F. Characterization of type 12 17 β -hydroxysteroid dehydrogenase, an isoform of type 3 17 β -hydroxysteroid dehydrogenase responsible for estradiol formation in women. *Mol. Endocrinol.* **2006**, *20*, 437-443.
24. Napoli, J. L. 17 β -Hydroxysteroid dehydrogenase type 9 and other short-chain dehydrogenases/reductases that catalyze retinoid, 17 β - and 3 α -hydroxysteroid metabolism. *Mol. Cell. Endocrinol.* **2001**, *171*, 103-109.
25. Nokelainen, P.; Peltoketo, H.; Vihko, R.; Vihko, P. Expression cloning of a novel estrogenic mouse 17 β -hydroxysteroid dehydrogenase/ 17-ketosteroid reductase (m17HSD7), previously described as a prolactin receptor-associated protein (PRAP) in rat. *Mol. Endocrinol.* **1998**, *12*, 1048-1059.
26. Peltoketo, H.; Isomaa, V.; Mäentausta, O.; Vihko, R. Complete amino acid sequence of human placental 17 β -hydroxysteroid dehydrogenase deduced from cDNA. *FEBS Lett.* **1988**, *239*, 73-77.
27. Wu, L.; Einstein, M.; Geissler, W. M.; Chan, H. K.; Elliston, K. O.; Andersson, S. Expression cloning and characterization of human 17 beta-hydroxysteroid dehydrogenase type 2, a microsomal enzyme possessing 20 alpha-hydroxysteroid dehydrogenase activity. *J. Biol. Chem.* **1993**, *268*, 12964-12969.
28. X.Z. Li, K.; Smith, R. E.; Krozowsk, Z. S. Cloning and expression of a novel tissue specific 17 β -hydroxysteroid dehydrogenase. *Endocr. Res.* **1998**, *24*, 663-667.
29. Adamski, J.; Jakob, F. J. A guide to 17 β -hydroxysteroid dehydrogenases. *Mol. Cell. Endocrinol.* **2001**, *171*, 1-4.
30. Day, J. M.; Tutill, H. J.; Purohit, A. 17Beta-hydroxysteroid dehydrogenase inhibitors. *Minerva Endocrinol.* **2010**, *35*, 87-108.
31. Day, J. M.; Tutill, H. J.; Purohit, A.; Reed, M. J. Design and validation of specific inhibitors of 17beta-hydroxysteroid dehydrogenases for therapeutic

- application in breast and prostate cancer, and in endometriosis. *Endocr. Relat. Cancer*. **2008**, *15*, 665-692.
32. Ghosh, D.; Pletnev, V. Z.; Zhu, D.-W.; Wawrzak, Z.; Duax, W. L.; Pangborn, W.; Labrie, F.; Lin, S.-X. Structure of human estrogenic 17 β -hydroxysteroid dehydrogenase at 2.20 Å resolution. *Structure* **1995**, *3*, 503-513.
 33. Moghrabi, N.; Andersson, S. 17 β -Hydroxysteroid dehydrogenases: Physiological roles in health and disease. *Trends Endocrin. Met.* **1998**, *9*, 265-270.
 34. Vihko, P.; Isomaa, V.; Ghosh, D. Structure and function of 17 β -hydroxysteroid dehydrogenase type 1 and type 2. *Mol. Cell. Endocrinol.* **2001**, *171*, 71-76.
 35. Labrie, F.; Luu-The, V.; Lin, S.-X.; Simard, J.; Labrie, C. Role of 17 β -hydroxysteroid dehydrogenases in sex steroid formation in peripheral intracrine tissues. *Trends Endocrin. Met.* **2000**, *11*, 421-427.
 36. Azzi, A.; Rehse, P. H.; Zhu, D.-W.; Campbell, R. L.; Labrie, F.; Lin, S.-X. Crystal structure of human estrogenic 17 β -hydroxysteroid dehydrogenase complexed with 17 β -estradiol. *Nat. Struct. Mol. Biol.* **1996**, *3*, 665-668.
 37. Negri, M.; Recanatini, M.; Hartmann, R. W. Insights in 17 β -HSD1 enzyme kinetics and ligand binding by dynamic motion investigation. *PLoS ONE* **2010**, *5*, e12026.
 38. Zhang, C.-Y.; Chen, J.; Yin, D.-C.; Lin, S.-X. The contribution of 17 β -hydroxysteroid dehydrogenase type 1 to the estradiol-estrone ratio in estrogen-sensitive breast cancer cells. *PLoS ONE* **2012**, *7*, e29835.
 39. Miyoshi, Y.; Ando, A.; Shiba, E.; Taguchi, T.; Tamaki, Y.; Noguchi, S. Involvement of up-regulation of 17 β -hydroxysteroid dehydrogenase type 1 in maintenance of intratumoral high estradiol levels in postmenopausal breast cancers. *Int. J. Cancer* **2001**, *94*, 685-689.
 40. Salhab, M.; Reed, M.; Al Sarakbi, W.; Jiang, W.; Mokbel, K. The role of aromatase and 17 β -hydroxysteroid dehydrogenase type 1 mRNA expression in predicting the clinical outcome of human breast cancer. *Breast Cancer Res. Tr.* **2006**, *99*, 155-162.
 41. Frotscher, M.; Ziegler, E.; Marchais-Oberwinkler, S.; Kruchten, P.; Neugebauer, A.; Fetzter, L.; Scherer, C.; Müller-Vieira, U.; Messinger, J.; Thole, H.; Hartmann, R. W. Design, synthesis, and biological evaluation of (hydroxyphenyl)naphthalene and -quinoline derivatives: Potent and selective nonsteroidal inhibitors of 17 β -hydroxysteroid dehydrogenase type 1 (17 β -HSD1) for the treatment of estrogen-dependent diseases. *J. Med. Chem.* **2008**, *51*, 2158-2169.
 42. Bey, E.; Marchais-Oberwinkler, S.; Kruchten, P.; Frotscher, M.; Werth, R.; Oster, A.; Algül, O.; Neugebauer, A.; Hartmann, R. W. Design, synthesis and biological evaluation of bis(hydroxyphenyl) azoles as potent and selective nonsteroidal inhibitors of 17 β -hydroxysteroid dehydrogenase type 1 (17 β -HSD1) for the treatment of estrogen-dependent diseases. *Bioorg. Med. Chem.* **2008**, *16*, 6423-6435.
 43. Allan, G. M.; Vicker, N.; Lawrence, H. R.; Tutill, H. J.; Day, J. M.; Huchet, M.; Ferrandis, E.; Reed, M. J.; Purohit, A.; Potter, B. V. L. Novel inhibitors of 17 β -hydroxysteroid dehydrogenase type 1: Templates for design. *Bioorg. Med. Chem.* **2008**, *16*, 4438-4456.
 44. Vicker, N.; Lawrence, H. R.; Allan, G. M.; Bubert, C.; Smith, A.; Tutill, H. J.; Purohit, A.; Day, J. M.; Mahon, M. F.; Reed, M. J.; Potter, B. V. L. Focused libraries of 16-substituted estrone derivatives and modified E-ring steroids:

- Inhibitors of 17 β -hydroxysteroid dehydrogenase type 1. *ChemMedChem* **2006**, *1*, 464-481.
45. Allan, G. M.; Bubert, C.; Vicker, N.; Smith, A.; Tutill, H. J.; Purohit, A.; Reed, M. J.; Potter, B. V. L. Novel, potent inhibitors of 17 β -hydroxysteroid dehydrogenase type 1. *Mol. Cell. Endocrinol.* **2006**, *248*, 204-207.
 46. Hillisch, A.; Gege, C.; Regenhardt, W.; Rosinius, A.; Adamski, J.; Moeller, G. Novel 2-substituted estra-1,3,5(10)-trien-17-ones used in a form of inhibitors of 17 β -hydroxysteroid dehydrogenase of type 1. PCT Int. Appl. WO2006/003013A2, Jan 12, 2006 (Also US2006/0009434A1).
 47. Gege, C.; Regenhardt, W.; Peters, O.; Hillisch, A.; Adamski, J.; Möller, G.; Deluca, D.; Elger, W.; Schneider, B. Novel 2-substituted D-homo-estra-1,3,5(10)-trienes as inhibitors of 17 β -hydroxysteroid dehydrogenase type 1. PCT Int. Appl. WO2006/003012A1, Jan 12, 2006.
 48. Zhu, B. T.; Lee, A. J. NADPH-dependent metabolism of 17 β -estradiol and estrone to polar and nonpolar metabolites by human tissues and cytochrome P450 isoforms. *Steroids* **2005**, *70*, 225-244.
 49. Allan, G. M.; Lawrence, H. R.; Cornet, J.; Bubert, C.; Fischer, D. S.; Vicker, N.; Smith, A.; Tutill, H. J.; Purohit, A.; Day, J. M.; Mahon, M. F.; Reed, M. J.; Potter, B. V. L. Modification of estrone at the 6, 16, and 17 positions: Novel potent inhibitors of 17 β -hydroxysteroid dehydrogenase type 1. *J. Med. Chem.* **2006**, *49*, 1325-1345.
 50. Poirier, D.; Dionne, P.; Auger, S. A 6 β -(thiaheptanamide) derivative of estradiol as inhibitor of 17 β -hydroxysteroid dehydrogenase type 1. *J. Steroid Biochem. Mol. Biol.* **1998**, *64*, 83-90.
 51. Tremblay, M. R.; Boivin, R. P.; Luu-The, V.; Poirier, D. Inhibitors of type 1 17 β -hydroxysteroid dehydrogenase with reduced estrogenic activity: Modifications of the positions 3 and 6 of estradiol. *J. Enzym. Inhib. Med. Ch.* **2005**, *20*, 153-163.
 52. Messinger, J.; Thole, H.-H.; Husen, B.; Van Steen, B. J.; Schneider, G.; Hulshof, J. B. E.; Koskimies, P.; Johansson, N.; Adamski, J. Novel 17 β -hydroxysteroid dehydrogenase type 1 inhibitors. PCT Int. Appl. WO 2005/047303A2, May 26, 2005.
 53. Messinger, J.; Husen, B.; Schoen, U.; Thole, H. H.; Koskimies, P.; Unkila, M. Substituted estratrien derivatives as 17 β -HSD inhibitors. PCT INT. Appl. WO2008/065100, June 05, 2008.
 54. Messinger, J.; Husen, B.; Koskimies, P.; Hirvelä, L.; Kallio, L.; Saarenketo, P.; Thole, H. Estrone C15 derivatives: A new class of 17 β -hydroxysteroid dehydrogenase type 1 inhibitors. *Mol. Cell. Endocrinol.* **2009**, *301*, 216-224.
 55. Pelletier, J. D.; Poirier, D. Synthesis and evaluation of estradiol derivatives with 16 α -(bromoalkylamide), 16 α -(bromoalkyl) or 16 α -(bromoalkynyl) side chain as inhibitors of 17 β -hydroxysteroid dehydrogenase type 1 without estrogenic activity. *Bioorg. Med. Chem.* **1996**, *4*, 1617-1628.
 56. Qiu, W.; Campbell, R. L.; Gangloff, A.; Dupuis, P.; Boivin, R. P.; Tremblay, M. R.; Poirier, D.; Lin, S.-X. A concerted, rational design of type 1 17 β -hydroxysteroid dehydrogenase inhibitors: estradiol-adenosine hybrids with high affinity. *FASEB J.* **2002**, *16*, 1829-1831.
 57. Fournier, D.; Poirier, D.; Mazumdar, M.; Lin, S. X. Design and synthesis of bisubstrate inhibitors of type 1 17 β -hydroxysteroid dehydrogenase: Overview and perspectives. *Eur. J. Med. Chem.* **2008**, *43*, 2298-2306.

58. Vicker, N.; Allan, G. M.; Lawrence, H. R. R.; Day, J. M.; Purohit, A.; Reed, M. J.; Potter, B. V. L. Diaryl compounds as non-steroidal inhibitors of 17- β -hydroxysteroid dehydrogenase and/or steroid sulphatase for the treatment of oestrogen-related diseases such as hormone dependent breast cancer. PCT Int. Appl. WO2007096647.
59. Marchais-Oberwinkler, S.; Wetzel, M.; Ziegler, E.; Kruchten, P.; Werth, R.; Henn, C.; Hartmann, R. W.; Frotscher, M. New drug-like hydroxyphenylnaphthol steroidomimetics as potent and selective 17 β -hydroxysteroid dehydrogenase type 1 inhibitors for the treatment of estrogen-dependent diseases. *J. Med. Chem.* **2010**, *54*, 534-547.
60. Marchais-Oberwinkler, S.; Kruchten, P.; Frotscher, M.; Ziegler, E.; Neugebauer, A.; Bhoga, U.; Bey, E.; Müller-Vieira, U.; Messinger, J.; Thole, H.; Hartmann, R. W. Substituted 6-phenyl-2-naphthols. Potent and selective nonsteroidal inhibitors of 17 β -hydroxysteroid dehydrogenase type 1 (17 β -HSD1): Design, synthesis, biological evaluation, and pharmacokinetics. *J. Med. Chem.* **2008**, *51*, 4685-4698.
61. Marchais-Oberwinkler, S.; Frotscher, M.; Ziegler, E.; Werth, R.; Kruchten, P.; Messinger, J.; Thole, H.; Hartmann, R. W. Structure–activity study in the class of 6-(3'-hydroxyphenyl)naphthalenes leading to an optimization of a pharmacophore model for 17 β -hydroxysteroid dehydrogenase type 1 (17 β -HSD1) inhibitors. *Mol. Cell. Endocrinol.* **2009**, *301*, 205-211.
62. Bey, E.; Marchais-Oberwinkler, S.; Werth, R.; Negri, M.; Al-Soud, Y. A.; Kruchten, P.; Oster, A.; Frotscher, M.; Birk, B.; Hartmann, R. W. Design, synthesis, biological evaluation and pharmacokinetics of bis(hydroxyphenyl) substituted azoles, thiophenes, benzenes, and aza-benzenes as potent and selective nonsteroidal inhibitors of 17 β -hydroxysteroid dehydrogenase type 1 (17 β -HSD1). *J. Med. Chem.* **2008**, *51*, 6725-6739.
63. Bey, E.; Marchais-Oberwinkler, S.; Negri, M.; Kruchten, P.; Oster, A.; Klein, T.; Spadaro, A.; Werth, R.; Frotscher, M.; Birk, B.; Hartmann, R. W. New insights into the SAR and binding modes of bis(hydroxyphenyl)thiophenes and -benzenes: influence of additional substituents on 17 β -hydroxysteroid dehydrogenase type 1 (17 β -HSD1) inhibitory activity and selectivity. *J. Med. Chem.* **2009**, *52*, 6724-6743.
64. Oster, A.; Klein, T.; Werth, R.; Kruchten, P.; Bey, E.; Negri, M.; Marchais-Oberwinkler, S.; Frotscher, M.; Hartmann, R. W. Novel estrone mimetics with high 17 β -HSD1 inhibitory activity. *Bioorg. Med. Chem.* **2010**, *18*, 3494-3505.
65. Alho-Richmond, S.; Lilienkamp, A.; Wähälä, K. Active site analysis of 17 β -hydroxysteroid dehydrogenase type 1 enzyme complexes with SPROUT. *Mol. Cell. Endocrinol.* **2006**, *248*, 208-213.
66. Vihko, P.; Isomaa, V. Method for prognosticating the progress of breast cancer and compounds useful for prevention or treatment thereof. U.S. Patent Appl. US2006/0057628A1, Mar 16, 2006.
67. Lilienkamp, A.; Karkola, S.; Alho-Richmond, S.; Koskimies, P.; Johansson, N.; Huhtinen, K.; Vihko, K.; Wähälä, K. Synthesis and biological evaluation of 17 β -hydroxysteroid dehydrogenase type 1 (17 β -HSD1) inhibitors based on a thieno[2,3-d]pyrimidin-4(3H)-one core. *J. Med. Chem.* **2009**, *52*, 6660-6671.
68. Starčević, S. t.; Brožič, P.; Turk, S.; Cesar, J. k.; Lanišnik Rižner, T.; Gobec, S. Synthesis and biological evaluation of (6- and 7-phenyl) coumarin derivatives as selective nonsteroidal inhibitors of 17 β -hydroxysteroid dehydrogenase type 1. *J. Med. Chem.* **2010**, *54*, 248-261.

69. Starčević, Š.; Kocbek, P.; Hribar, G.; Lanišnik Rižner, T.; Gobec, S. Biochemical and biological evaluation of novel potent coumarin inhibitor of 17 β -HSD type 1. *Chem. Biol. Interact.* **2011**, *191*, 60-65.
70. Brožič, P.; Kocbek, P.; Sova, M.; Kristl, J.; Martens, S.; Adamski, J.; Gobec, S.; Lanišnik Rižner, T. Flavonoids and cinnamic acid derivatives as inhibitors of 17 β -hydroxysteroid dehydrogenase type 1. *Mol. Cell. Endocrinol.* **2009**, *301*, 229-234.
71. Evans, R. M. The steroid and thyroid hormone receptor superfamily. *Science* **1988**, *240*, 889-895.
72. Giguere, V. Orphan nuclear receptors: from gene to function. *Endocr. Rev.* **1999**, *20*, 689-725.
73. Giguere, V.; Yang, N.; Segui, P.; Evans, R. M. Identification of a new class of steroid hormone receptors. *Nature* **1988**, *331*, 91-94.
74. Sullivan, A. A.; Thummel, C. S. Temporal profiles of nuclear receptor gene expression reveal coordinate transcriptional responses during *Drosophila* development. *Mol. Endocrinol.* **2003**, *17*, 2125-2137.
75. Bardet, P. L.; Schubert, M.; Horard, B.; Holland, L. Z.; Laudet, V.; Holland, N. D.; Vanacker, J. M. Expression of estrogen-receptor related receptors in amphioxus and zebrafish: implications for the evolution of posterior brain segmentation at the invertebrate-to-vertebrate transition. *Evol. Dev.* **2005**, *7*, 223-233.
76. Baker, M. E. Trichoplax, the simplest known animal, contains an estrogen-related receptor but no estrogen receptor: Implications for estrogen receptor evolution. *Biochem. Biophys. Res. Co.* **2008**, *375*, 623-627.
77. Stein, R. A.; McDonnell, D. P. Estrogen-related receptor α as a therapeutic target in cancer. *Endocr. Relat. Cancer* **2006**, *13*, S25-S32.
78. Delhon, I.; Gutzwiller, S.; Morvan, F.; Rangwala, S.; Wyder, L.; Evans, G.; Studer, A.; Kneissel, M.; Fournier, B. Absence of estrogen receptor-related- α increases osteoblastic differentiation and cancellous bone mineral density. *Endocrinology* **2009**, *150*, 4463-4472.
79. Bonnelye, E.; Saltel, F.; Chabadel, A.; Zirngibl, R. A.; Aubin, J. E.; Jurdic, P. Involvement of the orphan nuclear estrogen receptor-related receptor α in osteoclast adhesion and transmigration. *J. Mol. Endocrinol.* **2010**, *45*, 365-377.
80. Ranhostra, H. S. The estrogen-related receptors: orphans orchestrating myriad functions. *J. Recept. Sig. Transd.* **2012**, *32*, 47-56.
81. Gallet, M.; Vanacker, J.-M. ERR receptors as potential targets in osteoporosis. *Trends Endocrin. Met.* **2010**, *21*, 637-641.
82. Ju, D.; He, J.; Zhao, L.; Zheng, X.; Yang, G. Estrogen related receptor α -induced adipogenesis is PGC-1 β -dependent. *Mol. Biol. Rep.* **2012**, *39*, 3343-3354.
83. Ariazi, E. A.; Jordan, V. C. Estrogen-related receptors as emerging targets in cancer and metabolic disorders. *Curr. Top. Med. Chem.* **2006**, *6*, 203-215.
84. Luo, J.; Sladek, R.; Carrier, J.; Bader, J. A.; Richard, D.; Giguere, V. Reduced fat mass in mice lacking orphan nuclear receptor estrogen-related receptor α . *Mol. Cell. Biol.* **2003**, *23*, 7947-7956.
85. Tremblay, A. M.; Giguere, V. The NR3B subgroup: an ovERRview. *Nuclear receptor signaling* **2007**, *5*, e009.
86. Bonnelye, E.; Aubin, J. E. An energetic orphan in an endocrine tissue: A revised perspective of the function of estrogen receptor-related receptor α in bone and cartilage. *J. Bone Miner. Res.* **2013**, *28*, 225-233.

87. Mirebeau-Prunier, D.; Le Pennec, S.; Jacques, C.; Fontaine, J.-F.; Gueguen, N.; Boutet-Bouzamondo, N.; Donnart, A.; Malthiery, Y.; Savagner, F. Estrogen-related receptor alpha modulates lactate dehydrogenase activity in thyroid tumors. *PLoS ONE* **2013**, *8*, e58683.
88. Ao, A.; Wang, H.; Kamarajugadda, S.; Lu, J. Involvement of estrogen-related receptors in transcriptional response to hypoxia and growth of solid tumors. *P. Natl. Acad. Sci. USA* **2008**, *105*, 7821-7826.
89. Bianco, S.; Sailland, J.; Vanacker, J.-M. ERRs and cancers: Effects on metabolism and on proliferation and migration capacities. *J. Steroid Biochem. Mol. Biol.* **2012**, *130*, 180-185.
90. Fradet, A.; Sorel, H.; Bouazza, L.; Goehrig, D.; Dépalle, B.; Bellahcène, A.; Castronovo, V.; Follet, H.; Descotes, F.; Aubin, J. E.; Clézardin, P.; Bonnelye, E. Dual function of ERR α in breast cancer and bone metastasis formation: implication of VEGF and osteoprotegerin. *Cancer Res.* **2011**, *71*, 5728-5738.
91. Stein, R. A.; Chang, C.-y.; Kazmin, D. A.; Way, J.; Schroeder, T.; Wergin, M.; Dewhirst, M. W.; McDonnell, D. P. Estrogen-related receptor α is critical for the growth of estrogen receptor-negative breast cancer. *Cancer Res.* **2008**, *68*, 8805-8812.
92. Pancholi, S.; Lykkesfeldt, A. E.; Hilmi, C.; Banerjee, S.; Leary, A.; Drury, S.; Johnston, S.; Dowsett, M.; Martin, L.-A. ERBB2 influences the subcellular localization of the estrogen receptor in tamoxifen-resistant MCF-7 cells leading to the activation of AKT and RPS6KA2. *Endocr. Relat. Cancer* **2008**, *15*, 985-1002.
93. Ariazi, E. A.; Kraus, R. J.; Farrell, M. L.; Jordan, V. C.; Mertz, J. E. Estrogen-related receptor α 1 transcriptional activities are regulated in part *via* the ErbB2/HER2 signaling pathway. *Mol. Cancer Res.* **2007**, *5*, 71-85.
94. Deblois, G.; Hall, J. A.; Perry, M.-C.; Laganière, J.; Ghahremani, M.; Park, M.; Hallett, M.; Giguère, V. Genome-wide identification of direct target genes implicates estrogen-related receptor α as a determinant of breast cancer heterogeneity. *Cancer Res.* **2009**, *69*, 6149-6157.
95. Riggins, R. B.; Mazzotta, M. M.; Maniya, O. Z.; Clarke, R. Orphan nuclear receptors in breast cancer pathogenesis and therapeutic response. *Endocr. Relat. Cancer* **2010**, *17*, R213-R231.
96. Ariazi, E. A.; Clark, G. M.; Mertz, J. E. Estrogen-related receptor α and estrogen-related receptor γ associate with unfavorable and favorable biomarkers, respectively, in human breast cancer. *Cancer Res.* **2002**, *62*, 6510-6518.
97. Chisamore, M. J.; Wilkinson, H. A.; Flores, O.; Chen, J. D. Estrogen-related receptor- α antagonist inhibits both estrogen receptor- α positive and estrogen receptor-negative breast tumor growth in mouse xenografts. *Molecular Cancer Therapeutics* **2009**, *8*, 672-681.
98. Jarzabek, K.; Koda, M.; Kozlowski, L.; Sulkowski, S.; Kottler, M.-L.; Wolczynski, S. The significance of the expression of ERR α as a potential biomarker in breast cancer. *J. Steroid Biochem. Mol. Biol.* **2009**, *113*, 127-133.
99. Lu, X.; Peng, L.; Lv, M.; Ding, K. Recent advance in the design of small molecular modulators of estrogen-related receptors. *Curr. Pharm. Design* **2012**, *18*, 3421-3431.
100. Zhao, Y.; Li, Y.; Lou, G.; Zhao, L.; Xu, Z.; Zhang, Y.; He, F. MiR-137 targets estrogen-related receptor alpha and impairs the proliferative and migratory capacity of breast cancer cells. *PLoS ONE* **2012**, *7*, e39102.

101. Kallen, J.; Lattmann, R.; Beerli, R.; Blechschmidt, A.; Blommers, M. J. J.; Geiser, M.; Ottl, J.; Schlaeppli, J.-M.; Strauss, A.; Fournier, B. Crystal structure of human estrogen-related receptor α in complex with a synthetic inverse agonist reveals its novel molecular mechanism. *J. Biol. Chem.* **2007**, *282*, 23231-23239.
102. Tremblay, G. B.; Kunath, T.; Bergeron, D.; Lapointe, L.; Champigny, C.; Bader, J.-A.; Rossant, J.; Giguère, V. Diethylstilbestrol regulates trophoblast stem cell differentiation as a ligand of orphan nuclear receptor ERR α . *Gene Dev.* **2001**, *15*, 833-838.
103. Chao, E. Y. H.; Collins, J. L.; Gaillard, S.; Miller, A. B.; Wang, L.; Orband-Miller, L. A.; Nolte, R. T.; McDonnell, D. P.; Willson, T. M.; Zuercher, W. J. Structure-guided synthesis of tamoxifen analogs with improved selectivity for the orphan ERR γ . *Bioorg. Med. Chem. Lett.* **2006**, *16*, 821-824.
104. Wang, J.; Fang, F.; Huang, Z.; Wang, Y.; Wong, C. Kaempferol is an estrogen-related receptor alpha and gamma inverse agonist. *FEBS Lett.* **2009**, *583*, 643-647.
105. Busch, B. B.; Stevens, W. C.; Martin, R.; Ordentlich, P.; Zhou, S.; Sapp, D. W.; Horlick, R. A.; Mohan, R. Identification of a selective inverse agonist for the orphan nuclear receptor estrogen-related receptor α . *J. Med. Chem.* **2004**, *47*, 5593-5596.
106. Prentis, R. A.; Lis, Y.; Walker, S. R. Pharmaceutical innovation by the seven UK-owned pharmaceutical companies (1964-1985). *Brit. J. Clin. Pharmacol.* **1988**, *25*, 387-396.
107. Kola, I.; Landis, J. Can the pharmaceutical industry reduce attrition rates? *Nat. Rev. Drug. Discov.* **2004**, *3*, 711-716.
108. Lipinski, C. A.; Lombardo, F.; Dominy, B. W.; Feeney, P. J. Experimental and computational approaches to estimate solubility and permeability in drug discovery and development settings. *Adv. Drug. Deliver. Rev.* **2001**, *46*, 3-26.
109. Leese, M. P.; Jourdan, F.; Dohle, W.; Kimberley, M. R.; Thomas, M. P.; Bai, R.; Hamel, E.; Ferrandis, E.; Potter, B. V. L. Steroidomimetic tetrahydroisoquinolines for the design of new microtubule disruptors. *ACS Med. Chem. Lett.* **2011**, *3*, 5-9.
110. Topliss, J. G. Utilization of operational schemes for analog synthesis in drug design. *J. Med. Chem.* **1972**, *15*, 1006-1011.
111. Nagasawa, Y.; Ueoka, R.; Yamanokuchi, R.; Horiuchi, N.; Ikeda, T.; Rotinsulu, H.; Mangindaan, R. E. P.; Ukai, K.; Kobayashi, H.; Namikoshi, M.; Hirota, H.; Yokosawa, H.; Tsukamoto, S. Isolation of Salsolinol, a tetrahydroisoquinoline alkaloid, from the marine sponge *Xestospongia vansoesti* as a proteasome inhibitor. *Chem. Pharm. Bull.* **2011**, *59*, 287-290.
112. Bracca, A. B. J.; Kaufman, T. S. Synthetic approaches to carnegine, a simple tetrahydroisoquinoline alkaloid. *Tetrahedron* **2004**, *60*, 10575-10610.
113. Stöckigt, J.; Antonchick, A. P.; Wu, F.; Waldmann, H. The Pictet–Spengler reaction in nature and in organic chemistry. *Angew. Chem. Int. Ed.* **2011**, *50*, 8538-8564.
114. Pan, L.; Chen, R.; Ni, D.; Xia, L.; Chen, X. An approach to the synthesis of enantiopure tetrahydroisoquinoline *via* a key asymmetric Ugi reaction. *Synlett* **2013**, *24*, 241-245.
115. Chrzanowska, M.; Grajewska, A.; Meissner, Z.; Rozwadowska, M.; Wiatrowska, I. A concise synthesis of tetrahydroisoquinoline-1-carboxylic acids using a Petasis reaction and Pomeranz–Fritsch–Bobbitt cyclization sequence. *Tetrahedron* **2012**, *68*, 3092-3097.

116. Deng, X.; Liang, J. T.; Liu, J.; McAllister, H.; Schubert, C.; Mani, N. S. A practical synthesis of enantiopure 7-alkoxy-4-aryl-tetrahydroisoquinoline, a dual serotonin reuptake inhibitor/histamine H3 antagonist. *Org. Process Res. Dev.* **2007**, *11*, 1043-1050.
117. Bevis, M. J.; Forbes, E. J.; Naik, N. N.; Uff, B. C. The synthesis of isoquinolines, indoles and benzthiophen by an improved Pomeranz-Fritsch reaction, using boron trifluoride in trifluoroacetic anhydride. *Tetrahedron* **1971**, *27*, 1253-1259.
118. Awuah, E.; Capretta, A. Strategies and synthetic methods directed toward the preparation of libraries of substituted isoquinolines. *J. Org. Chem.* **2010**, *75*, 5627-5634.
119. Bergstrom, F. W. Heterocyclic nitrogen compounds. Part IIA. Hexacyclic compounds: pyridine, quinoline, and isoquinoline. *Chem. Rev.* **1944**, *35*, 77-277.
120. Abdel-Magid, A. F.; Carson, K. G.; Harris, B. D.; Maryanoff, C. A.; Shah, R. D. Reductive amination of aldehydes and ketones with sodium triacetoxyborohydride. Studies on direct and indirect reductive amination procedures. *J. Org. Chem.* **1996**, *61*, 3849-3862.
121. Pomeranz, C. Über eine neue Isochinolinsynthese. *Monatsh. Chem. Verw. Tl.* **1893**, *14*, 116-119.
122. Fritsch, P. Synthesen in der Isocumarin- und Isochinolinreihe. *Ber. Dtsch. Chem. Ges.* **1893**, *26*, 419-422.
123. Bobbitt, J. M.; Moore, T. E. Synthesis of isoquinolines. VIII. 3,4,11,11a-tetrahydro-1*H*-benzo[b]quinolizin-2(6*H*)-ones. *J. Org. Chem.* **1968**, *33*, 2958-2959.
124. Hutait, S.; Biswas, S.; Batra, S. Efficient synthesis of maxonine analogues from *N*-substituted benzyl-1-formyl-9*H*- β -carboline. *Eur. J. Org. Chem.* **2012**, *2012*, 2453-2462.
125. Naciuk, F. F.; Milan, J. C.; Andreão, A.; Miranda, P. C. M. L. Exploitation of a tuned oxidation with *N*-haloimides in the synthesis of caulibugulones A–D. *J. Org. Chem.* **2013**, *78*, 5026-5030.
126. Suzuki, T.; Takamoto, M.; Okamoto, T.; Takayama, H. Acid-catalyzed double-cyclization reactions of *N,N*-dibenzylamino-acetaldehyde dialkyl acetals and related compounds: General synthesis of 7, 12-dihydro-5*H*-6, 12-methanodibenz-[c, f]azocines and related compounds. *Chem. Pharm. Bull.* **1986**, *34*, 1888-1900.
127. Kütt, A.; Rodima, T.; Saame, J.; Raamat, E.; Mäemets, V.; Kaljurand, I.; Koppel, I. A.; Garlyauskayte, R. Y.; Yagupolskii, Y. L.; Yagupolskii, L. M.; Bernhardt, E.; Willner, H.; Leito, I. Equilibrium acidities of superacids. *J. Org. Chem.* **2010**, *76*, 391-395.
128. Meot-Ner, M. The ionic hydrogen bond. *Chem. Rev.* **2005**, *105*, 213-284.
129. Nordlander, J. E.; Catalane, D. B.; Kotian, K. D.; Stevens, R. M.; Haky, J. E. Synthesis of indoles from *N*-(trifluoroacetyl)-2-anilino acetals. *J. Org. Chem.* **1981**, *46*, 778-782.
130. Sundberg, R. J.; Laurino, J. P. Cyclization of 2-[*N*-(methylsulfonyl)anilino]acetaldehyde diethyl acetals to indoles. Evidence for stereoelectronic effects in intramolecular electrophilic aromatic substitution. *J. Org. Chem.* **1984**, *49*, 249-254.
131. Shirasaka, T.; Takuma, Y.; Shimpuku, T.; Imaki, N. Practical synthesis of 5,6,7,8-tetrahydro-4-methoxy-6-methyl-1,3-dioxolo[4,5-*g*]isoquinolin-5-ol (cotarnine). *J. Org. Chem.* **1990**, *55*, 3767-3771.

132. Harrowven, D. C.; Dainty, R. F. The sliding cyclohexane rearrangement. *Tetrahedron* **1997**, *53*, 15771-15786.
133. Sassaman, M. B.; Surya Prakash, G. K.; Olah, G. A.; Donald, P.; Loker, K. B. Ionic hydrogenation with organosilanes under acid-free conditions. Synthesis of ethers, alkoxysilanes, thioethers, and cyclic ethers *via* organosilyl iodide and triflate catalyzed reductions of carbonyl compounds and their derivatives. *Tetrahedron* **1988**, *44*, 3771-3780.
134. Parnes, Z. N.; Kalinkin, M. I. Ionic hydrogenation of organic compounds (review). *Pharm. Chem. J.* **1979**, *13*, 846-852.
135. Adlington, M. G.; Orfanopoulos, M.; Fry, J. L. A convenient one-step synthesis of hydrocarbons from alcohols through use of the organosilane-boron trifluoride reducing system. *Tetrahedron Lett.* **1976**, *17*, 2955-2958.
136. Nimmagadda, R. D.; McRae, C. A novel reduction reaction for the conversion of aldehydes, ketones and primary, secondary and tertiary alcohols into their corresponding alkanes. *Tetrahedron Lett.* **2006**, *47*, 5755-5758.
137. Jackson, A. H.; Johnston, P.; Kenner, G. W.; Berry, R. W. H.; Brocklehurst, P.; Cheeseman, G. H.; Nunn, E. K.; Wright, E. H. M.; Thomas, E.; Hay, R. W.; Williams, P. P.; Finch, A. C. M.; Berlin, K. D.; Sturm, G. P.; Nield, P. G.; Austin, J. D.; Eaborn, C. Organosilicon compounds. Part XXIX. The stereochemical course of the reaction of a silicon hydride with chlorotriphenylmethane. *J. Chem. Soc. (Resumed)* **1964**, 2262-2280.
138. Sommer, L. H.; Bauman, D. L. Stereochemistry of asymmetric silicon. XIV. The SN₂-Si mechanism and racemization of an optically active fluorosilane without displacement of fluoride ion. *J. Am. Chem. Soc.* **1969**, *91*, 7045-7051.
139. Weissman, S. A.; Zewge, D. Recent advances in ether dealkylation. *Tetrahedron* **2005**, *61*, 7833-7863.
140. Greene, T. W.; Wuts, P. G. M. Greene's protective groups in organic synthesis. Fourth edition. **2007**, 24-165, 370-406.
141. Chrzanowska, M.; Rozwadowska, M. D. Asymmetric synthesis of isoquinoline alkaloids. *Chem. Rev.* **2004**, *104*, 3341-3370.
142. Pictet, A.; Spengler, T. Über die Bildung von Isochinolin-derivaten durch Einwirkung von Methylal auf Phenyl-äthylamin, Phenyl-alanin und Tyrosin. *Ber. Dtsch. Chem. Ges.* **1911**, *44*, 2030-2036.
143. Zhurakulov, S. N.; Vinogradova, V. I.; Levkovich, M. G. Synthesis of 1-aryltetrahydroisoquinoline alkaloids and their analogs. *Chem. Nat. Compd.* **2013**, *49*, 70-74.
144. Bischler, A.; Napieralski, B. Zur Kenntniss einer neuen Isochinolinsynthese. *Ber. Dtsch. Chem. Ges.* **1893**, *26*, 1903-1908.
145. Dempsey, A. M.; Hough, L. The reaction of phosphorus pentachloride with amides, in particular 2-acetamido-2-deoxyaldohexopyranoses. *Carbohydr. Res.* **1975**, *41*, 63-76.
146. Brun, E. M.; Gil, S.; Mestres, R.; Parra, M. Lithium enediolates and dienediolates of carboxylic acids in synthesis: Alkylation with secondary halides. *Tetrahedron* **1998**, *54*, 15305-15320.
147. Nahm, S.; Weinreb, S. M. *N*-methoxy-*N*-methylamides as effective acylating agents. *Tetrahedron Lett.* **1981**, *22*, 3815-3818.
148. Niu, T.; Zhang, W.; Huang, D.; Xu, C.; Wang, H.; Hu, Y. A powerful reagent for synthesis of weinreb amides directly from carboxylic acids. *Org. Lett.* **2009**, *11*, 4474-4477.

149. Graham, S. L.; Scholz, T. H. A new mode of reactivity of *N*-methoxy-*N*-methylamides with strongly basic reagents. *Tetrahedron Lett.* **1990**, *31*, 6269-6272.
150. Giannis, A.; Sandhoff, K. LiBH₄(NaBH₄)/Me₃SiCl, an unusually strong and versatile reducing agent. *Angew Chem. Int. Edit.* **1989**, *28*, 218-220.
151. Olmstead, W. N.; Margolin, Z.; Bordwell, F. G. Acidities of water and simple alcohols in dimethyl sulfoxide solution. *J. Org. Chem.* **1980**, *45*, 3295-3299.
152. Bordwell, F. G.; Algrim, D. J. Acidities of anilines in dimethyl sulfoxide solution. *J. Am. Chem. Soc.* **1988**, *110*, 2964-2968.
153. Novak, A.; Humphreys, L. D.; Walker, M. D.; Woodward, S. Amide bond formation using an air-stable source of AlMe₃. *Tetrahedron Lett.* **2006**, *47*, 5767-5769.
154. Woodward, S. Design versus discovery in synthetic applications of organoalanes. *Synlett* **2007**, *2007*, 1490-1500.
155. Poirier, D.; Boivin, R. P.; Tremblay, M. R.; Bérubé, M.; Qiu, W.; Lin, S.-X. Estradiol-adenosine hybrid compounds designed to inhibit type 1 17 β -hydroxysteroid dehydrogenase. *J. Med. Chem.* **2005**, *48*, 8134-8147.
156. Dunigan, D. D.; Waters, S. B.; Owen, T. C. Aqueous soluble tetrazolium/formazan MTS as an indicator of NADH- and NADPH-dependent dehydrogenase activity. *Biotechniques* **1995**, *19*, 640-649.
157. Aka, J.; Lin, S.-X. Comparison of functional proteomic analyses of human breast cancer cell lines T47D and MCF7. *PLoS ONE* **2012**, *7*, e31532.
158. Karey, K. P.; Sirbasku, D. A. Differential responsiveness of human breast cancer cell lines MCF-7 and T47D to growth factors and 17 beta-estradiol. *Cancer Res.* **1988**, *48*, 4083-4092.
159. Desta, Z.; Ward, B. A.; Soukhova, N. V.; Flockhart, D. A. Comprehensive evaluation of tamoxifen sequential biotransformation by the human cytochrome P450 system in vitro: Prominent roles for CYP3A and CYP2D6. *J. Pharmacol. Exp. Ther.* **2004**, *310*, 1062-1075.
160. Faff, O.; Murray, A. B.; Schmidt, J.; Leib-Mosch, C.; Erfle, V.; Hehlmann, R. Retrovirus-like particles from the human T47D cell line are related to mouse mammary tumour virus and are of human endogenous origin. *J. Gen. Virol.* **1992**, *73* (Pt 5), 1087-1097.
161. Soto, A. M.; Murai, J. T.; Siiteri, P. K.; Sonnenschein, C. Control of cell proliferation: evidence for negative control on estrogen-sensitive T47D human breast cancer cells. *Cancer Res.* **1986**, *46*, 2271-2275.
162. Horwitz, K. B.; Mockus, M. B.; Lessey, B. A. Variant T47D human breast cancer cells with high progesterone-receptor levels despite estrogen and antiestrogen resistance. *Cell* **1982**, *28*, 633-642.
163. Chen, Y.; Alman, B. A. Wnt pathway, an essential role in bone regeneration. *J. Cell. Biochem.* **2009**, *106*, 353-362.
164. Lim, G. E.; Brubaker, P. L. Glucagon-like peptide 1 secretion by the L-cell: The view from within. *Diabetes* **2006**, *55*, S70-S77.
165. Dungan, K.; Buse, J. B. Glucagon-like peptide 1-based therapies for type 2 diabetes: A focus on exenatide. *Clinical Diabetes* **2005**, *23*, 56-62.
166. Chan, D. A.; Giaccia, A. J. Harnessing synthetic lethal interactions in anticancer drug discovery. *Nat. Rev. Drug. Discov.* **2011**, *10*, 351-364.
167. Markowitz, S. D.; Bertagnolli, M. M. Molecular basis of colorectal cancer. *New Engl. J. Med.* **2009**, *361*, 2449-2460.

168. Chu, Z.-L.; Jones, R. M.; He, H.; Carroll, C.; Gutierrez, V.; Lucman, A.; Moloney, M.; Gao, H.; Mondala, H.; Bagnol, D.; Unett, D.; Liang, Y.; Demarest, K.; Semple, G.; Behan, D. P.; Leonard, J. A role for β -cell-expressed G protein-coupled receptor 119 in glycemic control by enhancing glucose-dependent insulin release. *Endocrinology* **2007**, *148*, 2601-2609.
169. Overton, H. A.; Babbs, A. J.; Doel, S. M.; Fyfe, M. C. T.; Gardner, L. S.; Griffin, G.; Jackson, H. C.; Procter, M. J.; Rasamison, C. M.; Tang-Christensen, M.; Widdowson, P. S.; Williams, G. M.; Reynet, C. Deorphanization of a G protein-coupled receptor for oleoylethanolamide and its use in the discovery of small-molecule hypophagic agents. *Cell Metab.* **2006**, *3*, 167-175.
170. Falcão-Pires, I.; Ladeiras-Lopes, R.; Leite-Moreira, A. F. The apelinergic system: a promising therapeutic target. *Expert Opin. Ther. Tar.* **2010**, *14*, 633-645.
171. Tatemoto, K.; Hosoya, M.; Habata, Y.; Fujii, R.; Kakegawa, T.; Zou, M.-X.; Kawamata, Y.; Fukusumi, S.; Hinuma, S.; Kitada, C.; Kurokawa, T.; Onda, H.; Fujino, M. Isolation and characterization of a novel endogenous peptide ligand for the human APJ receptor. *Biochem. Bioph. Res. Co.* **1998**, *251*, 471-476.
172. ter Haar, E.; Koth, C. M.; Abdul-Manan, N.; Swenson, L.; Coll, J. T.; Lippke, J. A.; Lepre, C. A.; Garcia-Guzman, M.; Moore, J. M. Crystal structure of the ectodomain complex of the CGRP receptor, a class-B GPCR, reveals the site of drug antagonism. *Structure* **2010**, *18*, 1083-1093.
173. Recober, A.; Russo, A. F. Calcitonin gene-related peptide: an update on the biology. *Curr. Opin. Neurol.* **2009**, *22*, 241-246.
174. Gasparini, F.; Spooren, W. Allosteric modulators for mGlu receptors. *Curr. Neuropsychopharmacol.* **2007**, *5*, 187-194.
175. Witkin, J. M.; Eiler II, W. J. A. Antagonism of metabotropic glutamate group II receptors in the potential treatment of neurological and neuropsychiatric disorders. *Drug Dev. Res.* **2006**, *67*, 757-769.
176. Scatena, R.; Bottoni, P.; Pontoglio, A.; Mastrototaro, L.; Giardina, B. Glycolytic enzyme inhibitors in cancer treatment. *Expert Opin. Inv. Drug.* **2008**, *17*, 1533-1545.
177. Chase, A.; Cross, N. C. P. Aberrations of EZH2 in cancer. *Clin. Cancer Res.* **2011**, *17*, 2613-2618.
178. Sneeringer, C. J.; Scott, M. P.; Kuntz, K. W.; Knutson, S. K.; Pollock, R. M.; Richon, V. M.; Copeland, R. A. Coordinated activities of wild-type plus mutant EZH2 drive tumor-associated hypertrimethylation of lysine 27 on histone H3 (H3K27) in human B-cell lymphomas. *P. Natl. Acad. Sci. USA* **2010**, *107*, 20980-20985.
179. Tzschucke, C. C.; Murphy, J. M.; Hartwig, J. F. Arenes to anilines and aryl ethers by sequential iridium-catalyzed borylation and copper-catalyzed coupling. *Org. Lett.* **2007**, *9*, 761-764.
180. Ullrich, T.; Sulek, P.; Binder, D.; Pyerin, M. A new route to 4-ethynyl-N-hydroxy-2-imidazolidinones via oxime addition. *Tetrahedron* **2000**, *56*, 3697-3701.
181. Waltz, F.; Pillette, L.; Verhaeghe, E.; Ambroise, Y. Synthesis and structure-activity relationships of a class of sodium iodide symporter function inhibitors. *ChemMedChem* **2011**, *6*, 1775-1777.
182. Giovenzana, G. B.; Imperio, D.; Penoni, A.; Palmisano, G. Reductive amination with zinc powder in aqueous media. *Beilstein J. Org. Chem.* **2011**, *7*, 1095-1099.

183. Samec, J. S. M.; Mony, L.; Bäckvall, J.-E. Efficient ruthenium catalyzed transfer hydrogenation of functionalized imines by isopropanol under controlled microwave heating. *Can. J. Chem.* **2005**, *83*, 909-916.
184. Cheng, C.; Sun, J.; Xing, L.; Xu, J.; Wang, X.; Hu, Y. Highly chemoselective Pd-C catalytic hydrodechlorination leading to the highly efficient *N*-debenzylation of benzylamines. *J. Org. Chem.* **2009**, *74*, 5671-5674.
185. Shu, X.-Z.; Xia, X.-F.; Yang, Y.-F.; Ji, K.-G.; Liu, X.-Y.; Liang, Y.-M. Selective functionalization of sp³ C-H bonds adjacent to nitrogen using (diacetoxyiodo)benzene (DIB). *J. Org. Chem.* **2009**, *74*, 7464-7469.
186. Schaper, W.; Blume, E.; Raether, W.; Dittmar, W. 1-(1,3-Dioxolan-2-ylmethyl)-azole, German Patent DE3308554 A1.
187. Barlaam, B.; Dantzman, c. WO 02/46164 A1.
188. Ruiz Espelt, L.; Wiensch, E. M.; Yoon, T. P. Brønsted acid cocatalysts in photocatalytic radical addition of α -amino C-H bonds across Michael acceptors. *J. Org. Chem.* **2013**, *78*, 4107-4114.
189. Zhang, G.; Ma, Y.; Wang, S.; Zhang, Y.; Wang, R. Enantioselective metal/organo-catalyzed aerobic oxidative sp³ C-H olefination of tertiary amines using molecular oxygen as the sole oxidant. *J. Am. Chem. Soc.* **2012**, *134*, 12334-12337.
190. Erb, J.; Strull, J.; Miller, D.; He, J.; Lectka, T. The Diels-Alder cyclization of ketenimines. *Org. Lett.* **2012**, *14*, 2191-2193.
191. Cameron, K. O.; Jardine, P. A. Estrogen agonists/antagonists; WO 96/21656.
192. Jones, G.; Stanforth, S. P. The Vilsmeier reaction of non-aromatic compounds. In *Org. Reactions*, John Wiley & Sons, Inc.: 2004.
193. Kulkarni, C. L.; Shenoy, S. J.; Nagarajan, K.; Shah, R. K.; Talwalker, P. K.; Prabhu, S. S. Antiimplantation agents: part II - 1,2-diaryl-1,2,3,4-tetrahydroisoquinolines. *Indian J. Chem., Sect A* **1985**, *24B*, 83-97.
194. Wee, A. G. H.; Liu, B.; McLeod, D. D. Steric and electronic influences on the diastereoselectivity of the Rh₂(OAc)₄-catalyzed C-H insertion in chiral ester diazoanilides: Synthesis of chiral, nonracemic 4-substituted 2-pyrrolidinones. *J. Org. Chem.* **1998**, *63*, 4218-4227.
195. Chesworth, R.; Groton, C. Tetrahydroisoquinoline compounds as estrogen agonists/antagonists; EP1113007A1.
196. Bhagwat, S. S.; Gayo-Fung, L. M.; Stein, B. M.; Chao, Q.; Gangloff, A. R.; McKie, J. A.; Rice, K. D. Compounds and methods for modulation of estrogen receptors; US6563322B1.
197. Ghosh, A. K.; Martyr, C. D.; Xu, C.-X. TiCl₄-Promoted tandem carbonyl or imine addition and Friedel-Crafts cyclization: synthesis of benzo-fused oxabicyclooctanes and nonanes. *Org. Lett.* **2012**, *14*, 2002-2005.
198. Ackermann, L.; Mehta, V. P. Palladium-catalyzed mono- α -arylation of acetone with aryl imidazolylsulfonates. *Chem. Eur. J.* **2012**, *18*, 10230-10233.
199. Villani, F. J.; Ellis, C. A.; Tavares, R. F.; Steinberg, M.; Tolksdorf, S. Hypocholesteremic agents. I. Substituted stilbazoles and dihydrostilbazoles. *J. Med. Chem.* **1970**, *13*, 359-366.
200. Elderfield, R. C.; Burgess, K. L. The Reaction of o-phenylenediamines with ketones. V. Further studies with dibenzyl ketones. *J. Am. Chem. Soc.* **1960**, *82*, 1975-1981.
201. Schrittwieser, J. H.; Resch, V.; Sattler, J. H.; Lienhart, W.-D.; Durchschein, K.; Winkler, A.; Gruber, K.; Macheroux, P.; Kroutil, W. Biocatalytic

enantioselective oxidative C-C coupling by aerobic C-H activation. *Angew. Chem. Int. Ed.* **2011**, *50*, 1068-1071.

Appendix A
Crystallographic data for compound 164j

Table 1. Crystal data and structure refinement for 1.

Identification code	k12farm2
Empirical formula	C ₁₆ H ₁₆ Cl N O
Formula weight	273.75
Temperature	150(2) K
Wavelength	0.71073 Å
Crystal system	Orthorhombic
Space group	P2 ₁ cn
Unit cell dimensions	a = 6.5270(1) Å alpha = 90°
	b = 8.1320(1) Å beta = 90°
	c = 26.0040(4) Å gamma = 90°
Volume	1380.23(3) Å ³
Z	4
Density (calculated)	1.317 Mg/m ³
Absorption coefficient	0.268 mm ⁻¹
F(000)	576
Crystal size	0.50 x 0.25 x 0.20 mm
Theta range for data collection	4.00 to 27.50°
Index ranges	-7 ≤ h ≤ 8; -10 ≤ k ≤ 10; -33 ≤ l ≤ 33
Reflections collected	15160
Independent reflections	3094 [R(int) = 0.0505]
Reflections observed (>2sigma)	2704
Data Completeness	0.997
Absorption correction	Semi-empirical from equivalents
Max. and min. transmission	0.925 and 0.857
Refinement method	Full-matrix least-squares on F ²
Data / restraints / parameters	3094 / 1 / 174
Goodness-of-fit on F ²	1.039
Final R indices [I>2sigma(I)]	R1 = 0.0359 wR2 = 0.0827
R indices (all data)	R1 = 0.0458 wR2 = 0.0879
Absolute structure parameter	0.14(6)
Largest diff. peak and hole	0.257 and -0.176 eÅ ⁻³

Table 2. Atomic coordinates ($\times 10^4$) and equivalent isotropic displacement parameters ($\text{\AA}^2 \times 10^3$) for 1.U(eq) is defined as one third of the trace of the orthogonalized U_{ij} tensor.

Atom	x	y	z	U(eq)
Cl(1)	3053(1)	5163(1)	-1546(1)	41(1)
O(1)	7675(3)	10123(2)	2348(1)	42(1)
N(2)	2499(2)	8397(2)	503(1)	30(1)
C(1)	4054(3)	7980(2)	883(1)	30(1)
C(3)	534(3)	8813(3)	739(1)	37(1)
C(4)	695(3)	10373(3)	1050(1)	37(1)
C(5)	2653(3)	11364(2)	1834(1)	34(1)
C(6)	4335(3)	11363(2)	2156(1)	34(1)
C(7)	5915(3)	10255(2)	2064(1)	32(1)
C(8)	5772(3)	9167(2)	1652(1)	29(1)
C(9)	4088(3)	9179(2)	1329(1)	27(1)
C(10)	2493(3)	10289(2)	1414(1)	31(1)
C(11)	8019(4)	11336(3)	2736(1)	45(1)
C(1')	2552(3)	7537(2)	32(1)	27(1)
C(2')	1147(3)	7910(2)	-360(1)	31(1)
C(3')	1269(3)	7144(2)	-837(1)	32(1)
C(4')	2804(3)	6016(2)	-932(1)	31(1)
C(5')	4196(3)	5611(2)	-553(1)	33(1)
C(6')	4056(3)	6347(2)	-71(1)	31(1)

Table 3. Bond lengths [Å] and angles [°] for 1.

Cl(1)-C(4')	1.7505(17)	O(1)-C(7)	1.371(2)
O(1)-C(11)	1.427(2)	N(2)-C(1')	1.410(2)
N(2)-C(1)	1.457(2)	N(2)-C(3)	1.461(3)
C(1)-C(9)	1.515(2)	C(3)-C(4)	1.509(3)
C(4)-C(10)	1.509(3)	C(5)-C(6)	1.381(3)
C(5)-C(10)	1.403(3)	C(6)-C(7)	1.390(3)
C(7)-C(8)	1.392(3)	C(8)-C(9)	1.382(3)
C(9)-C(10)	1.396(3)	C(1')-C(2')	1.404(3)
C(1')-C(6')	1.404(3)	C(2')-C(3')	1.390(3)
C(3')-C(4')	1.380(3)	C(4')-C(5')	1.380(3)
C(5')-C(6')	1.392(3)		
C(7)-O(1)-C(11)	117.28(16)	C(1')-N(2)-C(1)	117.18(14)
C(1')-N(2)-C(3)	120.04(15)	C(1)-N(2)-C(3)	112.35(14)
N(2)-C(1)-C(9)	112.34(15)	N(2)-C(3)-C(4)	111.04(17)
C(10)-C(4)-C(3)	110.71(17)	C(6)-C(5)-C(10)	122.10(17)
C(5)-C(6)-C(7)	118.99(17)	O(1)-C(7)-C(6)	125.34(17)
O(1)-C(7)-C(8)	114.96(17)	C(6)-C(7)-C(8)	119.70(18)
C(9)-C(8)-C(7)	121.04(18)	C(8)-C(9)-C(10)	120.08(16)
C(8)-C(9)-C(1)	118.13(16)	C(10)-C(9)-C(1)	121.78(17)
C(9)-C(10)-C(5)	118.09(17)	C(9)-C(10)-C(4)	120.63(17)
C(5)-C(10)-C(4)	121.23(17)	C(2')-C(1')-C(6')	117.86(16)
C(2')-C(1')-N(2)	120.47(16)	C(6')-C(1')-N(2)	121.60(16)
C(3')-C(2')-C(1')	120.89(18)	C(4')-C(3')-C(2')	119.88(17)
C(5')-C(4')-C(3')	120.61(17)	C(5')-C(4')-Cl(1)	119.77(15)
C(3')-C(4')-Cl(1)	119.55(14)	C(4')-C(5')-C(6')	119.82(18)
C(5')-C(6')-C(1')	120.88(17)		

Symmetry transformations used to generate equivalent atoms:

Table 4. Anisotropic displacement parameters ($\text{\AA}^2 \times 10^3$) for 1. The anisotropic displacement factor exponent takes the form: $-2 \pi^2 [h^2 a^{*2} U_{11} + \dots + 2 h k a^* b^* U_{12}]$

Atom	U11	U22	U33	U23	U13	U12
Cl(1)	54(1)	39(1)	30(1)	-5(1)	-7(1)	-1(1)
O(1)	46(1)	40(1)	39(1)	-9(1)	-12(1)	5(1)
N(2)	27(1)	35(1)	27(1)	-1(1)	-2(1)	4(1)
C(1)	30(1)	31(1)	28(1)	0(1)	0(1)	6(1)
C(3)	30(1)	40(1)	41(1)	-6(1)	0(1)	2(1)
C(4)	32(1)	39(1)	41(1)	-1(1)	1(1)	9(1)
C(5)	35(1)	33(1)	35(1)	-2(1)	8(1)	7(1)
C(6)	42(1)	30(1)	28(1)	-2(1)	5(1)	-3(1)
C(7)	38(1)	30(1)	27(1)	3(1)	-3(1)	-1(1)
C(8)	33(1)	25(1)	30(1)	1(1)	1(1)	2(1)
C(9)	30(1)	25(1)	26(1)	3(1)	2(1)	0(1)
C(10)	30(1)	33(1)	30(1)	3(1)	5(1)	0(1)
C(11)	50(1)	46(1)	37(1)	-10(1)	-8(1)	-1(1)
C(1')	28(1)	26(1)	28(1)	4(1)	1(1)	-3(1)
C(2')	31(1)	30(1)	32(1)	4(1)	-4(1)	1(1)
C(3')	32(1)	33(1)	31(1)	6(1)	-7(1)	-3(1)
C(4')	40(1)	27(1)	27(1)	1(1)	-4(1)	-6(1)
C(5')	38(1)	28(1)	33(1)	1(1)	-2(1)	5(1)
C(6')	33(1)	30(1)	29(1)	2(1)	-7(1)	4(1)

Table 5. Hydrogen coordinates ($\times 10^4$) and isotropic displacement parameters ($\text{\AA}^2 \times 10^3$) for 1.

Atom	x	y	z	U(eq)
H(1A)	5415	7972	716	36
H(1B)	3785	6860	1016	36
H(3A)	89	7900	964	45
H(3B)	-511	8957	467	45
H(4A)	864	11323	817	45
H(4B)	-583	10535	1249	45
H(5)	1570	12116	1900	41
H(6)	4412	12108	2437	40
H(8)	6848	8405	1591	35
H(11A)	6978	11228	3005	67
H(11B)	7932	12435	2582	67
H(11C)	9382	11180	2885	67
H(2')	99	8696	-298	37
H(3')	298	7397	-1098	39
H(5')	5247	4833	-621	40
H(6')	4990	6039	192	37

Table 6. Dihedral angles [$^{\circ}$] for 1.

Atom1 - Atom2 - Atom3 - Atom4	Dihedral
C(1') - N(2) - C(1) - C(9)	169.66(16)
C(3) - N(2) - C(1) - C(9)	-45.3(2)
C(1') - N(2) - C(3) - C(4)	-150.30(17)
C(1) - N(2) - C(3) - C(4)	65.8(2)
N(2) - C(3) - C(4) - C(10)	-50.4(2)
C(10) - C(5) - C(6) - C(7)	-0.5(3)
C(11) - O(1) - C(7) - C(6)	-7.3(3)
C(11) - O(1) - C(7) - C(8)	172.51(17)
C(5) - C(6) - C(7) - O(1)	179.54(18)
C(5) - C(6) - C(7) - C(8)	-0.2(3)
O(1) - C(7) - C(8) - C(9)	-179.27(16)
C(6) - C(7) - C(8) - C(9)	0.5(3)
C(7) - C(8) - C(9) - C(10)	-0.1(3)
C(7) - C(8) - C(9) - C(1)	178.97(17)
N(2) - C(1) - C(9) - C(8)	-164.97(16)
N(2) - C(1) - C(9) - C(10)	14.1(2)
C(8) - C(9) - C(10) - C(5)	-0.5(3)
C(1) - C(9) - C(10) - C(5)	-179.61(17)
C(8) - C(9) - C(10) - C(4)	176.98(17)
C(1) - C(9) - C(10) - C(4)	-2.1(3)
C(6) - C(5) - C(10) - C(9)	0.8(3)
C(6) - C(5) - C(10) - C(4)	-176.66(18)
C(3) - C(4) - C(10) - C(9)	19.8(3)
C(3) - C(4) - C(10) - C(5)	-162.75(18)
C(1) - N(2) - C(1') - C(2')	-177.84(17)
C(3) - N(2) - C(1') - C(2')	39.9(2)
C(1) - N(2) - C(1') - C(6')	-1.0(2)
C(3) - N(2) - C(1') - C(6')	-143.22(19)
C(6') - C(1') - C(2') - C(3')	-1.2(3)
N(2) - C(1') - C(2') - C(3')	175.83(17)
C(1') - C(2') - C(3') - C(4')	-0.8(3)
C(2') - C(3') - C(4') - C(5')	1.5(3)
C(2') - C(3') - C(4') - Cl(1)	-175.66(15)
C(3') - C(4') - C(5') - C(6')	-0.1(3)
Cl(1) - C(4') - C(5') - C(6')	177.04(15)
C(4') - C(5') - C(6') - C(1')	-2.0(3)
C(2') - C(1') - C(6') - C(5')	2.6(3)
N(2) - C(1') - C(6') - C(5')	-174.40(18)

Symmetry transformations used to generate equivalent atoms:

Appendix B

NCI raw data

		163e	163i	163q	163s	170e	170i	170q	170s
Type of cancer	Cell line								
Leukemia	CCRF-CEM	0,7	-2,3	4,2	-0,5	5,5	12,7	5,5	6,5
Leukemia	HL-60(TB)	20,4	18,8	19,6	11,0	6,1	7,7	9,2	1,5
Leukemia	K-562	22,2	19,7	22,2	15,6	18,0	23,9	4,1	5,2
Leukemia	MOLT-4	8,4	19,1	9,6	11,5	11,5	32,4	5,9	11,9
Leukemia	RPMI-8226	-6,2	3,4	8,0	5,3	2,9	5,8	2,7	7,5
Leukemia	SR	8,2	9,0	6,8	2,2	2,7	6,6	0,8	2,4
Non-Small Cell Lung Cancer	A549/ATCC	4,4	1,4	4,4	6,0	7,7	7,8	3,7	
Non-Small Cell Lung Cancer	EKVX	-1,6	19,9	3,9	13,4	4,7	9,5	-0,6	-6,3
Non-Small Cell Lung Cancer	HOP-62	-2,1	-13,1	-7,2	1,6	-3,5	-7,6	-9,8	-6,1
Non-Small Cell Lung Cancer	HOP-92				27,2	9,4			
Non-Small Cell Lung Cancer	NCI-H226	-10,6	-2,7	-9,9	5,2	3,2	-2,0	1,0	-2,6
Non-Small Cell Lung Cancer	NCI-H23	4,6	8,7	3,4	-1,4	-3,1	2,0	-5,7	11,8
Non-Small Cell Lung Cancer	NCI-H322M	-3,3	-4,0	1,6	6,0	0,8	13,9	1,8	-9,8
Non-Small Cell Lung Cancer	NCI-H460	-14,5	-3,5	-6,0	-4,4	-1,8	-6,2	2,4	-2,5
Non-Small Cell Lung Cancer	NCI-H522	13,5	34,7	27,7	23,1	18,5	20,3	6,7	31,7
Colon Cancer	COLO 205	-17,6	-14,5	-10,9	-5,2	-15,9	-9,3	-10,1	-13,6
Colon Cancer	HCC-2998								
Colon Cancer	HCT-116	-6,7	7,5	8,8	2,0	-5,0	-2,0	-1,5	9,4
Colon Cancer	HCT-15	5,9	4,8	2,1	3,9	-2,4	6,3	-1,0	10,7
Colon Cancer	HT29	19,4	25,6	23,0	19,7	-0,2	10,1	4,8	6,1
Colon Cancer	KM12	1,0	-5,9	-10,2	7,8	3,5	-7,2	-5,7	12,1
Colon Cancer	SW-620	0,9	6,5	3,1	8,0	-3,4	2,5	3,5	3,0
CNS Cancer	SF-268	-5,1	-11,8	-6,7	1,9	-1,1	6,8	0,5	-2,1
CNS Cancer	SF-295	9,2	0,7	6,7	1,5	4,8	-2,8	0,6	-4,1
CNS Cancer	SF-539	-6,8	-5,8	-8,8	-11,8	-2,6	0,3	-12,8	25,7
CNS Cancer	SNB-19	-1,2	2,4	-4,6	-3,2	6,0	0,8	6,5	-2,2
CNS Cancer	SNB-75	8,4	7,5	-6,7	8,3	13,4	16,5	-0,5	5,5
CNS Cancer	U251	4,6	24,4	2,9	3,0	2,0	0,4	-0,9	
Melanoma	LOX IMVI	4,2	0,1	-2,6	0,0	-0,9	1,5	1,0	11,1
Melanoma	M14	1,8	-1,8	-3,2	-2,7	-6,0	-8,2	-8,0	2,6
Melanoma	MALME-3M								
Melanoma	MDA-MB-435	9,6	3,8	6,4	0,4	-0,1	-1,9	0,3	5,5
Melanoma	SK-MEL-2								
Melanoma	SK-MEL-28	-9,1	-7,8	-13,6	-3,5	-4,7	-11,2	-11,5	-8,8
Melanoma	SK-MEL-5	-0,7	6,3	7,2	12,3	2,6	3,5	-0,3	15,9
Melanoma	UACC-257	-3,8	-7,4	-3,1	-5,3	-7,9	-1,8	24,4	18,0
Melanoma	UACC-62	3,4	13,1	7,9	6,7	0,9	8,0	0,1	16,4
Ovarian Cancer	IGROV1	-4,7	-0,9	-2,0	-2,9	-11,6	0,4	-11,3	-16,0
Ovarian Cancer	NCI/ADR-RES	-1,9	-2,9	-2,6	1,1	-1,8	-7,6	-7,0	19,6
Ovarian Cancer	OVCAR-3	-4,3	-12,0	-11,1	-0,2	-2,8	-13,4	-4,8	-15,2
Ovarian Cancer	OVCAR-4	6,4	6,2	-2,1	5,0	-6,6	2,8	-4,7	6,6
Ovarian Cancer	OVCAR-5	-3,9	10,0	5,4	2,6	-0,8	5,3	-11,7	-7,1
Ovarian Cancer	OVCAR-8	-0,5		1,5	-1,5	-6,1	4,1	-8,3	
Ovarian Cancer	SK-OV-3	-4,7	-3,5	-1,2	4,9	-7,1	-11,3	-13,2	-8,5
Renal Cancer	786-0	7,7	12,7	9,5	9,3	7,0	11,4	7,7	11,8
Renal Cancer	A498	9,0	34,0	28,6	28,8	3,5	39,1	6,6	12,4
Renal Cancer	ACHN	-12,3	-3,7	-5,8	-6,5	-3,0	-3,4	-20,8	70,3
Renal Cancer	CAKI-1	4,5	9,2	18,7	12,4	2,3	3,0	-2,0	42,2
Renal Cancer	RXF 393	-0,7	-0,9	-21,0	0,0	-1,9	10,5	-6,3	-3,5
Renal Cancer	SN12C	6,6	2,1	-1,5	1,4	-1,2	0,8	-12,6	0,4
Renal Cancer	TK-10	7,4	24,0	26,7	26,3	12,6	18,7	7,1	4,5
Renal Cancer	UO-31	7,1	10,7	8,4	16,5	11,0	27,2	5,0	8,1
Prostate Cancer	DU-145	-4,0	-2,1	-4,2	1,0	5,5	-5,9	-7,1	5,5
Prostate Cancer	PC-3	-9,2	8,8	3,2	11,6	-1,6	10,1	-5,5	23,8
Breast Cancer	BT-549	1,7	4,2	4,3	4,8	6,9	-4,1	-3,8	22,1
Breast Cancer	HS 578T	-6,6	-23,5	7,8	11,0	-7,5	0,0	-2,2	-30,3
Breast Cancer	MCF7	-0,2	1,2	-0,7	-0,7	-10,8	-4,3	-5,2	-0,8
Breast Cancer	MDA-MB-231/ATCC	-2,6	-2,5	-13,8	-17,2	-14,1	4,2	-7,0	20,5
Breast Cancer	MDA-MB-468	-10,6	-12,6	7,8	20,1	-4,9	2,5	7,1	1,0
Breast Cancer	T-47D	2,1	9,2	7,9	11,5	3,8	13,2	2,8	-3,0

		163u	163w	163t	163v	164j	165j	163aa	143z
Type of cancer	Cell line								
Leukemia	CCRF-CEM	-9,9	0,7	72,8	1,5		16,0	2,3	-2,0
Leukemia	HL-60(TB)	1,9	20,1	46,4	12,8	112,8	4,6	18,6	41,7
Leukemia	K-562	13,7	30,5	51,7	39,6	47,1	7,8	20,0	24,8
Leukemia	MOLT-4	12,4	13,0	71,0	12,2	130,7	20,6	11,8	12,6
Leukemia	RPMI-8226	1,0	6,9	14,3	6,4	15,5	6,5	17,6	6,3
Leukemia	SR	8,9	22,2	56,9	22,7	121,4	36,2	8,6	17,1
Non-Small Cell Lung Cancer	A549/ATCC	-1,5	8,8	1,9	6,1	9,8	1,4	8,5	-0,1
Non-Small Cell Lung Cancer	EKVX								
Non-Small Cell Lung Cancer	HOP-62	-6,3	-6,0	-2,8	-20,3	-3,7	-0,4	-4,6	-9,2
Non-Small Cell Lung Cancer	HOP-92	-3,1	9,4	-7,7	2,1	6,0	14,0	9,3	-20,1
Non-Small Cell Lung Cancer	NCI-H226								
Non-Small Cell Lung Cancer	NCI-H23	2,8	-1,3	13,4	7,0	20,6	11,3	16,5	5,1
Non-Small Cell Lung Cancer	NCI-H322M	2,1	5,7	1,3	-2,8	15,4	10,1	7,9	8,2
Non-Small Cell Lung Cancer	NCI-H460	-5,4	-3,9	-1,7	-10,2	37,9	0,6	1,6	-13,4
Non-Small Cell Lung Cancer	NCI-H522								
Colon Cancer	COLO 205	0,0	-11,2	-4,4	-9,0	-9,4	5,3	0,8	-18,3
Colon Cancer	HCC-2998	-10,3	0,1	-0,7	2,2	-8,9	1,4	-0,9	2,6
Colon Cancer	HCT-116	-9,4	-1,3	1,0	-9,0	92,6	6,5	8,7	-2,4
Colon Cancer	HCT-15	1,1	1,1	9,3	7,4	35,2	1,8	12,0	4,5
Colon Cancer	HT29	-9,2	4,6	14,1	4,7	94,5	5,6	17,2	4,9
Colon Cancer	KM12	6,1	-4,5	24,2	4,5	131,2	7,5	9,8	3,0
Colon Cancer	SW-620	-2,4	-4,5	16,9	-0,5	182,6	9,3	4,4	-7,6
CNS Cancer	SF-268	6,0	5,2	-0,9	3,7	93,9	19,0	-3,3	-5,3
CNS Cancer	SF-295	6,5	10,1	-36,1	7,7	9,8	4,0	14,1	22,0
CNS Cancer	SF-539	5,3	12,1	2,7	6,9	1,2	9,8	1,8	0,0
CNS Cancer	SNB-19								
CNS Cancer	SNB-75	-7,1	-18,0	-8,1	-11,3	-20,5	-11,1	-31,1	-3,8
CNS Cancer	U251	-3,1	4,8	1,8	3,8	34,3	2,9	12,8	2,7
Melanoma	LOX IMVI	-5,9	-6,1	7,4	3,6	160,6	11,4	5,2	0,5
Melanoma	M14	-6,8	-7,8	-0,8	-6,0	3,5	3,2	1,8	-16,7
Melanoma	MALME-3M	6,1	9,8	4,9	-2,7	27,3	7,1	20,0	14,1
Melanoma	MDA-MB-435	-1,7	-1,3	53,9	7,1	179,9	-0,9	1,3	2,4
Melanoma	SK-MEL-2								
Melanoma	SK-MEL-28	-9,1	-8,0	1,2	-1,6	-9,7	-2,3	-10,0	-16,7
Melanoma	SK-MEL-5	6,5	-9,0	4,8	8,3	-1,1	8,2	-8,8	1,4
Melanoma	UACC-257	21,7	13,6	14,6	12,0	12,9	89,3	7,6	10,5
Melanoma	UACC-62	2,3	8,0	9,5	8,7	14,1	13,7	19,1	9,3
Ovarian Cancer	IGROV1	5,0	-0,6	-7,9	-4,6	12,1	14,6	15,8	8,0
Ovarian Cancer	NCI/ADR-RES	-2,6	-6,0	-6,1	-7,2	21,5	-1,5	-3,6	-9,4
Ovarian Cancer	OVCAR-3	-6,1	-12,9	-1,4	-4,0	188,8	-1,3	0,3	-6,5
Ovarian Cancer	OVCAR-4	-8,2	-10,6	-2,4	-8,0	1,4	1,0	4,5	0,8
Ovarian Cancer	OVCAR-5	4,5	2,8	8,2	15,1	12,5	4,6	3,7	9,2
Ovarian Cancer	OVCAR-8	0,0	-2,7	10,0	2,3	117,1	2,2	-12,0	-10,0
Ovarian Cancer	SK-OV-3	2,1	-3,2	-4,0	-9,0	3,4	-0,8	10,9	-5,1
Renal Cancer	786-0	-2,6	1,1	-4,8	3,6	4,8	-1,3	2,0	-2,0
Renal Cancer	A498	8,3	30,6	7,8	1,2	19,9	15,7	1,9	10,0
Renal Cancer	ACHN	-4,6	-4,5	2,4	-2,3	16,2	1,8	0,2	1,2
Renal Cancer	CAKI-1	1,6	4,0	-2,4	13,8	28,5	17,3	9,3	4,7
Renal Cancer	RXF 393	5,8	25,5	-29,1	3,6	4,0	-4,0	-5,4	-4,1
Renal Cancer	SN12C	1,1	5,9	-7,4	-6,9	5,0	-5,6	5,6	4,5
Renal Cancer	TK-10								
Renal Cancer	UO-31	20,9	6,9	27,9	13,9	42,7	21,7	26,4	21,1
Prostate Cancer	DU-145	-4,9	-3,7	-1,5	-1,2	64,5	2,8	0,6	-4,6
Prostate Cancer	PC-3	-2,8	-1,0	-5,8	3,1	100,0	16,9	9,3	6,0
Breast Cancer	BT-549	-15,3	0,0	-3,6	-4,7	-3,2	7,6	-0,9	-14,7
Breast Cancer	HS 578T	-0,7	-10,1	-2,6	-5,3	-8,2	7,7	-4,7	-14,9
Breast Cancer	MCF7	-1,8	-8,1	3,2	-19,9	-1,2	5,7	11,9	-3,4
Breast Cancer	MDA-MB-231/ATCC	0,0	-7,1	15,7	3,7	11,1	11,4	7,7	-0,9
Breast Cancer	MDA-MB-468	0,4	1,4	11,1	7,7	0,0	-3,8	21,3	3,9
Breast Cancer	T-47D	-7,3	-13,7	6,4	5,7	9,7	14,4	21,6	4,5

		166i	170aa	170t	170u	146x	167	168	166s
Type of cancer	Cell line								
Leukemia	CCRF-CEM	5,2	68,1	22,6	-15,1		-0,3	-9,6	-1,2
Leukemia	HL-60(TB)	25,6	62,4	36,1	-3,8	-2,3	6,5	17,8	21,8
Leukemia	K-562	42,6	50,1	76,5	4,6	10,9	3,6	27,6	23,3
Leukemia	MDLT-4	21,6	66,8	36,2	-5,1	1,8	-4,5	-8,4	8,9
Leukemia	RPMI-8226	27,7	27,6	2,8	-10,3	-15,7	-1,5	3,7	8,1
Leukemia	SR	20,7	29,9	35,5	-16,4	9,7	8,2	26,3	-1,7
Non-Small Cell Lung Cancer	A549/ATCC	2,1	16,8	-3,5	-6,1	-1,0	1,4	2,6	-0,7
Non-Small Cell Lung Cancer	EKVX								
Non-Small Cell Lung Cancer	HOP-62	-11,0	-2,9	-1,4	-10,2	-8,4	-9,1	-5,9	-3,3
Non-Small Cell Lung Cancer	HOP-92	-1,9	16,3	-6,6	-24,9	-10,6	-9,5	6,8	-15,5
Non-Small Cell Lung Cancer	NCI-H226								
Non-Small Cell Lung Cancer	NCI-H23	4,3	10,3	0,6	1,6	-3,0	-1,9	-5,0	7,0
Non-Small Cell Lung Cancer	NCI-H322M	3,2	14,5	5,9	-11,9	6,9	0,1	2,1	6,8
Non-Small Cell Lung Cancer	NCI-H460	-8,0	2,6	-6,2	-14,0	-12,6	-7,8	-7,3	-14,9
Non-Small Cell Lung Cancer	NCI-H522								
Colon Cancer	COLO 205	-11,5	-20,6	-16,4	-11,0	-20,8	-18,6	-12,1	-13,5
Colon Cancer	HCC-2998	-4,2	3,1	-13,9	-6,5	-10,7	2,3	-2,1	-17,6
Colon Cancer	HCT-116	-4,4	17,8	-9,8	-10,6	-8,5	-5,4	-4,1	-2,7
Colon Cancer	HCT-15	2,5	14,3	8,8	2,5	0,8	-3,1	0,9	0,8
Colon Cancer	HT29	15,6	-2,5	5,2	-4,0	-1,4	8,0	3,4	2,7
Colon Cancer	KM12	7,6	12,4	23,2	1,4	6,2	4,5	2,0	1,7
Colon Cancer	SW-620	-0,9	5,3	2,0	-8,3	-14,0	-6,5	-6,3	-2,8
CNS Cancer	SF-268	6,6	23,7	7,0	2,3	2,1	9,5	-6,9	-2,9
CNS Cancer	SF-295	16,4	3,5	-37,6	1,3	13,6	13,4	27,4	10,1
CNS Cancer	SF-539	6,7	9,2	1,5	5,2	-1,7	0,1	3,1	1,0
CNS Cancer	SNB-19								
CNS Cancer	SNB-75	-6,9	-12,0	7,4	11,6	-6,2	-1,5	-1,6	-2,1
CNS Cancer	U251	-1,6	9,6	0,4	-1,2	-1,9	-2,3	-0,3	0,1
Melanoma	LOX IMVI	-6,8	10,9	0,5	1,6	-7,7	-4,2	-5,7	-0,6
Melanoma	M14	-19,9	-6,6	-2,2	-13,8	-12,3	-9,0	-9,3	-11,5
Melanoma	MALME-3M	0,6	3,2	-0,7	-3,2	5,1	-8,0	10,5	18,3
Melanoma	MDA-MB-435	4,6	6,2	83,3	-2,9	1,7	-5,3	5,5	-5,6
Melanoma	SK-MEL-2								
Melanoma	SK-MEL-28	-11,0	-14,5	-6,4	-11,9	-11,4	-20,0	-3,4	-11,1
Melanoma	SK-MEL-5	10,4	-1,1	33,4	-9,2	1,4	8,0	26,0	6,8
Melanoma	UACC-257	2,9	16,9	-4,0	3,3	7,7	3,1	8,6	9,9
Melanoma	UACC-62	9,0	27,2	4,0	-1,0	-3,5	-1,6	8,4	7,1
Ovarian Cancer	IGROV1	4,8	15,3	-20,6	-7,2	-0,8	-10,2	0,0	7,9
Ovarian Cancer	NCI/ADR-RES	-10,0	2,8	-3,7	-6,5	-8,8	-7,4	-4,0	-9,5
Ovarian Cancer	OVCAR-3	1,4	-3,0	-7,1	-2,7	-11,1	-9,6	-11,1	-3,2
Ovarian Cancer	OVCAR-4	-5,3	2,9	-2,4	-11,9	-6,0	-4,7	-9,9	-6,0
Ovarian Cancer	OVCAR-5	8,8	-0,3	2,0	4,9	-3,5	1,4	6,9	2,8
Ovarian Cancer	OVCAR-8	-0,2	8,1	-3,7	-0,4	-6,8	-4,0	-20,0	-5,7
Ovarian Cancer	SK-OV-3	-9,4	-6,7	0,1	-3,6	-0,6	-3,8	0,1	3,9
Renal Cancer	786-0	-2,8	4,2	-6,9	-5,7	-0,5	-3,1	1,6	-9,4
Renal Cancer	A498	-20,3	-3,1	-0,3	-15,5	11,7	10,4	29,4	3,9
Renal Cancer	ACHN	-6,9	6,9	3,5	1,2	-2,1	-4,8	-3,9	-4,9
Renal Cancer	CAKI-1	9,9	8,0	8,6	6,7	12,3	-1,5	8,5	0,6
Renal Cancer	RXF 393	7,6	-35,5	-18,6	-0,5	-15,3	-6,2	0,9	-10,5
Renal Cancer	SN12C	1,9	14,3	-3,8	-10,6	-1,4	-8,3	0,9	0,6
Renal Cancer	TK-10								
Renal Cancer	UO-31	30,2	43,6	31,1	20,9	16,4	-0,1	15,1	17,4
Prostate Cancer	DU-145	-2,8	2,5	-10,0	-8,4	-6,9	0,5	-7,7	-10,0
Prostate Cancer	PC-3	9,0	32,8	-10,9	-7,5	-2,6	6,1	7,7	8,5
Breast Cancer	BT-549	-15,1	6,3	-4,2	-8,7	-10,8	2,6	-1,2	-14,9
Breast Cancer	HS 578T	-9,7	-2,4	4,6	-1,1	-21,2	-20,2	-15,4	-2,1
Breast Cancer	MCF7	-0,4	13,6	-0,3	-10,1	-1,0	-9,8	-8,5	-0,8
Breast Cancer	MDA-MB-231/ATCC	-10,4	29,4	19,6	1,4	0,4	-11,3	-5,1	-5,6
Breast Cancer	MDA-MB-468	1,3	16,1	-2,4	-2,2	2,9	1,9	5,9	0,8
Breast Cancer	T-47D	2,6	8,7	6,0	3,1	0,9	-0,7	3,3	5,1

		176x	181a	181e	181f	191a	191e	190f	181c
Type of cancer	Cell line								
Leukemia	CCRF-CEM	21,0	2,6	4,1	7,9		13,6	1,3	30,0
Leukemia	HL-60(TB)	91,0	1,5	34,6	36,3	6,0	-8,6	-0,5	50,0
Leukemia	K-562	69,0	28,9	51,3	45,5	24,8	12,2	33,0	34,6
Leukemia	MOLT-4	31,6	20,0	35,0	25,7	32,7	17,1	13,7	24,9
Leukemia	RPMI-8226	73,6	21,7	48,5	44,5	-6,3	5,2	10,2	65,3
Leukemia	SR	54,1	19,5	27,6	33,9	14,0	7,8	30,5	36,3
Non-Small Cell Lung Cancer	A549/ATCC	31,6	7,7	0,2	-0,8	3,5	4,2	0,1	12,2
Non-Small Cell Lung Cancer	EKVX								
Non-Small Cell Lung Cancer	HOP-62	12,8	-1,6	-1,4	-10,3	-8,6	2,1	2,6	12,7
Non-Small Cell Lung Cancer	HOP-92	48,3	19,6	1,2	2,1	1,3	6,8	8,5	37,0
Non-Small Cell Lung Cancer	NCI-H226								14,0
Non-Small Cell Lung Cancer	NCI-H23	29,0	7,5	11,5	12,0	0,8	0,8	9,4	36,9
Non-Small Cell Lung Cancer	NCI-H322M	3,2	-0,7	-3,6	-6,0	13,3	-0,3	8,6	5,4
Non-Small Cell Lung Cancer	NCI-H460	12,3	-2,4	2,6	-7,0	-9,2	-4,3	4,4	7,0
Non-Small Cell Lung Cancer	NCI-H522								35,6
Colon Cancer	COLO 205	46,8	-18,3	-4,0	-3,6	-12,5	-9,3	1,7	5,9
Colon Cancer	HCC-2998	37,6	6,8	1,9	1,4	-10,2	-12,5	-1,1	4,5
Colon Cancer	HCT-116	21,7	3,8	12,2	19,8	3,8	5,1	27,2	27,0
Colon Cancer	HCT-15	-0,9	-1,4	9,1	7,0	3,5	-6,1	9,0	-0,8
Colon Cancer	HT29	12,5	9,5	24,0	25,6	-15,2	4,9	20,6	14,5
Colon Cancer	KM12	73,8	-0,7	3,4	8,1	7,9	5,3	27,0	21,7
Colon Cancer	SW-620	22,2	-0,8	0,0	5,1	-12,0	-10,5	9,6	10,0
CNS Cancer	SF-268	43,6	1,5	4,0	6,8	16,2	16,9	9,2	12,7
CNS Cancer	SF-295	25,8	6,0	-40,5	6,4	3,1	7,5	1,2	5,7
CNS Cancer	SF-539	16,1	3,3	0,3	4,0	5,1	4,4	9,8	9,5
CNS Cancer	SNB-19								11,0
CNS Cancer	SNB-75	8,6	-3,0	-4,6	-0,9	2,7	3,8	1,2	10,2
CNS Cancer	U251	37,9	4,6	4,3	1,0	1,0	0,5	6,7	32,9
Melanoma	LOX IMVI	9,7	-4,6	-0,6	-1,9	2,7	0,2	2,2	14,3
Melanoma	M14	5,6	-11,3	-1,6	-7,9	-8,2	-2,4	6,0	2,7
Melanoma	MALME-3M	42,6	12,7	11,8	5,3	10,5	-4,3	7,5	21,3
Melanoma	MDA-MB-435	59,2	-6,5	8,7	2,0	-1,0	-10,9	-5,2	17,3
Melanoma	SK-MEL-2								10,6
Melanoma	SK-MEL-28	18,5	-17,9	-6,5	-9,4	-10,5	-10,9	-4,6	2,4
Melanoma	SK-MEL-5	6,2	-2,3	6,9	2,5	3,7	104,6	0,2	4,2
Melanoma	UACC-257	11,0	1,7	6,5	14,3	-3,5			10,6
Melanoma	UACC-62	48,5	15,8	8,1	12,3	5,3	-2,4	14,3	22,8
Ovarian Cancer	IGROV1	36,8	6,8	-15,8	8,1	3,7	5,8	24,0	23,8
Ovarian Cancer	NCI/ADR-RES	-8,1	-6,2	-8,5	-8,0	-7,5	-3,2	-4,3	3,7
Ovarian Cancer	OVCAR-3	66,9	-7,5	7,0	17,3	-7,8	5,9	14,3	31,3
Ovarian Cancer	OVCAR-4	31,7	0,1	1,5	0,5	3,4	5,4	7,3	11,0
Ovarian Cancer	OVCAR-5	8,6	0,1	4,4	11,2	1,1	0,0	4,5	6,1
Ovarian Cancer	OVCAR-8	22,6	0,1	-3,4	-6,2	-2,9	-1,4	-19,6	23,3
Ovarian Cancer	SK-OV-3	4,7	4,8	-1,9	-3,8	-11,9	-1,6	3,4	-7,2
Renal Cancer	786-0	2,4	-0,2	-2,7	3,2	-1,0	-5,5	2,4	1,2
Renal Cancer	A498	2,8	6,7	-2,9	4,2	11,3	2,5	-18,9	19,4
Renal Cancer	ACHN	-0,8	-6,3	-1,0	-5,1	1,5	-0,2	3,6	0,5
Renal Cancer	CAKI-1	3,4	0,4	1,1	7,7	20,7	-0,5	9,4	9,0
Renal Cancer	RXF 393	18,0	-15,1	-14,2	14,3	-8,2	-7,7	-3,1	-7,7
Renal Cancer	SN12C	28,9	0,7	-2,1	-7,5	2,5	-5,6	2,0	13,3
Renal Cancer	TK-10								-7,8
Renal Cancer	UO-31	21,7	9,2	32,0	19,5	35,0	12,9	25,3	39,0
Prostate Cancer	DU-145	25,8	-3,1	-2,6	-2,7	-0,1	3,6	-3,4	0,1
Prostate Cancer	PC-3	62,9	2,1	-7,3	7,1	4,1	12,7	6,6	36,6
Breast Cancer	BT-549	46,0	-3,6	-7,5	-10,2	-5,0	-4,0	-14,9	36,3
Breast Cancer	HS 578T	13,3	-8,4	-5,4	-10,5	-4,9	-10,6	-9,5	
Breast Cancer	MCF7	52,2	-6,5	-16,2	-13,1	-19,3	-19,5	1,9	5,0
Breast Cancer	MDA-MB-231/ATCC	12,9	-6,7	-8,5	-5,4	10,7	-10,0	4,5	19,9
Breast Cancer	MDA-MB-468	94,4	-2,2	6,8	22,1	-1,4	-6,7	0,2	59,6
Breast Cancer	T-47D	61,7	6,2	14,0	14,0	-6,1	3,5	29,1	24,9

		191b	191c	191f	173	174	143n	175n	145h
Type of cancer	Cell line								
Leukemia	CCRF-CEM	15,7	14,0	5,8	21,6	30,1	-0,3	116,7	-4,3
Leukemia	HL-60(TB)	19,4	19,9	21,8	15,0	9,7	9,5	103,0	15,7
Leukemia	K-562	15,1		11,7	15,7	18,2	-4,1	84,3	-4,8
Leukemia	MOLT-4	28,4		27,4	3,6	10,0	1,9	109,3	1,4
Leukemia	RPMI-8226	32,0	29,4	14,3	11,1	-0,3	-6,0	109,5	-4,4
Leukemia	SR	31,2	22,2	6,9	-21,7	5,5	-6,8	125,4	11,1
Non-Small Cell Lung Cancer	A549/ATCC	27,1	22,1	22,4	11,1	12,1	7,9	37,5	12,6
Non-Small Cell Lung Cancer	EKVX								
Non-Small Cell Lung Cancer	HOP-62	5,4	2,4	-5,5	6,8	-1,1	-10,0	26,9	-1,0
Non-Small Cell Lung Cancer	HOP-92	32,7	33,4	10,9	5,6			110,9	-7,6
Non-Small Cell Lung Cancer	NCI-H226	-1,5	15,7	8,5	1,5	7,7	0,0	26,0	8,7
Non-Small Cell Lung Cancer	NCI-H23	18,0	30,4	15,9	13,2	2,2	3,5	109,9	5,7
Non-Small Cell Lung Cancer	NCI-H322M	-0,4	6,2	8,3	10,2	-5,4	0,0	21,1	0,1
Non-Small Cell Lung Cancer	NCI-H460	3,5	6,0	2,1	-0,8	-3,8	-3,1	87,5	1,4
Non-Small Cell Lung Cancer	NCI-H522	10,2	24,5	20,6	61,4	31,0	4,0	90,1	1,3
Colon Cancer	COLO 205	-7,3	-7,8	-5,4	-6,2	-2,6	-2,9	90,0	1,0
Colon Cancer	HCC-2998	-6,1	-1,7	4,0	4,5	-2,2	-1,5	55,5	-7,6
Colon Cancer	HCT-116	14,8	28,4	15,1	-6,0	14,0	6,5	159,8	9,5
Colon Cancer	HCT-15	4,6	17,3	14,9	15,9	6,1	1,7	147,0	0,3
Colon Cancer	HT29	3,2	21,3	8,8	3,3	9,7	-15,0	149,5	3,3
Colon Cancer	KM12	18,2	12,5	6,6	20,3	-5,4	-15,1	142,0	-0,6
Colon Cancer	SW-620	11,2	4,7	3,2	0,1	0,8	-6,0	171,4	2,7
CNS Cancer	SF-268	8,5	5,1	6,8	5,1	28,9	-17,0	95,5	-5,3
CNS Cancer	SF-295	-3,4	0,7	5,6	5,2	1,1	0,1	23,7	-3,8
CNS Cancer	SF-539	7,4	9,6	0,0	15,5	10,0	-11,8	33,4	-4,1
CNS Cancer	SNB-19	-11,9	-10,6	-0,2	3,6	0,2	-1,2	30,5	8,7
CNS Cancer	SNB-75	16,0	25,2	11,9	13,2	39,6	1,0	47,8	12,7
CNS Cancer	U251	7,1	9,3	9,0	9,0	11,7	11,5	153,5	8,7
Melanoma	LOX IMVI	8,0	9,8	10,3	20,0	5,5	3,1	154,2	4,7
Melanoma	M14	6,9	5,3	0,9	0,6	9,8	-6,8	73,2	-6,9
Melanoma	MALME-3M	6,0	19,8	8,9	8,8	0,8	-6,1	128,8	1,8
Melanoma	MDA-MB-435	10,4	10,4	2,8	7,3	8,5	-0,3	167,7	-7,1
Melanoma	SK-MEL-2	6,3	1,6	-9,0	0,5	0,3	-9,1	56,9	-8,7
Melanoma	SK-MEL-28	5,5	1,7	-10,1	-6,0	3,6	-18,3	122,2	-8,8
Melanoma	SK-MEL-5	-3,3	8,6	-1,6	2,6	-0,4	-4,0	7,5	0,9
Melanoma	UACC-257	6,3	1,6	-9,0	0,5	0,3	-9,1	56,9	-8,7
Melanoma	UACC-62	17,1	10,4	17,4	7,9	-2,3	5,4	77,7	1,3
Ovarian Cancer	IGROV1	-14,9	8,0	3,6	-15,5	-3,4	-1,8	81,9	0,6
Ovarian Cancer	NCI/ADR-RES	6,0	12,5	4,1	7,7	0,3	-0,2	70,0	-4,5
Ovarian Cancer	OVCAR-3	2,3	0,0	-1,6	-7,2	25,3	-18,9	176,0	-13,3
Ovarian Cancer	OVCAR-4	19,8	26,3	8,2	2,9	16,4	-9,0	67,9	4,3
Ovarian Cancer	OVCAR-5	2,5	1,2	-5,8	-6,3	-13,6	-26,4	25,2	-9,7
Ovarian Cancer	OVCAR-8	8,1	13,4	4,4	4,6	7,3	2,6	119,2	2,2
Ovarian Cancer	SK-OV-3	-16,3	-10,0	-22,9	-9,1	-0,7	0,3	35,2	-10,9
Renal Cancer	786-0	5,0	5,6	5,4	-0,7	13,1	2,9	68,1	-12,2
Renal Cancer	A498	11,6	0,7	32,6	21,5	40,7	45,2	73,4	25,1
Renal Cancer	ACHN	-10,6	1,4	4,1	14,8	12,0	-5,5	109,7	-1,7
Renal Cancer	CAKI-1	7,0	2,9	7,3	16,8	4,0	-0,1	87,0	6,3
Renal Cancer	RXF 393	0,4	7,8	5,9	0,9	60,2	-1,2	56,7	-14,3
Renal Cancer	SN12C	11,1	19,4	6,9	2,1	18,2	-3,5	88,2	5,6
Renal Cancer	TK-10	9,6	-20,4	-1,3	-3,3	-3,1	-13,4	64,0	-21,0
Renal Cancer	UO-31	27,6	39,7	32,9	23,3	30,3	27,2	99,7	38,3
Prostate Cancer	DU-145	-9,5	-1,0	-3,3	11,3	-3,8	-10,2	39,8	-9,0
Prostate Cancer	PC-3	22,4	25,3	18,2	12,7	3,1	-0,4	89,0	18,9
Breast Cancer	BT-549	7,4	-10,5	-7,6	13,2	-0,5	-2,2	99,2	-0,4
Breast Cancer	HS 578T		9,5	4,9	-13,8	9,9	-2,5	61,9	-4,9
Breast Cancer	MCF7	-8,2	15,2	-2,0	8,5	15,2	3,5	75,3	13,9
Breast Cancer	MDA-MB-231/ATCC	9,5	9,2	3,7	16,7	15,9	-0,7	122,8	14,7
Breast Cancer	MDA-MB-468	-7,7	-6,1	9,1	10,7	12,9	11,2	104,2	-21,4
Breast Cancer	T-47D	14,6	32,0	27,2	13,6	15,8	6,3	82,0	10,3

		144h	181g	181i	228a	228b	228d	234e	234a
Type of cancer	Cell line								
Leukemia	CCRF-CEM	8,6	13,8	26,9	9,5	11,6	9,0	15,6	5,7
Leukemia	HL-60(TB)	12,3	23,8	57,0	20,1	25,2	17,3	15,8	23,6
Leukemia	K-562	-3,9		30,5	-9,1	14,0	7,3	22,3	3,3
Leukemia	MOLT-4	-3,3		6,2	-1,6	3,8	2,7	4,5	3,9
Leukemia	RPMI-8226	-2,0	23,2	53,6	6,3	8,5	4,9	6,8	11,0
Leukemia	SR	7,4	12,3	51,3	0,4	13,6	7,9	5,7	1,7
Non-Small Cell Lung Cancer	A549/ATCC	19,2	12,9	10,6	3,3	10,0	9,2	6,5	12,5
Non-Small Cell Lung Cancer	EKVX								
Non-Small Cell Lung Cancer	HOP-62	-1,6	1,6	-18,6	-7,0	-5,7	-6,1	-11,0	-16,3
Non-Small Cell Lung Cancer	HOP-92	11,0	11,5	22,2	5,5			24,8	-1,3
Non-Small Cell Lung Cancer	NCI-H226	12,8	13,9	10,1	7,5	3,8	6,8	1,5	-0,7
Non-Small Cell Lung Cancer	NCI-H23	6,8	17,8	35,6	15,6	6,8	18,7	4,0	8,8
Non-Small Cell Lung Cancer	NCI-H322M	1,0	-11,5	-10,6	-18,7	-10,2	-3,5	0,8	-2,7
Non-Small Cell Lung Cancer	NCI-H460	-3,1	0,0	2,6	-4,0	-1,6	-2,6	-3,5	-1,2
Non-Small Cell Lung Cancer	NCI-H522	10,8	20,5	29,5	25,7	25,7	10,2	19,2	10,9
Colon Cancer	COLO 205	-4,7	4,4	16,1	-4,6	2,3	5,1	-2,3	-1,0
Colon Cancer	HCC-2998	-11,5	-4,9	15,4	-3,4	-3,5	-0,9	-8,9	-6,2
Colon Cancer	HCT-116	5,8	30,2	32,8	15,8	25,6	28,8	-3,3	15,7
Colon Cancer	HCT-15	4,1	13,6	14,4	17,2	13,8	15,8	3,0	11,3
Colon Cancer	HT29	-10,7	36,8	36,1	23,2	25,2	21,4	-2,7	19,5
Colon Cancer	KM12	-6,8	-4,6	5,3	-2,2	-9,0	-5,8	-2,5	-7,7
Colon Cancer	SW-620	-3,6	10,1	10,6	3,8	0,3	5,7	-0,9	3,4
CNS Cancer	SF-268	-10,2	-1,2	0,4	-7,5	-2,0	-17,4	3,4	-12,2
CNS Cancer	SF-295	-7,1	-3,4	5,7	3,7	2,1	-1,0	0,7	-2,1
CNS Cancer	SF-539	-2,2	1,3	2,0	-6,6	-3,8	-6,1	2,4	-5,1
CNS Cancer	SNB-19	4,3	6,6	5,8	4,4	0,4	-0,1	-4,7	7,5
CNS Cancer	SNB-75	12,0	14,2	15,0	-2,9	15,1	4,9	16,2	-2,2
CNS Cancer	U251	11,6	7,0	15,2	1,4	10,4	7,6	5,8	7,9
Melanoma	LOX IMVI	7,2	11,0	7,5	0,4	-0,1	3,3	2,6	-1,6
Melanoma	M14	0,3	-1,1	4,1	-3,7	6,5	-1,7	-10,3	-12,4
Melanoma	MALME-3M	0,1	5,1	14,3	6,5	-3,1	-3,7	1,5	6,2
Melanoma	MDA-MB-435	0,6	-1,2	12,4	7,1	2,1	4,7	-0,5	4,8
Melanoma	SK-MEL-2	-7,9	-4,5	-4,8	-1,5	5,9	0,7	-12,9	-2,0
Melanoma	SK-MEL-28	-8,9	-5,6	-0,8	-0,7	-9,9	-16,1	-3,8	-3,8
Melanoma	SK-MEL-5	2,2	-2,2	1,3	5,4	12,1			
Melanoma	UACC-257	-7,9	-4,5	-4,8	-1,5	5,9	0,7	-12,9	-2,0
Melanoma	UACC-62	1,7	5,0	18,8	13,5	12,3	23,3	4,4	16,7
Ovarian Cancer	IGROV1	-10,4	9,0	12,4	-19,1	-1,2	14,5	-11,6	-1,7
Ovarian Cancer	NCI/ADR-RES	-5,7	5,0	3,4	-6,7	-0,9	2,6	-5,1	-5,1
Ovarian Cancer	OVCAR-3	-15,0	-19,1	1,8	-17,2	-14,1	-25,4	-12,6	-20,1
Ovarian Cancer	OVCAR-4	-9,4	8,6	40,2	13,7	21,3	17,2	7,4	9,6
Ovarian Cancer	OVCAR-5	11,7	2,7	-4,7	-2,2	-1,0	-20,1	-4,4	-12,1
Ovarian Cancer	OVCAR-8	4,7	6,8	3,9	-1,0	3,8	0,6	0,8	7,4
Ovarian Cancer	SK-OV-3	0,4	0,7	-3,7	-8,8	-9,1	7,2	-10,6	-16,0
Renal Cancer	786-0	-12,2	-4,1	5,2	0,4	6,0	0,7	-2,6	-1,6
Renal Cancer	A498	31,2	38,2	44,5	44,5	26,9	31,3	15,0	40,4
Renal Cancer	ACHN	5,7	3,6	-5,3	-9,4	1,8	-2,8	5,1	-4,2
Renal Cancer	CAKI-1	9,5	9,6	-0,6	0,1	4,6	12,3	3,3	-1,8
Renal Cancer	RXF 393	-3,9	-1,5	18,8	-4,6	-0,2	-3,9	-2,1	-16,2
Renal Cancer	SN12C	12,3	7,0	0,8	-2,9	1,0	8,9	6,6	7,7
Renal Cancer	TK-10	-8,3	-16,0	-7,2	-4,3	-13,2	-23,4	-12,7	5,8
Renal Cancer	UO-31	19,2	28,2	15,7	14,4	12,8	9,4	15,4	15,5
Prostate Cancer	DU-145	-12,7	-12,4	-4,7	-7,2	-7,0	-14,7	-10,1	-9,4
Prostate Cancer	PC-3	19,1	7,6	12,2	6,7	4,8	-1,2	10,5	22,3
Breast Cancer	BT-549	-4,9	-14,1	12,5	-9,8	-12,4	-2,2	-18,4	-2,4
Breast Cancer	HS 578T	-3,9	-2,4	0,6	-12,1	-10,3	-4,5	-3,3	-0,1
Breast Cancer	MCF7	13,9	4,0	7,6	3,1	4,0	9,6	-6,8	-1,0
Breast Cancer	MDA-MB-231/ATCC	19,7	8,1	0,1	-2,9	5,4	1,4	-5,5	5,7
Breast Cancer	MDA-MB-468	2,9	0,7	79,4	-9,1	1,4	12,0	-22,7	-2,5
Breast Cancer	T-47D	8,7	22,8	37,7	14,5	14,6	18,2	13,8	11,9

		234c	234f	234h	191g	191h	191i
Type of cancer	Cell line						
Leukemia	CCRF-CEM	3,6	6,5	-3,4	5,5	7,5	-3,9
Leukemia	HL-60(TB)	14,1	16,5	20,4	9,7	11,3	21,5
Leukemia	K-562	12,2		-11,4	2,2	5,0	-1,6
Leukemia	MOLT-4	3,3		-3,2	1,9	7,3	-15,2
Leukemia	RPMI-8226	3,5	26,3	0,0	17,9	17,7	9,3
Leukemia	SR	-13,9	8,1	-14,9	-12,6	-20,2	-26,8
Non-Small Cell Lung Cancer	A549/ATCC	20,1	22,3	-1,4	7,6	24,8	10,9
Non-Small Cell Lung Cancer	EKVX						
Non-Small Cell Lung Cancer	HOP-62	-8,3	-19,7	-15,4	-8,1	-14,0	-13,4
Non-Small Cell Lung Cancer	HOP-92	12,5	11,4	5,5	28,5		
Non-Small Cell Lung Cancer	NCI-H226	12,6	-1,1	3,0	11,7	9,5	-0,5
Non-Small Cell Lung Cancer	NCI-H23	2,7	9,3	-6,8	19,4	11,8	1,6
Non-Small Cell Lung Cancer	NCI-H322M	1,6	9,8	-9,1	-5,5	-4,3	-8,5
Non-Small Cell Lung Cancer	NCI-H460	-2,8	0,5	-2,7	8,0	3,4	-2,8
Non-Small Cell Lung Cancer	NCI-H522	2,8	12,0	-5,0	29,9	15,3	1,3
Colon Cancer	COLO 205	-11,1	-14,9	-17,0	-8,2	-5,2	-7,0
Colon Cancer	HCC-2998	-17,1	-8,5	-4,6	-7,0	-4,6	-9,4
Colon Cancer	HCT-116	2,2	13,2	-6,1	40,0	18,1	1,5
Colon Cancer	HCT-15	3,3	7,7	2,7	17,4	9,4	-2,0
Colon Cancer	HT29	-8,7	-4,1	-7,7	20,6	8,1	-23,2
Colon Cancer	KM12	-7,6	-2,3	-14,0	5,8	2,3	-18,7
Colon Cancer	SW-620	-4,5	3,9	-2,1	12,0	2,4	-10,2
CNS Cancer	SF-268	-9,4	8,2	-12,9	0,3	-4,0	-23,7
CNS Cancer	SF-295	-11,8	-5,8	1,2	-0,9	-2,8	-4,6
CNS Cancer	SF-539	-1,3	-1,3	-0,3	-3,2	-2,5	-11,2
CNS Cancer	SNB-19	4,5	3,1	-4,3	0,5	2,2	7,9
CNS Cancer	SNB-75	13,6	12,9	-0,4	20,3	24,4	14,7
CNS Cancer	U251	17,9	1,5	-0,3	1,9	12,6	3,5
Melanoma	LOX IMVI	4,5	5,6	0,5	5,2	0,7	0,0
Melanoma	M14	-9,4	-6,8	-14,1	-6,9	6,6	-14,0
Melanoma	MALME-3M	-17,3	-6,1	-10,2	7,8	4,6	-11,6
Melanoma	MDA-MB-435	1,0	5,8	-3,3	6,0	9,1	1,9
Melanoma	SK-MEL-2	-15,3	-6,3	-24,4	1,3	0,7	-18,2
Melanoma	SK-MEL-28	-5,6	-3,2	-17,3	-2,8	-3,7	-31,9
Melanoma	SK-MEL-5						
Melanoma	UACC-257	-15,3	-6,3	-24,4	1,3	0,7	-18,2
Melanoma	UACC-62	12,7	15,9	0,2	27,2	29,6	8,6
Ovarian Cancer	IGROV1	-11,6	-5,5	-18,1	-9,4	3,0	-20,0
Ovarian Cancer	NCI/ADR-RES	-8,5	8,2	-8,7	-0,2	1,9	1,1
Ovarian Cancer	OVCAR-3	-17,5	-17,7	-19,6	-9,2	-8,2	-17,3
Ovarian Cancer	OVCAR-4	-4,3	10,1	-2,1	20,2	5,4	-17,1
Ovarian Cancer	OVCAR-5	-7,1	-5,0	-2,2	10,8	10,2	-20,5
Ovarian Cancer	OVCAR-8	4,9	9,3	2,1	3,4	11,0	7,8
Ovarian Cancer	SK-OV-3	-12,8	-16,2	-27,0	-22,0	-17,9	-14,9
Renal Cancer	786-0	-6,2	-2,5	-8,9	-3,0	3,8	-15,5
Renal Cancer	A498	30,6	9,5	29,9	18,2	27,9	58,7
Renal Cancer	ACHN	4,9	4,9	-0,9	0,1	8,1	-1,8
Renal Cancer	CAKI-1	13,8	8,7	-1,5	18,6	13,7	-4,8
Renal Cancer	RXF 393	-2,1	0,6	0,7	-3,4	7,8	-20,3
Renal Cancer	SN12C	8,7	1,2	-7,1	11,0	8,4	8,8
Renal Cancer	TK-10	-24,9	-11,9	-14,4	-6,1	-20,2	-49,4
Renal Cancer	UO-31	12,2	18,9	9,6	26,6	20,1	12,1
Prostate Cancer	DU-145	-18,6	-16,7	-13,8	-6,6	-10,9	-18,0
Prostate Cancer	PC-3	19,0	13,8	1,4	16,0	21,1	12,4
Breast Cancer	BT-549	-12,2	-11,4	-29,1	-16,7	-19,0	2,1
Breast Cancer	HS 578T	-6,2	2,5	0,4	-2,1	2,5	-11,8
Breast Cancer	MCF7	10,0	4,7	-8,0	-3,5	-8,0	-10,0
Breast Cancer	MDA-MB-231/ATCC	13,4	10,8	-8,5	16,0	9,1	9,3
Breast Cancer	MDA-MB-468	11,3	-4,1	2,9	-17,3	7,2	15,9
Breast Cancer	T-47D	25,5	22,9	-0,3	26,7	30,9	-3,7

Graphic data by cancer type

